THE SEARCH FOR CORRELATED ROTATION IN STERICALLY HINDERED, MULTI-n-BLADED $C_nAr_n^{x\pm}$ (n = 5, 6 and 7) PROPELLERS: FROM MODELS TO MOLECULES

By

STACEY BRYDGES, B.Sc.

A Thesis

Submitted to the School of Graduate Studies

in Partial Fulfillment of the Requirements

for the Degree

Doctor of Philosophy

McMaster University

MULTI-n-BLADED C_nAr_n PROPELLERS: FROM MODELS TO MOLECULES

DOCTOR OF PHILOSOPHY (2003) McMaster University

(Chemistry) Hamilton, Ontario, CA

TITLE: The Search for Correlated Rotation in Sterically Hindered, Multi-n-Bladed $C_nAr_n^{x\pm}$ (n = 5, 6 and 7) Propellers: From Models to Molecules

AUTHOR: Stacey Brydges

SUPERVISOR: Professor M. J. McGlinchey

NUMBER OF PAGES: xvi, 308

ABSTRACT

Crystallographically independent structures possessing persubstituted cyclopentadiene (C_5Ar_4X, $C_5Ar_4X_2$) and –dienyl (C_5Ar_5) moieties were retrieved from the Cambridge Structural Database, and the torsional angles of selected diaryl frames presented in the form of conformational plots. Semi-empirical (AM1) calculations of the corresponding potential energy surfaces reproduced the conformational trends observed in the solid state. By the Structure Correlation principle, the internal oscillations of nearest (1,2-) and next-nearest (1,3-) aryl rings in all pseudo-propeller subunits were found to be only partially correlated. These solid-state data sets, in combination with energetic predictions of the molecules $C_5Ph_5^-$ **1.18**, $C_5Ph_4H^-$ **2.1**, $C_4Ph_4C{=}O$ **1.53** and $C_4Ph_4CH_2$ **2.2**, indicate that a *delayed n-ring-flip* (where n = 5, X = 0-2 in $C_nAr_{n-m}X_m$), which is otherwise unobservable via NMR spectroscopic methods, is the threshold rotational mechanism in propeller systems of this type.

The least linear motion path associated with the reorientation of a single terminal phenyl group in the parent C_6Ph_6, **1.125**, has been mapped with the use of semi-empirical molecular orbital, ab initio Hartree Fock and hybrid density functional theory, in combination with numerous basis sets (STO-3G to cc-pVDZ). The superior energetic performance of the less common yet appropriately balanced B3PW91/6-31G(d,p) model chemistry compares favourably with the AM1 Hamiltonian in a conformational analysis of **1.125**. To evaluate the energetic and structural implications of replacing a phenyl group with different sterically anisotropic fragments, a series of polyarylated benzenes of the formula C_6Ar_5X have been synthesized by the Diels-Alder cycloaddition of the appropriate diarylacetylenes to tetraarylcyclopentadienones and subsequent extrusion of carbon monoxide. The X-ray structure determinations of perphenylphenylferrocene (**3.19**), 1-(pentaphenylphenyl)benzene-2-phenylacetylene (**3.26**), 1-(1,2-Z-dibromo-2-phenyl)vinyl-2,3,4,5,6-pentaphenylbenzene (**3.35**) and 1-(2-born-2,3-en-2-yl)-2,3,4,5,6-pentaphenylbenzene (**3.40**) are correlated with the NMR measurements of rotational isomerism in solution.

The solid-state characterization of the heptaphenylcycloheptatrienyl cation, $C_7Ph_7^+$, **1.139**, in $[C_7Ph_7^+][CF_3CO_2^-]\cdot 2CF_3CO_2H$, represents the *first nondisordered* structure solution of a *free* tropylium cation and ends a formidable, three decade long crystallographic quest. The conformational features of **1.139** and other polysubstituted $C_7R_{7-m}H_m$ (where $4 \leq m \geq 0$, R = Ph, Me) derivatives have been rationalized by semi-empirical (AM1) calculations, and reveal a compromise between steric congestion and the fractional loss in aromaticity as the central ring distorts from planarity. A correlation of the ^{13}C-NMR chemical shift with the computed electron density for $C_nH_n^{x\pm}$ and $C_nAr_n^{x\pm}$ species (n = 3 to 7) yields a proportionality factor of approximately 21 and 22 ppm per extra 0.1 electron at the central ring carbons, respectively. The steric capacity of the Diels-Alder cycloaddition reaction has been corroborated by the synthesis of C_7Ph_6FcH, **4.38**, for which the structural perturbations induced by the ferrocenyl fragment were quantified on both static (X-ray crystallography) and dynamic (variable-temperature NMR) levels. Subsequent attempts to study π-delocalization effects in the α-stabilized organometallic cation, $[C_7Ph_6Fc]^+$, were thwarted by the apparent inaccessibility of the methine hydrogen in **4.38** by appropriate reagents. An X-ray diffraction analysis confirmed the formation of $[C_7Ph_6FcH]^+$ $[SbCl_6]^-$, **4.44**, via an electron abstraction at the metal center.

ACKNOWLEDGEMENTS

I would like to thank my doctorate supervisor, Dr. Michael McGlinchey, for empowering me to become an independent practitioner of science, for providing me with the guidance and freedom to explore and discover new research avenues and interests, and for enabling and encouraging me to nurture my passion for science in other pursuits, including literacy, teaching, and writing. MJM: in your unwavering support of and trust in my professional and personal endeavours, I have grown as both a scientist and an individual. Know that your infectious love of chemistry and rhetoric are two, of among many, distinctions that I will always strive to uphold.

Over the course of my doctoral studies, I've had the great fortune to interact with and learn from many ardent and adept scientists. I wish to extend my gratitude to the members of my Ph.D. committee, Drs. Gary Schrobilgen and John Warkentin, for their helpful suggestions and careful critique of my graduate research. My early years in the laboratory were marked by challenging interchanges with Drs. Suzie Rigby and David Pole, whose respective expertise in NMR spectroscopy and computational chemistry invited new directions and encouraged my interests in both subject areas. The latter, in particular, led to a fruitful and exciting collaboration with Drs. Kim Baldridge and Jay Siegel at the San Diego Supercomputing Center (SDSC) and University of California at San Diego (UCSD). I am indebted to Kim for allowing me the incredible experience of working at SDSC/UCSD, and for her time, tutelage and friendship. Kim's dedication and tenacity in research, as well as her support of women in science, are truly inspiring. Of equal import were my discussions with Professor Hans-Beat Bürgi of the Universitaet Bern, Switzerland, who impressed upon me the importance of chemical intuition and mathematics, and who so graciously provided guidance in his Structure Correlation theory. I also wish to acknowledge the valuable discourse regarding computational chemistry given me by Professor Robert Pascal of Princeton University. Finally, I am grateful to Drs. Ignacio Vargas-Baca and Paul Berti of McMaster University, who in the past year-and-a-half, have both lent an

ear and eye toward my research and future goals. For helping me to keep my eyes open during this transition, I give thanks to my friends and colleagues, Drs. Alex Adronov and John Valliant.

There are many individuals in the Department of Chemistry at McMaster that contribute 'behind the lines' to our success and growth as researchers. For sharing their wealth of knowledge and technical command, I am indebted to: Dr. Don Hughes and Mr. Brian Sayer of the NMR spectroscopy facility; Drs. Richard Smith (past) and Kirk Green (present) of mass spectrometry; and finally, Dr. Jim Britten in X-ray crystallography, who is also a good friend and advocate. I must credit Mike Mallot for his tireless assistance in the computational arena: Mike, you have come to the rescue more times than I can list, and always with a smile and great counsel. Last, but not least, I wish to recognize all of the past and present members of the office and chemistry stores, including Carol Dada, Josie Petrie, Marilyn McIntyre and Barbra DeJean, for their selfless efforts and daily doses of sunshine!

A significant part of this experience has comprised my lab mates, both past and present, of ABB-357: Drs. Suzie Rigby, David Pole, Ralph Ruffolo, Jamie Dunn, Pippa Lock, Mark Stradiotto, Hari Gupta, Sonya Balduzzi, Yannick Ortin, as well as Laura Harrington, John Kaldis, Francis Ogini, Nada Reginato, and the many undergraduate and visiting students. Thank you for your warm fellowship and the great pleasure I've had working alongside and learning from each of you. In relation to SDSC/UCSD, I extend my sincere appreciation to Laura Gregerson for sharing her office space and computational talents, and to Roie Yerushalmi (Weizmann Institute) and Dr. Jerry Greenberg (SDSC) for also showing me the ropes.

Financial assistance, including scholarships or funding opportunities from NSERC of Canada, the Ontario Government, Dow Chemical of Canada and the Department of Chemistry, School of Graduate Studies, Dean of Science, and Center for Leadership in Learning at McMaster University, was gratefully received. CPU time was provided through the SDSC/UCSD and the Biomolecular Interactions Initiative at McMaster.

On a personal note, there are so many people that have impacted and enriched this part of my life journey. To the team members of the Anal Chemists, Bricklayers, Easy Lay-Ins, 200

Toes of Fury and guys on the early morning basketball court, I thank you for the great camaraderie and recreational outlet. In the halls of ABB, on the Phoenix patio, and elsewhere on this campus over the years, I have encountered too many wonderful individuals to name here.

I've been blessed with remarkable friends - a band of angels - who've cheered, motivated, guided and simply awed me by their depths. To Trac: from the grand challenges to the simple daily pleasures, I can't imagine not sharing this road with you! There aren't words enough to thank you. And also to Pip: I've grown by your grace and faith. To Jo: I admire your strength and vision. To Frank: your spirit, insight and laughter are gifts in my life. To Jules, Stacie (s^2-1), Leona, Christina, Nicola and the Bond St. babes - Ang, Di and Kim: your support and 'life' perspectives from the outside have been appreciated during this process. And to MJS, who was an original inspiration: thanks for sharing the handshake of your soul.

It has also been a privilege and unexpected joy to share in the warm embrace of many Southern Ontario families. To the Stradiotto relations, the Locks, Simmons and Felthams(-to-be), the Morkins, and the Hilemans, Pat and Ed: I've been moved by the incredible generosity, kindness and love that you have shown me over the years. And the Valley has always been within reach, thanks to the extended Brydges and Dittburner clan. For their added lessons of courage and compassion, I humbly acknowledge my grandmothers, Emily and Irene, as my mentors in ife and guardian angels beyond.

Lastly, to Mom, Dad, Byron (Mo) and Joel (Kelly): There has never been a time or place when I haven't felt you by my side. With every call across the miles, "card made and play laid", life chat along the 401, home-cooked meal and Valley adventure (fish shack and all!), your love has sustained me and given me the freedom to dream and the courage to leap. With my deepest love, respect and gratitude ... this one's for you.

"And then there's that thing that seems to be more than a dream; It's almost like a map, a map that you live by, that you trade your days for, knowing that some day you're going to stand on top of that mountain, holding everything you saw in your head right there in your hands." My final shout-out to GB for "The River" and the unforgettable moments that it has marked.

TABLE OF CONTENTS

Chapter One: Introduction

Chapter Five: From Iconic Models to Molecular Bevel Gears: Future Work & Perspectives

Chapter Six: Experimental and Computational Details

LIST OF TABLES

LIST OF FIGURES

LIST OF COMMONLY USED SYMBOLS AND ACRONYMS

NMR:	Nuclear Magnetic Resonance
T:	Temperature
E_a:	Activation Energy (Arrhenius)
$\Delta G^{\ddagger}$:	Gibb's Free Energy of Activation (Eyring)
IR:	Infra Red
PES:	Potential Energy Surface
SC:	Structure-Correlation
HF:	Hartree-Fock
HDFT:	Hybrid Density Functional Theory
Cp:	Cyclopentadienyl
PAH:	Polycyclic Aromatic Hydrocarbons
Fc:	Ferrocene

CHAPTER ONE

Introduction

"I held them in every light. / I turned them in every attitude. / I surveyed their characteristics. / I dwelt upon their peculiarities. I pondered upon their conformation. / I mused upon the alteration in their nature." (Edgar Allan Poe, "Berenice", 1835)

1.1 Forward

The detection and control of rotational motion about molecular bonds are themes that have permeated the chemical literature for more than a century. Fundamental issues, such as circumrotation around the carbon-carbon bond in ethane[1-3] or the metal-ligand coordination axis,[4-7] have been advanced and even supplanted gradually by more subtle aspects of modern conformational analysis and complex stereochemical phenomena.[8] Aided by recent paradigm shifts, the abstract linkages between macromechanical principles of motion and molecular-scale systems have provided fertile grounds for such innovations as molecular gears,[9-11] switches,[12;13] shuttles,[14;15] brakes,[16] turnstiles,[17] gyroscopes and compasses,[18;19] and even a mill.[20]

At both the macroscopic and microscopic levels, the arrest and promotion of movement are intricately tied to structure and constitution. With their attendant opportunities for restricted, or even coupled, molecular motions,[8] their suggested roles as micro-machines,[21;22] and their consequent relevance to nanotechnology,[23-26] *sterically crowded molecules*[27] offer a nexus between the two scales of size, property and dynamic function. Within this sweeping category of compounds, *molecular propellers* have provided a platform for exciting conceptual and experimental advances.

1.2 Conformational Analyses: The Time-Dependent Spatial Structure of Molecules

Molecular structure is typically described by a rigid point group formalism. Inasmuch as this approach neglects the effect of time, it is ambiguous when applied to molecules possessing a

number of thermally accessible structures that, under the appropriate conditions, may interconvert via rearrangements of an *intramolecular* character, such as rotation or inversion. Such being the case, the designation *stereochemically non-rigid* is given to systems that undergo rapid, internal processes which enable the permutation of nuclear positions.[28] If the interconverting species are chemically and structurally equivalent (i.e. no net stereochemical change), the compound is termed fluxional.[29]

The concept of free rotation about single bonds was unchallenged until the later part of the nineteenth century. Following the contributions of Van't Hoff, Le Bel and Bischoff,[30] the first definitive example of restricted mobility induced by the presence of bulky substituents was provided in 1922 when Christie and Kenner[31] resolved stable isomers of 2,2'-dinitro-6,6'-diphenic acid, **1.1**. Antithetically, it was not until 1956 that Wilkinson and Piper[32;33] provided experimental proof of the non-rigid nature of organometallic complexes. Rapid site exchange of the σ-cyclopentadiene moiety was attributed to "ring-whizzing" or [1,5] sigmatropic shifts of the metal fragment in $(\eta^5\text{-}C_5H_5)(\sigma\text{-}C_5H_5)Fe(CO)_2$, **1.2**.[34]

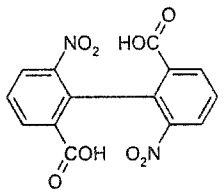

1.1

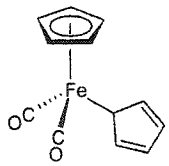

1.2

Scheme 1.1: *The study of internal rotation in **1.1** and **1.2** provided new insight into the conformational analysis of organic and organometallic compounds, respectively.*

Modern conformational systems comprised of alkyl, aryl and ML_n groups bonded to a central framework may be analysed on a multidimensional level. The emphasis is on the shapes of molecules in their energy minima, the heights of barriers separating them, and the low- (and occasionally high-) energy pathways interconnecting the minima.[35] To represent properly a molecular ensemble, the structural model must match a particular set of observations, which will depend on the lifetime of the molecular configurations present and the conditions of the relevant

physical (or chemical) measurement. Of course, the latter may vary for the same molecular system according to the time scale of observation, physical state (through which ground-state structures may vary) and instrumental sensitivity.[36] In this regard, any detailed stereochemical description of a non-rigid molecule or ion can benefit from the fruitful interaction between theory and experiment, which comprises a variety of structural techniques.

1.2.1 X-ray Crystallography

In the determination of X-ray structures, the molecule is approximated as a rigid body that is in fact a three-dimensional equilibrium arrangement of atoms vibrating about time-averaged positions on the X-ray diffraction time scale (10^{-18} s). While this static model corresponds to a single minimum on the potential-energy hypersurface (PES), approaches to extracting dynamic information from crystallographic data have been conceived in the past two decades. Structure-Correlation theory[37] is highly complementary to, among others, variable-temperature Nuclear Magnetic Resonance (NMR) spectroscopic and quantum mechanical methods.

1.2.2 Dynamic NMR Spectroscopy

The time-dependent conformations of a molecule that occupies more than one low-lying minimum on the PES may invoke both static and dynamic representations. Intramolecular rearrangements (i.e. rotations, inversions) typically occur on a time frame that is quite long relative to vibrational (IR, Raman) methods (10^{-13} s) but comparable to NMR spectroscopic experiments (10^{-1} to 10^{-9} s). Under conditions of dynamic equilibrium when a chemical exchange process is proceeding at a detectable rate, the resultant NMR spectral differences may be used in the determination of rate constants for the particular interconversion.[38] As such, dynamic NMR methods span three exchange regimes: fast ($k_{rate} \geq 10^5$ s^{-1}), which entail the evaluation of molecular correlation times obtained from relaxation or cross-relaxation experiments; intermediate ($k_{rate} \sim 1$ to 10^5 s^{-1}), which require measurement by total-band shape analyses; and, slow ($k_{rate} \sim 10^{-3}$ to 10^2 s^{-1}), which are of similar magnitude to the spin-lattice relaxation times (T_1)

for the exchanging sites, and thus make use of one-dimensional magnetization transfer techniques or two-dimensional exchange spectroscopy (2D-EXSY).

One-dimensional total band-shape analysis takes advantage of the fact that a transition from the slow to fast exchange regimes (or vice-versa) is accompanied by changes in NMR lineshapes (i.e. the functional relationship between signal intensity and frequency). In the slow motion region the exchanging sites show resolved, separated signals, whereas in the fast motion range the dynamic process causes one line at the population weighted average frequency of the individual sites; in the intermediate regime, the lines merge, that is collapse and broaden, sometimes to the point of being invisible, at the coalescence temperature, T_c. A comparison of the experimentally obtained NMR spectra (recorded at various temperatures) with a series of simulated spectra generated using assigned rate values, allows for an estimation of the rearrangement rate at *each* temperature from visual inspection. Following, the statistical analysis of rate data requires application of the Arrhenius activation theory (equation 1.1) to calculate the activation energy (E_a),

$$\ln(k_{rate}) = \ln(A) - E_a/RT \qquad \text{(Eq. 1.1)}$$

The more standard procedure relies on the use the absolute rate theory developed by Eyring (revised to give equation 1.2) to extract the enthalpic and entropic terms, $\Delta H^{\ddagger}$ and $\Delta S^{\ddagger}$, and thus, the free energy of activation, $\Delta G^{\ddagger}$ at a specified temperature:

$$\ln(k_{rate}/T) = (-\Delta H^{\ddagger}/R)(1/T) + \Delta S^{\ddagger}/R + \ln(k_b/h) \qquad \text{(Eq. 1.2)}$$

$$\Delta G^{\ddagger} = \Delta H^{\ddagger} - T\Delta S^{\ddagger} \qquad \text{(Eq. 1.3)}$$

The *coalescence temperature approximation* is a less-time consuming, albeit less rigorous, adaptation of the former approach. For two equally populated, non-coupled sites (at equilibrium), separated by a frequency difference, $\Delta\nu$ (in Hertz), in the absence of exchange, the rate constant, k_c, at the coalescence temperature, T_c, is given by:

$$k_c = \pi\Delta\nu/2^{0.5} \qquad \text{(Eq. 1.4)}$$

The free energy of activation at a *specific* coalescence temperature, $\Delta G_c^{\ddagger}$, can be determined by use of the Eyring equation (1.2):

$$k_c = \kappa(k_b T_c/h)\exp(-\Delta G_c^{\ddagger}/RT_c) \qquad \text{(Eq. 1.5)}$$

Rearrangement of equation 1.5 and substitution for k_c (Eq. 1.4) yields equation 1.7,

$$\Delta G_c^{\ddagger} = (-RT_c)\ \ln[k_c h/(\kappa k_b T_c)] \qquad \text{(Eq. 1.6)}$$

$$\Delta G_c^{\ddagger} = (-RT_c)\ \ln[h\pi\Delta\nu/2^{0.5})/(\kappa k_b T_c)] \qquad \text{(Eq. 1.7)}$$

where κ is the transmission coefficient (usually assumed to be unity), k_b is the Boltzmann constant (1.3807×10^{-23} JK^{-1}), h is the Planck constant (6.6262×10^{-34} Js), and R is the ideal gas constant (8.3144 $JK^{-1}mol^{-1}$). Typically, values of $\Delta G_c^{\ddagger}$ are quoted in units of kilocalories per mole (1 J = 0.23901 cal). Since the temperature at which coalescence occurs must be qualitatively identified from experimental spectra, an error range of at least ± 2 K is assumed.

It should be emphasized that the lineshape depends on the exchange rate, k, and thus on the time spent by the nuclei in a particular environment. This in turn is a function of the external magnetic field (to which chemical shifts are proportional) and the applied temperature; as such, the available instrumentation offers various strengths (60 to 900 MHz) and operational ranges (-150 to 150 °C). While dynamic processes are commonly investigated using ^{1}H NMR spectroscopy, the greater chemical shift range of other nuclides (^{19}F, ^{31}P, ^{13}C) are also employed. Beyond these factors, a successful experiment may be hampered by the spectral complexities associated with multi-site systems or the thermal limits (i.e. high-temperature instability or low-temperature insolubility) of a chemical sample.

In sum, DNMR spectroscopy allows access to a wide range of free energies of activation (5 to 25 kcal mol^{-1}). However, as a technique that deals exclusively with the phenomenon of site exchanges among nuclei, it is uninformative with respect to ground states or transition states; instead, it provides data on the energy gap between these two states, and in some instances, evidence for preferred interconversion pathways.[39] In addition to structure elucidation, theoretical

calculations can be of help in understanding the steric, coulombic and electronic effects on the rates of rearrangement.

1.2.3 Quantum Mechanical Methods

Computational chemistry has emerged from the fundamentals of theoretical chemistry as a complex blend of new methodologies, enhanced predictive theories, and high-performance computing strategies applied to scientifically challenging problems. Combined programs of computational prediction and experimental verification continue to advance our understanding of molecular properties and the design principles for molecular construction. From problem identification, to selection of model, relevant calculations and interpretation of results, the assessment of quantum chemical methodologies requires knowledge of the premises and limitations of the underlying principles.[40]

The goal of most quantum mechanical calculations is to find a molecular wavefunction, which then allows the determination of molecular orbitals, the associated energy and derivative properties. This necessitates solution of the time-independent Schrödinger equation, which in short-hand operator form is given as

$$\mathbf{H}\Psi = E\Psi \qquad \text{(Eq. 1.8)}$$

where E is the total energy, Ψ is the *wave function*, and H is the *Hamiltonian operator*. The computational practicality of exact solutions to equation 1.8 does not extend beyond the H_2^+ molecule, and similar one-electron systems; electronic structure methods are therefore characterized by the type and derivation of the mathematical approximations, which in some cases include empirical data, employed in the solution of the Schrödinger equation. In contrast to semi-empirical approaches, methods that do not employ parametrization are termed *ab initio* ("from scratch") and encompass Hartree-Fock (HF) or molecular orbital (MO) theory, configuration interaction (CI) theory, and perturbation theory (PT). Although it is occasionally

(and incorrectly) included in the latter description, density functional theory (DFT) constitutes a third class of methods.

In the *Born-Oppenheimer* model of molecular structure, it is assumed that the electron distribution within a system depends on the positions of the nuclei, and not on their momenta. This assumption motivates the view that electrons move in electronic wave functions (for example, orbitals) that smoothly 'traverse' the molecule's atomic framework. The complete Hamiltonian is comprised of kinetic and potential energy terms,

$$H_{TOT} = [T_n] + [T_e + V_{ne} + V_{ee} + V_{nn}] \qquad \text{(Eq. 1.9)}$$

allowing for the separate derivation of the electronic wavefunction for a fixed nuclear geometry, which in turn serves as an effective potential for the subsequent analysis of the nuclear wavefunction. In neglecting the kinetic energy term for the nuclei, which is necessary for the generation of molecular vibrational and rotational energy levels, the solution to the electronic Schrödinger equation yields the potential energy surface associated with nuclear motion. A slice through such a surface (*i.e.* a plot of the energy as a function of two out of 3N-6 coordinates for a non-linear polyatomic molecule having N atoms) is shown below, with selected features detailed.

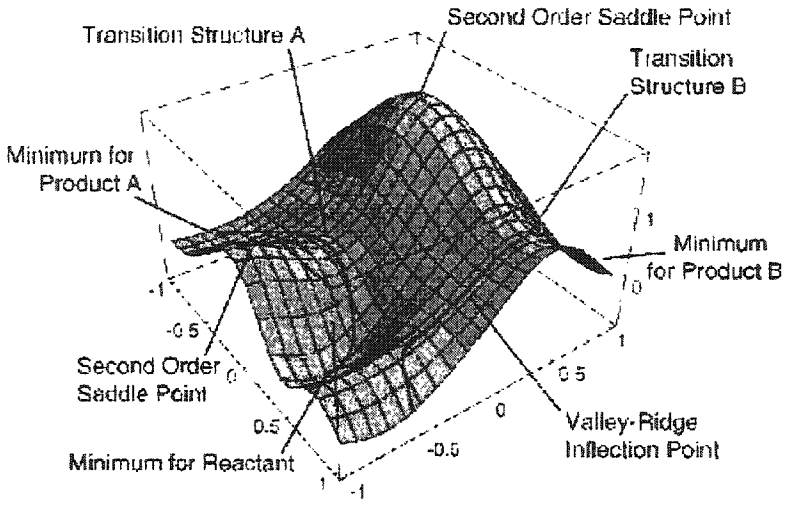

***Figure 1.1**: A slice of the potential energy surface for a polyatomic molecule.*

After taking into account the normalization and antisymmetric restrictions placed on the wave function, the orbital approximation yields the many-electron wave function, Ψ, as the determinant of constituent three-dimensional spin-orbital functions (ϕ_i) (only closed-shell systems are considered here). These unknown molecular orbitals are further expanded as a linear combination (LCAO approach) of pre-defined one-electron orbital or basis functions (χ_i) centered on the atomic nuclei (Eq. 1.10). Typically, exponential Slater (STO) or radial Gaussian (GTO) type basis functions are used in electronic structure calculations.

$$\Psi = |\,\phi_1(r_1)\bar{\phi}_1(r_2)\phi_2(r_3)\bar{\phi}_2(r_4)\ldots\phi(r_{2\theta-1})\bar{\phi}_\theta(r_{2\theta})\,| \text{ where } \phi i = \sum c_{ik}\chi_k \qquad \text{(Eq. 1.10)}$$

The variational principle is used to derive the Hartree-Fock equations, which in turn give rise to the Roothaan-Hall secular equations that describe the molecular orbital expansion coefficients (c_μ) as related to the Fock, density and overlap matrices. The set of coefficients that minimize the energy of the resultant wave function are generated via an iterative Self-Consistent Field (SCF) procedure. The total energy, which is *not* simply a sum of MO orbital energies, can be represented as:

$$E_{HF} = \sum_{i=1}^{N} h_i + 1/2\sum_{i=1}^{N}\sum_{j=1}^{N}(J_{ij} - K_{ij}) + V_{nn} \qquad \text{(Eq. 1.11)}$$

where h_i, the one-electron operator, describes the motion of electron *i* in the field of all the nuclei, *J* is the coulomb integral, *K* is the exchange integral and V_{nn} accounts for the nuclear-nuclear repulsion.

Such a solution produces a total of M (= number of basis functions) MOs, which increase in accuracy towards the limit of the *complete* basis set. Practically, this is offset by the computational effort associated with the one-electron integrals (on the order of M^2) and two-electron integrals (proportional to M^4) required to construct the Fock matrix.

1.2.3.1 Semi-Empirical Methods

Semi-empirical methods are based on (a) the central assumption of the *Zero Differential Overlap* approximation, which neglects all products of basis functions depending on the same

electron coordinates when located on different atoms (i.e. elimination of all three- and four-center two-electron integrals), and (b) parameterization of the remaining integrals. Reducing the number of integrals and further considering only the valence electrons explicitly, by way of a minimum basis set, significantly decreases the computational effort associated with this methodology.

1.2.3.2 Post SCF Methods

Under Hartree-Fock treatment, the approximation of a single Slater determinant as the trial wavefunction generates solutions to the Schrödinger equation where the real electron-electron repulsion is replaced by an average interaction. Post-SCF methods attempt to remedy this inadequate treatment of the correlated motion of electrons, particularly that associated with electrons of opposite spin. The *Electron Correlation* energy represents the remaining energy error between the limiting HF energy and the true total energy in a given basis, taking into account the relativistic effect. CI methods expand the single determinant HF wavefunction by selectively substituting occupied orbitals for virtual orbitals (*i.e.* equivalent to electron excitations) in the determinant, allowing for mixing of the electronic states of the molecule. Alternatively, Møller-Plesset perturbation theory provides second-order and higher energy corrections by expanding (via a Taylor series) the wavefunction.

1.2.3.3 DFT Methods

Whereas the many-body wavefunction (in the form of a Slater determinant) is fundamental in HF theory, the density functional theory approach is based upon a strategy of modeling electron correlation via general functionals (a function whose definition is itself a function) of an observable quantity, the electron density. Practical implementation of DFT leads to effective one-electron equations based on the Kohn-Sham formalism, where the orbital dependent exchange operator of the HF equations is formally replaced by exchange ($E_x[\rho]$) and correlation ($E_c[\rho]$) functionals that depend only on electron density (and spin density in spin-polarized calculations), as depicted in equation 1.12.

$$E_{KS} = \sum_{i=1}^{N} h_i + 1/2 \sum_{i=1}^{N} \sum_{j=1}^{N} J_{ij} + V_{nm} + E_x[\rho] + E_c[\rho] \qquad \text{(Eq. 1.12)}$$

Thus, HF theory is considered to be a special case of DFT, with $E_x[\rho]$ given by the exchange integral, -1/2<P*K*(P)> and $E_c = 0$.

While it has been proven that each density yields a unique ground-state energy, the explicit functional form of the exchange-correlation potential has remained elusive. The goal of DFT methods is to design such functionals, which are typically classified as local (depending only on ρ) and gradient-corrected (depending on ρ and its gradient, $\nabla\rho$). By varying the component functionals, different paired functionals, $E_{xc}[\rho]$, are constructed.

In actual practice, self-consistent Kohn-Sham DFT calculations are performed in an iterative manner that is analogous to an HF-SCF computation. From this noted similarity in methodology has emanated *Hybrid DFT* methods, which are based on a formulation in which the exchange functional is represented as a linear combination of HF exchange and a DFT exchange-correlation. The conceptual definition of E_{xc} is provided by equation 1.13, where c represents a constant.

$$E_{HYBRID}^{XC} = c_{HF} E_{HF}^{X} + c_{DFT} E_{DFT}^{X} \qquad \text{(Eq. 1.13)}$$

Essentially all calculations employ an expansion of the KS orbitals in an atomic basis set, which are typically the same functions as those used in wave mechanics for expanding the HF orbitals (see below). While the computational effort of DFT is similar to that of HF methods, DFT provides an improved treatment of systems comprised of transition metals and corresponding pseudopotentials. Whereas relatively little is known about the systematic performance of DFT applied to typical organic molecules, it is a potentially good choice for the accurate description of electronic and structural properties of solids, surfaces and interfaces.

1.2.3.4 Basis Set Considerations

One of the approximations inherent in essentially all *ab initio* methods is the introduction of a basis set. Expanding an unknown function, such as a molecular orbital, in a set of known

functions is not an estimation if the basis is complete. When a finite basis is employed, only the components of the MO along those coordinate axes corresponding to the selected basis are represented. Both HF and DFT methods are one-dimensional in that increasing the size of the basis set allows for a better and better description of the respective orbitals. Thus, following selection of the type of function (STO/GTO) and the location (nuclei), the most important factor is the number of functions that is applied.

A *minimum basis set* encompasses only enough functions to contain all the electrons of the neutral atom(s). For example, a second row element is represented by three *s*-functions (1*s*, 2*s* and 3*s*) and two sets of *p*-functions (2*p* and 3*p*). *Double Zeta* (DZ) type basis sets, which double all basis functions, constitute the next improvement in methodology. A DZ basis thus employs six *s*-functions (1*s*, 1*s*', 2*s*, 2*s*', 3*s*, and 3*s*') and four (by 3) *p*-functions for second row elements. The DZ designation often includes, as a variation of the DZ basis, a *split valence* basis, which neglects to double the core orbitals that are independent of the chemical environment and bonding. Further multiplication of orbitals gives rise to Triple Zeta (TZ) basis sets and beyond. The inclusion of higher angular momentum functions, termed *polarization functions*, allows for the improved description of electron distribution differences along and orthogonal to a bond. Thus, the addition of a single set of polarization functions (*p*-functions on hydrogens and *d*-functions on heavy atoms) to the DZ basis forms a *Double Zeta plus Polarization* (DZP) type basis. Generally, the number of functions of a given type should at most be one less than the type with one lower angular momentum (i.e. a 3*s*2*p*1*d* basis is balanced, but a 3*s*2*p*2*d*2*f*1*g* basis is too heavily polarized). Failure to consider basis set balance may produce artefacts in wavefunctions (and possibly geometry) as the optimization procedure attempts to compensate for inadequacies in the selected basis. Lastly, for systems containing lone pairs, anions and/or excited states, basis augmentation with *diffuse functions* is an important consideration.

Basis set contraction, which combines the full set of basis functions, known as primitive GTOs, into a smaller set of functions by forming fixed linear combinations, is founded in the fact that many basis functions serve to describe the energetically important, but chemically insignificant, core electrons. The previously introduced acronynms DZP, *etc.* refer to the number of contracted basis functions. The specification of a basis set in terms of primitive and contracted functions is given by the notation (10*s*4*p*1*d*/4*s*1*p*) → [3*s*2*p*1*d*/2*s*1*p*], respectively, where the heavy atoms (first row elements) appear before, and hydrogen after, the slash. Pople-style, Dunning-Huzinaga, atomic natural orbitals and correlation consistent basis sets are among the many different contracted basis sets which are available in the literature and computational programs.

Finally, for molecular systems comprised of elements from the third row or higher in the periodic table, there are two issues which must be addressed: (1) relativistic effects; and (2) the fact that a proper description (expansion) of the valence orbitals requires a large number of basis functions, whereas many of the corresponding core orbitals are (in general) chemically irrelevant. A simultaneous 'solution' is offered by *Effective Core Potentials* (ECPs) (also termed *pseudopotentials*), which allow for core electrons to be modeled by a suitable potential but treat valence electrons explicitly using nodeless pseudo-orbitals.

1.3 Modern Stereochemistry and Molecular Machinery

Our understanding of molecular spatial structure and its consequences, which are central to issues of reactivity, property and function, could not have evolved without the dramatic progress in physical and theoretical methods of structure elucidation. In turn, the extraordinary growth and impact that stereochemistry has had in all facets of the chemical enterprise persists as the borders of this discipline expand and diffuse into many related fields, including nanoscience.

1.3.1 Molecular Propellers

From bacteria flagella to aerodynamics, propeller designs are prevalent in nature as well as scientific and technological domains. On the molecular level, the propeller designation is given to a generic class of compounds comprised of two or more subunits ("blades") arranged in a helical fashion about a central core (the "hub" or propeller axis). It is the corresponding sense of twist, and not the twist angle, that is the defining structural feature of these architectures, which, in the absence of substitution, possess a skeleton of D_n or C_n ($n > 1$) symmetry.[41] This deliberately flexible description encompasses a wide variety of structures, as exemplified in Scheme 1.2. Although constitutionally diverse, such multi-bladed systems are typically related by their static and dynamic stereochemistry.

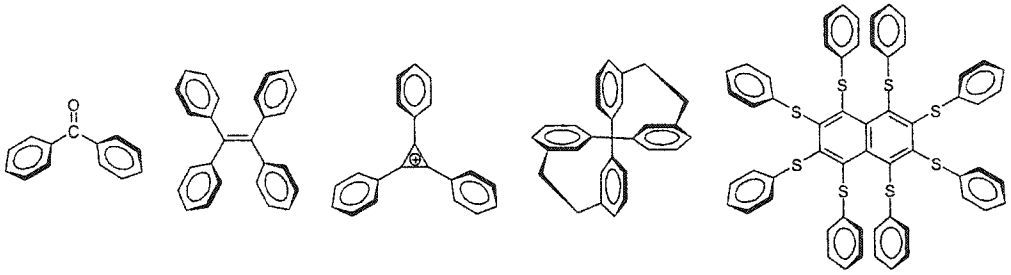

Scheme 1.2: *Selected examples of molecular propellers.*[42]

1.3.1.1 Static Stereochemistry

Conducted by Gust and Mislow[43;44] in the early 1970s, the extensive analyses of interconversion processes in di- and triaryl propeller structures presenting restricted conformational equilibria were pivotal to the development of modern stereochemical concepts. In the ground state, the number and symmetry of isomers can be enumerated mathematically and depend on the degenerate features of each molecule. According to the principle of chirality, the topological property of handedness of a given structure, there are three independent elements of stereoisomerism that may serve as specification: the center, axis and plane of chirality.* [36;45] To

---

* These three stereogenic units are the basis for the generally accepted CIP (Cahn-Ingold-Prelog) system. By definition, an object is chiral if it is not superimposable on its mirror image; otherwise it is achiral.[36]

illustrate, consider a molecule of the type Ar_3Z that is represented by the generalized structures **1.3** or **1.4**, wherein the three carbons attached to Z define a plane (the reference plane). By virtue of its propeller shape, *axial chirality* or *helicity* allows for only two enantiomeric states in either unlabeled or completely degenerate systems such as **1.3**. *Planar chirality* is induced by ortho or meta substitution of one or more aryl groups; in the absence of a local C_2 axis coincident with the Z-C bond, such labels may reside on either side of the reference plane. In **1.4**, where A ≠ B ≠ C, a separate conformation results from each of these edge interchanges, for a total stereoisomer count (N) of 2^4 (eight diasteromeric *dl* pairs), the product of the number and multiplicity of the stereogenic units. For the related tetrahedral systems Ar_3ZX, where X is any moiety with conical symmetry on the time scale of observation and all aryl rings are constitutionally distinct, the configuration at the *chiral center* accounts for a third form of stereogenicity. In combination with edge differentiation, there are thus 16 x 2 = 2^5 possible isomers (16 *dl* pairs) in the case depicted by **1.5**. By analogy, this reduction of structural features can be extended to isomerism in other propeller molecules.

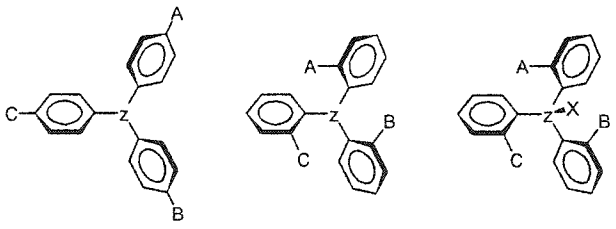

1.3 **1.4** **1.5**

Scheme 1.3: *Three elements of chirality (an axis, plane and center) or combination thereof may give rise to isomerism in the generic triaryl systems **1.3**, **1.4** and **1.5**.*

1.3.1.2 Dynamic Stereochemistry

Finally, the reader should take note that the stereochemical nomenclature used here and throughout the remainder of the document reflects the evolution of ideas in this area; presently, terms such as "planar chirality" are considered obsolete and often ambiguous.

The interconversion of isomers may occur by rotations of the aryl group about the C-Z bonds, which in principle, could constitute any number of reaction trajectories. A consideration of viable rearrangement alternatives identified the flip mechanisms, first proposed by Kurland et al.,[46] in which helicity reversal may be effected by disrotatory or conrotatory ring motion that involves passage through the reference plane, with concomitant edge interchange, or through a direction perpendicular to the propeller plane (denoted as a ring flip). Among the four classes of ring flips, the *two-ring flip*, whereby two rings are simultaneously orthogonal to and the other coplanar with the reference plane in the transition state, has been firmly established as the isomerization pathway of lowest energy in systems of the type Ar_3Z and Ar_3ZX (Scheme 1.4),[47] with one exception cited to date.[48;49] Since the flip mechanisms have no effect on the configuration of the chiral center, an additional pathway – pyramidal inversion – is incorporated into the description of internal dynamics in relevant Ar_3ZX molecules.

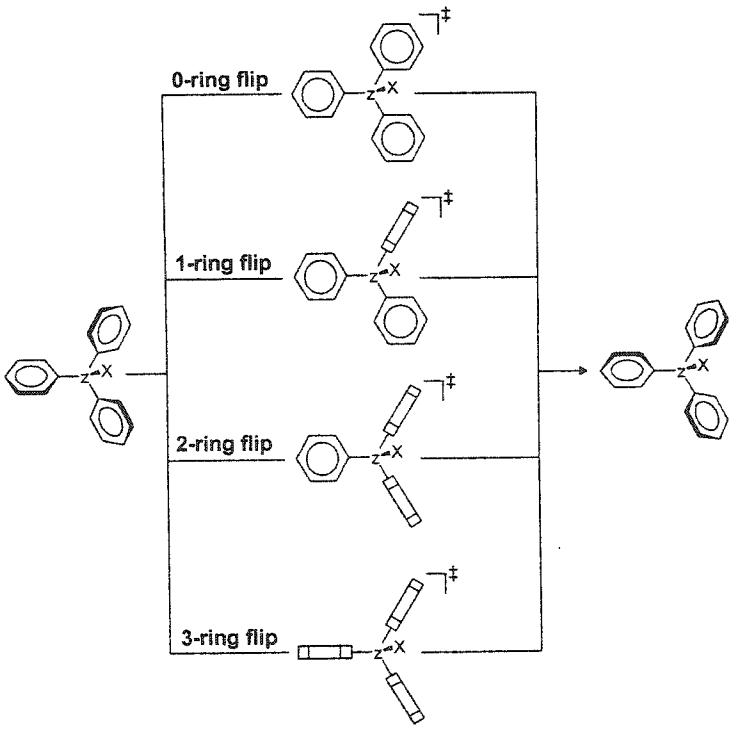

Scheme 1.4: *Stereoisomerization in triarylmethanes is conventionally distinguished by correlated ("n-ring flip") rotational pathways.*

Pending the disclosure of these studies, Mislow and co-workers advanced the powerful and unifying theory of *stereochemical correspondence*,[41] which identifies relationships among various groups of constitutionally dissimilar propeller molecules. For example, triarylboranes (Ar_3B) and the transition metal tris-chelates are intrinsically associated by the number and kind of both stereoisomers and respective n-ring flip or Rây-Dutt and trigonal twist (Bailar) rearrangements. Such an abstract, mathematical model equates static (point groups) and dynamic (permutational groups) stereochemical features, but does not provide information concerning the stabilities of ground-state structures or the actual physical mechanisms of the transformations. That (the lowest-energy) enantiomerization of trans forms of tris(2-methyl-1-naphthyl)borane, **1.6**, and tris(α-isopentyltropolonato)cobalt(III), **1.7**, is achieved by the two-ring flip and trigonal twist (three-ring flip equivalent), respectively, does not alter the isomorphic association of these two systems.

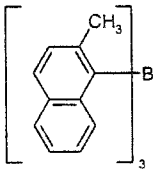

1.6

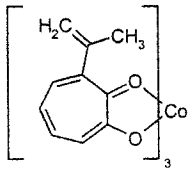

1.7

Another important and general phenomenon, *residual stereoisomerism*, was first adduced for *maximally labeled* Ar_3Z and Ar_3ZX moieties.[44;50] On a particular time-scale, the observation of closed subsets of interconverting isomers, separated by substantial barriers, emerges as a fascinating consequence of *correlated ring rotation.* Whereas there are no restrictions on the individual torsional angles, the interdependent motion of all three rings imposes a constraint on the relationship between torsional angles, thus blocking a number of isomerization pathways among the full set of conformers. For example, it is possible to separate chromatographically two achiral diastereomers (*dl* pairs) of (2-methoxynaphthyl)(2-methylnaphthyl)(3-methyl-2,4,6-trimethoxyphenyl)methane, **1.8**, despite the rapid spinning of all

aryl groups under the full operation of the two-ring flip; at temperatures in excess of 373 K, stereomutation occurs by a distinct rotational mechanism ($\Delta G^{\ddagger}$ = 30.5 kcal mol^{-1}).[50] In representing the structures of these residual isomers, reaction graphs or the equivalent group theoretical formalisms are required in the place of static models.

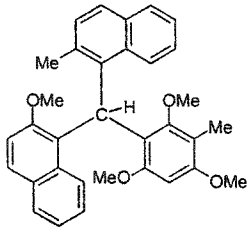

1.8

Scheme 1.5: *As an example of stable torsional isomers, diastereomers of* ***1.8*** *are separable at room temperature.*

The experimental realization of such novel stereochemistry suffices as a conditional test for sympathetic or coupled torsional motion, which is energetically favoured over the independent rotation of individual groups. Conformational changes exclusively following correlated pathways or a 'cog-wheeling circuit' have been revealed in numerous two- and three-bladed propeller prototypes, including diaryl-sulfoxides, -sulfones, -ethanols and -ethers[51-53] di- and triarylboranes;[54,55] triarylmethanes and triarylcarbenium ions;[47-49,56-60] trialkoxymethanes;[61] triarylamines;[62] triarylphosphines and derivatives;[63,64] polyarylethanes and ethylenes;[65,66] and complex, multiple propeller units.[67-70]

1.3.2 The Metamorphosis to Molecular Bevel Gears

By the late 1970s, the research groups of Mislow and Iwamura[71] had contemporaneously recognized the astonishing resemblance between correlated disrotation in three-bladed molecular propellers and the coupled behaviour of meshed gears. Already pervading the chemical literature were examples of the *static gear effect*, the interlocking of alkyl groups or n-fold rotors in the ground state "by virtue of cooperative non-bonded repulsions" induced under conditions of intramolecular crowding.[35] In extending the analogy to *dynamic gearing*,[72] the intermeshing of a

chemical rotor with a neighbouring group is manifested in the mechanical selection rules (disrotatory allowed, conrotatory disallowed) and the observation of residual stereoisomerism attributable to the conservation of phase relationships in an appropriately labeled molecule (later termed 'phase isomerism').* Despite apparent similarities, Mislow cautioned that the cogwheel metaphor was flawed for molecular propellers since the two-fold nature of the aryl rings precludes the obligatory tongue-and-groove interaction.[21] Ideal candidates for highly mobile (with rotation rates on the order of 10^9 s^{-1}) and tightly meshed bevel gears proved to be Tp_2X (X=CH_2, etc.) systems **1.9** comprised of 9-triptycyl (Tp) moieties, previously shown by Oki[8] to possess exceptionally large three-fold torsional barriers (Scheme 1.6).

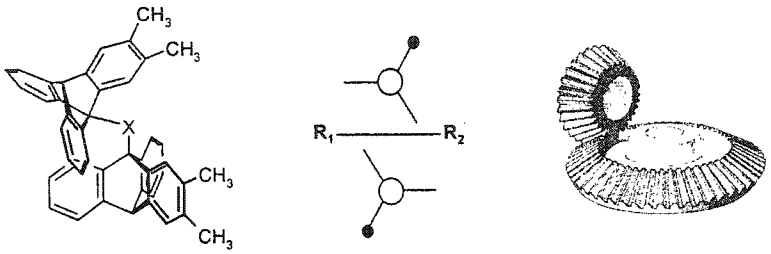

1.9

Scheme 1.6: *A labeled Tp_2X (Tp=9-triptycyl; X = CH_2, O, CO, etc.) molecule (**1.9**) and its analogic resemblance to macroscopic bevel gears. Under conditions of rapid disrotatory cogwheeling, three phase isomers (meso, dl) remain.*

A unique marriage of the propeller and gear models was unveiled in the triskelion species, Tp_3XZ (X=Ge, Z = Cl **1.10**; X=C^+, Z=ClO_4^- **1.11**), for which structural rigidity was induced by the odd number of securely interlocked rotors.[9] The transmission of cooperative torsional motions along macromolecular chains of suitably meshed N-chemical gears is governed by the parity rule for gear trains, which dictates correlated disrotation of the terminal gears if N is even and conrotatory interactions if N is odd.[21;67] Thus, in arranging an odd number of gears in a cyclic array, dynamic gearing is disallowed and immobilization of the rotors can be expected. The strict

---

* Phase isomerism is a special case of residual stereoisomerism, generated under the operation of correlated rotation. Labeling a cog in each wheel establishes a unique phase relationship between the two cogs that remains fixed as long as the barriers to gear slippage are sufficiently high.

specificity of cogwheeling under steric control and in the absence of gear-slippage, which requires activation energies of 30-40 kcal mol^{-1}, is illustrated in these molecular gear systems, particularly the 'frustrated' cogwheel-propellers, **1.10** and **1.11** (Scheme 1.7).[9] As the genesis of what is now termed triptycene-based 'technomimetics',[11] such bevel gear designs are among the most successful examples of conventionally synthesized molecular architectures that mimic desired mechanical and electronic devices.

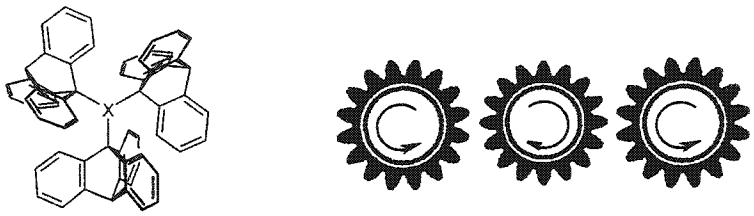

1.10: X = GeCl
1.11: X = C^+, Z = ClO_4^-

Scheme 1.7: *Immobilization of the rotors in the tris-(9-triptycyl) propeller-gear Tp_3XZ (**1.10**, **1.11**) is a consequence of the parity restriction on dynamic gearing.*

1.3.3 Macromechanical Models

Since broached by Richard Feynman in his 1959 historic address, *"There is Plenty of Room at the Bottom"*,[73] the notion of applying mechanical principles at the molecular level has enticed practitioners from numerous realms of chemistry to tackle the problem of constructing an artificial "molecular machine". By definition, a machine is a device "consisting of two or more resistant, relatively constrained parts, which, by a certain predetermined intermotion, may serve to transmit or modify force and motion so as to produce some given effect or to do some desired kind of work."[74] In analogous molecular systems, large-amplitude movements induced by external (photochemical, chemical, electrochemical or other) stimuli lead to real translocation of selective parts of the compound, effecting *reversible* transformations that are (hopefully) detectable by some intrinsic property (electronic absorption, luminescence, NMR signals, electrochemical potentials, *et cetera*).[75] "This metamorphosis of molecule to model requires a process of abstraction and selective emphasis" of nontrivial mechanical parameters, and therefore entails,

according to Mislow, "a deliberate falsification of the object that the model supposedly represents."[21] As highlighted by the earlier examples, it is important to distinguish between static or *iconic* models, and those which possess the additional feature of internal mobility (such as molecular propellers), termed *analogic*.[21]

Although the design and construction of molecular devices has been routinely regarded as a curiosity-driven quest,[76] several recent reports of prototypical structural units demonstrate that it is possible to devise analogic models of machines.[77;78] The motivation for such studies is derived in part from the desire (a) to mimic, and therefore further comprehend, essential biological processes involving motion,[79] such as the rotary motor adenosine triphosphatase[80-82] or the myosin-actin linear motor present in muscles;[83] and (b) to fabricate artificial systems which may perform tasks as varied as catalysis, nanoscale manipulation, information storage, processing and replication. To date, most efforts have focused on controlled submolecular motion that involves either biomolecular recognition[84] or translocation between two or more active sites.[85-87] However, two striking examples of propeller-type models have honed strategies and provided further confirmation that macromechanical features, including those that enable continuous, unidirectional motion, may be incorporated into molecular-scale assemblies.

In a modification to an earlier ratchet proposal[88;89] which would have violated the second law of thermodynamics,[90] Kelly et al.[91;92] have devised a system (**1.12**) that relies on chemical energy to activate and bias a thermally induced isomerization reaction, and thereby achieve unidirectional rotation. Comprised of a three-bladed triptycene ('wheel') moiety connected via a single bond ('axle') to a curved, asymmetric [4]helicene ('brake'), controlled rotary motion by $\pi/3$ radians is effected by the introduction of an urethane tether. It is the reaction of a phosgene-activated isocyanate on triptycene and a hydroxypropyl substituent on the helicene which energetically favours this clockwise rotation ($\Delta G^{\ddagger}$ = 25 kcal mol^{-1}) prior to urethane cleavage and regeneration of a low-energy rotamer (Scheme 1.8). By shortening the hydroxyalkyl group

attached to the helicene, the urethane-linked molecule is trapped in an even higher energy conformational state, thereby accelerating the rate of rotation (*cf.* $t_{1/2}$ 5 min. versus 3 h. for the 2-carbon and 3-carbon tethers, respectively).[93]

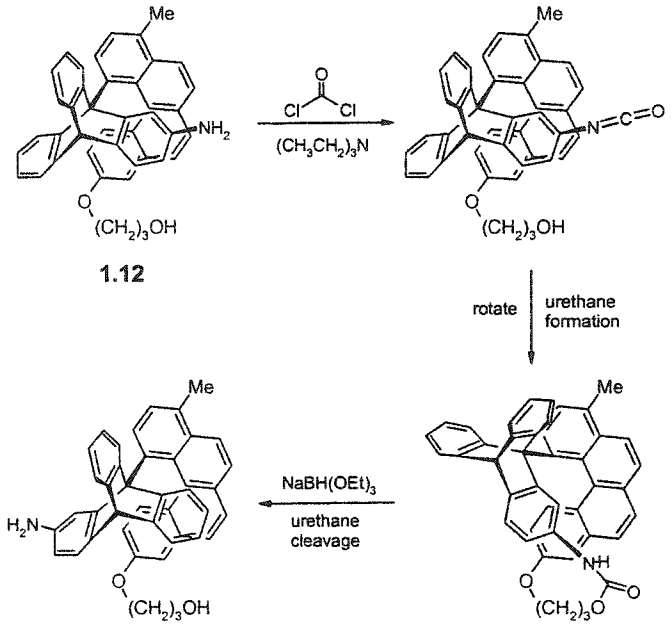

Scheme 1.8: *Unidirectional motion is chemically promoted in the chiral triptycenyl-helicene unit* ***1.12****.*

In the elegant propeller system advanced by Ferringa and co-workers,[94] monodirectional rotation is photochemically promoted. The 2π radian revolution of a helical olefin (**1.13**) is achieved for three full cycles, each comprising four discrete steps of consecutive cis-trans photoisomerizations and irreversible, thermally induced helicity inversions (Scheme 1.9a). It is the molecular architecture of **1.13**, which features the unique combination of axial chirality about the adjoining carbon-carbon double bond and two stereogenic centers in the identical phenanthryl-derived halves, that facilitates the concerted rotary behaviour. Second generation rotor models **1.14a**, comprising two distinct upper and lower parts, namely (2*R*)-methyl-2,3-dihydronaphthothiopyran and heteroatom-bridged xanthene, respectively, have provided additional structural details (Scheme 1.95b). Not only is a single stereogenic center a sufficient

condition for unidirectional motion, but the thermal isomerization barriers, which govern the rotation rate, may be tuned by appropriate steric modifications ($\Delta G^{\ddagger}$ = 21.9 to 25.3 kcal mol^{-1}).[95-97] In a variation on this assembly, an asymmetric donor-acceptor substitution in **1.14b** allows excitation by visible light.[98]

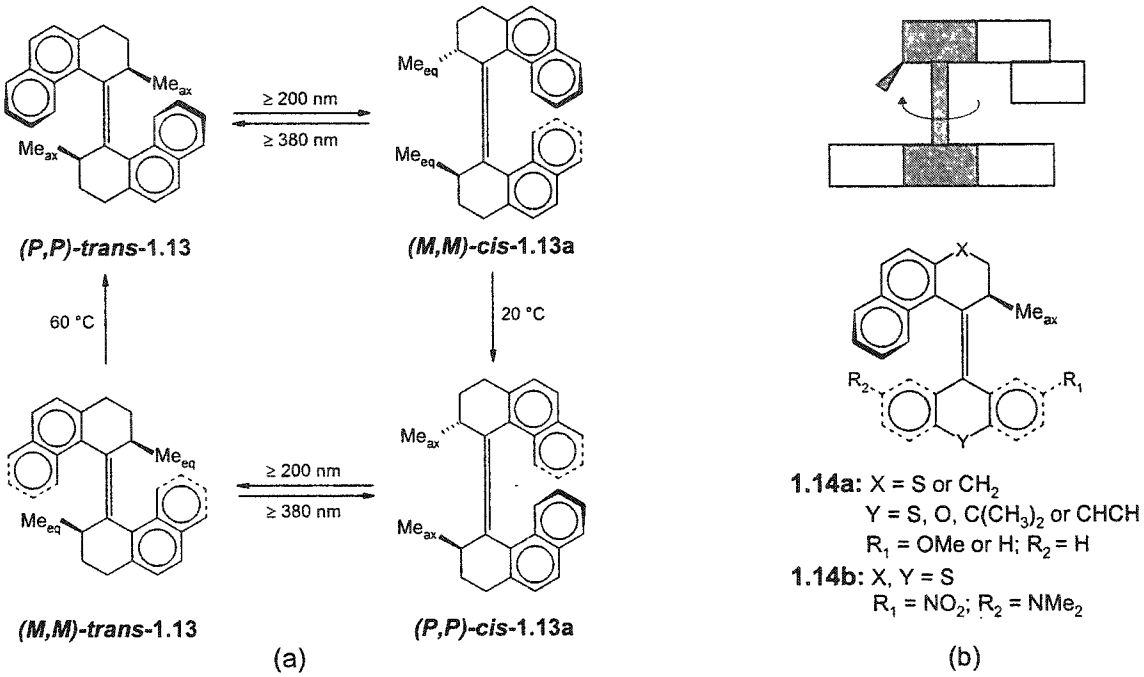

Scheme 1.9: *(a) Unidirectional rotary motion is realized in a photochemically activated and thermally driven helical alkene **1.13** and (b) its second generation analogues, **1.14**.*

Despite their disparate structural compositions, the molecular motors of Kelly (**1.12**)[91,92] and Ferringa (**1.13** and **1.14**)[94] are conceptually related, both employing chirality as the fundamental basis for unidirectional rotary motion.[99,99] Interestingly, nature makes use of this essential principle by using a helical proton channel to define the sense of spinning axle in ATP synthase. Rotation is further guided and abetted in **1.12** - **1.14** by restricting the internal degrees of freedom of each system, ensuring a potential gradient, and providing an influx of external energy which activates the submolecular components to move with respect to each other in a predetermined manner. Although these prototypes represent important strides toward the seductive goal of a molecular motor that rivals in controllable speed and continual operation its

biological and mechanical counterparts, design complexities and synthetic challenges maintain the gap between the two realities. New perspectives continue to emerge at the interface of the sciences, and include such formulas as hybrid 'organic-inorganic' rotors. Restricted rotation of planar aromatic, hexa-tert-butyl decacyclene deposited on a copper surface has been examined by atomic force microscopy,[100] while a CCD video camera has been used to monitor the functional dependence of a nickel post anchored to a recombinant version of ATP synthase that powers peptide-labelled nanopropellers.[78] In both 'nanoscale devices', the crucial component is a *high-symmetry paddle-wheel unit*!

1.4 Multi-n-Rotor (n = 5, 6 and 7) Molecular Propellers

Architectures comprised of contiguous groups attached to a planar central framework, as opposed to a central atom, extend the symmetry limits inherent in the second of the two systems. Indeed, molecules of the type $C_nR_n^{x\pm}$ (n = 3 to 7) endowed with a propeller form (R= aryl) or gear-meshed ground states (R = alkyl) present torsional circuits which may be greatly influenced by the non-bonded repulsions of voluminous substituents. One may view this particular series in terms of the reciprocal relationship between n and the angle ω subtended by adjacent moieties at the center of the internal ring (ω = 360°/n = 120°, 90°, 72°, 60°, to 51.4°, respectively). Although increasing the ring size lengthens the radial distance of the external groups from the center of the molecule, this is more than compensated for by the diminishing value of ω. As a result of cyclic expansion, the peripheral rotors are successively placed in a more crowded locale.

Despite differences at the conformational level, these metric relations underscore a gross, unifying feature of such organic substrates. The concept of aromaticity (and aromatic character), whether applied globally to structure or property, has continued to evolve since the 1865 Kekulé[101] and the more general 1866 Erlenmeyer[102] formulations. However, more than a century later there is still no singular and generally accepted definition, and the quantification of various aromaticity criteria and their interrelationships is persistently challenged by the complexity

of molecular systems (e.g. open shelled fragments or extended polycycles) and the inability to dissect aromaticity effects from other influences. Typically, any of six indices are employed in the designation of aromatic compounds possessing ground-state properties that are derived from:[103;104]

(i) an *electronic* nature that may be characterized (with well known exceptions) by the presence of (4n+2) Hückel π-electron cyclic conjugation, where n = 0,1,2 ...;

(ii) an *energetic* vantage, wherein the cyclic delocalization of mobile electrons stabilizes a system (relative to its chain analogue) and results in a larger HOMO-LUMO gap;

(iii) *geometric* considerations that favour the equalization of bond lengths, which is purportedly induced by the σ-imposed framework (as in the case of benzene);

(iv) *magnetic* effects leading to diatropic (low field) ^{1}H NMR chemical shifts, large magnetic susceptibility exaltations, and negative nucleus-independent chemical shifts (NICS);

(v) *spectroscopic* observables, such as low energy UV and high symmetry IR/Raman spectra; and,

(vi) in relation to the transition state, a *reactive* preference for electrophilic substitution to addition and hence, retention of the π-electron structure.

Thus, within the more classical Hückel scheme of aromatic molecules are featured neutral, anionic and cationic planar, monocyclic hydrocarbons of the formulae $C_3H_3^+$, $C_4H_4^{2+}$ (n = 1) and $C_5H_5^-$, C_6H_6 and $C_7H_7^+$ (n = 2), as depicted in Figure 1.2.

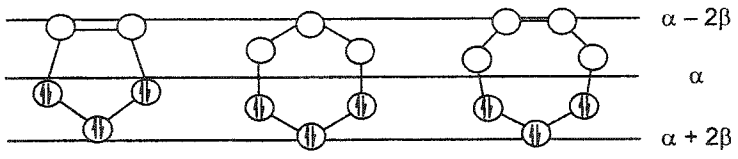

Figure 1.2: *Hückel Molecular Orbital (HMO) energy levels of the closed-shell, 6π-electron $C_5H_5^-$, C_6H_6 and $C_7H_7^+$ monocyclic aromatic species.*

Depending on their substitution patterns (R = alkyl, aryl), these hydrocarbon π ligands may offer multiple coordination sites for metals and therefore, the opportunity to study the influence of complexation on rotational barriers. Toward this end, there is only one example of a $C_nR_n^{\pm}$ (R = Ph, n = 4) ligand deliberately incorporated into a molecular gear formulation. Richards et al.[105;106] have integrated two rotors with incongruent rotational periods of three and four in the compound [(9-triptycylethynyl)cyclopentadienyl](tetraphenylcyclobutadiene)cobalt, **1.15**. However, there was no spectral indication of coupled torsional motions of any of the metallocene fragments (Tp, C_4–ML_n, C_4–Ar) on the NMR time-scale (260 to 203 K), suggesting that the steric contacts in **1.15** are ineffective. Earlier evidence of impeded C_4–Ar rotation effected by either steric hindrance of the groups neighbouring a pivot bond in **1.16** or a "chiral pin" on the C_5 ring in **1.17** has been cited by the research groups of Rausch[107;108] and Takahashi,[109] respectively.

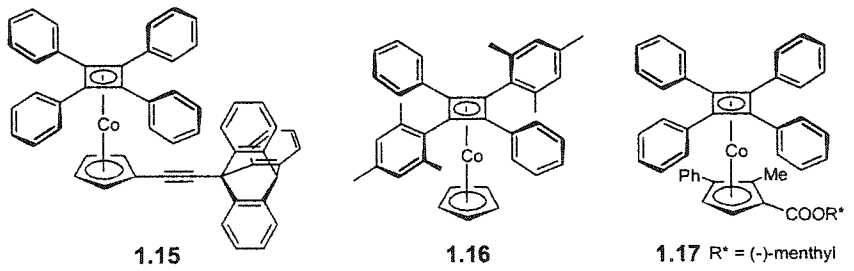

1.15 **1.16** **1.17** R* = (-)-menthyl

Scheme 1.10: *An organometallic gearing array (**1.15**) comprised of a 4-toothed metallocene and a 3-toothed 9-triptycenyl moiety may be compared to two other C_4Ar_4 systems, **1.16** and **1.17**.*

From propeller to gear train, the transfer of angular momentum at the molecular level via structurally programmed ("correlated") motions is rendered more likely when the internal rotors are tightly intermeshed.[71] On a more fundamental level than perhaps that bestowed by the powerful aesthetic appeal of the gear analogy, a $C_nR_n^{x\pm}$ conformational framework that incorporates the effects of ring size constraints, metal complexation and organic substituents, both planar and polyhedral, would be extremely edifying. Since an analysis of such scope has not been conducted, this critical review (vide infra) seeks to combine and abridge an expansive number of reports detailing (either or both) the static and dynamic aspects of the more sterically encumbered $C_5R_5^-$, C_6R_6, and $C_7R_7^+$

systems and their organometallic derivatives. Although a conscientious effort has been made to cite all relevant studies, the more imperative purpose is to highlight the breadth and depth of a topic that spans a variety of fields, and to bring to the forefront the work that provides a context for the thesis research to follow. In order to place the literature in a proper perspective, the chronology of this survey does not necessarily coincide with the timeline of publication.

1.4.1 Persubstituted Cyclopentadienyls: C_nR_n, where n = 5

Somewhat in contrast to the higher C_nR_n propeller analogues, polysubstituted cyclopentadienyl (Cp) systems have been the subject of intense scrutiny. The development of Cp chemistry was first marked by the serendipitous discovery of ferrocene in 1951,[110;111] and has been subsequently expedited by its modification. Notwithstanding the much more common and frequently studied C_5H_5 and its permethylated derivative, C_5Me_5,[112] sterically demanding Cps such as the pentaphenylcyclopentadienyl ligand (C_5Ph_5 **1.18**) have been found to confer novel properties on transition metal centers, including: (i) a high kinetic stability imparted through its large volume;[113;114] (ii) a wider variety of accessible oxidation states, presumably reflecting the ability of the aryl substituents to buffer electronic changes at the metal center;[115] and, (iii) a rich and diverse chemistry, including potential applications in enantioselective synthesis[116;117] and catalysis.[118;119]

1.4.1.1 Tetraarylcyclopentadienone and Pentaarylcyclopentadienyl Derivatives

In 1971, Hayward-Farmer and Battiste[120] provided the first evidence that central ring size influences restricted inter-annular rotation in biphenyl-like molecules. The free energies of activation for stereoisomerization of 3,4-bis(*o*-tolyl)-2,5-diphenylcyclopentadienone (**1.19**) and 1,2-bis(*o*-tolyl)-3,6-diphenylbenzene (**1.20**) by rotation of the *o*-tolyl rings were determined to be 21.8 and > 25.6 kcal mol^{-1}, respectively. As quantitative models, however, these polyaryl systems presented certain shortcomings, including incommensurate substituents and Hückel $4n$ versus $4n$ + 2 electron counts. To expand upon these concepts, Fagan and Gust[121] examined the analogous

6-π–electron pentaarylpyrroles, which eliminate complications caused by the presence of an unpaired electron ($C_5Ph_5^{\bullet}$) or a negative charge ($C_5Ph_5^{-}$) and associated cation. Utilizing the stereochemical framework proposed for hexaarylbenzenes (Section 1.4.2.2),[122;123] the barriers to diastereomerization of 3,4-bis(*o*-tolyl)-2,5-diphenylpyrrole (**1.21**) and 1,2-bis(*o*-tolyl)tetraphenylbenzene (**1.22**) were found to be 19.9 and 38 kcal mol^{-1} by VT-NMR line shape analyses and classical kinetic methods, respectively. The $\Delta G^{\ddagger}$ difference of approximately 18 kcal mol^{-1} was ascribed to decreased steric interactions in the C_s-symmetric rotational transition state of **1.21** relative to **1.22**, which are in turn a consequence of the larger angle subtended by adjacent rings. Conversely, the 2.1 kcal mol^{-1} difference in rotational barriers for **1.19** and **1.21** was argued not only on the premise of disparate steric influences of the carbonyl and phenyl groups, but variations in bond lengths, bond angles, and central ring deformability of the 5-membered ring systems (Scheme 1.11).

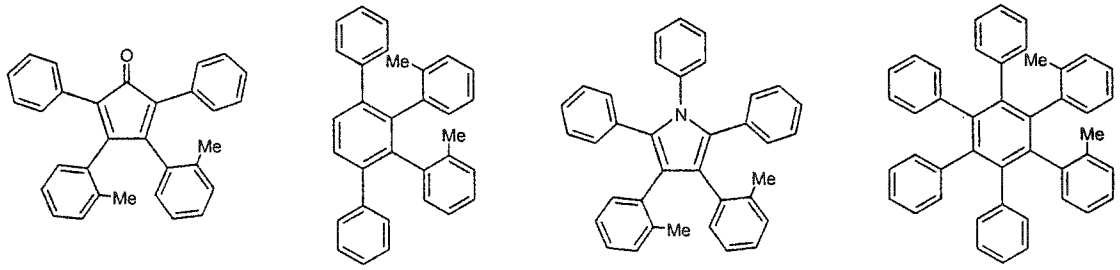

1.19 **1.20** **1.21** **1.22**

Scheme 1.11: *Original (**1.19**, **1.20**) and ensuing (**1.21**, **1.22**) model systems for evaluating the effect of ring size on the magnitude of the energy barrier to rotation of the peripheral rings in C_5 and C_6 systems.*

Notwithstanding energy barrier magnitudes, the aforementioned studies failed to address any stereochemical variations between the constitutionally distinct C_5Ar_4O and C_5Ar_5 ligands. Whereas a small phenyl group oscillation about the planes orthogonal to the C_5 ring of the neutral pentaphenylcyclopentadienyl radical was deduced from EPR spectroscopy in 1964,[124] the conformational features of tetraarylcyclopentadienones remained relatively ambiguous until 1981. By analogy with C_6Ar_6 propellers (Section 1.4.2.2), Willem et al.[125] proposed a static, C_{2v}

symmetric skeleton in which the four aryl groups are orthogonal to the central C_5-ring, at least on the laboratory time-scale. A variable-temperature NMR analysis of the maximally labeled tetra-*o*-tolylcyclopentadienone, **1.23**, which exists as a mixture of ten rotamers, revealed two coalescence regions, below and above room temperature. From a consideration of all possible rearrangement modes, the spectral data were attributed to two dynamic processes: an uncorrelated alpha-one-ring rotation in the direction of the carbonyl moiety, corresponding to the threshold isomerization pathway, and a more sterically demanding, uncorrelated beta-one-ring rotation ($\Delta G^{\ddagger} \approx 20$ kcal mol^{-1}) (Scheme 1.12).[126] As previously established by Gust and co-workers[127] for C_6Ar_5X systems, rings adjacent to an "X" substituent can be expected to rotate much more rapidly than the other rings if "X" is less bulky than an aryl group. In placing these results in the context of earlier studies, Willem and co-workers[125] proposed, perhaps prematurely, that uncorrelated, one-ring rotations constitute the threshold mechanism for all molecules containing peripheral aryl substitutents attached to a central ring.

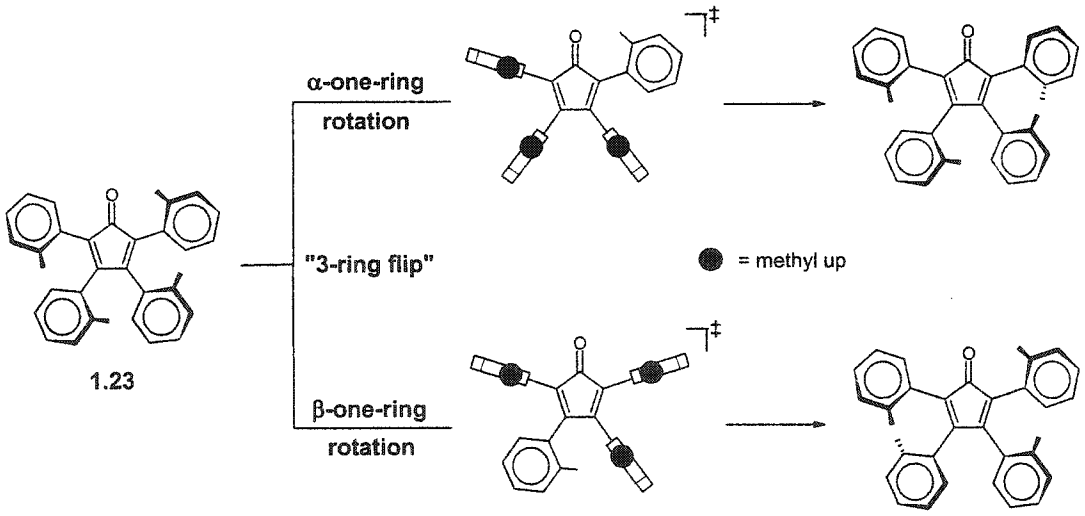

Scheme 1.12: *The two rearrangement modes adduced for tetraarylcyclopentadienones involve a combination of alpha-ring (low energy) and beta-ring (higher energy) rotations.*

Comparative studies of rotational dynamics in metal-ligated systems comprising tetrahapto $Ar_4C_4C{=}O$ and pentahapto Ar_4C_5OH, Ar_4C_5H and C_5Ar_5 platforms can be found scattered among the plethora of reports pertaining to the preparation, physical properties and reactivity of polyarylated Cp-based complexes, spanning both early and late transition metals. In the uncomplexed ligand C_5Ph_5, **1.18**, free rotation of the peripheral aryl substituents imparts effective D_{5h} symmetry; in contrast, hindered libration imposes cyclic directionality on the ring and the effective symmetry of the enantiomeric system is reduced to D_5. This propeller conformation is also manifested in the solid state (cf. C_5Ph_5 radical with torsional angles of ~50°),[128] and represents a compromise between stabilizing orbital overlap and destabilizing steric interactions. Furthermore, the preferential labeling of one face of the Cp ring with an organometallic fragment (ML_n) lowers the maximum symmetry to C_{5v} and in principle, allows for the detection of restricted phenyl rotation since the edges of each arene ring are differentiable by their proximal and distal positioning relative to the metal. The addition of a second stereogenic element, via a chiral metal auxiliary, renders inequivalent the Cp ring carbons in the event of steric inhibition of the tripodal rotation about the fivefold axis. The resulting molecular asymmetry may manifest itself in both the solution and the solid state; if C_5–ML_n and phenyl rotation are incidentally slowed on the NMR time-scale, the degeneracy of all 30 phenyl ring carbons in *each* diastereomer is removed. Commensurate activation barriers for the two fluxional processes – rotation about both the Cp plane-metal vector and the Cp-substituent bond – would substantiate the cooperative, gearing interaction of the π-bonded ML_n moiety with the C_5Ph_5 pentacycle. As highlighted earlier, the detection of correlated behaviour in the chiral aryl array alone would require the incorporation of appropriate NMR probes on adjacent phenyl substituents. In the absence of arene edge labels, it is more challenging to measure the barrier to peripheral ring rotation since, even on a high field spectrometer, there is considerable overlap of ^1H and ^{13}C resonances, making spectral simulation a non-trivial task. Of course, the substitution of a peripheral phenyl ring to give Ar_4C_5OH, Ar_4C_5H

and $Ar_4C_5R^*$ (R* = menthyl, neomenthyl,[117] for example) has static and dynamic stereochemical consequences which must be considered in distinction to the preceding logic.

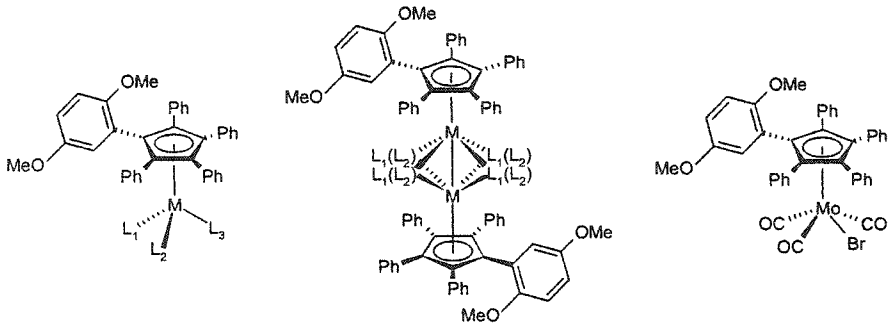

1.24: M = Mo; $L_1 = L_2 = O$; L_3 = OR (R = Me, Et, ^{i}Pr, ^{t}Bu)
1.25: M = Ru; $L_1 = L_2$ = CO; L_3 = Br
1.40: M = Mo; $L_1 = L_2 = O$; L_3 = Br

1.26: L_1 = CO; L_2 = Br
1.27: $L_1 = L_2$ = Br

1.41

Scheme 1.13: *Pentaarylcyclopentadienylmetal systems containing the 2,5-dimethoxyphenyl substituent.*

As solid-state evidence for the stereochemical nonrigidity of the C_5Ar_5 moiety, Colbran et al.[129] cite the occurrence of both the proximal and distal orientations of the 2,5-dimethoxyphenyl substituent (R) in X-ray crystallographic structures of $[M(C_5Ph_4R)L_1L_2L_3]$ complexes (M = Mo, L_1,L_2 = O, L_3 = OMe **1.24**; M = Ru, L_1,L_2 = CO, L_3 = Br **1.25**[129]) and respective dimers, $\{[M(C_5Ph_4R)L_1L_2]_2\}$ (M = Mo, L_1 = μ-CO, L_2 = μ-Br **1.26**; M = Mo, $L_1 = L_2$ = Br **1.27**) (Scheme 1.13).[130] Additionally, the splitting of the solution C-O stretching absorptions in the solid state IR spectra of several chiral complexes, including $[Fe(\eta^5\text{-}C_5Ph_5)(CO)(PMe_3)Br]$ (**1.28**)[131] and $[Os(\eta^5\text{-}C_5Ph_5)(CO)(L)Br]$, where L = PMe_2Ph (**1.29**), $P(OEt)_3$ (**1.30**) and $P(OCH_2)_3CCH_3$ (**1.31**),[132] has been rationalized on the basis of diastereoisomerism arising from the propeller helicity. In agreement with the presence of two diastereomers in the solid, and hindered rotation of both the tripod and the phenyl groups, the solid-state ^{13}C NMR spectrum of **1.28** displayed a 1:1:2:1:1:1:1:2 peak pattern corresponding to 10 distinct Cp ring carbon atoms.[131] Finally, the reduced molecular motion resulting from restricted libration of the phenyl groups has been

suggested as an explanation for the extreme insolubility of decaphenylmetallocenes, $(C_5Ph_5)_2M$ (M = Fe **1.32**,[133] Ni **1.33**,[134] W^+ **1.34**,[135] Ge **1.35**, Sn **1.36**, Pb **1.37**[136]).

Accounts of the dynamic behaviour of pentaarylcyclopentadienyl metal complexes in solution reveal that, in general, the aryl substituents rotate freely about their bonds to the central C_5-plane at ambient temperature. One exception provided by Adams et al.[116] is $Ru(C_5Ph_5)(CO)(PPh_3)Br$ (**1.38**), which exists as a mixture of diastereomers on the NMR time-scale, as evidenced by two $^{31}P\{^1H\}$ NMR signals. Unfortunately, the instability of **1.38** in solution at elevated temperatures, in the absence of an excess of triphenylphosphine, precluded attempts to acquire activation parameters by use of VT-NMR spectroscopy. In replacing the triphenylphosphine ligand with the less bulky $P(OMe)_3$ or $P(OPh)_3$, the intramolecular steric interactions, and hence rotational barriers, associated with the polyaryl array were significantly reduced. Similarly, the room temperature ^1H NMR spectrum of $Fe(\eta^5\text{-}(o\text{-tolyl})C_5Ph_4)(CO)_2Br$ (**1.39**) exhibited two resonances for the methyl groups in the ratio of 7:4, consistent with the presence of proximal and distal rotamers.[137] While no VT-NMR data were provided by Field, Masters and colleagues, this example established that substituents of at least the size of a methyl moiety can be accommodated at the aryl ortho position of these half sandwich compounds.

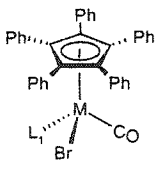

1.28: M = Fe; $L_1 = PMe_3$
1.29: M = Os; $L_1 = PMe_2Ph$
1.30: M = Os; $L_1 = P(OEt)_3$
1.31: M = Os; $L_1 = P(OCH_2)_3CCH_3$
1.38: M = Ru; $L_1 = PPh_3$

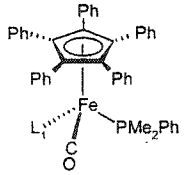

1.47: L_1 = COEt
1.48: L_2 = COMe

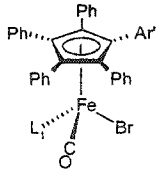

1.39: Ar' = o-tolyl; L_1 =CO
1.49: Ar' = m-xylyl; L_1 =PMe_3

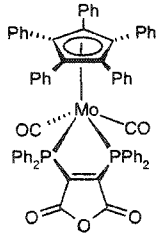

1.46

Scheme 1.14: *A selection of pentaarylcyclopentadienyl half-sandwich complexes.*

The rotational barrier for the 2,5-dimethoxyphenyl substituent (R) in $[Mo(C_5Ph_4R)O_2(Br)]$ (**1.40**), was calculated to be 16.4 ± 0.2 kcal mol^{-1}.[115] In progressing from the static (300 K) to dynamic (370 K) limit, the four ^1H NMR signals attributable to the methoxy moiety gradually coalesced to two resonances, while concomitant changes were also observed in the phenyl spectral region. Whereas the underlying exchange phenomenon could be attributed to either hindered rotation of the labeled aryl ring or of the metal tripod, Colbran and co-workers[115] argued the former fluxional mechanism on the premise that $\Delta G^{\ddagger}$ values in related C_5Ph_5 and C_5Ph_4H systems are much lower for the latter process. Interestingly, this interconversion of proximal and distal rotamers is mentioned but not quantified in earlier reports of $[Ru(C_5Ph_4R)(CO)_2(Br)]$ (**1.25**),[129] $[Mo(C_5Ph_4R)(CO)_3(Br)]$ (**1.41**),[130] and analogues. In the dimers $[Mo(C_5Ph_4R)(\mu\text{-}CO)(\mu\text{-}Br)]_2$ (**1.26**) and $[Mo(C_5Ph_4R)(\mu\text{-}Br)_2]_2$ (**1.27**),[130] the dimethoxyphenyl groups remained static but the phenyl substituents exhibited restricted rotation over the 500 MHz ^1H-NMR experimental temperature range. Once again, however, $\Delta G^{\ddagger}$ estimates for these systems were not provided by the researchers.[130]

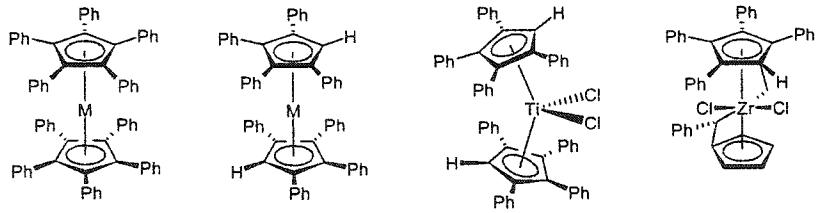

1.32: M = Fe
1.33: M = Ni
1.34: M = W*
1.35: M = Ge
1.36: M = Sn
1.37: M = Pb

1.42: M = Fe
1.44: M = Ru

1.43

1.45

Scheme 1.15: *C_5Ph_5 and C_5Ph_5H linear and bent metallocene derivatives.*

There was no evidence (293 to 178 K) for hindered rotation about the two Cp-ML_n bonds in the linear and bent bis(tetraphenylcyclopentadienyl) complexes $Fe(C_5Ph_4H)_2$ (**1.42**) [138] and $[Ti(C_5Ph_4H)_2Cl_2]$ (**1.43**),[139] respectively. Analysis of the temperature dependence of the 500 MHz ^1H-NMR spectra of **1.42** yielded a barrier of 9 ± 1 kcal mol^{-1} for (beta) phenyl ring rotation, with

alpha and beta substituents adopting coplanar and perpendicular conformations, respectively, relative to the central C_5 ring. A concomitant high frequency shift of the Cp proton was attributed to the deshielding from ring currents of the adjacent coplanar aryl groups.[138] Within experimental error of the free energy of activation determined for **1.42**, the dynamic ^{1}H-NMR studies of **1.43** gave a commensurate value ($\Delta G^{\ddagger}$ = 9.8 ± 0.2 kcal mol^{-1}) for the restricted libration of the phenyl rings.[139] Whereas the low temperature limiting spectrum of $Ru(C_5Ph_4H)_2$, **1.44**, could not be accessed before the solvent freezing point, allowing only for a $\Delta G^{\ddagger}$ extrapolation of ~ 9 kcal mol^{-1},[140] the paramagnetic nature of the other octaphenylmetallocenes with M = V, Cr, Co and Ni did not lend themselves to NMR studies. In the ^{1}H VT-NMR spectra (293 to 183 K) of the related ansa-metallocene complex, rac-[1-(η^5-Cp)-1-Ph-(η^5-C_5Ph_4)Et]$ZrCl_2$, **1.45**, the slowed rotation of the beta phenyl substituents (273 K) was detected in advance of the sterically less hindered alpha phenyl groups (253 K) (Scheme 1.15).[141]

In 1989, Tyler et al.[142] approximated the barrier to Cp–ML_n rotation as 9.1 kcal mol^{-1} from the dynamic ESR spectrum of Mo(η^5-C_5Ph_5)$(CO)_2L_2$, where L_2 = (2,3-bis(diphenylphosphino)maleic anhydride), **1.46**. The large, negative activation entropy ($\Delta S^{\ddagger}$ = -22.9 ± 0.3 cal K^{-1} mol^{-1}) was noted as additional justification of free Cp rotation, since this process necessitates cooperative 'gearing' of the phenyl substituents on the Cp periphery and phosphorus ligand and a corresponding transition state structure which is highly organized. The second observation of steric inhibition of tripodal rotation in a persubstituted cyclopentadienyl half-sandwich complex was reported by Brégaint et al.[131] in 1992. The ^{13}C VT-NMR data for [(η^5-C_5Ph_5)Fe(CO)(PMe_2Ph)(C(O)Et)] (**1.47**), from 293 to 163 K (the lowest accessible temperature owing to poor solubility), revealed a decoalescence phenomenon whereby the single resonance of the C_5 ring split into four distinct signals in the ratio of 1:2:1:1. To date, the only solution state NMR-derived free activation energy of C_5Ar_5–ML_n rotation has been adduced by Li, et al.[143] Evaluation of the temperature-dependent ^{13}C NMR spectral changes (293 to 173 K) associated

with the Cp ring nuclei of [(C_5Ph_5)Fe(CO)(PMe_2Ph)(C(O)Me)] (**1.48**) yielded an E_a value of 8.7 ± 0.3 kcal mol^{-1}. A second, non-coupled fluxional process (E_a = 11.7 ± 0.3 kcal mol^{-1}) was measured from the splitting of the diastereotopic phosphorus-coupled methyl resonances (from two ^{13}C signals at room temperature to four at 173 K), and ascribed to either slowed libration of the peripheral phenyls or the phosphine ligand (Scheme 1.14). Indeed, the dimethylphenylphosphine ligand may not serve as an innocent probe for chirality inversion in the C_5Ph_5 moiety if it introduces an additional source of asymmetry. Unfortunately, attempts to clarify the steric contributions of these moieties via the VT-NMR study of (C_5Ph_4-*m*-C_6H_3-Me_2)Fe(CO)(PMe_3)(Br), **1.49**, incorporating an *m*-xylyl substituent and a small, symmetrical phosphine were unsuccessful, either because the PMe_3 does not gate the phenyl rotations or because the methyl ^{13}C chemical shift differences are too small to be observed in solution. In hindsight, the inability to detect exchange between distal and proximal rotamers could likely have been circumvented by ortho, as opposed to meta, aryl labeling of the C_5Ar_5 ligand.

In all cases of hindered Cp–substituent bond rotations featured above, an uncorrelated, stepwise or one-ring interconversion, as opposed to a correlated, synchronous rotational mechanism has been postulated. Moreover, rotary motion about the Cp–ML_n bond is clearly effected by the interannular repulsion of the bulky ring substituents in metallocenes, or a ring-substituent metal-ligand steric interaction in half-sandwich complexes. Despite the numerous accounts of metal-ligated cyclopentadienones generated either indirectly by metal carbonyl-promoted alkyne oligomerizations[144-146] or less frequently via direct metallation methods,[147] few investigations have considered the stereochemical features of such systems. The exclusive formation of [(η^5-(C_5Ph_5)Co(η^4-(C_4-2,4-Mes_2-3,5-Ph_2C=O)] (**1.50**) and the corresponding cyclobutadiene complex (refer to the introduction of Section 1.4) from the reaction of $CpCo(CO)_2$ and mesitylphenylacetylene was noted in a 1979 report by Rausch and co-workers.[107] At ambient temperatures, the ^1H NMR spectrum of **1.50** exhibited six methyl resonances in the

aliphatic region, consistent with impeded rotation about the mesityl-cyclopentadienone bonds in both the alpha and beta positions. Although it would have been particularly instructive to compare activation parameters for the alpha- and beta-ring rotations (cf. tetra-*o*-tolylcyclopentadienone, **1.23**), even in the presence of a metal moiety, no dynamic NMR studies were conducted. In 1993, Adams and co-workers[148] related the synthesis and ^{31}P VT-NMR of complexes $[Mo(CO)_2(L\text{-}L)(\eta^4\text{-}(C_4Ph_4C{=}O))]$ (L-L = $Ph_2PCH_2PPh_2$, **1.51**; or L-L = $Ph_2PCH_2CH_2PPh_2$, **1.52**) (Scheme 1.16). Whereas the low-temperature limiting spectrum of **1.51** could not be accessed, transformation of the dppe ^{31}P AB pattern to a singlet over the temperature range of 193 to 308 K allowed for an activation energy (E_a) of 11.6 kcal mol^{-1} to be estimated for **1.52**. More recently, the McGlinchey laboratory[147;149] has provided several examples of enhanced conformational rigidity in $(C_4Ar_4C{=}O)ML_n$ complexes resulting in cyclopentadienone–ML_n rotational barriers measurable by dynamic NMR methods.

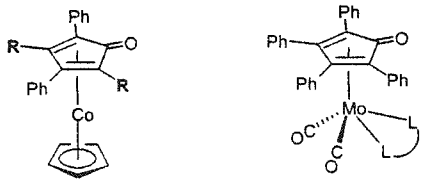

1.50: R = mesityl **1.51**: L-L = $Ph_2PCH_2PPh_2$
1.52: L-L = $Ph_2PCH_2CH_2PPh_2$

Scheme 1.16: *η^4-Tetraarylcyclopentadienone cobalt and molybdenum complexes that exhibit hindered Cp–Ar and Cp–ML_n rotation on the NMR time-scale, respectively.*

The separate treatment of tetracyclone, **1.53**, and its organometallic analogue, 3-ferrocenyl-2,4,5-triphenylcyclopentadienone, **1.54**, with $Fe_2(CO)_9$ afforded η^4-$(C_4Ph_4C{=}O)Fe(CO)_3$ (**1.55**) and the novel complex, η^4-$(C_4Ph_3FcC{=}O)Fe(CO)_3$ (**1.56**), respectively (Scheme 1.17).[147] Whereas in the X-ray crystal structure of **1.55** the peripheral aryl rings adopt the conventional propeller conformation with average interplanar angles of ~49°, the orientations of the aryl blades in **1.56** are markedly influenced by the nearly coplanar C_5H_4 ring of the *exo* ferrocenyl moiety. These solid-state structural incongruities are also apparent in the solution

behaviour of both complexes. In accordance with earlier studies by Kruczynski and Takats,[150] a low barrier to tripodal rotation in **1.55** precluded the observation of this dynamic process in the experimental limit (167 K) of the ^{13}C NMR regime. In contrast, the ^{1}H and ^{13}C VT-NMR (173 to 300 K) spectral patterns of the ferrocenyl derivative **1.56** indicated an unequal isomeric distribution of 80:20, possibly corresponding to Fc *exo* and *endo* positions; an activation barrier of 12.5 ± 0.5 kcal mol^{-1} was extracted from the decoalescence data (177 K) of the ^{13}CO resonance of the major rotamer.

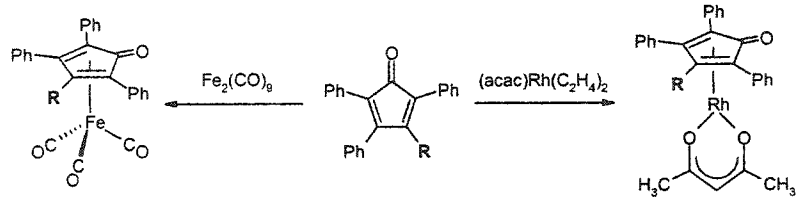

1.55: R = Ph
1.56: R = Fc

1.53: R = Ph
1.54: R = Fc

1.57: R = Ph
1.58: R = Fc

Scheme 1.17: *Organometallic derivatives of tetraarylcyclopentadienones **1.53** and **1.54**.*

Similarly, η^4-(C_4Ph_4C=O)Rh(acac), **1.57**, and η^4-(C_4Ph_3FcC=O)Rh(acac), **1.58**, were synthesized by gentle reflux of the appropriate ligand **1.53** or **1.54** with (acac)Rh(C_2H_4)$_2$.[147] X-ray crystallographic studies revealed that **1.57** adopts a head-to-tail dimeric arrangement with the individual dienones possessing a cup-shaped, as opposed to a helical, arrangement of phenyl rings about their periphery. In solution, the Rh–acetylacetonate moiety was presumed to straddle the molecular mirror plane, thereby preventing the detection of restricted rotation about the Cp–ML_n axis. On the other hand, the monomeric form of **1.58** was enforced by the presence of the bulky ferrocenyl substituent, which again disturbs the propeller conformation and appropriately desymmetrizes the system. At low temperature the methyl groups of the acac ligand were rendered magnetically non-equivalent, yielding a rotational barrier of 12.5 ± 0.5 kcal mol^{-1} for the Rh-acac moiety. Apparently, there is little distinction between the steric interplay of the $Fe(CO)_3$ and Rh(acac) fragments with the peripheral substituents of **1.54**, owing perhaps to the

comparable M–diene carbon distances in **1.56** (2.061(2) to 2.136(3) Å) and **1.58** (2.098(5) to 2.165(6) Å).

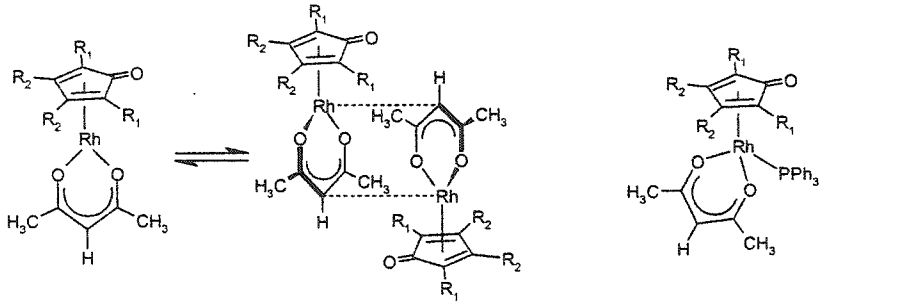

1.61: R_1 = phenyl; R_2 = 2-naphthyl **1.62:** R_1 = phenyl; R_2 = 2-naphthyl
1.63: R_1 = *m*-xylyl; R_2 = 2-naphthyl **1.64:** R_1 = *m*-xylyl; R_2 = 2-naphthyl

Scheme 1.18: *Rhodium complexes (**1.61 – 1.64**) of 3,4-di(2-naphthyl)-2,5-diarylcyclopentadienones.*

In a related 2002 study by Harrington et al.,[149] the diastereotopic methyl groups of the acetylacetonate ligand were utilized as an indirect probe for the hindered rotation of asymmetric 2-naphthyl appendages in rhodium complexes of 3,4-di(2-naphthyl)-2,5-diarylcyclopentadienone (aryl = Ph, **1.59**; or aryl = m-xylyl, **1.60**) (Scheme 1.18). As in **1.57**, **1.61** and **1.63** exist as head-to-tail dimers in the solid state and undergo a rapid monomer-dimer equilibrium in solution at ambient temperature. The anticipated presence of several proximal-distal conformers (maximum of 7) with overlapping resonances was revealed in both the ^{1}H and ^{13}C VT-NMR regimes at low temperatures. Subsequent reaction of **1.61** (or **1.63**) with triphenylphosphine afforded the monomeric species **1.62** (or **1.64**), thereby limiting the number of possible rotamers to three (distal-distal, proximal-distal, and proximal-proximal). From the ^{31}P VT-NMR of both **1.62** and **1.64**, activation enthalpies of 8.2 ± 0.5 kcal mol^{-1} were extracted for (beta) naphthyl rotation. This value is 13.6 kcal mol^{-1} less than the free energy of activation for stereoisomerization of tetraarylcyclopentadienone **1.19** by rotation of the (beta) *o*-tolyl rings and reflects both the differing steric requirements of ring substituents and the electronic effects of metal complexation.[120] That the magnitude of the barrier height is the same in **1.62** and **1.64** is not

surprising, given the comparable steric profiles of *m*-xylyl and phenyl rings. To eliminate the possibility of restricted Cp–ML_n rotation as an explanation for the spectral attributes, the ^{31}P-NMR temperature invariance (298 to 162 K) of the corresponding tetracyclone complex was demonstrated.

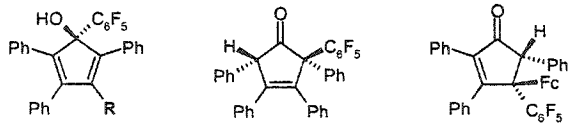

1.65: R = Ph
1.66: R = Fc

1.67

1.68

Scheme 1.19: *Products from the reaction of pentafluorophenyllithium with* ***1.53*** *and* ***1.54.***

In an endeavour to systematically and collectively quantify the fluxional properties of $(C_5Ar_5)ML_n$ derivatives, McGlinchey and co-workers have also sought to develop methods of incorporating ^{19}F NMR probes, which have larger chemical shift dispersions than do ^{1}H or ^{13}C nuclei. The derivatization of an already sterically demanding C_5-ring system such as tetracyclone, **1.53**, via treatment with aryl Grignard reagents offers synthetic access to C_5Ar_5 pentacycles and their organometallic complexes (see Scheme 1.30). As a first entry point to fluorinated analogues, Gupta et al.[151] have examined the syntheses, structures and dynamic behaviour of pentafluorophenyl-containing Cp systems. The reaction of pentafluorophenyllithium with cyclopentadienones **1.53** and **1.54** yielded, in both cases, the cyclopentadienols **1.65** and **1.66** as a result of 1,2 additions, and the cyclopentenones **1.67** and **1.68**, as the products of 1,6 and 1,4 additions, respectively (Scheme 1.19). X-ray crystallographic characterization of **1.65**, **1.67** and **1.68** clarified the regiochemistry of these adducts and the non-bonded environments of the pentafluorophenyl moiety. The observation of five different resonances in the room temperature ^{19}F NMR spectra of **1.65**, **1.66** and **1.68** further corroborated the conformational rigidity induced by the steric crowding about the C_6F_5 rings. However, the barriers to pentafluorophenyl ring rotation could not be evaluated directly from line-broadening measurements because the expansive chemical shifts of both the ortho and meta fluorines

prevented the observation of complete peak coalescence. Rather, the approximate $\Delta G^{\ddagger}$ values of 20 ± 1, 21 ± 1, and 19 ± 1 kcal mol^{-1}, respectively, were obtained by simulation of the variable temperature 282 MHz ^{19}F-NMR spectra. Ultimately, the demonstration of restricted rotation of C_6F_5 groups in synthetically feasible peraryl-substituted organic platforms, such as the cyclopentadienols **1.65** and **1.66**, offers promise for the design of gated organometallic complexes.

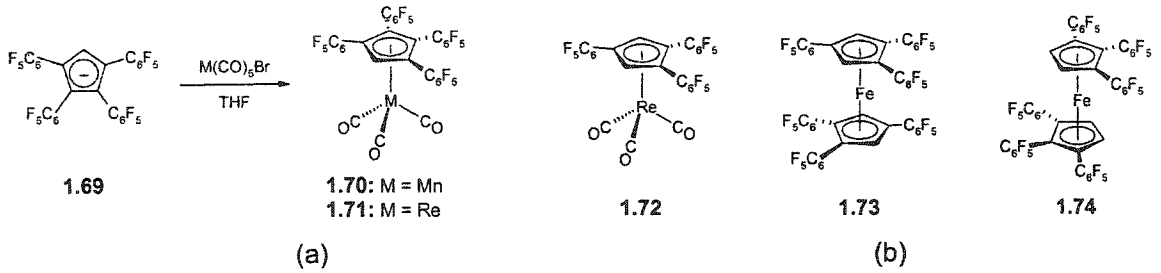

Scheme 1.20: *(a) The synthesis of transition metal half-sandwich complexes comprising the tetrakis(pentafluorophenyl)cyclopentadienyl ligand,* ***1.69****. (b) Various metallocene and piano-stool derivatives (****1.72-1.74****) of tris(pentafluorophenyl)cyclopentadienyl ligands.*

Relevant to both the interest in ancillary perfluoroaryl groups and the C_5Ar_4H metallocene derivatives **1.42-1.45**, a 2001 report by Deck and associates[152] outlines the synthesis and characterization of piano stool complexes derived from the tetrakis(pentafluorophenyl)cyclopentadienyl ligand, **1.69**. The diene was isolated from the reaction of sodium cyclopentadienide with excess hexafluorobenzene and sodium hydride in refluxing diglyme, and readily converted to $[(C_6F_5)_4C_5H]Na$ **1.69(Na)** upon treatment with sodium hydride in THF. Whereas attempts to generate the octaarylated Fe(II) and Co(II) metallocenes by use of standard methods failed, the $[(C_6F_5)_4C_5H]M(CO)_3$ (M=Mn **1.70**; M = Re **1.71**) complexes were prepared in moderate yields from **1.69(Na)** and the corresponding metal carbonyls, $M(CO)_5Br$ (Scheme 1.20a). In the solid state, the molecular structures of **1.69**, **1.70** and **1.71** display a helical arrangement of the C_6F_5 groups, as evinced from single crystal X-ray diffraction data. Dynamic ^{19}F NMR studies (173 to 298 K) of **1.70** and **1.71** revealed that the beta C_6F_5 moieties are in slow exo(distal)-endo(proximal) exchange at all temperatures, while rotation of the

alpha rings is not frozen out until 198 K. Accompanying Eyring analyses afforded the same activation parameters ($\Delta G^{\ddagger}$ = 8.0 ± 0.2 kcal mol^{-1}) for both complexes. Moreover, there was no evidence for hindered libration about the Cp–M(CO)$_3$ axes within the experimental limits.

Earlier fluxional analyses of a homologous series of mono-, bis- and tris(pentafluorophenyl)cyclopentadienyl complexes (Scheme 1.20b) established that "isolated" C_6F_5 rings undergo rapid rotation on the NMR timescale, whereas vicinal C_6F_5 groups in [1,2,4-$(C_6F_5)_3C_5H_2$]Re(CO)$_3$, **1.72**, display temperature-dependent rotational behaviour, with an associated E_a of 9 ± 1 kcal mol^{-1} ($\Delta G^{\ddagger} \approx$ 8.4 kcal mol^{-1}).[153] In the related metallocene, [1,2,4-$(C_6F_5)_3C_5H_2]_2$Fe, **1.73**, both Cp–C_6F_5 and Cp–Fe rotational processes can be monitored by use of ^{19}F VT-NMR, yielding an activation energy of 11 ± 2 kcal mol^{-1} ($\Delta G^{\ddagger} \approx$ 11.4 kcal mol^{-1}) for the latter racemization. In the case of three contiguous aryl moieties in [1,2,3-$(C_6F_5)_3C_5H_2]_2$Fe, **1.74**, the rotational barrier (E_a) for the "outer" C_6F_5 rings was calculated to be 10 ± 1 kcal mol^{-1} ($\Delta G^{\ddagger} \approx$ 9.2 kcal mol^{-1}), whereas the central ring is conformationally locked. The buttressing effects engendered by the anisotropic steric profile of C_6F_5 groups are significantly different than for a phenyl substituent, as evidenced by the fast exo-endo edge exchange of the beta rings in Fe$(C_5Ph_4H)_2$, **1.42**, at ambient temperature.[138] As a rationale for the stereochemical behaviour of perfluoroarylated metallocenes, Deck[153] invoked a qualitative model of transannular Cp–Fe steric interactions coupled (synchronized) with torsional Cp–C_6F_5 strain.

In yet another pertinent article by Thépot and Lapinte in 2001,[154] the preparation and characterization of several bromopentaarylcyclopentadienes of the formula $C_5Ar_4Ar'Br$, **1.75**, (Ar = C_6H_5 or 3,5-$C_6H_3Me_2$ and Ar' = C_6H_5, 3-C_6H_5X, 3,5-$C_6H_3X_2$, 2,4-$C_6H_3X_2$, 2,4,6-$C_6H_2X_3$ where X = methyl; 3-C_6H_5X, 3,5-$C_6H_3X_2$, 2,6-$C_6H_3X_2$ where X = fluorine) have been detailed. Treatment of the tetraarylcyclopentadienones with the corresponding lithium-aryl (Ar'Li) reagents in THF allowed for the systematic introduction of the fifth aryl moiety. Conversion of the tetraarylcyclopentadienols into their bromo derivatives **1.75** was achieved by reaction with $SOBr_2^-$

pyridine, and resulted in three different positional isomers (1:2:1 for **A**:**B**:**C**) when the Ar' and Ar groups were different, but only a single, sterically moderated beta-product, **1.75C**, in the di-ortho-substituted Ar' cases (Scheme 1.21). With the exception of systems containing di-ortho-substituted arene rings, bromopentaarylcyclopentadienes allow facile access to iron piano stool complexes via a formal oxidative addition of pentacarbonyliron(0) and subsequent ligand exchange.[155] While the presence of meta (fluoro or methyl) moieties is apparently ineffective in impeding free aryl rotation, the differential labeling methods should eventually enable quantification of the dynamic processes in these diversely substituted metal-Cp arrays.

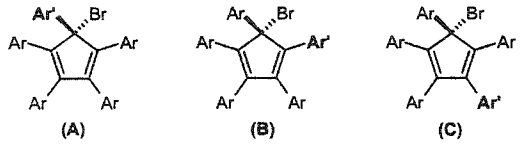

1.75

Scheme 1.21: *Conversion of methyl- and fluorine-containing pentaarylcyclopentadienols to bromopentaarylcyclopentadienes* ***1.75*** *gives a regio-isomeric distribution of products when Ar and Ar' groups are different.*

1.4.1.2 Pentaalkylcyclopentadienyl Derivatives

The study of rotational dynamics in peralkylated cyclopentadienyl π-complexes has emulated the corresponding analyses of C_6 homologs (refer to Section 1.4.2.1) and since reviewed earlier by Janiak and Schumann,[113] will only be considered briefly here. The barriers ($\Delta G^{\ddagger}$) to enantiomerization in the penta(isopropyl)- and penta(neopentyl)cobalticinium salts, $[C_5(^{i}Pr)_5]CoCp^{+}$, **1.76**, (17.1 ± 0.2 kcal mol^{-1}) and $[C_5(CEt_2H)_5]CoCp^{+}$, **1.77**, (19.4 ± 0.2 kcal mol^{-1}), respectively, were reported in 1990 by Gloaguen and Astruc.[156] Coalescence temperatures of 338 and 373 K were extracted from the variable-temperature ^{1}H- and ^{13}C-NMR spectra of **1.76** and **1.77**, which displayed features consistent with metallocenic chirality arising from hindered Cp–R rotation at room temperature. The methyl protons are rendered diastereotopic by the pentacycle helicity and sense the clockwise-counterclockwise exchange of alkyl groups, which occurs via a stepwise, uncorrelated mechanism deemed prevalent for gear-meshed systems.[35]

In the related half-sandwich complex $[C_5(^iPr)_5]Mo(CO)_3CH_3$, **1.78**, the activation energy for this interconversion process was estimated to be 13 ± 1 kcal mol^{-1}, with an associated ^1H VT-NMR coalescence temperature of 288 K.[157] A further decrease in rotational barrier was noted in the silicon analogue, $[C_5(SiMe_2H)_5]Mn(CO)_3$, **1.79**, which yielded an approximate $\Delta G^{\ddagger}$ value of 9.5 kcal mol^{-1}.[158] A combination of differing steric and electronic requirements in these sym-metallocenes and piano stool complexes undoubtedly accounts for these trends in isomerization barriers. In the absence of solid-state structural data for **1.76** and **1.78**, one might speculate that the Cp–M distance is significantly decreased in **1.76** (*cf.* **1.78**) given its electronically deficient metal center, while **1.78** and **1.79** might be expected to possess unequal ML_n cone angles and Cp–R (R = C or Si) bond lengths. Similar steric predictions are realized in the fluxional behaviour of pentabenzyl-Cp based bent metallocenes, $[C_5(CH_2Ph)_5]_2M$ (M = Ge **1.80**,[159] Sn **1.81**, Pb **1.82**[160]) and half-sandwich complexes $(PhCH_2)_5C_5M$ (M = Tl **1.83**, In **1.84**,[161] $Co(CO)_2$ **1.85**,[162] $Mn(CO)_3$ **1.86**[163]), which exhibit both free Cp–ML_n and Cp–CH_2Ph rotation at ambient temperature, in contrast to the stereorigid, linear decabenzylferrocene, **1.87**, and its derivatives.[163-166] In the absence of computational or VT-NMR spectroscopic data, it has been argued that the deca-anti benzyl arrangement, which is found crystallographically, also persists in the solution state of **1.87** because of severe transannular repulsions (Scheme 1.22).[164]

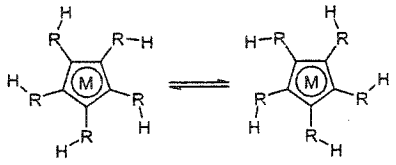

1.76: M = $CoCp^+$; R = CMe_2
1.77: M = $CoCp^+$; R = CEt_2
1.78: M = $Mo(CO)_3CH_3$; R = CMe_2
1.79: M = $Mn(CO)_3$; R = $SiMe_2$

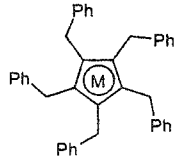

1.80: M = $Ge[C_5(CH_2Ph)_5]$
1.81: M = $Sn[C_5(CH_2Ph)_5]$
1.82: M = $Pb[C_5(CH_2Ph)_5]$
1.83: M = Tl
1.84: M = In
1.85: M = $Co(CO)_2$
1.86: M = $Mn(CO)_3$

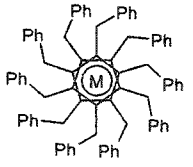

1.87: M = Fe

Scheme 1.22: *A selection of chiral peralkyl-cyclopentadienyl metal π-complexes (**1.76 – 1.87**).*

1.4.2 Persubstituted Arenes: C_nR_n, where n = 6

With their sterically diverse, radially functionalized hexagonal cores, C_6R_6 scaffolds have adopted key roles in various fields of research. From a synthetic vantage, persubstituted benzenes are products of two of the most intensely studied, useful transformations: namely, the metal (e.g. Co(0))[167-169] or non-metal (e.g. Si_2Cl_6)[170;171] catalyzed trimerization of alkynes, and the [4+2] Diels-Alder cycloaddition of cyclopentadienones and ethynyl moieties.[172;173] Conferred with novel optical and electronic properties, these highly alkylated and arylated 6-π electron centers have been exploited as (a) synthons for polyaromatic hydrocarbons or graphite building blocks,[174-176] complex, highly branched dendrimers,[177-180] and nanosize homogeneous catalysts,[181;182] (b) polymeric side chains,[183] (c) room-temperature discotic nematic liquid crystals,[184] (d) hosts in self-assembled supramolecular networks,[185;186] (e) ligands in organometallic complexes, (f) subjects of theoretical studies,[187] and (g) candidates for stereochemical analyses (*vide infra*).

1.4.2.1 Hexaalkylbenzenes

In the molecular ground state and under the appropriate conditions of intramolecular crowding, the arrangement of neighbouring alkyl groups around the arene periphery can be compared to a system of meshed gears, as delineated by Mislow.[21] The static and dynamic stereochemistry of several persubstituted arenes (C_6R_6) have been reported, including R = isopropyl **1.88**;[188-191] dimethylsilyl **1.89**;[192] bis(1-bromoethyl), tetraisopropyl **1.90**;[193] dichloromethyl **1.91**;[194] bis(bromochloromethyl), tetraisopropyl **1.92**;[195] and dimethylamino **1.93**.[196] Among these, hexaisopropylbenzene, **1.88**, has served as a spectacular example of the precise interlocking of contiguous groups via bisected conformations to generate a helical C_{6h} structure (Scheme 1.23). While **1.88** resists metal complexation, its symmetry was reduced by selective deuteration, and the barrier to homomerization (attendant rotation of isopropyl substituents by π radians) estimated to have a lower limit of 22 kcal mol^{-1} by VT-NMR methods (298 to 398 K). Empirical force field (EFF)

calculations corroborated that the threshold mechanism for stereoisomerization in prototype **1.88** and its derivatives is a stepwise, uncorrelated rotation (or inversion, in the case of **1.93**) of individual side chains. This dynamic circuit follows the pattern observed or calculated for tetraisopropylethylene[197] and other statically geared systems (*vide infra*),[35] and corresponds, with the exception of **1.93**, to slippage of one gear at a time in the mechanical counterpart.[21] However, in an extension of the parity rule for gear trains, all hexaalkylbenzenes are *in principle* capable of correlated disrotation, even if these conformational interconversions are associated with high-energy regions of the potential energy surface.[21] Only if the three-fold alkyl rotors possess deep grooves is gear slippage suppressed, as has been exemplified by hexamethylbenzene, **1.94**, which engages in correlated, internal rotations, but only at very low temperatures.[198]

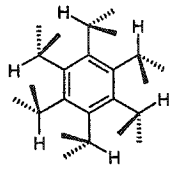

1.88

Scheme 1.23: *The static gear effect is most strikingly exhibited by hexaisopropylbenzene,* ***1.88****.*

Hexamethylbenzene is the parent representative of a subclass of hexaalkylbenenes (also including R = ethyl **1.95**; cyclopropyl **1.96**;[199] trimethylsilylmethyl **1.97**;[200] bromomethyl **1.98**;[201] neopentyl **1.99**[27;202]; benzyl **1.100**[203] and others) in which the alkyl groups adopt antiparallel conformations, so as to impart approximate D_{3d} or S_6 symmetry to the molecule. For almost two decades, the static and dynamic stereochemistry of hexaethylbenzene, **1.95** (HEB), and its organometallic derivatives fostered a vigorous debate between several research groups, including that of McGlinchey.[204] In 1980, Hunter et al.[205;206] established by use of X-ray crystallography that the ethyl groups project alternately above and below the ring plane in the hydrocarbon **1.95**, and that ligated $Cr(CO)_3$ (**1.101**) and $Mo(CO)_3$ (**1.102**) tripods eclipse the distal ethyl groups of the D_{3d} conformer, confirming the earlier claims by Maricq and co-workers.[207] The

barrier to site exchange of the diastereotopic ethyl groups in **1.101** (and **1.102**) was measured as 11.5 kcal mol^{-1} by dynamic NMR spectroscopy and attributed by EFF studies to uncorrelated side chain rotation.[206] Despite the energetic preference of the 1,3,5-distal-2,4,6-proximal isomer, this arrangement is not always found in the solid state or solution, as was first demonstrated by the hexa-distal (C_{6v}) HEB conformation and the ^{13}C-NMR spectral temperature invariance (298 to 189 K) of [(HEB)Cr(CO)$_2$PPh$_3$], **1.103**.[206;208] The results of these and many subsequent studies raised questions regarding the effect of metal complexation on the barrier to topomerization, thereby prompting the evaluation of barriers to metal tripod rotation (Scheme 1.24).

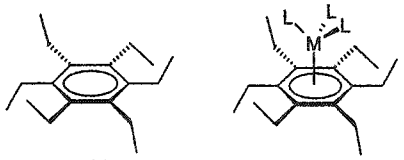

1.95

1.101: $ML_3 = Cr(CO)_3$
1.102: $ML_3 = Mo(CO)_3$
1.103: $ML_3 = Cr(CO)_2PPh_3$
1.104: $ML_3 = Cr(CO)_2CS$
1.106: $ML_3 = [Cr(CO)(CS)(NO)][BF_4]$
1.107: $ML_3 = [Cr(CO)_2(NO)][BF_4]$

Scheme 1.24: *The alternate 'up-down' conformational preference of hexaethylbenzene,* ***1.95****, and a selection of its transition-metal complexes, for which different Et group arrangements may be adopted.*

Steric inhibition of tripodal rotation is only detectable if the C_{3v} symmetry of **1.101** and its congeners is reduced, either by carbonyl ligand exchange or arene substitution (*i.e.* to generate C_6Et_5X). Jointly with colleagues in France, McGlinchey and co-workers[209] thus prepared [(HEB)Cr(CO)$_2$CS], **1.104**, which closely parallels **1.101** in its solid-state structure, and which exhibits a C_s-consistent 2:1:2:1 pattern for each of the aromatic ring carbon, methylene and methyl environments in the static (solution) ^{13}C-NMR regime. Even with comparable solid-state ^{13}C-NMR data,[210] the interpretation of slowed tripodal rotation was challenged by Hunter and Mislow,[211] who raised the possibility of a solution-state 1,2,3,5-distal-4,6-proximal conformer in which HEB itself possesses C_s symmetry. To validate the assertion of restricted rotation about the arene-ML_n axis, it was necessary to establish that the desymmetrization source was not the altered orientation of HEB in solution. Temporarily circumventing this particular issue, Downton

and co-workers from the McGlinchey laboratory[212] applied the alternate substitution scheme to the generation and combined X-ray crystallographic and NMR spectroscopic characterization of $[(C_6Et_5COMe)Cr(CO)_3]$, **1.105** (Scheme 1.25). While the complex adopts the successive proximal-distal conformation in both phases, the 2:1 splitting pattern of the $Cr(^{13}CO)_3$ signal in the solid state and in solution at 173 K unequivocally demonstrated the cessation of tripodal rotation ($\Delta G^{\ddagger} \approx 9$ kcal mol^{-1}). Having distinguished the resonance assignments for proximal and distal ethyl environments, Mailvaganam et al.[213] refocused on the analogous C_6Et_6 species. The cationic derivatives $[(HEB)Cr(CO)(CS)(NO)][BF_4]$, **1.106**, and $[(HEB)Cr(CO)_2(NO)][BF_4]$, **1.107**, both exhibit the 1,3,5-distal-2,4,6-proximal arrangement in the solid state. In solution, the behaviour of the former is consonant with that of the thiocarbonyl species **1.104**, whereas the chiral tripod in the latter complex renders inequivalent all six ethyl substituents in the unperturbed C_s symmetric HEB ligand. These observations, together with data on **1.104**, are rationalized in terms of two independent fluxional processes: tripodal rotation ($\Delta G^{\ddagger} \approx 9.5$ kcal mol^{-1}), and uncorrelated rotation of the ethyl groups ($\Delta G^{\ddagger} \approx 11.5$ kcal mol^{-1}; cf. **1.101** and **1.102**).[213]

To allow for independent yet concomitant evaluation of these two interconversion pathways, Kilway and Siegel[214;215] elegantly extended the aforementioned desymmetrization concepts to the design of 1,4-R_2-2,3,5,6-tetraethylbenzene ligands (R = 4,4-Me_2-3-oxypentyl **1.108**; OMe **1.109**; CH_2OMe **1.110**; neohexyl **1.111**) (Scheme 1.25). Nearly commensurate barriers to alkyl rotation in the free and $Cr(CO)_3$-complexed systems, **1.108(Cr)** to **1.111(Cr)**, were attributed to a cogwheel-like ("lock and key") complementarity of rotation between the ethyl substituents and the metal tripod.[215] This apparent dynamic correlation is not manifested in the energetic requirements of the two pathways, however; for **101.8** the free energies of activation for alkyl rotation (11.3 kcal mol^{-1} in **1.108** and 11.5 kcal mol^{-1} in **1.108(Cr)**) and tripodal rotation (9.5 kcal mol^{-1}) are obviously disproportionate,[214] as evinced by the earlier systems (**1.106**, **1.107**).[213] In further support of the innocuous role of the metal in the stereodynamics of **1.101**, Gottlieb and

co-workers[216;217] have recently provided VT-NMR and computational (MM3 force field) data for a series of pentaethylated benzenes, C_6Et_5X (X=H, Br, $OCOCH_3$, C_6Et_5, *et cetera*) **1.112-1.117**, for which the diastereotopic methylene hydrogens of the ortho and meta ethyl groups serve as rotational probes (Scheme 1.25). A re-examination of the interconversion pathway established that in the *consecutive (step-wise)* rotation of contiguous alkyl groups, the third (4^{th}-alkyl),[217] as opposed to the first (2^{nd}-alkyl),[206] step is rate-determining. In its entirety, the hexaethylbenzene narrative is a powerful example of the need to apply rigorous symmetry and steric principles in the selection of candidates for stereochemical analyses.

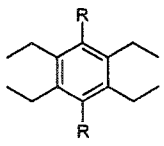

1.108: R = $CH_2CH_2COCMe_3$
1.109: R = OMe
1.110: R = CH_2OMe
1.111: R = $CH_2CH_2CMe_3$
1.118: R = Br
1.119: R = $CH_2NHCOMe$
1.120: R = $CH_2CH_2NO_2$
1.121: R = CH_2Cl
1.122: R = CH_2SMe
1.123: R = CH_2CN
1.124: R = CH_2NH_2

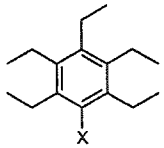

1.112: X = H
1.113: X = Br
1.114: X = OCOMe
1.115: X = OCOPh
1.116: X = C_6Et_5
1.117: X = COMe

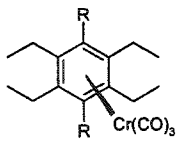

1.105: R_1 = Et, R_2 = COMe
1.108(Cr): $R_1 = R_2 = CH_2CH_2COCMe_3$
1.109(Cr): $R_1 = R_2$ = OMe
1.110(Cr): $R_1 = R_2 = CH_2OMe$
1.111(Cr): $R_1 = R_2 = CH_2CH_2CMe_3$

Scheme 1.25: *Mono- and di-(1,4)-substituted analogues of hexaethylbenzene, including metal-ligated derivatives of the latter systems.*

For example, both the static-gearing effects and the stereodynamics of the pendant alkyl groups will determine the utility of hexaethylbenzene derivatives as preorganized templates for the supramolecular assembly of nanomaterials with tailored physical properties, or as building blocks for large, maximally alkylated polycyclic aromatic hydrocarbons. In 2001, Kilway and Siegel[218] broadened the scope of this area by demonstrating how cooperative conformational networks can control the proximity and direction of functional groups in surrogates of HEB (Scheme 22). Variable-temperature ^{1}H-NMR studies of 1,4-disubstituted-2,3,5,6-

tetraethylbenzenes (**101.8**, **1.110**, **1.111**, **1.118-1.124**), for which the diastereotopic geminal methylene protons of the ethyl groups served as a spectroscopic probe for alkyl motion, established that in the static (solution) limit all isomers adopt the divergent C_{2h} conformation, as in the solid state. Furthermore, the free energies of activation ($\Delta G^{\ddagger}$), calculated by use of the Gutowsky-Holm approximation, were distinctly influenced by the effective steric bulk of the substituents. Taking into account the relative interaction of each position (α, β, γ) with relation to the arene carbon on which the group resides, it was found that the barrier height is directly correlated with the van der Waals radius of the α and β locales, with the exception of CH_2CN, which is best described by its Taft parameter. On the other hand, the γ moiety does not bias the energetics of the vicinal ethyl group rotation but instead serves as a magnetic perturbation to desymmetrize the system. Repulsive van der Waals interactions also serve as the major conformational determinant of polyethylated hydrocarbon analogues. Gottlieb, Biali, and co-workers[219-221] have applied the HEB model to the study of sp^2-sp^3 rotational barriers in persubstituted biphenylene, anthracene, fluorene and triptycene derivatives. The appropriate quantification of structural features (size, arrangement) and the identification of corresponding $\Delta G^{\ddagger}$ trends within these C_6R_6 subsets provide critical calibration points for the future design of conformationally controlled architectures.

1.4.2.2 Hexaarylbenzene and Derivatives

In the solid state, the nascent six-bladed propeller, hexaphenylbenzene, **1.125**, adopts a helical conformation with interplanar angles of approximately 65(75)°[222;223] between the peripheral phenyl substituents and the central ring. Earlier gas phase electron diffraction studies revealed an essentially orthogonal form, with phenyl oscillations of ±10°.[224] Correspondingly, the fluxional nature of C_6Ar_6 molecules in solution is rationalized by an effective NMR time-averaged D_{6h} perpendicular arrangement.[122] In order to observe restricted rotation about the sp^2-sp^2 bonds joining the central and peripheral aromatic rings, proper substitution of the aryl rings is required. The pioneering

stereochemical studies of C_6Ar_6 systems by Gust and Patton[122;123] established that isomerization occurs via a mechanism wherein an individual peripheral ring rotates in an uncorrelated fashion by approximately π radians (Scheme 1.26). Rotational barriers of ~ 33, 38 kcal mol^{-1} or 17 kcal mol^{-1} are engendered by the incorporation of ortho or meta (methoxy, methyl) substituents, respectively (**1.21**, **1.126-1.129**). Whereas the differing steric requirements of *ortho*-positioned groups are evidently manifested in the interconversion barriers, the influences of electronically and spatially dissimilar meta substituents are minimal, such that $\Delta G^{\ddagger}$ values of the latter species indirectly reflect the interactions of ortho hydrogens on adjacent aryl rings. Rotating rings also detect the non-bonded repulsions from remote sites around the circumference of the central benzene ring. Such buttressing effects were evinced by the free energies of activation for pentaarylbenzene (C_6Ar_5X) derivatives, **1.130-1.135**, bearing various substituents, which ranged from 15.5 (X=H) to 18.7 ($X=C(CH_3)_3$) kcal mol^{-1}.[122;127] In all of the C_6Ar_6 and C_6Ar_5X systems reported to date (Scheme 1.27), the $\Delta G^{\ddagger}$ values have been ascribed to diastereomeric interconversions, since enantiomerization necessarily involves rotation of *all* substituted rings and is therefore energetically more demanding. A particularly striking example is provided by the extended propeller 1,3,5-tris{[3,4-bis(4-methoxyphenyl)-2,5,6-triphenyl]phenyl}benzene, **1.136**, which yielded a barrier ($\Delta G^{\ddagger}_{333\,K}$) of 18.9 kcal mol^{-1} for C_3 to C_1 diastereomerization achieved by 180° rotation about one of the Ph_5Ph–benzene bonds.[225]

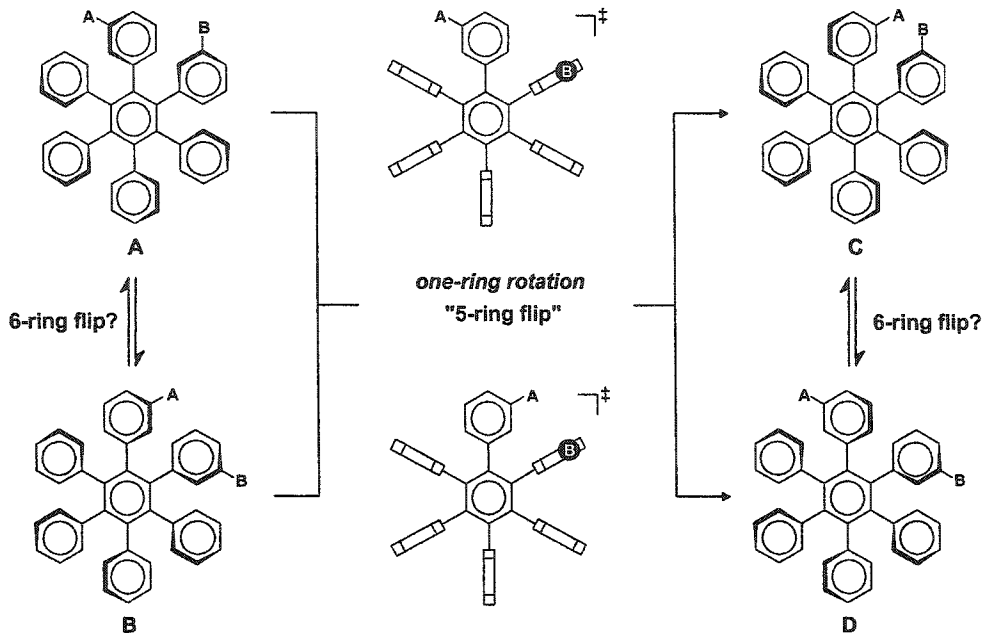

Scheme 1.26: *Stereoisomerization in hexaarylbenzenes is conventionally distinguished by uncorrelated (180° edge-interchange of an individual ring) rotational pathways. Since helicity inversion is only inferred, syn-anti interconversion may theoretically occur by two diverse mechanisms: 180°-one-ring rotation (A → C; B → D) or a five-ring flip (A → D; B → C).*

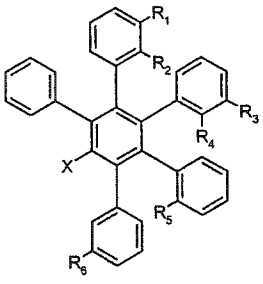

1.126: X = Ph; R_2 = OMe; R_4 = Me
1.127: X = Ph; R_2,R_5,R_6 = Me; R_4 = OMe
1.128: X = Ph; R_1 = R_3 = OMe
if R_1,R_3 = Me:
1.129: X = Ph
1.130: X = H
1.131: X = $CH(CH_3)_2$
1.132: X = CH_3
1.133: X = CH_2CH_3
1.134: X = $CH(OH)CH_3$
1.135: X = $C(CH_3)_3$
Otherwise, R_n = H

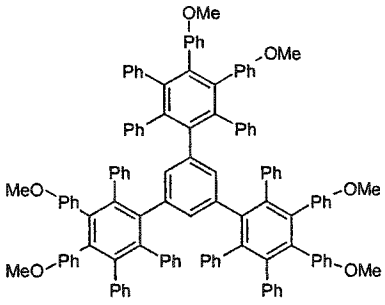

1.136

Scheme 1.27: *Suitably substituted penta- and hexaarylbenzenes (**1.126-1.136**) that have demonstrated rotational stereoisomerization on the NMR time-scale.*

These experiments have subsequently been extended to complexes of the type $(C_nAr_n)ML_x$ whereby the π-bonded organometallic fragment(s) render inequivalent the *faces* rather than the *edges* of the aryl rings. Both desymmetrization methods were employed simultaneously by Weissensteiner et al.,[226] in order to compare the rotational barriers of propeller complexes of the type Ar_2X (X = CR_2,

C=O) and their mono- and bis(tricarbonylchromium) derivatives. In the same year (1987), McGlinchey and co-workers demonstrated the fecundity of this approach by attaching one, two and three $Cr(CO)_3$ pendant functionalities to the periphery of 1,3,5-triphenylbenzene, which exists as a non-propeller in its ground state.[227] Whereas the X-ray crystallographic characterization of 1,3,5-tris[(η^6-C_6H_5)$Cr(CO)_3$]benzene, **1.137**, revealed a radially-disposed (two-up, one-down) trimetallic system of moderate congestion (Scheme 1.28), the VT-NMR spectra (298 to 183 K) provided no evidence of hindered rotation of the labeled aryl rings. Otherwise, chromium tricarbonyl complexes of arenes typically display metal-tripod rotations with barriers less than 3 kcal mol^{-1}, well below the detectable limits of NMR methods.[4;204;228;229] In order to slow the libration of either the organometallic domain or the propeller blades[230] it is therefore necessary to employ extremely bulky arenes.

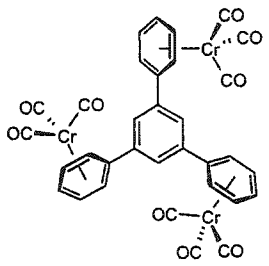

1.137

Scheme 1.28: *The effectively C_{3h}-symmetric tris(tricarbonylchromium(0)) complex of 1,3,5-triphenylbenzene,* ***1.137****.*

Accordingly, efforts were directed towards functionalization of the more sterically encumbered perarylated benzene **1.125**, for which both in-plane splaying and hydrogen interactions are negated.[127] Ligation of a tricarbonylchromium moiety to an external ring in (C_6Ph_6)$Cr(CO)_3$, **1.138**, was achieved, albeit in low isolable yields, following treatment of **1.125** with $Cr(CO)_6$.[231] A dynamic ^{13}C-NMR spectroscopic analysis yielded a $\Delta G^{\ddagger}$ value of 12.2 kcal mol^{-1} for the independent rotation of the metal-substituted ring relative to the central plane. Although not discernable under the experimental conditions, a concomitant isomerization process involving a low energy oscillation which inverts the handedness of the enantiomerically related chiral propellers was proposed. Thus, **1.138**

exists in two stereoisomeric forms, namely a *d,l* pair each having C_1 symmetry, which may only be observed as a NMR time-averaged C_s isomer at low temperature (193 K) and as an effective C_{2v} conformation at 300 K (Scheme 1.29). This rationale is in agreement with the peak splitting patterns for all ortho, meta and para carbons, which indicate that the rapid libration of the metal-complexed ring in the dynamic limit equilibrates both the σ-related halves and top and bottom faces of the molecule. On lowering the temperature, signal decoalescence (*i.e.* 2:2:1 to 1:1:1:1:1 for para carbons of uncomplexed rings) reveals six differentiable, yet locally C_2-equivalent, peripheral ring environments arising from a rotamer in which the $(\eta^6\text{-}C_6H_5)Cr(CO)_3$ ring is perpendicularly disposed to the central arene plane. Since the ortho and meta carbons in any particular aryl ring are magnetically equivalent in both the static and dynamic regimes, restricted rotation of the non-complexed rings is unobservable in the absence of further substitution. Interestingly, the measured activation energy for this isomerization process is ~ 5 kcal mol^{-1} less than the associated barrier in the free 1,2-bis(*m*-tolyl)-3,4,5,6-tetraphenylbenzene, **1.129**.[122;123] Contrary to earlier claims,[230] these differences are likely a combination of ground-state destabilization through repulsive steric interactions and electronic stabilization of the transition state engendered by metal complexation.

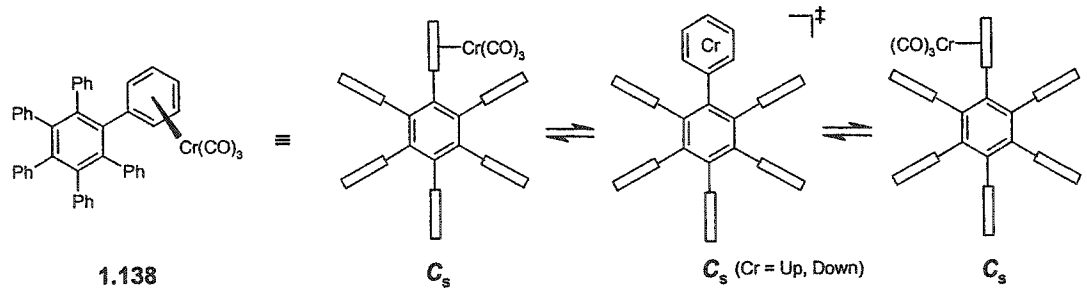

1.138 C_s C_s (Cr = Up, Down) C_s

Scheme 1.29: *The fluxional behaviour of $C_6Ph_6Cr(CO)_3$, **1.138**, is rationalized in terms of the interconversion of average C_s (low T) and C_{2v} (high T) symmetric conformations, excluding the low energy oscillation of the peripheral aryl rings that interconverts enantiomers.*

1.4.3 Persubstituted Cycloheptatrienyls: C_nR_n, where n = 7

In the development and modification of sterically demanding perarylated and peralkylated and $C_nR_n^{x\pm}$ (n = 5 to 7) templates and their diverse applications in organotransition metal chemistry,

π-coordinated cycloheptatriene and -enyl systems have evaded experimentalists until just recently. This is perhaps surprising, given that the parent aromatic cations, $C_7Ph_7^+$, **1.139**, and $C_7Me_7^+$, **1.140**, have been known for decades. [232;233] As one of the most stable carbenium species (pK_a value of 4.75[234]), the tropylium cation ($C_7H_7^+$, **1.141**) itself has been incorporated as part of host-guest architectures,[235-237] intramolecular charge-transfer complexes,[238;239] extended macrocyclic frameworks[240;241] and metal coordination compounds.[242-244] Despite these exciting advances, the expansion of the tropylium ion series has been restricted by the challenging syntheses, leading to a significant dearth of both static and dynamic structural details of $C_7R_7^+$ systems.

1.5 Global Aim of Study

1.5.1 Overview

Within the context of the retrospective overview provided in Section 1.4 is detailed the progressive evolution of a long-term research goal (of the McGlinchey laboratory) to realize the formulation of sterically crowded molecules offering routes to gear systems. Indeed, insight into the static and dynamic stereochemical complexities of $C_nR_n^{x\pm}$ and $(C_nR_n)ML_x$ (where R = alkyl or aryl, n = 5, 6 or 7, and ML_x is an organometallic fragment) propellers may eventually corroborate the topological parameters necessary to effect hindered, and possibly even intercoupled, rotations on the laboratory time scale, and therefore found a more direct morphological relationship to macroscopic devices. As emphasized in this introduction, such pursuits draw upon multi-disciplinary concepts and implement combined programs of synthetic methodology, X-ray crystallography, variable-temperature and multi-dimensional NMR spectroscopy, and computational theory. The elucidation of novel structures, physical (e.g. steric, electronic) attributes and dynamic properties (e.g. barriers to rotation) are fundamental to all studies, which, of course, begin with molecular design.

1.5.2 Framework: Design Considerations and Synthetic Template

Since both the structure and its internal motions must be controlled with regard to symmetry, sterics and strain, there are numerous design complexities associated with the detailed conformational studies of such extended, aromatic arrays. The observation of stereoisomerism crucially depends on the appropriate desymmetrization, or substitution on, the basic molecular framework. Furthermore, the complementary steric interplay between the n-fold rotors and hence, the detection of interconversion processes (with barriers typically in the range of 5-25 kcal mol^{-1}) by use of variable-temperature NMR spectroscopy, is promoted by the judicious selection of organic fragments and their ligating metal moieties. Taking these factors into account, our preparative schemes concentrically feature tetrasubstituted cyclopentadienones, versatile synthons which offer avenues to the 5-, 6- and 7-membered ring systems, and which themselves serve as candidates for fluxional studies. As featured in the generalized Scheme 1.30, the condensation of a substituted diketone **1.142** with appropriately 1,3-derivatized propanones **1.143** affords the desired cyclopentadienone **1.144**, which (usually) resists Diels-Alder dimerization because of its bulky periphery. Access to cyclopentadienes **1.146** (and the corresponding cyclopentadienide salts, **1.147**) is gained via aryl- or alkyl-Grignard treatment of **1.144**, and subsequent reduction of the intermediate cyclopentadienols **1.145**. Conversely, the [4 + 2] cycloaddition of **1.144** with alkynes or cyclopropenes, followed by decarbonylation of the respective bicyclic and tricyclic systems, gives the persubstituted arenes, **1.148**, or cycloheptatrienes, **1.149**. Organometallic transformations of **1.147**-**1.149** lead to architectures with the potential for engaged gearing interactions of the C_nR_n and ML_n components.

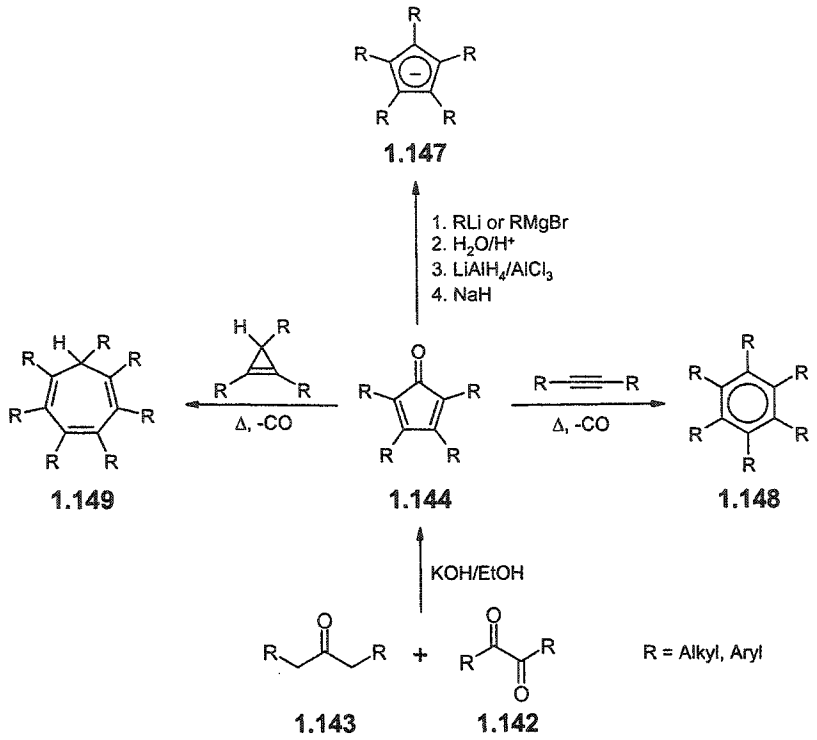

Scheme 1.30: *A general synthetic template for C_nR_n systems, where n = 5, 6 and 7.*

1.5.3 Objectives of the Thesis

In an effort to develop a more rigorous conformational model of $C_nAr_n^{x\pm}$ (n = 5, 6 and 7) propellers that is inclusive of metal complexation, this doctoral study concentrates on different aspects of the three ring systems in tandem.

To begin, the stereochemical attributes of Ar_3Z/ Ar_3ZX and C_nAr_n molecular propellers are closely correspondent, as their graphical representations would suggest. Although this equivalence relation was noted by Willem, Pepermans and co-workers in 1983,[65] the conformational dichotomy of these two propeller types has persisted in the literature for over two decades. In bridging this fundamental gap, it may be possible to acquire a better understanding of isomerism and stereodynamics in the latter systems, by way of model abstracting. As a complement to prior dynamic NMR analyses (Section 1.4.1), Chapter Two features a survey of the potential energy surface associated with low-energy rotational pathways in $C_5Ar_{5-m}X_m$ (m = 0,

1) compounds, which has been enabled by the unique application of Structure Correlation methods in combination with detailed computations.

As evinced in the foregoing sections, C_6Ar_6 propellers have provided the essential reference frame for interpreting stereochemical patterns within this class of structures. Computational standards for molecules of (at least) this size and constitution are critical to our understanding of the conformational subtleties associated with increased dimensions and functionalization. In Part One of Chapter Three, the least linear motion path associated with the reorientation of terminal phenyl groups in the parent C_6Ph_6, **1.125**, is mapped using semi-empirical, *ab initio* (RHF) and hydrid density functional (HDFT) methods. The structural perturbations induced by the systematic incorporation of different planar and polyhedral substituents represent an important extension of this work. Accordingly, the second part of Chapter Three describes the preparation and conformational analysis of a series of C_6Ph_5X derivatives, wherein "X" represents selected aryl, alkyl and organometallic groups.

The study of nonbonded interactions on molecular structure and internal mobility in persubstituted C_7-ring platforms has been confined to a few olefin precursors and annelated tropylium derivatives. The heptaphenylcycloheptatrienyl cation, $C_7Ph_7^+$ (**1.139**), is the last species in the series of $C_nAr_n^{x\pm}$ (n = 3 to 7) molecular paddle-wheels to be crystallographically characterized, either as a free ion or molecule, or as an organometallic ligand. Furthermore, minimal attention has been given to the steric and electronic effects of metal derivatization of both the core and periphery of the covalent tropilidene and its corresponding cationic π-system. To this end, the theoretical trends and experimental considerations, including synthesis, characterization and conformational dynamics, of novel C_7Ar_7H and $C_7Ar_7^+$ analogues are presented in Chapter Four.

CHAPTER TWO

Persubstituted Cyclopentadienes and –dienyls: $C_nAr_{n-m}X_m$ where n = 5, X = 0-2. A Conformational Analysis

"C'est la dissymétrie qui crée le phénomène." (Pierre Curie, Paris, 1894)

2.1 Preface

The entwined concept of symmetry and chirality derives its relevance in experiment, and as such, any molecular model must suit the occasion of its use.[36] In representing the static and dynamic aspects of molecular propellers, it is customary to distinguish between compounds comprised of two or more substituents arranged in a helical fashion about either a central atom (type I) or a planar, polyatomic framework (type II). On the NMR time-scale of observation, the former species generally exist in a chiral array (triphenylmethane, with its low enantiomerization barrier, is a notable exception[47,56-60]) whereas derivatives of the latter type effectively possess an achiral, orthogonal perimeter. Analysis of torsional isomerism in appropriately substituted propeller units has revealed two seemingly disparate modes of rearrangements:* correlated and uncorrelated ring rotation. To reiterate, helicity inversion in type I systems is achieved by means of "n-ring-flip" mechanisms that involve conrotatory rotation of n rings through a direction perpendicular to the propeller plane, while the non-flipping rings, if any, pass in a disrotatory fashion through the reference plane, with concomitant edge interchange (see Scheme 1.4). For type II molecules, the topomerization pathway (i.e. process of site exchange) of lowest energy consists of the independent rotation of a single peripheral ring by 180°, and proceeds with indeterminate helicity, at least by NMR spectroscopy (Scheme 1.26). However, Willem, Pepermans et al.[65] have reasoned that the two

---

* A mode of rearrangement is a set of elementary pathways (cf. 'mechanism') which are indistinguishable because either they are characterized by the same initial and final configuration states, they occur with the same rate constant by reason of symmetry equivalence, or they are related to each other by a combination of both correlations.[125] As such, the mode corresponding to the suite of highest rate constants (lowest activation energies) is termed the threshold mode.

models are equivalent from a permutational perspective, since the one-ring rotation of the perpendicular conformation and the (n-1)-ring flip of the propeller forms are stereochemically correspondent.[41] In accordance with this unified classification scheme, the threshold mode of isomerization of *all* n-aryl propeller systems is either a (n) or (n-x, where $x \leq m$)-ring flip.

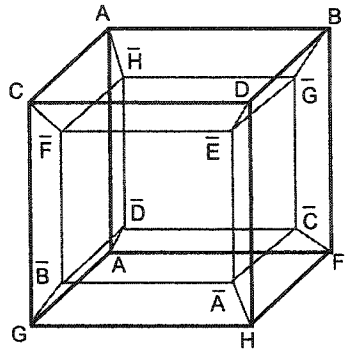

Figure 2.1: *The stereochemical correspondence of Type I (ex. Ar_3Z) and II (ex. C_6Ar_6) propellers is reflected in the graph portraying the results of their isomerizations. The vertices of the hypercube represent isomers and the edges rearrangements.*

Such a dynamic analogy implies that the effective NMR time-averaged perpendicular conformation of C_nAr_n and $C_nAr_{n-m}X_m$ propeller systems represents an idealized transition state for the low-energy interconversion of helical forms via a concerted n-ring flip. Notwithstanding the intuitive logic of this rotational phenomenon, incompatible time-scale considerations have precluded its experimental verification. In order to circumvent this issue, previous analyses of torsional behaviours of particular di- and triaryl systems, including 1,1- and 1,2-diarylethenes,[245;246] benzophenones,[247] and triphenylphosphine oxides,[248] have employed the structure correlation (SC) method.

2.1.1 Structure-Correlation Theory and Conformational Analyses

With ever-advancing technologies, applications and database capacities, the contributions of X-ray crystallography to three-dimensional structure determination and the molecular paradigm have propelled, in turn, the coalescence of numerous scientific domains and important interdisciplinary discoveries. Although the time-scale of this technique (~ 10^{-18} s)

greatly exceeds that of molecular rearrangements, the dynamic interpretation of static aspects has been realized in the form of two distinct solid-state (crystalline) observables: atomic displacement amplitudes[249-251] and systematic structural deformations.[37;249]

A data survey of the latter type requires an examination of the perturbation of a precisely defined fragment geometry within different intra- and intermolecular frameworks (steric settings, crystal packing arrangements), allowing for a series of crystallographic 'snapshots' of the chemical transformation under investigation. In the low-energy regions of n-dimensional space there should be a concentration of sample points corresponding to the equilibrium atomic arrangements; as the energy rises, the *reaction* or *response* path becomes increasingly less populated in the vicinity of the associated 'transition state'. As stated by Bürgi and Dunitz, "if a correlation can be found between two or more independent parameters describing the structure of a given molecular fragment in various environments, then the correlation function maps a minimum energy path in the corresponding parameter space."[249] From the fundamentals of fragment definition, data retrieval, statistical treatments and (often subtle) physical/chemical interpretations, this theory is widely applicable to organic, inorganic and biochemical reactions, including bond-breaking or bond-making processes as well as conformational interconversions.

The concept of configurational space provides an immediate connection with the molecular potential energy hypersurface (see Figure 2.2), and is restricted to those coordinates necessary to describe the invariant part of the structural formulae under study. For non-rigid molecules, a complete set of isometric (properly or improperly congruent) conformations,[252] equivalent to the non-Abelian super-group order, is obtained by combining the 'isodynamic' operations[253] of a rotor group (related to crystallographic translation groups, in n dimensions, with n the number of flexible degrees of freedom) and the frame group (related to point group symmetries) transformations on the relevant internal parameters. Data expansion of this type establishes the one-to-one correspondence between familiar crystallographic concepts and

molecular symmetry; the pattern that is produced is a finite (of modulo 2π) representation of an infinite n-dimensional lattice, and can be characterized by a standard unit cell with its general and special positions. To illustrate these properties, the periodic configuration space and set of corresponding operations pertaining to diphenylmethane, with two degrees of internal rotation, are depicted in Figure 2.1 and Table 2.1, respectively.[37] Although the quantitative details of such a scatterplot are not explicit, the effect of energy perturbations is most apparent if the reference surface is shallow. Thus, in examining the static deformations that a molecular fragment of interest manifests collectively over a large sampling of chemically different compounds in a variety of crystal structures, space groups serve as an essential tool to visualize conformational variation and eliminate artificial distributions of geometrical values.

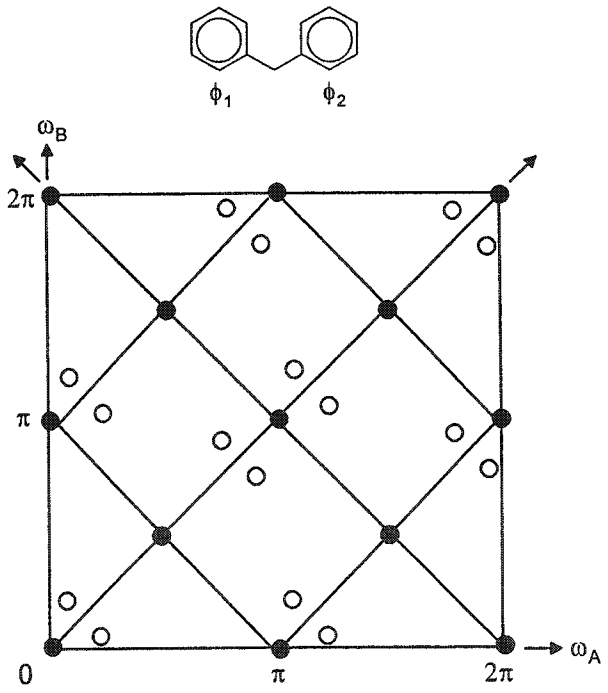

Table 2.1. Elements of the frame and rotor groups for CH_2Ph_2 combine to give 16 operations (the isometric conformations).*

Operation	ω_A	ω_B
E	ϕ_1	ϕ_2
R_A	$\phi_1 + \pi$	ϕ_2
R_B	ϕ_1	$\phi_2 + \pi$
R_{AB}	$\phi_1 + \pi$	$\phi_2 + \pi$
C_2	ϕ_2	ϕ_1
R_AC_2	$\phi_2 + \pi$	ϕ_1
R_BC_2	ϕ_2	$\phi_1 + \pi$
$R_{AB}C_2$	$\phi_2 + \pi$	$\phi_1 + \pi$
$\sigma(xz)$	$-\phi_1$	$-\phi_2$
$R_A\sigma(xz)$	$-\phi_1 + \pi$	$-\phi_2$
$R_B\sigma(xz)$	$-\phi_1$	$-\phi_2 + \pi$
$R_{AB}\sigma(xz)$	$-\phi_1 + \pi$	$-\phi_2 + \pi$
$\sigma(yz)$	$-\phi_2$	$-\phi_1$
$R_A\sigma(yz)$	$-\phi_2 + \pi$	$-\phi_1$
$R_B\sigma(yz)$	$-\phi_2$	$-\phi_1 + \pi$
$R_{AB}\sigma(yz)$	$-\phi_2 + \pi$	$-\phi_1 + \pi$

* $F\ (E, C_2, \sigma(xz), \sigma(yz))$; $R\ (E, R_A, R_B, R_{AB})$.

Figure 2.2: *Conformational map of diphenylmethane, depicting (open circles) the 16 equivalent positions (images of its isometric conformations) with different values of the two torsional angles, ϕ_1 and ϕ_2. This particular unit cell is primitive (defined by $0 \leq \omega_A < \pi$ and $0 \leq \omega_B < \pi$), whereas the alternate non-primitive lattice is based on translation vectors and comprises the plane group cmm.*

2.1.2 Overview of Study

With such a compass to facilitate structural investigations, it is proposed that a succession of static X-ray structures of C_5Ar_5 and C_5Ar_4X derivatives should permit a survey of the potential energy surface associated with inter-annular rotations, and therefore heighten our understanding of the stereoisomerization processes exhibited by these systems. Foregoing considerations of the sort, the fluxional properties of these systems have been interpreted using the stereochemical framework devised for hexaarylbenzenes (see Section 1.4.2.2), thus perpetuating the "oft-stated dichotomy" of the two propeller models. However, the SC method is particularly relevant for low barrier rotational pathways for which the slow exchange NMR regime cannot be accessed experimentally. As a supplement to the activation parameters that have been acquired by use of dynamic NMR, the following study explores the conformational preferences and associated threshold rotational pathways of persubstituted cyclopentadiene and –dienyl moieties by application of structure correlation principles.[254]

2.2 Results and Discussion

2.2.1 Statistical, Numerical and Theoretical Approaches

2.2.1.1 Conformational Maps and Computational Methods.

The torsional preferences and variability of C_5Ar_5 and C_5Ar_4X molecules can be conveniently analyzed by means of a conformational map[255] (*c.f.* also a Ramachandran-type plot[256]), which depicts the relative energy as a function of the central-to-peripheral interplanar angles (ϕ_n) of interest. The symmetry properties of the two-dimensional rotational potential energy surface reflect the symmetry of the nonrigid molecular fragment, which is isomorphous to either C_{2v} {[1,2-], [1,3-] (C_5Ar_5); [2,3-], [1,4-] (C_5Ar_4X)} or C_s {[1,2-], [1,3-] (C_5Ar_4X)} for the idealized diaryl frames. The relative energies of $C_5Ph_5^-$ **1.18**, $C_5Ph_4H^-$ **2.1**, $C_4Ph_4C{=}O$ **1.53** and $C_4Ph_4CH_2$ **2.2** were calculated at the semi-empirical level of theory (AM1 Hamiltonian)[257] by

systematically altering the two selected angles ϕ_n in 10° increments (dihedral driver option in SPARTAN V5.1[258]) from 0° to 90° and 0° to 180°, while allowing all other torsional degrees of freedom to minimize accordingly. For comparative purposes, the conformational plots were also generated using molecular mechanics methods (MMFF94[259] and Sybyl[260] force fields) and have been provided as supplementary data (see Appendix). To confirm the nature of specific stationary points along the PES of **1.18**, **2.1**, **1.53** and **2.2** (Table 2.2), geometry optimizations and subsequent frequency analyses were performed using the AM1 Hamiltonian as implemented in the GAUSSIAN98 program suite.[261]

Table 2.2. Calculated (AM1) conformational energies of molecules **1.18**, **2.1**, **1.53** and **2.2**.

	Interconversion Process[a]	E (a.u.)	ΔE (kcal mol^{-1})[b]	Ph–C_5 ∠ (°)
1.18-D_5		0.213809	0.0 *	46.3
1.18-D_{5h}	5-ring flip	0.205231	5.4	90.0
1.18-C_{2v}	4-ring flip	0.214266	5.7	90.0, 0.0
1.18-TS1	*Sequential-5-ring flip*	0.207888	1.7 **	109.4, 75.2 (α), 40.5 (β)
2.1-C_2		0.161710	0.0 *	30.3 (α), 47.1 (β)
2.1-C_s		0.162971	0.8 **	25.1 (α), 72.6 (β)
2.1-C_{2v}	4-ring flip	0.174078	7.8	90.0
2.1-C_s	[α, β, β]-3-ring flip	0.169106	4.6	90.0, 0.0 (α)
2.1-C_s'	[α, α, β]-3-ring flip	0.173318	7.3	90.0, 0.0 (β)
2.1-TS1	*Sequential-4-ring flip*	0.165666	2.5 **	110.0 (α), 51.0, 41.9 (β), 31.5 (α)
1.53-C_2		0.198769	0.0 *	30.4 (α), 76.9 (β)
1.53-C_s		0.198916	0.1 *	30.8 (α), 81.0 (β)
1.53-C_{2v}	4-ring flip	0.204465	3.6	90.0
1.53-C_s	[α, β, β]-3-ring flip	0.203215	2.8	90.0, 0.0 (α)
1.53-C_s'	[α, α, β]-3-ring flip	0.209080	6.5	90.0, 0.0 (β)
1.53-TS1	*Sequential-4-ring flip*	0.201328	1.6 **	110.3 (α), 73.9, 77.0 (β), 31.4 (α)
2.2-C_2		0.222599	0.0 *	30.3 (α), 79.3 (β)
2.2-C_s		0.222696	0.1 *	30.0 (α), 81.5 (β)
2.2-C_{2v}	4-ring flip	0.226683	2.6	90.0
2.2-C_s	[α, β, β]-3-ring flip	0.225049	1.5	90.0, 0.0 (α)
2.2-C_s'	[α, α, β]-3-ring flip	0.231271	5.4	90.0, 0.0 (β)
2.2-TS1	*Sequential-4-ring flip*	0.224236	1.0 **	106.4 (α), 60.3, 80.4 (β), 30.4 (α)

[a] Abbreviated titles are used here (see text). [b] Second derivative analyses have confirmed that these stationary points are either a local minimum* or a transition state**; otherwise, the structures represent higher nth-order saddle points (n negative eigenvalues).

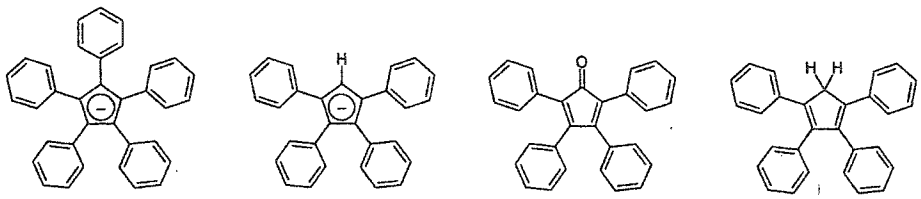

1.18 2.1 1.53 2.2

2.2.1.2 Database Retrieval.

A Cambridge Structural Database (July 2001 version)[262] search was conducted of molecular fragments possessing C_5Ar_4X ($X \neq Ar$) and C_5Ar_5 formulations, and incorporated those with peripheral aryl substitution, metal coordination, charged species and geometrically non-constrained (i.e. non-fused aromatics) frameworks. For the initial study, cyclopentadienyl species displaying a deviation from planarity of the central C_5-ring > 0.05 Å and a crystallographic agreement R factor > 0.10 were excluded; no further restrictions were placed on the non-bonding interactions (packing phenomena).

2.2.1.3 Data Treatment.

Atomic coordinates of 62 crystallographically independent substructures derived from 48 C_5Ar_5 units were retrieved using the CSD programs QUEST and CONQUEST (see supplementary data tables). Likewise, data for 100 substructures were acquired from 86 C_5Ar_4X fragments (where $X \neq Ar$). The C_5Ar_4X subset was further divided into two structural classes, comprising either aromatic (cyclopentadienyl) or non-aromatic (cyclopentadiene) systems. The torsional angles (defined as the angle between the mean planes of the peripheral ring and internal C_5-ring (C_5Ar_5 or C_5Ar_4X) or diene fragment (C_5Ar_4X), and denoted as ϕ_1, ϕ_2, ϕ_3, ϕ_4, ϕ_5, where the X substituent is always designated at position 5 for consistency) were analyzed manually, selecting as the reference frame the z-axis as directed along the ML_n-central Cp bond. Since published coordinates refer to an optional sense of chirality, ϕ_n values were initially adjusted between (plus/minus) 0 and 90°, which correspond respectively to situations in which an aryl ring is coplanar with the central ring or perpendicular to it. To eliminate the arbitrariness inherent in

labeling the directionality of the interplanar angles, isometric conformations were generated by application of the symmetry operations of the molecular frame. A comparison of several molecular fragments requires each specimen to be considered as a representative point (terminus of vector) in an n-dimensional hyperspace, with one dimension for each internal coordinate of interest. The simultaneous analysis of the five or four peripheral rings in C_5Ar_5 and C_5Ar_4X structures would therefore necessitate a 5^{th} (4^{th}) dimensional mathematical (principal component or cluster analysis) treatment and presentation (hyperstereoscopic unit cell, for example) of the data. Obviously there is a practical limitation to this approach, given the difficulties associated with visualization, and hence interpretation, of the results. In reducing the problem to two- or three-dimensional parameter space, the chemical questions that may be addressed by such a study are significantly modified. Rather than portraying the interdependence of all aryl substituents, a two-dimensional correlation of torsional angles of nearest (or next-nearest) neighbours (*c.f.* histogram or conformational map) highlights the conformational relationship of such fragments exclusively. The latter graphical method requires that each C_5Ar_5 or C_5Ar_4X moiety contribute not one, but five or four data points, respectively, exclusive of its isometric conformations. Whereas this precludes the direct investigation of a threshold rotational mechanism in these systems, it provides insight into contiguous group effects and the preferred arrangement of such molecules. *As the torsional angle of a peripheral aryl ring-to-central plane changes, what influence, if any, does this have on neighbouring aryl groups? Does the variation in molecular geometry provide any evidence of gearing motion or correlated rotation in these systems?*

2.2.2 Histogram Analysis

The histograms depicted in Figure 2.3 were generated from the absolute values of peripheral aryl-to-central ring interplanar angles for the collective crystallographic sets of C_5Ar_5 and C_5Ar_4X molecules. A comparison of the distribution of angles reveals comparable medians

(*c.f.* 51.1° (C_5Ar_5), 50.1° (dienyl) and 51.0° (diene), respectively), whereas the range of values is much greater in the latter systems (*c.f.* 77.5° (dienyl), 73.6° (diene) and 61.6°(C_5Ar_5)). Moreover, the relatively peaked distribution (kurtosis* = 1.97) displayed by the C_5Ar_5 systems is in contrast to the more uniform dispersion (kurtosis = -0.70 for dienyl species and -0.78 for diene fragments) that characterizes the C_5Ar_4X fragments. If the entire series of C_5Ar_4X interplanar angles is partitioned into two subsets comprising aryl groups positioned alpha (1,4) and beta (2,3) to the 'X' substituent, a significantly different distribution is apparent (Figure 2.3c). 1,4-Interplanar angles are scattered over a range of 75.6°, with a median of 40.5° and associated kurtosis of 0.19. Centered at 56.7°, the 2,3-interplanar angles envelop a smaller region (60.2°) with a kurtosis (–0.30) reflective of the skew towards an orthogonal orientation. These trends confirm our simple chemical intuition that aryl-flanked beta rings are more sterically encumbered than alpha rings (*i.e.* when X is less bulky than an aryl group), which exhibit a heightened rotational response to intra- and intermolecular non-bonded interactions.

2.2.3 C_5Ar_5 Systems

In all pentaarylcyclopentadienyl systems thus far examined by use of dynamic NMR, independent peripheral ring rotation by ~ π radians has been invoked as the stereoisomerization mechanism of lowest observable energy. However, as disclosed in Section 1.4.1.1, the shorter timescale of EPR (relative to NMR) spectroscopy has permitted the observation of a small phenyl group oscillation about the planes orthogonal to the C_5 ring of the neutral C_5Ph_5 radical.[124] Furthermore, the splitting of the solution C-O stretching absorptions in the solid-state IR spectra

---

* $Kurtosis = \left(\frac{\sum (X-\mu)^4}{N\sigma^4} \right) - 3$ where μ is the mean, σ is the standard deviation, and N is the number of data points. Kurtosis is based on the size of a distribution's tails, with values corresponding to a high peak (> 0), a flat-topped curve (< 0), or a normal distribution (= 0).

of several chiral (η^5-C_5Ph_5)ML_3 complexes (**1.28 - 1.31**) has been rationalized on the basis of diastereoisomerism, arising from axial chirality.[131,132]

The symmetry-extended conformations of C_5Ar_5 fragments possessing two internal rotational degrees of freedom are mapped in Figure 2.4. With the exception of values corresponding to three moieties,** the solid-state data points (Table A.1, Appendix A) lie in the region where both torsional angles have the same sign, which is the condition for a propeller structure. This arrangement is typically favoured as a result of a compromise between energy reducing conjugation effects (maximal when the peripheral aryl substituents are coplanar with the central ring) and energy increasing repulsive steric effects (minimal when the aryl groups are perpendicular to the C_5 ring). From the pronounced clustering of points around (~50°,~50°), sparsely populated symmetry-related paths corresponding to torsional angles of opposite sign {via regions (~90°,~50°) to (~130°,~50°)} interconnect enantiomeric conformations (e.g. (50°,50°) and (-50°,-50°)=(130°,130°)). The same trend is exhibited by both adjacent (1,2-) and next-nearest (1,3-) aryl groups (Figures 2.4a and 2.4b, respectively), although there is a wider data spread in the latter case. As a plausible description of the stereomutation process that is manifested here, uncorrelated rotation can be discounted since minima of identical helicities are segregated. Furthermore, the absence of points near the (~90°,~90°), (~0°,~90°) and (~90°,~0°) regions suggests that helicity inversion of the propeller molecule is neither distinguished by a classical (concomitant) conrotatory nor disrotatory pathway. Instead the data, which encapsulate all C_5Ar_5 interplanar angles, are more readily interpreted in terms of a delayed 5-fold motion; at a critical torsional angle, which likely coincides with the van der Waals distance, an instantaneous

---

** While there are no obvious steric interactions that may explain the helical distortions in two of the organometallic derivatives (HOGPAU, SIRMIP), in the third case (HAYMEZ) it is the presence of a palladium-bound 2,6-dimethylphenylisocyanido ring wedged in between two contiguous peripheral phenyl groups that appears to engender the non-propeller C_5Ph_5 array in one of its crystallographic forms.

(conrotatory) ring flip occurs. Accordingly, this analysis provides the first evidence for a *non-classical* n-ring (n = 5) flip interconversion process operative in these types of propeller systems.

The dynamic behaviour of more complex C_5Ar_5 fragments may be qualitatively interpreted from the calculated potential energy surfaces of C_5Ph_5, **1.18**, in view of the correspondence between the contour maps and the preferred solid-state geometry of the molecules comprising the diversely substituted C_5Ar_5 subset. The PES regions of lowest ($\phi_1 = \phi_2 = 50 \pm 10°$; $\phi_1 = \phi_3 = 50 \pm 10°$) and highest ($\phi_1 = \phi_2 < 40°$; $\phi_1 = \phi_3 < 40°$) energy are consistent with the concentrated and uninhabited areas of the crystallographic scatterplots, respectively. The barriers to enantiomerization (helicity inversion) of the selected frames (1,2-Ar_2 and 1,3-Ar_2) may be estimated as 2-3 kcal mol^{-1} from the plots. In extrapolating the mechanistic information to the entire molecule, a more precise assessment of the energetics of this process requires characterization of the actual saddle point(s) separating the ground-state propellers of **1.18** (*vide infra).*

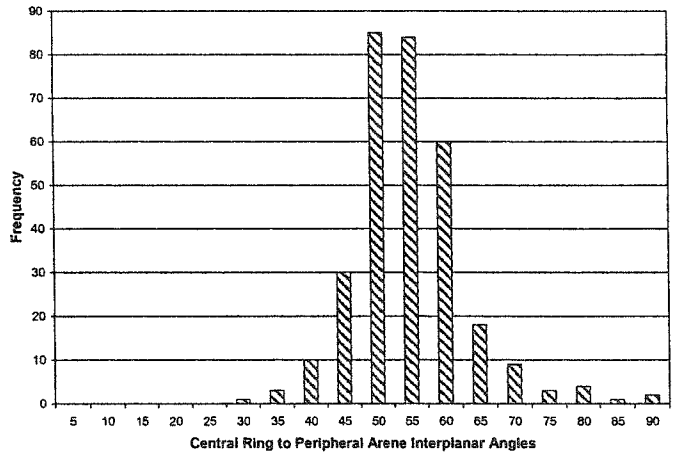

(a)

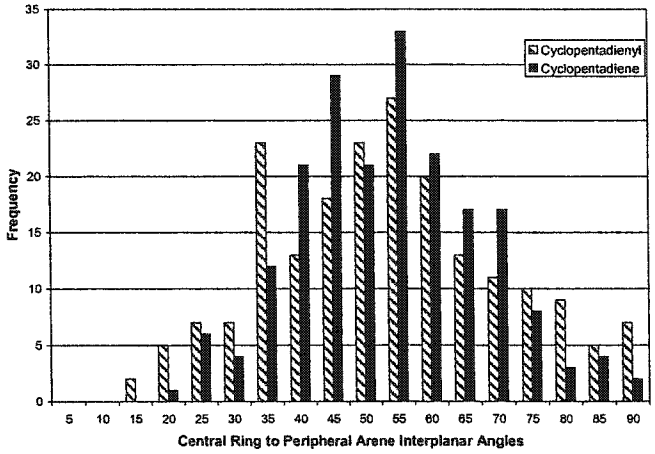

(b)

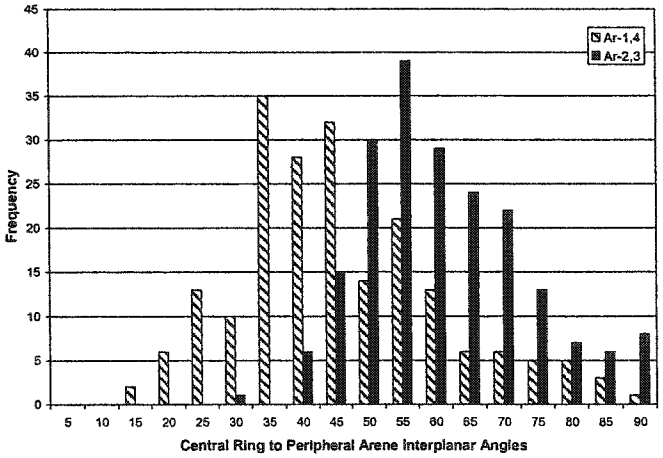

(c)

Figure 2.3: *Distribution of interplanar angles (with bin sizes of 5° increments) for all aryl substituents in (a) C_5Ar_5 and (b) C_5Ar_4X systems, with alpha (1,4) and beta (2,3) aryl groups also depicted separately in (c) for the latter case.*

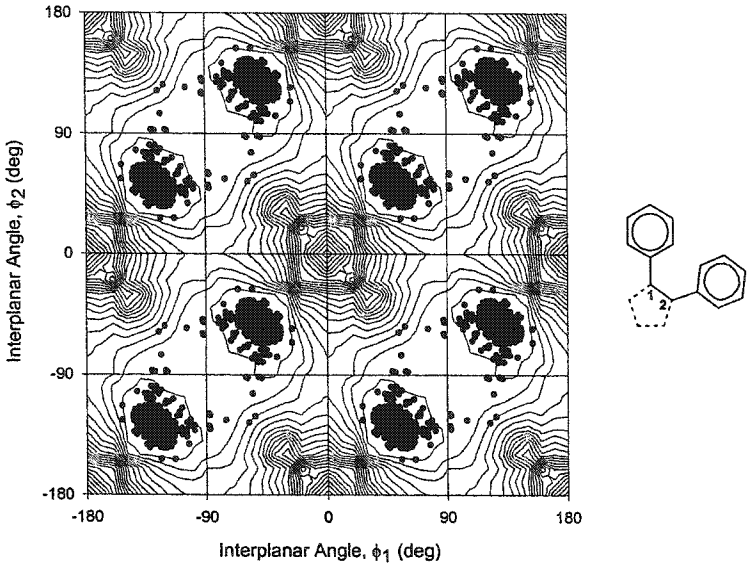

(a)

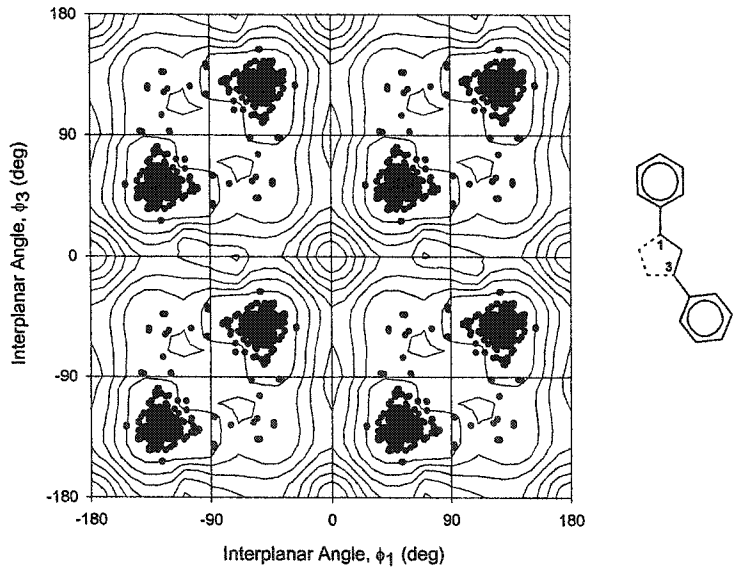

(b)

Figure 2.4: *Conformational maps of torsional angles of 2 peripheral aryl rings (or rotors) constituting part of a C_5Ar_5 frame, featuring (a) adjacent (1,2) aryl groups, and (b) next-nearest neighbouring (1,3) aryl groups. In both maps a denser population of points can be observed in the region of (~50°,~50°), corresponding to the low-energy conformation of pentaarylcyclopentadienyl species. The overlaid contours (at 1 kcal mol^{-1}) represent the calculated (AM1) equipotential energy regions associated with $C_5Ph_5^-$,* ***1.18.***

2.2.4 C_5Ar_4X Systems (Aromatic)

Tetraarylcyclopentadienyl derivatives bearing 'X' substituents also display restricted rotation on the NMR time-scale. However, analogous to polyarylbenzenes,[127] steric buttressing effects can influence the isomerization pathway and associated barrier heights, as exemplified by the differing alpha and beta ring torsional responses in the the linear metallocene, $Fe(C_5Ph_4H)_2$, **1.42**, and the ansa-metallocene complex, rac-[1-(η^5-Cp)-1-Ph-(η^5-C_5Ph_4)Et]$ZrCl_2$, **1.45** (Section 1.4.1.1). If qualitative parallels are drawn, peripheral substitution of the C_5 framework might also be expected to alter the conformational model for helicity inversion.

Semi-empirical calculations of the tetraphenylcyclopentadienyl ligand (**2.1**) indicate that the molecule adopts a propeller orientation of C_2 symmetry, with interplanar angles of 30° (alpha) and 47° (beta). As a conformational option, the C_s rotamer (ϕ_{alpha} ~ 25° and ϕ_{beta} ~ 73°) is only 0.8 kcal mol^{-1} higher in energy than the global minimum, and is associated with one imaginary vibrational frequency. When the various skeletal fragments are considered separately, the projected activation energies of this process are in the range of 2-3 kcal mol^{-1}.

The C_5Ar_4X ($X \neq Ar$) subset is comprised of fifty data points (Table A.2, Appendix A), wherein twenty-six fragments assume a propeller conformation, nine adopt a non-propeller arrangement (with only one aryl substituent canted in the opposite direction), and fifteen possess a pseudo-mirror structure (with aryl groups 1 and 2 oppositely inclined to aryl rings 3 and 4). In comparison to C_5Ar_5 systems, the structural deformations within this class are more pronounced, attributable in part to the two sets of aryl groups (alpha and beta to the X substituent) residing in differing steric environments. The sampling of C_5Ar_4X moieties therefore provides increased conformational coverage and the potential for further probing the stereodynamic details of these multi-rotor arrays.

The crystallographic data points for all C_5Ar_4X fragments are superimposed on the AM1 calculated PES for $C_5Ph_4H^-$ (**2.1**) in Figure 2.5, which depicts diaryl [1,2-/4,3-], [2,3-], [1,3-] and

[1,4-] frameworks. For the symmetry inequivalent 1,2/4,3 model, most of the points congregate in the vicinity of (~40°,~60°), and represent both propeller and pseudo-mirror structures. The path linking equilibrium conformations is formed by non-propeller fragments and proceeds via (~120°,~75°), suggesting that alpha ring libration induces the beta ring to flip. Although energetically accessible according to calculations, the (90°,90°) region is void of data. Interestingly, three non-propeller moieties yield rotational values that approach (0°,90°), the *idealized* transition state for either an independent alpha-one-ring rotation (a process for which VT-NMR data have only been reported for the crowded derivatives $[(C_6F_5)_4C_5H]M(CO)_3$, M = Mn, **1.70**; or Re, **1.71**)[152] or a correlated alpha,beta,beta-3-ring flip.

In considering the 2,3-vicinal aryl substituents (Figure 2.5b), propeller and non-propeller moieties both give rise to the enantiomeric clusters at (~60°,~60°) and (~120°,~120°), which are interconnected by symmetry-related pathways {via regions (~90°,~60°) to (~120°,~90°)} densely populated by pseudo-mirror structures. Once again, the progressive rotation of one ring through the orthogonal position gradually effects the helicity reversal of the adjacent ring. The asymmetry of this torsional circuit should not be overlooked; whereas alpha aryl substituents must traverse at least 100° to achieve enantiomerization, the rotational span of beta aryl groups is only ~60°.

The transformation of 1,3-diaryl enantiomeric conformations {(~40°,~60°) to (~140°,~120°), and (~40°,~120°) to (~140°,~60°)} proceeds via linear routes corresponding to a sequential 2-ring flip, wherein the inversion of the second aryl group appears instantaneous (Figure 2.5c). Extending the torsional scope to the least sterically encumbered (when 'X' is less bulky than an aryl group) 1,4-diaryl interactions, the associated conformational map (Figure 2.5d) depicts separate enantiomeric clusters of propellers {(~40°,~40°), (~140°,~140°)} and pseudo-mirror structures {(~40°,~140°), (~140°,~40°)}, linked by non-propeller fragments along a (90°,~60°);(~120°,90°) curvature.

The picture that emerges when all sets of torsional data are amassed suggests that helicity inversion in tetraarylated cyclopentadienyl systems is achieved by means of a *delayed* oscillation. Despite the fact that alpha and beta aryl groups experience different buttressing effects, both immediate and long-range correlations may be ascribed to a lowest energy stereoisomerization pathway that is equivalent to a *non-synchronous* 4-ring flip, in agreement with calculations. The flatness of the PE landscape near the dominant propeller conformation easily lends to deformations, with pseudo-mirror fragments corresponding to an energy transition, as predicted computationally.

2.2.5 C_5Ar_4X Systems (Non-aromatic)

The stereochemical scaffold for all substituted tetrahapto and pentahapto C_5Ar_4X ligands was derived from the detailed conformational analysis of the maximally labeled tetra-*o*-tolylcyclopentadienone, **1.23** (see Scheme 1.12). In assuming a $Ph_4C_4C{=}O$ perpendicular skeleton with C_{2v} symmetry, the VT-NMR spectral data of **1.23** were ascribed to two dynamic processes: a low energy, uncorrelated alpha-one-ring rotation (cf. alpha,beta,beta-3-ring flip) in the direction of the carbonyl moiety, and a more sterically demanding, uncorrelated beta-one-ring rotation ($\Delta G^{\ddagger} \approx 20$ kcal mol^{-1}; *c.f.* alpha,alpha,beta-3-ring flip). As conceded by Willem, Pepermans, et al.,[125] a model that embraces the interconversion of propeller configurations lends itself to the same combination of rearrangement modes and experimental rationales, provided the threshold rotational pathway is a concerted four-ring flip *or approximation thereof.* In probing this inversion process from a SC vantage, Hückel 4n systems present not only disparate steric influences of an 'X' substituent relative to an aryl moiety, but additional electronic differences (and accompanying variations in bond lengths, bond angles, central ring deformability and central-to-peripheral ring conjugative effects) that may have stereochemical consequences.

The tetraarylcyclopentadiene solid-state subset is also comprised of fifty data points (Table A.3, Appendix A), with a conformational partitioning of twenty-nine propeller, five non-

propeller and sixteen pseudo-mirror fragments. With reference to the hybridization of the C(5) center, both sp^2 (twenty-two) and sp^3 (twenty-eight) derivatives have been included in this structural class. Statistically, more than half the $Ar_4C_4C{=}X$ moieties are cup-shaped, whereas almost seventy percent of the $Ar_4C_4CX_2$ units assume a helical arrangement.

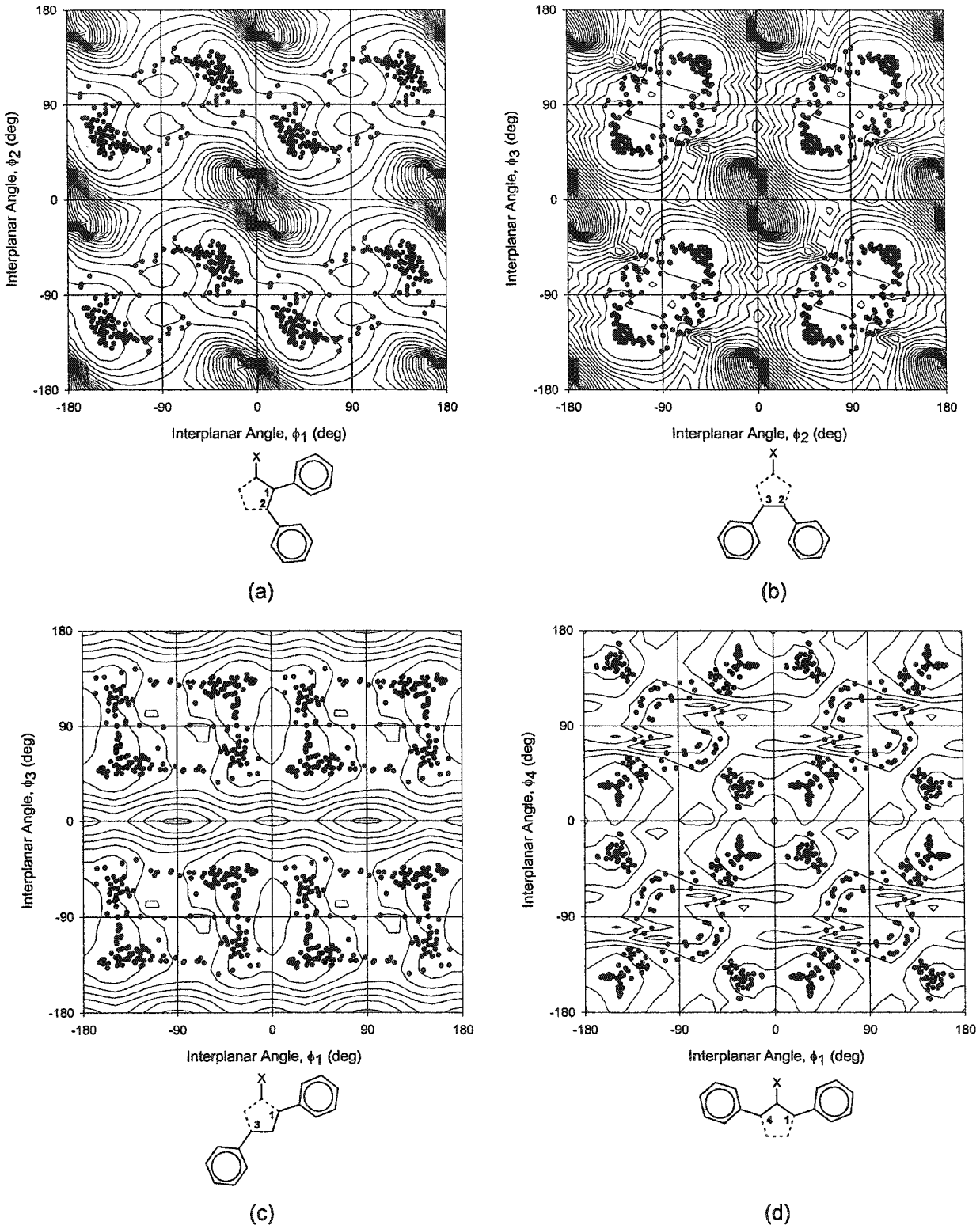

Figure 2.5: *Conformational maps of torsional angles of 2 peripheral aryl rings (or rotors) constituting part of a C_5Ar_4X ($X \neq Ar$) frame, featuring vicinal (a) (1,2/4,3) and (b) (2,3), as well as next-nearest (c) (1,3) and (d) (1,4) interactions. The overlaid contours (at 1.5 kcal mol^{-1}) represent the calculated (AM1) equipotential energy regions associated with $C_5Ph_4H^-$,* ***2.1.***

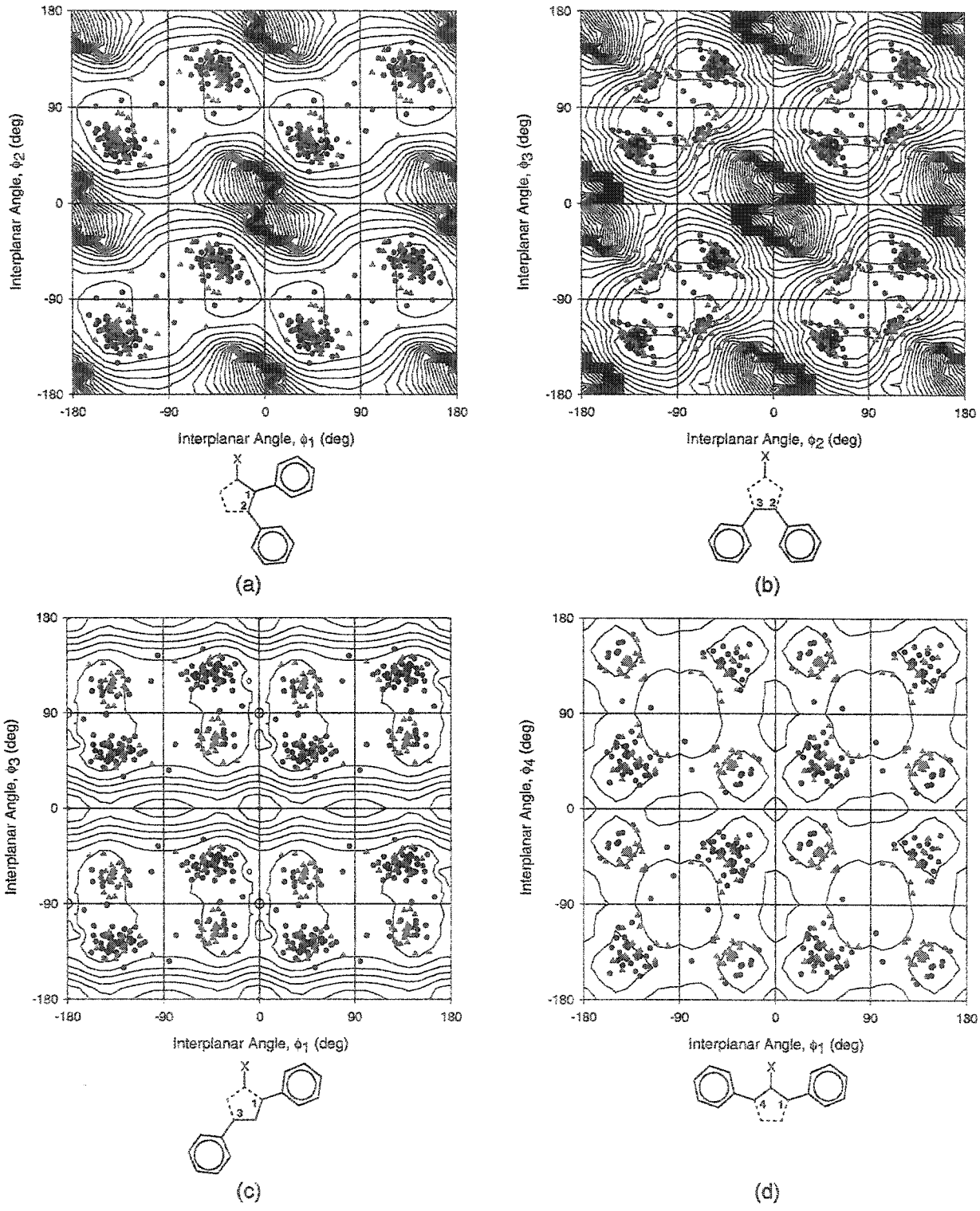

Figure 2.6: *Conformational maps of torsional angles of 2 peripheral aryl rings constituting part of a Ar_4C_4CX frame ($X \neq Ar$; C-X = sp^2 (triangles) and sp^3 (circles) hybridized), featuring vicinal (a) (1,2/4,3) and (b) (2,3), as well as next-nearest (c) (1,3) and (d) (1,4) interactions. The overlaid contours (at 1.5 kcal mol^{-1}) represent the calculated (AM1) equipotential energy regions associated with $C_4Ph_4C{=}O$,* ***1.53.***

AM1 calculations of tetraphenylcyclopentadienone, **1.53**, predict a chiral C_2 isomer with angles of ~ 30° and 77° (cf. values of 27.4, 60.5, 47.7 and 36.1° in the experimentally observed propeller[263]), as well as an almost equally accessible C_s-symmetric structure (ϕ_{alpha} ~ 30° and ϕ_{beta} ~ 81°). These two conformations are essentially isoenergetic in tetraphenylcyclopentadiene, **2.2**, which adopts a pseudo-mirror structure with interplanar angles of 33.1, 69.4, 69.6 and 23.5° in the solid state.[264]

Figure 2.6 features the experimental solid state torsional values superimposed on the calculated PES of **1.53** for the various diaryl frames. Patterns similar to the C_5Ar_4X subset are manifested in all four plots, however, the data are generally more scattered, and the pathways connecting enantiomeric clusters are much less clearly defined. A survey of vicinal interactions (1,2/4,3 and 2,3) reveals that certain $Ar_4C_4CX_2$ structures contribute isometric angles which approach the (90°,90°) region. Overall, the rotational trajectory is less evident from this data set, making it unreasonable to speculate about any stereochemical variations between the constitutionally distinct $Ar_4C_4C{=}X/Ar_4C_4CX_2$ and C_5Ar_5 ligands.

2.2.6 Threshold Rotational Mechanism

Having arranged the pillars of a dynamic model from the conformational energy landscapes of **1.18**, **2.1**, **1.53** and **2.2**, a more rigorous analysis of the degenerate inversions is now feasible. In the **1.18-*D*$_5$** ⇌ **1.18-*D*$_5$'** isomerization, three transition states and two intermediates, differing in energy by less than 0.7 kcal mol^{-1}, have been identified (Scheme 2.1a). Scheme 2.2a depicts the sequential flipping process (overall barrier of 1.7 kcal mol^{-1}), symmetrically disposed about the transition state **1.18**-TS2 in which one of two adjacent aryl groups has completely reversed helicity and the buttressing phenyl substituents are approaching orthogonality. The rearrangement of **2.1-*C*$_2$** ⇌ **2.1-*C*$_2$'** also constitutes three steps (Schemes 2.1b and 2.2b), with a slightly steeper energy profile and a barrier height of 2.5 kcal mol^{-1}. The corresponding inversion of configuration of propellers **1.53** and **2.2** has not been completely

characterized, but by analogy, the relative energies of the first transition structures (**1.53-TS1**, **2.2-TS1**), wherein an alpha ring has rotated beyond its perpendicular orientation, are 1.6 and 1.0 kcal mol^{-1}, respectively. Particularly noteworthy is the agreement of the calculated angles in the various saddle points with the crystallographic orientations of the peripheral blades along the gearing trajectories evinced in the two-dimensional conformational maps. In all four molecules, concerted n-ring (see **1.18-D_{5h}**, **2.1-C_{2v}**, **1.53-C_{2v}**, **2.2-C_{2v}**) and (n-1)-ring flip mechanisms are easily discounted given the number of imaginary vibrational frequencies associated with the relevant stationary points. So while the earlier suppositions of Pepermans et al.[65] are confirmed herein, we have also extended the model beyond the permutational sense, which is devoid of all mechanistic details.

There is one final corollary that should not be overlooked. According to the parity restriction on dynamic gearing, uncorrelated as well as correlated rotation is mechanically disallowed in a closed cyclic array consisting of an odd number of securely meshed gears, thus inducing immobility.[21] Whereas the operation of this rule has precedent in triptycyl-based molecules,[9;71] propeller frameworks comprised of aryl rings (two-fold rotors) may not present the obligatory "tongue and groove interactions" for such interdependent rotation, allowing for *gear slippage* in the dynamic regime.[168;190;191] Furthermore, the efficient transmission of information via cooperative torsional motions along a macromolecular chain of coupled rotors is limited not only by the extent of steric interplay, but by the length of the propeller chain and the inversely related energy gap between uncorrelated and correlated rotational pathways (Scheme 2.3).[67;265] By deductive reasoning $C_5Ar_5^-$ systems are exempt from the strict specificity of cog-wheeling, and therefore, exhibit a preference for successive localized (con/dis)rotations of adjacent rings over concerted ring-flip mechanisms. Alas, there is no disparity in the parity principle!

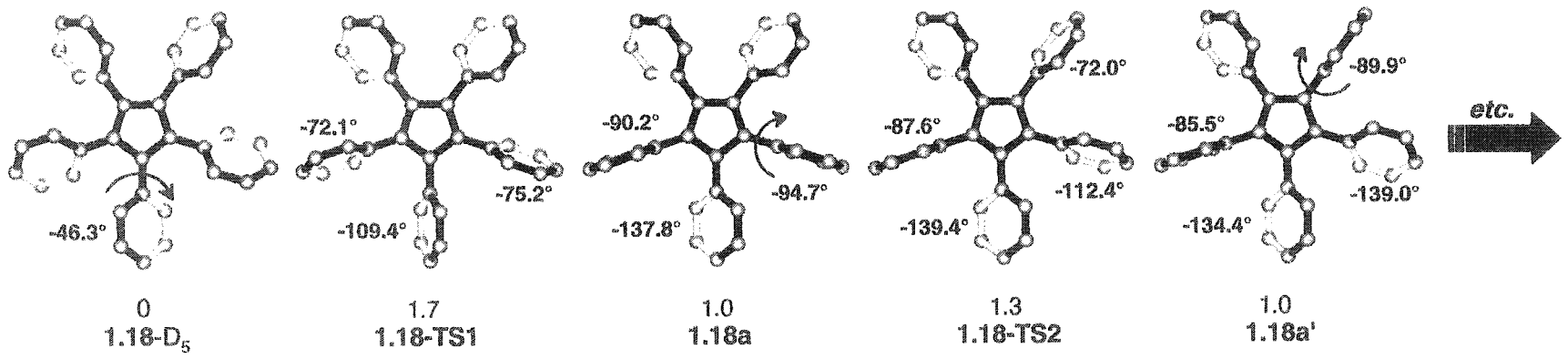

0 1.7 1.0 1.3 1.0
1.18-D_5 **1.18-TS1** **1.18a** **1.18-TS2** **1.18a'**

(a)

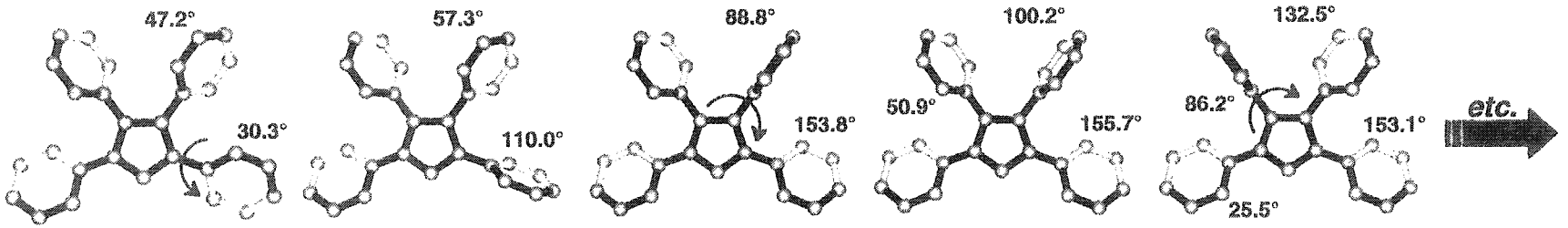

0 2.5 0.4 0.7 0.4
2.1-C_2 **2.1-TS1** **2.1a** **2.1-TS2** **2.1a'**

(b)

Scheme 2.1: *The intermediate and transition structures (AM1 Hamiltonian) involved in the flipping processes (a)* ***1.18-D_5*** *⇌* ***1.18-D_5'*** *and (b)* ***2.1-C_2*** *⇌* ***2.1-C_2'****, as viewed along the 5-fold or perpendicular to the 2-fold symmetry axes in* ***1.18-D_{5h}*** *and* ***2.1-C_{2v}****, respectively.*[a]

[a]*The dihedral angles (∠) = C_5(alpha)-C_5(ipso)-C_6(ipso)-C_6(alpha) are measured counterclockwise around the C_5 ring. The relative energies are given in kcal mol^{-1}.*

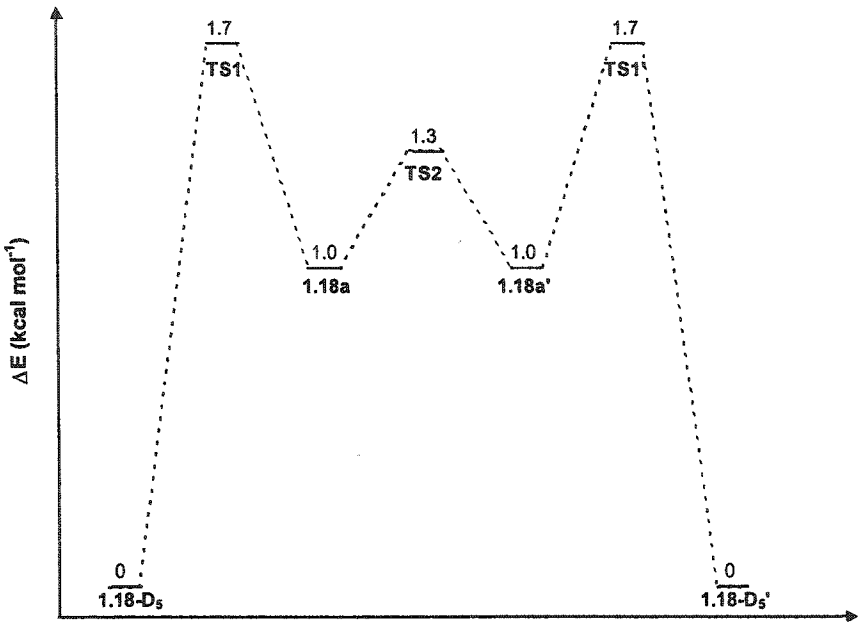

(a)

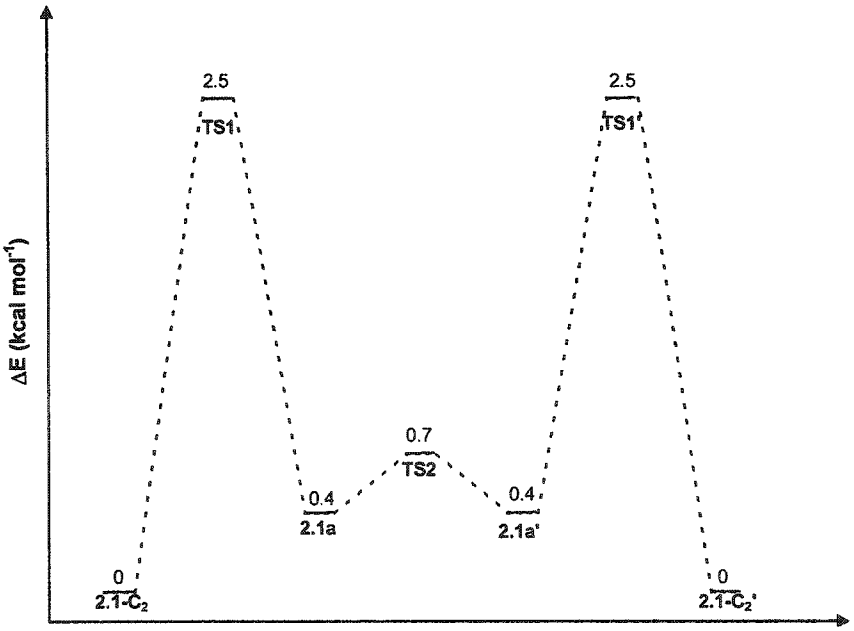

(b)

Scheme 2.2: *Graphical representation of the potential energy surfaces associated with the correlated inversion of propeller forms of (a)* ***1.18*** *and (b)* ***2.1****.*

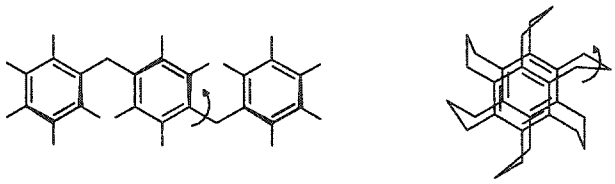

2.3 2.4

Scheme 2.3: *(a) Computations confirm that successive localized disrotations of two adjacent rings, as opposed to concerted ring flips, are responsible for the enantiomerization of the linear propeller systems (such as* ***2.3****) possessing two or three diarylmethyl moieties. (b) Similarly, the correlated inversion of [3$_6$](1,2,3,4,5,6)cyclophane,* ***2.4****, occurs via a sequential flipping process with an extremely flat potential energy surface.*

2.3 Summary and Outlook

Analysis of C_5Ar_5 and C_5Ar_4X moieties by the Structure Correlation method indicates an equilibrium propeller orientation, although species belonging to the latter class exhibit increased conformational flexibility by virtue of different alpha and beta steric environments. Based on the qualitative agreement between the AM1 calculated potential energy surfaces and the experimental distribution of data points generated from the diaryl (C_{2v} and C_s symmetric) models, an extended torsional itinerary corresponding to an entropically favoured non-synchronous (i.e. delayed) n-ring flip has been constructed for all tetra- and pentacycles.[254] Without an index of comparison (i.e. empirical data) to evaluate the quality of our computations or our description of this stereoisomerization process, we can only submit that the highly organized transition states associated with a concerted mechanism are much less probable. The observation of helicity reversal by use of dynamic NMR methods requires the incorporation of diastereotopic probes, such as pendant para-$CH^{19}F_2$ groups on the peripheral aryl rings, that are rendered enantiotopic (and therefore necessarily isochronous in an achiral solvent) in a symmetrized environment. In the absence of increased repulsive nonbonded interactions of the flipping rings (such as mesityl or 2,6-xylyl substituents), however, the calculated rotational barriers are well below the range accessible by such techniques. In an endeavor to transcend the time-scale limitations of NMR spectroscopy, the challenge remains for experimentalists to devise variable-temperature EPR studies that might further probe the generality of this correlated inversion process in propeller systems comprised of a central planar, polyatomic framework.

CHAPTER THREE

Persubstituted Arenes: C_nAr_n where n = 6

"The important thing in science is not so much to obtain new facts as to discover new ways of thinking about them." (William Bragg Sr., 1862 - 1942)

3.1 Preface

Benzene as a core in $C_nAr_n^{x\pm}$ propellers provides hexagonal symmetry, anisotropy and functional versatility that allows for the introduction of an even number of rotors in a closed cyclic π array, thus fulfilling the parity requirements of gear trains. As mentioned in Section 1.4.2, the polyarylated molecular analogs are available by the transition-metal-catalyzed cyclotrimerization of suitable diarylacetylenes or by the intermolecular [4+2] Diels-Alder cycloaddition of such diarylacetylenes with tetraarylcyclopentadienones followed by in situ decarbonylation at high temperatures. The former approach leads exclusively to the uniform functionalization of all aryl groups in C_6Ar_6, whereas the scope and utility of the latter synthetic transformation permits varied substitution patterns (Scheme 3.1).

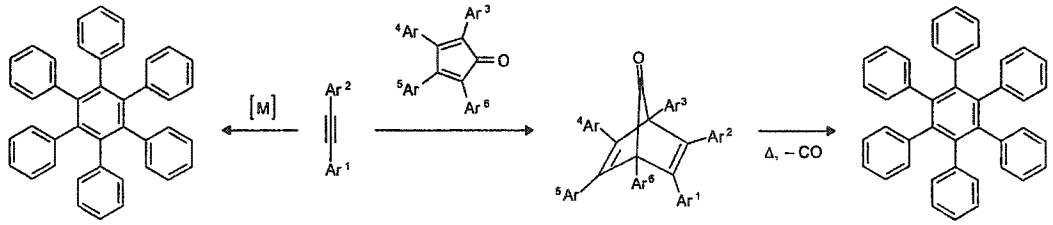

Scheme 3.1: *Classical trimerization (left) and cycloaddition (right) reactions to produce (un)symmetrically substituted benzenes.*

From an historical perspective, synthetic stimulation in this area was first provided by Ogliaruso,[173;266;267] Reid,[268] and Stille and co-workers,[269] who contributed a multitude of unsubstituted oligophenylenes and polyphenylenes, respectively, in the 1960s. Since 1986, Pascal et al.[225;270-272] have employed a series of cyclopentadienone derivatives together with

various ethyne and aryne compounds in cycloaddition reactions to produce sterically congested PAHs. These studies continue to form the basis for understanding the structures and properties of more complex, polyphenyl systems, the interest in which was rekindled by Müllen and co-workers in 1997.[273-275] The use of protection/deprotection sequences and oligomeric starting materials with multiple dienophilic and dienic functions has allowed for an exceptional diversity of linear, branched and dendritic derivatives. As precursors to 'polyphenylene nanostructures', significant strides have already been made toward the preparation of such a library of ensembles of varying geometry, size, stereochemistry, and periphery (cf. hexaphenylbenzene diameter of 1.14 nm).[276;277]

Table 3.1.[278-284]

3.1

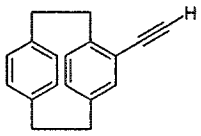

3.3

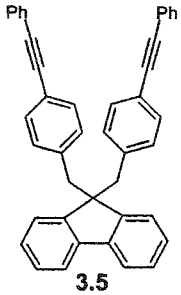

3.5

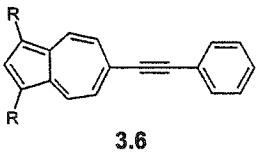

3.6

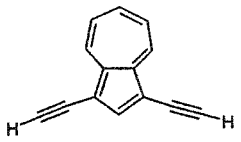

3.2

3.4

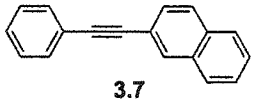

3.7

Table 3.2.[225;278;285]

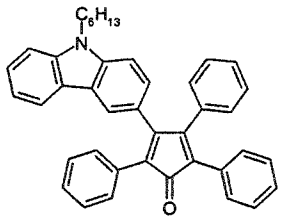

3.8

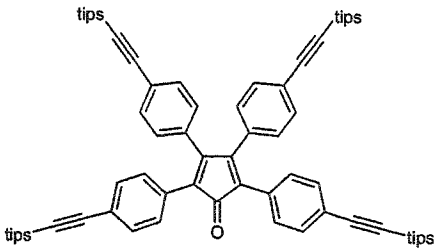

3.9

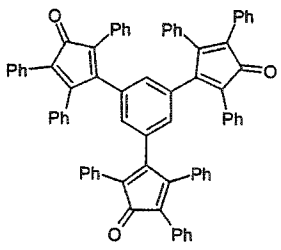

3.10

In support of this endeavour, acetylene chemistry is itself a very active area of research, and new or improved synthetic methods for symmetrical and unsymmetrical disubstituted platforms are regularly advanced.[286-288] Beyond their obvious role in Scheme 3.1, alkynes may also be oxidized by a variety of reagents (for example, permanganate) to generate 1,2-diketones

that, when condensed with 1,3-diarylacetones, yield the desired tetracyclone. An assortment of acetylenes and tetraarylcyclopentadienones that have recently been employed in the production of polyarylated benzenes is featured in Tables 3.1 and 3.2, respectively. Despite the collection of organic systems that can be found in the current literature, only a relatively small number of crystallographic and computational analyses have cast any light upon their conformational preferences. In probing the motional processes of polyphenylene dendrimers with use of advanced solid-state NMR techniques, it was found that the localized, restricted reorientation of single terminal phenyl groups is limited to an angular excursion of either 60° (msec. to sec.) or 20° (μsec. timescale), as opposed to the 180° edge interchanges observed in comparatively smaller propellers in the solution phase.[289]

The dynamic NMR studies of metal-complexed hexaarylbenzenes are thus far confined to $(C_6Ph_6)Cr(CO)_3$, **1.138**, notwithstanding the fact that a few molecules of this type have been prepared and structurally characterized (Scheme 3.2). In connection with the cobalt-catalyzed cyclotrimerization of alkynes, Biagini and associates[290] have described the irreversible disproportionation of $[Co(py)_6][BF_4]$ in the presence of diphenylacetylene, **3.11**, to give $(\eta^6\text{-}C_6Ph_6)Co(\eta^2\text{-}C_2Ph_2)$, **3.12**, as one of two products. From a generalized synthetic route to sterically crowded ruthenium arene cations, Crocker, Green et al.[291] have employed **3.11** in a photochemically promoted ring expansion reaction with an η^4-cyclobutadiene complex, $[CpRu(CO)(\eta^4\text{-}C_4Ph_4)][BF_4]$, yielding $[CpRu(\eta^6\text{-}C_6Ph_6)][BF_4]$, **3.13**. Quamby and co-workers[292] have recently reported the corresponding molybdenum 17-electron mixed-sandwich metallocene, $CpMo(\eta^6\text{-}C_6Ph_6)$, **3.14**, generated from the thermolysis of $CpMo(CH_2Ph)(\eta^2\text{-}PhC_2Ph)[P(OMe)_3]$ and diphenylacetylene, **3.11**. In contrast to the three aforementioned complexes, in which the metal fragments are bound in a η^6-fashion to the central arene ring of HPB, Munakata[293;294] has provided examples of the varied (η^1, η^2) coordination topologies of silver(I) ions around the peripheral rings of the propeller ligand, including $[Ag_4(HPB)(ClO_4)_4]$, **3.15**, and $[Ag_2(HPB)(ClO_4)_2(THF)_2]$, **3.16**. The collaborative efforts of Constable,

Fenske, and Housecroft[295] have led to the realization of yet another supramolecular utility of these six-spoked cartwheels, namely metallostars **3.17** comprised of hexaalkyne arms possessing multiple $\{C_2Co_2(CO)_6\}$ cluster motifs. Finally, van Koten et al.[181;182] have capitalized on the rigid aromatic hydrocarbon skeleton of HPB to generate multimetallic (tris)pincer compounds, such as $[C_6\{3,5\text{-}(CH_2SPh)_2\}_6C_6H_2\text{-}4\text{-}(PdCl)]$, **3.18**, and analogues, with homogeneous Lewis-acid catalytic capabilities.

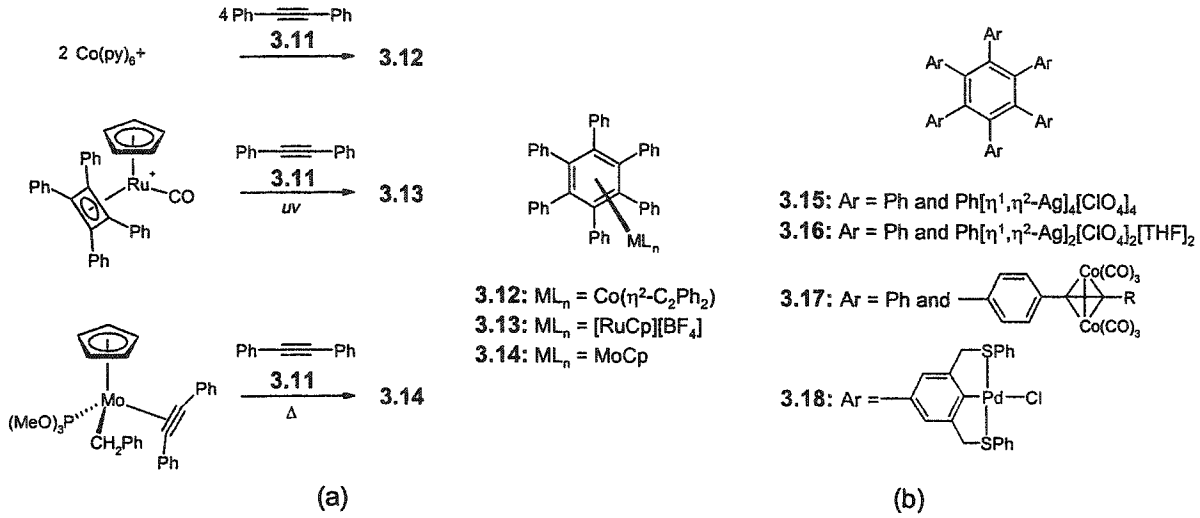

Scheme 3.2: *Hexaarylbenzenes centrally (a) or peripherally (b) coordinated with various early and late transition metal fragments.*

3.1.1 Overview of Study

At the nucleus of stereochemical logic for polyaryl frameworks of all dimensions and substitution patterns, including polyphenylene nanostructures, are C_6Ar_6 molecular propellers. Any advances in dynamic gear design thus require a clear description of the gross static and dynamic features of these systems. While NMR spectroscopy provides an expansive window for the measurement of rotational isomerism in solution, both high-resolution X-ray crystallography and quantum mechanical calculations can yield reliable and rigorous structural data. These approaches are used in concert in the following study to evaluate the electronic and geometrical

implications of replacing a peripheral phenyl group with varied substituents, both organic and organometallic in nature.

3.2 Results and Discussion

Part 1: Modeling the Dynamic Stereochemistry of Hexaarylbenzenes

The pioneering stereochemical studies of hexaarylbenzenes conducted by Gust et al.[123] consisted initially of a group theoretical permutation treatment to determine all possible modes of rearrangements of the maximally (meta) substituted molecular skeleton. Scheme 3.3 features the idealized transition states for rotational mechanisms corresponding to the 13 identified modes; hexagons represent aryl rings that undergo rotation by π radians during the interconversion in question, whereas rectangles denote rings that remain essentially perpendicular to the plane of the central arene on the NMR timescale.

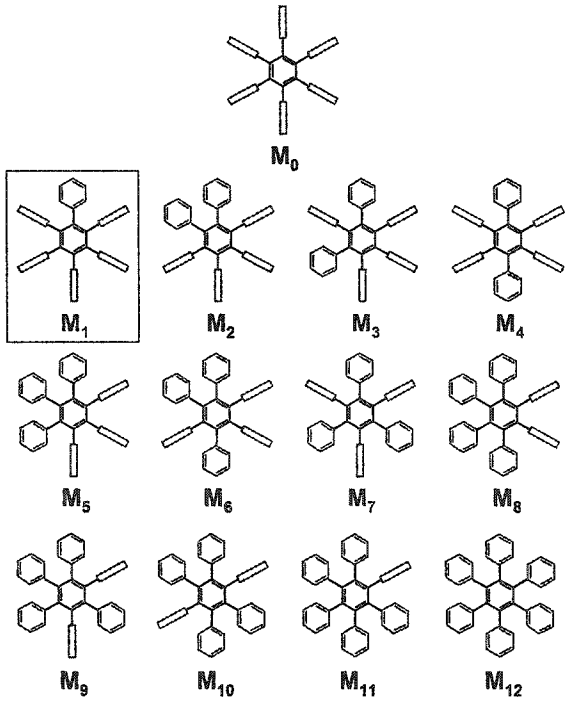

Scheme 3.3: *Idealized transition states for rotational mechanisms corresponding to the 13 rearrangement modes for C_6Ar_6.*

For example, M_0 is the identity rearrangement, for which no net isomerization occurs, whereas M_{12} results in pairwise interchange of all ortho and all meta substituents, and signifies enantiomerization in the absence of secondary chiral features. As already highlighted in Chapter 1, extensive dynamic NMR analyses enabled Gust to distinguish the preferred interconversion pathway(s) for C_6Ar_6 derivatives, which were exclusively consistent with mode M_1 only, the simplest and most intuitively reasonable mechanism. However, depending on the molecular labeling patterns, certain classes of rearrangements are impossible to differentiate by use of DNMR; these and other ambiguities associated with this rotational model can be clarified computationally.

3.2.1 Theoretical Probe of the C_6Ph_6 Torsional PES

Rigid potential energy surface scans, consisting of single point energy evaluations, were conducted for the M_0 to M_1 C_6Ph_6 rearrangement (Scheme 3.4). The peripheral phenyl to central arene torsional angle, ϕ, was increased in 10° increments from 90 to 180°, starting from the B3PW91/6-31G(d,p) optimized geometry. In addition to mapping the least linear motion path associated with such a conformational change, an exhaustive basis set (STO-3G, 3-21G, 3-21G*, 6-31G(d), 6-31G(d,p), cc-pVDZ) and theory (semi-empirical, RHF, HDFT) analysis had the added benefit of establishing an accurate methodology with which to pursue the full analysis of this class of polyaryl compounds, containing over 40 non-hydrogen atoms.

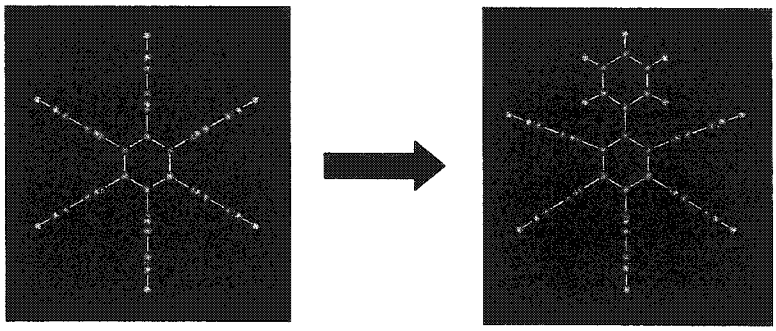

Scheme 3.4: *M_0 (left) to M_1 (right) rearrangement for C_6Ph_6,* ***1.125.***

The two plots in Figure 3.1 depict the change in energy as a function of dihedral angle for semi-empirical, restricted Hartree-Fock[296] and HDFT methods[297] (refer also to tables in Appendix C), the latter of which was represented by Becke's three parameter hybrid exchange functional[298] in combination with the Perdew and Wang 1991 gradient-corrected nonlocal correlation expression, B3PW91.[299;300] Independent of the level of theory, the systematic extension of basis set flexibility is reflected in the total energy for all steps, which decreases considerably from STO-3G[301;302] to 3-21G and 3-21G*,[303;304] and incrementally for the 6-31G(d), 6-31G(d,p)[305;306] and cc-pVDZ[307;308] basis sets. In considering the shape of the curves, the energy differences associated with the minimal STO-3G yielded the largest gradient over the torsional range that was explored. The poor aspects of small split valences are illustrated in the form of the 3-21G and 3-21G* Pople basis sets, particularly for the last data point which either did not reach convergence (RHF) or deviated significantly (HDFT). Since the set of *d* primitives are only added to second row elements for the 3-21G* basis, it yields results identical to the 3-21G basis for this particular test set. In both expanding the size of the orbitals in the double zeta suite and introducing *d* functions on the carbon atoms [6-31G(d)] and additional *p* functions on the hydrogen atoms [6-31G(d,p)], the energetic gains derived from polarization are confirmed. Dunning's correlation consistent polarized basis set (cc-pVDZ), a [3*s*,2*p*,1*d*] contraction of a (9*s*,4*p*,1*d*) primitive set, which is further optimized to recover the correlation energy of the valence electrons, offers only a slight improvement over the other DZP type basis. Interestingly, the combinations of these latter three basis sets with the hybrid B3PW91 functional predict a final decrease in energy for the coplanar M_1 system, reflecting (perhaps) enhanced conjugative effects. At both RHF and HDFT, energy convergence is essentially approached with the two largest DZP basis sets, 6-31G(d,p) and cc-pVDZ. However, in comparing the two levels of theory, and hence the contributions of dynamic correlation, the HDFT computations generally produced lower relative energies. Based on these data, B3PW91/6-31G(d,p) has been selected as a reliable and appropriately balanced (with *both*

p and *d* functions) model chemistry for the complete set of $C_nAr_{n-m}X_m$ molecules. The energetic performance of semi-empirical techniques using the AM1 Hamiltonian (refer to Figure 3.1b), which closely paralleled (with the exception of the last scan step) the higher HDFT methods, should not be overlooked.

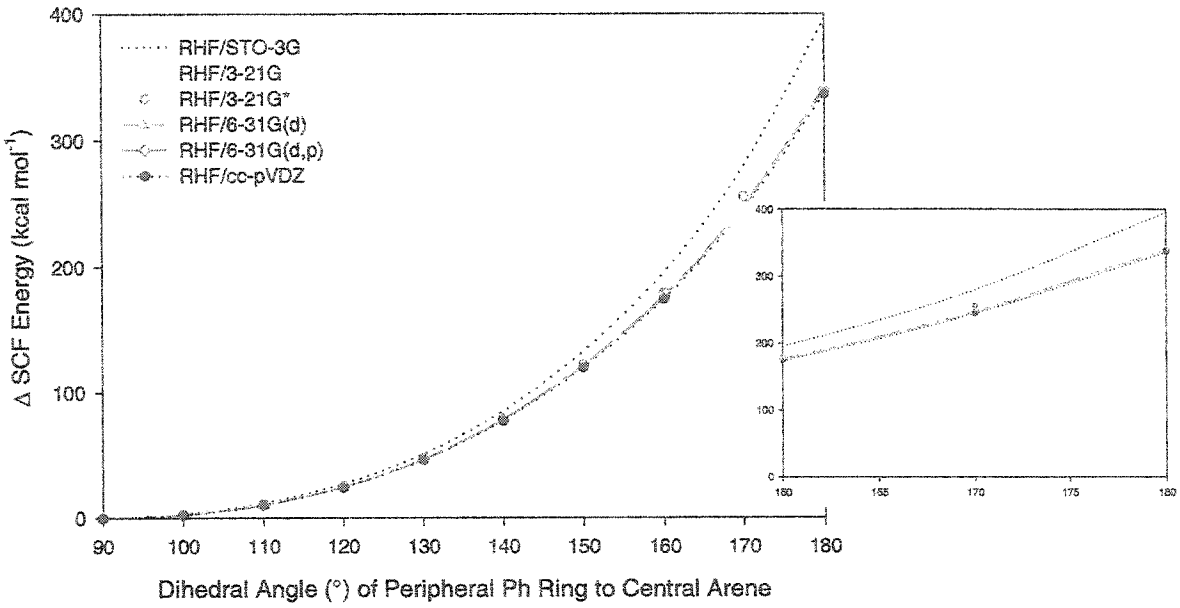

(a)

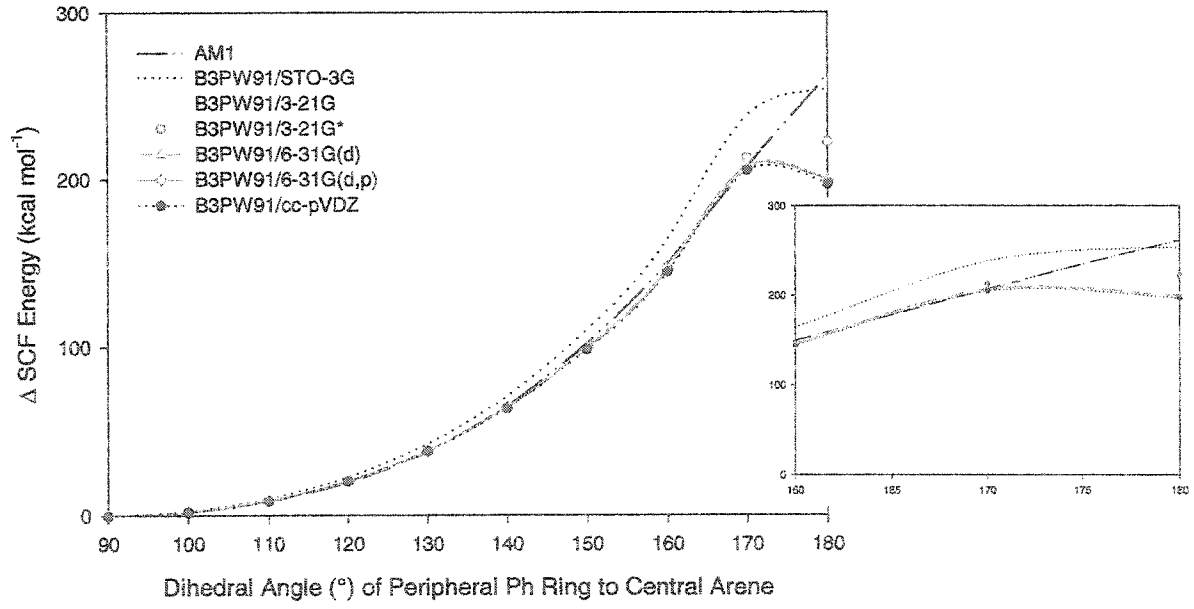

(b)

Figure 3.1: *Rigid potential energy surface of the M_0 to M_1 rearrangement for C_6Ph_6 employing various (a) RHF and (b) semi-empirical or HDFT methods.*

The aforementioned evaluation of theoretical models provided only a qualitative description of the region of the potential energy surface associated with the *one-ring rotation* (or 5-ring flip; see Scheme 1.25 in Chapter One) and served to identify the approximate location of both minimum (D_{6h}-symmetric) and maximum energy (C_{2v}-symmetric) structures. To gain a more quantitative profile of this torsional process, the C_6Ph_6 molecular geometry was subsequently allowed to relax during the PES scan. In stepping over the same rectangular grid on the torsional PES at the semi-empirical (AM1) level, two features are apparent from the corresponding curve (Figure 3.2): (1) the relative energies have improved significantly (cf. E_{max} (M_1) 14.7 (relaxed) to 262 kcal mol^{-1} (restricted)); and (2) the initial energy gradient has diminished. Although the AM1 Hamiltonian was shown to be an energetically adequate method, its ability to predict accurate molecular geometries is not assessable from this constrained optimization.

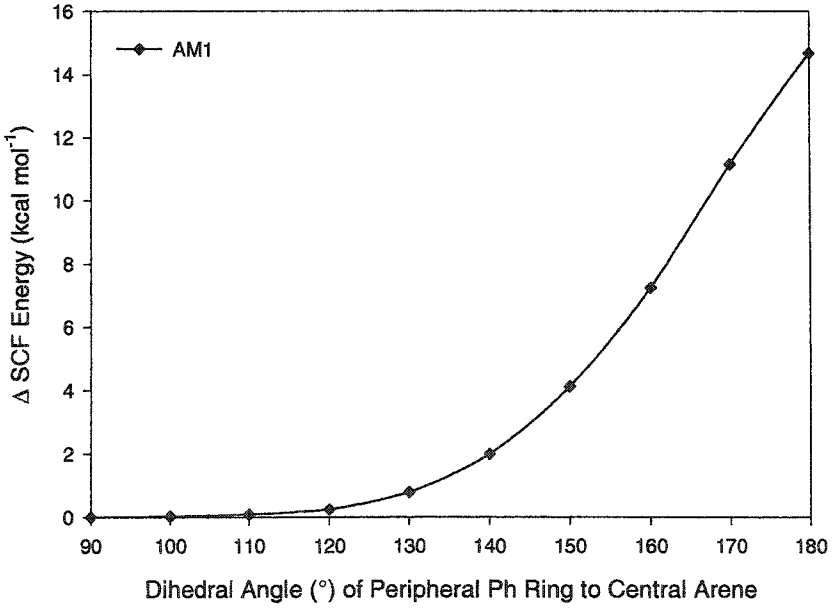

Figure 3.2: *Relaxed torsional potential energy surface (AM1) of the M_0 to M_1 rearrangement for C_6Ph_6,* ***1.125.***

Since each unique pairing of basis set with method represents a different approximation to the Schrödinger equation, one may question, *post facto*, whether the decision to employ B3PW91/6-31G(d,p) was appropriate. In an endeavour to improve their predictive values (with respect to accurate molecular energies and geometries), the calibration of many quantum mechanical methods has typically relied on test sets weighted with small (often non-complex) molecules containing only a limited number of non-hydrogen atoms.[309] The MP2(FC)/6-31G(d) method[310] has been an accepted standard for reliable geometries, but because of its computational demands, it is rarely used for molecules with more than 25 non-hydrogen atoms. Instead, the much more efficient B3LYP/6-31G(d) method seems to have replaced MP2 model chemistries for the routine determination of organic molecular geometries and energies.* Notwithstanding the statistics, the current popularity of this HDFT method has been challenged in a very recent evaluation of modern computational options conducted by Pascal.[309] For an illustrative, albeit judiciously selected, test set of molecules (with corresponding high-quality X-ray structures) containing only hydrogen and first-row elements (6-18 atoms), superior results were attained using the B3PW91/6-31G(d) and the less common B3PW91/cc-pVDZ methods. Interestingly, the accuracy of both these model chemistries exceeded that of conventional B3LYP/6-31G(d) and MP2/6-31G(d) methods for geometry optimizations. Although our comparative analysis (1) omitted the B3LYP functional[311] and (2) was limited in the extent and manner of dynamic correlation treatment by reason of molecular size (i.e. MP2 is much too expensive), Pascal's study offers further endorsement of our model selection, differing only in polarization functionality.

---

* A survey of the Quantum Chemistry Literature DataBase (QCLDB), which contains 51432 records, gave 413 hits for the B3LYP functional compared to only 26 hits for the B3PW91 functional for the years 1978-2000, not distinguishing between inorganic and organic systems. As for American Chemical Society journals in the last four years, the B3LYP functional has been noted in 5418 papers compared to 368 citations for the B3PW91 functional.

3.2.2 *Rotational Isomerism in C_6Ph_6*

Having established a reliable computational standard for large, unconstrained polycyclic aromatic hydrocarbons, our aim was to provide a theoretical verification of rotational isomerism in the nascent C_6Ph_6, **1.125**, and in turn, to map the related energy profile. Based on the topological arguments presented by Gust,[123] the C_1- and D_6-symmetric skeleton structures, as well as the rotamers representing the idealized rearrangement modes M_0, M_1, M_3, M_4 and M_7 (refer to Scheme 3.3) were selected as viable candidates for this conformational analysis. Structure and energy parameters derived from geometry optimizations (GAUSSIAN98) [261] conducted at both HDFT (B3PW91/6-31G(d,p)) and semi-empirical (AM1 Hamiltonian) levels of theory are summarized in Table 3.3.

Table 3.3. Energies (Hartrees and relative kcal mol^{-1}) and Structural Data corresponding to the Principal Stationary Points on the Conformational Hypersurface of Hexaphenylbenzene, **1.125**.

	AM1				B3PW91/6-31G(d,p)			
Mode / Sym	E (a.u.)	ΔE * (kcal mol^{-1})	d (Å)[a]	γ (°)[b]	E (a.u.)	ΔE[a] (kcal mol^{-1})	d (Å)[b]	γ (°)[c]
1.125-C_1	0.316553	1.1 *	1.47	65.9	-1617.9779	0.0 *	1.50	65.9
1.125-D_6	0.314795	0.0 *	1.47	89.76	-1617.9782	0.2 *	1.50	65.43
M_0, D_{6h}	0.314796	0.0		90.0	-1617.9735	3.1		90.0
M_1, C_{2v}	0.342143	17.2			-1617.9476	19.4		
M_3, C_{2v}	0.383641	43.2			-1617.9079	44.3		
M_4, D_{2h}	0.372618	36.3			-1617.9165	38.9		
M_7, D_{3h}	0.452865	86.6			-1617.8460	83.1		

[a] Second derivative analyses have confirmed that these stationary points are either a local minimum* or a transition state**; otherwise, the structures represent higher nth-order saddle points (n negative eigenvalues). [b] The bond distance from central to ipso carbon atoms. [c] The torsional angle between the central and peripheral aryl rings, which is an averaged value in the case of X-ray crystallography.

From among these relevant stationary points, the HDFT-derived D_6 isomer, with central to peripheral ring torsional angles of 65.4°, is only 0.2 kcal mol^{-1} higher in energy than the minimum C_1-symmetric gas phase electron diffraction structure, with torsional angles ranging from 64.3 to 68.8° (*avg.* 65.9°). At a 3.1 kcal mol^{-1} energy difference is the orthogonal M_0-D_{6h} identity rearrangement, which also corresponds to the *idealized* transition state for the correlated

inversion of propeller helicity (6-ring flip). In fact, this value represents the upper limit for a process which is sequential, rather than concerted, in nature, as already established in Chapter Two for C_5Ar_5 and C_5Ar_5X propeller systems. In accordance with experimental results, a consideration of the topomerization pathways characterized by modes M_1, M_3, M_4 and M_7 finds that the one-ring rotation (5-ring flip) is the lowest energy trajectory in this region of the hypersurface.

Typically, rotational isomerism in C_6Ar_6 systems arises when two or more of the peripheral aryl rings bear substituents in either the meta or ortho positions such that at least one of the rings lacks the local C_2-axis coincident with the bond joining it to the central arene. In the latter case, the observed barriers (~17.0 kcal mol^{-1}) indirectly reflect the non-bonded repulsions of ortho hydrogens on adjacent aryl rings. In eliminating *all* substitution effects, the computationally derived (B3PW91/6-31G(d,p)) energy difference of the C_1-symmetric and M_1-C_{2v} rotamers has a value of 19.4 kcal mol^{-1}, without taking into account thermodynamic (zero-point energy) corrections. This is in good agreement with experiment, particularly in the absence of strict saddle point location (see number of imaginary frequencies listed in Appendix C), which would require the torsional relaxation of all aryl groups. The energetic performance of the AM1 Hamiltonian is once again consonant with, and even slightly superior to, the applied HDFT methodology (ΔE_{rot} = 17.2 kcal mol^{-1}).

From the data it is also possible to quantify the two types of buttressing effects displayed by this polyaryl system. Such indirect steric perturbations are induced by a bulky substituent adjacent to an already sterically crowded environment, and typically affect the rotational barriers (and even reactivity or equilibria) by hindering modes of steric relief, such as bond angle widening.[66] The interaction of an orthogonal aryl group flanked by both a perpendicular and planar aryl moiety (**1.125-M_1**) is approximated by 19 kcal mol^{-1}. In **1.125-M_4** such steric interplay is represented twice and auspiciously, is additive in value (cf. 38 kcal mol^{-1}). The second

buttressing type effect is manifest in **1.125-M_3**, wherein an orthogonal aryl group is sandwiched between two coplanar arenes, with an estimated energy of 25 kcal mol^{-1} (by difference). However, the triple sum of this buttressing effect does not coincide with the computed energy of **1.125-M_7** (cf. 75 to 83 kcal mol^{-1}), suggesting that other (non-steric) factors affect this higher-order transition state.

Characterization of the more elaborate features of the conformational PES of hexaarylbenzenes is ongoing. Angular displacements within other parts of the molecule other than the rotating ring(s), as well as the difference in dis/conrotatory (with reference to the helical twist of the propeller) dynamics, particularly under conditions of spatial overcrowding caused by aryl substitution, are microscopic yet essential aspects of the torsional pathway. Regardless, the added dimensions of secondary chirality can invoke conflicting stereochemical interpretations, as in the case of $(C_6Ph_6)Cr(CO)_3$, **1.138**. The DNMR site exchange phenomenon was explained by a sterically unfavourable, limiting C_s-symmetric rotamer in which the chromium-complexed ring is arrested in an orthogonal orientation relative to the central ring (cf. M_0).[231] However, large amplitude libration (of less than 90°) of the η^6-$(C_6H_5)Cr(CO)_3$ fragment about a maximum equivalent to M_1, with rapid reorientation of the unlabelled phenyl groups (cf. M_2, M_3 or M_4, or some combination thereof, as transition states) can also account for the observed spectral properties. In the static regime, motion of the labelled ring is again restricted while the remaining phenyl groups must be presumed to rotate freely. Whether the perpendicular arrangement is energetically accessible (see ambiguous barrier height represented by TS-2 or TS-6 in Scheme 3.5) *cannot* be discerned experimentally without further desymmetrization of the molecular system. Depending on edge or facial differentiation of an arene ring, the energetic and steric components of this conformational argument may vary; an examination of different pentaaryl derivatives may help to resolve these stereochemical distinctions.

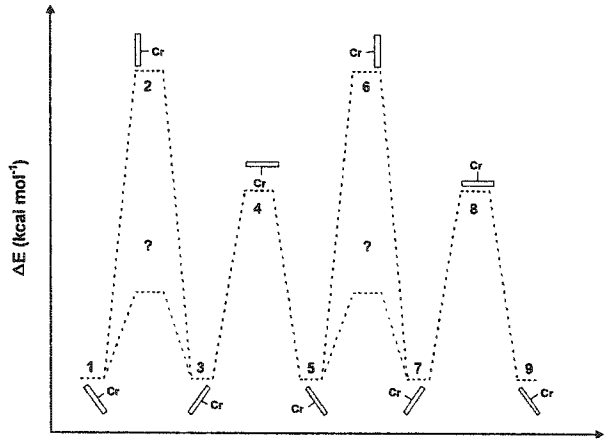

Scheme 3.5: *Are all regions of the torsional PES energetically accessible in C_6Ph_5X systems? The rotation of "X" = η^6-$(C_6H_5)Cr(CO)_3$ relative to the central benzene ring is featured, whereas all other Ph groups are presumed to rotate freely.*

Part 2: Syntheses and Characterization of Novel C_6Ph_5X Platforms

Systematic modification of the molecular periphery of C_6Ar_6 cyclic arrays by the introduction of "X" pendant groups is expected to have static and dynamic stereochemical consequences. The choice of "X" is primarily dependent on appropriately asymmetric and sterically anisotropic achiral and chiral fragments which (a) possess sufficient bulk in advance of metal complexation, but may have the potential to bind to metal moieties, and which (b) include NMR "signatures" for monitoring the internal fluxional processes. Synthetic targets containing a variety of single residues that may augment the non-bonded repulsions between peripheral aryl rotors attached to the benzene core are thus explored.

3.2.3 Ferrocenylpentaphenylbenzene

The incorporation of different sterically demanding organometallic domains in C_6Ar_5X can either be achieved by metalation procedures that precede the construction of the organic core, as in the case of $(C_6Ph_6)Cr(CO)_3$, **1.138**, or by direct linkage of the metal centers to the molecular framework. Employing the latter strategy, the preparation of ferrocenyl-substituted pentaphenylbenzene, C_6Ph_5Fc, **3.19**, by the Diels-Alder cycloaddition of 2,3,4,5-tetraphenylcyclo-2,4-pentadien-1-one, **1.53**, to ferrocenylphenylacetylene, **3.20**, and subsequent decarbonylation of the intermediate bicyclic ketone, was reported by Rausch and Siegel[312] in 1978. We elected to

synthesize **3.19**, for which no structural or dynamic data were available, *via* a complementary Diels-Alder approach involving diphenylacetylene, **3.11**, and the versatile synthon, 3-ferrocenyl-2,4,5-triphenylcyclopentadienone, **1.54** (Scheme 3.6).[313] The mixed benzoin condensation of formylferrocene, **3.21**, and benzaldehyde yields the intermediate acyloin, which is oxidized to the diketone **3.22** with activated manganese dioxide at elevated temperatures in chloroform solution. Treatment of **3.22** with dibenzyl ketone in refluxing ethanolic potassium hydroxide affords the diene as a light blue amorphous solid.[314] Besides six-membered ring systems, this latter methodology allows access to fluorinated analogues and metal complexes of **1.54**, or substituted cycloheptatrienes, as described in Chapters One and Four (vide infra), respectively.

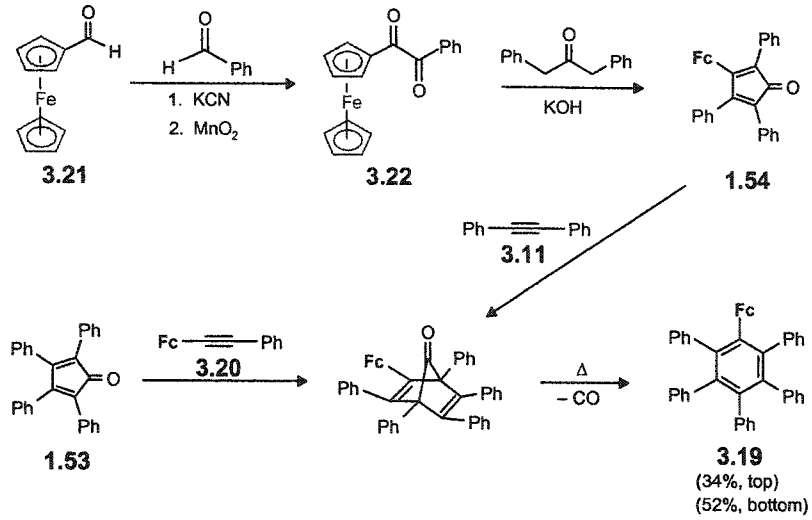

Scheme 3.6: *Synthetic routes to C_6Ph_5Fc,* ***3.19****.*

The X-ray crystal structure of C_6Ph_5Fc, **3.19**, appears as Figure 3.3; the accompanying crystallographic refinement parameters and selected structural data are provided in the tables of Appendix B. Non-bonded repulsions undoubtedly influence the molecular geometry of **3.18**, which does not adopt a regular propeller type conformation. Instead, the peripheral substituents exhibit an incremental progression of twist angles relative to the central ring, marked by values of 51°, 64°, 70°, 81°, 89° and 120°, from C(1) to C(6), respectively. The net effect is to provide a series of rotors each displaced slightly more than its immediately preceding neighbour. These orientations about the

C(sp^2)-C(sp^2) pivot bonds are significantly different from the average 67° phenyl cant in the sixfold symmetric C_6Ph_6, **1.125** (see Figure 3.4b).[222] In replacing a phenyl group with a hydrogen, the helical arrangement is not restored in C_6Ph_4FcH, **3.23**.[315] This differs from the molecular structure of the related 1,1'-(tetraphenyl-*o*-phenylene)ferrocene, **3.24**, wherein the cyclopentadienyl rings are internally constrained at 91° and 95° to the central benzene and the outer phenyl groups adopt interplanar angles of 57°, 65°, 62° and 66°.[316] Although one cannot dismiss the presence of symmetry artefacts or the potential influences of crystal packing forces, it is tempting to postulate that the 'domino' phenomenon in **3.19** is a manifestation of the low energy oscillation process that interconverts helical forms. Indeed, the (intra)molecular configuration of **3.19** is solid-state evidence for the non-synchronous n-ring flip proposed in Chapter Two. Unfortunately, there are too few X-ray crystallographic solutions of C_6Ar_6 and C_6Ar_5X structures to probe the likelihood of this process by application of Structure Correlation theory.[37]

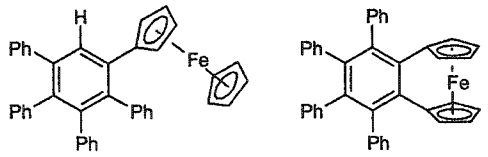

3.23 **3.24**

Scheme 3.7: *Ferrocenyl-substituted polyarylbenzenes **3.23** and **3.24**.*

In this regard, one may question whether there is another conformational option available to **3.19**. Full geometry optimization of a C_1 symmetric starting point using hybrid density functional methods (B3LYP)[311] in combination with the LANL2DZ effective core potential/basis set[317] finds only one potential minimum, corresponding to the experimentally observed conformation. The gas-phase predicted orientations of the peripheral aryl group closely agree with the solid-state values, as seen in Figure 3.5a. Failed attempts to locate a propeller ground state (at least at this level of theory) suggest that the non-helical form is indeed the preferred geometry.

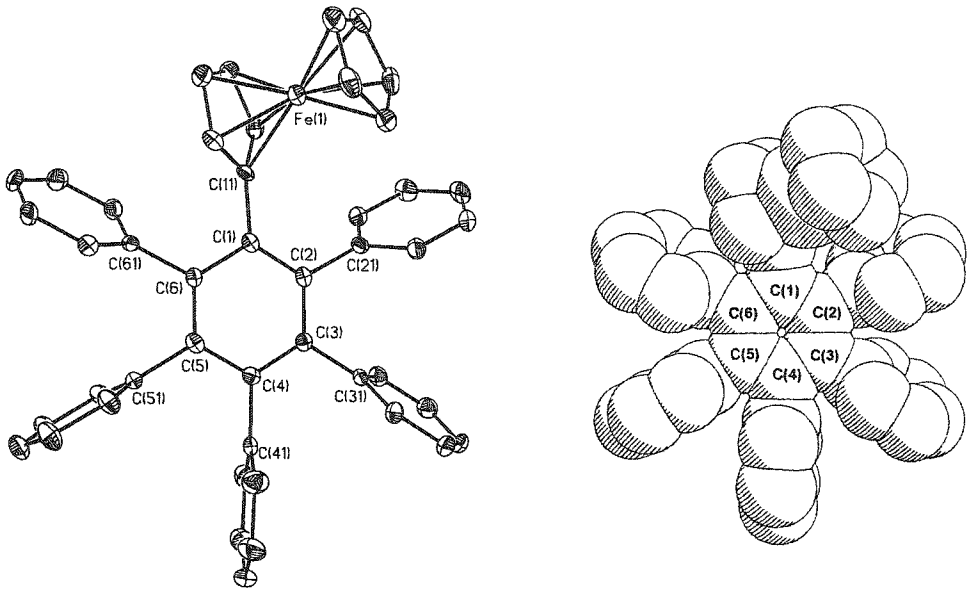

Figure 3.3: *(a) Top view of the molecular structure of C_6Ph_5Fc,* ***3.19****, (30% thermal ellipsoids), with hydrogen atoms omitted for clarity, and (b) its space-filling representation.*

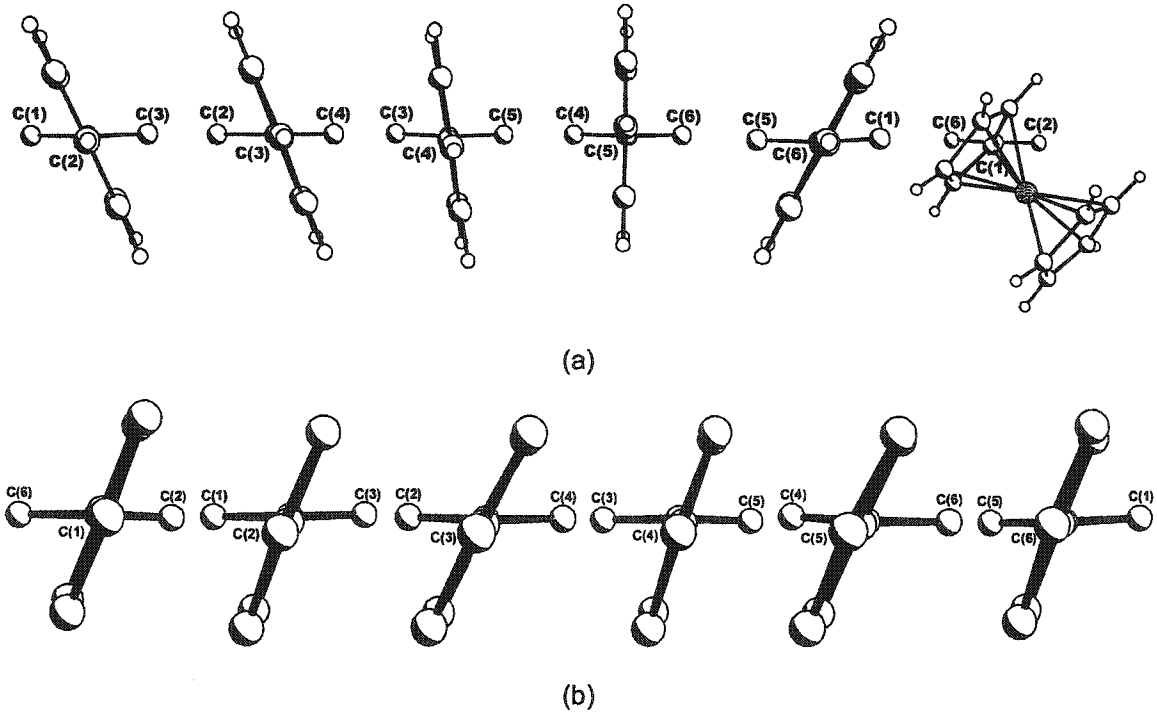

Figure 3.4: *Views along successive peripheral ring – central axes in (a) C_6Ph_5Fc,* ***3.19****, (top) and (b) C_6Ph_6,* ***1.125****, (bottom), depicting the differences in phenyl ring orientations.*

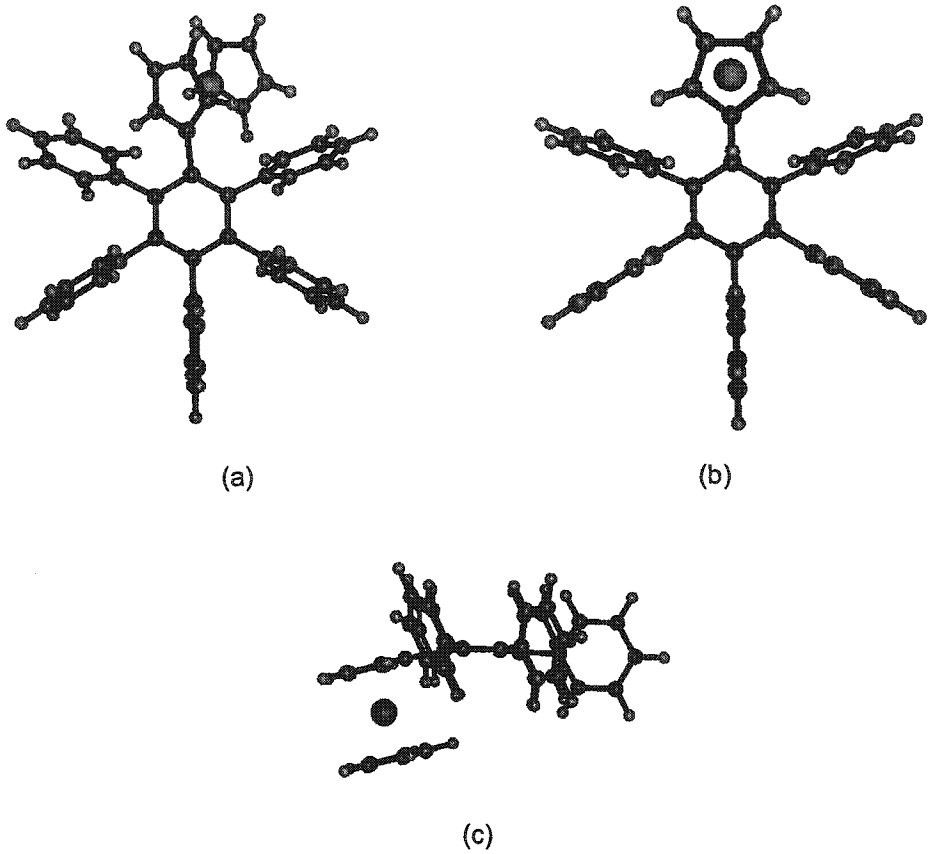

Figure 3.5: *Computed structures (B3LYP/LANL2DZ) of C_6Ph_5Fc, corresponding to a C_1 minimum,* ***3.19****, (a) and C_s transition state,* ***3.19-TS****, as viewed from the top (b) and side (c).*

Perhaps surprisingly, the 500 MHz ^{1}H and 125 MHz ^{13}C data on **3.19** indicate that the interconversion processes previously detailed for $(C_6Ph_6)Cr(CO)_3$, **1.138**, (see Section 1.4.2.2)[231] are fast on the NMR time-scale. Even at the lowest attainable temperature (188 K), the ^{13}C spectrum of the phenyl rings remains essentially unchanged from its appearance at room temperature; apparently, the overall effect of replacing a $(C_6H_5)Cr(CO)_3$ substituent by a ferrocenyl fragment is to lower substantially the barriers to rotational isomerism, thus rendering more difficult the generation of a chiral propeller. In retrospect, the typical cone volume of a $Cr(CO)_3$ moiety (~21 Å^3) is somewhat greater than that of its ferrocenyl counterpart (~17 Å^3), on account of the spatial extension engendered by the carbonyl ligands.* To achieve hindered rotation about the single bond joining the central and

* Ligand cone volumes ($\pi r^2 h/3$) were estimated from the structural data of several organometallic complexes, utilizing the dimensions defined by the ligand base (r) and the centroid of the C_nH_n ring to the centroid of the ligand base (h).

peripheral aryl groups, the steric influence imparted by a fragment, organometallic or otherwise, must be reflected in *both* of the relevant dimensions.

Whereas the 'reaction coordinates' of **3.19** are NMR indistinguishable, the energy and structure of the transition state associated with isomerization of the unlabelled molecule can be verified computationally. Geometry optimization and subsequent frequency analyses (B3LYP/LANL2DZ) have identified one of two possible C_s rotamers as a first order saddle point (Figure 3.5b). The shallow boat conformation of the central arene ring and the out-of-plane bending (~ 15°) of the ferrocenyl (Fc) moiety are apparent in the side view of **3.19-TS** (Figure 3.5c). The other C_s isomer, in which the Fc fragment assumes an orthogonal orientation to the benzene core, does not converge to a chemically meaningful structure. In further support of the torsional potential energy description offered in Section 3.2.2 (see Scheme 3.5), the small calculated ΔE value of 1.7 kcal mol^{-1} is compatible with the experimental observations.

3.2.4 2,3,4,5,6-Pentaphenyltolan and Derivatives

Since it is known that carbon-carbon triple bonds can supply up to six electrons to as many as four metal centers and can assist in cluster reinforcement, the introduction of an alkyne unit (as "X" in C_6Ph_5X) was deemed a fertile route to metal-rendered sterically encumbered propellers. 1-(pentaphenylphenyl)-2-phenylacetylene (2,3,4,5,6-pentaphenyltolan), **3.26**, was originally synthesized by Dilthey et al.[318] in 1935. In heating together (240 - 250 °C under nitrogen) the commercially available reagents, tetraphenylcyclopentadienone, **1.53**, and 1,4-diphenyl-1,3-butadiyne, **3.25**, the loss of carbon monoxide from the Diels-Alder adduct yields $C_6Ph_5C{\equiv}CPh$ directly. A second, albeit sterically very demanding, [4+2] cycloaddition results in decaphenylbiphenyl, **3.27**, as reported by Ogliaruso and Becker[267] in 1965 (Scheme 3.8a). The acute crowding in **3.27** was confirmed by Pascal and co-workers[272] only in 1998, as part of an X-ray crystallographic study of highly congested polyphenyl PAHs. In the solid-state, **3.27** adopts an asymmetric (C_1) geometry in which one of the central benzene rings is distorted into a boat

shape; this is in contrast to the D_2 conformation exhibited by biphenyls that lack the buttressing effects from substituents meta to the central bond. In 2001, the conformational subtleties of these polyphenylene nanostructures were further realized by the X-ray structure solution of 1,3-bis(nonaphenyl-3-biphenylyl)benzene, **3.29**, which was one of two possible isomers isolated from the Diels-Alder reaction of two equivalents of **3.26** with the biscyclopentadienone **3.28** (Scheme 3.8b).[319] Quite remarkably, the degree of steric relief provided by the alkyne moiety in the maximally arylated precursor **3.26** has never been quantified.

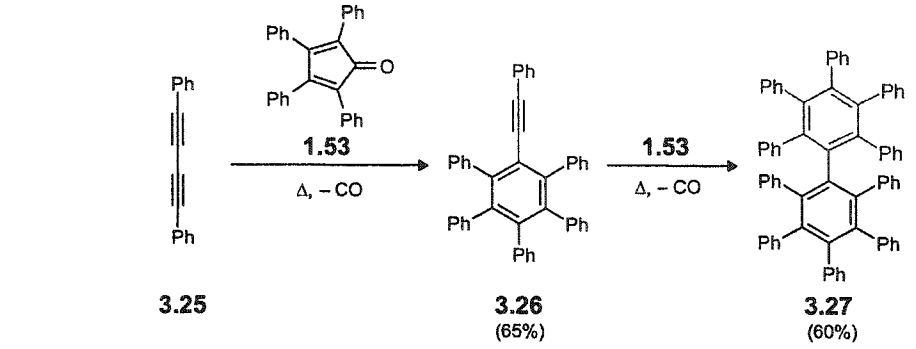

(a)

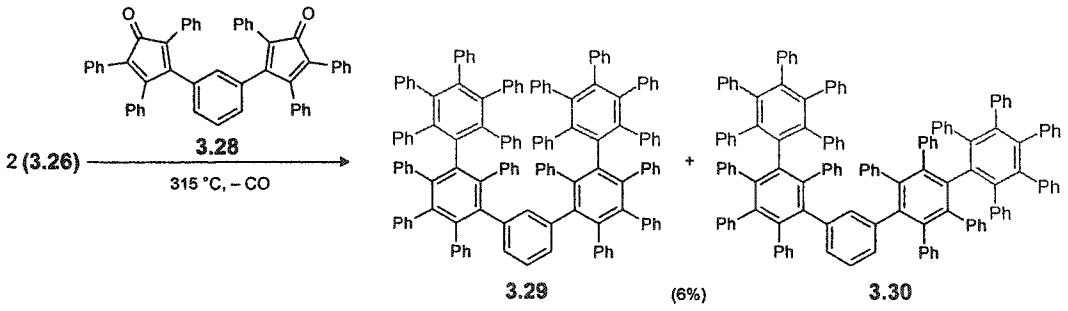

(b)

Scheme 3.8: *Single and double Diels-Alder additions comprising **3.26** as a product and /or a reagent.*

Thus, Dilthey's[318] synthesis of $C_6Ph_5C{\equiv}CPh$, **3.26**, was repeated without difficulty and single, white crystals suitable for an X-ray diffraction experiment were obtained from the acetone:dichloromethane (50:50) solvate. Structure solution and refinement in the triclinic space group *P*(-1) revealed the presence of two independent, and geometrically unique, molecules in the

asymmetric unit, as illustrated in Figures 3.6a and 3.6b. In the approximately C_2-symmetric **3.26a**, rings A and B are essentially coplanar (at 3.4°); the phenyl rotors attached to the former arene consecutively adopt dihedral angles of 68°, 61°, 70°, 56° and 61°, from C(2) to C(6). In the other solid-state C_1 conformer, **3.26b**, ring B is oriented 24° relative to the central plane of A, which is surrounded by a "picket fence" of phenyl groups in a non-propeller arrangement marked by individual torsional angles of 97°, 85°, 61°, 66° and 63° (C(20) to C(60)). These structural features are most likely coupled to the bending deformation of the acetylenic unit, which is characterized by bond angles of 175.6° and 173.2° at C(170) and C(180), respectively. The latter is smaller than the typical values for sp carbons among nonconjugated cyclic alkynes.* For example, average angles of 178° are exhibited in the molecular structure of the related phenyl(pentamethylphenyl)acetylene, prepared by Bosch et. al.[320] via the palladium catalyzed coupling of the corresponding aryl iodide and aryl acetylene. In solution, bond-angle strain typically results in the deshielding of the *sp* carbon atoms in the ^{13}C-NMR spectrum because of rehybridization.[321] This is certainly the case in **3.26,** wherein one of the *sp* carbon signals, at δ 97.0 (cf. other C(sp) at δ 89.6), is shifted to higher frequency relative to the unstrained diphenylacetylene, (cf. δ 89.3 Ph–C≡C–Ph). In the solid state, it is more difficult to distill the effects of intermolecular interactions on the observed geometries. Despite the inherent non-symmetry of the cell, it can be seen from the packing diagram in Figure 3.4 that molecules of **3.26** are ordered in a fashion which closely resembles the 'sandwich-herringbone' morphology exemplified by the fused aromatic hydrocarbons pyrene and perylene.[322]

---

* A search of the Cambridge Crystallographic Database (Version 5.24, Nov. 2002) for non-complexed alkynes of the form C(sp^2)–C(sp)≡C(sp)–C(sp^2) gave 19 structures in which at least one bond angle was smaller than 174.° Of this sample, 12 possessed ortho-functional groups (170.9–173.4°) and the remainder contained either para substituents or heterosubstituted rings (165.5–171.2°).

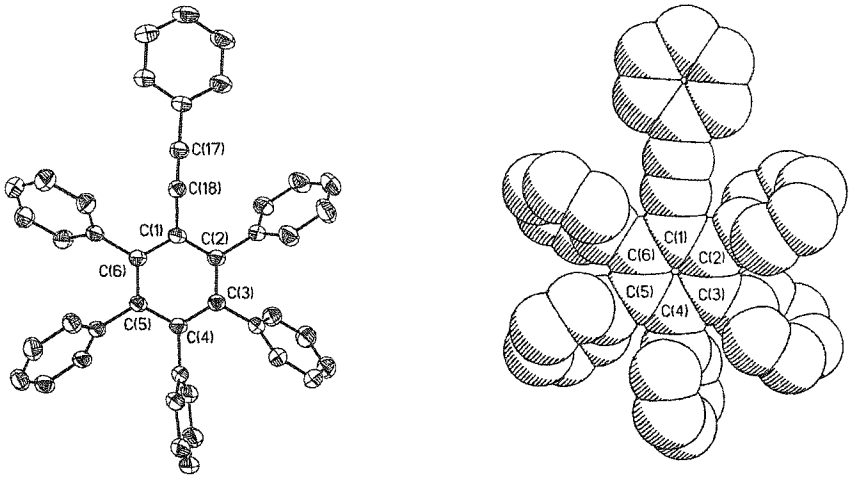

(a)

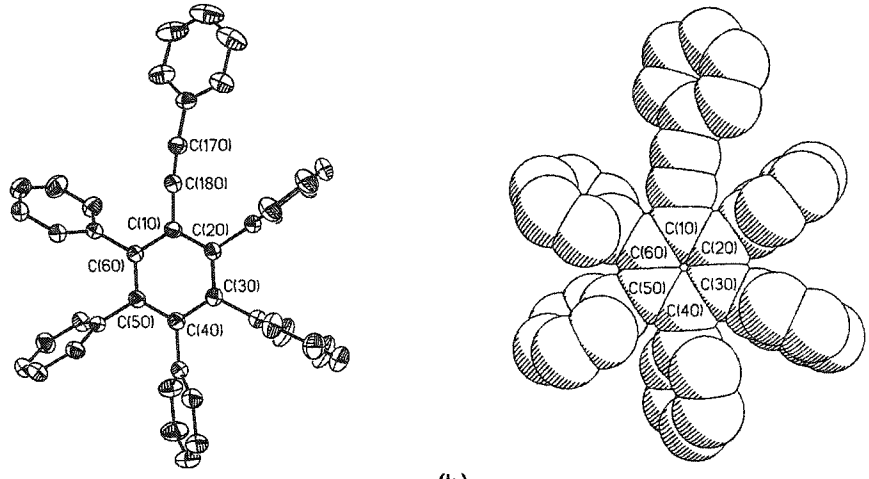

(b)

Figure 3.6: *The molecular structures (30% thermal ellipsoids) and space-filling representations of 1-(pentaphenylphenyl)-2-phenylacetylene,* **3.26a** *(a) and* **3.26b** *(b), determined by X-ray diffraction. Hydrogen atoms have been omitted for clarity.*

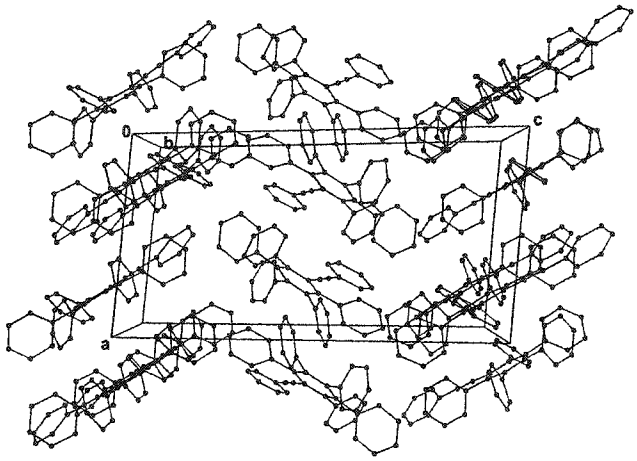

Figure 3.7: *Projection of the crystal structure of* **3.26** *down the crystallographic b axis.*

The degree to which **3.26** is susceptible to deformations as a result of environmental influences is related to the topology of its potential energy hypersurface. Full geometry optimization (B3PW91/6-31G(d,p)) of **3.26** yields an effectively C_2-symmetric conformational minimum, which closely corresponds to **3.26a** in the solid state. The minor steric penalties and/or subtle variations in inter-ring conjugation associated with **3.26b** have yet to be assessed, although one might expect that such effects will translate into a small energy difference for this molecular system. For example, there is a ΔE of 2.25 kcal mol^{-1} between the C_{2v} and C_2 rotamers of **3.26**.

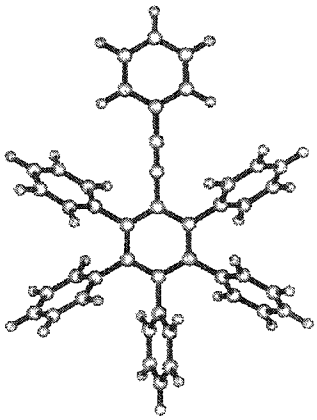

Figure 3.8: *B3PW91/6-31G(d,p) geometry-optimized structure of* ***3.26****.*

Both the alkyne curvature and twist of phenyl group B are not without influence on the adjacent phenyl substituents in the solid state. Rings ortho (C), meta (D) and para (E) to the arylethynyl fragment rotate a difference of +65°, +25° and -9°, respectively, from **3.26a** to **3.26b**, reflecting the progressive transmission of non-bonded repulsions. As noted by Patton, Dirks and Gust,[127] the steric interactions between "X" and the adjacent rings in pentaarylbenzene derivatives, C_6Ph_5X, is mainly a "side-by-side" contact such as is observed between 1,3-axial groups in cyclohexane, rather than the "end-to-end" interplay in biaryls (see **3.27**). If "X" is less sterically demanding than a phenyl substituent, it is reasonable to assume that aryl groups ortho

and meta to X will experience less steric hindrance to rotation than will an aryl group in the para position. The solid-state alterations in **3.26** provide evidence for this effect, as the plane E is most limited in its response to the orientation of the arylethynyl moiety. That these deformations are enhanced in the molecular structure of C_6Ph_5Fc, **3.19**, is not surprising (see Figure 3.3), since the corresponding C-X bond is shortened and the effective size of the ferrocenyl moiety exceeds that of -C≡CPh. It should be re-emphasized, however, that the steric requirements of the former anisotropic "X = Fc" group relative to a phenyl ring in such systems has not been established (vide supra).

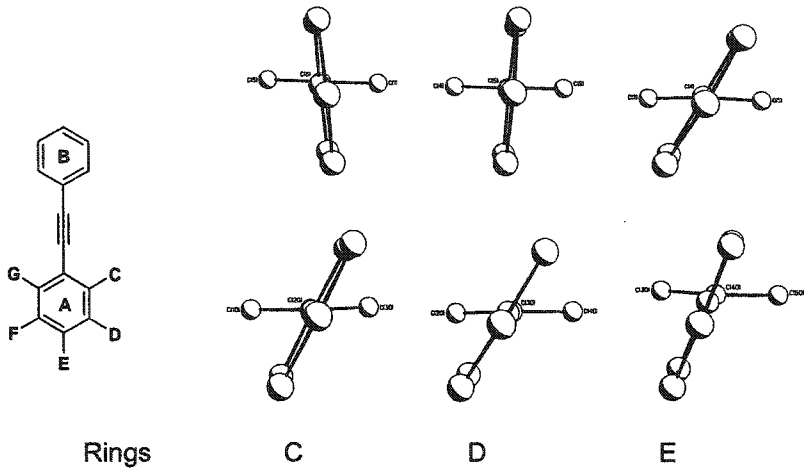

Figure 3.9: *Ortho, meta and para phenyl arrangements, relative to the central arene ring in* ***3.26b*** *(top) and* ***3.26a*** *(bottom).*

In order to verify the mechanistic intimations of these 'static' data, extensive labelling studies would be necessary. Ultimately, it would be highly instructive to correlate the solution-state barriers to ortho, meta and para ring rotation (diastereomerization) in both **3.26** and **3.18** to the well-known $-\Delta G°$ scale implemented by Gust et al.[127] Since the "A value" or $-\Delta G°$ of the same substituent in the axial-equatorial cyclohexane equilibrium was found to obey a linear relationship with $\Delta G^{\ddagger}_{293}$ for rotation of an aryl group in C_6Ph_5X derivatives, it is possible to estimate a torsional

barrier of 15.6 kcal mol^{-1} for this process in **3.26**.* While the trends in activation energies for such conformational interconversions are usually attributed to differences in transition states, ground state effects may influence the barrier heights in **3.18**. Apart from the buttressing changes associated with the torsional motion of peripheral rings, rotation about the acetylenic axis (C(*sp*)–C(sp^2)) in **3.26** is essentially frictionless without additional steric bulk.** The incorporation of organometallic domains into these carbon-rich frameworks may be exploited for such design, as discussed next.

3.2.4.1 Transition Metal Motifs

Following the dissolution of **3.26** and excess dicobalt octacarbonyl in dry THF, the mixture was stirred at room temperature for 48 hours. Upon solvent removal and purification of the dark brown-red residue by column chromatography, the (IR, NMR) spectroscopic data of the collected fractions were inconsistent with the formation of the desired product, **3.31** (Scheme 3.9). Typically, reactions of this type are accompanied by significant structural changes as the alkyne is converted into its $[Co_2(CO)_6RCCR]$ cluster. Crystallographic data for the derivatives $[Co_2(CO)_6C_2Ph_2]$,[323] $[1,4\text{-}\{Co_2(CO)_6C_2H\}_2C_6H_4]$[324] and $[(CO)_6Co_2C_2H(1,4\text{-}C_6H_4)CH_2(1,4\text{-}C_6H_4)HC_2Co_2(CO)_6]$,[324] which have similar, albeit less crowded, environments circa the RCCR fragment, reveal a C_{Ph}-C-C bond angle (α in Scheme 3.9 insert) of ~ 140°. It is not possible to distinguish whether functionalization of the alkyne moiety in **3.31** is prohibited by steric shielding or rendered unstable by the severe strain of the metallatetrahedrane. Certainly, the crowding in **3.31** would be significantly greater than that encountered in the second and third generation polyalkyne arms of the C_6Ar_6 metallostars (**3.17**).[295] In a nearly diametric experiment, Dickson and Michel[325] have observed that the thermal degradation of μ,μ-1,4-diphenylbutadiyne-

---

* This value has been calculated using the linear equation advanced by Gust et al.,[127] $\Delta G^{\ddagger}_{293} = 0.599(-\Delta G^{\ddagger}) + 15.35$, and the $-\Delta G^{\ddagger}$ values (0.18, 0.5) for -C≡CH listed in the table of conformational energies provided by Hirsch.[2]

** The barrier to rotation about the alkynyl–aryl single bond is very low, estimated at less than 1 kcal mol^{-1}.[462]

tetrakis(tricarbonylcobalt) (from **3.25**) in the presence of diphenylacetylene affords **3.26**, amongst other products. Curiously, the melting point (110 °C) and purple colouration of this solid are inconsistent with the literature data for **3.26**.

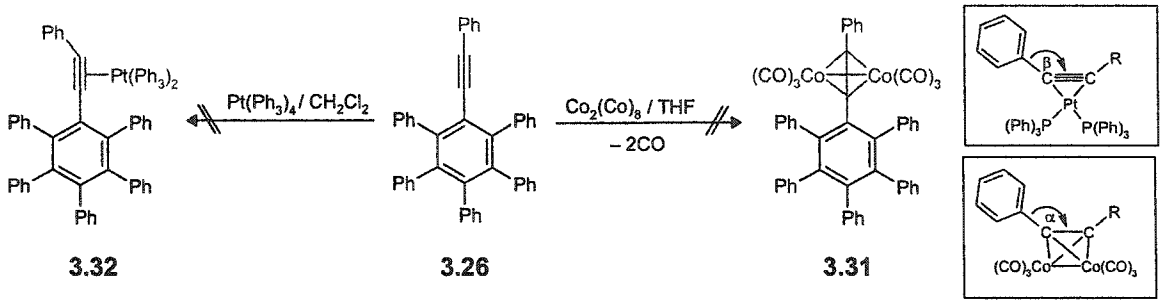

Scheme 3.9: *Attempted transition metal complexations of the alkyne moiety in* ***3.26****.*

Distinct from the cluster motif, the structural modifications afforded by other metallation procedures maintain the triple bond character of the alkyne linkage. Yamazaki et al.[326] have reported the quantitative formation of the diyne mono-complex, $[Pt(\eta^2\text{–}PhC{\equiv}CC{\equiv}CPh)(PPh_3)_2]$, by the reaction of **3.25** with $[Pt(PPh_3)_4$. With the exception of reaction times, which were increased from 10 min. to 24 hours, **3.26** was subjected to the same treatment, albeit to no avail.[327] Neither the IR absorptions nor the NMR signals of the pale yellow solid that was isolated after workup were implicative of a platinum alkyne complex such as **3.32** (Scheme 3.9). Typically, complexes of this type have a square planar geometry with the donor phosphine groups occupying cis coordination sites. As for the conformation of the organic ligand, significant bending about the C(*sp*)–C(sp^2) bonds (angle β in ~ 140° in Scheme 3.9 insert)[326] and reorientation of the peripheral phenyl substituents would be expected in order to accommodate the metal fragment and in particular, the splaying of the triphenylphosphine groups.

One may wonder whether the arylethynyl functionality in **3.26** is accessible to any metal reagent. Recently, Pascal and co-workers[328] addressed this query by refluxing **3.26** with (η^5-cyclopentadienyl)dicarbonylcobalt, first for 72 hours, according to the conditions outlined by Rausch[107] for the preparation of **1.16**, and again for 144 hours on a larger scale. Surprisingly, a

C–C bond cleavage route proved to be more than competitive with the simpler cyclization reactions, yielding 1,2,3,4-tetraphenylfluorene **3.33** as a major product (Scheme 3.10), rather than the anticipated tetraarylcyclobutadiene. The speculative mechanistic scheme that was put forward by the authors invokes an initial activation of **3.26** by cobalt complexation and ortho metallation; these intermediates are significantly less crowded than the cobaltacycle generated in cyclooligomerizations.[329]

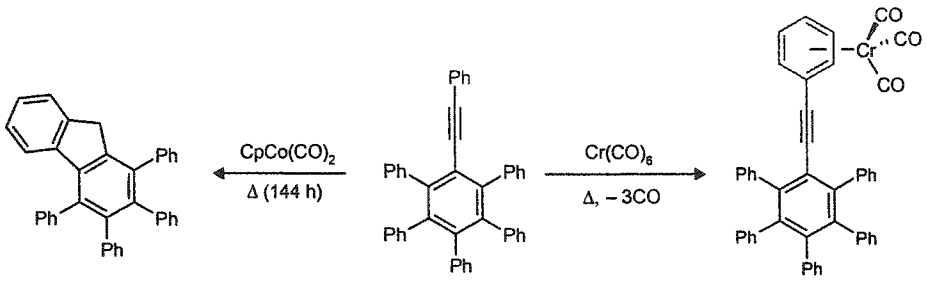

3.33 **3.26** **3.34**

Scheme 3.10: *Additional transition-metal reactions of* ***3.26****.*

As a final consideration, it may be possible to gain advantage over the steric shielding of the pentaphenylphenyl group by the pyrolysis of chromium hexacarbonyl in the presence of **3.26**, but π-complexation of the least hindered aryl ring is unlikely to alter the stereodynamics in this system (see **3.34** in Scheme 3.10). Moreover, this synthetic methodology is recognized to be much less tolerant of alkynylarenes and has been superseded by superior chemo- and regioselective coupling alternatives.[330;331] It is also expected that the thermal instability of most metal fragments would render the complexation of 1,4-diphenyl-1,3-butadiyne prior to the Diels-Alder cycloaddition an unsuitable route, since temperatures in excess of 250 °C are required to drive the final decarbonylation reaction.

3.2.4.2 Organic Reactivity

As a dienophile, the asymmetric alkyne **3.26** is obviously not so sterically shrouded that it resists both single and double Diels-Alder reactions. Metal reactivity aside, halogenation of the carbon-carbon triple bond is another way in which the organic chemistry of **3.26** might be

extended. It was thus encouraging to observe the gradual discolouration of a solution of **3.26** in bromine and carbon tetrachloride; mass spectrometric data of the resulting yellow solid (DEI MS *m/z* 716 $[M]^+$) confirmed that the reaction was indeed a success.

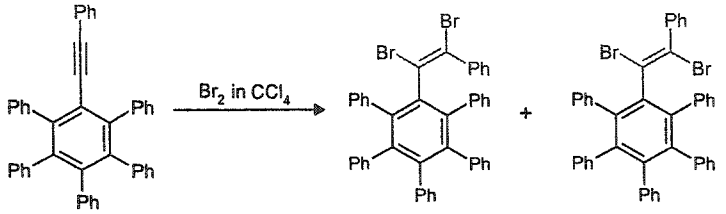

3.26 **cis-3.35** **trans-3.35**

Scheme 3.11: *Bromination of **3.26** may yield either or both the cis, trans stilbene derivatives of **3.35**.*

Distinct from most alkyl derivatives, the electrophilic bromine addition to aryl-substituted substrates proceeds via a vinyl cation intermediate that permits both *syn* and *anti* products, with the proportion of the latter increased in the presence of an excess of bromide ion and bulky substituents.[332] In 1999, Espenson et al.[333] provided definitive solid-state proof for the exclusive formation of the trans isomer of dibromostilbene, **3.36**, from the methyltrioxorhenium-catalyzed stoichiometric reaction of Br^-, H_2O_2 and diphenylacetylene. More recently in 2002, Barnes and Chudek[334] have reported the X-ray crystal structure of *cis*-1,2-dibromostilbene–diphenylethene (2:1). Although details of its original preparation (in *ca.* 1965) were unknown, it was conjectured that spontaneous and partial debromination of the less stable cis isomer, **3.37**, had occurred over the sample's thirty year span of storage in the dark. In the case of **3.35**, the 500 MHz ^{1}H-NMR spectrum consists of a number of overlapping aromatic mutliplets in the region δ 6.6–7.3, corresponding to an isomeric distribution of 18:82. Given the apparent nonstereospecificity of this reaction, it was especially gratifying when single crystals of **3.35** were isolated from a solution of dichloromethane:acetone. The assumption, of course, is that the sample selection was of the major isomer.

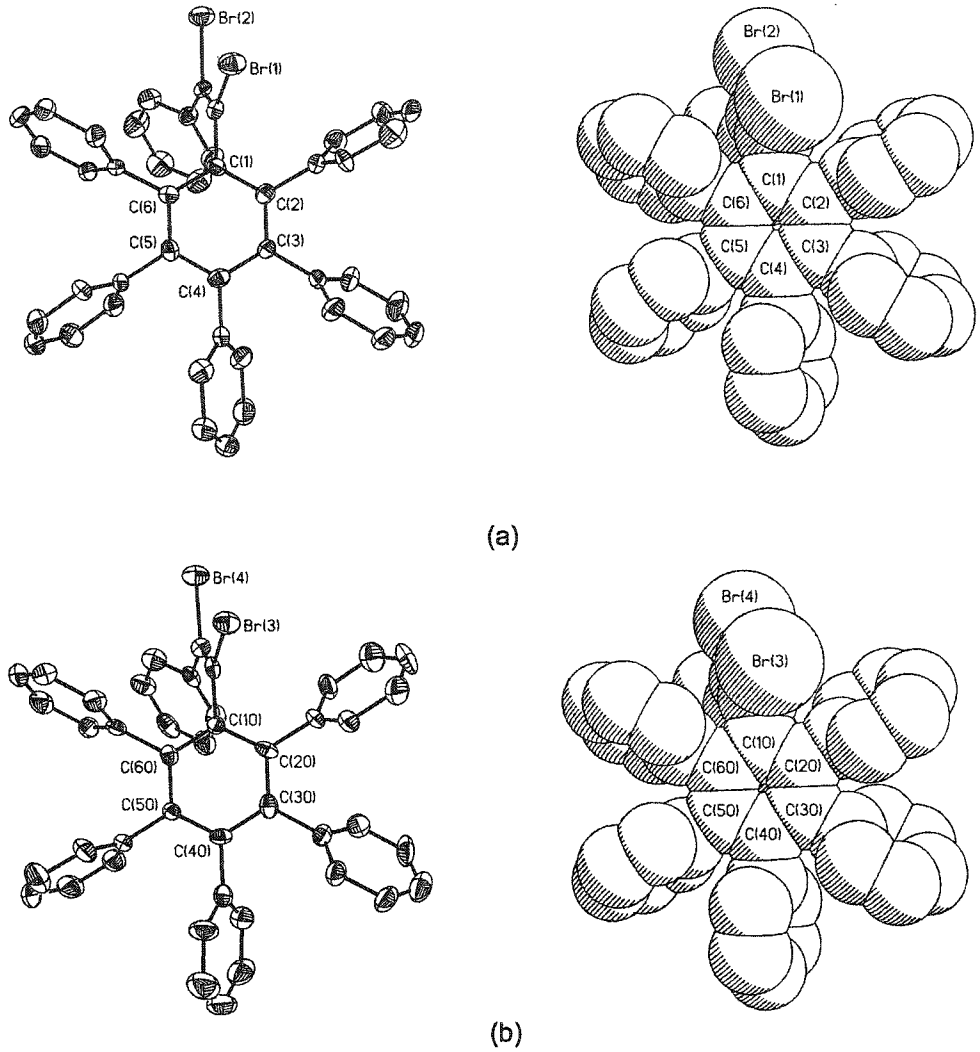

Figure 3.10: *Molecular structures (thermal ellipsoids at the 30% probability level) of the brominated adduct of 1-(pentaphenylphenyl)-2-phenylacetylene,* ***cis-3.35****, depicting an atomic numbering scheme consistent with previous C_6Ar_5X systems. The space-filling representations of* ***3.35a*** *(top) and* ***3.35b*** *(bottom) are also featured. Note that hydrogen atoms have been omitted for the sake of clarity.*

The cis configuration of the crowded dibromostilbene derivative **3.35** was revealed by its X-ray structure determination. Projections of the separate, yet geometrically similar, molecules that appear in the asymmetric unit (space group *P*(-1)) are displayed in Figure 3.10. In both C_1 conformers, the peripheral phenyls adopt a propeller arrangement that is characterized by interplanar angles of 74°, 70°, 70°, 75°, 66° (C(2) to C(6) in **cis-3.35a**) and 62°, 58°, 70°, 77°, 73°

(C(20) to C(60) in **cis-3.35b**). Relative to the diene fragment, the phenyl rings A and B are oriented very differently. A summary of the pertinent torsional values is given in Table 3.4, and may be compared to the only other solid-state data available for a non-cyclized cis-1,2-dibromoethene (**3.37**) and its chloro analogue.

Table 3.4. Torsional angles (°) in *cis*-stilbene derivatives.

Compound (re: vinyl group)	C6-C5-C2-C1[a]	C4-C3-C1-C2[b]	C3-C1-C2-C5[c]
3.35a; 1,2-Br_2-1,2-Ph,C_6Ph_5	135.8	110.3	0.0
3.35b; 1,2-Br_2-1,2-Ph,C_6Ph_5	143.9	107.0	-3.1
3.37; 1,2-Br_2-1,2-Ph_2	144.5	112.9	-4.4
3.38; 1,2-Cl_2-1,2-Ph_2	133.7	111.3	-8.7

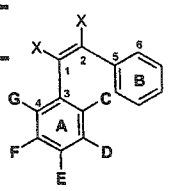

[a] Ring B orientation. [b] Ring A orientation. [c]Diene Planarity.

How does the steric impact of the (1,2-dibromo-2-phenyl)vinyl moiety in **3.35** measure relative to the organometallic fragments in **1.138** and **3.19**? In the dynamic limit, the ^{13}C NMR spectrum should exhibit 22 signals in the aromatic region, of which eight (downfield) correspond to aromatic non-hydrogen bearing sp^2 carbons (4 ipso and 4 central ring of intensities 1:2:2:1 each) and 14 (upfield) to aromatic C-H carbons (4 ortho (2:4:4:2), 4 meta (2:4:4:2), 4 para, (1:2:2:1)) and the two vinyl carbons. That this number of resonances (and relative intensities) is exceeded at ambient temperatures in the 125 MHz ^{13}C regime suggests some form of conformational rigidity. Upon cooling (303 K to 179 K), the various sets of (de)coalescence patterns are somewhat obscured by the accidental superposition of signals. All told, it appears as though **3.35** undergoes more than one distinct class of rotational processes, which cannot be discriminated without appropriate arene labels. Similar to the arguments presented for **1.138** and **3.18**, whether the angular displacement of the vinyl group is unrestricted or limited to a "windshield wiper" motion will not break the symmetry of the molecule unless rotation of one or more of the aryl rings is inhibited.

3.2.5 *(2-Pentaphenylphenyl-1,7,7-trimethyl)norborn-2-ene*

Although they lack metal binding sites, terpenes as an auxiliary chiral and bulky source have not been exploited thus far in propeller design. Spontaneous extrusion of carbon monoxide from the intermediate Diels-Alder cycloadducts should yield a C_6Ph_5X derivative as a pair of diastereomers or as an enantiomeric pair of diastereomers, depending on whether the natural source employed is enantiomerically pure or racemic, respectively.

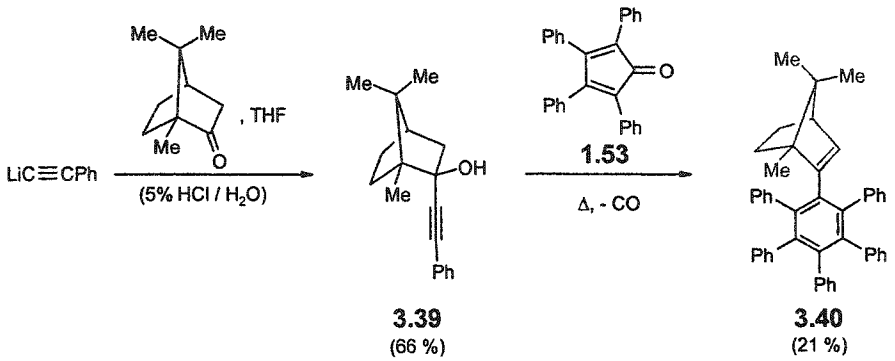

Scheme 3.12: *2-phenylethynylnorborneol,* ***3.39,*** *as a dienophile in a Diels-Alder cycloaddition with the diene* **1.53.**

With this in mind, the addition of lithium phenylacetylide to 1*R*-(+)-camphor gave 2-endo-(phenylethynyl)-2-exo-hydroxybornane, **3.39**, as a white crystalline solid after work-up.[335] The propensity of reagents to approach the ketonic carbon from the less-hindered α face (opposite to the dimethyl bridge) is well established.[336-338] Single crystals of **3.39** suitable for X-ray diffraction were grown from slow evaporation of a deuterated chloroform (NMR) sample. The molecular structure of **3.39** is featured in Figure 3.11a; this is one of two independent, yet closely related, molecules that appear as (O–H···O) hydrogen-bonded dimers in the asymmetric unit of the non-centrosymmetric space group $P2_1$. As featured in Figure 3.11b, atom O2A in molecule 1 acts as an H-bond donor to O2B in molecule 2, yielding H-bond dimensions of 2.05 Å (H···A), 2.872(6) Å (D···A) and 165.9° (D–H···A). This interaction between hydroxy functions of alternately arranged neighbours provides directionality along the b-direction of the crystalline lattice (Figure 3.11). As such, **3.39** represents one-half the constitution of Korkas and co-workers'[339] optically active

inclusion hosts, derived from a central 'axle' and large terpenoid diol groups as terminal 'wheels'. In addition to an infinite H-bond chain, 3-dimensional control is achieved in these latter systems in the presence of a guest molecule; the enantioselective co-crystallization of (*S*)-(+)-phenyloxirane with (anthracene-9,10-diethynyl)(2,2'-bis(2-hydroxybornane)) allows for complementary aromatic stacking in this clathrate. Although there is no evidence of direct π–π associations in **3.39**, the off-parallel alignment of phenyl groups forms an "aromatic sandwich" between interlocking aliphatic regions, as depicted in Figure 3.12.

When the dehydration of **3.39** under mild acidic conditions did not proceed, the isoborneol was allowed to react directly with tetraphenylcyclopentadienone, **1.53**, at > 200 °C for 1.5 hours. After addition of diphenyl ether, precipitation in pentane and several washing cycles, a white solid was obtained in 21% yield; optimization of this value would likely require increased reaction times. Mass spectrometric and NMR (^{1}H, ^{13}C) spectroscopic data suggested that loss of water had occurred concomitantly with cycloaddition and decarbonylation. The constitution of this olefinic product was later confirmed by its X-ray structure determination.

In a continuing trend, the optically pure chiral compound **3.40** crystallizes as two independent molecules in the asymmetric unit of the monoclinic space group *C*2 (Figure 3.9). The C_1-symmetric rotamers, **3.40a** and **3.40b**, each possess a non-propeller arrangement that is characterized by approximate peripheral-to-central interplanar values of 85°, 74°, 67°, 73°, 98° (C(2) to C(6)) and 97°, 79°, 66°, 65°, 78° (C(20) to C(60)), respectively. Unfortunately, the small crystal dimensions (0.2 x 0.14 x 0.02 mm^3) resulted in such weak diffraction that it was not possible to refine the data with use of anisotropic temperature factors (*R*1 = 14%).

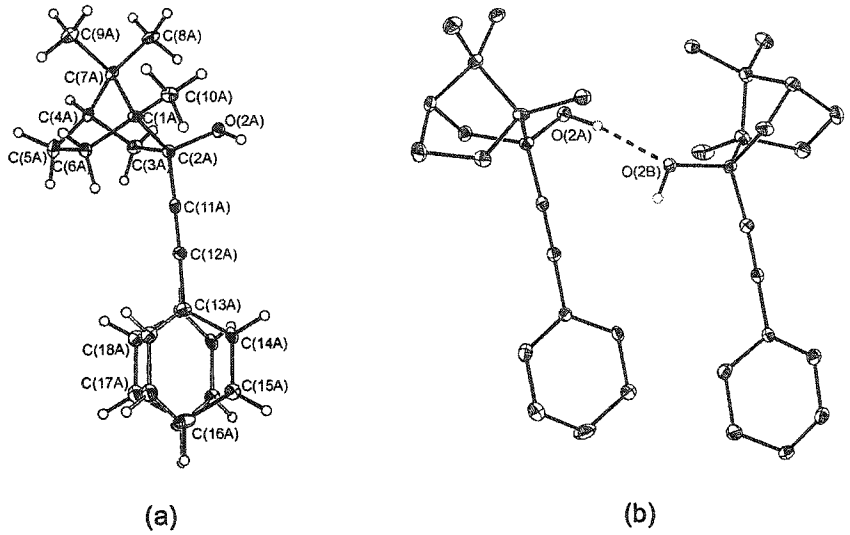

Figure 3.11: *(a) One of the crystallographically determined structures of* ***3.39****, showing the atom-labelling scheme and the two orientations of the disordered phenyl group (50:50 occupancy, wherein atoms C13 – C18 are not marked). (b) Dimeric units in the asymmetric unit are linked by a O2A–H2A···OB' bond. For the sake of clarity, hydrogen atoms have been omitted and only one phenyl conformation is featured. In both diagrams, the displacement ellipsoids are drawn at the 30% probability level.*

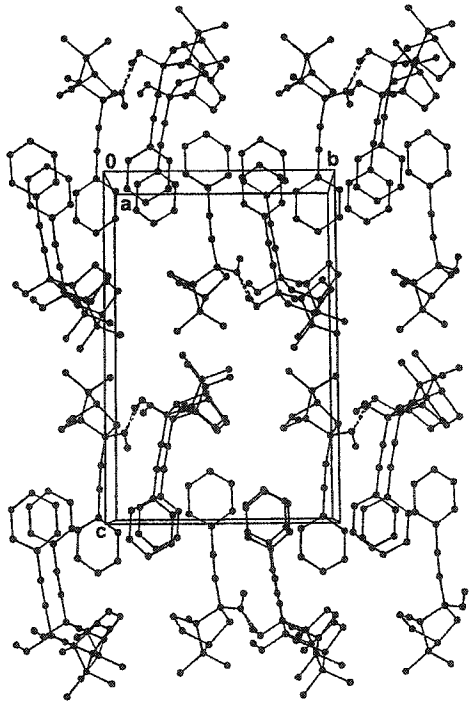

Figure 3.12: *An aliphatic-aromatic-aliphatic bilayer is enforced by a hydrogen bonding (O–H···O) network that extends parallel to the b axis in crystalline* ***3.39****.*

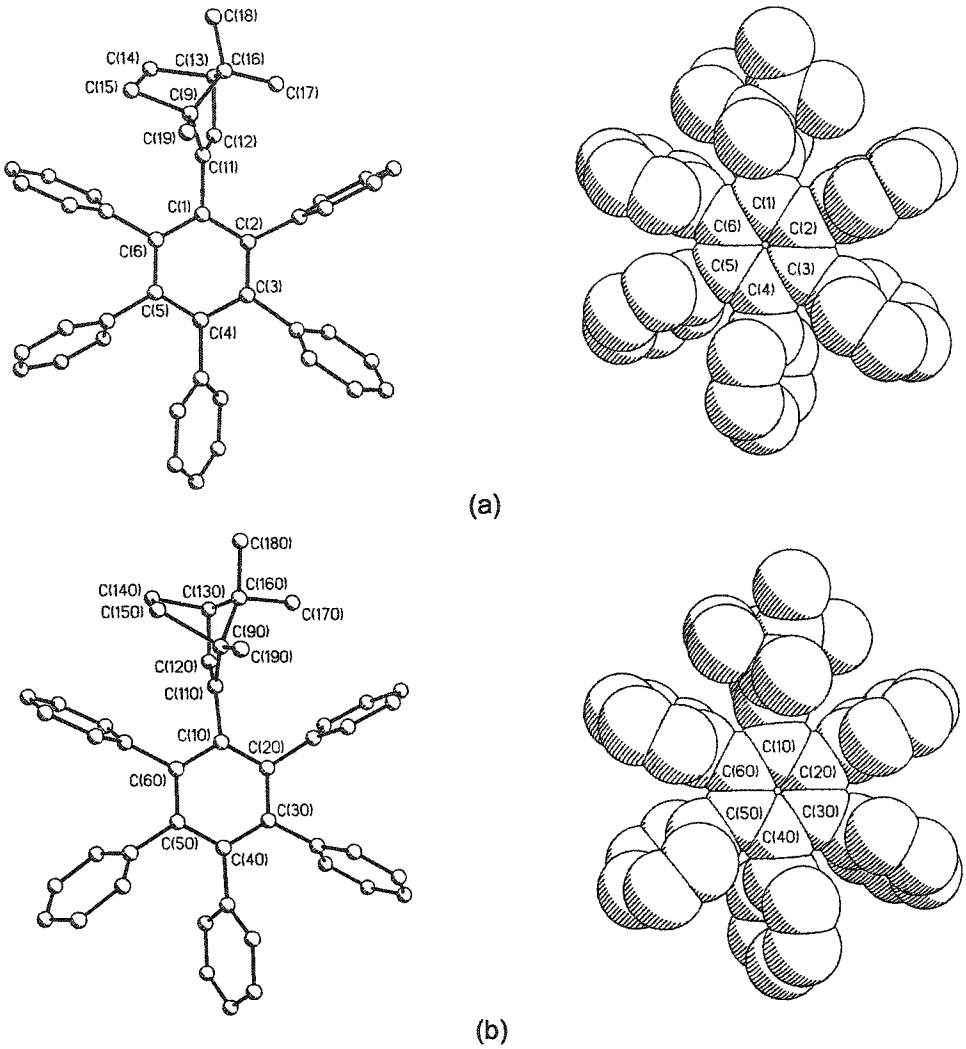

Figure 3.13: *The two independent C_1-symmetric molecular structures of* ***3.40****, depicting the atom connectivity (left) and the space-filling models (right). In both representations, hydrogen atoms have been omitted for clarity. The atom-labelling scheme employed is consistent with previous C_6Ph_5X models.*

Even though **3.40** is of comparatively low molecular weight ($C_{46}H_{40}$), the growth of suitably sized and well-ordered crystals has hampered the crystallographic characterization of many oligophenylenes.[340] In part, this is attributed to the high degrees of rotational freedom associated with these polyaryl frameworks. Regardless, the solid-state deformations induced by the norbornenyl fragment in **3.40** are still valid and assessable; relative to **3.18**, **3.26** and **3.35**, the

ortho phenyl groups in **3.40** exhibit the most heightened conformational response to an "X" substituent.

In solution at ambient temperature, **3.40** adopts a time-averaged C_s-symmetric conformation arising from rapid (presumably uncorrelated) rotation of both the norbornenyl and phenyl groups. We have yet to examine the dynamic NMR behaviour of **3.40**, which should yield a relatively high energy barrier to diasteromeric interconversion (i.e. gear slippage) if the solid-state predictions are correct. To date, the only other sterically encumbered aromatic molecule of this type has been generated by Oguma et al.[341] by means of a catalytic "merry-go-round" multiple alkylation process. The reaction of phenylboronic acid and 2-norbornene in the presence of [RhCl(cod)]$_2$/[1,3-bis(diphenylphosphino)propane] and a base, yields primarily tetra(2-exo-norbornyl)benzene, **3.41**, as shown in Scheme 3.13. Neither X-ray crystallgraphic nor VT-NMR data have been reported for this hydrocarbon substrate.

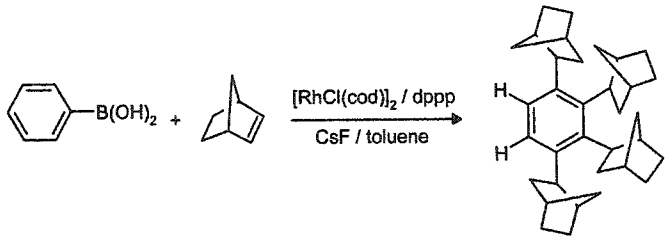

3.41

Scheme 3.13: *Catalytic "merry-go-round" alkylation to give **3.41**.*

3.2.6 Potentially New π-Systems Incorporating the Indenyl Moiety

As an asymmetric "X" substituent in C_6Ph_5X systems, indene (C_9H_8) is highly attractive in that it possesses a planar carbocyclic architecture with both an olefinic unit and acidic protons available for subsequent functionalization. Moreover, its capacity to bind to metals in a variety of modes, most notably through the C_5 and C_6 rings, is well established.[342-346] The pH dependent haptotropic rearrangement between the pentahapto (favoured) and hexahapto isomers of indenyl-ML_n

complexes presents an additional dynamic (mechanical) function that may be controlled by an external input other than temperature (see Scheme 3.14).

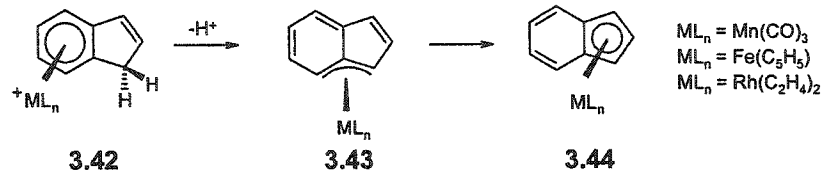

3.42 **3.43** **3.44**

Scheme 3.14: *η^6-to-η^5 haptotropic shift in the indenyl systems,* ***3.42 – 3.44.***

It is equally viable to incorporate the indenyl moiety as part of the Diels-Alder diene or dienophile, and by points of attachment that comprise the different steric profiles of either the C_5 or C_6 ring. Recently, the research groups of Elwahy[282] and Ito[281] have employed the related 10-π–electron aromatic azulene in such an approach (see **3.2** and **3.6**, for example, in Table 3.1). A survey of the synthetic repertoire pertaining to ethynylindenes has revealed the untapped potential of these skeletons, particularly the 3-substituted derivatives (cf. reports of 2-ethynylindene[347;348]). Thus, dehydration of the indanol, prepared from 1-indanone and lithium phenylacetylide, furnished the hitherto unknown 3-(phenylethynyl)indene, **3.45** (72%). Preliminary attempts to react **3.45** with tetracyclone (**1.53**), either neat in a glass ampoule (heated at 220 °C for 28 hours) or in diphenyl ether (reflux, 12 hours), have failed to yield the desired pentaphenylbenzene derivative, **3.46**. In the former instance, **1.53** was reduced to 2,3,4,5-tetraphenylcyclopenta-2-en-1-one,[349] as confirmed by an X-ray diffraction analysis.

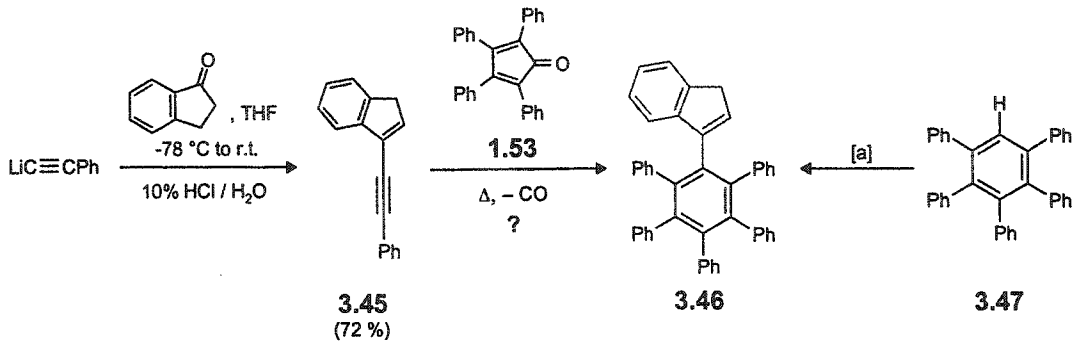

3.45 (72 %) **3.46** **3.47**

Scheme 3.15: *Two possible synthetic pathways to 3-(pentaphenylphenyl)indene,* ***3.46.***
[a] 1. *n*BuLi / THF, -78 °C; 2. 1-indanone, -78 °C to r.t.; 3. 10% HCl

Future efforts to determine the optimal conditions required for this cycloaddition should also help to clarify the thermal stability of **3.45**. To circumvent this concern altogether, it may be possible to access **3.46** via the sterically shrouded pentaphenylbenzenide, **3.47**, as shown in Scheme 3.15. Ultimately, metalation of the parent propeller will give rise to enantiomeric pairs of C_1 symmetric diastereomers, given the stereogenicity engendered by the (η^n-indenyl)ML_n (n = 5 or 6) moiety. As we tend towards maximally differentiated C_6Ar_6 substrates, a logical progression in the construction of novel cyclic π-conjugated systems might utilize 3-(ferrocenylethynyl)indene, **3.48**, previously prepared by Chung and co-workers[350] (Scheme 3.16). The corresponding (cyclopentadienyliron)indene system is extremely air sensitive and decomposes easily, thus reducing the likelihood of obtaining an oligoferrocene by way of the "CpFe transfer method". Nonetheless, the increased 'wingspan' offered by the indenyl group adjacent to the ferrocenyl moiety in **3.49** provides both steric bulk and the necessary 'edge label' to detect restricted rotary motion. Together with the stereochemical arguments advanced for **3.19**, we can expand our conformational model of organometallic cogwheels.

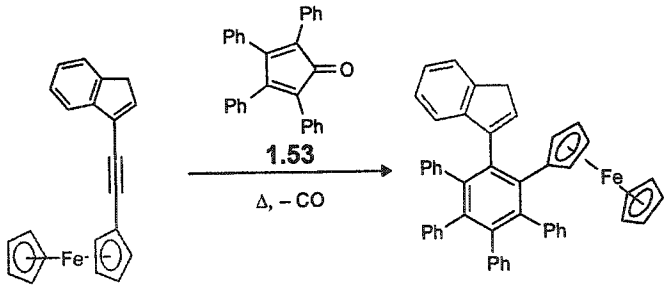

3.48 **3.49**

Scheme 3.16: *The C_6Ar_6 analogue* **3.49** *contains both an indenyl and ferrocenyl fragment.*

3.3 Summary and Outlook

The juxtaposition of experiment and theory continues to challenge the frontiers of complex, yet addressable scientific queries, including those pertaining to isolated molecules possessing high degrees of freedom and a large number of potentially accessible and

energetically similar conformers. As underscored herein, such programs are only as effective as the availability of the former results and the confirmed predictive value of the latter methodologies. To this end, the superior energetic performance of the less common B3PW91/6-31G(d,p) model chemistry has been advanced, but its ability to determine, accurately and consistently, the experimentally observed conformations of polyarylated systems requires further assessment. Pascal et al.[319] have found that a wide range of methods (from MM to HDFT) can be used to locate the appropriate potential minima of the even larger hydrocarbons **3.27** and **3.29**; however, the results did not converge for either molecule and no level of theory and basis set combination correctly predicted the lowest-energy geometries of both molecules. Interestingly, B3PW91/6-31G(d,p) was not among the methods which were tested in this latter study.

Of great import to computational developments is the availability of crystallographic data for molecules of increasing size and functionality, both organic and organometallic in nature. With the aid of a non-rigorous cluster analysis,[37] conformational anomalies associated with different substitution patterns may be distinguished from the dominant structural motif(s). In this regard, the π MOs of benzene may be used to represent the four prototypical structures for C_6Ar_5X systems. As featured in Scheme 3.17, the peripheral rotors may possess the same helicity (as in A), a mid-inverted form (as in B), opposite cants separated by two nodes equivalent to 90° orientations (as in C), or alternating helicity (see D). A search of the Cambridge Structural Database (Version 5.24)[351] reveals that of the 21 C_6Ar_6 / C_6Ar_5X (sub)structures (33 fragments) filed to date, the preferred ground state geometry is indeed that of a molecular propeller (Appendix A). However, 10 examples of type B were found, confirming that other geometrical patterns are accessible in the solid state. This structural variance is realized in the four polyarylbenzenes presented in Part Two of this chapter.

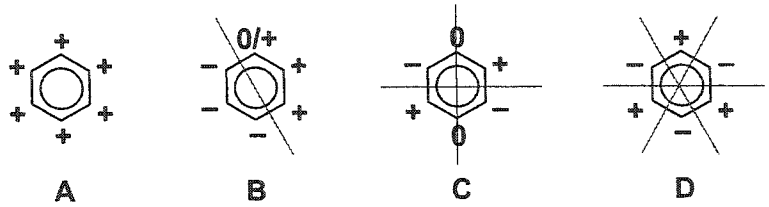

Scheme 3.17: *Viable structural models for C_6Ar_6 and C_6Ar_5X systems, where + and - refers to the cant of the aryl groups, may be considered for a non-rigorous cluster analysis.*

On a dynamic level, it is difficult to measure the steric and electronic impact of different pendant groups in C_6Ph_5X without further desymmetrization of the molecular frame. There are a number of directions that should be pursued, from the intriguing stereochemical profile of ferrocene, to the metal complexing abilities of alkynes, the polyhedral form of terpenes and the unique chemistry of the indenyl ligand. Inasmuch as our design potential is not necessarily limited by the synthetic concept, methods comprising alkyne coupling[352] or metathesis,[353] the cyclotrimerization of symmetric acetylenes[169] and the generation of linked cyclopentadienones,[266] have yet to be applied in this context. Ultimately, structural and mechanistic studies involving more highly substituted C_6R_6 (R = alkyl, aryl, organometallic) derivatives should clarify any subtle isomerization phenomena, such as that portrayed in Scheme 3.5, and thus aid in establishing the features necessary for 'freezing' internal rotation.

CHAPTER FOUR

Persubstituted Cycloheptatrienyls: C_nAr_n where n = 7

"In fact it happens also in chemistry as in architecture that 'beautiful' edifices, that is, symmetrical and simple, are also the most sturdy: in short, the same thing happens with molecules as with the cupolas of cathedrals or the arches of bridges."
(P. Levi, Il Sistema Periodico, Einaudi, Torino, 1975)

4.1 Preface

Molecules possessing both closed circuits of mobile electrons and positive charge(s) present unique electronic and structural vantages to numerous research domains. Since the 1931 prediction by Hückel[354] and 1954 preparation by Doering and Knox,[355] various advances in the chemistry of the cycloheptatrienyl cation **1.141** and its derivatives have been reviewed by Vol'pin (1960),[356] Kolomnikova and Parnes (1967),[357] Pietra (1973)[242], Deganello (1979)[358] and Green and Ng (1995).[243] Typically, such properties are attributed to the π-electrons whereas the σ-framework serves to control the shape of the aromatic system. However, functionalization may allow for both inductive effects and σ-π conjugation, the results of which are reflected by the thermodynamic stability, and hence pK_R+ value, of the carbocycle.[359]

To assess the stabilizing potential of a given alkyl or aryl substituent it is necessary to consider the conjugation energies of *both* the covalent tropilidene system and the corresponding cation.[357] It has been established that the acidity of the tropylium ions increase and decrease respectively in the presence of more powerful electron-acceptor and electron-donor groups linked by single σ-bonds, whereas the reverse relationship is maintained upon the introduction of condensed rings. These trends in pK_R+ values, and subtle variations thereof, are exemplified in Table 4.1.

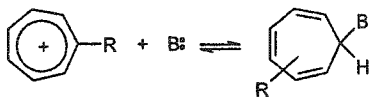

Table 4.1. Empirical stability trends (pK_R^+ values) exhibited by selected polysubstituted $C_7R_{7-m}H_m$ (where $7 \leq m \geq 0$, R = alkyl, aryl) derivatives.

Tropylium Derivative	pK_R^+	Solvent	Ref.
1.141, $C_7H_7^+$	4.75	H_2O	355
	4.01	50% MeCN:H_2O	360
4.1, $C_7H_6(C{\equiv}CPh)$	2.40	50% MeCN:H_2O	364
4.2, $C_7H_6Ph^+$	3.87	50% MeCN:H_2O	360
4.3, 1,2,3,4-$C_7H_3Ph_4^+$	0.13[a]	MeOH:H_2SO_4	361
4.4, $C_7HPh_6^+$	-1.11[a]	MeOH:H_2SO_4	361
1.139, $C_7Ph_7^+$	-0.54[a]	MeOH:H_2SO_4	361
4.5, $C_7HMe_6^+$	6.60	50% MeCN:H_2O	365
1.140, $C_7Me_7^+$	4.86	50% MeCN:H_2O	365
4.6, 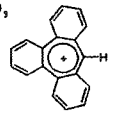	-7.4	50% MeCN:H_2O	366
4.7, 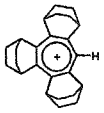	13.0	50% MeCN:H_2O	363
4.8, 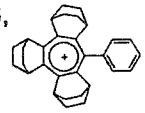	12.0	50% MeCN:H_2O	241
4.9, 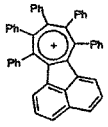	n.a.		362
4.10, $C_7H_7Cr(CO)_3$	6.30	H_2O	357
4.11, $C_7H_7Fe(CO)_3$	4.50	H_2O	357

[a] values adjusted to the water scale.

Thus, the electron-donor methyl moiety enhances the stability of the tropylium ion, in contrast to the triple bond, which acts as a strong electron-acceptor substituent. Despite its frequently cited electronic duality, phenyl group destabilization in relation to **1.141** is rationalized on the basis of decreased π-conjugation (a negative inductive effect) resulting from its non-coplanar arrangement with the central ring.[232;360] The effects, although marked, are not necessarily additive;[361] multiple substitution may invoke competing steric factors, as demonstrated for both the perphenylated and permethylated ions, **1.139** and **1.140**, respectively

(cf. the corresponding hexasubstituted compounds). Unfortunately, there are no thermodynamic data available for the pentaphenyl derivative of the cyclohepta(a)acenaphthylene cation, **4.9**, with an unique ring fusion that allows for extensive charge delocalization.[362] To date, the highest thermodynamic stability has been achieved in the case of **4.7**, whereby maximum annelation with bicyclo[2.2.2]octene units has allowed for steric and electronic design to be implemented synergistically.[363]

4.1.1 Precursors to Persubstituted Tropylium Ions

4.1.1.1 Synthetic Entries and Dynamic Properties

Whereas the trends in thermodynamic stability relate to reactivity, the aromaticity of tropylium ions is manifested in their ease of formation. Excluding other less common routes, synthetic entries to (un)substituted cycloheptatrienyl salts typically comprise hydride abstraction from, or oxidation of, the respective cycloheptatrienes by a variety of reagents.[242;357] Access to the tropilidene species themselves has been made feasible by either [4+2] Diels-Alder cycloaddition or ring-expansion reactions. Construction of the only known peralkyl platform ($C_7Me_7^+$, **1.140**)[233;367] and its corresponding chlorocarbon ($C_7Cl_7^+$, **4.12**)[368] have relied on this latter method, while the utility of the former concept has been established for maximally arylated precursors.

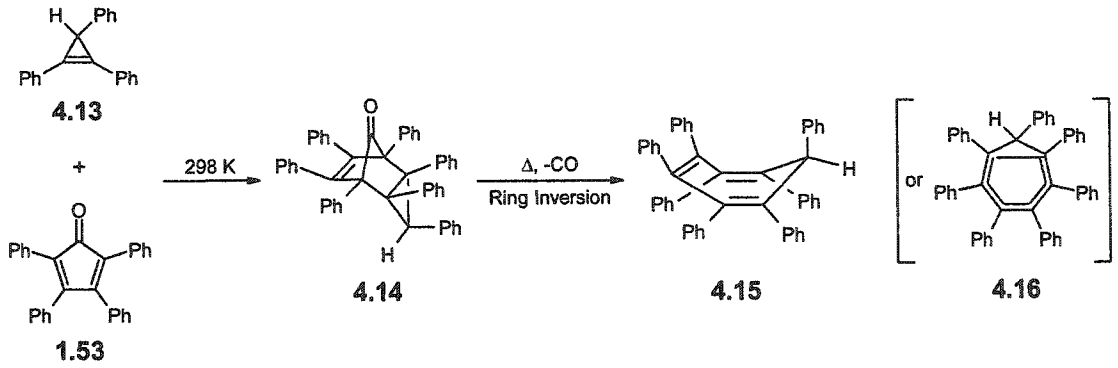

Scheme 4.1: *Under the appropriate in situ conditions, an equimolar reaction of diene **1.53** and dienophile **4.13** yields the cycloheptatriene **4.15** directly.*

Heptaphenylcycloheptatriene, C_7Ph_7H **4.15**, originally synthesized by Battiste in 1961,[369] was structurally characterized only in 1995 by Chao, Gupta and co-workers of our research laboratory,[370] as was its precursor, the tricyclic Diels-Alder adduct (**4.14**) of 2,3,4,5-tetraphenylcyclo-2,4-pentadien-1-one **1.53** and 1,2,3-triphenylcyclopropene **4.13** (Scheme 4.1). As a dienophile **4.13** has proven to be considerably more effective than *trans*-stilbene or tolane and roughly comparable to styrene in its Diels-Alder reactivity with **1.53**.[369] The definitive bond length alternation in the central ring of the perphenylated tropilidene refutes the earlier claims[369] that **4.15** might possess a structure commensurate with **4.16**, which allows for the 1,6-π interaction first conjectured by Doering.[371] The later syntheses of two novel classes of hydrocarbons, the covalent derivatives of the cyclohepta(a)acenaphthylene cation **4.9** (Table 4.1) and a series of bis(heptaphenylcycloheptatrienes) **4.17** with phenyl, diphenyl, diphenylmethane and diphenylether as linking groups, attest to the versatility and steric scope of the Diels-Alder approach.[362;372]

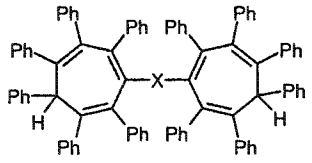

4.17

NMR studies of di-*p*-tolylpentaphenylcycloheptatriene, **4.18**, have corroborated the intermediacy of a boat isomer in which the phenyl substituent at the sp^3 position occupies the sterically hindered pseudo-equatorial site (as it does in the ketonic precursor **4.14**) prior to a conformational ring inversion that reorients it pseudo-axially, impeding further (symmetry-allowed) [1,5]-suprafacial sigmatropic hydrogen shifts.[370] The energy barriers associated with the former process are quite low for the unsubstituted tropilidene (est. 6 kcal mol^{-1})[373;374] and its tris(bicyclo[2.2.2]octeno) analogue (8.5 kcal mol^{-1}),[375] but exceed 20 kcal mol^{-1} for the 1,2,3,4,5,6-hexamethyl,[375] 2,5-dimethyl-1,3,4,6,7-pentaphenyl[370] and tribenzo[376] derivatives. Destabilization of the planar transition state for the boat-to-boat flip is ascribed to non-bonded interactions and angle

strain,[375] two factors which are undoubtedly augmented in the persubstituted systems, with equilibrium rate constants reflecting a preference for exo (relative to the unique hydrogen) isomers. Regardless, the finite lifetime of the endo conformation allows for a final isomeric product distribution that can be correlated with the differing steric environments of the triolefin periphery, as exemplified by **4.18** (4 isomers) and $C_7Ph_5Me_2H$, **4.19** (1 isomer). In the case of the parent cycloheptatriene **4.15**, Harvey and Ogliaruso[372] have provided spectral and melting point evidence which suggests that [1,5]-transannular phenyl rearrangements can also occur under thermal conditions. Similar metallotropic migrations, usually affiliated with cyclopentadienyl and indenyl compounds,[377] have been observed in cycloheptatrienylmetal complexes (vide infra).[243]

Torsional isomerism (C_{sp2}-C_{sp2}) is yet another dynamic process potentially revealed in both aryl-substituted cycloheptatrienes and cycloheptatrienyl systems. Despite the reduced steric interactions in the exo conformer **4.15**, the rings alpha, beta and gamma to the methine hydrogen, with solid-state dihedral angles of ~ 50°, 63 ± 4°, and 92°/87°, respectively, are sufficiently encumbered so as to engender slowed rotation in solution at low temperatures. An evaluation of the ^1H and ^{13}C VT-NMR spectra yielded torsional barriers of 11.0 ± 0.5 kcal mol^{-1} (beta ring), ~ 9.1 kcal mol^{-1} (gamma ring) and ≈ 9 kcal mol^{-1} (alpha ring), thereby excluding a correlated interconversion pathway.[370]

4.1.1.2 Transition Metal π-Complexes

The transition metal chemistry of simple $C_7H_{8-m}R_m$ (and derivatives thereof, including tropone, heptafulvene, azulene, heptalene and sesquifulvalene) and $C_7H_{7-m}R_m$ ligands (where m = 0 - 4) has been developed significantly since the first π-complexes were prepared in 1958.[378;379] While lower hapticity tends to dominate in compounds of the late transition metals, the early (groups IV to VI) metals coordinate in an η^6-triene and η^7-C_7H_7 mode that after much dispute, has been described as the interaction between three metal electrons and a trivalent, 7-electron donor (as opposed to 6-electron ligand with a +1 formal charge).[243] Convenient preparations of η^6-

cycloheptatriene and η^7-cycloheptatrienylmetal complexes employ the olefin and either metal carbonyls, metal atoms or metal chlorides as starting materials. Examples of mononuclear and dinuclear systems, $[\eta^7\text{-}(1,2,4,6\text{-}Me_4C_7H_3)Mo(CO)_3]^+[BF_4]^-$ **4.23** and $\mu\text{-}(1\text{–}3\text{-}\eta\text{:}4\text{–}7\text{-}\eta\text{-}C_7H_7)Fe(CO)_3Rh(CO)_2$[Fe-Rh] **4.25**, respectively, are featured in Scheme 4.2.[380;381] Prior to hydride abstraction, the formation of η^6-isomers **4.21** and **4.22** may be ascribed to sequential 1,5-shifts of the 7-*endo*-hydrogen in **4.20**. As a rule, the reaction of tropylium cation with a substitution-labile metal species does not yield the $(\eta^7\text{-}C_7H_7)ML_n$ species.[243]

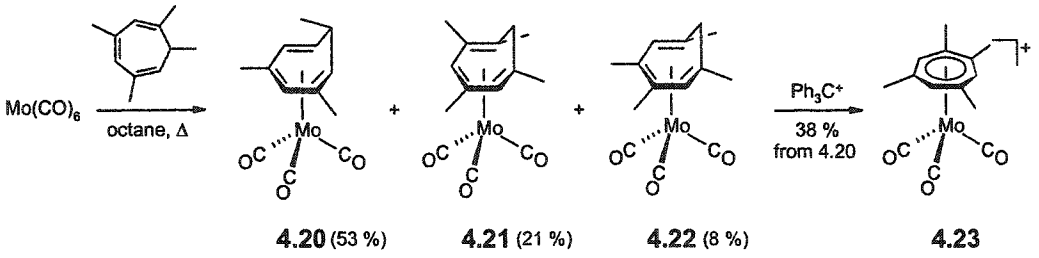

(a)

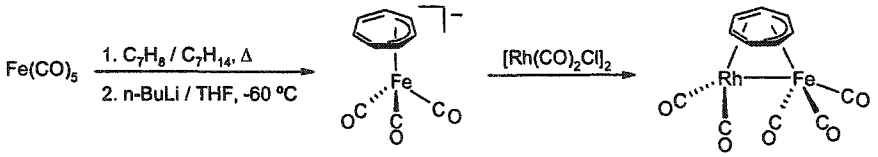

(b)

Scheme 4.2: *Synthetic examples of cycloheptatriene and –enyl complexes comprising (a) early and (b) late transition metals.*

In 1995, Chao et al.[370] attempted to extend these direct metalation procedures to perarylated ligands. The reaction of **4.15** (or **4.19**) with metal carbonyls, notably $Cr(CO)_6$, $Mo(CO)_6$ and $W(CO)_3(CH_3CN)_3$, furnished a definitive, stable product in the first case only (Scheme 4.3). As opposed to η^6-coordination to the cycloheptatriene, the metal moiety in **4.26** and **4.27** was found to attach to the unique sp^3-based aryl ring (cf. $C_6Ph_6)Cr(CO)_3$, **1.138**), either directly because of steric accessibility or indirectly as a result of hydrogen migration after ligation. Unfortunately, a comparison

of the fluxional properties of **4.15** and **4.26** (or **4.27**) was not possible owing to low yields. In a variation of these synthetic designs, efforts where directed toward the complexation of a metal tricarbonyl fragment to the open face of the tricyclic ketone **4.14**, in the expectation that subsequent metal-assisted cyclopropane ring opening and decarbonylation would yield the hexahapto species **4.28**. Instead, treatment of **4.14** with hexacarbonylmolybdenum(0) afforded the retro Diels-Alder product (η^5-C_5Ph_4OH)$Mo(CO)_2(C_3Ph_3H_2)$, **4.29**, as confirmed by mass spectrometric, NMR spectroscopic and X-ray crystallographic analyses. Subsequently, it was demonstrated that **4.29** and the dimethyl analogue **4.30** may be obtained from the reaction of $Mo(CO)_6$, 1,2,3-triphenylcyclopropene and the appropriate cyclopentadienone (**1.53**, **4.31**) in refluxing toluene (Scheme 4.3; see also Section 1.4.1.1). Prior to the ensuing study, these experiments represented the only applications of maximally substituted C_7-ring synthons to the preparation of metal π complexes.

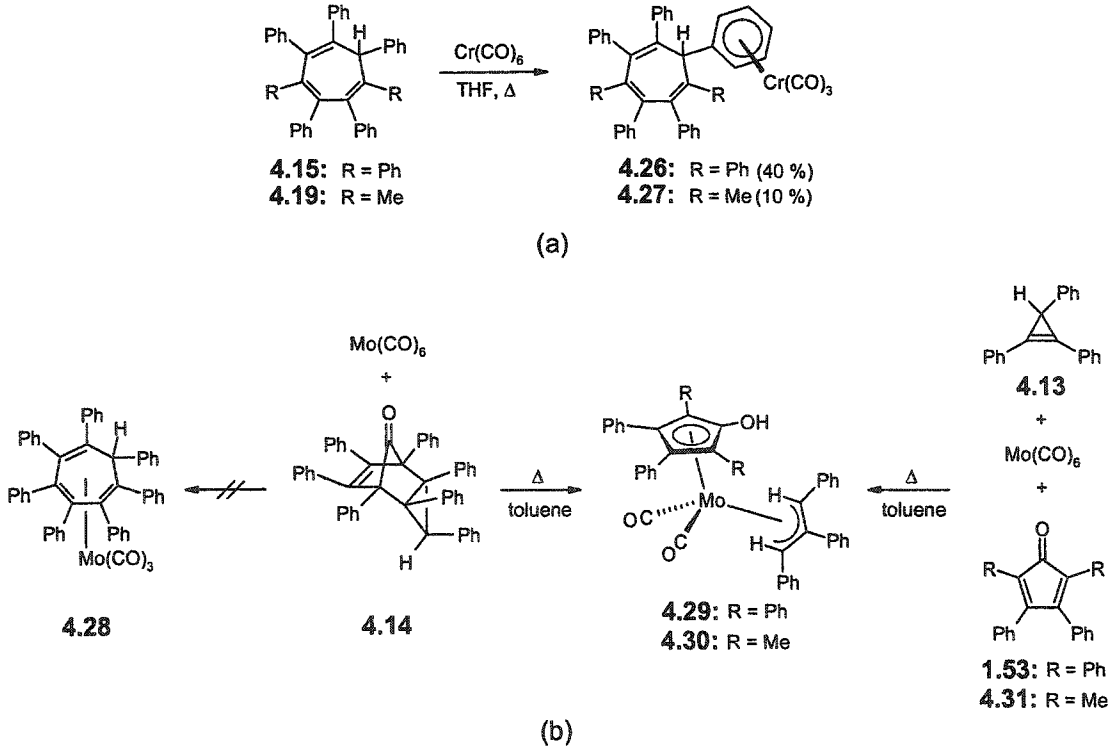

Scheme 4.3: *Reactions of metal carbonyls with (a) C_7Ph_7H **4.15**, $C_7Ph_5Me_2H$ **4.19** and (b) C_7Ph_7HCO **4.14**.*

4.1.2 Overview of Study

Notwithstanding its synthesis in the early 1960s,[232] the heptaphenylcycloheptatrienyl cation, $C_7Ph_7^+$ (**1.139**), is the last species in the series of $C_nAr_n^{x\pm}$ (n = 3 to 7) molecular paddle-wheels to be crystallographically characterized, either as a free ion or molecule, or as an organometallic ligand. Beyond a general and even fundamental interest, high-quality structures of the peralkyl and peraryl derivatives of common hydrocarbons provide important calibration points for theoretical work,[272] as evinced in the earlier chapters. In turn, computational studies of this nonbenzenoid 6π-electron model may clarify further aspects of the structure-property concepts of aromaticity. Experimental support may be garnered in the form of metal derivatization, which is expected to endow new kinetic (i.e. sterics) and thermodynamic properties to the original π-system, and thus aid in illuminating the effects of structural modifications to the cycloheptatriene and -enyl center and periphery. In the broader context of our long-term objectives, seven-membered ring platforms may possess the appropriate geometric features (i.e. extreme steric encumbrance) required to induce the conformational immobility predicted by the parity rule for gear trains.

4.2 Results and Discussion

4.2.1 The Heptaphenyltropylium Cation: An X-ray Crystallographic Study

In accord with an earlier protocol,[232] treatment of heptaphenylcycloheptatriene, C_7Ph_7H (**4.15**), with bromine and subsequent dehydrobromination under conditions of mild pyrolysis yielded the orange-red compound $C_7Ph_7^+Br^-$. In addition to the monobromide, salts of the tribromide, [232] triiodide,[382;383] potassium[382;383] and fluroroborate[232] ions have been reported. Thus, hydrolysis (or methanolysis) and subsequent reaction with HBF_4-ether afforded crystals of $C_7Ph_7^+BF_4^-$ (Scheme 4.4). Several X-ray data sets were acquired for both the bromide and tetrafluoroborate complexes but, despite the determined efforts of a number of crystallographers both in Europe and in North America, no structural information was forthcoming because of an unresolvable disorder problem. Subsequent counter-ion exchange by slow solvent evaporation from a solution containing $C_7Ph_7^+Br^-$

in trifluoroacetic acid produced crystals of X-ray quality, which solved to give the trifluoroacetate salt $[C_7Ph_7^+][CF_3CO_2^-]\cdot 2CF_3CO_2H$, of **1.139**.[384]

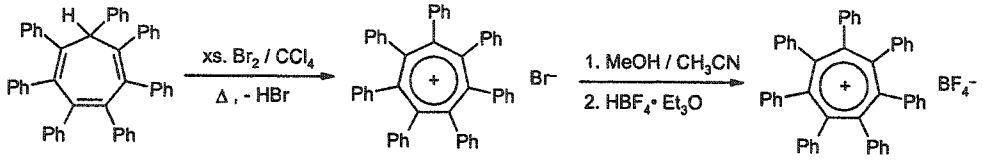

4.15 **1.139(Br)** **1.139(BF_4)**

Scheme 4.4: *Doering's[355] method is effective in the formation of salts of the heptaphenyltropylium ion,* ***1.139.***

Figure 4.1 depicts the structure of the cation and reveals that the seven-membered ring is not flat but rather adopts a shallow boat conformation. The bend angles, γ and ϕ, are most pronounced for the planes containing C(6)-C(7)-C(1) [plane 1], C(1)-C(2)-C(5)-C(6) [plane 2], and C(2)-C(3)-C(4)-C(5) [plane 3], and yield values of 13° ([plane 1]/[plane 2]) and 18° ([plane 2]/[plane 3]), respectively. These may be compared with the corresponding interplanar angles in C_7Ph_7H (or C_7Cl_8), for which γ is 55°(52°) and ϕ is 35°(32°)[370;385] Thus, $C_7Ph_7^+$, **1.139**, retains some vestiges of its boat-like precursor, C_7Ph_7H, **4.15**. It is noteworthy that this distortion from planarity has been previously observed in the molecular structures of [7]circulene **4.32**[386] and the bis[tris(bicyclo[2.2.2]octeno)tropylium]acetylene dication **4.33**.[387] In this regard, X-ray measurements of heptaphenyl-7-borabicyclo[2.2.1]heptadiene **4.34** would be extremely informative given the isoelectronic relationship between the borepin and **1.139**, its aromatic carbocylic counterpart.[388]

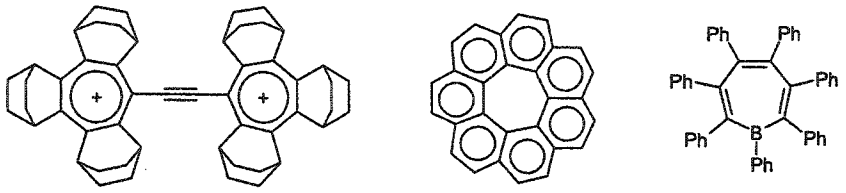

4.32 **4.33** **4.34**

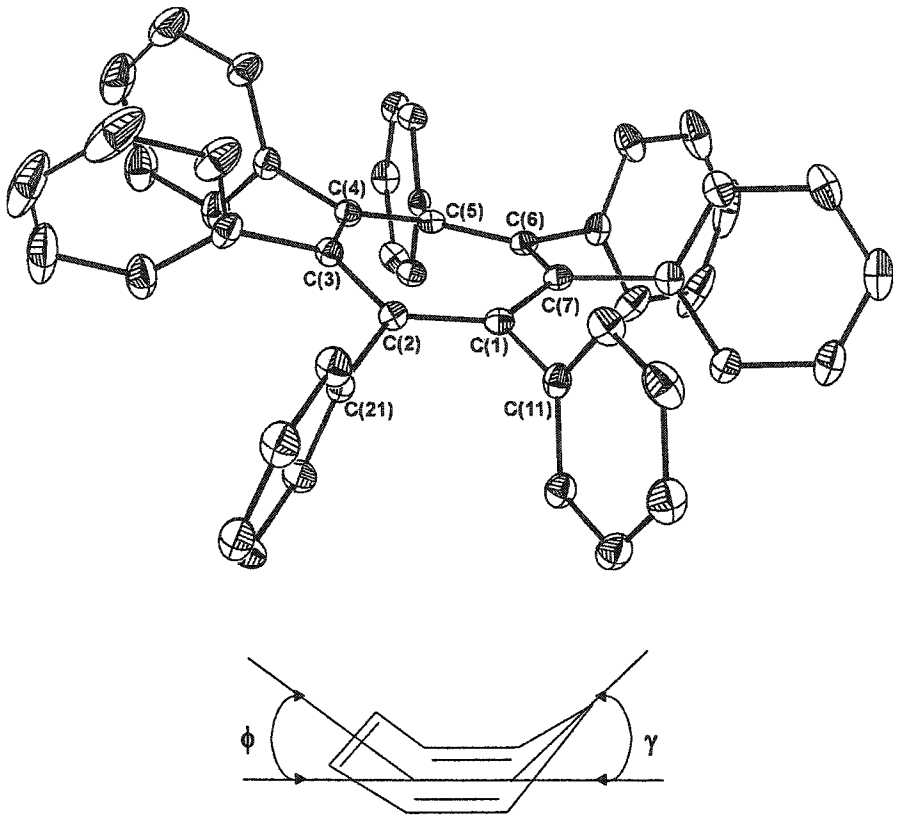

Figure 4.1: *Molecular structure of* ***1.139*** *(thermal ellipsoids at 20% probability) with hydrogen atoms omitted for clarity. The average interplanar angles for* γ *([plane 1]/[plane 2]) and* ϕ *([plane 3]/[plane 2]) are 12.8° and 10.7°, respectively.*

* Selected bond distances (Å) and bond angles (deg.): C_7-ring [C1 – C2 1.404(4), C2 – C3 1.412(4), C3 – C4 1.411(4), C4 – C5 1.415(4), C5 – C6 1.411(4), C6 – C7 1.414(4), C1 – C7 1.414(4); C2-C1-C7 127.4(3), C1-C2-C3: 127.7(3), C4-C3-C2 127.5(3), C3-C4-C5 127.1, C6-C5-C4 127.1(3), C5-C6-C7 128.5(3), C1-C7-C6 126.8(3)]; Typical C_7-ring to Ph [C1 – C11 1.510(4); C1-C2-C21 117.0(3), C3-C2-C21 115.2(3)].

The space-filling representation of the cation **1.139** in Figure 4.2 shows how each peripheral phenyl group is twisted very markedly out of the plane containing its attached central ring carbon and neighbouring ring atoms. These dihedral angles range from 76° to 82° (average 80°), and may be compared to the mean θ values of 75°(67°) for C_6Ph_6 **1.125**,[222;223] ~ 50° for (η^5-C_5Ph_5)ML_n complexes,[116;133;143] ~ 36° (15.3 to 81.5°) for various (η^4-C_4Ph_4)ML_n complexes,[389;390] and ~ 5° for the free $C_3Ph_3^+$ cation.[391]

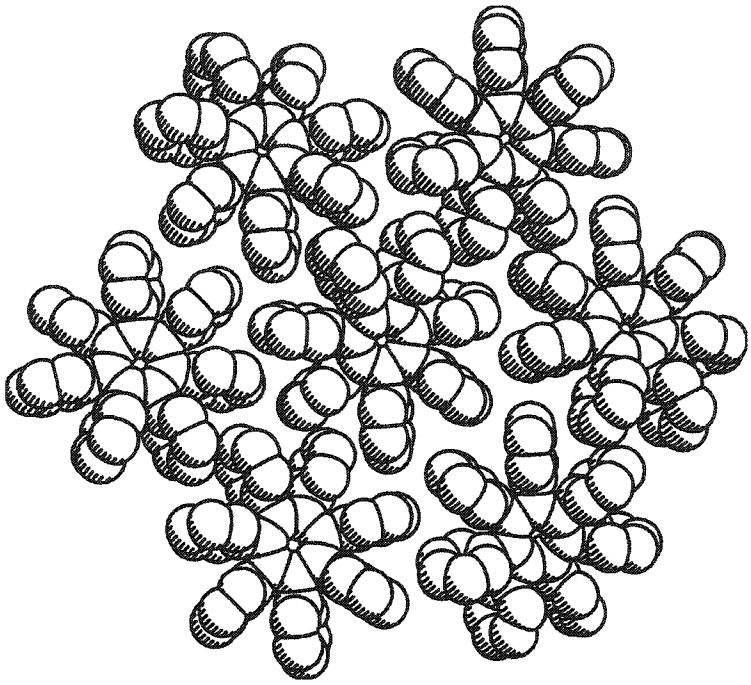

Figure 4.2: *Space-filling representation of a section of a cationic layer, showing the hexagonal packing of $C_7Ph_7^+$ ions, in* ***1.139****.*

One can rationalize the propensity of this system to form well-defined single crystals in terms of a hydrogen bonded network of trifluoroacetates and trifluoroacetic acid molecules which lies between the layers of close-packed disks of cations and provides a stabilization of the crystalline edifice.[392;393] This interlocking motif between the anion, solvates, and cation can be viewed in Figure 4.3. It is likely that the relatively strong and directional O-H···O interactions between each anion and two separate trifluoroacetic acid molecules (2.52 Å and 2.60 Å) that lie parallel to the (101) plane are responsible for the cohesion in the molecular salt. Interestingly, many of the previous X-ray crystallographic determinations of tropylium salts have been of disordered crystals (cf. C_7H_7Cl[394], $C_7H_7ClO_4$,[395] C_7H_7I[396] and $C_7H_7PF_6$[397]). Only those complexes that involve transannular stabilization of the tropylium moiety *via* charge transfer interactions[238;239;398;399] or the encapsulation of $C_7H_7^+$ into the large cavity of a crown ether in order to fix the ion orientation[235;236] have avoided the structurally unfavorable disorder that seems to be associated with the tropylium cation and its analogues.

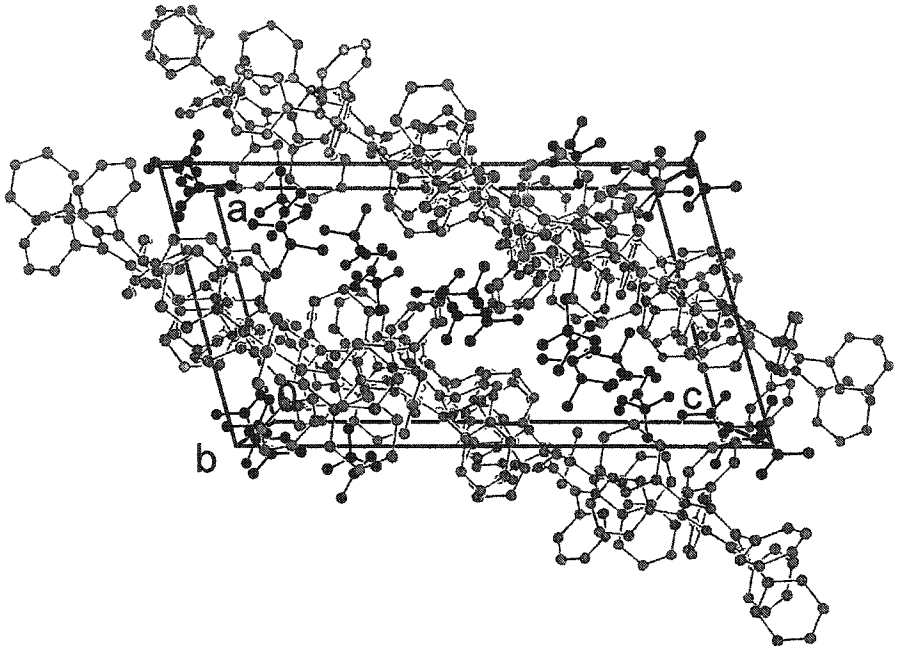

Figure 4.3: *View of the unit cell of* ***1.139*** *depicting the alternating layers of cations and anions/solvates parallel to the (101) plane.*

It has been emphasized by Braga and Grepioni that in crystals of ionic species, the distribution of anions and cations is controlled primarily by the relative size and shape of component ions.[392] Bromide and tetrafluoroborate anions may be likened to molecular "ball-bearings" and, when such species are introduced into a crystal lattice that contains layers of disc-shaped $C_7Ph_7^+$ cations, it is reasonable to infer that the coulombic interactions lack directionality and are insufficient in providing cohesion. On the other hand, the intermolecular links afforded by the trifluoroacetate anions and trifluoroacetic acid molecules serve to more efficiently fix the discoidal cations in the crystal lattice, resulting in a discrete, ordered, low energy solid-state structure.

4.2.2 C_7 Computational Analysis

In order to ascertain whether the conformational anomalies observed in the solid-state structure of **1.139** are a response to steric or electronic factors, we conducted semi-empirical MO calculations using the AM1 Hamiltonian[257] available in the Spartan computational package.[258] The

general features of the X-ray structure were reproduced in the ground-state optimized C_1 geometry of $C_7Ph_7^+$, with average (maximum) interplanar angles of 9° (12°) and 11° (16°) for γ and ϕ, respectively. It is noteworthy that a search of conformational space also yielded a separate potential minimum corresponding to the D_{7h} form of $C_7Ph_7^+$, which is only 0.2 kcal mol^{-1} higher in energy than the aforementioned C_1 isomer. The existence of two energetically accessible (gas-phase) equilibrium structures, one planar and one non-planar, implies that the system is conformationally flexible. In turn, it supports the dynamic symmetry that is observed in both the ^{1}H and ^{13}C NMR regimes of **1.139** (cf. $C_5Ph_5^-$ **1.18** and C_6Ph_6 **1.125**) and the postulate that solid-state packing effects may influence the geometry of the seven-membered ring in $C_7Ph_7^+$.

In fact, the archetypal aromatic system – benzene – itself in the solid state at 15 K is not planar.[400] Its slight chair conformation is caused by weak intermolecular interactions in the crystal lattice, which are estimated by Kitaygorodsky[401] to be in the range of 1-3 kcal mol^{-1}. From the diametric perspective, this out-of-plane bending does not require much energy;[402] for example, in studies of sodium p-nitrobenzoate trihydrate, the significant deformations of the ring were found to be proportional to the strength of the intracrystalline contacts.[403] In a recent survey of molecular models, Krygowski and Cyranski[103] established that even appreciable distortions from planarity may effect only minimal changes in aromaticity, as approximated by HOMA (harmonic oscillator model of aromaticity) values.

Further calculations (Table 4.2) revealed that consecutive replacement of the phenyl substituents with hydrogens results in a decrease in the dihedral angle between the peripheral phenyls and the central C_7-ring (from 88° for $C_7Ph_7^+$, **1.139**, to 42° for $C_7PhH_6^+$, **4.2**, cf. LCAO-Hückel value of 45–50° estimated by Jutz[360]), and an accompanying increase in the planarity of the tropylium ring. For example, in the C_2-optimized structure of the 1,2,4,6-tetraphenyltropylium cation, **4.35**, the central ring is essentially planar and the phenyl-to-central ring dihedral angles are 58° and 45° for the two adjacent phenyl moieties, 1 and 2, and phenyls 4 and 6, respectively. Steric

repulsions between the central C_7-ring hydrogens and the *ortho*-hydrogens of the phenyl moieties prevent the electronically optimal coplanar arrangement between the two types of π systems. Such a disposition of the rings diminishes resonance stabilization within the ion, and has been cited as one of the factors contributing to the increased acidity of this series (see section 4.1.1). One might also surmise that any non-planar substituent would pucker the central C_7 ring, as evinced by the average calculated (AM1) interplanar angles of 18° (γ) and 22° (ϕ) for the ground-state C_s-optimized structure of the permethylated derivative, $C_7Me_7^+$ (**1.140**), which is almost 15 kcal mol^{-1} more stable than its planar conformer. At the time of these studies, no crystallographic studies had been conducted on this latter system (vide infra). Ultimately, these results indicate that the geometrical features observed in the solid state structure of $C_7Ph_7^+$ arise because of a compromise between steric congestion and the fractional loss in aromaticity one might anticipate as the ring distorts from planarity. Given the complex interaction between molecular structure and (an)isotropic crystal packing forces, it is plausible that a planar crystal form of $C_7Ph_7^+$ may eventually be realized.

Table 4.2. Conformational features of polysubstituted $C_7R_{7-m}H_m$ (where $4 \leq m \geq 0$, R = Ph, Me) derivatives.

Compound	Pt. Symmetry	γ (°)*	ϕ (°)*	Ph–C_7 $\angle$ (°)*	ΔH_f (kcal mol^{-1})
4.15, C_7Ph_7H [a]		55	35	--	--
4.15, C_7Ph_7H [b]	C_1	50	35	--	248.01
1.139, $C_7Ph_7^+$ [a]		11	13	79	--
1.139, $C_7Ph_7^+$ [b]	C_1	9	11	88	419.52
1.139, $C_7Ph_7^+$ [b]	D_{7h}	0	0	90	419.71
4.35, 1,2,4,6-$C_7H_3Ph_4^+$ [b]	C_2	~0	~0	45, 58	309.24
4.35, 1,2,4,6-$C_7H_3Ph_4^+$ [b]	C_1	3	3	46, 56	309.48
4.36, 1,3,5-$C_7H_4Ph_3^+$ [b]	C_1	0	0	46	279.35
4.2, $C_7H_6Ph^+$ [b]	C_1	0	0	42	232.52
1.140, $C_7Me_7^+$ [b]	C_s	18	22	*na*	168.53
1.140, $C_7Me_7^+$ [b]	C_{7h}	0	0	*na*	183.47
4.37, 1,3,5-$C_7H_4Me_3^+$ [b]	C_s	0	0	*na*	182.46

[a] X-ray crystallographic data. [b] Calculated (AM1 Hamiltonian) data. * The averaged value is quoted.

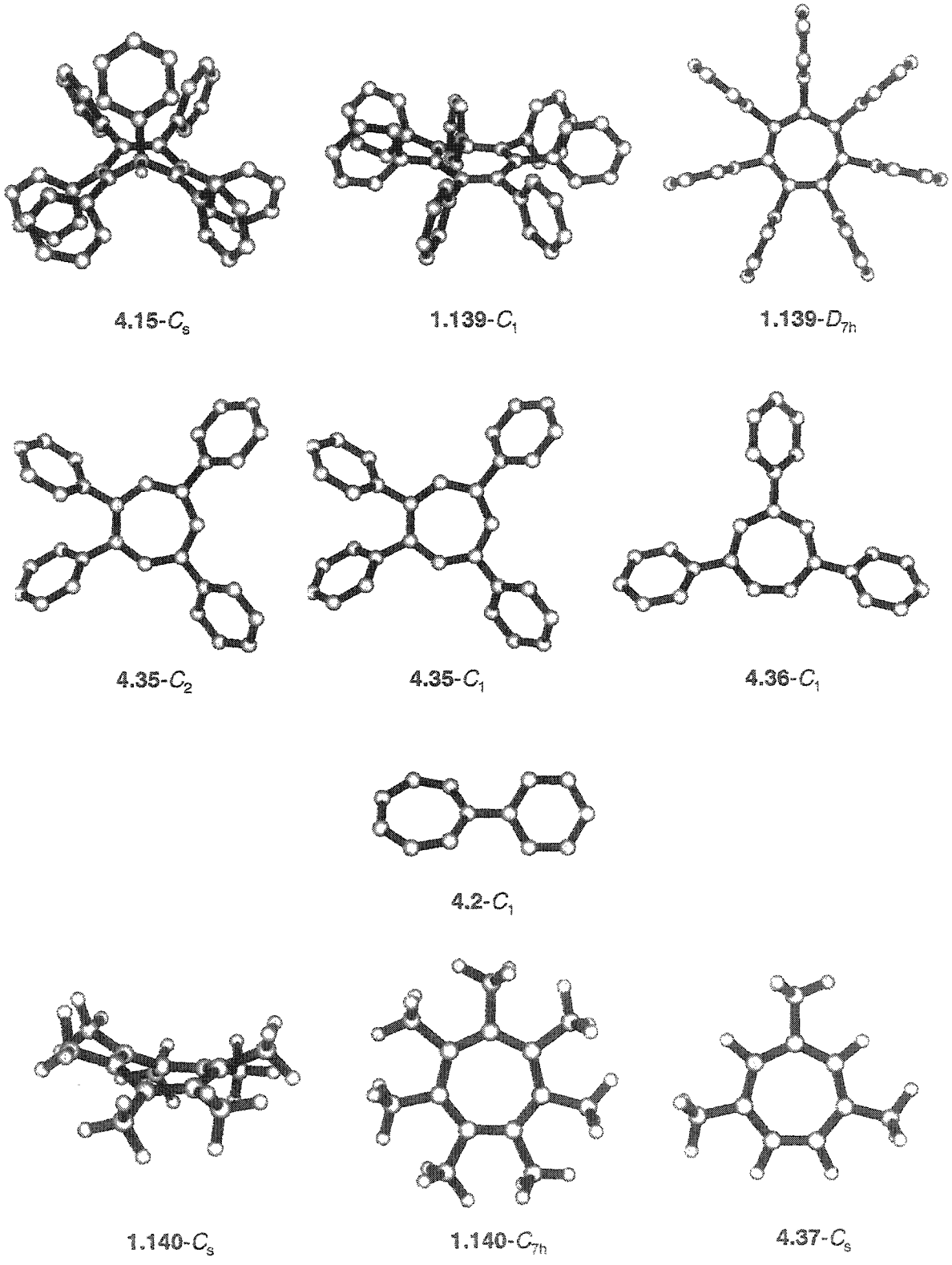

Figure 4.4: *Calculated (AM1 Hamiltonian) structures for select $C_7R_{7-m}H_m$ (where $4 \leq m \geq 0$, R = Ph, Me) cations.*

4.2.3 ^{13}C NMR Chemical Shift Correlations

It is well established that the proton and carbon environments associated with points of unsaturation within a hydrocarbon experience deshielding, which in turn increases the effective magnetic field at the nuclei and thus, their corresponding NMR chemical shift(s). More specific to cyclic conjugated systems, chemical shift variations have been attributed to diatropic ring current contributions, although neighbour anisotropy and substituent effects may also govern.[404] In 1961, Spiesecke and Schneider[405] demonstrated the striking parallelism of the linear relationships [as defined by $\delta_H^1 = 10.6\rho$, $\delta_C^{13} = 160\rho$] between the π-electronic charge distribution (ρ) at the local carbon centers and the resonance of both the proton and carbon nuclei in the nonalternant $C_nH_n^{x\pm}$ series (n = 5 to 8). The validity of the ^{13}C chemical shift correlation was later substantiated by Olah,[406] with a slope of 140 ppm per unit charge obtained from simple Hückel calculations for both positive and negative species with two, six and ten π-electrons. The model has since been tested for a variety of polycyclic aromatic compounds (including heterocycles), yielding values as high as 210 ppm per π electron.[407]

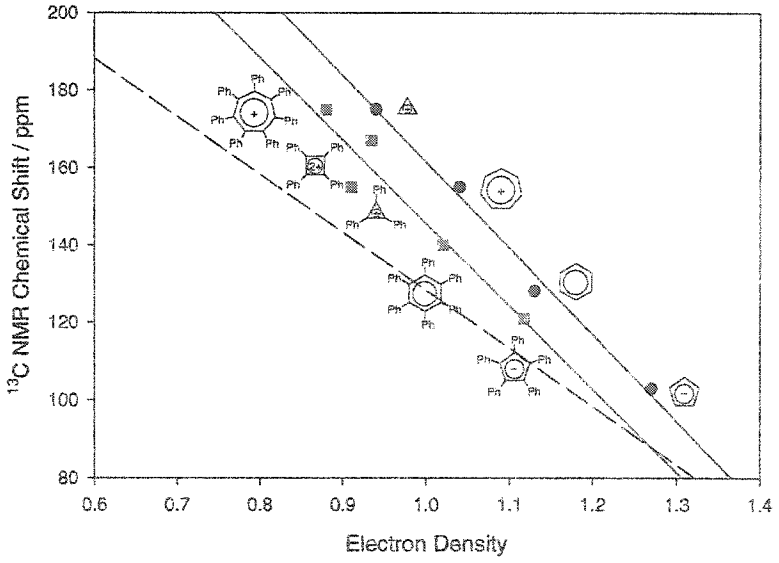

Figure 4.5: *^{13}C NMR chemical shifts versus calculated (HMO ···,[406] AM1 —) charge densities for aromatic $C_nR_n^{x\pm}$, where R = H (●)or Ph (■).*

How does the charge density vary at different levels of theoretical approximation and for aromatic scaffolds of increasing complexity? In applying the AM1 Hamiltonian (cf. other semi-empirical methods, such as CNDO/2 or INDO[404]) and Mulliken charges for the central ring carbons, we have found that the original correlation (for n = 3 to 9) is maintained but that the proportionality factor is approximately 21 ppm per extra 0.1 electron (see Figure 4.5). We further extended this quantitative relationship to the $C_nPh_n^{x+}$ series (n = 3 through 7), since phenyl substitution is apt to influence the charge delocalization within each system. Because of the dominance of the local paramagnetism in ^{13}C shieldings, ^{13}C chemical shifts are quite sensitive to changes in the electronic density at the carbon.[404] In contrast to the earlier HMO studies,[406] all analyses were performed on energy-minimized (AM1 Hamiltonian) structures, since for the larger rings, the peripheral phenyls are clearly not coplanar with the central ring. Computation of the Mulliken charges in the perphenylated series again revealed a reasonable correlation, with a ^{13}C NMR shielding of approximately 22 ppm per extra 0.1 electron at the central ring carbons (Figure 4.5). In improving the level of theory, from simple Hückel to semi-empirical methods, the results indicate that a particular change in ^{13}C chemical shift corresponds to a smaller change in electron density (pi and sigma inclusive). The added effects of basis set augmentation and (the extent of) applied electron correlation have yet to be explored. We also emphasize that the NMR data for such a series of anionic, neutral and cationic species cannot be acquired in the same solvent medium, a factor which introduces a degree of uncertainty in the relationship between ^{13}C resonances and electron density.

4.2.4 Synthesis and Characterization of Hexaphenylferrocenylcycloheptatriene

In principle, enhanced π-delocalization in $C_7Ph_7^+$ may be achieved by complexation of the perphenylated cation with selected transition metal fragments.[408-412] Whereas numerous η^6-$(C_7H_{8-m}R_m)ML_n$ and η^7-$(C_7H_{7-m})ML_n$ (m = 0 - 4) derivatives have been reported,[243] all attempts to coordinate a metal moiety to the central C_7-ring in heptaphenylcycloheptatriene and -enyl salts have thus far been thwarted (refer to Section 4.1.1.2). Therefore, to circumvent any steric impediments that may

be associated with metal binding, we elected to incorporate the organometallic fragment as part of the molecular periphery.

In extending the synthetic versatility of the Diels-Alder reaction, a particularly attractive template is 3-ferrocenyl-2,4,5-triphenylcyclopentadienone, **1.54**. The inclusion of ferrocene, an electron donating group, is not only expected to enhance the thermodynamic stability of the corresponding tropylium ion, but it should also impart improved crystallinity to its compounds. In the event, treatment of **1.54** with 1,2,3-triphenylcyclopropene, **4.13**, and subsequent cheletropic loss of carbon monoxide resulted in the corresponding polyphenylated species, C_7Ph_6FcH, **4.38**, as a red-orange crystalline solid in a 68% yield.[313] Despite the complexity of the ^1H- and ^{13}C-NMR spectra, only one of several possible isomers (as depicted in Scheme 4.5) appeared to be present, and the identification of this product was realized by X-ray crystallography. From the two views of the molecular structure of **4.38** that are provided in Figure 4.6, it is evident that the ferrocenyl substituent is positioned at C(1), adjacent to the sp^3-hybridized carbon of the CHPh unit.

Clearly, such an isomer must have arisen as the result of a [1,5]-transannular shift of hydrogen after decarbonylation but prior to endo-exo (relative to the unique hydrogen) inversion of the cycloheptatriene ring. Comparison of the structure of **4.38** with that of C_7Ph_7H, **4.15**, reveals that the ferrocenyl unit is located in the sterically least demanding site. According to the dynamic NMR data of **4.15**, the phenyls at C(2)/C(5) have relatively high rotational barriers relative to the phenyls positioned at C(1)/C(6) and C(3)/C(4), and presumably reside in the most hindered locale (Section 4.1.1.2).[370]

Consistent with the solid-state geometries of other C_nAr_n systems, the peripheral aryl substitutents are oriented in a twisted fashion relative to the central ring in C_7Ph_6FcH, **4.38**, affording dihedral angles of 56°, 82°, 81°, 68°, 55°, 132° and 142° with the plane defined by the attached central ring carbons C(1) to C(7), respectively, and neighbouring ring atoms. Moreover, the seven-membered carobocycle in **4.38** adopts a boat conformation that it is distinguished by

the planes containing C(6)-C(7)-C(1) [plane 1], C(1)-C(2)-C(5)-C(6), [plane 2], and C(2)-C(3)-C(4)-C(5) [plane 3]. The interplanar angles of 54° ([plane 1]/[plane 2]) and 34° ([plane 2]/[plane 3]) are consonant with the values that have been reported previously for other cycloheptatrienes bearing very bulky substituents.[370;385]

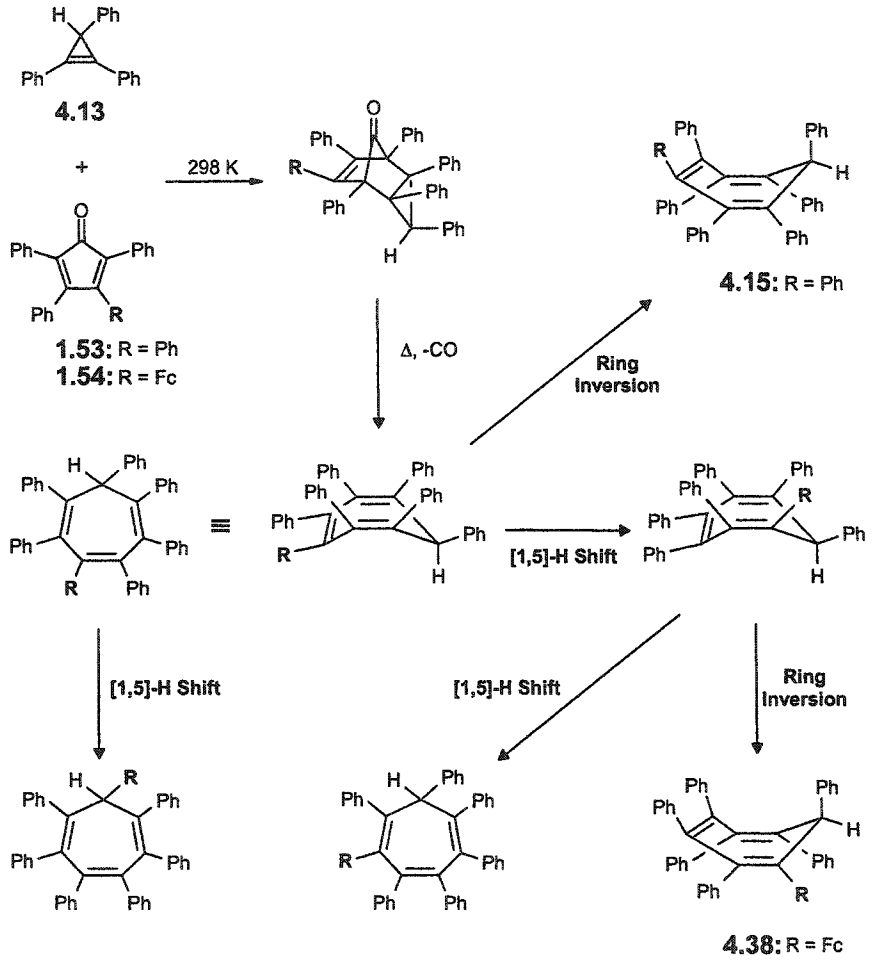

Scheme 4.5: *Preparation of and thermal isomerization processes in C_7Ar_6FcH, **4.38**, and its organic analogue **4.15**.*

As a complement to these crystallographic studies, the conformational flexibility of C_7Ph_6FcH, **4.38**, in solution was probed by VT-NMR spectroscopy. The room temperature 500 MHz ^1H- and ^{13}C-NMR spectra of **4.38** were completely assigned (with the exception of phenyl rings 3 and 4, which can not be differentiated) by means of ^1H-^1H COSY and ^1H-^{13}C shift-

correlated experiments. In its perphenylated analogue, C_7Ph_7H, **4.15**, the rotation of phenyl 7 could not be monitored because the mirror plane renders its *ortho* and *meta* protons equivalent at any temperature. This symmetry is disrupted in **4.38** and, on warming the sample, the pair of doublets (at 7.71 and 8.08 ppm) attributable to the *ortho* protons of phenyl 7 (H72/H76) broaden and converge to give a doublet at 7.97 ppm. These coalescence data, obtained at 202 K, yield a rotational barrier of 9.3 (± 0.5) kcal mol^{-1}. Likewise, the ortho protons of phenyl 4 (H42/H46), which at 193 K resonate at 5.59 and 6.16 ppm, exhibited coalescence at 223 K, corresponding to a free energy of activation of 10.1 (± 0.5) kcal mol^{-1} for the analogous process. Libration of the other phenyls in **4.38** is also clearly slowed on the NMR time scale (refer to Figure 4.7), but overlapping resonances leave the assignments less certain. In the absence of these data, it is difficult to correlate the magnitude of the rotational barriers in **4.38** and **4.15**. Whether there is a larger degree of congestion in the former vis-à-vis the latter system can hardly be distilled from the available barriers to gear slippage (9.1 to 11.0 kcal mol^{-1}), especially with the associated error limits.

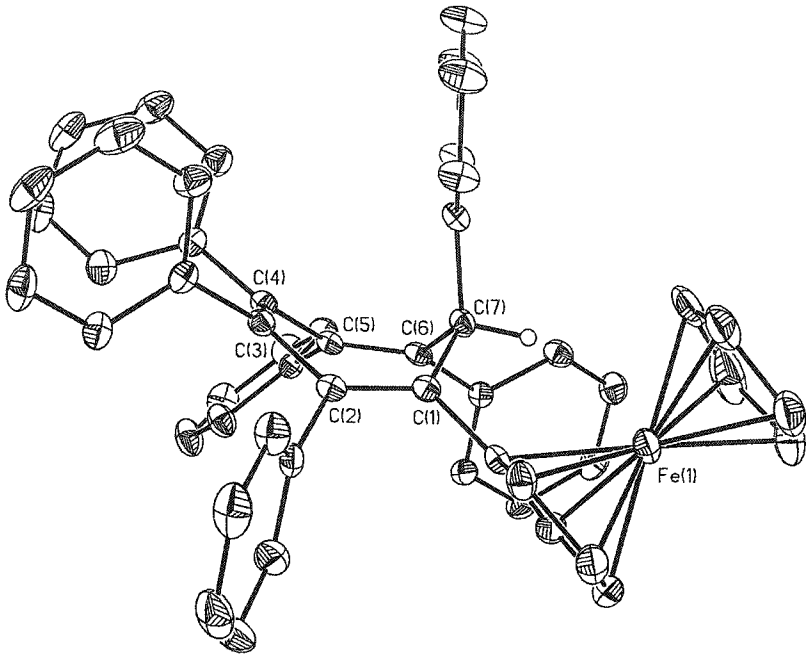

(a)

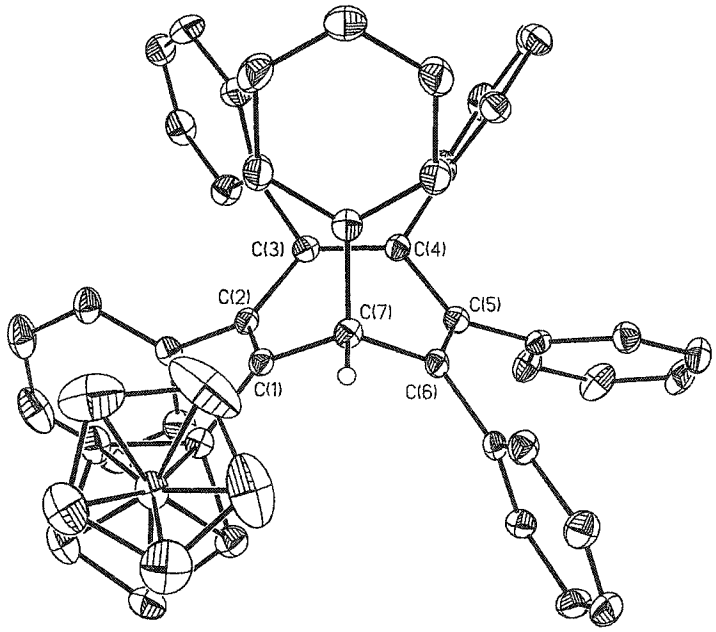

(b)

Figure 4.6: *(a) Side and (b)"Bow" to "Stern" views of the molecular structure of C_7Ph_6FcH,* ***4.38****, (30% thermal ellipsoids), depicting the atom numbering scheme.*

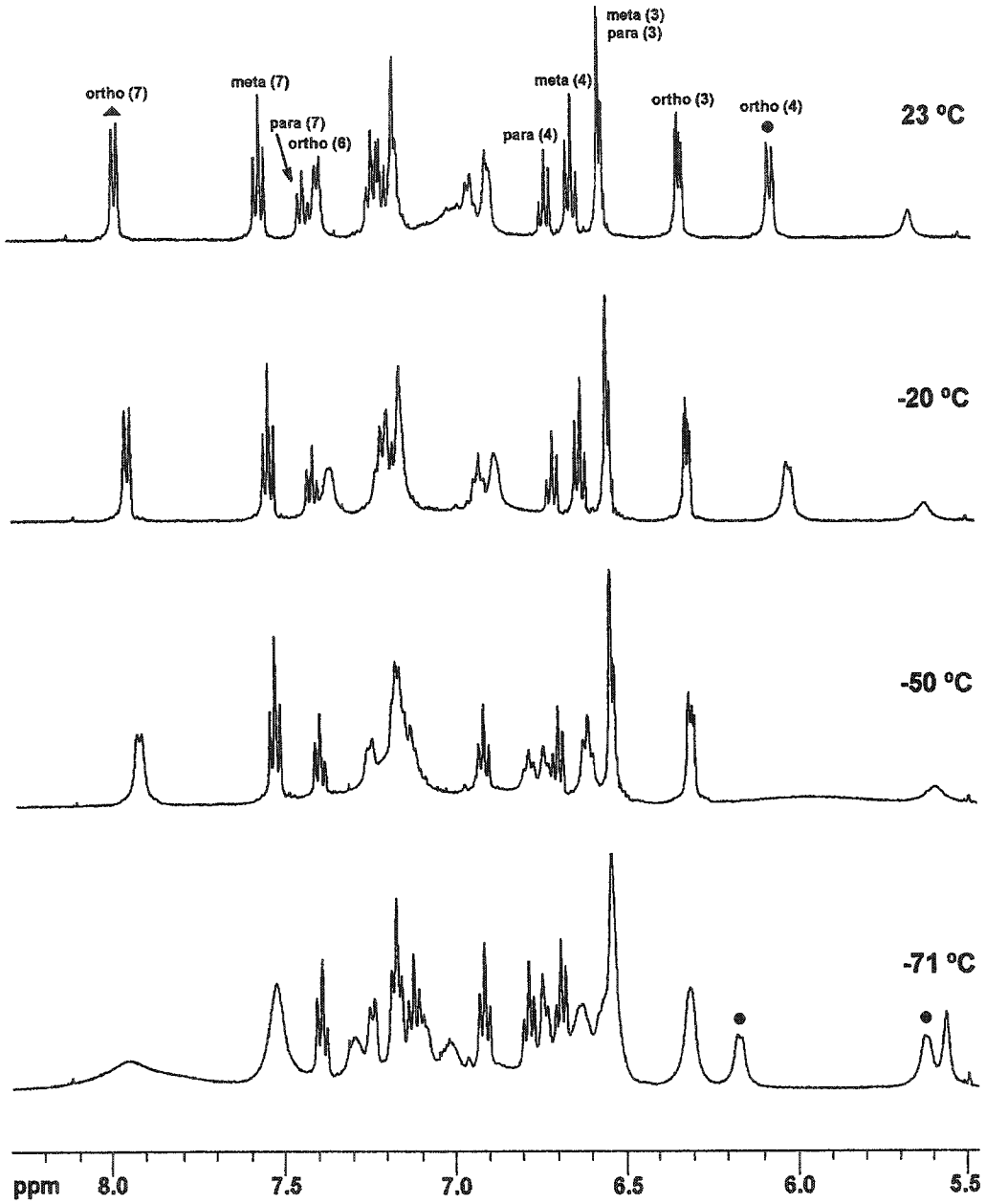

Figure 4.7: *Variable-temperature 500 MHz ^{1}H NMR spectra of C_7Ph_6FcH,* ***4.38****.*

4.2.5 *In Pursuit of an Organometallic Carbenium Ion: Synthesis and Characterization of Ferricinium-Hexaphenylcycloheptatriene*

One of our aims in preparing C_7Ph_6FcH, **4.38**, was to attempt the isolation of the corresponding cation $[C_7Ph_6Fc]^+$, **4.39**, in order to compare its geometrical features with those of $[C_7Ph_7]^+$, **1.139**,[384] and with other ferrocenyl cations (see **4.40**).[413] The ability of group 8 metallocenes, in addition to other cluster-based organometallic units, to alleviate electron deficiency at a neighbouring carbocationic center has been well-established.[408-411;414] This is generally accomplished by allowing the formally positive α-site to bend towards the metal atom so as to optimize the orbital overlap between the vacant *p* orbital on carbon and a filled *d* orbital on the relatively electron-rich metal, effectively augmenting the HOMO–LUMO gap.[415] In the extreme, one may view the resulting structure as a fulvene coordinated to a $[(C_5H_5)M]^+$ moiety, as in **4.40b**, wherein the exocyclic double bond is displaced by ~ 25-40° (see Scheme 4.6).

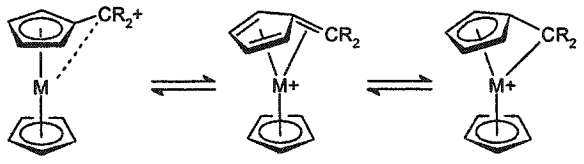

4.40 M = Ru, Fe

Scheme 4.6: *Resonance structures of α-metallocenyl cations.*

On the contrary, if the carbocation does not require anchimeric assistance from the L_nM residue, it is reasonable to infer that the organometallic fragment will effect minimal geometric distortions in the adjacent organic ligand. For instance, it has been confirmed crystallographically that cationic Hückel-type systems that are thermodynamically stable (and therefore isolable), retain their planarity and characteristic bond lengths even when an α-organometallic group is introduced. Examples include the pyrylium and unsubstituted tropylium ions, **4.42**[416] and **4.43**,[397] respectively, which lack the metal participation evinced by a 15° C_5–C_3-ring incline in the ferrocenyldiphenylcyclopropenium cation **4.41**.[417;418]

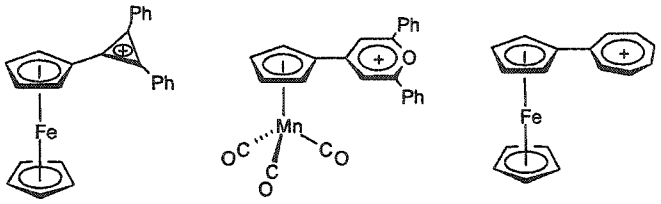

4.41 **4.42** **4.43**

Scheme 4.7: *Aromatic analogues of organometallic carbenium ions,* ***4.41 - 4.43.***

In our efforts to generate the organometallic cation $[C_7Ph_6Fc]^+$, **4.39**, from its covalent precursor C_7Ph_6FcH, **4.38**, several approaches were considered: attempted removal of the unique hydrogen by use of the trityl cation (see synthesis of 1,2,3,4-$C_7H_3Ph_4^+$, **4.3**),[361] or *via* successive replacement of this hydrogen by bromine and methoxy substituents (as was done with C_7Ph_7H, **4.15**)[232] proved fruitless. Limited success was eventually achieved by treatment of **4.38** with triethyloxonium hexachloroantimonate, $[Et_3O]^+[SbCl_6]^-$, which is known to be an excellent reagent for hydride abstractions.[419]

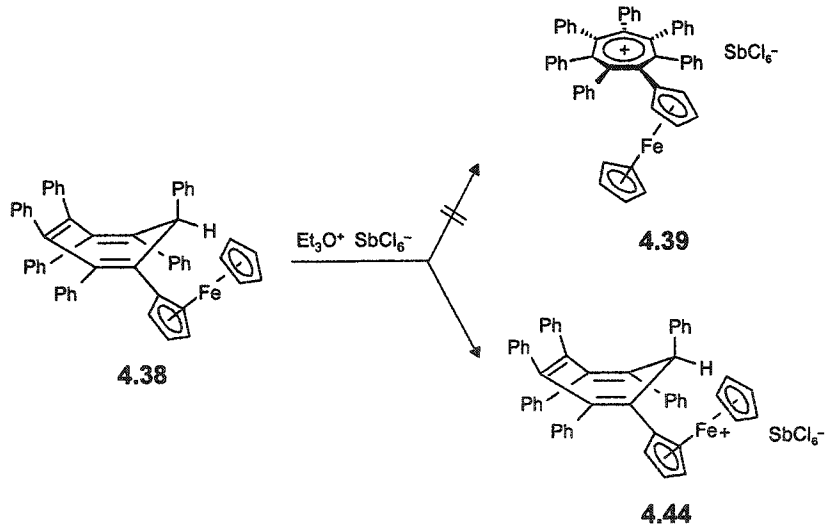

Scheme 4.8: *Unanticipated generation of* $[C_7Ph_6FcH]^+$ $[SbCl_6]^-$, ***4.44.***

From the supernatant, dark blue prismatic crystals suitable for structural determination by single-crystal X-ray diffraction were carefully isolated. Figure 4.8 features the molecular structure of the product, which is not the anticipated ferrocenyl-hexaphenyltropylium cation but rather $[C_7Ph_6FcH]^+[SbCl_6]^-$, **4.44**, the ferricinium salt of the starting material! The characteristic boat

conformation of the seven-membered ring is maintained, and the unique hydrogen attached to the sp^3-carbon was also readily located. The major differences between **4.38** and **4.44**, apart from the presence of the hexachloroantimonate counter-anion, are found in the ferrocenyl unit where the average Fe-C distance has lengthened from 2.04 Å to 2.08 Å, a value that is typical for ferricinium systems.[420] Given the success of the aforementioned reactions with C_7Ph_7H, it is plausible that the steric bulk of the ferrocenyl unit in **4.38** hinders the approach of any reagent that might abstract hydride, such that an electron transfer process intervenes. For future consideration, Takeuchi et al.[233] have found phosphorus pentachloride to be superior to triphenylcarbenium ion in its capacity to remove a sterically encumbered C_7 hydrogen (cf. formation of $C_7Me_7^+$, **1.140**). Oxidation of **4.44** to ferricinium-hexaphenyltropylium (a dication) was not attempted, although this would constitute a logical next experimental step. In any case, attempts to desymmetrize $C_7Ph_7^+$, **1.139**, by metal complexation and thus study stereodynamic phenomena within this propeller system have not been entirely successful.

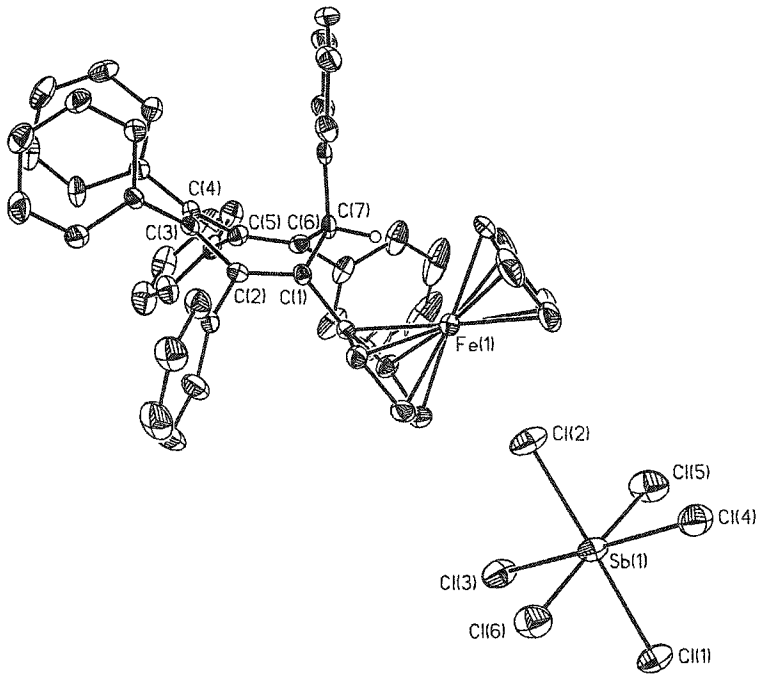

Figure 4.8: *Side view of $[C_7Ph_6FcH]^+[SbCl_6]^-$, **4.44**, (30% thermal ellipsoids), depicting the atom numbering scheme.*

4.2.6 Addendum: Polyalkylcycloheptatrienyl Species

The applications of multi-alkyl substituted cycloheptatrienyl ligands in organotransition metal chemistry have been advanced significantly since the completion and publication of the research profiled in Sections 4.2.1 - 4.2.5.[313;384] In lieu of the multistep preparation reported by Knoche in 1964,[367] an improved synthetic protocol for heptamethylcycloheptatriene, **4.45**, was introduced by Tamm and co-workers in 2000.[421] The diazoethane-promoted ring expansion of hexamethylbenzene **1.94** afforded **4.45** in nearly quantitative yields (based on recovery and reuse of **1.94**). Hydride transfer from **4.45** to phosphorus pentachloride and subsequent dissolution in acetic acid/anhydride and hydrogen tetrafluoroborate furnished **1.140**(BF_4) (Scheme 4.9). The X-ray crystallographic characterization of the heptamethylcycloheptatrienyl cation **1.140** provides only the second solid state example of an unconstrained, persubstituted C_7R_7 ($R \neq H$) platform. The static gear effect is manifested in the molecular structure of **1.140**, which possesses an intermeshed arrangement of methyl groups along the π-periphery of a non-planar ($\phi \approx 29°$, $\gamma \approx 21°$; cf. **1.139** in Figure 4.1) Hückel $4n + 2$ system, in accordance with our earlier estimations of a global minimum of C_s symmetry ($\phi \approx 22°$, $\gamma \approx 8°$).[384] The computational prediction that persubstitution of the C_7 border with n-fold rotors ($n > 2$) would induce central ring deformations is therefore validated.

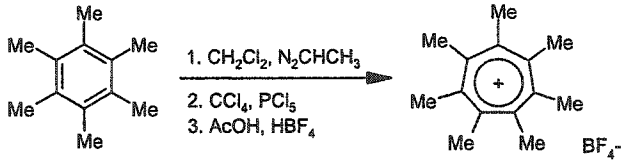

1.94 **1.140**(BF_4)

Scheme 4.9: *Synthetic route to the hexamethylcycloheptatrienyl cation **1.140**, based on a ring-expansion of hexamethylbenzene (**1.94**).*

Given the literature precedent for cycloheptatrienyl metal complexes of the type $[(\eta^7\text{-}1,2,4,6\text{-}C_7H_3R_4)M(CO)_3]^+$ or $[(\eta^7\text{-}1,2,4,6\text{-}C_7H_3R_4)M(CO)_2X]$ (where M = Mo, W; X = Br, I),[422;423] Tamm et al.[424] attempted analogous synthetic routes with the $C_7Me_7^+$ ligand. However, the

reaction of **1.140**(BF_4) with *fac*-[$W(CO)_3(NEt)_3$] in the presence of a catalytic quantity of [Cp_2Fe][PF_6] and subsequent treatment of the cationic intermediate with sodium iodide did not yield [η^7-(C_7Me_7)$W(CO)_2I$], **4.46**, as anticipated. Instead, the stable, isolated complex was identified by spectroscopic (IR, NMR) and single crystal X-ray diffraction methods as [η^5-(C_7Me_7)$W(CO)_3I$], **4.47** (Scheme 4.10). With its pendant double bond, the η^5-bound cycloheptatrienyl retains vestiges of its original boat conformation,[421] which likely imparts unusual reactivity to **1.140**.

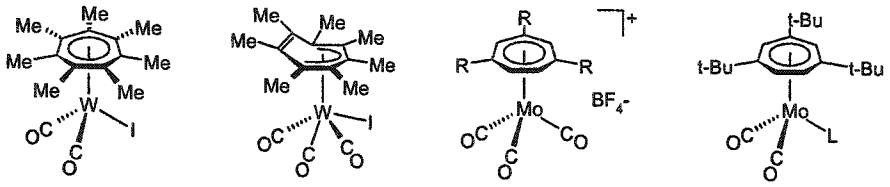

Scheme 4.10: *Proposed (**4.46**) and isolated metal complexes containing the hepta- (**4.47**) and 1,3,5-trisubstituted (**4.50 – 4.52**) tropylium ligands.*

Whereas no other bonding modes have yet to be demonstrated for (C_7Me_7)ML_n complexes, Tamm and co-workers[425] have prepared symmetrically η^7-ligated 1,3,5-alkylsubstituted cycloheptatrienyl species. Concomitant arene exchange - molybdenum tricarbonyl transfer from [(η^6-*p*-xylene)$Mo(CO)_3$] to (1,3,5-$C_7H_4R_3$)BF_4 (R = tert-butyl **4.48**; R = isopropyl **4.49**) produced the cationic species [(η^7-1,3,5-$C_7H_4R_3$)$Mo(CO)_3$][BF_4] (**4.50**; **4.51**), and upon reaction of the former with the appropriate alkali metal halide, the neutral complexes [(η^7-1,3,5-$C_7H_4{}^tBu_3$)$Mo(CO)_2X$] (X = Cl or Br), **4.52** (Scheme 4.10). The solid-state structures of both **4.48** and **4.52** reveal an effectively planar, C_s-symmetric tropylium platform, in agreement with our theoretical predictions for the related 1,3,5-trimethylcycloheptatrienyl cation, **4.37** (see Section 4.2.3).[384] One notable distinction is the significant bond length alternation in the central ring of **4.48** (1.368(4) - 1.417(4) Å); although this geometric detail is not manifested in the calculated structure of **4.37**, it has been attributed to an unsymmetric substitution pattern (cf. **1.140**).[425]

Since dynamic NMR data for **4.47, 4.50 - 4.52** have not been documented, a comparison with the corresponding arene systems, and thus an evaluation of the effect of ring size on the barrier to rotation, is not possible.

4.3 Summary and Outlook

Beyond their topological interest, sterically demanding C_7R_7H and $C_7R_7^+$ molecules allow for the possibility of incorporating multimetallic fragments with markedly different spatial and electronic properties. Despite the counsel of Haywood-Farmer and Battiste in 1971,[120] there remains a paucity of information pertaining to the static and dynamic structural properties of these systems, attributable in part to the belated development of their derivatization and metal coordination chemistries. Yet even within the confines of successful studies, the merits of X-ray crystallography have been repeatedly undermined by the prerequisite for suitable single crystals of ordered morphology. The solid-state characterization of **1.139** represents the *first* non-disordered structure of a *free* tropylium cation and provides unambiguous geometric data in support of aromaticity arguments. Whether proximal transition metals (e.x. the α-ferrocenyl group in **4.38 / 4.44**) reduce or enhance the cyclic π-electron delocalization of the persubstituted tropylium ion is still unresolved. Alternatively, the unique nature of the M-(η^7-C_7H_7) bond is well understood, but steric hindrance to metal complexation of the central ring has posed significant difficulties. There is precedent in simpler tropilidene systems to suggest that it may be possible to promote, photochemically or thermally, the σ- to π-rearrangement of an organometallic fragment, starting from the 4n π-electron heptaphenylcycloheptatrienyl anion.[426-428] In the anticipation that cycloheptatrienyl metal complexes will eventually share the same level of significance as η-cyclopentadienyl and η-arene analogues, alkyl and aryl-based structural modifications are among the many possibilities for the future expansion of C_7-ring chemistry.

For example, strain alleviation in the maximally arylated C_7-ring may be advanced by the marriage of Pascal's *albatrossenes*[225] and the annelated bis(tris(bicyclo[2.2.2]octeno)-

tropyliumyl]phenylene dications (**4.32**), reported by Kagayama and co-workers,[387] to produce perphenylated tropylium-based arenes from *para*- and *meta*-linked bistetracyclones and 1,3,5-tristetracyclones. Indications of liquid crystal behaviour in the bis(heptaphenylcycloheptatrienes), **4.17**, prepared by Harvey and Ogliaruso,[372] make related olefin precursors even more attractive synthetic candidates. To extend the quantification of rotational barriers beyond the geometry-constrained cycloheptatriene precursors, Gust's[122;123] labelling approach may be adopted in lieu of metal desymmetrization methods. Indeed, cycloheptatrienyl derivatives originating from a manifold of cyclopentadienone building blocks bearing substituents (fluoro, alkyl or alkoxy groups, or fused rings) in the ortho or meta positions of adjoining aryl rings should give rise to distinguishable stereochemical features.

CHAPTER FIVE

From Iconic Models to Molecular Bevel Gears: Future Work and Perspectives

"We shall not cease from exploration / And the end of all our exploring / Will be to arrive where we started / And know the place for the first time." (T. S. Eliot, Little Gidding, Four Quartets, 1942)

5.1 Synopsis

Beyond the aesthetic appeal of sterically crowded organometallic molecules, our interest in $(C_nR_n)ML_x$ cyclic arrays has evolved from their potential transformation into functional molecular bevel gears. As both convergent and divergent domains for facial and peripheral metal binding, we seek to establish the precise substitution patterns that will enable control of their static structure and dynamic capabilities. Although challenging, our modular synthetic strategy (Scheme 1.30) is tolerant of many functional groups and has allowed us to expand the repertory of stereochemical data that is available for persubstituted cyclopentadienyl, arene and cycloheptatrienyl systems. Notwithstanding these advancements, the gap between propeller molecule and gear entity persists, attributable in part to the dichotomies of the iconic and analogic models. Central to this thematic shift is coupled torsional motion, an obligatory feature that is derived from the tight intermeshing of component parts. As confirmed by the trends in rotational barriers,[429] the torsional itinerary is significantly influenced by the spatial disposition of the rotor axes (5 < 6 < 7 central rings), and the proximity and variations in 'tooth size' of the interacting n-fold rotors. Besides gear slippage, design considerations are further governed by the parity restriction for dynamic gearing, which in effect limit us to the use of n > 2-fold rotors and C_5R_4X, C_6R_6 or C_7R_6X fragments, respectively. Ultimately, we must formulate methods of (a) interlinking gears to enable the transmission of conformational information, and (b) interfacing the molecular arrays to the macroscopic world (i.e. on surfaces or at interfaces) to effect either parallel or serial concerted action. This is a formidable task, in that the transition between different lengths of

scale, from individual molecules to supramolecular structures and objects relevant to nanoscience, must necessarily involve the integration of rotary function. In continuing to probe these possibilities, persubstituted benzenes offer many exciting experimental directions.

5.2 Experimental Directions

5.2.1 Extended Fulvalene-linked Polyaryl Arrays

Insofar as the chemistry of indenyl platforms has been little explored (see Section 3.2.6), their unique design and properties may be considered for other discrete molecular architectures. For example, the $CuCl_2$-mediated oxidative coupling of two arylethynyl-substituted indenide anions, generated from deprotonation of either **3.45** or **3.48**, would afford an isomeric mixture of the *d,l* and/or *meso* 1,1'-, 1,3'- and 3,3'-biindenyl species, **5.1**.[430]. Subsequently, the dianion of **5.1** could be oxidized to the dibenzo[*a,f*]fulvalene, **5.2**, by treatment with iodine.[431] With its extensive 38 π-electron carbon network, **5.2** represents a spatially and directionally well-defined scaffold of significant structural, as well as electronic and optical, interest. Although its stability is less certain, the corresponding dibenzoferrocene, **5.3**, may be prepared by trapping of the anion of **3.45** (or **3.48**) with one-half an equivalent of iron(II) chloride-tetrahydrofuran complex $[FeCl_2{\cdot}(THF)_2]$ (Scheme 5.1).

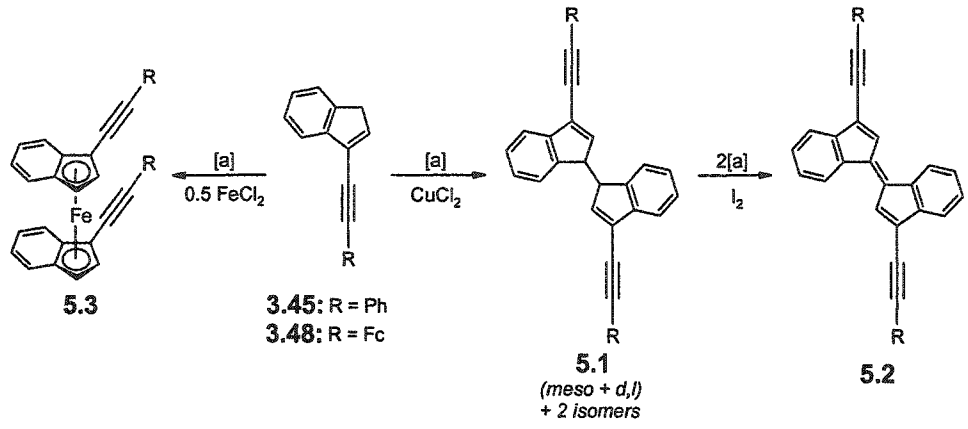

Scheme 5.1: *Oxidative coupling and salt metathesis methods employing **3.45** or **3.48**. [a] nBuLi / THF, -78 °C.*

Diels-Alder cycloadditions of the aforementioned dienophiles **5.1–5.3** to tetraphenylcyclopentadienone, **1.53**, should allow access to the more complex polyphenylated systems **5.4**, **5.5** and **5.6**, respectively. These extended hydrocarbons are attractive candidates for comparative structural studies, in that the conformation of the pentaphenylbenzene units may depend greatly on the hybridization and the capacity for free rotation about the indenyl-indenyl bond. Independent of metal complexation, the electron-transfer properties of **5.4** and **5.5** may also allow for interconversion between these bistable states, as a chirochemical or chiroptical switching mechanism[432] that involves a twisted configuration and the hitherto unutilized, planar dibenzofulvalene form with conducting capabilities.

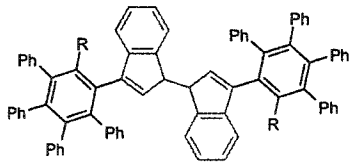

5.4
(meso + d,l)

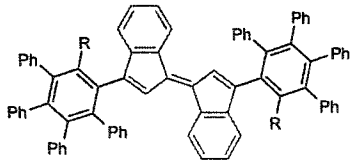

5.5
R = Ph or Fc

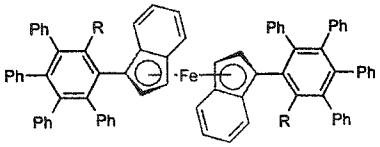

5.6
(meso + rac)

5.2.2 Ferrocenylalkynes to Oligoferrocenylphenyls

The utility of ferrocenylalkynes in systematically expanding the series of Fc-substituted benzenes, as well as cyclopentadienes and cycloheptatrienes, has yet to be exploited. In addition to their stereochemical intrigue (see **3.19**), these unique organometallic arrays may be targeted for their non-linear optical properties, as the oxidation state, redox behaviour and potential for metal-ligand or ligand-metal charge transfer of the ferrocenyl centers can be altered.[433] From a synthetic vantage, improved access to unsymmetrical bis(aryl)acetylenes bearing a ferrocenyl group has been made possible via transition metal mediated coupling between an aryl halide and terminal acetylene, or a single step procedure involving inexpensive chlorophosphonates.[287] These substrates can be used directly as dienophiles or converted to tetraarylcyclopentadienones. In this latter role, ferrocenyl-oligoalkynes are versatile intermediates. As a representative example, 1,1'-bis(phenylethynyl)ferrocene (cf. **5.7** to **5.3**), may

be oxidized to the tetraketone **5.8** and then condensed with two equivalents of a 1,3-diaryl acetone derivative to furnish the double Diels-Alder diene, **5.9** (Scheme 5.2). The Diels-Alder reactivity of this new class of ferrocenyl-linked bistetracyclones may be profitably compared to that of their hydrocarbon analogues.[266;267]

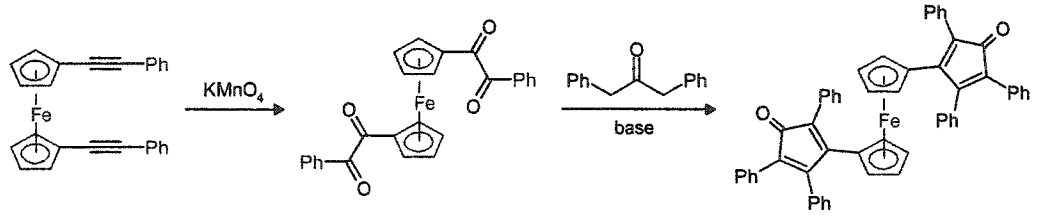

5.7 **5.8** **5.9**

Scheme 5.2: *Unsymmetrical ferrocenylalkynes offer a synthetic route to bistetracyclones, as exemplified by* ***5.9****.*

In testing the scope of cyclotrimerization methods, the catalytic activity of the methylidynetricobalt nonacarbonyl cluster relative to the parent dicobalt octacarbonyl may be a consideration.[434] The regioselective cyclization of 1,4-diphenyl-1,3-butadiyne, **3.25**, to give a 1,3,5-triphenyl substituted benzene suggests that the conjugated ferrocenyldiyne **5.10** will tolerate the same reaction, as depicted in Scheme 5.3. The electronic and stereochemical differences between **5.11** and the known 1,3,5-triferrocenylbenzene[435] are of interest, as is the steric accessibility of the triple bonds to metal ligating moieties and Diels-Alder dienes.

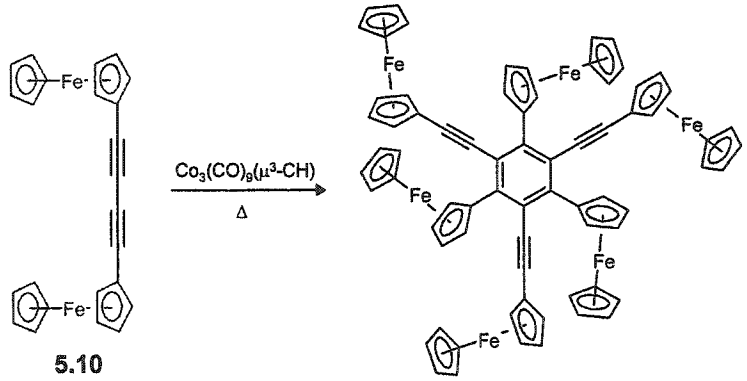

5.10 **5.11**

Scheme 5.3: *The cyclotrimerization of symmetrical ferrocenylalkynes to 1,3,5-$C_6Fc_3R_3$, such as* **5.11****.**

Another appealing target of study is hexaferrocenylbenzene, **5.14**, which is expected to manifest the most pronounced conformational preferences of this series on account of its persubstituted periphery. According to a 1967 report by Rosenblum et al.,[436] diferrocenylacetylene (**5.12**) reacts with dicobalt octacarbonyl to give $[Co_2(CO)_6(\mu\text{-}\eta^2{:}\eta^2\text{-}$ bis(ferrocenyl)acetylene)], which is easily oxidized to ferrocil, FcCOCOFc, and on treatment with **5.12** affords the blue tetraferrocenylcyclopentadienone, **5.13**. Subsequent attempts to induce **5.13** to enter into a Diels-Alder cycloaddition with diferrocenylacetylene at elevated temperatures failed. Although it may be the case that extreme steric crowding hinders the transformation to **5.14**, or its Dewar benzene isomer, it may also be possible to achieve favourable results using improved Diels-Alder reaction conditions (different solvents, increased reaction times) or cyclotrimerization methods (Scheme 5.4). In the end, whether the polyhedral organometallic moieties retain a thermodynamically favoured propeller or alternating *ababab* geometry is relevant to the next proposal.

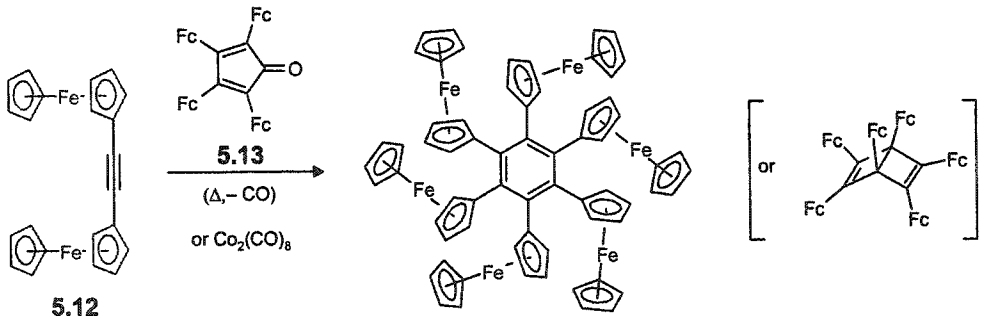

5.12 **5.14**

Scheme 5.4: *Synthesis of an organometalic pinwheel,* **5.14**.

5.2.3 Oligonuclear Coordination Compounds from Self-Assembly

The current chemical literature is replete with reports describing the use of persubstituted benzenes as sterically predisposed platforms for macrocycles and supramolecular assemblies.[437] The unique 1,3,5- versus 2,4,6-facial segregration that is observed in hexaethylbenzene and its derivatives (see Section 1.4.2.1) is the design principle which has inspired these varied tridentate

binding units. A similar stereochemical concept has been implemented in triarylmesitylenes, wherein the methyl groups were intended to enforce conformational rigidity.[438] Despite the geometry and overall dimensions of propeller derivatives, their potential for building supramolecular architectures has been overlooked, with the exception of Munakata's[293;294] organosilver(I) complexes of hexaphenylbenzene (**3.15**, **3.16**) and Kobayashi's[185;186] two-dimensional hexagonal hydrogen-bonded networks.

To promote the self-assembly of C_6Ar_6 domains, a coordination motif that involves dative bonding between transition metal fragments or ions and appropriate lone-pair-bearing ligands may be employed. Accordingly, the introduction of N-, S- or O-based functionalities into oligophenyls requires a modification of the classical synthetic protocols. Tetracyclones incorporating pyridine, thiophene, furan, pyrrole and carbazole have been reported,[285] as have many heteroaromatic derivatives of tolane. There are also examples which substantiate the Diels-Alder activity of these precursors,[173;439] including the recent pyrimidine-substituted benzenes prepared by Draper and co-workers.[283] Müllen has also expressed interest in thiol-terminated dendrimers capable of giving stable chemisorbed surface layers (on Au).[276] Using either the 'symmetry interaction' or 'molecular library' strategies for metal-ligand assembly,[440;441] new ensembles of various sizes, shapes and dimensions may be constructed. As a preliminary effort, trans palladium dichloride and n-pyridyl substituted benzenes may be assembled into linear or cyclic oligomers, as well as two-dimensional sheets with applications in crystal engineering (see Schemes 5.5 - 5.7, respectively).

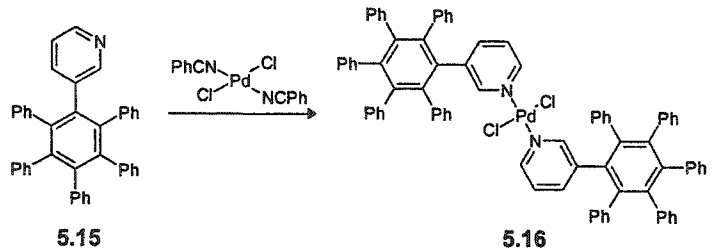

5.15 **5.16**

Scheme 5.5: *The palladium-based monometallic dimer* ***5.16*** *contains a single 3-pyridyl linker.*

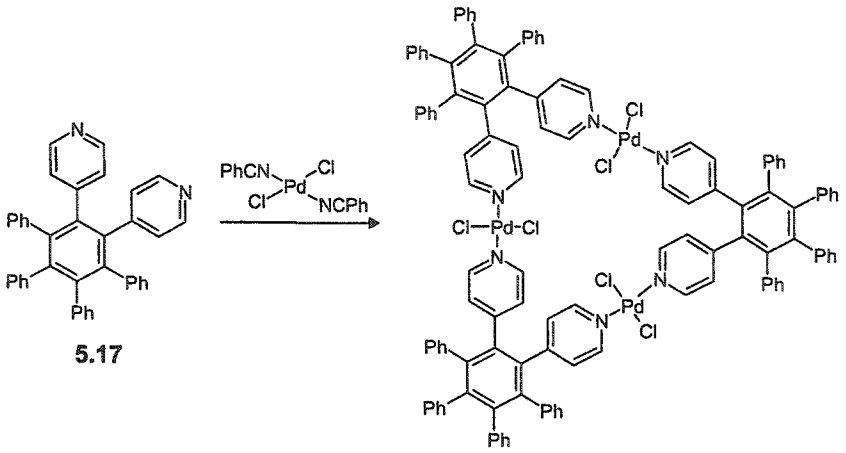

5.17

5.18

Scheme 5.6: *The trimeric oligomer* ***5.18*** *formed from 1,2-bis(4-pyridyl)-3,4,5,6-tetraphenylbenzene (****5.17****) and trans-Pd(NCPh)$_2$Cl$_2$.*

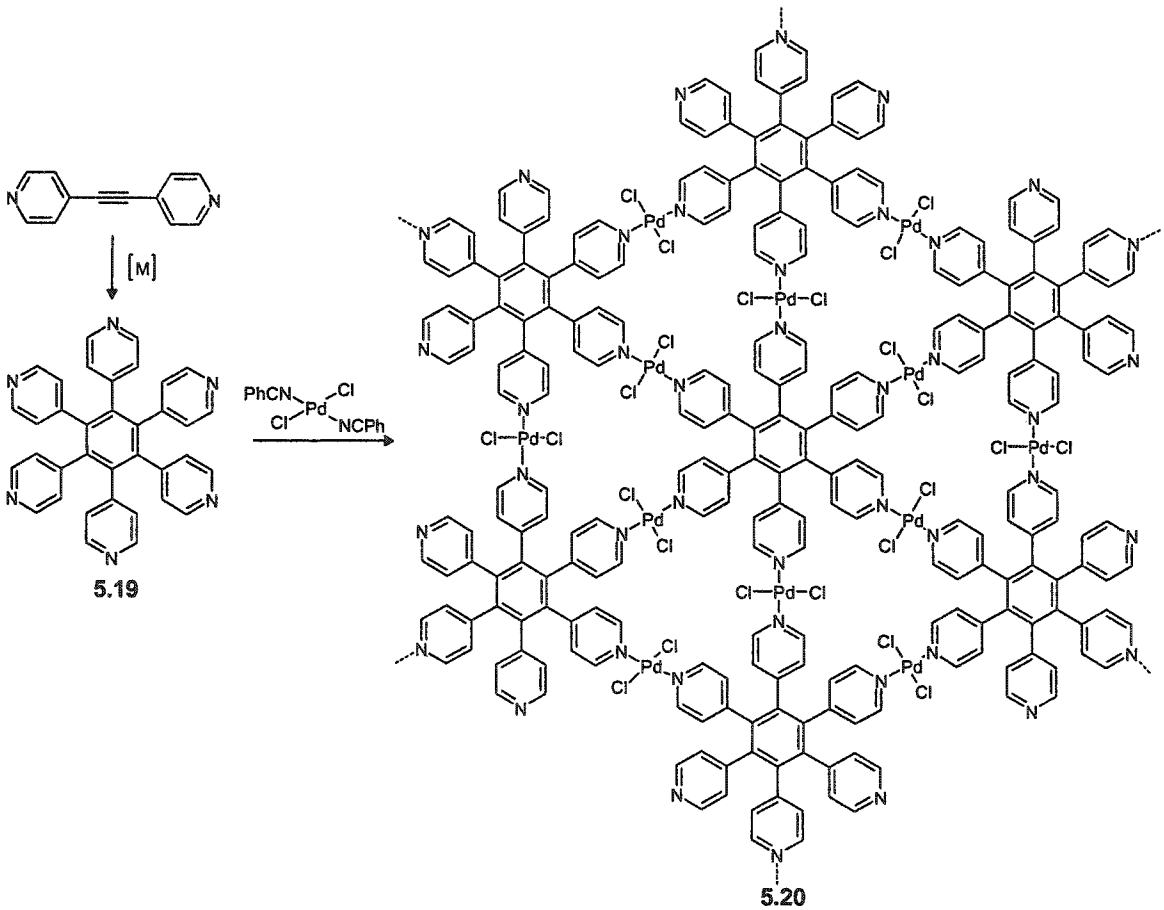

5.19

5.20

Scheme 5.7: *A 2-D C$_6$Ar$_6$ lattice assembled from trans-Pd(NCPh)$_2$Cl$_2$ and hexakis(4-pyridyl)benzene.*

5.3 With an Eye to the Future: Societal Implications of Nanoscience

The extension of macroscopic concepts of a device or machine to the molecular level is of interest not only for basic research, but also for the growth of nanoscience and the evolution of nanotechnology.[26] As the latter has only just begun, it is difficult to predict whether the impact on society will be revolutionary or insignificant.[442] Scientific opportunities have been rapidly advanced by the emergence and refinement of tools for the study of phenomena, and the fabrication of structures, at the nanoscale level.[443] While the potential transfer of this knowledge into practical applications is the basis for popular enthusiasm in this multidisciplinary arena, the anticipation presently has reached beyond the ability of the field to deliver. Along with creativity and daring ideas, future outcomes are dependent on clear strategies that encompass education and training, changes in policy related to funding, national programs, international security, privacy issues and public perception, and ongoing assessment of the short and long-term implications and risks of the new "nano" technologies.[444]

CHAPTER SIX

Experimental and Computational Details

6.1 General Synthetic Protocol

All syntheses were performed under an atmosphere of dry nitrogen utilizing conventional benchtop and glovebag techniques. Solvents were dried and distilled according to standard procedures.[445] Unless otherwise specified, reagents were purchased from either Aldrich Chemicals Company, Inc., Strem Chemical, Inc. (hexacarbonylchromium and octacarbonyldicobalt) or Cambridge Isotope Laboratories (deuterated NMR solvents) and used as received. Silica gel (particle size: 20 - 45 μm) was employed for flash column chromatography.

6.2 Physical Methods

6.2.1 Melting Points

Melting points (uncorrected) were recorded on either a Thomas Hoover Unimelt capillary or a Fisher-Jones melting point apparatus.

6.2.2 Elemental Analyses

Microanalyses were performed by Guelph Chemical Laboratories (Guelph, Ontario, Canada).

6.2.3 IR Spectroscopy

Infrared spectra were obtained from liquid samples on a Bio-Rad FTS-40 FT-IR spectrometer using 0.1 mm NaCl windows.

6.2.4 Mass Spectrometry

Low-resolution mass spectra were collected on either the VG analytical ZAB-E or the Finnigan 4500 Quadrupole instrument by direct electron impact and direct chemical ionization (NH_3) methods. High-resolution EI measurements were obtained on the VG ZAB-R instrument.

Electrospray ionization (ESI), atmospheric pressure chemical ionization (APcI) and MS/MS spectra were acquired on a Micromass Quattro-LC triple quadrupole mass spectrometer. For pneumatically assisted electrospray, samples were injected into a mobile phase consisting of 50/50 CH_3CN/H_2O flowing at 10 μl/min. Typical experimental conditions included a source temperature of 80°C, an ESI probe voltage of 3.1 kV, and gas flow rates (N_2 at 100 psi) of approximately 600 l/hour for the drying gas and 60 L/hr for the ESI nebulising gas. MS/MS experiments were performed utilizing argon as the target gas, at a pressure of 1.9×10^{-3} mbar and a collision energy of 20 eV. ApcI samples were dissolved in acetonitrile or $MeOH/H_2O$ and injected at a 50 μL/min flow rate with a discharge needle (3.2-3.2 kV) and temperature of usually 450°C.

6.2.5 NMR Spectroscopy

Ambient-temperature ^1H- and ^{13}C-NMR spectra were acquired by use of a Bruker AC-200 (^1H: 200.13 MHz; ^{13}C: 50.34 MHz) or Avance DRX-500 (^1H: 500.13 MHz, ^{13}C: 125.76 MHz) spectrometer on spinning, or non-spinning samples, respectively, locked to a deuterated solvent signal. ^{19}F NMR spectra were collected with use of a Bruker AC 300 spectrometer (^{19}F: 282.4 MHz). Variable-temperature NMR spectra were recorded on a Bruker Avance DRX-500 spectrometer equipped with an 11.74 T superconducting magnet, a Bruker B-VT 2000 temperature controller, and a 5 mm broad-band inverse probe with triple axis gradient capability. One-dimensional ^1H and ^{13}C NMR spectra, as well as two-dimensional ^1H-^1H COSY, ^1H-^{13}C shift correlated, and long range ^1H-^{13}C shift correlated spectra were recorded on spinning samples (except during the acquisition of 2-D spectra), locked to a solvent signal. In all cases, NMR resonances were referenced to an external trichlorofluoromethane signal or a residual proton or ^{13}C signal of the solvent.

6.2.6 X-Ray Crystallography

Single crystal samples, mounted on a glass fiber, were employed in all X-ray crystallographic experiments. Data for compounds **3.18**, **3.26**, **3.35**, **3.39**, **3.40**, **1.139**, **4.38** and

4.44 were collected using a P4 Siemens diffractometer, equipped with a Siemens SMART 1K Charge-Coupled Device (CCD) Area Detector (employing the program SMART[446]) and a rotating anode utilizing graphite-monochromated Mo-Kα radiation (λ = 0.71073 Å). The crystal-to-detector distance was 3.991 or 4.987 cm, and the data acquisition was carried out in 512 x 512 pixel mode, employing 2 x 2 pixel binning. The initial unit cell parameters were determined by a least-squares fit of the angular settings of the strong reflections, measured by a 4.5 / 12 degree scan in 15 / 40 frames over three different parts of reciprocal space (45 / 120 frames in total).* One complete hemisphere of data was collected, to better than 0.8 Å resolution (**3.40** is an exception). At this time and only if necessary, the first 50 frames were recollected in order to improve the decay analysis. Data processing was carried out by use of the program SAINT,[447] which applied Lorentz and polarization corrections to three-dimensionally integrated diffraction spots. The program SADABS[448] was utilized for the scaling of diffraction data, the application of a decay correction, and an empirical absorption correction based on redundant reflections. All structures were solved by use of the direct method procedure outlined in the Siemens SHELXTL program library,[449] followed by full-matrix least squares refinement on F^2 with anisotropic thermal parameters for all non-hydrogen atoms. Unless otherwise indicated, hydrogen atoms were added as fixed contributors at calculated positions, and refined using a riding model with isotropic thermal parameters based on the atoms to which they were bonded. To confirm that no extra crystallographic symmetry was overlooked in the structure solution, all data sets were checked with use of the program PLATON.[450;451] For cell parameters and intensity collection refer to the Tables provided in the Appendix B.

After attempts to model the orientational disorder associated with an acetone solvent in **3.35**, the electron density associated with the molecules (two per unit cell) was removed from the

---

* The first conditions apply to compounds **3.18**, **3.26**, **3.35**, **1.139**, **4.38**, and **4.44** and the latter details to **3.39** and **3.40**.

difference map with use of the SQUEEZE/BYPASS function[452] implemented in the program PLATON,[451] and the resulting data refined accordingly.

The absolute structure of **3.39** was set to the known configuration and confirmed by the Flack parameter. With the beta angle approximately equal to 90°, pseudo-orthorhombic twinning about the c axis was modeled by the matrix (-1000-10001) with a final fractional contribution (BASF) of 3.8%. Phenyl group disorders in both molecules (C13A – C18A and C13 – C18; C13B – C18B and C13' – C18') of the asymmetric unit were modeled with use of an EADP constraint and a fixed occupancy factor of 50% (confirmed as a free variable). The hydrogens atoms for each unique component of the conformational disorder were added at calculated positions and allowed to refine based on the carbon atoms to which they were attached. A rotating group refinement was employed for the two OH hydrogens.

No significant diffraction was observed beyond 1.05 Å resolution for the crystal sample of **3.40**, resulting in an incomplete refinement of the corresponding data; the phenyl rings were modeled as ideal hexagons and all atoms were treated isotropically.

In the case of **1.139**, rotational disorder of the fluorine atoms F7, F8 and F9 in one of the CF_3CO_2H molecules and a conformational disorder involving C82, O3 and O4 in the other solvate molecule was established by refinement of the population factors F7, F8, F9 and F7A, F8A, F9A and C82, O3, O4 and C82A, O3A and O4A, respectively, with a final occupancy ratio of approximately 50:50.

6.3 Syntheses and Characterization of Compounds

$(C_6Ph_5\text{-}C_5H_4)Fe(C_5H_5)$, 3.19. In a modification of the synthesis published by Siegel and Rausch,[312] diphenylacetylene, **3.11** (0.018 g, 1.0 mmol) and 3-ferrocenyl-2,4,5-triphenylcyclopentadienone, **1.54** (0.492 g, 1.0 mmol), which was prepared according to the literature procedure[314] from the reaction of ferrocenylphenylglyoxal[453] and dibenzyl ketone in

refluxing ethanolic potassium hydroxide, were sealed under vacuum in a glass tube and heated at 200 °C for 48 hours. The reaction mixture was subsequently cooled to room temperature, the tube broken carefully, and the residue extracted with CH_2Cl_2 (~ 50 mL) and filtered. The addition of hexanes (~ 50 mL) to the filtrate facilitated the precipitation of a dark solid. After removal of the solvent the recovered material was subjected to flash chromatography on silica gel. Elution with hexane/CH_2Cl_2 (50:50, 25:75, 0:100) afforded an orange-yellow band which was collected and evaporated to give **3.19** as an orange-yellow solid, mp > 265 °C (0.215 g, 0.335 mmol, 34%). ^{1}H NMR (CD_2Cl_2, 500 MHz, 25°C): δ = 7.07 (m, 10H, H(*aromatic*)), 6.81 (m, 15H, H(*aromatic*)), 3.85 (m, 2H, C_5H_4), 3.75 (m, 2H, C_5H_4), 3.71 (s, 5H, C_5H_5); ^{13}C NMR (CD_2Cl_2, 125 MHz, 25°C): δ = 132.6 (4C), 131.7 (4C), 131.5 (2C), 127.0 (4C), 126.7 (2C), 126.6 (4C), 126.1 (2C), 125.4 (1C), 125.3 (2C), 69.0 (2C, C_5H_4), 68.5 (5C, C_5H_5), 68.0 (2C, C_5H_4); LRMS (DEI): *m/z* (%) = 642 (64) $[M]^+$, 577 (74) $[M - C_5H_5]^+$, 120 (100) $[M - C_6Ph_5(C_5H_5)]^+$, 55 (88); LRMS (DCI): *m/z* (%) = 643 (100) $[M + H]^+$, 577 (25). A sample suitable for structural determination by single-crystal X-ray diffraction was obtained by recrystallization from hexane/CH_2Cl_2.

1-(pentaphenylphenyl)-2-phenylacetylene, 3.26. According to the procedure outlined by Dilthey et al.[318] 2,3,4,5-tetraphenylcyclopentadienone, **1.53** (0.385 g, 1.0 mmol) and 1,4-diphenylbutadiyne, **3.25** (0.204 mg, 1.0 mmol), were heated at 250 °C in an atmosphere of N_2 for 4.5 hours. After cooling, the residue was washed with 40 mL of hexanes and filtered. The off-white solid was then dissolved in 15 mL of CH_2Cl_2 and following the addition of 20 mL of hexanes to this solution, it was left for recrystallization over several days. It is from this blend that white needles of the title compound, **3.26**, were isolated. Yield: 0.360 g (0.65 mmol, 65%); m.p. 260, lit. 258 (±1) °C.[318] ^{1}H NMR (CD_2Cl_2, 500 MHz, 25 °C): δ = 7.30 - 7.28 (m, 4H), 7.25 - 7.09 (m, 9H), 6.94 - 6.86 (m, 15H), 6.69 - 6.67 (m, 2H); ^{13}C NMR (CD_2Cl_2, 125 MHz, 25°C): δ = 143.8 (2C), 142.0 (1C) 141.2 (2C), 140.9 (2C), 140.8 (1C), 140.6 (2C) (C-*ipso* and 3 C_6-central ring), 131.9 (4C), 131.8 (2C), 131.5 (2C),

131.4 (4C), 128.6 (2C), 128.5 (1C), 127.6 (4C), 127.3 (4C), 127.1 (2C), 127.0 (2C), 126.1 (2C), 126.0 (1C), 123.9 (1C), 123.2 (1C) (C-*ortho*, C-*meta*, C-*para*, 2 C_6-central/terminal ring), 97.3 (1C, C≡C), 89.9 (1C, C≡C); LRMS (DEI): *m/z* (%) = 558 (100) $[M]^+$; HRMS: *m/z* calcd for $C_{44}H_{30}$ 558.2348 $[M]^+$, found 558.2327. Crystals suitable for X-ray diffraction studies were carefully grown at low temperatures from a 1:1 solution of CH_2Cl_2/acetone.

Reaction of 3.26 and $Co_2(CO)_8$: 1-(pentaphenylphenyl)-2-phenylacetylene, **3.26**, (0.249 g, 0.45 mmol) and hexacarbonylchromium (0.150 g, 0.45 mmol) were dissolved in freshly distilled THF (~ 10 mL) and stirred under an atmosphere of N_2 at ambient temperature for 48 hours. After solvent evaporation the residue was subjected to column chromatography on silica gel with hexanes/CH_2Cl_2 combinations (100/0 to 50/50) as the eluent. Of the two pale yellow bands that were collected, the second was identified by ^{1}H-, ^{13}C-NMR and MS data as the starting material.

Reaction of 3.26 and $Pt(Ph_3)_4$: 1-(pentaphenylphenyl)-2-phenylacetylene, **3.26**, (0.279 g, 0.50 mmol) and $[Pt(PPh_3)_4]$ (0.622 g, 0.50 mmol), prepared in advance according to the literature procedure,[327] were dissolved in CH_2Cl_2 (20 mL) and the solution stirred under N_2 at ambient temperature for 24 hours. No precipitation was observed upon volume reduction and addition of hexanes, suggesting that the reaction was not a success. Chromatographic purification on a silica gel column resulted in the recovery of the starting material only, as confirmed by spectroscopic (^{1}H-, ^{13}C-NMR and IR) and spectrometric (MS) data.

1-(1,2-*Z*-dibromo-2-phenylvinyl)-2,3,4,5,6-pentaphenylbenzene, 3.35. To 1-(pentaphenyl-phenyl)-2-phenylacetylene, **3.26**, (0.279 g, 0.50 mmol) dissolved in CCl_4 (10 mL) was added two to three drops of Br_2 (large excess); the solution was stirred vigorously at room temperature for five days. Following solvent removal the isolated solid was washed with CCl_4 and later acetone, and

then dried *in vacuo*. Recrystallization in CH_2Cl_2/acetone produced a light yellow solid. Yield: 358 mg (0.49 mmol, 98%); mp > 250 °C. The presence of two components was verified when a sample dissolved in ~ 90:10 acetonitrile:H_2O was ejected into a 4.6 x 150 mm HPLC analytical column at 2 ml/min, 85% acetonitrile:H_2O composition operating at 254 nm. ^{1}H NMR (CD_2Cl_2, 500 MHz, 25 °C):* δ = 7.26 - 7.29 (m, 2H), 7.25 - 7.14 (m, 8H), 7.09, (m, 2H), 6.90 - 6.93 (m, 4H), 6.82 - 6.86 (m, 8H), 6.75 - 6.77 (m, 4H), 6.49 - 6.51 (m, 2H). ^{13}C NMR (CD_2Cl_2, 125 MHz, 25°C): δ = 143.4 (1C), 142.3 (2C), 140.8 (1C), 140.6 (2C), 140.5 (2C), 139.7 (1C), 138.6 (1C), 137.3 (1C) (C-*ipso* and C_6-central ring) 132.0, 131.8, 131.4, 131.1, 130.7, 130.7, 129.1, 129.0, 128.7, 128.6, 127.5, 127.4, 127.2, 127.1, 126.9, 126.4, 126.0 (C-*ortho*, C-*meta*, C-*para*, C=C)*; LRMS (DEI): *m/z* (%) = 716 (10) $[M]^+$, 639 (5) $[M - Br]^+$, 557 (100) $[M - 2Br]^+$, 481 (25) $[M - 2Br - Ph)]^+$, 403 (20) $[M - 2Br - 2Ph)]^+$; LRMS (DCI): *m/z* (%) = 716 (15) $[M]^+$, 639 (5) $[M - Br]^+$, 558 (100) $[M - 2Br]^+$, 481 (30) $[M - 2Br - Ph)]^+$ (Peaks quoted correspond to the lowest mass (^{79}Br); isotopic distribution is evident); HRMS: *m/z* calcd for $C_{44}H_{30}Br_2$ 716.0714 $[M]^+$, found 716.0616. *Resonances corresponding to a second isomer (~18%) were also observed in the ^{1}H spectrum. X-ray quality crystals of the *cis* isomer, presumably the major product, were isolated from the CH_2Cl_2/hexanes supernatant.

2-(phenylethynyl)isoborneol, 3.39. To phenylacetylene (26.2 mmol, 2.88 mL) in freshly distilled THF (20 mL) under nitrogen at -78 °C was added dropwise *n*-BuLi (~ 14.8 mL, 1.6 M). The resulting solution was warmed to room temperature and stirred for 3 hrs. Upon re-cooling to - 78 °C, (1R)-(+)-camphor (26.2 mmol, 4.0 g) in dry THF (20 mL) was slowly added. A pale creamy to orange colour change was noted as the mixture warmed to room temperature while stirring overnight. Removal of THF and re-dissolution in diethyl ether was followed by quenching with 5% aqueous HCl (3 x 30 mL), neutralization with 10% $NaHCO_3$ (30 mL) and drying of the organic layer over anhydrous $MgSO_4$. Chromatographic purification of the residue on a silica gel column with hexanes as the eluent yielded **3.39** (rather than its dehydrated form) as a white crystalline solid, (4.39 g, 17.3 mmol, 66%). ^{1}H and

^{13}C NMR chemical shifts are consistent with published data.[335] LRMS (DEI): *m/z* (%) = 254 (25) $[M]^+$, 237 (35) $[M - OH]^+$, 144 (95) $[M - C_5H_5(Me)_3]^+$, 95 (55) $[C_7H_{11}]^+$; LRMS (DCI): *m/z* (%) = 254 (7) $[M + H - H]^+$; 237 (100) $[M - OH]^+$, 144 (70) $[M - C_5H_5(Me)_3]^+$, 95 (45) $[C_7H_{11}]^+$; HRMS: *m/z* calcd for $C_{18}H_{22}O$ 254.1671 $[M]^+$, found 254.1652. A crystalline sample suitable for X-ray structure determination was produced by slow growth from a refrigerated aliquot dissolved in hexanes.

1-(2β-born-2,3-en-2-yl)-2,3,4,5,6-pentaphenylbenzene, 3.40. 2α-Phenylethynyl-2β-hydroxy-bornane, **3.39** (0.666 g, 2.62 mmol) and 2,3,4,5-tetraphenylcyclopentadienone, **1.53** (0.600 g, 1.56 mmol) were combined neat in an open flask and flame heated (> 200 °C). After approximately 40 min. the molten mixture appeared to have changed from magenta to dark brown in colour, and diphenyl ether (10 mL) was added to the melt. To effect precipitation, hexanes (20 mL) were added dropwise to the cooled reaction mixture. The product was filtered under suction, re-precipitated in ethanol until the red colour of unreacted **1.53** had disappeared, and then dried *in vacuo* to give an off-white solid. Yield: 0.157 g (0.26 mmol, 17%); mp > 250 °C. ^1H NMR ($CDCl_3$, 200 MHz, 25 °C): δ = 6.59 - 7.09 (m, 25H), 5.91 (m, 1H, C3-H), 2.15 (m, 2H), 1.51 (m, 2H), 1.09 (m, 1H), 0.75 (s, 3H, CH_3), 0.40 (s, 3H, CH_3), 0.2 (s, 3H, CH_3); ^{13}C NMR ($CDCl_3$, 50 MHz, 25 °C): δ = 140.9, 136.5 (weak C-*ipso* or C_6-central ring) 131.7, 131.4, 130.6, 126.7, 126.4, 125.9, 124.8 (C-*ortho*, C-*meta*, C-*para*, C=C), 29.7, 25.3, 20.3, 17.7, 13.7, 12.8 (bornene ring). LRMS (DEI): *m/z* (%) = 592 (100) $[M]^+$, 564 (45) $[M - C_2H_4]^+$, 549 (25) $[M - C_3H_7]^+$; LRMS (DCI): *m/z* (%) = 592 (100) $[M]^+$, 564 (30) $[M - C_2H_4]^+$, 469 (10) $[C_6Ph_5C]^+$; HRMS: *m/z* calcd for $C_{46}H_{40}$ 592.3101 $[M]^+$, found 592.3130. The growth of appropriately sized crystals for an X-ray diffraction study proved to be difficult, although data was eventually collected on a sample of **3.40** extracted from an NMR tube (deuterated chloroform) stored in refrigeration.

3-phenylethynylindene, 3.45. Following the dropwise addition of *n*-BuLi (~ 32.8 mL, 1.6 M) to phenylacetylene (58.3 mmol, 6.40 mL) in dry THF (20 mL) under nitrogen at -78 °C, the resulting solution was stirred at room temperature for 3 hours prior to its re-cooling. To lithium phenylacetylide at - 78 °C was slowly cannulated 1-indanone (29.1 mmol, 3.85 g) dissolved in dry THF (20 mL). The mixture was allowed to gradually warm to room temperature and stirred overnight, after which time it had assumed a deep orange-red colour. The residue was then reduced in volume, re-dissolved in diethyl ether, quenched with 5% aqueous HCl (3 x 30 mL) and neutralized with 10% $NaHCO_3$ (30 mL). The organic layer was collected, dried over anhydrous $MgSO_4$, concentrated and subjected to flash column chromatography on silica gel using 100% hexanes and later hexanes:CH_2Cl_2 eluent combinations of increasing polarity. The second fraction to elute, an orange-yellow band, was collected and evaporated to give **3.45** as an orange-yellow oily solid, m.p. 115-117 °C (4.51 g, 20.9 mmol, 72%). ^{1}H NMR (CD_2Cl_2, 200 MHz, 25°C): δ = 3.60 (d, 2H, J = 2.2), 6.96 (t, 1H, J = 1.7), 7.39 - 7.75 (m, 9H); ^{13}C NMR ($CDCl_3$, 50 MHz, 25°C): δ = 143.9 (1C), 142.7 (1C), 138.3 (2C), 131.8 (2C), 128.5 (3C), 126.6 (1C), 126.5 (1C), 125.6 (1C), 123.8 (1C), 123.3 (*C-1*), 120.4 (1C), 93.0 (*C*=*C*), 83.6 (*C*=*C*), 38.7 (*C-3*); LRMS (DEI): *m/z* (%) = 216 (100) $[M]^+$; LRMS (DCI): *m/z* (%) = 217 (100) $[M + H]^+$; HRMS: *m/z* calcd for $C_{17}H_{12}$ 216.0939 $[M]^+$, found 216.0942.

Reaction of 3.45 and tetracyclone: 3-phenylethynylindene, **3.45** (0.114 g, 0.50 mmol) and 2,3,4,5-tetraphenylcyclopentadienone, **1.53** (0.203 g, 0.50 mmol) were sealed under vacuum (following deoxygenation by a series of freeze-pump-thaw cycles) in a glass ampoule and heated at 220 (±10)°C for 28 hours. Despite the prevailing magenta colour, the reaction was cooled to room temperature, the tube broken carefully and the residue extracted with CH_2Cl_2. Column chromatography on silica gel, with hexanes/CH_2Cl_2 eluent combinations of 100/0 to 50/50, afforded numerous fractions, but none were identified as the desired product, 1-(pentaphenylphenyl)indene, **3.46**. Instead, from a dark orange band was isolated the reduced form of **1.53**, 2,3,4,5-tetraphenylcyclopenta-2-en-1-one, as

confirmed by mass spectrometric and X-ray diffraction analyses.[349] In a second attempt to generate **3.46**, a mixture of **3.45** (1.320 g, 6.10 mmol) and **1.53** (2.346 g, 6.10 mmol) was refluxed for 12 hours in diphenyl ether (10 mL) under an N_2 atmosphere. No solid product was isolated upon work-up (cooling, addition of hexanes and filtration).

$[C_7Ph_7^+][CF_3CO_2^-]\cdot 2CF_3CO_2H$, 1.139. Bright orange-red needles of $C_7Ph_7^+Br^-$ were prepared from C_7Ph_7H and bromine in CCl_4, followed by treatment with acetonitrile containing 6% acetone, as outlined in the literature.[232] Subsequent digestion of $C_7Ph_7^+Br^-$ (352 mg, 0.50 mmol) in a solution of trifluoroacetic acid proceeded by filtration and slow solvent evaporation over several days produced red plates of the title compound, **1.139**. Yield: 260 mg (0.27 mmol, 54%, based on $C_7Ph_7^+Br^-$); m.p. 160 °C; ^{1}H NMR (CD_3CN, 500 MHz, 25 °C): δ = 6.89 (d of d, ^1J = 8.1 Hz, ^2J = 1.6 Hz, 14H, H(*ortho*)), 6.83 (m, 21H, H(*meta*) and H(*para*); ^{13}C NMR (CD_3CN, 125 MHz, 25 °C): δ = 167.2 (C_7-ring)), 141.5 (C-*ipso*)), 130.4 (C-*ortho*), 127.8 (C-*para*), 127.5 (C-*meta*); ^{19}F NMR (CD_3CN, 282.4 MHz, 25°C): δ = -76.2 (s); MS (+ESI): *m/z* (%) = 623.2 (100) $[M]^+$; MS (ESI MS/MS of $[M]^+$ ion): *m/z* (%) = 545.2 (100) $[M - C_6H_6]^+$, 533.2 (7) $[M - C_7H_6]^+$, 467.2 (18) $[M - 2C_6H_6]^+$, 455.2 (8) $[M - 2C_7H_6]^+$, 367.1 (11), 343.1 (6), 291.1 (8), 166.9 (35); $C_{55}H_{37}F_9O_6$ (964.85): calcd. C 68.47, H 3.86, found C 68.49, H 4.00.

$(\eta^5\text{-}C_5H_5)Fe(\eta^5\text{-}C_5H_4\text{-}C_7Ph_6H)$, 4.38. 3-Ferrocenyl-2,4,5-triphenylcyclopentadienone, **1.54**, (0.049 g, 0.10 mmol),[314] was combined with 1,2,3-triphenylcyclopropene, **4.13**, (0.027 g, 0.10 mmol) in 5 mL of dry xylene. The reaction mixture was refluxed at approximately 170 °C in an atmosphere of N_2 for 48 hours, and then cooled to room temperature. Thereafter, the reaction flask was stored at -20 °C for 72 hours, yielding red-orange crystals of **4.38**, which were isolated by filtration, washed with hexanes (~ 5 mL) and dried *in vacuo*, mp > 265 °C (0.045 g, 0.062 mmol, 62%). ^{1}H NMR (CD_2Cl_2, 500 MHz, 25 °C): δ = 7.97 (d, 2H, ^3J = 8.2 Hz, H(72A) and H(76A)

(*ortho*)), 7.54 (t, 2H, ^3J = 8.0 Hz, H(73A) and H(75A) (*meta*)) 7.43 (t, 1H, ^3J = 7.1 Hz, H(74A) (*para*)), 7.39 (d, 2H, ^3J = 6.4 Hz, H(62A) and H(66A) (*ortho*)), 7.20 (m, 3H, H(63A), H(65A) (*meta*) and H(64A) (*para*)), 7.15 (m, 3H, H(23A), H(25A) (*meta*) and H(24A) (*para*)), 6.90 - 7.10 (m, 5H, H(52A), H(56A) (*ortho*), H(53A), H(55A) (*meta*) and H(54A) (*para*)), 6.88 (m, 2H, H(22A) and H(26A) (*ortho*)), 6.71 (t, 1H, ^3J = 7.3 Hz, H(44A) (*para*)), 6.64 (t, 2H, ^3J = 7.9 Hz, H(43A) and H(45A) (*meta*), 6.55 (m, 3H, H(33A), H(35A) (*meta*) and H(34A) (*para*)), 6.31 (m, 2H, H(32A) and H(36A) (*ortho*)), 6.05 (d, 2H, ^3J = 7.3 Hz, H(42A) and H(46A) (*ortho*)), 5.64 (s, 1H, sp^3-H (H(7A))), 3.88 (s, 5H, η^5-C_5H_5 (H(16A), H(17A), H(18A), H(19A), H(20A))), 3.90 (s, 1H, η^5-C_5H_4), 3.82 (s, 1H, η^5-C_5H_4), 3.78 (s, 1H, η^5-C_5H_4), 3.22 (s, 1H, η^5-C_5H_4); ^{13}C NMR (CD_2Cl_2, 125 MHz, 25 °C): δ = 144.2, 143.7, 143.4, 141.4, 141.2, 140.8, 136.5 (C-*ipso* and C_7-ring), 131.7, 131.1, 131.0, 130.8, 130.7, 128.1, 127.7, 127.3, 127.2, 127.0, 126.6, 126.1, 125.8, 124.9, 124.6 (C-*ortho*, C-*meta*, C-*para*), 68.5 (η^5-C_5H_5, C(16-C(20)), 68.9, 68.5, 67.9, 67.8 (η^5-C_5H_4, C(11)-C(15)), 56.3 (sp^3-C, C(7));* LRMS (DEI): *m/z* (%) = 732 (75) $[M]^+$; LRMS (DCI): *m/z* (%) = 733 (100) $[M + H]^+$, 141 (86); $C_{53}H_{40}Fe$ (732.70): calcd. C 86.88, H 5.50, found C 87.00, H 5.76. Single crystals suitable for X-ray diffraction studies were selected directly from the xylene solution. (**Note:* Definitive NMR assignment of phenyl rings 3 and 4 was not possible; it should be recognized that the chemical shift assignments could be interchanged.)

[(η^5-C_5H_5)Fe(η^5-C_5H_4-C_7Ph_6H]$^+$[$SbCl_6$]$^-$, 4.44. (η^5-C_5H_5)Fe(η^5-C_5H_4-C_7Ph_6H), **4.38**, (0.073 g, 0.1 mmol) and triethyloxonium hexachloroantimonate (0.044 g, 0.1 mmol) were dissolved in freshly distilled CH_2Cl_2 (~ 5 mL) and stirred under an atmosphere of N_2 at ambient temperature for 24 hours. The reaction mixture was filtered, and from the filtrate dark blue-green crystals of **4.44** were isolated after several days of slow solvent evaporation at reduced temperatures, mp: decomposes on heating (0.026 g, 0.062 mmol, 24%). Crystals suitable for structural determination by single-crystal X-ray diffraction were carefully selected.

6.4 Computational Methods

6.4.1 C_5Ar_5 and C_5Ar_4X Study

The relative energies of $C_5Ph_5^-$ **1.18**, $C_5Ph_4H^-$ **2.1**, $C_4Ph_4C{=}O$ **1.53** and $C_4Ph_4CH_2$ **2.2** were calculated at the semi-empirical level of theory (AM1 Hamiltonian)[257] by systematically altering the two selected angles ϕ_n in 10° increments (dihedral driver option in SPARTAN V5.1)[258] from 0° to 90° and 0° to 180°, while allowing all other torsional degrees of freedom to minimize accordingly. For comparative purposes, the conformational plots were also computed using molecular mechanics methods (MMFF94[259] and Sybyl[260] force fields). To confirm the nature of specific stationary points along the PES of **1.18**, **2.1**, **1.53** and **2.4**, geometry optimizations and subsequent frequency analyses were performed using the AM1 Hamiltonian as implemented in the GAUSSIAN98 program suite.[261] The visualization and depiction of structures was enabled with QMView.[454]

6.4.2 C_6Ar_6 and C_6Ar_5X Study

High-level (*ab initio* and otherwise) computations were performed on a series of hexaarylbenzene derivatives with the aid of analytically determined gradients and search algorithms contained within the GAMESS and GAUSSIAN98 software programs.[261;455] Restricted Hartree-Fock (RHF),[296] hybrid density functional (HDFT)[297] and second-order Moller-Plesset perturbation (MP2)[456] methods were investigated in conjunction with a variety of basis sets (STO-3G, 3-21G(nd), 6-31G(nd,mp), cc-pVDZ, where n,m=0,1).** Such a comparative study enabled the structural and energetic sensitivity to dynamic correlation and polarization functionality to be assessed. The HDFT methods employed Becke's 3-parameter exchange functional,[298] in combination with either the nonlocal correlation provided by either the Lee-Yang-Parr expression (B3LYP),[457;458] which contains both local and nonlocal terms, or the Perdew 91 expression (B3PW91).[300;459] For hydrocarbons of this size and constitution, HDFT techniques

offer a significant advantage over conventional *ab initio* methods, as they implicitly incorporate electron correlation effects at considerable savings in computational time.

**In order to establish an accurate methodology with which to pursue the full analysis of this class of compounds, an exhaustive basis set and method analysis was conducted in the form of *rigid* potential energy surface scans. For each model chemistry [AM1, RHF/STO-3G, RHF/3-216, RHF/3-21G*, RHF/6-31G(d), RHF/6-31G(d,p), RHF/cc-pVDZ, B3PW91/3-216, B3PW91/3-21G*, B3PW91/6-31G(d), B3PW91/6-31G(d,p), B3PW91/cc-pVDZ] single point energy evaluations were performed over a rectangular grid involving the selected internal coordinates corresponding to the M_0 to M_1 rearrangement (i.e. 10° steps from 90° to 180° for a single phenyl group). A *relaxed* PES scan at the AM1 level of theory demonstrated the energetic advantages of partial geometry optimizations.

The organometallic analogues were treated with the relativistic effective core potentials (RECP) proposed by Hay and Wadt,[460] for which the computational efficacy has been established for most first- to third-row transition metals.[461] In this case, two specific core potential/basis set combinations were tested: LANL2DZ (Los Alamos National Laboratory 2-double-ζ) and SDD (Stuttgart/Dresden RECP).[317] The LANL2DZ basis set is of double-ζ-quality in the valence and 'valence-1' shells, which are treated explicitly, whereas the RECP contains Darwin and mass-velocity contributions.

Unless otherwise stated, full geometry optimizations were performed on all systems. The nature of each stationary point was uniquely characterized by analytically calculating and diagonalizing the matrix of energy second derivatives (Hessian) and subsequently evaluating the number of imaginary frequencies (>1,1, and 0 corresponding to a higher order saddle point, a transition state, or a stationary point, respectively). Once again, the assessment of results was aided with the quantum mechanical pre- and post-processing analysis tool QMView.[454]

6.4.3 $C_7R_{7-n}X_n$ (n = 0 - 7, X = Aryl, Alkyl, H) Study

All computed $C_7R_{7-n}X_n$ structures were geometry optimized with use of the Restricted Hartree-Fock assumption using the AM1 Hamiltonian[257] found in the Spartan computational package.[258] Mulliken point charges were calculated on the resultant wavefunctions and stationary points were confirmed to be minima by vibrational frequency analysis. Planar structures were attained for all members of the $C_nH_n^{x\pm}$ (n = 3 to 7) and the $C_nPh_n^{x\pm}$ (n = 3 to 6) series. In the latter systems, all species possessed a propeller-like arrangement of the peripheral phenyl rings such that the dihedral angle between the phenyl rings and the central ring of the molecule increased as the value of n increased. Conformational searches were conducted for $C_7H_{7-n}Ph_n^+$ (n = 1,3,4, and 7) cations, utilizing symmetry constraints to identify the higher symmetry molecules. Two conformers of $C_7Ph_7^+$, **1.139**, were located, (ΔH_f (C_1) = 419.52 and ΔH_f (D_{7h}) = 419.71 kJ mol^{-1}) and based on the energy difference between the two stationary points, the puckered C_1 structure represents the global minimum on the potential energy surface for the heptaphenylcycloheptatrienyl cation. Of the two conformers of 1,2,4,6-$C_7H_3Ph_4^+$, **4.35**, that were identified, (ΔH_f (C_2) = 309.24 and ΔH_f (C_1) = 309.48 kJ mol^{-1}), the planar configuration is slightly preferred over its non-planar form. It is evident from the results pertaining to **1.139** and **4.35** that the potential energy surface near each of the minima is flat, and accordingly, the convergence criteria were altered and the maximum step size reduced during the geometry optimization in order to prevent premature identification of the minima. Given the small energy differences that separate the equilibrium structures, it should be emphasized that the topology of these regions may be sensitive to changes in the level of calculation. Limited computational resources made it impossible to verify this assertion at the time the study was conducted.

REFERENCES

1. Bischoff, C.A. *Chem. Ber.* **1890**, *23*, 620.
2. Hirsch, J.A. *Top. Stereochem.* **1967**, *1*, 199.
3. Pophristic, V.; Goodman, L. *Nature* **2001**, *411*, 565.
4. Albright, T.A.; Hofmann, P.; Hoffmann, R. *J. Am. Chem. Soc.* **1977**, *99*, 7546.
5. Albright, T.A.; Hoffmann, R.; Thibeault, J.C.; Thorn, D.L. *J. Am. Chem. Soc.* **1979**, *101*, 3801.
6. Albright, T.A.; Hoffmann, R.; Tse, Y.-C.; D'Ottavio, T. *J. Am. Chem. Soc.* **1979**, *101*, 3812.
7. Albright, T.A. *Acc. Chem. Res.* **1982**, *15*, 149.
8. Oki, M. *Top. Stereochem.* **1983**, *14*, 1.
9. Chance, J.M.; Geiger, J.H.; Mislow, K. *J. Am. Chem. Soc.* **1989**, *111*, 2326.
10. Clayden, J.; Pink, J.H. *Angew. Chem., Int. Ed. Engl.* **1998**, *37*, 1937.
11. Gakh, A.A.; Sachleben, R.A.; Bryan, J.C. *Chemtech* **1997**, 26.
12. Fabbrizzi, L.; Licchelli, M.; Pallavicini, P. *Acc. Chem. Res.* **1999**, *32*, 846.
13. Pease, A.R.; Jeppesen, J.O.; Stoddart, J.F.; Luo, Y.; Collier, C.P.; Heath, J.R. *Acc. Chem. Res.* **2001**, *34*, 433.
14. Kawaguchi, Y.; Harada, A. *Org. Lett.* **2000**, *2*, 1353.
15. Brouwer, A.M.; Frochot, C.; Gatti, F.G.; Leigh, D.A.; Mottier, L.; Paolucci, F.; Roffia, S.; Wurpel, G.W.H. *Science* **2001**, *291*, 2124.
16. Kelly, T.R.; Bowyer, M.C.; Bhaskar, K.V.; Bebbington, D.; Garcia, A.; Lang, F.; Kim, M.H.; Jette, M.P. *J. Am. Chem. Soc.* **1994**, *116*, 3657.
17. Bedard, T.C.; Moore, J.S. *J. Am. Chem. Soc.* **1995**, *117*, 10662.
18. Dominguez, Z.; Dang, H.; Strouse, M.J.; Garcia-Garibay, M.A. *J. Am. Chem. Soc.* **2002**, *124*, 2398.
19. Dominguez, Z.; Dang, H.; Strouse, M.J.; Garcia-Garibay, M.A. *J. Am. Chem. Soc.* **2002**, 7719.
20. Asfari, Z.; Naumann, C.; Kaufmann, G.; Vicens, J. *Tetrahedron Lett.* **1998**, *39*, 9007.
21. Mislow, K. *Chemtracts: Org. Chem.* **1989**, *2*, 151.

22. Stoddart, J.F. *Acc. Chem. Res.* **2001**, *34*, 409-410 (Molecular Machines Special Issue).

23. Coontz, R.; Szuromi, P. *Science* **2000**, *290*, 1523-1523.

24. Dagani, R. Building from the Bottom Up. *Chem. Eng. News* **2000**, 78(42), 27-32.

25. *Sci. Am.* **2001**, *285*, Special Issue on Nanotechnology.

26. Balzani, V.; Credi, A.; Venturi, M. *Chem. Eur. J.* **2002**, *8*, 5525.

27. Tidwell, T.T. *Tetrahedron* **1978**, *34*, 1855.

28. Muetterties, E.L. *Inorg. Chem.* **1965**, *4*, 769.

29. Doering, W.v.E.; Roth, W.R. *Angew. Chem., Int. Ed. Engl.* **1963**, *2*, 115.

30. Orville-Thomas, W.J. *Internal Rotation in Molecules*; John Wiley & Sons Ltd.: London, England, 1974; pp 1-17.

31. Christie, G.H.; Kenner, J. *J. Chem. Soc.* **1922**, *121*, 614..

32. Wilkinson, G.; Piper, T.S. *J. Inorg. Nucl. Chem.* **1956**, *2*, 32.

33. Wilkinson, G.; Piper, T.S. *J. Inorg. Nucl. Chem.* **1956**, *3*, 104.

34. Bennett, M.A.; Cotton, F.A.; Davison, A.; Faller, J.W.; Lippard, S.J.; Morehouse, S.M. *J. Am. Chem. Soc.* **1966**, *88*, 4371.

35. Berg, U.; Liljefors, T.; Roussel, C.; Sandström, J. *Acc. Chem. Res.* **1985**, *18*, 80.

36. Mislow, K. *Top. Stereochem.* **1999**, *22*, 1.

37. Bürgi, H.B.; Dunitz, J.D. *Structure Correlation*; VCH: Weinheim, New York, 1994.

38. Sandström, J. *Dynamic NMR Spectroscopy*; Academic Press: Toronto, 1982.

39. Oki, M. *Applications of Dynamic NMR Spectroscopy to Organic Chemistry*; VCH Publishers, Inc.: Deerfield Beach, 1985.

40. Jensen, F. *Introduction to Computational Chemistry*; John Wiley & Sons Ltd.: West Sussex, England, 1999.

41. Mislow, K.; Gust, D.; Finocchiaro, P.; Boettcher, R.J. *Fortschr. Chem. Forsch.* **1974**, *47*, 1.

42. Meurer, K.P.; Vögtle, F. *Top. Curr. Chem.* **1985**, *127*, 3.

43. Gust, D.; Mislow, K. *J. Am. Chem. Soc.* **1973**, *95*, 1535.

44. Mislow, K. *Acc. Chem. Res.* **1976**, *9*, 26.

45. Mislow, K.; Siegel, J. *J. Am. Chem. Soc.* **1984**, *106*, 3319.

46. Kurland, R.J.; Schuster, I.I.; Colter, A.K. *J. Am. Chem. Soc.* **1965**, *87*, 2279.

47. Gust, D.; Mislow, K. *J. Am. Chem. Soc.* **1973**, *95*, 1535.

48. Ito, S.; Morita, N.; Asao, T. *Tetrahedron Lett.* **1992**, *44*, 6669.

49. Ito, S.; Morita, N.; Asao, T. *Bull. Chem. Soc. Jpn.* **1995**, *68*, 1409.

50. Finocchiaro, P.; Gust, D.; Mislow, K. *J. Am. Chem. Soc.* **1974**, *96*, 3198.

51. Casarani, D.; Grilli, S.; Lunazzi, L.; Mazzanti, A. *J. Org. Chem.* **2001**, *66*, 2757.

52. Grilli, S.; Lunazzi, L.; Mazzanti, A.; Casarani, D.; Femoni, C. *J. Org. Chem.* **2001**, *66*, 488.

53. Grilli, S.; Lunazzi, L.; Mazzanti, A. *J. Org. Chem.* **2001**, *66*, 5853.

54. Blount, J.F.; Finocchiaro, P.; Gust, D.; Mislow, K. *J. Am. Chem. Soc.* **1973**, *95*, 7019.

55. Blount, J.F.; Finocchiaro, P.; Gust, D.; Mislow, K. *J. Am. Chem. Soc.* **1973**, *95*, 7029.

56. Finocchiaro, P.; Gust, D.; Mislow, K. *J. Am. Chem. Soc.* **1974**, *96*, 2165.

57. Andose, J.D.; Mislow, K. *J. Am. Chem. Soc.* **1974**, *96*, 2168.

58. Finocchiaro, P.; Gust, D.; Mislow, K. *J. Am. Chem. Soc.* **1974**, *96*, 2176.

59. Finocchiaro, P.; Gust, D.; Mislow, K. *J. Am. Chem. Soc.* **1974**, *96*, 3205.

60. Levendis, D.C.; Bernal, I. *Structural Chem.* **1997**, *8*, 263.

61. Willem, R.; Hoogzand, C. *Org. Magn. Reson.* **1979**, *12*, 55.

62. Glaser, R.; Blount, J.F.; Mislow, K. *J. Am. Chem. Soc.* **1980**, *102*, 2777.

63. Howell, J.A.S.; Palin, M.G.; Yates, P.C.; McArdle, P.; Cunningham, D.; Goldschimdt, Z.; Gottlieb, H.E.; Hezroni-Langerman, D. *J. Chem. Soc., Perkin Trans.II* **1992**, 1769.

64. Howell, J.A.S.; Fey, N.; Lovatt, J.D.; Yates, P.C.; McArdle, P.; Cunningham, D.; Sadeh, E.; Gottlieb, H.E.; Goldschimdt, Z.; Hursthouse, M.B.; Light, M.E. *J. Chem. Soc., Dalton Trans.* **1999**, 3015.

65. Willem, R.; Pepermans, H.; Hallenga, K.; Gielen, M.; Dams, R. *J. Org. Chem.* **1983**, *48*, 1890.

66. Rappoport, Z.; Biali, S.E. *Acc. Chem. Res.* **1997**, *30*, 307.

67. Lindner, A.B.; Grynszpan, F.; Biali, S.E. *J. Org. Chem.* **1993**, *58*, 6662.

68. Selzer, T.; Rappoport, Z. *J. Org. Chem.* **1996**, *61*, 7326.

69. Sedó, J.; Ventosa, N.; Molins, M.A.; Pons, M.; Rovira, C.; Veciana, J. *J. Org. Chem.* **2001**, *66*, 1567.

70. Sedó, J.; Ventosa, N.; Molins, M.A.; Pons, M.; Rovira, C.; Veciana, J. *J. Org. Chem.* **2001**, *66*, 1579.

71. Iwamura, H.; Mislow, K. *Acc. Chem. Res.* **1988**, *21*, 175.

72. Hounshell, W.D.; Iroff, L.D.; Iverson, D.J.; Wroczynski, R.J.; Mislow, K. *Isr. J. Chem.* **1980**, *20*, 65.

73. Feynman, R.P. *Eng. Sci.* **1960**, *23(5)*, 22.

74. *Webster's New International Dictionary*; G. & C. Merriam Co.: Springfield, MA, 1938; pp 1474.

75. Ballardini, R.; Balzani, V.; Credi, A.; Gandolfi, M.T.; Venturi, M. *Acc. Chem. Res.* **2001**, *34*, 445.

76. Freemantle, M. Two Ways to Drive Molecular Motors. *Chem. Eng. News* **1999**, 77(37), 6-7, 9-13.

77. Yurke, B.; Turberfield, A.J.; Mills, A.P., Jr.; Simmel, F.C.; Neumann, J.L. *Nature* **2000**, *406*, 605.

78. Soong, R.K.; Bachand, G.D.; Neves, H.P.; Olkhovets, A.G.; Craighead, H.G.; Montemagno, C.D. *Science* **2000**, *290*, 1555.

79. Feringa, B.L. *Nature* **2000**, *208*, 151.

80. Nedelec, F.J.; Surrey, T.; Maggs, A.C.; Leibler, S. *Nature* **1997**, *389*, 305.

81. Alberts, B. *Cell* **1998**, *92*, 291.

82. Boyer, P.D. *Angew. Chem., Int. Ed.* **1998**, *37*, 2296.

83. Kitamura, K.; Tokunaga, M.; Iwane, A.H.; Yanagida, T. *Nature* **1999**, *397*, 129.

84. Mao, C.; Sun, W.; Shen, Z.; Seeman, N.C. *Nature* **1999**, *397*, 144.

85. Balzani, V.; Gómez-López, M.; Stoddart, J.F. *Acc. Chem. Res.* **1998**, *31*, 405.

86. Sauvage, J.-P. *Acc. Chem. Res.* **1998**, *31*, 611.

87. Balzani, V.; Credi, A.; Raymo, F.M.; Stoddart, J.F. *Angew. Chem. Int. Ed.* **2000**, *39*, 3348.

88. Kelly, T.R.; Tellitu, I.; Sestelo, J.P. *Angew. Chem. Int. Ed. Engl.* **1997**, *36*, 1866.

89. Kelly, T.R.; Sestelo, J.P.; Tellitu, I. *J. Org. Chem.* **1998**, *63*, 3655.

90. Davis, A.P. *Angew. Chem. Int. Ed.* **1998**, *37*, 909.

91. Kelly, T.R.; De Silva, H.; Silva, R.A. *Nature* **1999**, *401*, 150.

92. Kelly, T.R.; Silva, R.A.; De Silva, H.; Jasmin, S.; Zhao, Y. *J. Am. Chem. Soc.* **2000**, *122*, 6935.

93. Kelly, T.R. *Acc. Chem. Res.* **2001**, *34*, 514.

94. Koumura, N.; Zijlstra, R.W.J.; van Delden, R.A.; Harada, N.; Feringa, B.L. *Nature* **1999**, *401*, 152.

95. Koumura, N.; Geertsema, E.M.; Meetsma, A.; Feringa, B.L. *J. Am. Chem. Soc.* **2000**, *122*, 12005.

96. Feringa, B.L. *Acc. Chem. Res.* **2001**, *34*, 504.

97. Koumura, N.; Geertsema, E.M.; van Gelder, M.B.; Meetsma, A.; Feringa, B.L. *J. Am. Chem. Soc.* **2002**, *124*, 5037.

98. van Delden, R.A.; Koumura, N.; Schoevaars, A.; Meetsma, A.; Feringa, B.L. *Org. Biomol. Chem.* **2003**, *1*, 33.

99. Schalley, C.A.; Beizai, K.; Vögtle, F. *Acc. Chem. Res.* **2001**, *34*, 465.

100. Gimzewski, J.K.; Joachim, C.; Schlittler, R.R.; Langlais, V.; Tang, H.; Johannsen, I. *Science* **1998**, *281*, 531.

101. Kekulé, A. *Bull. Soc. Chim. Fr.* **1865**, *3*, 98.

102. Erlenmeyer, E. *Ann. Chem. Pharm.* **1866**, *137*, 327.

103. Krygowski, T.M.; Cyranski, M.K. *Chem. Rev.* **2001**, *101*, 1385.

104. Allen, A.D.; Tidwell, T.T. *Chem.Rev.* **2001**, *101*, 1333.

105. Stevens, A.M.; Richards, C.J. *Tetrahedron Lett.* **1997**, *38*, 7805.

106. Richards, C.J.; Butler, D.C.D. *Abstr. Pap.- Am. Chem. Soc.* **2001**, *221st*, ORGN-367.

107. Rausch, M.D.; Westover, G.F.; Mintz, E.; Reisner, G.M.; Bernal, I.; Clearfield, A.; Troup, J.M. *Inorg. Chem.* **1979**, *18*, 2605.

108. Clearfield, A.; Rudolf, P.; Bernal, I.; Rausch, M.D. *Inorg. Chim. Acta* **1980**, *42*, 17.

109. Uno, M.; Shirai, K.; Ando, K.; Komatsuzaki, N.; Tanaka, T.; Sawada, M.; Takahashi, S. *Chem. Lett.* **1995**, 7.

110. Kealy, T.J.; Pauson, P.L. *Nature* **1951**, *168*, 1039.

111. Wilkinson, G.; Rosenblum, M.; Whiting, M.C.; Woodward, R.B. *J. Am. Chem. Soc.* **1952**, *74*, 2125.

112. King, R.B.; Bisnette, M.B. *J. Organomet. Chem.* **1967**, *8*, 287.

113. Janiak, C.; Schumann, H. *Adv. Organomet. Chem.* **1991**, *33*, 291.

114. Okuda, J. *Top. Curr. Chem.* **1991**, *160*, 97.

115. Harrison, W.M.; Saadeh, C.; Colbran, S.B.; Craig, D.C. *J. Chem. Soc., Dalton Trans.* **1997**, 3785.

116. Adams, H.; Bailey, N.A.; Browning, A.F.; Ramsden, J.A.; White, C. *J. Organomet. Chem.* **1990**, *387*, 305.

117. Ramsden, J.A.; Milner, D.J.; Adams, H.; Bailey, N.A.; Smith, A.J.; White, C. *Organometallics* **1995**, *14*, 2575.

118. Matt, D.; Huhn, M.; Fischer, J.; De Cian, A.; Kläui, W.; Tkatchenko, I.; Bonnet, M.C. *J. Chem. Soc., Dalton Trans.* **1993**, 1173.

119. Matt, D.; Huhn, M.; Bonnet, M.; Tkatchenko, I.; Englert, U.; Kläui, W. *Inorg. Chem.* **1995**, *34*, 1288.

120. Haywood-Farmer, J.; Battiste, M.A. *Chem. Ind.* **1971**, 1232.

121. Fagan, M.W.; Gust, D. *J. Org. Chem.* **1981**, *46*, 1499.

122. Gust, D. *J. Am. Chem. Soc.* **1977**, *99*, 6980.

123. Gust, D.; Patton, A. *J. Am. Chem. Soc.* **1978**, *100*, 8175.

124. Möbius, K. *Z. Naturforsch.* **1965**, *20A*, 1117.

125. Willem, R.; Pepermans, H.; Hoogzand, C.; Hallenga, K.; Gielen, M. *J. Am. Chem. Soc.* **1981**, *103*, 2299.

126. Willem, R.; Jans, A.; Hoogzand, C.; Gielen, M.; Van Binst, G.; Pepermans, H. *J. Am. Chem. Soc.* **1985**, *107*, 28.

127. Patton, A.; Dirks, J.W.; Gust, D. *J. Org. Chem.* **1979**, *44*, 4749.

128. Janiak, C.; Weimann, R.; Gõrlitz, F. *Organometallics* **1997**, *16*, 4933.

129. Colbran, S.B.; Craig, D.C.; Harrison, W.M.; Grimley, A.E. *J. Organomet. Chem.* **1991**, *408*, C33.

130. Saadeh, C.; Colbran, S.B.; Craig, D.C.; Rae, A.D. *Organometallics* **1993**, *12*, 133.

131. Brégaint, P.; Hamon, J.-R.; Lapinte, C. *Organometallics* **1992**, *11*, 1417.

132. Field, L.D.; Hambley, T.W.; Humphrey, P.A.; Masters, A.F.; Turner, P. *Polyhedron* **1998**, *17*, 2587.

133. Schumann, H.; Lentz, A.; Weimann, R.; Pickardt, J. *Angew. Chem. Int. Ed. Engl.* **1994**, *33*, 1731.

134. Schott, A.; Scott, H.; Wilker, G.; Brandt, J.; Hoberg, H.; Hoffmann, E.G. *Liebigs Ann. Chem.* **1973**, 508.

135. Yeh, W.-Y.; Peng, S.-M.; Lee, G.-H. *J. Organomet. Chem.* **1999**, *572*, 125.

136. Hegg, M.J.; Herber, R.H.; Janiak, C.; Zuckerman, J.J.; Schumann, H.; Manders, W.J. *J. Organomet. Chem.* **1988**, *346*, 321.

137. Field, L.D.; Masters, A.F.; Gibson, M.; Latimer, D.R.; Hambley, T.W.; Buys, I.E. *Inorg. Chem.* **1993**, *32*, 211.

138. Castellani, M.P.; Wright, J.M.; Geib, S.J.; Rheingold, A.L.; Trogler, W.C. *Organometallics* **1986**, *5*, 1116.

139. Castellani, M.P.; Geib, S.J.; Rheingold, A.L.; Trogler, W.C. *Organometallics* **1987**, *6*, 2524.

140. Hoobler, R.J.; Adams, J.V.; Hutton, M.A.; Fransisco, T.W.; Haggerty, B.S.; Rheingold, A.L.; Castellani, M.P. *J. Organomet. Chem.* **1991**, *412*, 157.

141. Rieger, B.; Steimann, M.; Fawzi, R. *Chem. Ber.* **1992**, *125*, 2373.

142. Mao, F.; Sur, S.K.; Tyler, D.R. *J. Am. Chem. Soc.* **1989**, *111*, 7627.

143. Li, L.; Decken, A.; Sayer, B.G.; McGlinchey, M.J.; Brégaint, P.; Thépot, J.-Y.; Toupet, L.; Hamon, J.-R.; Lapinte, C. *Organometallics* **1994**, *13*, 682.

144. Potenza, J.A.; Johnson, R.J.; Chirico, R.; Efraty, A. *Inorg. Chem.* **1977**, *16*, 2354.

145. Burke, M.R.; Funk, T.; Takats, J.; Day, V.W. *Organometallics* **1994**, *13*, 2109.

146. Yamazaki, S.; Taira, Z. *J. Organomet. Chem.* **1999**, *578*, 61.

147. Gupta, H.K.; Rampersad, N.; Stradiotto, M.J.; McGlinchey, M.J. *Organometallics* **2000**, *19*, 184.

148. Adams, H.; Bailey, N.A.; Hempstead, P.D.; Morris, M.J.; Riley, S.; Beddoes, R.L.; Cook, E.S. *J. Chem. Soc., Dalton Trans.* **1993**, 91.

149. Harrington, L.E.; Britten, J.F.; Hughes, D.W.; Bain, A.D.; Thépot, J.-Y.; McGlinchey, M.J. *J. Organomet. Chem.* **2002**, *656*, 243.

150. Kruczynski, L.; Takats, J. *Inorg. Chem.* **1976**, *15*, 3140.

151. Gupta, H.K.; Stradiotto, M.J.; Hughes, D.W.; McGlinchey, M.J. *J. Org. Chem.* **2000**, *65*, 3652.

152. Thornberry, M.P.; Slebodnick, C.; Deck, P.A.; Fronczek, F.R. *Organometallics* **2001**, *20*, 920.

153. Thornberry, M.P.; Slebodnick, C.; Deck, P.A.; Fronczek, F.R. *Organometallics* **2000**, *19*, 5352.

154. Thépot, J.-Y.; Lapinte, C. *J. Organomet. Chem.* **2001**, *627*, 179.

155. Thépot, J.-Y.; Lapinte, C. *J. Organomet. Chem.* **2002**, *656*, 146.

156. Gloaguen, B.; Astruc, D. *J. Am. Chem. Soc.* **1990**, *112*, 4607.

157. Sitzmann, H. *Chem. Ber.* **1990**, *123*, 2311.

158. Sünkel, K.; Hofmann, J. *Organometallics* **1992**, *11*, 3923.

159. Schumann, H.; Janiak, C.; Hahn, E.; Loebel, J.; Zuckerman, J.J. *Angew. Chem. Int. Ed. Engl.* **1985**, *24*, 773.

160. Schumann, H.; Janiak, C.; Hahn, E.; Kolax, C.; Loebel, J.; Rausch, M.D.; Zuckerman, J.J.; Heeg, M.J. *Chem. Ber.* **1986**, *119*, 2656.

161. Schumann, H.; Janiak, C.; Görlitz, F.; Loebel, J.; Dietrich, A. *J. Organomet. Chem.* **1989**, *363*, 243.

162. Chambers, J.W.; Baskar, A.J.; Bott, S.G.; Atwood, J.L.; Rausch, M.D. *Organometallics* **1986**, *5*, 1635.

163. Rausch, M.D.; Tsai, W.-M.; Chambers, J.W.; Rogers, R.D.; Alt, H.G. *Organometallics* **1989**, *8*, 816.

164. Schumann, H.; Janiak, C.; Köhn, R.D.; Loebel, J.; Dietrich, A. *J. Organomet. Chem.* **1989**, *365*, 137.

165. Zanello, P.; Cinquantini, A.; Mangani, S.; Opromolla, G. *J. Organomet. Chem.* **1994**, *471*, 171.

166. Schumann, H.; Sühring, K.; Weimann, R. *J. Organomet. Chem.* **1995**, *496*, C5.

167. Hübel, W.; Hoogzand, C. *Chem. Ber.* **1961**, *94*, 2817.

168. Arnett, E.M.; Bollinger, J.M. *J. Am. Chem. Soc.* **1964**, *86*, 4729.

169. Vollhardt, K.P.C. *Acc. Chem. Res.* **1977**, *10*, 1.

170. Yang, J.; Verkade, J.G. *J. Am. Chem. Soc.* **1998**, *120*, 6834.

171. Yang, J.; Verkade, J.G. *Organometallics* **2000**, *19*, 893.

172. Allen, C.F.H. *Chem. Rev.* **1962**, *62*, 653.

173. Ogliaruso, M.A.; Romanelli, M.G.; Becker, E.I. *Chem. Rev.* **1965**, *65*, 261.

174. Ito, S.; Herwig, P.T.; Böhme, T.; Rabe, J.B.; Rettig, W.; Müllen, K. *J. Am. Chem. Soc.* **2000**, *122*, 7698.

175. Ito, S.; Brand, J.D.; Gherghel, L.; Müllen, K. *J. Am. Chem. Soc.* **2000**, *122*, 7707.

176. Enkelmann, V.; Wegner, G.; Müllen, K. *J. Mater. Chem.* **2000**, *10*, 879.

177. Morgenroth, F.; Kübel, C.; Müllen, K. *J. Mater. Chem.* **1997**, *7*, 1207.

178. Morgenroth, F.; Müllen, K. *Tetrahedron* **1997**, *53*, 15349.

179. Morgenroth, F.; Berresheim, A.J.; Wagner, M.; Müllen, K. *Chem. Commun.* **1998**, 1139.

180. Nlate, S.; Nieto, Y.; Blais, J.-C.; Ruiz, J.; Astruc, D. *Chem. Eur. J.* **2002**, *8*, 171.

181. Dijkstra, H.P.; Steenwinkel, P.; Grove, D.M.; Lutz, M.; Spek, A.L.; van Koten, G. *Angew. Chem. Int. Ed.* **1999**, *38*, 2186.

182. Dijkstra, H.P.; Meijer, M.D.; Patel, J.; Kreiter, R.; van Klink, G.P.M.; Lutz, M.; Spek, A.L.; Canty, A.J.; van Koten, G. *Organometallics* **2001**, *20*, 3159.

183. Kübel, C.; Chen, S.-L.; Müllen, K. *Macromolecules* **1998**, *31*, 6014.

184. Kumar, S.; Varshney, S.K. *Angew. Chem. Int. Ed.* **2000**, *39*, 3140.

185. Kobayashi, K.; Shirasaka, T.; Sato, A.; Horn, E.; Furukawa, N. *Angew. Chem. Int. Ed.* **1999**, *38*, 3483.

186. Kobayashi, K.; Shirasaka, T.; Horn, E.; Furukawa, N. *Tetrahedron Lett.* **2000**, *41*, 89.

187. Eshdat, L.; Ayalon, A.; Beust, R.; Shenhar, R.; Rabinovitz, M. *J. Am. Chem. Soc.* **2000**, *122*, 12637.

188. Arnett, E.M.; Bollinger, J.M. *J. Am. Chem. Soc.* **1964**, *86*, 4729.

189. Siegel, J.; Mislow, K. *J. Am. Chem. Soc.* **1983**, *105*, 7763.

190. Siegel, J.; Gutiérrez, A.; Schweizer, W.B.; Ermer, O.; Mislow, K. *J. Am. Chem. Soc.* **1986**, *108*, 1569.

191. Biali, S.E.; Gutiérrez, A.; Mislow, K. *J. Org. Chem.* **1988**, *53*, 1316.

192. Schuster, I.I.; Weissensteiner, W.; Mislow, K. *J. Am. Chem. Soc.* **1986**, *108*, 6661.

193. Singh, M.D.; Siegel, J.; Biali, S.E.; Mislow, K. *J. Am. Chem. Soc.* **1987**, *109*, 3397.

194. Kahr, B.; Biali, S.E.; Schaefer, W.; Buda, A.B.; Mislow, K. *J. Org. Chem.* **1987**, *52*, 3713.

195. Biali, S.E.; Mislow, K. *J. Org. Chem.* **1988**, *53*, 1318.

196. Chance, J.M.; Kahr, B.; Buda, A.B.; Toscano, J.P.; Mislow, K. *J. Org. Chem.* **1988**, *53*, 3226.

197. Ermer, O. *Angew. Chem. Int. Ed. Engl.* **1983**, *22*, 998.

198. Melissas, V.; Faegri, K., Jr.; Almolöf, J. *J. Am. Chem. Soc.* **1985**, *107*, 4640.

199. Bar, I.; Bernstein, J.; Christensen, A. *Tetrahedron* **1977**, *33*, 3177.

200. Bock, H.; Kaim, W. *Chem. Ber.* **1978**, *111*, 3552.

201. Marsau, M.P. *Acta Crystallogr.* **1965**, *18*, 851.

202. Iverson, D.J.; Mislow, K. *Organometallics* **1982**, *1*, 3.

203. Frampton, C.S.; Gall, J.H.; MacNicol, D.D. *Acta Crystallogr.* **2000**, *C56*, e22.

204. McGlinchey, M.J. *Adv. Organomet. Chem.* **1992**, *34*, 285.

205. Hunter, G.; Iverson, D.J.; Mislow, K.; Blount, J.F. *J. Am. Chem. Soc.* **1980**, *102*, 5942.

206. Iverson, D.J.; Hunter, G.; Blount, J.F.; Damewood, J.R., Jr.; Mislow, K. *J. Am. Chem. Soc.* **1981**, *103*, 6073.

207. Maricq, M.M.; Waugh, J.S.; Fletcher, J.L.; McGlinchey, M.J. *J. Am. Chem. Soc.* **1978**, *100*, 6902.

208. Hunter, G.; Blount, J.F.; Damewood, J.R., Jr.; Iverson, D.J.; Mislow, K. *Organometallics* **1982**, *1*, 448.

209. McGlinchey, M.J.; Fletcher, J.L.; Sayer, B.G.; Bougeard, P.; Faggiani, R.; Lock, C.J.L.; Bain, A.D.; Rodger, C.A.; Kuendig, E.P.; Astruc, D.; Hamon, J.-P.; LeMaux, P.; Top, S.; Jaouen, G. *J. Chem. Soc., Chem. Commun.* **1983**, 634.

210. McGlinchey, M.J.; Bougeard, P.; Sayer, B.G.; Hofer, R.; Lock, C.J.L. *J. Chem. Soc., Chem. Commun.* **1984**, 789.

211. Hunter, G.; Mislow, K. *J. Chem. Soc., Chem. Commun.* **1984**, 172.

212. Downtown, P.A.; Mailvaganam, B.; Frampton, C.S.; Sayer, B.G.; McGlinchey, M.J. *J. Am. Chem. Soc.* **1990**, *112*, 27.

213. Mailvaganam, B.; Frampton, C.S.; Top, S.; Sayer, B.G.; McGlinchey, M.J. *J. Am. Chem. Soc.* **1991**, *113*, 1177.

214. Kilway, K.V.; Siegel, J.S. *J. Am. Chem. Soc.* **1991**, *113*, 2332.

215. Kilway, K.V.; Siegel, J.S. *J. Am. Chem. Soc.* **1992**, *114*, 255.

216. Marks, V.; Gottlieb, H.E.; Biali, S.E. *J. Am. Chem. Soc.* **1997**, *119*, 9672.

217. Gottlieb, H.E.; Ben-Ari, C.; Hassner, A.; Marks, V. *Tetrahedron* **1999**, *55*, 4003.

218. Kilway, K.V.; Siegel, J.S. *Tetrahedron* **2001**, *57*, 3615.

219. Taha, M.; Marks, V.; Gottlieb, H.E.; Biali, S.E. *J. Org. Chem.* **2000**, *65*, 8621.

220. Marks, V.; Gottlieb, H.E.; Melman, A.; Byk, G.; Cohen, S.; Biali, S.E. *J. Org. Chem.* **2001**, *66*, 6711.

221. Marks, V.; Nahmany, M.; Gottlieb, H.E.; Biali, S.E. *J. Org. Chem.* **2002**, *67*, 7898.

222. Bart, J.C.J. *Acta Cryst.* **1968**, *B24*, 1277.

223. Larson, E.M.; Von Dreele, R.B.; Hanson, P.; Gust, J.D. *Acta Cryst.* **1990**, *C46*, 784.

224. Almenningen, A.; Bastiansen, O.; Skancke, P.N. *Acta Chem. Scand.* **1958**, *12*, 1215.

225. Tong, L.; Ho, D.M.; Vogelaar, N.J.; Schutt, C.E.; Pascal, R.A., Jr. *J. Am. Chem. Soc.* **1997**, *119*, 7291.

226. Weissensteiner, W.; Scharf, J.; Schlögl, K. *J. Org. Chem.* **1987**, *52*, 1210.

227. Mailvaganam, B.; McCarry, B.E.; Sayer, B.G.; Perrier, R.E.; Faggiani, R.; McGlinchey, M.J. *J. Organomet. Chem.* **1987**, *335*, 213.

228. Albright, T.A. *Acc. Chem. Res.* **1982**, *15*, 149.

229. Rogers, R.D.; Atwood, J.L.; Albright, T.A.; Lee, W.A.; Rausch, M.D. *Organometallics* **1984**, *3*, 263.

230. Malisza, K.L.; Chao, L.C.F.; Britten, J.F.; Sayer, B.G.; Jaouen, G.; Top, S.; Decken, A.; McGlinchey, M.J. *Organometallics* **1993**, *12*, 2462.

231. Mailvaganam, B.; Sayer, B.G.; McGlinchey, M.J. *J. Organomet. Chem.* **1990**, *395*, 177.

232. Battiste, M.A. *J. Am. Chem. Soc.* **1961**, *83*, 4101.

233. Takeuchi, K.; Yokomichi, Y.; Okamoto, K. *Chem.Lett.* **1977**, 1177.

234. Ritchie, C.D.; Fleischaur, H. *J. Am. Chem. Soc.* **1972**, *94*, 3841.

235. Lämsä, M.; Suorsa, T.; Pursiainen, J.; Huuskonen, J.; Rissanen, K. *Chem.Commun.* **1996**, 1443.

236. Lämsä, M.; Pursiainen, J.; Rissanen, K.; Huuskonen, J. *Acta Chem.Scand.* **1998**, *52*, 563.

237. Lämsä, M.; Kiviniemi, S.; Kettukangas, E.-R.; Nissinen, M.; Rissanen, J.P.K. *J. Phys. Org. Chem.* **2001**, *14*, 551.

238. Yamamura, K.; Nakatsu, K.; Nakao, K.; Nakazawa, T.; Murata, I. *Tetrahedron Lett.* **1979**, *52*, 4999.

239. Tsuji, R.; Komatsu, K.; Takeuchi, K.; Shiro, M.; Cohen, S.; Rabinovitz, M. *J. Phys. Org. Chem.* **1993**, *6*, 435.

240. Mills, O.S.; Mooney, N.J.; Robinson, P.M.; Watt, C.I.F.; Box, B.G. *J. Chem. Soc., Perkin Trans.II* **1995**, 697.

241. Komatsu, K. *Eur. J. Org. Chem.* **1999**, 1495.

242. Pietra, F. *Chem. Rev.* **1973**, *73*, 334.

243. Green, M.L.H.; Ng, D.K.P. *Chem. Rev.* **1995**, *95*, 439.

244. Tamm, M.; Baum, K.; Fröhlich, R.; Saarenketo, P. *Organometallics* **2001**, *20*, 1376.

245. Kaftory, M.; Nugiel, D.A.; Biali, S.E.; Rappoport, Z. *J. Am. Chem. Soc.* **1989**, *111*, 8181.

246. Gur, E.; Kaftory, M.; Biali, S.E.; Rappoport, Z. *J. Org. Chem.* **1999**, *64*, 8144.

247. Rappoport, Z.; Biali, S.E.; Kaftory, M. *J. Am. Chem. Soc.* **1990**, *112*, 7742.

248. Bye, E.; Schweizer, W.B.; Dunitz, J.D. *J. Am. Chem. Soc.* **1982**, *104*, 5893.

249. Bürgi, H.-B.; Dunitz, J.D. *Acc. Chem. Res.* **1983**, *16*, 153.

250. Bürgi, H.B. *Ann. Rev. Phys. Chem.* **2000**, *51*, 275.

251. Bürgi, H.B.; Capelli, S.C. *Acta Crystallogr.* **2000**, *A56* , 403.

252. Bauder, A.; Meyer, R.; Günthard, H.H. *Molec. Phys.* **1974**, *28*, 1305.

253. Altmann, S.L. *Molec. Phys.* **1971**, *21*, 587-607.

254. Brydges, S.; McGlinchey, M. J. *J. Org. Chem.* **2002**, *67*, 7688.

255. Dunitz, J.D. *X-ray Analysis and the Structure of Organic Molecules*; Cornell University Press: Ithaca, NY, 1979; Chapter 10.

256. Ramachandran, G.N.; Sasisekharan, V. *Adv. Protein Chem.* **1968**, *23*, 283.

257. Dewar, M.J.S.; Zoebisch, E.G.; Healy, E.F.; Stewart, J.J.P. *J. Am. Chem. Soc.* **1985**, *107*, 3902.

258. *SPARTAN SGI,* Version 5.1.1; Irvine, California, USA, Wavefunction, Inc., 2001.

259. Halgren, T.A. *J. Comput. Chem.* **1996**, *17*, 490.

260. Clark, M.; Cramer III, R.D.; Van Opdenbosch, N.J. *J. Comput. Chem.* **1989**, *1989*, 982.

261. Frisch, M.J.; Trucks, G.W.; Schlegel, H.B.; Scuseria, G.E.; Robb, M.A.; Cheeseman, J.R.; Zakrzewski, V.G.; Montgomery, J.A.; Stratmann, R.E.; Burant, J.C.; Dapprich, S.; Millam, J.M.; Daniels, A.D.; Kudin, K.N.; Strain, M.C.; Farkas, O.; Tomasi, J.; Barone, V.; Cossi, M.; Cammi, R.; Mennucci, V.; Pomelli, C.; Adamo, C.; Clifford, S.; Ochterski, J.; Petersson, G.A.; Ayala, P.Y.; Cui, Q.; Morokuma, K.; Malick, D.K.; Rabuck, A.D.; Raghavachari, K.; Foresman, J.B.; Cioslowski, J.; Ortiz, J.V.; Baboul, A.G.; Stefanov, B.B.; Liu, G.; Liashenko, A.; Piskorz, P.; Komaromi, V.; Gomperts, R.; Martin, R.L.; Fox, D.J.; Keith, T.; Al-Laham, M.A.; Peng, C.Y.; Nanayakkara, A.; Challacombe, M.; Gill, P.M.W.; Johnson, B.; Chen, W.; Wong, M.W.; Andres, J.L.; Gonzalez, C.; Head-Gordon, M.; Replogle, E.S.; Pople, J.A.*GAUSSIAN98, Rev. A.9*; Gaussian: Pittsburgh, PA, 1998.

262. *CSD, July Release V5.21 2001*; Cambridge Crystallographic Data Center: University Chemical Laboratory, Cambridge, England, 2001.

263. Alvarez-Toledano, C.; Baldovino, O.; Espinoza, G.; Toscano, R.A.; Gutiérrez-Pérez, R.; García-Mellado, O. *J. Organomet. Chem.* **1997**, *540*, 41.

264. Evrard, P.G.; Piret, P.; Germain, G.; van Meerssche, M. *Acta Crystallogr.* **1971**, *B27*, 661.

265. Bettinger, H.F.; Schelyer, P.v.R.; Schaeffer, H.F.I. *J. Am. Chem. Soc.* **1998**, *120*, 1074.

266. Ogliaruso, M.A.; Shadoff, L.A.; Becker, E.I. *J. Org. Chem.* **1963**, *28*, 2725.

267. Ogliaruso, M.A.; Becker, E.I. *J. Org. Chem.* **1965**, *30*, 3354.

268. Reid, W.; Saxena, V.B. *Angew. Chem., Int. Ed. Engl.* **1968**, *7*, 378.

269. Noren, G.K.; Stille, J.K. *Macromol. Rev.* **1971**, *5*, 385.

270. Pascal, R.A., Jr.; McMillan, W.D.; Van Engen, D. *J. Am. Chem. Soc.* **1986**, *108*, 5652.

271. Pascal, R.A., Jr.; McMillan, W.D.; Van Engen, D.; Eason, R.G. *J. Am. Chem. Soc.* **1987**, *109*, 4660.

272. Tong, L.; Lau, H.; Ho, D.M.; Pascal, R.A., Jr. *J. Am. Chem. Soc.* **1998**, *120*, 6000.

273. Iyer, V.S.; Wehmeier, M.; Brand, J.D.; Keegstra, M.A.; Müllen, K. *Angew. Chem., Int. Ed. Engl.* **1997**, *36*, 1604.

274. Müller, M.; Iyer, V.S.; Kübel, C.; Enkelmann, V.; Müllen, K. *Angew. Chem., Int. Ed. Engl.* **1997**, *36*, 1607.

275. Iyer, V.S.; Yoshimura, K.; Enkelmann, V.; Epsch, R.; Rabe, J.P.; Müllen, K. *Angew. Chem., Int. Ed. Engl.* **1998**, *37*, 2696.

276. Berresheim, A.J.; Müller, M.; Müllen, K. *Chem. Rev.* **1999**, *99*, 1747.

277. Watson, M.D.; Fechtenkötter, A.; Müllen, K. *Chem. Rev.* **2001**, *101*, 1267.

278. Simpson, C.D.; Brand, J.D.; Berresheim, A.J.; Przybilla, L.; Müllen, K. *Chem. Eur. J.* **2002**, *8*, 1424.

279. Sankararaman, S.; Hopf, H.; Dix, I.; Jones, P.G. *Eur. J. Org. Chem.* **2000**, 2711.

280. Setayesh, S.; Grimsdale, A.C.; Weil, T.; Enkelmann, V.; Müllen, K.; Meghdadi, F.; List, E.J.W.; Leising, G. *J. Am. Chem. Soc.* **2001**, *123*, 946.

281. Ito, S.; Inabe, H.; Okujima, T.; Morita, N.; Watanabe, M.; Imafuku, K. *Tetrahedron Lett.* **2000**, *41*, 8343.

282. Elwahy, A.H.M. *Tetrahedron Lett.* **2002**, *43*, 711.

283. Draper, S.M.; Gregg, D.J.; Madathil, R. *J. Am. Chem. Soc.* **2002**, *124*, 3486.

284. Samanta, S.R.; Mukherjee, A.K.; Bhattacharyya, A.J. *Curr.Sci.* **1988**, *57*, 926.

285. Walsh, C.J.; Mandal, B.K. *J. Org. Chem.* **1999**, *64*, 6102.

286. Pschirer, N.G.; Bunz, U.H.F. *Tetrahedron Lett.* **1999**, *40*, 2481.

287. Muthiah, C.; Kumar, K.P.; Mani, C.A.; Swamy, K.C.K. *J. Org. Chem.* **2000**, *65*, 3733.

288. Katritzky, A.R.; Abdel-Fattah, A.A.A.; Wang, M. *J. Org. Chem.* **2002**, *67*, 7526.

289. Wind, M.; Wiesler, U.M.; Saalwächter, K.; Müllen, K.; Spiess, H.W. *Adv. Mater.* **2001**, *13*, 752.

290. Biagini, P.; Funaioli, T.; Fachinetti, G.; Laschi, F.; Zanazzi, P.F. *J. Chem. Soc., Chem. Commun.* **1989**, 405.

291. Crocker, M.; Green, M.; Orpen, A.G.; Thomas, D.M. *J. Chem. Soc., Chem. Commun.* **1984**, 1141.

292. Quarmby, I.C.; Hemond, R.C.; Feher, F.J.; Green, M.; Geiger, W.E. *J. Organomet. Chem.* **1999**, *577*, 189.

293. Ning, G.L.; Munakata, M.; Wu, L.P.; Maekawa, M.; Kuroda-Sowa, T.; Suenaga, Y.; Sugimoto, K. *Inorg. Chem.* **1999**, *38*, 1376.

294. Ning, G.L.; Munakata, M.; Wu, L.P.; Maekawa, M.; Suenaga, Y.; Kuroda-Sowa, T.; Sugimoto, K. *Inorg. Chem.* **1999**, *38*, 5668.

295. Constable, E.C.; Eich, O.; Fenske, D.; Housecraft, C.E.; Johnston, L.A. *Chem. Eur. J.* **2000**, *6*, 4364.

296. Roothaan, C.C.J. *Rev. Mod. Phys.* **1951**, *23*, 69.

297. Parr, R.G.; Yang, W. *Density Functional Theory of Atoms and Molecules*; Oxford University Press: New York, 1989.

298. Becke, A.D. *J. Chem. Phys.* **1993**, *98*, 5648.

299. Perdew, J.P.; Chevary, J.A.; Vosko, S.H.; Jackson, K.A.; Pederson, M.R.; Singh, D.J.; Fiolhais, C. *Phys. Rev. B* **1992**, *46*, 6671.

300. Perdew, J.P.; Burke, K.; Wang, Y. *Phys. Rev. B* **1996**, *54*, 16533.

301. Hehre, W.J.; Stewart, R.F.; Pople, J.A. *J. Chem. Phys.* **1969**, *51*, 2657.

302. Collins, J.B.; Schleyer, P.v.R.; Binkley, J.S.; Pople, J.A. *J. Chem. Phys.* **1976**, *64*, 5142.

303. Binkley, J.S.; Pople, J.A.; Hehre, W.J. *J. Am. Chem. Soc.* **1980**, *102*, 939.

304. Dobbs, K.D.; Hehre, W.J. *J. Comp. Chem.* **1987**, *8*, 880.

305. Ditchfield, R.; Hehre, W.J.; Pople, J.A. *J. Chem. Phys.* **1971**, *54*, 724.

306. Binning, R.C., Jr.; Curtiss, L.A. *J. Comp. Chem.* **1990**, *11*, 1206.

307. Dunning, T.H. *J. Chem. Phys.* **1989**, *90*, 1007.

308. Woon, D.E.; Dunning, T.H., Jr. *J. Chem. Phys.* **1993**, *98*, 1358.

309. Pascal, R.A., Jr. *J. Phys. Chem.A* **2001**, *105*, 9040.

310. Hehre, W.J.; Radom, L.; Schleyer, P.v.R.; Pople, J.A. *Ab Initio Molecular Orbital Theory*; John Wiley & Sons: New York, 1986; pp 63-100.

311. Barone, V. *Chem. Phys. Lett.* **1994**, *226*, 392.

312. Siegel, A.; Rausch, M.D. *Synth. React. Inorg. Met.-Org. Chem.* **1978**, *8*, 209.

313. Gupta, H.K.; Brydges, S.; McGlinchey, M.J. *Organometallics* **1999**, *18*, 115.

314. Rausch, M.D.; Siegel, A. *J. Org. Chem.* **1968**, *33*, 4545.

315. Draper, S. M. Personal communication re: C_6Ph_4FcH. 2003.

316. Yasufuku, K.; Aoki, K.; Yamazaki, H. *Inorg. Chem.* **1977**, *16*, 624.

317. Dunning, T.H., Jr.; Hay, P.J.*Modern Theoretical Chemistry*; Plenum: New York, 1976.

318. Dilthey, W.; Schommer, W.; Höschen, W.; Dierichs, H. *Ber.* **1935**, *68*, 1159.

319. Pascal, R.A., Jr.; Hayashi, N.; Ho, D.M. *Tetrahedron* **2001**, *57*, 3549.

320. Bosch, E.; Hubig, S.M.; Lindeman, S.V.; Kochi, J.K. *J. Org. Chem.* **1998**, *63*, 592.

321. Toyota, S.; Yamamori, T.; Makino, T. *Tetrahedron* **2001**, *57*, 3521.

322. Desiraju, G.R. *Chem. Commun.* **1997**, 1475.

323. Gregson, D.; Howard, J.A.K. *Acta Crystallogr.* **1983**, *C39*, 1024.

324. Housecraft, C.E.; Johnson, B.F.G.; Khan, M.S.; Lewis, J.; Raithby, P.R.; Robson, M.E.; Wilkinson, D.A. *J. Chem. Soc., Dalton Trans.* **1992**, 3171.

325. Dickson, R.S.; Michel, L.J. *Aust. J. Chem.* **1975**, *28*, 1957.

326. Yamazaki, S.; Deeming, A.J.; Speel, D.M. *Organometallics* **1998**, *17*, 775.

327. Ugo, R.; Cariati, F.; La Monica, G. *Inorg. Synth.* **1968**, *11*, 105.

328. Hayashi, N.; Ho, D.M.; Pascal, R.A., Jr. *Tetrahedron Lett.* **2000**, *41*, 4261.

329. Elwahy, A.H.M.; Hafner, K. *Tetrahedron Lett.* **2000**, *41*, 2859.

330. Müller, T.J.J.; Linder, H.J. *Chem. Ber.* **1996**, *129*, 607.

331. Müller, T.J.J.; Ansorge, M.; Linder, H.J. *Chem. Ber.* **1996**, *129*, 1433.

332. Schmid, G.H.; Modro, A.; Yates, K. *J. Org. Chem.* **1980**, *45*, 665.

333. Espenson, J.H.; Zhu, Z.; Zauche, T.H. *J. Org. Chem.* **1999**, *64*, 1191.

334. Barnes, J.C.; Chudek, J.A. *Acta Cryst.* **2002**, *E58*, o703.

335. Bright, S.T.; Coxon, J.M.; Steel, P.J. *J. Org. Chem.* **1990**, *55*, 1338.

336. Cuingnet, E. *Bull. Soc. Chim. Fr.* **1955**, 91.

337. Capmau, M.-L.; Chodkiewicz, W.; Cadiot, P.; Fayet, A.-M. *Bull. Soc. Chim. Fr.* **1968**, 3238.

338. Brittelli, D.R.; Boswell, G.A., Jr. *J.Org.Chem.* **1981**, *46*, 312.

339. Korkas, P.P.; Weber, E.; Czugler, M.; Náray-Szabó, G. *Chem. Commun.* **1995**, 2249.

340. Bauer, R.E.; Enkelmann, V.; Wiesler, U.M.; Berresheim, A.J.; Müllen, K. *Chem. Eur. J.* **2002**, *8*, 3858.

341. Oguma, K.; Miura, M.; Satoh, T.; Nomura, M. *J. Am. Chem. Soc.* **2000**, *122*, 10464.

342. Treichel, P.M.; Johnson, J.W. *J. Organomet. Chem.* **1975**, *88*, 207.

343. Salzer, A.; Täschler, C. *J. Organomet. Chem.* **1984**, *291*, 261.

344. Clark, D.T.; Mlekuz, M.; Sayer, B.G.; McCarry, B.E.; McGlinchey, M.J. *Organometallics* **1987**, *6*, 2201.

345. Veiros, L.F. *J. Organomet. Chem.* **1999**, *587*, 221.

346. Veiros, L.F. *Organometallics* **2000**, *19*, 3127.

347. Bavin, P.M.G.; Ganellin, C.R.; Loynes, J.M.; Spickett, R.G.W. *J. Med. Chem.* **1969**, *12*, 513.

348. Wentrup, C.; Wentrup-Byrne, E.; Müller, P.; Becker, J. *Tetrahedron Lett.* **1979**, *44*, 4249.

349. Sonntag, N.O.V.; Linder, S.; Becker, E.I.; Spoerri, P.E. *J. Am. Chem. Soc.* **1953**, *75*, 2283.

350. Lee, S.-G.; Lee, S.S.; Chung, Y.K. *Inorg. Chim. Acta* **1999**, *286*, 215.

351. *CSD, November Release V5.24 2002*; Cambridge Crystallographic Data Center: University Chemical Laboratory, Cambridge, England, 2002.

352. Siemsen, P.; Livingston, R.C.; Diederich, F. *Angew. Chem. Int. Ed.* **2000**, *39*, 2632.

353. Bunz, U.H.F. *Acc. Chem. Res.* **2001**, *34*, 998.

354. Hückel, E. *Z. Physik* **1931**, *70*, 204.

355. Doering, W. E.; Knox, L. H. *J. Am. Chem. Soc.* **1954**, *76*, 3203.

356. Vol'pin, M. E. *Russ. Chem. Rev.* **1960**, 129.

357. Kolomnikova, G. D.; Parnes, Z. N. *Russ. Chem. Rev.* **1967**, *36*, 735.

358. Deganello, G. *Transition Metal Complexes of Cyclic Polyolefins*; Academic Press: London, 1979; pp Chapter 1.

359. Freedman, H.E.In *Carbonium Ions*; Olah, G.A., Schleyer, P.v.R., Eds.; Wiley-Interscience: New York, 1973;

360. Jutz, C.; Voithenleitner, F. *Ber.* **1964**, *97*, 29.

361. Battiste, M.A.; Barton, T.J. *Tetrahedron Lett.* **1968**, *25*, 2951.

362. Battiste, M. A. *J. Am. Chem. Soc.* **1963**, *85*, 2175.

363. Komatsu, K.; Akamatsu, H.; Jinbu, Y.; Okamoto, K. *J. Am. Chem. Soc.* **1988**, *110*, 633.

364. Jutz, C.; Voithenleitner, F. *Chem. Ber.* **1964**, 97, 1337.

365. Okamoto, K., Takeuchi, K., Komatsu, K., Kubota, Y., Ohara, R., Arima, M., Takahashi, K., Waki, Y., and Shirai, S. *Tetrahedron* **1983**, *39*, 4011.

366. Stiles, M.; Libbey, A. J. *J. Org. Chem.* **1957**, *22*, 1243.

367. Knoche, H. *Chem. Ber.* **1966**, *99*, 1097.

368. Kusuda, K.; West, R.; Rao, V. N. M. *J. Am. Chem. Soc.* **1971**, *93*, 3627.

369. Battiste, M.A. *Chem. Ind.* **1961**, 550.

370. Chao, L.C.F.; Gupta, H.K.; Hughes, D.W.; Britten, J.F.; Rigby, S.S.; Bain, A.D.; McGlinchey, M.J. *Organometallics* **1995**, *14*, 1139.

371. Doering, W. von E.; Laber, G.; Vonderwahl, R.; Chamberlain, N. F.; Williams, R. B. *J. Am. Chem. Soc.* **1956**, *78*, 5448.

372. Harvey, J. A.; Ogliaruso, M. A. *J. Org. Chem.* **1976**, *41*, 3374.

373. Anet, F. A. L. *J. Am. Chem. Soc.* **1964**, *86*, 458.

374. Jensen, F. R.; Smith, L. A. *J. Am. Chem. Soc.* **1964**, *86*, 956.

375. Aonuma, S.; Komatsu, K.; Takeuchi, K. *Chem. Lett.* **1989**, 2107.

376. Nógrádi, M.; Ollis, W. D.; Sutherland, I. O. *Chem. Commun.* **1970**, 158.

377. Stradiotto, M. J.; McGlinchey, M. J. *Coord. Chem. Rev.* **2001**, *219-221*, 311.

378. Abel, E. W.; Bennett, M. A.; Burton, R.; Wilkinson, G. *J. Chem. Soc.* **1958**, 4559.

379. Dauben, H. J.; Honnen, L. R. *J. Am. Chem. Soc.* **1958**, *80*, 5570.

380. Green, M. L. H.; Ng, D. K. P. *J. Chem. Soc., Dalton Trans.***1993**, *17*.

381. Bennett, M.J.; Pratt, J.L.; Simpson, K.A.; Li Shing Man, L.K.K.; Takats, J. *J. Am. Chem. Soc.* **1976**, *98*, 4810.

382. Battiste, M.A. *J. Am. Chem. Soc.* **1962**, *84*, 3780.

383. Breslow, R.; Chang, H. W. *J. Am. Chem. Soc.* **1962**, *84*, 1484.

384. Brydges, S.; Britten, J.F.; Chao, L.C.F.; Gupta, H.K.; McGlinchey, M.J.; Pole, D.L. *Chem. Eur. J.* **1998**, *4*, 1201.

385. Dunn, J. A.; Gupta, H. K.; Bain, A. D.; McGlinchey, M. J. *Can. J. Chem.* **1996**, *74*, 2258.

386. Yamamoto, K.; Harada, T.; Okamoto, Y.; Chikamatsu, H.; Nakazaki, M.; Kai, Y.; Nakao, T.; Tanaka, M.; Harada, S.; Kasai, N. *J. Am. Chem. Soc.* **1988**, *110*, 3578.

387. Kagayama, A.; Komatsu, K.; Nishinaga, T.; Takeuchi, K.; Kabuto, C. *J. Org. Chem.* **1994**, *59*, 4999.

388. Eisch, J. J.; Gale, J. E. *J. Am. Chem. Soc.* **1975**, *97*, 4436.

389. Iyoda, M.; Sultana, F.; Sasaki, S.; Butenschön, H. *Tetrahedron Lett.* **1995**, *36*, 579.

390. Bailey, P.J.; Blake, A.J.; Dyson, P.J.; Ingham, S.L.; Johnson, B.F.G. *J. Chem. Soc., Chem. Commun.* **1994**, 2233.

391. Borgias, B.A.; Scarrow, R.C.; Seidler, M.D.; Weiner, W.P. *Acta Cryst.* **1985**, *C41*, 476.

392. Braga, D.; Grepioni, F. *Chem. Commun.* **1996**, 571.

393. Braga, D.; Grepioni, F.; Desiraju, G.R. *Chem. Rev.* **1998**, *98*, 1375.

394. Gould, E.S. *Acta Cryst.* **1955**, *8*, 657.

395. Kitaigorodshii, A. I.; Khotsyanova, T. L.; Struchkov, Y. T. *Acta Crystallogr.***1957**, *10*, 797.

396. Kitaigorodshii, A.I.; Struchkov, Yu.T.; Khotsyanova, T.L.; Volpin, M.E.; Kursanov, D.N. *Izv. Akad. Nauk. SSSR, Ser. Khim.* **1960**, 39.

397. Brownstein, S.K.; Gabe, E.J.; Hynes, R.C. *Can. J. Chem.* **1992**, *70*, 1011.

398. Bruce, M.I.; Humphrey, P.A.; Skelton, B.W.; White, A.H. *Aust. J. Chem.* **1986**, *39*, 165.

399. Takahashi, Y.; Sankararaman, S.; Kochi, J.K. *J. Am. Chem. Soc.* **1989**, *111*, 2954.

400. Jeffrey, G. A.; Ruble, J. R.; McMullan, R. K.; Pople, J. A. *Proc. R. Soc. London* **1987**, *A414*, 47.

401. Kitaygorodsky, A.I. *Molecular Crystals and Molecules*; Academic Press: New York, 1973.

402. Lipkowitz, K. B.; Peterson, M. A. *J. Comput. Chem.* **1993**, 14, 121.

403. Krygowski, T. M.; Turowska-Tyrk, I. *Chem. Phys. Lett.* **1987**, *138*, 90.

404. Memory, J.D.; Wilson, N.K. *NMR of Aromatic Compounds*; John Wiley & Sons, Inc.: New York, 1982.

405. Spiesecke, H.; Schneider, W.G. *Tetrahedron Lett.* **1961**, 468.

406. Olah, G.A.; Mateescu, G.D. *J. Am. Chem. Soc.* **1970**, *92*, 1430.

407. Nelson, G. L.; Williams, E. A. *Prog. Phys. Org. Chem.* **1976**, *12*, 229.

408. Hill, E.A.; Wiesner, R. *J. Am. Chem. Soc.* **1969**, *91*, 510.

409. Gleiter, R.; Seeger, R.; Binder, H.; Fluck, E.; Cais, M. *Angew. Chem. Int. Ed. Engl.* **1972**, *11*, 1028.

410. Dannenberg, J.J.; Lavenberg, M.K.; Richards, J.H. *Tetrahedron* **1973**, *29*, 1575.

411. McGlinchey, M.J.; Girard, L.; Ruffolo, R. *Coord. Chem. Rev.* **1995**, *143*, 331.

412. El Amouri, H.; Gruselle, M. *Chem. Rev.* **1996**, *96*, 1077.

413. Harrington, L.E.; Vargas-Baca, I.; Reginato, N.; McGlinchey, M.J. *Organometallics* **2003**, *22*, 663.

414. Caffyn, A.J.M.; Nicholas, K.M. In *Comprehensive Organometallic Chemistry II*; Wilkinson, G., Stone, F.G.A., Abel, E.W., Eds.; Pergamon: Oxford, U.K., 1995; pp 685-702.

415. Barlow, S.; Cowley, A.; Green, J. C.; Brunker, T. J.; Hascall, T. *Organometallics* **2001**, 20, 5351.

416. Malisza, K.L.; Top, S.; Vaissermann, J.; Caro, B.; Sénéchal-Tocquer, M.-C.; Sénéchal, D.; Saillard, J.-Y.; Triki, S.; Kahlal, S.; Britten, J.F.; McGlinchey, M.J.; Jaouen, G. *Organometallics* **1995**, *14*, 5273.

417. Sime, R. L.; Sime, R. J. *J. Am. Chem. Soc.* **1974**, *96*, 892.

418. Cais, M.; Dani, S.; Herbstein, F. H.; Kapon, M. *J. Am. Chem. Soc.* **1978**, *100*, 5554.

419. Crabtree, R.H. *The Organometallic Chemistry of the Transition Metals*; Wiley: New York, N.Y., 1993; pp 131.

420. Deeming, A.J. In *Comprehensive Organometallic Chemistry*; Wilkinson, G., Stone, F.G.A., Abel, E.W., Eds.; Pergamon: Oxford, U.K., 1982; pp 479.

421. Tamm, M.; Dre□el, B.; Fröhlich, R. *J. Org. Chem.* **2000**, *65*, 6795.

422. Roberts, A.; Whiteley, M.W. *J. Organomet. Chem.* **1993**, *458*, 131.

423. Schwed, E.; Hund, H.-U.; Bosch, H.W.; Berke, H. *Helv. Chim. Acta* **1991**, *74*, 189.

424. Tamm, M.; Dreβel, B.; Fröhlich, R.; Bergander, K. *Chem. Commun.* **2000**, 1731.

425. Tamm, M.; Bannenberg, T.; Dressel, B. *Organometallics* **2001**, *20*, 900.

426. Whitesides, T. H.; Budnik, R. A. *Chem. Commun.* **1971**, 1514.

427. Whitesides, T. H.; Budnik, R. A. *Inorg. Chem.* **1976**, *15*, 874.

428. Breslow, R.; Chang, H.W. *J. Am. Chem. Soc.* **1965**, *87*, 2200.

429. Brydges, S.; Harrington, L.E.; McGlinchey, M.J. *Coord. Chem. Rev.* **2002**, *232-234*, 75.

430. Nicolet, P.; Sanchez, J.-Y.; Benaboura, A.; Abadie, M.J.M. *Synthesis* **1987**, 202.

431. Müllen, K.; Simmross, U. *Chem. Ber.* **1993**, *126*, 969.

432. Feringa, B.L.; van Delden, R.A.; Koumura, N.; Geertsema, E.M. *Chem. Rev.* **2000**, *100*, 1789.

433. Verbiest, T.; Houbrechts, S.; Kauranen, M.; Clays, K.; Persoons, A. *J. Mater. Chem.* **1997**, *7*, 2175.

434. Sugihara, T.; Wakabayashi, A.; Nagai, Y.; Takao, H.; Imagawa, H.; Nishizawa, M. *Chem. Commun.* **2002**, 576.

435. Gupta, H.K.; Reginato, N.; Ogini, F.O.; Brydges, S.; McGlinchey, M.J. *Can. J. Chem.* **2002**, *80*, 1546.

436. Rosenblum, M.; Brawn, S.; S.J.; King, B. *Tetrahedron Lett.* **1967**, *45*, 4421.

437. Hennrich, G.; Anslyn, E.V. *Chem. Eur. J.* **2002**, *8*, 2219.

438. Katz, H.E. *J. Org. Chem.* **1987**, *52*, 3932.

439. Ried, W.; Freitag, D. *Angew. Chem., Int. Ed. Engl.* **1968**, *7*, 835.

440. Leininger, S.; Olenyuk, B.; Stang, P.J. *Chem. Rev.* **2000**, *100*, 853.

441. Sweigers, G.F.; Malefetse, T.J. *Chem. Rev.* **2000**, *100*, 3483.

442. Whitesides, G.M.; Love, J.C. In *Societal Implications of Nanoscience and Nanotechnology*; Roco, M.C., Bainbridge, W.S., Eds.; Kluwer Academic Publishers: Dordrecht, The Netherlands, 2000; pp 129-145.

443. Drexler, K.E. *Nanosystems: Molecular Machinery, Manufacturing and Computation*; John Wiley & Sons, Inc.: New York, 1992.

444. Crow, M.M.; Sarewitz, D. In *Societal Implications of Nanoscience and Nanotechnology*; Roco, M.C., Bainbridge, W.S., Eds.; Kluwer Academic Publishers: Dordrecht, The Netherlands, 2000; pp 55-67.

445. Perrin, D.D.; Armarego, W.L.F.; Perrin, D.R. *Purification of Laboratory Chemicals*; Pergamon Press: New York, 1980.

446. SMART, Version 4.05. 1996. Madison, WI 53711, Bruker AXS. Inc.

447. SAINT, Version 4.05. 1996. Madison, WI 53711, Bruker AXS Inc.

448. Sheldrick, G. M. SADABS. 1996.

449. Sheldrick, G. M. SHELXTL, Version 5.03. 1994. Madison, WI 53711, Bruker AXS Inc.

450. Spek, A.L. *Acta Cryst.* **1990**, *A46*, C-34.

451. Spek, A. L. PLATON, Program for the Automated Analysis of Molecular Geometry. (Version 20501). 2001. Utrecht University, Netherlands.

452. Van der Sluis, P.; Spek, A.L. *Acta Cryst.* **1990**, *A46*, 194.

453. Broadhead, G.D.; Osgerby, J.M.; Pauson, P.L. *J. Chem. Soc.* **1958**, 650.

454. Baldridge, K.K.; Greenberg, J.P. *J. Mol. Graphics* **1995**, *13*, 63.

455. Schmidt, M.W.; Baldridge, K.K.; Boatz, J.A.; Elbert, S.T.; Gordon, M.S.; Jensen, J.H.; Koseki, S.; Matsunaga, N.; Nguyen, K.A.; Su, S.; Windus, T.L.; Dupuis, M.; Montgomery, J.A. *J. Comput. Chem.* **1993**, *14*, 1347.

456. Møller, C.; Plesset, M.S. *Phys. Rev.* **1934**, *46*, 618.

457. Lee, C.; Yang, W.; Parr, R.G. *Phys. Rev. B* **1988**, *37*, 785.

458. Miehlich, B.; Savin, A.; Stoll, H.; Preuss, H. *Chem. Phys. Lett.* **1989**, *157*, 200.

459. Perdew, J.P.; Chevary, J.A.; Vosko, S.H.; Jackson, K.A.; Pederson, M.R.; Singh, D.J.; Fiolhais, C. *Phys. Rev. B* **1993**, *48*.

460. Hay, P.J.; Wadt, W.R. *J. Chem. Phys.* **1985**, *82*, 284.

461. Merlic, C.A.; Walsh, J.C.; Tantillo, D.J.; Houk, K.N. *J. Am. Chem. Soc.* **1999**, *121*, 3596.

462. Inoue, K.; Takeuchi, H.; Konaka, S. *J. Phys. Chem. A* **2001**, *105*, 6711.

APPENDIX A: Structure Correlation Data

Cambridge Structural Database Results

Table A.1. Supplementary Structure Correlation Data [CSD Version 5.21, April 2001], C_5Ar_5_Aromatic Fragments

Nfrag	Refcode	ANG1*	ANG2*	ANG3*	ANG4*	ANG5*	Designation
1	CIZHOI	58.788	51.404	48.676	48.572	47.734	Propeller
2	DAYPIC	60.286	54.936	45.627	54.245	44.339	Propeller
3	FAFZAN	51.820	52.090	65.224	49.375	55.476	Propeller
4	GAHRUC	48.898	64.198	51.702	50.439	55.185	Propeller
5	GOFFIQ	55.936	47.164	69.619	50.030	43.119	Propeller
6	GOTJII	45.952	51.885	55.439	48.052	59.649	Propeller
7	GOTJOO	47.490	39.771	63.949	51.454	50.174	Propeller
8	HAYMEZ	49.331	48.623	51.936	49.214	52.969	Propeller
9	HAYMEZ	55.682	-75.483	-43.116	-58.532	53.760	Non-Prop
10	HEDRAJ	44.364	61.891	55.866	45.549	52.343	Propeller
11	HESLOG	50.642	58.253	49.113	57.759	50.706	Propeller x2
12	HESLUM	57.701	47.267	51.047	48.919	43.737	Propeller x2
13	HESLUM	35.907	57.754	43.400	45.115	63.285	Propeller x2
14	HOGPAU	60.073	39.479	60.598	-88.030	51.118	Non-Prop
15	HOGPEY	54.689	44.687	56.024	56.394	51.029	Propeller
16	JEFKUA	45.020	59.637	46.847	49.968	37.245	Propeller
17	JIVFEZ	50.547	49.969	64.536	40.666	46.922	Propeller
18	KECDOL	44.505	50.558	62.581	50.330	48.092	Propeller
19	KECDOL	51.956	45.322	43.560	53.492	58.569	Propeller
20	KESSAC	55.778	26.415	66.151	53.417	52.724	Propeller
21	KIDLAK	44.879	71.689	49.424	71.468	64.870	Propeller
22	KOLLAY	58.939	56.500	57.155	47.212	67.671	Propeller
23	KOLLAY	80.841	51.749	50.728	49.780	47.971	Propeller
24	KOLLEC	45.451	53.543	54.486	59.401	55.937	Propeller
25	LELJER	52.074	48.570	50.817	52.648	50.094	Propeller
26	NICDIM	46.819	45.315	51.346	49.878	66.579	Propeller
27	NOWYON	64.423	45.806	57.709	52.576	52.058	Propeller
28	PAVFUN	59.306	42.402	52.866	43.132	50.940	Propeller
29	POHQUY	52.472	49.004	51.739	43.869	49.827	Propeller x2
30	POHQUY	44.277	59.529	38.111	57.607	49.083	Propeller x2
31	POHXAL	52.325	48.610	57.261	40.262	52.043	Propeller x2
32	POHXAL	45.165	60.568	34.970	59.921	49.532	Propeller x2
33	PURCOU	58.465	50.967	60.461	51.185	52.362	Propeller
34	RAQZUE	47.995	51.092	54.711	49.990	51.907	Propeller
35	RAQZUE	55.562	45.599	56.760	54.958	47.689	Propeller
36	RURLUL	55.908	46.888	35.052	55.026	55.365	Propeller
37	RURLUL	50.066	66.932	49.524	47.463	50.851	Propeller
38	SIRMIP	37.197	59.336	-87.376	49.057	59.709	Non-Prop
39	SOKLUZ	48.825	52.863	46.584	50.147	47.252	Propeller
40	SOKLUZ	57.934	43.111	48.557	46.219	50.928	Propeller
41	TINBEX	65.355	50.721	45.563	50.137	54.548	Propeller
42	TOZLAV	42.830	58.693	34.767	57.243	43.036	Propeller x2

43	TOZLAV	48.228	56.263	44.551	49.870	50.866	Propeller x2
44	TOZLEZ	51.793	48.060	52.572	42.626	49.700	Propeller x2
45	TOZLEZ	43.088	59.902	36.327	58.113	48.022	Propeller x2
46	TOZLID	43.763	59.865	34.906	57.595	43.538	Propeller x2
47	TOZLID	48.821	56.807	45.798	51.242	52.129	Propeller x2
48	TUPQAW	55.385	62.392	47.057	65.512	39.197	Propeller
49	VIVLIV	47.991	56.244	47.943	55.350	51.423	Propeller
50	VIXKIW	43.484	59.802	55.543	48.008	74.925	Propeller
51	VORGIS	45.282	56.767	52.511	49.713	57.990	Propeller
52	VORGOY	55.053	51.467	46.381	48.629	52.090	Propeller
53	WAFKIX	55.390	48.003	47.798	55.771	78.055	Propeller x2
54	WAFKOD	45.406	48.136	48.345	53.590	75.304	Propeller x2
55	WAFMAR	51.837	52.685	61.552	59.338	42.128	Propeller
56	WAFMEV	47.688	52.562	46.622	54.297	52.781	Propeller
57	WAFMEV	49.338	48.177	51.676	43.387	66.063	Propeller
58	WAHVEG	47.712	54.173	57.433	49.668	61.947	Propeller
59	YECHIX	45.834	54.602	47.066	51.078	57.211	Propeller
60	YECHIX01	44.807	51.770	47.248	59.588	60.305	Propeller
61	YOGKAG	46.478	52.473	44.561	60.963	41.703	Propeller
62	YOGKAG	76.856	50.704	51.800	52.741	37.575	Propeller

Statistics:	*Mean*	51.398	52.696	51.430	52.513	52.925
	Minimum	35.907	26.415	34.767	40.262	37.245
	Maximum	80.841	75.483	87.376	88.030	78.055
	No. of Propellers:		59			
	No. of Non-Propellers:		3			
	No. of Mirror Structures:		0			

Notes:

1. **DATA RETRIEVAL:**
- Included C_5Ar_5 fragments with: peripheral aryl substitution; metal coordination; charged species; no geometrical constraints
- Excluded C_5Ar_5 fragments with: ESD planarity of central C5-ring > 0.05 Å; R-factor > 0.10

2. **DATA TREATMENT:**
* Absolute values converted to arbitrary +/-
* Angles calculated from plane of central C_5 ring

Table A.2. Supplementary Structure Correlation Data [CSD Version 5.21, April 2001], C_5Ar_4X_Aromatic (X ≠ Ar) Fragments

Nfrag	C5-Center (X)	Refcode	ANG1*	ANG2*	ANG3*	ANG4*	Designation
1	Br	BTPCYP	31.330	67.450	-73.604	-35.081	Mirror
2	OMe	COVQIN	48.693	53.694	48.031	76.756	Propeller
3	OH	COVQOT	51.603	50.150	58.175	42.914	Propeller
4	OR	COVREK	79.014	49.460	48.543	63.943	Propeller x2
5	OMe	*COVTEM	58.042	50.699	49.475	51.546	Propeller
6	H	DULNUT	32.996	47.461	77.213	15.244	Propeller x2
7	H	FOCJAI	31.664	46.771	67.234	23.677	Propeller x2
8	H	FOCJEM	31.892	46.840	69.887	19.673	Propeller x2
9	H	FOCJIQ	32.594	46.027	71.113	18.788	Propeller x2
10	H	FOCJOW	31.810	46.169	64.817	22.651	Propeller x2
11	OCOR	FUBVAZ	59.553	51.769	60.255	43.743	Propeller
12	H	HADPUX	41.684	39.725	-85.795	-37.161	Mirror
13	H	HAYMID	23.050	73.308	-54.283	-30.918	Mirror
14	H	HAYMID	32.686	59.332	-89.937	-36.912	Mirror
15	SMe	HOBWOK	41.210	59.556	50.810	59.175	Propeller
16	H	JEDPEN	34.786	44.583	79.810	-13.026	Non-Prop
17	H	JEDPEN	36.007	43.947	72.172	-20.737	Non-Prop
18	H	JIWDOI	33.908	49.816	77.725	17.258	Propeller x2
19	OH	KOMYUG	44.262	88.555	-70.235	-41.045	Mirror
20	OH	KOMYUG	36.915	82.131	60.174	34.736	Propeller
21	OH	KUWJAN	43.335	66.515	-67.637	-37.510	Mirror
22	OH	KUWJAN	47.882	63.955	-65.474	-41.934	Mirror
23	H	NUZSUW	26.230	87.208	-59.411	-22.652	Mirror
24	H	NUZSUW	25.073	75.749	-68.647	-24.444	Mirror
25	CR	PAPMAU	71.191	-58.485	-48.306	-55.215	Non-Prop
26	CR	PAPMAU	56.647	46.887	62.429	-64.618	Non-Prop
27	H	PECTUM	38.883	70.017	-52.743	-31.208	Mirror
28	H	PECTUM	29.978	52.729	-75.020	-28.962	Mirror
29	H	PECTUM	31.154	80.174	-56.608	-31.249	Mirror
30	H	PECTUM	25.619	55.282	-64.664	-35.359	Mirror
31	H	RATNIJ	33.997	51.441	48.291	34.353	Propeller
32	OR	REVHEF	50.681	52.512	59.555	44.104	Propeller
33	OH	REVHIJ	54.931	55.537	50.071	46.889	Propeller
34	$OSnPh_3$	SNCPMN	49.525	51.638	46.910	87.963	Propeller
35	H	*SUHLEM	33.600	59.100	82.600	-12.400	Non-Prop
36	H	SUHLOW	22.897	70.684	42.190	35.745	Propeller x2
37	H	TUFVAR	43.295	43.788	62.110	54.977	Propeller
38	H	VERPEN	33.876	56.110	59.236	26.583	Propeller
39	H	WEYBIL	28.588	63.335	-63.184	-32.578	Mirror x2
40	pyr+	YORCUD	54.483	44.827	54.652	37.336	Propeller
41	OH	YOSXAF	41.227	50.133	60.766	38.742	Propeller
42	H	YOSZUB	33.540	50.016	77.173	19.467	Propeller x2

43	cyclohexyl	ZAFVAD	56.744	48.690	45.027	74.096	Propeller
44	cyclohexyl	ZAFVEH	54.517	51.429	-89.615	-67.982	Mirror
45	cyclohexyl	ZAFVEH	77.516	36.381	89.036	-50.524	Non-Prop
46	CPhMe	ZAGVOS	65.900	47.026	53.061	-84.402	Non-Prop
47	H	ZAGZAI	32.097	55.265	53.078	44.234	Propeller x2
48	cyclohexyl	ZERCOO	83.511	-57.992	-48.449	-62.672	Non-Prop
49	cyclohexyl	ZERCOO	-69.735	68.684	48.531	71.939	Non-Prop
50	H	ZOZHOL	30.535	44.638	52.084	32.117	Propeller

Statistics:	*Mean*	43.218	56.273	62.717	40.745
	Minimum	22.897	36.381	42.190	12.400
	Maximum	83.511	88.555	89.937	87.963
	No. of Propellers:		26		
	No. of Non-Propellers:		9		
	No. of Mirror Structures:		15		

Notes:

1. **DATA RETRIEVAL:**
- Included C_5Ar_4X fragments with: peripheral aryl substitution; metal coordination; charged species; no geometrical constraints
- Excluded C_5Ar_4X fragments with: ESD planarity of central C5-ring > 0.05 Å; R-factor > 0.10

2. **DATA TREATMENT:**
* Absolute values converted to arbitrary +/-
* Angles calculated from plane of central C_5 ring

Table A.3. Supplementary Structure Correlation Data [CSD Version 5.21, April 2001], C_5Ar_4X_Non-Aromatic Fragments.

Nfrag	C5-Center (X)	Refcode	ANG1*	ANG2*	ANG3*	ANG4*	Designation
1	H, $AuPPh_3$	BAJZAN	35.065	57.871	59.380	38.831	Propeller
2	=O	BEJROX	35.780	65.018	-59.736	-52.806	Mirror
3	=O	CAGFIZ	20.647	51.692	-44.412	-50.165	Mirror
4	=O	*COVQUZ	38.865	53.461	63.184	41.024	Propeller
5	=O	*COVQUZ	50.700	41.400	57.300	79.000	Propeller
6	=O	CPMSCO	48.770	42.990	-72.633	-33.570	Mirror
7	spiro	DAKLAC	63.411	35.775	67.818	-84.811	Non-Prop
8	spiro	DITYUA	45.387	53.721	44.046	72.600	Propeller
9	spiro	DITYUA10	45.387	53.721	44.046	72.600	Propeller
10	=O	DOCCON	53.289	41.886	51.634	46.291	Propeller
11	=O	DOHQUM	44.148	48.803	50.916	50.869	Propeller
12	=O	DOHSOI	40.780	67.226	-65.761	-37.766	Mirror x2
13	=O	GIMWAA	43.065	84.417	-61.278	-38.511	Mirror
14	Ph, SC(S)OEt	HERBEL	32.924	51.143	60.044	67.885	Propeller
15	Ph, SC(S)OEt	HERBEL	61.593	52.470	54.895	31.347	Propeller
16	=C-Ph	JEDAIC	68.567	44.908	52.080	52.745	Propeller
17	=N=N	*JENPIB	52.353	37.859	58.786	45.244	Propeller
18	Ph, H	JUZSOM	15.598	74.523	83.751	-46.764	Non-Prop
19	=O	KIKTUT	27.296	60.542	47.777	36.123	Propeller
20	=O	KIKTUT01	27.485	60.525	47.721	36.290	Propeller
21	CH_3, $NHCH_2Ph$	KOPBAS	38.471	57.181	46.130	58.612	Propeller
22	Ph, H	KUKDEZ	31.501	70.764	-65.548	-32.883	Mirror
23	Ph, $SnCl_3$	NORKIO	53.363	58.878	46.929	40.819	Propeller
24	Ph, H	NOWYIH	36.891	58.406	89.185	-22.796	Mirror/Non-Prop
25	=O	PABPMO	52.508	79.859	-55.505	-33.992	Mirror
26	Ph, OH	PECXEA	35.217	51.833	60.941	40.401	Propeller
27	Ph, OH	PECXIE	48.989	48.293	54.897	41.500	Propeller
28	Ph, OH	PECXOK	48.958	54.356	60.663	26.513	Propeller
29	Ph, $(CPh)_3W(CO)(PhCCPh)$	*PEHJIV	52.372	68.253	29.701	41.860	Propeller
30	=O	PIXLEN	67.339	36.477	59.014	36.718	Propeller
31	H^-	RATNOP	34.004	53.602	38.559	44.401	Propeller
32	H^-	RATNUV	40.682	43.630	45.721	38.079	Propeller
33	H, Et(9-fluorenyl)	REHZAF	32.787	60.483	-73.703	-31.924	Mirror
34	Ph, $GeCl_3$	SAZSER	58.109	59.208	-72.673	-57.225	Mirror
35	CPh, $OC(O)CF_3$	SOSWUS	24.628	59.768	69.038	24.591	Propeller
36	=O	SOSXUT10	58.314	66.823	63.855	-54.925	Non-Prop
37	spiro	SUNGAJ	-78.518	88.137	60.130	36.643	Non-Prop
38	H, H	TPHCYP	23.524	69.581	-69.427	-33.088	Mirror
39	H^-	TUQWOR	32.242	45.257	47.552	36.836	Propeller
40	=O	VANHOH	40.256	65.554	-62.249	-43.221	Mirror x2
41	Ph, OH	YEBCUD	50.510	49.818	54.034	39.209	Propeller
42	Ph, OH	YEBDAK	58.077	52.776	63.475	31.106	Propeller

43	Ph, OH	YEBDAK	62.683	51.789	45.943	48.531	Propeller
44	spiro	ZANDEX	59.079	56.858	53.047	40.577	Propeller
45	spiro	ZOQKUL	53.072	43.801	65.886	22.052	Propeller
46	=O	**	43.400	70.100	-60.200	-41.000	Mirror
47	=O	**	40.000	60.200	-68.900	-41.100	Mirror
48	=O	**	55.200	53.500	-67.900	-40.900	Mirror
49	=O	**	43.900	52.200	-83.600	-47.400	Mirror
50	=O	**	43.400	58.000	-57.400	-43.700	Mirror

Statistics:	*Mean*	44.982	56.507	58.780	43.757
	Minimum	15.598	35.775	29.701	22.052
	Maximum	78.518	88.137	89.185	84.811

No. of Propellers:	29
No. of Non-Props:	5
No. of Mirror Strucs:	16
Sp2 centers:	22
Sp3 centers:	28

Notes:

1. **DATA RETRIEVAL:**
- Included C_5Ar_4X fragments with: peripheral aryl substitution; metal coordination; charged species; no geometrical constraints
- Excluded C_5Ar_4X fragments with R-factor > 0.10

2. **DATA TREATMENT:**
- Absolute values converted to arbitrary +/-
- Angles calculated from diene plane of central C_5 ring

** Not yet entered into CSD: Harrington, L.E.; Britten, J.F.; Hughes, D.J.; Bain, A.D.; Thepot, J.-Y.; McGlinchey, M.J. *J.Organomet.Chem.* **2002**, in press.

** Re NFrags: 31 (RATNOP), 32 (RATNUV), 39 (TUQWOR): These three cyclopentadienide structures have been included in this category (dienes) on the basis of their CSD classification and the fact that they do not have metal coordination (*c.f.* majority of dienyls); a third category of structures was not implemented in this study. In either case, the internal angles of all three fragments are similar to the median values and do not influence the conformational trends.

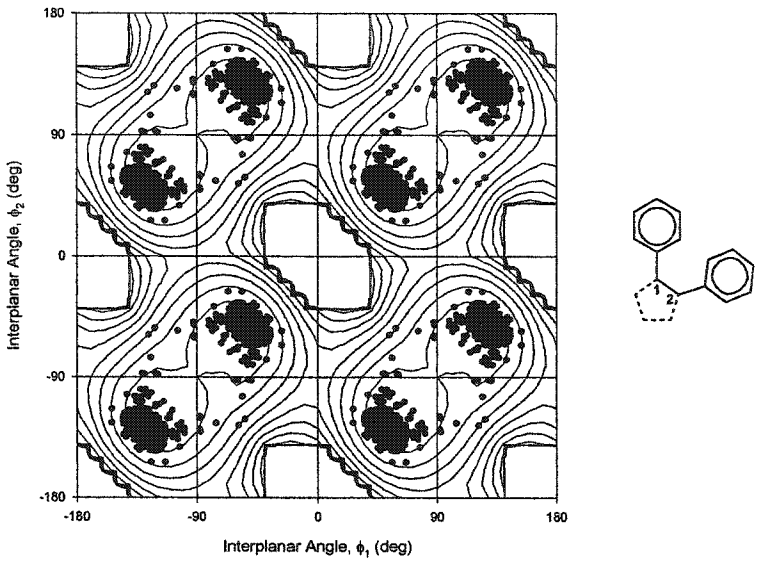

(a)

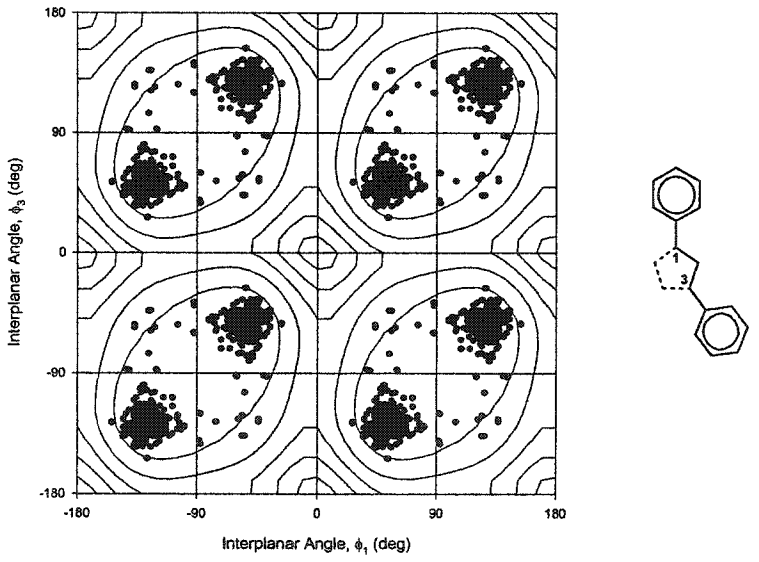

(b)

Figure A.1: *Conformational maps of torsional angles of 2 peripheral aryl rings attached to a rigid central C_5Ar_5 frame of C_{2v} symmetry, featuring (a) adjacent (1,2) aryl groups, and (b) next-nearest neighbouring (1,3) aryl groups. The overlayed contours (at 3 kcal mol^{-1}) represent the calculated (MMFF94) equipotential energy regions associated with $C_5Ph_5^-$* ***1.18.***

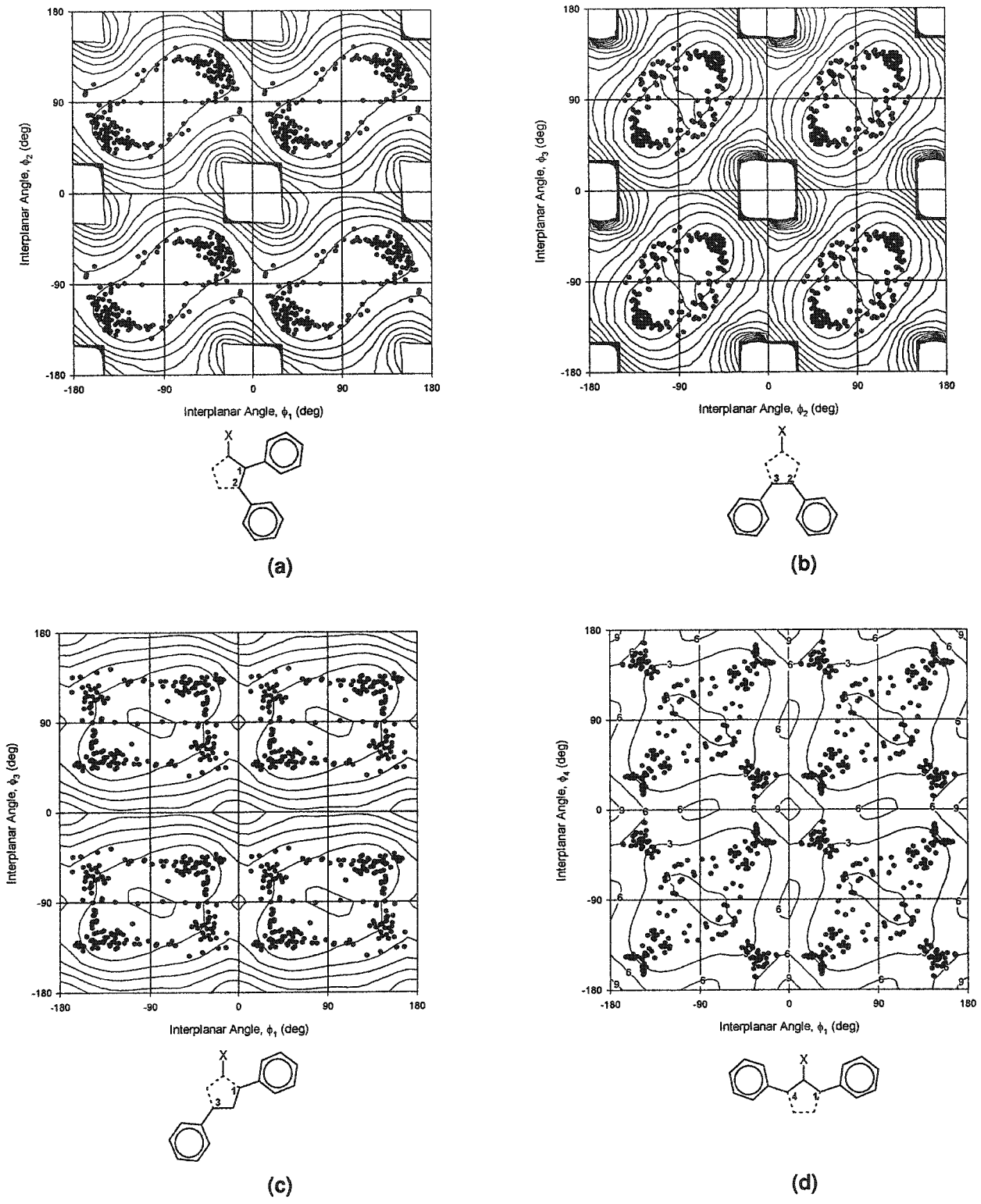

Figure A.2: *Conformational maps of torsional angles of 2 peripheral aryl rings (or rotors) attached to a rigid central C_5Ar_4X frame, featuring vicinal (a) (1,2/4,3) and (b) (2,3), as well as next-nearest (c) (1,3) and (d) (1,4) interactions. The overlayed contours (at 3 kcal mol^{-1}) represent the calculated (MMFF94) equipotential energy regions associated with C_5Ph_4H* ***2.1.***

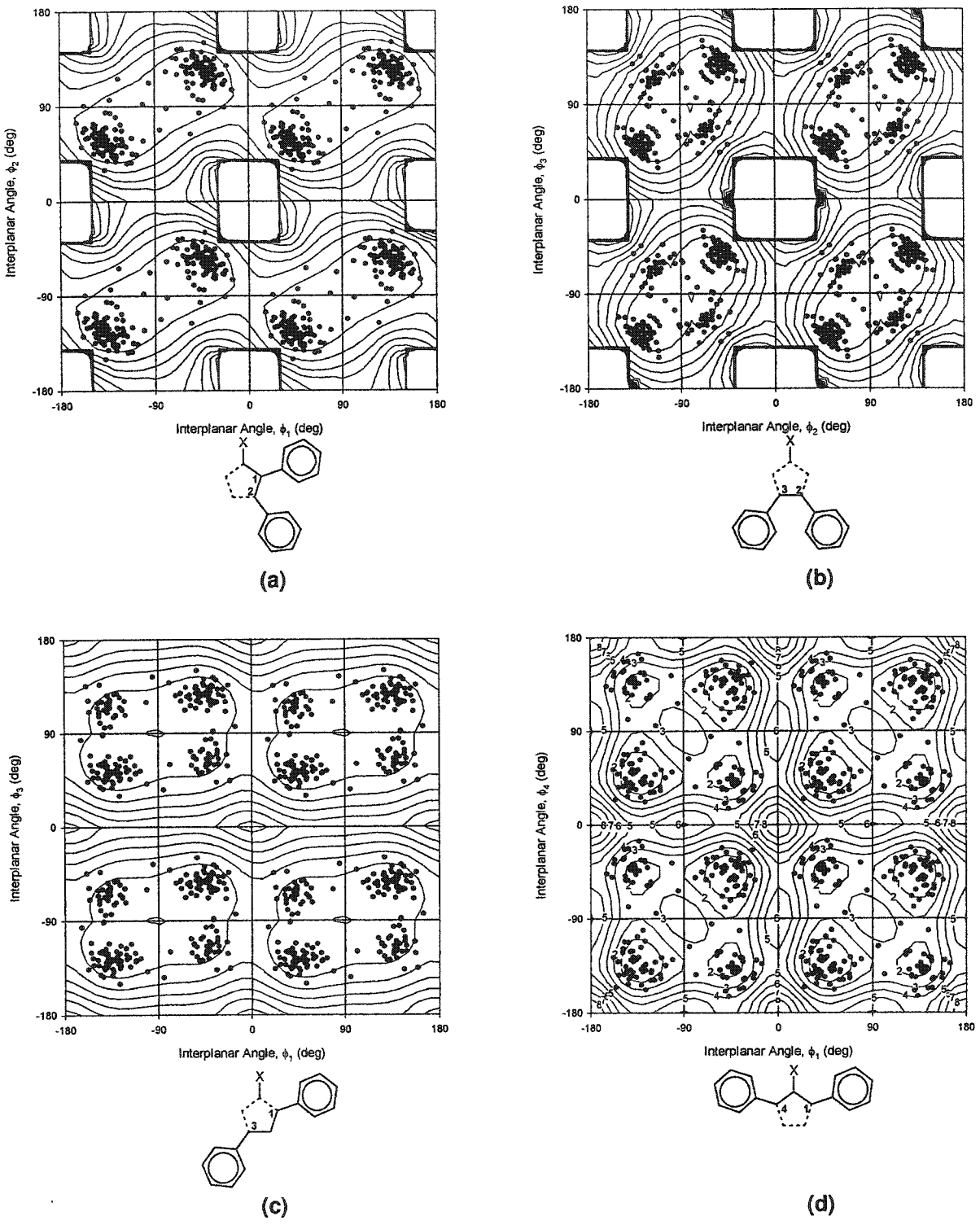

Figure A.3: *Conformational maps of torsional angles of 2 peripheral aryl rings attached to a rigid central Ar_4C_4CX (where X = sp^2 (triangles) and sp^3 (circles)) frame, featuring vicinal (a) (1,2/4,3) and (b) (2,3), as well as next-nearest (c) (1,3) and (d) (1,4) interactions. The overlayed contours (at 3 kcal mol^{-1}) represent the calculated (MMFF94) equipotential energy regions associated with $C_4Ph_4C{=}O$* ***1.53****.*

Table A.4. CSD [Version 5.24, Nov. 2002] Query of C_6Ar_6 and C_6Ar_5X Fragments

Refcode	ANG1*	ANG2*	ANG3*	ANG4*	ANG5*	ANG6*	TYPE**
DOCLIQ-1	88.601	94.825	93.401	91.399	85.175	86.599	B
FAWTUS	103.706	88.816	79.343	76.294	91.184	100.657	B
HOFVIH	61.398	66.935	61.398	66.935	61.398	66.935	A
HPHBNZ	65.848	67.357	70.695	61.962	68.546	68.806	A
HPHBNZ02	89.645	102.204	87.270	76.843	67.180	83.334	B
HUFJIB	99.179	96.219	94.837	80.821	83.781	85.163	B
JEGSIX-A	66.452	74.210	72.888	80.568	79.010	76.808	A
JEGSIX-B	93.958	86.779	73.130	73.955	76.609	72.442	B
KAHBOK	70.492	65.495	63.136	69.654	66.876	69.868	A
LAQJES	94.929	71.345	74.817	85.071	108.655	105.183	B
LAQJIW	79.042	78.938	85.582	76.879	85.963	89.717	A
METFOG	66.776	83.766	94.048	113.224	96.234	85.952	B
OCECII	59.994	66.984	69.193	66.652	58.094	64.260	A
PAWCAR-A	104.587	84.516	64.026	56.505	56.820	93.511	B
PAWCAR-B	57.006	70.219	76.466	72.325	65.047	86.489	A
QEYVIZ-A	98.732	110.553	116.574	85.902	80.119	76.491	B
QEYVIZ-B	67.658	61.222	64.109	67.122	63.048	74.144	A
QEZVUM-A	72.620	61.640	63.326	63.324	69.461	70.402	A
QEZVUM-B	66.485	63.848	68.748	69.351	72.843	76.841	A
QOWNEV-A	62.766	59.545	81.115	56.611	62.440	68.427	A
QOWNEV-B	64.123	50.305	81.115	53.892	58.869	74.638	A
RIQMUZ-A	70.877	70.761	69.394	74.160	72.730	56.892	A
RIQMUZ-B	75.687	71.717	63.623	68.224	71.371	57.242	A
RIQMUZ-C	69.776	66.190	68.039	69.114	69.103	60.197	A
RIQMUZ-D	76.233	77.691	58.968	64.064	74.180	55.545	A
RIQMUZ-E	75.384	72.977	60.410	73.559	71.152	57.971	A
RIQMUZ-F	64.678	73.129	73.076	78.813	72.495	58.434	A
RODCAO-A	65.532	71.043	70.532	67.450	74.659	58.845	A
RODCAO-B	65.532	71.043	70.532	67.450	74.659	58.845	A
FOQJOK		44.127	60.809	68.179	55.832	49.624	A
ICEJIJ		100.806	89.298	63.192	65.961	64.308	B
PUTVUV		58.191	69.593	65.549	79.960	60.937	A

*** Notes:**

DATA RETRIEVAL:

- Included C_6Ar_5X fragments with: peripheral aryl substitution; metal coordination; charged species; no geometrical constraints

DATA TREATMENT:

- Absolute values converted to arbitrary +/-
- Interplanar angles calculated from plane of central C_6 ring

**** Type: See discussion in Chapter Three.**

APPENDIX B: Supplementary X-Ray Crystallographic Data

Refinement Data and Metrical Parameters

Table B.1. Crystal Data and Structure Refinement Parameters for 3.19, 3.26 and 3.35.

	3.19	3.26	3.35
Empirical formula	$C_{46}H_{34}Fe$	$C_{44}H_{30}$	$C_{44}H_{30}Br_2$
Molecular weight	642.58	558.68	718.50
Description	red plate	colourless plate	colourless fragment
Crystal size, mm	0.05 X 0.15 X 0.30	0.50 x 0.24 x 0.05	0.14 x 0.18 x 0.28
Temperature, K	213(2)	299(2)	299(2)
Wavelength, Å	(Mo-Kα) 0.71073	0.71073	0.71073
Crystal system	orthorhombic	triclinic	triclinic
Space group	*Pccn*	$P(\bar{1})$	$P(\bar{1})$
a, Å	45.1814(1)	11.0833(3)	11.5433(5)
b, Å	11.6417(2)	13.3548(3)	16.1621(8)
c, Å	12.2057(2)	21.94640(10)	21.5017(10)
α, deg.	90.000	103.1890(10)	73.733(2)
β, deg.	90.000	94.800(2)	87.728(2)
γ, deg.	90.000	93.643(2)	71.871(2)
Volume, $Å^3$	6420.1(2)	3140.17(11)	3654.7(3)
Z	8	4	4
Calcd Density, g/cm^3	1.330	1.182	1.306
Abs Coeff, mm^{-1}	0.503	0.067	2.246
Scan Mode	ω-scans	ω-scans	ω-scans
F(000)	2688	1176	1456
θ-range, deg.	0.90 to 23.00	1.57 to 22.50	1.38 to 22.50
Index ranges	$-56 \le h \le 56$	$-11 \le h \le 11$	$-12 \le h \le 11$
	$-14 \le k \le 11$	$-14 \le k \le 14$	$-17 \le k \le 17$
	$-15 \le l \le 15$	$-23 \le l \le 23$	$-13 \le l \le 23$
No. Reflect. collected	36391	17565	18159
No. Independent reflect.	4472	8192	9565
R(int)	0.1962	0.0291	0.0886
Data / Restraints / Param.	4448 / 0 / 424	8192 / 0 / 794	9565 / 0 / 830
Goodness-of-fit on F^2	1.101	1.008	0.849
Final *R* indices (I>2σ(I))*	*R*1 = 0.0734;	*R*1 = 0.0447;	*R*1 = 0.0600;
	w*R*2 = 0.1110	w*R*2 = 0.1041	w*R*2 = 0.1314
R indices (all data)*	*R*1 = 0.1340;	*R*1 = 0.0779	*R*1 = 0.1443
	w*R*2 = 0.1316	w*R*2 = 0.1218	w*R*2 = 0.1520
Mean shift/error	<0.000	0.000	0.005
Max. shift/error	<0.000	0.000	-4.023
Ratio Min.:Max Trans.	0.66865	0.903802	na
Extinction coeff	0.0031(5)	0.0109(8)	0.0000
Largest diff. Peak, $e/Å^3$	0.288	0.198	0.556
Largest diff. Hole, $e/Å^3$	-0.337	-0.167	-0.372

Refinement method: Full-matrix least-squares on F^2,
Weighting Scheme: $w = 1/[\sigma^2Fo^2+(0.0597((Fo^2+2Fc^2)/3))^2]$

*$R1 = \Sigma(\|Fo\|-\|Fc\|)/\Sigma|Fo|$; $wR2 = [\Sigma[w(Fo^2-Fc^2)^2]/\Sigma[w(Fo^2)^2]]^{0.5}$; $P=(Fo^2+2Fc^2)/3$)

Table B.2. Atomic coordinates (x 10^4) and equivalent isotropic displacement parameters (A^2 x 10^3) for 3.19. U(eq) is defined as 1/3rd of the trace of the orthogonalized Uij tensor.

	x	y	z	U(eq)
Fe(1)	389(1)	6534(1)	3693(1)	32(1)
C(1)	1045(1)	5164(4)	3711(4)	23(1)
C(2)	1266(1)	6016(4)	3603(5)	23(1)
C(3)	1552(1)	5813(4)	4011(4)	24(1)
C(4)	1626(1)	4759(4)	4503(4)	24(1)
C(5)	1415(1)	3875(4)	4531(4)	24(1)
C(6)	1130(1)	4060(4)	4128(4)	21(1)
C(11)	724(1)	5314(4)	3466(5)	24(1)
C(12)	498(1)	4921(4)	4199(5)	32(2)
C(13)	223(1)	4919(4)	3641(6)	38(2)
C(14)	274(1)	5324(5)	2572(5)	36(2)
C(15)	580(1)	5570(4)	2454(5)	31(2)
C(16)	536(1)	8031(5)	4427(6)	43(2)
C(17)	304(1)	7533(5)	5049(6)	47(2)
C(18)	49(2)	7448(5)	4376(7)	52(2)
C(19)	121(2)	7895(5)	3330(6)	51(2)
C(20)	424(2)	8250(5)	3354(6)	46(2)
C(21)	1206(1)	7147(4)	3047(5)	26(1)
C(22)	1148(1)	7186(5)	1931(5)	33(2)
C(23)	1099(1)	8218(5)	1389(5)	42(2)
C(24)	1117(1)	9239(5)	1967(6)	44(2)
C(25)	1178(1)	9229(5)	3071(6)	39(2)
C(26)	1226(1)	8188(4)	3600(5)	33(2)
C(31)	1787(1)	6726(4)	3921(5)	25(1)
C(32)	1903(1)	7033(5)	2911(5)	33(2)
C(33)	2122(1)	7880(5)	2841(5)	39(2)
C(34)	2228(1)	8391(5)	3787(6)	39(2)
C(35)	2111(1)	8092(5)	4779(5)	36(2)
C(36)	1893(1)	7263(4)	4858(5)	30(2)
C(41)	1926(1)	4528(4)	4967(5)	30(2)
C(42)	2157(1)	4220(5)	4283(6)	44(2)
C(43)	2433(2)	3965(5)	4730(7)	59(2)
C(44)	2480(2)	4029(6)	5830(8)	64(3)
C(45)	2253(2)	4347(5)	6489(7)	64(2)
C(46)	1979(1)	4605(5)	6071(6)	48(2)
C(51)	1506(1)	2708(4)	4950(5)	24(1)
C(52)	1618(1)	1902(4)	4221(5)	32(2)
C(53)	1700(1)	807(5)	4578(6)	40(2)
C(54)	1665(1)	517(5)	5653(6)	43(2)
C(55)	1557(1)	1307(5)	6395(6)	47(2)
C(56)	1479(1)	2395(5)	6042(5)	36(2)
C(61)	918(1)	3057(4)	4066(5)	23(1)
C(62)	825(1)	2464(5)	4975(5)	35(2)
C(63)	636(1)	1539(5)	4887(6)	39(2)
C(64)	533(1)	1203(5)	3887(7)	48(2)
C(65)	624(1)	1791(5)	2958(6)	41(2)
C(66)	811(1)	2715(5)	3045(5)	34(2)

Table B.3. Complete List of Bond Lengths [Å] for 3.19.

Fe(1)-C(13)	2.027(5)	C(51)-C(56)	1.387(8)
Fe(1)-C(14)	2.032(6)	C(51)-C(52)	1.391(7)
Fe(1)-C(12)	2.036(5)	C(52)-C(53)	1.397(7)
Fe(1)-C(19)	2.044(6)	C(53)-C(54)	1.363(8)
Fe(1)-C(20)	2.047(5)	C(54)-C(55)	1.379(8)
Fe(1)-C(18)	2.049(6)	C(55)-C(56)	1.383(7)
Fe(1)-C(17)	2.059(6)	C(61)-C(62)	1.374(7)
Fe(1)-C(16)	2.068(6)	C(61)-C(66)	1.395(7)
Fe(1)-C(15)	2.070(6)	C(62)-C(63)	1.378(8)
Fe(1)-C(11)	2.093(5)	C(63)-C(64)	1.363(8)
C(1)-C(2)	1.412(7)	C(64)-C(65)	1.386(8)
C(1)-C(6)	1.434(7)	C(65)-C(66)	1.373(7)
C(1)-C(11)	1.493(7)		
C(2)-C(3)	1.403(7)		
C(2)-C(21)	1.506(7)		
C(3)-C(4)	1.406(7)		
C(3)-C(31)	1.506(7)		
C(4)-C(5)	1.403(7)		
C(4)-C(41)	1.496(7)		
C(5)-C(6)	1.396(7)		
C(5)-C(51)	1.509(7)		
C(6)-C(61)	1.510(7)		
C(11)-C(15)	1.427(7)		
C(11)-C(12)	1.434(7)		
C(12)-C(13)	1.417(7)		
C(13)-C(14)	1.408(8)		
C(14)-C(15)	1.421(7)		
C(16)-C(17)	1.418(8)		
C(16)-C(20)	1.426(9)		
C(17)-C(18)	1.420(9)		
C(18)-C(19)	1.417(9)		
C(19)-C(20)	1.431(8)		
C(21)-C(22)	1.388(7)		
C(21)-C(26)	1.390(7)		
C(22)-C(23)	1.389(7)		
C(23)-C(24)	1.385(8)		
C(24)-C(25)	1.375(8)		
C(25)-C(26)	1.391(7)		
C(31)-C(32)	1.386(7)		
C(31)-C(36)	1.388(7)		
C(32)-C(33)	1.399(7)		
C(33)-C(34)	1.386(8)		
C(34)-C(35)	1.365(8)		
C(35)-C(36)	1.385(7)		
C(41)-C(46)	1.371(8)		
C(41)-C(42)	1.383(8)		
C(42)-C(43)	1.392(8)		
C(43)-C(44)	1.362(10)		
C(44)-C(45)	1.355(10)		
C(45)-C(46)	1.376(8)		

Table B.4. Complete List of Bond Angles [deg] for 3.19.

C(13)-Fe(1)-C(14)	40.6(2)	C(1)-C(2)-C(21)	121.9(5)
C(13)-Fe(1)-C(12)	40.8(2)	C(2)-C(3)-C(4)	121.1(5)
C(14)-Fe(1)-C(12)	68.1(2)	C(2)-C(3)-C(31)	120.3(4)
C(13)-Fe(1)-C(19)	119.5(3)	C(4)-C(3)-C(31)	118.6(5)
C(14)-Fe(1)-C(19)	103.8(3)	C(5)-C(4)-C(3)	119.3(5)
C(12)-Fe(1)-C(19)	157.4(3)	C(5)-C(4)-C(41)	118.4(5)
C(13)-Fe(1)-C(20)	158.2(3)	C(3)-C(4)-C(41)	122.3(5)
C(14)-Fe(1)-C(20)	124.1(3)	C(6)-C(5)-C(4)	120.3(5)
C(12)-Fe(1)-C(20)	160.6(3)	C(6)-C(5)-C(51)	120.6(5)
C(19)-Fe(1)-C(20)	40.9(2)	C(4)-C(5)-C(51)	119.0(5)
C(13)-Fe(1)-C(18)	102.4(3)	C(5)-C(6)-C(1)	120.6(5)
C(14)-Fe(1)-C(18)	116.2(3)	C(5)-C(6)-C(61)	118.8(4)
C(12)-Fe(1)-C(18)	122.4(3)	C(1)-C(6)-C(61)	120.5(5)
C(19)-Fe(1)-C(18)	40.5(2)	C(15)-C(11)-C(12)	106.3(5)
C(20)-Fe(1)-C(18)	68.5(3)	C(15)-C(11)-C(1)	129.9(5)
C(13)-Fe(1)-C(17)	118.7(3)	C(12)-C(11)-C(1)	122.2(5)
C(14)-Fe(1)-C(17)	152.2(3)	C(15)-C(11)-Fe(1)	69.1(3)
C(12)-Fe(1)-C(17)	108.8(3)	C(12)-C(11)-Fe(1)	67.5(3)
C(19)-Fe(1)-C(17)	68.0(3)	C(1)-C(11)-Fe(1)	139.1(4)
C(20)-Fe(1)-C(17)	68.0(3)	C(13)-C(12)-C(11)	109.1(5)
C(18)-Fe(1)-C(17)	40.4(2)	C(13)-C(12)-Fe(1)	69.2(3)
C(13)-Fe(1)-C(16)	156.1(3)	C(11)-C(12)-Fe(1)	71.8(3)
C(14)-Fe(1)-C(16)	163.3(3)	C(14)-C(13)-C(12)	107.5(5)
C(12)-Fe(1)-C(16)	124.7(3)	C(14)-C(13)-Fe(1)	69.9(3)
C(19)-Fe(1)-C(16)	68.3(3)	C(12)-C(13)-Fe(1)	69.9(3)
C(20)-Fe(1)-C(16)	40.5(2)	C(13)-C(14)-C(15)	108.8(5)
C(18)-Fe(1)-C(16)	68.1(3)	C(13)-C(14)-Fe(1)	69.5(3)
C(17)-Fe(1)-C(16)	40.2(2)	C(15)-C(14)-Fe(1)	71.2(3)
C(13)-Fe(1)-C(15)	68.3(2)	C(14)-C(15)-C(11)	108.3(5)
C(14)-Fe(1)-C(15)	40.5(2)	C(14)-C(15)-Fe(1)	68.3(3)
C(12)-Fe(1)-C(15)	67.8(2)	C(11)-C(15)-Fe(1)	70.8(3)
C(19)-Fe(1)-C(15)	120.6(3)	C(17)-C(16)-C(20)	107.7(6)
C(20)-Fe(1)-C(15)	110.4(2)	C(17)-C(16)-Fe(1)	69.6(4)
C(18)-Fe(1)-C(15)	153.0(3)	C(20)-C(16)-Fe(1)	68.9(3)
C(17)-Fe(1)-C(15)	166.1(2)	C(16)-C(17)-C(18)	108.6(6)
C(16)-Fe(1)-C(15)	129.7(2)	C(16)-C(17)-Fe(1)	70.3(4)
C(13)-Fe(1)-C(11)	68.6(2)	C(18)-C(17)-Fe(1)	69.4(4)
C(14)-Fe(1)-C(11)	68.0(2)	C(19)-C(18)-C(17)	107.9(6)
C(12)-Fe(1)-C(11)	40.6(2)	C(19)-C(18)-Fe(1)	69.5(4)
C(19)-Fe(1)-C(11)	157.8(3)	C(17)-C(18)-Fe(1)	70.2(4)
C(20)-Fe(1)-C(11)	125.4(2)	C(18)-C(19)-C(20)	108.0(6)
C(18)-Fe(1)-C(11)	161.7(3)	C(18)-C(19)-Fe(1)	69.9(4)
C(17)-Fe(1)-C(11)	128.7(2)	C(20)-C(19)-Fe(1)	69.7(3)
C(16)-Fe(1)-C(11)	113.4(2)	C(16)-C(20)-C(19)	107.8(6)
C(15)-Fe(1)-C(11)	40.1(2)	C(16)-C(20)-Fe(1)	70.5(3)
C(2)-C(1)-C(6)	118.3(5)	C(19)-C(20)-Fe(1)	69.4(3)
C(2)-C(1)-C(11)	125.9(4)	C(22)-C(21)-C(26)	117.4(5)
C(6)-C(1)-C(11)	115.7(4)	C(22)-C(21)-C(2)	120.3(5)
C(3)-C(2)-C(1)	119.9(5)	C(26)-C(21)-C(2)	122.1(5)
C(3)-C(2)-C(21)	118.2(4)	C(21)-C(22)-C(23)	121.7(6)

Table B.4. Complete List of Bond Angles [deg] for 3.19 (continued).

C(24)-C(23)-C(22)	119.3(6)
C(25)-C(24)-C(23)	120.3(6)
C(24)-C(25)-C(26)	119.6(6)
C(21)-C(26)-C(25)	121.6(6)
C(32)-C(31)-C(36)	119.1(5)
C(32)-C(31)-C(3)	120.9(5)
C(36)-C(31)-C(3)	120.0(5)
C(31)-C(32)-C(33)	120.2(6)
C(34)-C(33)-C(32)	119.8(6)
C(35)-C(34)-C(33)	119.7(5)
C(34)-C(35)-C(36)	121.0(6)
C(35)-C(36)-C(31)	120.1(6)
C(46)-C(41)-C(42)	118.8(6)
C(46)-C(41)-C(4)	121.1(6)
C(42)-C(41)-C(4)	120.1(6)
C(41)-C(42)-C(43)	119.5(7)
C(44)-C(43)-C(42)	121.1(7)
C(45)-C(44)-C(43)	118.7(7)
C(44)-C(45)-C(46)	121.5(7)
C(41)-C(46)-C(45)	120.4(7)
C(56)-C(51)-C(52)	118.1(5)
C(56)-C(51)-C(5)	122.6(5)
C(52)-C(51)-C(5)	119.3(5)
C(51)-C(52)-C(53)	120.8(6)
C(54)-C(53)-C(52)	119.7(6)
C(53)-C(54)-C(55)	120.5(6)
C(54)-C(55)-C(56)	119.7(6)
C(55)-C(56)-C(51)	121.1(6)
C(62)-C(61)-C(66)	118.1(5)
C(62)-C(61)-C(6)	122.9(5)
C(66)-C(61)-C(6)	119.0(5)
C(61)-C(62)-C(63)	121.3(6)
C(64)-C(63)-C(62)	120.4(6)
C(63)-C(64)-C(65)	119.3(5)
C(66)-C(65)-C(64)	120.4(6)
C(65)-C(66)-C(61)	120.4(6)

Table B.5. Atomic coordinates (x 10^4) and equivalent isotropic displacement parameters (A^2 x 10^3) for 3.26. U(eq) is defined as 1/3rd of the trace of the orthogonalized Uij tensor.

	x	y	z	U(eq)
C(1)	2659(2)	5199(2)	-4926(1)	48(1)
C(2)	3299(2)	5327(2)	-4330(1)	48(1)
C(3)	3286(2)	4508(2)	-4034(1)	48(1)
C(4)	2558(2)	3590(2)	-4313(1)	47(1)
C(5)	1883(2)	3474(2)	-4902(1)	46(1)
C(6)	1961(2)	4274(2)	-5218(1)	47(1)
C(11)	2913(2)	7631(2)	-5743(1)	55(1)
C(12)	2347(3)	7579(2)	-6332(1)	78(1)
C(13)	2425(3)	8409(3)	-6600(2)	94(1)
C(14)	3083(3)	9297(3)	-6287(2)	92(1)
C(15)	3646(3)	9369(2)	-5700(2)	94(1)
C(16)	3556(2)	8540(2)	-5424(1)	78(1)
C(17)	2815(2)	6764(2)	-5467(1)	56(1)
C(18)	2731(2)	6036(2)	-5234(1)	51(1)
C(21)	3913(2)	6365(2)	-4009(1)	51(1)
C(22)	3446(2)	6938(2)	-3492(1)	72(1)
C(23)	3946(3)	7916(2)	-3201(1)	95(1)
C(24)	4928(3)	8330(2)	-3424(2)	95(1)
C(25)	5412(3)	7775(2)	-3934(2)	83(1)
C(26)	4906(2)	6795(2)	-4228(1)	65(1)
C(31)	4064(2)	4607(2)	-3430(1)	52(1)
C(32)	3597(2)	4519(2)	-2878(1)	63(1)
C(33)	4351(3)	4571(2)	-2337(1)	77(1)
C(34)	5591(3)	4715(2)	-2341(2)	86(1)
C(35)	6067(3)	4821(2)	-2883(2)	82(1)
C(36)	5313(2)	4761(2)	-3422(1)	66(1)
C(41)	2487(2)	2750(2)	-3965(1)	52(1)
C(42)	1441(2)	2517(2)	-3710(1)	63(1)
C(43)	1413(3)	1796(2)	-3346(1)	82(1)
C(44)	2421(4)	1289(2)	-3249(1)	95(1)
C(45)	3447(3)	1497(2)	-3511(2)	90(1)
C(46)	3491(2)	2221(2)	-3867(1)	69(1)
C(51)	1058(2)	2522(2)	-5175(1)	49(1)
C(52)	-170(2)	2596(2)	-5322(1)	60(1)
C(53)	-963(2)	1731(2)	-5547(1)	72(1)
C(54)	-544(3)	771(2)	-5635(1)	79(1)
C(55)	672(3)	674(2)	-5505(1)	72(1)
C(56)	1467(2)	1545(2)	-5276(1)	58(1)
C(61)	1324(2)	4150(2)	-5862(1)	50(1)
C(62)	437(2)	4782(2)	-5983(1)	66(1)
C(63)	-151(2)	4650(2)	-6577(1)	80(1)
C(64)	141(3)	3893(2)	-7062(1)	84(1)
C(65)	1010(3)	3259(2)	-6950(1)	79(1)
C(66)	1601(2)	3388(2)	-6357(1)	65(1)
C(10)	2405(2)	9369(2)	214(1)	49(1)
C(20)	2567(2)	8307(2)	90(1)	50(1)
C(30)	2149(2)	7719(2)	492(1)	50(1)
C(40)	1506(2)	8174(2)	995(1)	49(1)
C(50)	1335(2)	9232(2)	1112(1)	48(1)

Table B.5. Atomic coordinates (x 10^4) and equivalent isotropic displacement parameters (A^2 x 10^3) for 3.26. U(eq) is defined as 1/3rd of the trace of the orthogonalized Uij tensor (continued).

	x	y	z	U(eq)
C(60)	1798(2)	9838(2)	728(1)	47(1)
C(110)	3919(2)	10725(2)	-1043(1)	59(1)
C(120)	4822(2)	10204(2)	-1340(1)	81(1)
C(130)	5367(3)	10550(4)	-1802(2)	111(1)
C(140)	5015(3)	11389(4)	-1982(2)	112(1)
C(150)	4125(3)	11924(3)	-1702(2)	107(1)
C(160)	3574(2)	11594(2)	-1222(2)	86(1)
C(170)	3359(2)	10338(2)	-569(1)	58(1)
C(180)	2906(2)	9951(2)	-197(1)	54(1)
C(210)	3157(2)	7840(2)	-480(1)	54(1)
C(220)	4372(2)	7711(2)	-456(1)	83(1)
C(230)	4916(3)	7330(3)	-995(2)	97(1)
C(240)	4253(4)	7079(2)	-1560(2)	96(1)
C(250)	3049(3)	7202(3)	-1594(1)	106(1)
C(260)	2503(3)	7571(2)	-1058(1)	86(1)
C(310)	2392(2)	6600(2)	360(1)	55(1)
C(320)	3475(2)	6308(2)	582(1)	81(1)
C(330)	3729(3)	5292(3)	461(2)	98(1)
C(340)	2908(4)	4553(3)	111(2)	106(1)
C(350)	1840(4)	4820(3)	-115(2)	127(1)
C(360)	1580(3)	5843(2)	11(2)	97(1)
C(410)	939(2)	7507(2)	1377(1)	54(1)
C(420)	1616(2)	6949(2)	1718(1)	68(1)
C(430)	1051(3)	6303(2)	2039(1)	84(1)
C(440)	-177(3)	6217(2)	2032(2)	98(1)
C(450)	-849(3)	6781(3)	1715(2)	100(1)
C(460)	-304(2)	7415(2)	1384(1)	76(1)
C(510)	656(2)	9735(2)	1647(1)	48(1)
C(520)	1128(2)	9837(2)	2261(1)	59(1)
C(530)	523(2)	10328(2)	2755(1)	70(1)
C(540)	-564(3)	10711(2)	2640(1)	72(1)
C(550)	-1049(2)	10609(2)	2034(1)	72(1)
C(560)	-442(2)	10130(2)	1543(1)	62(1)
C(610)	1670(2)	10971(2)	854(1)	51(1)
C(620)	2197(2)	11635(2)	1400(1)	64(1)
C(630)	2069(3)	12686(2)	1507(1)	82(1)
C(640)	1412(3)	13074(2)	1071(2)	92(1)
C(650)	901(3)	12423(2)	530(2)	92(1)
C(660)	1020(2)	11382(2)	420(1)	69(1)

Table B.6. Complete List of Bond Lengths [Å] for 3.26.

C(1)-C(6)	1.404(3)	C(10)-C(60)	1.406(3)
C(1)-C(2)	1.404(3)	C(10)-C(20)	1.409(3)
C(1)-C(18)	1.434(3)	C(10)-C(180)	1.440(3)
C(2)-C(3)	1.395(3)	C(20)-C(30)	1.395(3)
C(2)-C(21)	1.495(3)	C(20)-C(210)	1.488(3)
C(3)-C(4)	1.407(3)	C(30)-C(40)	1.406(3)
C(3)-C(31)	1.494(3)	C(30)-C(310)	1.501(3)
C(4)-C(5)	1.410(3)	C(40)-C(50)	1.406(3)
C(4)-C(41)	1.495(3)	C(40)-C(410)	1.500(3)
C(5)-C(6)	1.402(3)	C(50)-C(60)	1.400(3)
C(5)-C(51)	1.492(3)	C(50)-C(510)	1.499(3)
C(6)-C(61)	1.495(3)	C(60)-C(610)	1.493(3)
C(11)-C(12)	1.374(3)	C(110)-C(160)	1.374(3)
C(11)-C(16)	1.375(3)	C(110)-C(120)	1.379(3)
C(11)-C(17)	1.428(3)	C(110)-C(170)	1.431(3)
C(12)-C(13)	1.370(4)	C(120)-C(130)	1.373(4)
C(13)-C(14)	1.358(4)	C(130)-C(140)	1.339(5)
C(14)-C(15)	1.362(4)	C(140)-C(150)	1.360(5)
C(15)-C(16)	1.381(4)	C(150)-C(160)	1.400(4)
C(17)-C(18)	1.198(3)	C(170)-C(180)	1.189(3)
C(21)-C(22)	1.376(3)	C(210)-C(260)	1.366(3)
C(21)-C(26)	1.381(3)	C(210)-C(220)	1.367(3)
C(22)-C(23)	1.375(4)	C(220)-C(230)	1.380(4)
C(23)-C(24)	1.367(4)	C(230)-C(240)	1.348(4)
C(24)-C(25)	1.365(4)	C(240)-C(250)	1.353(4)
C(25)-C(26)	1.380(4)	C(250)-C(260)	1.373(4)
C(31)-C(32)	1.383(3)	C(310)-C(360)	1.354(3)
C(31)-C(36)	1.383(3)	C(310)-C(320)	1.371(3)
C(32)-C(33)	1.379(3)	C(320)-C(330)	1.375(4)
C(33)-C(34)	1.376(4)	C(330)-C(340)	1.347(4)
C(34)-C(35)	1.374(4)	C(340)-C(350)	1.346(4)
C(35)-C(36)	1.374(3)	C(350)-C(360)	1.384(4)
C(41)-C(42)	1.376(3)	C(410)-C(460)	1.377(3)
C(41)-C(46)	1.383(3)	C(410)-C(420)	1.382(3)
C(42)-C(43)	1.386(3)	C(420)-C(430)	1.383(4)
C(43)-C(44)	1.369(4)	C(430)-C(440)	1.357(4)
C(44)-C(45)	1.358(4)	C(440)-C(450)	1.352(4)
C(45)-C(46)	1.377(4)	C(450)-C(460)	1.378(4)
C(51)-C(56)	1.384(3)	C(510)-C(520)	1.378(3)
C(51)-C(52)	1.387(3)	C(510)-C(560)	1.380(3)
C(52)-C(53)	1.374(3)	C(520)-C(530)	1.380(3)
C(53)-C(54)	1.369(4)	C(530)-C(540)	1.365(3)
C(54)-C(55)	1.375(4)	C(540)-C(550)	1.365(3)
C(55)-C(56)	1.382(3)	C(550)-C(560)	1.374(3)
C(61)-C(66)	1.379(3)	C(610)-C(620)	1.377(3)
C(61)-C(62)	1.383(3)	C(610)-C(660)	1.379(3)
C(62)-C(63)	1.377(3)	C(620)-C(630)	1.389(4)
C(63)-C(64)	1.368(4)	C(630)-C(640)	1.367(4)
C(64)-C(65)	1.364(4)	C(640)-C(650)	1.358(4)
C(65)-C(66)	1.377(3)	C(650)-C(660)	1.372(4)

Table B.7. Complete List of Bond Angles [deg] for 3.26.

C(6)-C(1)-C(2)	121.06(19)	C(56)-C(51)-C(52)	117.8(2)
C(6)-C(1)-C(18)	120.36(19)	C(56)-C(51)-C(5)	122.2(2)
C(2)-C(1)-C(18)	118.6(2)	C(52)-C(51)-C(5)	120.0(2)
C(3)-C(2)-C(1)	119.6(2)	C(53)-C(52)-C(51)	121.4(2)
C(3)-C(2)-C(21)	121.32(19)	C(54)-C(53)-C(52)	120.0(3)
C(1)-C(2)-C(21)	118.94(19)	C(53)-C(54)-C(55)	119.9(3)
C(2)-C(3)-C(4)	119.61(19)	C(54)-C(55)-C(56)	120.0(3)
C(2)-C(3)-C(31)	119.70(19)	C(55)-C(56)-C(51)	120.9(2)
C(4)-C(3)-C(31)	120.67(19)	C(66)-C(61)-C(62)	117.8(2)
C(3)-C(4)-C(5)	120.59(19)	C(66)-C(61)-C(6)	120.5(2)
C(3)-C(4)-C(41)	118.75(18)	C(62)-C(61)-C(6)	121.7(2)
C(5)-C(4)-C(41)	120.64(19)	C(63)-C(62)-C(61)	121.0(2)
C(6)-C(5)-C(4)	119.58(19)	C(64)-C(63)-C(62)	120.3(2)
C(6)-C(5)-C(51)	120.34(18)	C(65)-C(64)-C(63)	119.4(3)
C(4)-C(5)-C(51)	120.05(19)	C(64)-C(65)-C(66)	120.5(3)
C(5)-C(6)-C(1)	119.33(19)	C(65)-C(66)-C(61)	121.0(2)
C(5)-C(6)-C(61)	120.99(19)	C(60)-C(10)-C(20)	120.7(2)
C(1)-C(6)-C(61)	119.67(19)	C(60)-C(10)-C(180)	121.8(2)
C(12)-C(11)-C(16)	118.6(2)	C(20)-C(10)-C(180)	117.45(19)
C(12)-C(11)-C(17)	120.5(2)	C(30)-C(20)-C(10)	119.62(19)
C(16)-C(11)-C(17)	121.0(2)	C(30)-C(20)-C(210)	121.9(2)
C(13)-C(12)-C(11)	121.0(3)	C(10)-C(20)-C(210)	118.4(2)
C(14)-C(13)-C(12)	120.0(3)	C(20)-C(30)-C(40)	120.0(2)
C(13)-C(14)-C(15)	120.0(3)	C(20)-C(30)-C(310)	117.88(19)
C(14)-C(15)-C(16)	120.2(3)	C(40)-C(30)-C(310)	122.1(2)
C(11)-C(16)-C(15)	120.1(3)	C(50)-C(40)-C(30)	120.0(2)
C(18)-C(17)-C(11)	179.9(3)	C(50)-C(40)-C(410)	120.52(19)
C(17)-C(18)-C(1)	177.1(2)	C(30)-C(40)-C(410)	119.3(2)
C(22)-C(21)-C(26)	118.3(2)	C(60)-C(50)-C(40)	120.36(19)
C(22)-C(21)-C(2)	119.2(2)	C(60)-C(50)-C(510)	118.67(19)
C(26)-C(21)-C(2)	122.4(2)	C(40)-C(50)-C(510)	120.97(19)
C(23)-C(22)-C(21)	121.2(3)	C(50)-C(60)-C(10)	119.2(2)
C(24)-C(23)-C(22)	119.8(3)	C(50)-C(60)-C(610)	121.55(19)
C(25)-C(24)-C(23)	120.2(3)	C(10)-C(60)-C(610)	119.28(19)
C(24)-C(25)-C(26)	120.0(3)	C(160)-C(110)-C(120)	118.4(2)
C(25)-C(26)-C(21)	120.6(3)	C(160)-C(110)-C(170)	122.2(2)
C(32)-C(31)-C(36)	118.0(2)	C(120)-C(110)-C(170)	119.4(2)
C(32)-C(31)-C(3)	122.9(2)	C(130)-C(120)-C(110)	120.7(3)
C(36)-C(31)-C(3)	119.0(2)	C(140)-C(130)-C(120)	120.7(4)
C(33)-C(32)-C(31)	121.0(2)	C(130)-C(140)-C(150)	120.5(3)
C(34)-C(33)-C(32)	120.0(3)	C(140)-C(150)-C(160)	119.6(3)
C(35)-C(34)-C(33)	119.6(3)	C(110)-C(160)-C(150)	120.0(3)
C(36)-C(35)-C(34)	120.2(3)	C(180)-C(170)-C(110)	175.6(3)
C(35)-C(36)-C(31)	121.1(3)	C(170)-C(180)-C(10)	173.2(2)
C(42)-C(41)-C(46)	118.4(2)	C(260)-C(210)-C(220)	117.4(2)
C(42)-C(41)-C(4)	120.9(2)	C(260)-C(210)-C(20)	120.5(2)
C(46)-C(41)-C(4)	120.6(2)	C(220)-C(210)-C(20)	122.0(2)
C(41)-C(42)-C(43)	120.6(3)	C(210)-C(220)-C(230)	121.2(3)
C(44)-C(43)-C(42)	120.1(3)	C(240)-C(230)-C(220)	120.3(3)
C(45)-C(44)-C(43)	119.7(3)	C(230)-C(240)-C(250)	119.4(3)
C(44)-C(45)-C(46)	120.8(3)	C(240)-C(250)-C(260)	120.4(3)
C(45)-C(46)-C(41)	120.4(3)	C(210)-C(260)-C(250)	121.3(3)

Table B.7. Complete List of Bond Angles [deg] for 3.26 (continued).

C(360)-C(310)-C(320)	117.1(2)
C(360)-C(310)-C(30)	122.4(2)
C(320)-C(310)-C(30)	120.5(2)
C(310)-C(320)-C(330)	121.7(3)
C(340)-C(330)-C(320)	120.0(3)
C(350)-C(340)-C(330)	119.4(3)
C(340)-C(350)-C(360)	120.6(3)
C(310)-C(360)-C(350)	121.2(3)
C(460)-C(410)-C(420)	117.5(2)
C(460)-C(410)-C(40)	119.9(2)
C(420)-C(410)-C(40)	122.5(2)
C(410)-C(420)-C(430)	120.6(3)
C(440)-C(430)-C(420)	120.6(3)
C(450)-C(440)-C(430)	119.5(3)
C(440)-C(450)-C(460)	120.7(3)
C(410)-C(460)-C(450)	121.0(3)
C(520)-C(510)-C(560)	117.8(2)
C(520)-C(510)-C(50)	120.80(19)
C(560)-C(510)-C(50)	121.4(2)
C(510)-C(520)-C(530)	120.9(2)
C(540)-C(530)-C(520)	120.2(2)
C(550)-C(540)-C(530)	119.7(2)
C(540)-C(550)-C(560)	120.2(2)
C(550)-C(560)-C(510)	121.2(2)
C(620)-C(610)-C(660)	118.1(2)
C(620)-C(610)-C(60)	121.5(2)
C(660)-C(610)-C(60)	120.4(2)
C(610)-C(620)-C(630)	120.5(3)
C(640)-C(630)-C(620)	120.3(3)
C(650)-C(640)-C(630)	119.3(3)
C(640)-C(650)-C(660)	120.8(3)
C(650)-C(660)-C(610)	120.9(3)

Table B.8. Atomic coordinates (x 10^4) and equivalent isotropic displacement parameters (A^2 x 10^3) for 3.35. U(eq) is defined as 1/3rd of the trace of the orthogonalized Uij tensor.

	x	y	z	U(eq)
Br(1)	7399(1)	9998(1)	4368(1)	64(1)
Br(2)	9819(1)	8771(1)	5315(1)	66(1)
C(1)	8328(7)	8956(5)	3473(3)	38(2)
C(2)	7397(7)	8594(5)	3391(4)	41(2)
C(3)	7226(6)	8428(5)	2808(4)	38(2)
C(4)	8007(7)	8596(5)	2296(4)	44(2)
C(5)	8920(7)	8984(5)	2374(4)	42(2)
C(6)	9064(7)	9177(5)	2960(4)	38(2)
C(11)	10615(8)	7832(6)	4358(4)	45(2)
C(12)	11826(8)	7774(7)	4489(4)	63(3)
C(13)	12771(9)	7139(8)	4333(5)	85(3)
C(14)	12553(11)	6527(7)	4050(5)	87(3)
C(15)	11362(10)	6542(7)	3941(5)	81(3)
C(16)	10420(8)	7205(6)	4087(4)	58(3)
C(17)	8580(7)	9062(6)	4111(4)	43(2)
C(18)	9598(8)	8545(6)	4499(4)	44(2)
C(21)	6546(8)	8416(6)	3928(4)	44(2)
C(22)	5373(8)	8978(6)	3863(4)	53(3)
C(23)	4556(9)	8851(7)	4319(5)	78(3)
C(24)	4940(9)	8114(9)	4868(5)	79(4)
C(25)	6126(10)	7515(7)	4964(4)	77(3)
C(26)	6934(8)	7695(6)	4466(4)	63(3)
C(31)	6244(8)	8061(7)	2707(4)	45(2)
C(32)	5226(8)	8585(7)	2296(4)	65(3)
C(33)	4316(9)	8203(9)	2219(5)	79(3)
C(34)	4436(12)	7321(11)	2553(6)	98(5)
C(35)	5411(12)	6793(9)	2949(6)	96(4)
C(36)	6308(9)	7182(8)	3023(4)	72(3)
C(41)	7861(7)	8365(7)	1690(4)	50(2)
C(42)	7442(9)	9023(8)	1116(5)	83(3)
C(43)	7312(11)	8767(11)	536(5)	100(4)
C(44)	7610(12)	7880(13)	568(7)	107(6)
C(45)	8054(11)	7233(9)	1119(7)	99(4)
C(46)	8193(8)	7471(8)	1689(5)	72(3)
C(51)	9735(7)	9153(7)	1818(4)	45(2)
C(52)	9563(8)	10053(7)	1418(4)	62(3)
C(53)	10334(11)	10149(9)	905(5)	90(4)
C(54)	11202(10)	9403(10)	780(5)	78(4)
C(55)	11350(9)	8570(9)	1156(5)	79(3)
C(56)	10626(8)	8429(7)	1686(4)	65(3)
C(61)	9989(8)	9631(6)	3011(3)	42(2)
C(62)	9607(8)	10509(7)	3067(4)	59(3)
C(63)	10462(11)	10949(7)	3107(4)	68(3)
C(64)	11670(11)	10492(8)	3098(4)	74(3)
C(65)	12065(8)	9639(8)	3043(4)	67(3)
C(66)	11235(8)	9183(6)	3007(3)	48(2)
Br(3)	7358(1)	2623(1)	3534(1)	60(1)
Br(4)	5256(1)	4252(1)	3939(1)	68(1)
C(10)	5980(7)	3170(5)	2335(3)	37(2)

Table B.8. Atomic coordinates (x 10^4) and equivalent isotropic displacement parameters (A^2 x 10^3) for 3.35. U(eq) is defined as 1/3rd of the trace of the orthogonalized Uij tensor (continued).

	x	y	z	U(eq)
C(20)	6808(7)	3378(5)	1862(4)	41(2)
C(30)	6678(7)	3246(5)	1250(4)	45(2)
C(40)	5776(7)	2864(5)	1133(3)	42(2)
C(50)	5004(7)	2626(5)	1614(4)	36(2)
C(60)	5124(7)	2767(5)	2223(4)	38(2)
C(110)	4061(7)	4701(6)	2691(4)	44(2)
C(120)	2941(9)	4950(6)	2990(5)	70(3)
C(130)	1877(9)	5505(7)	2618(5)	74(3)
C(140)	1936(9)	5820(7)	1949(6)	75(3)
C(150)	3046(9)	5585(7)	1650(5)	73(3)
C(160)	4082(7)	5027(6)	2044(5)	59(3)
C(170)	6002(7)	3394(5)	2952(4)	41(2)
C(180)	5145(7)	4063(6)	3110(3)	41(2)
C(210)	7758(8)	3746(6)	1990(4)	46(2)
C(220)	8967(8)	3240(7)	1973(4)	61(3)
C(230)	9892(10)	3575(10)	2095(5)	91(4)
C(240)	9585(11)	4380(9)	2248(5)	90(4)
C(250)	8401(12)	4876(7)	2279(5)	84(3)
C(260)	7480(9)	4554(7)	2145(4)	63(3)
C(310)	7537(7)	3473(7)	721(4)	47(2)
C(320)	8303(7)	2790(7)	459(4)	61(3)
C(330)	9096(8)	3004(9)	-8(5)	80(4)
C(340)	9163(11)	3865(11)	-222(5)	97(5)
C(350)	8415(10)	4548(9)	20(5)	92(4)
C(360)	7629(8)	4342(7)	492(4)	65(3)
C(410)	5611(7)	2744(7)	484(4)	50(2)
C(420)	5874(9)	1898(8)	399(5)	78(3)
C(430)	5687(12)	1773(12)	-184(8)	123(6)
C(440)	5185(13)	2513(14)	-703(8)	124(7)
C(450)	4897(10)	3385(12)	-655(5)	108(5)
C(460)	5124(8)	3499(8)	-48(5)	72(3)
C(510)	4000(8)	2303(7)	1474(4)	46(2)
C(520)	4074(9)	1421(8)	1717(4)	67(3)
C(530)	3118(13)	1126(8)	1610(5)	95(4)
C(540)	2062(12)	1728(11)	1267(5)	91(4)
C(550)	1985(10)	2617(9)	1019(5)	82(3)
C(560)	2950(8)	2902(7)	1134(4)	61(3)
C(610)	4352(7)	2464(6)	2765(4)	40(2)
C(620)	4878(7)	1702(6)	3268(4)	52(2)
C(630)	4199(9)	1406(7)	3770(4)	63(3)
C(640)	2981(9)	1874(7)	3774(5)	66(3)
C(650)	2427(8)	2637(8)	3264(5)	69(3)
C(660)	3120(8)	2928(6)	2765(4)	49(2)

Table B.9. Complete List of Bond Lengths [Å] for 3.35.

Br(1)-C(17)	1.891(8)	Br(3)-C(170)	1.907(7)
Br(2)-C(18)	1.931(8)	Br(4)-C(180)	1.906(7)
C(1)-C(6)	1.401(9)	C(10)-C(60)	1.402(10)
C(1)-C(2)	1.411(10)	C(10)-C(20)	1.411(9)
C(1)-C(17)	1.480(10)	C(10)-C(170)	1.472(10)
C(2)-C(3)	1.388(9)	C(20)-C(30)	1.411(10)
C(2)-C(21)	1.510(10)	C(20)-C(210)	1.467(10)
C(3)-C(4)	1.416(10)	C(30)-C(40)	1.427(10)
C(3)-C(31)	1.481(10)	C(30)-C(310)	1.522(10)
C(4)-C(5)	1.419(10)	C(40)-C(50)	1.389(9)
C(4)-C(41)	1.482(11)	C(40)-C(410)	1.489(10)
C(5)-C(6)	1.407(10)	C(50)-C(60)	1.410(9)
C(5)-C(51)	1.510(10)	C(50)-C(510)	1.484(10)
C(6)-C(61)	1.494(10)	C(60)-C(610)	1.504(10)
C(11)-C(16)	1.379(11)	C(110)-C(160)	1.345(10)
C(11)-C(12)	1.406(10)	C(110)-C(120)	1.414(10)
C(11)-C(18)	1.457(10)	C(110)-C(180)	1.486(10)
C(12)-C(13)	1.351(12)	C(120)-C(130)	1.394(11)
C(13)-C(14)	1.384(13)	C(130)-C(140)	1.392(12)
C(14)-C(15)	1.396(12)	C(140)-C(150)	1.403(11)
C(15)-C(16)	1.365(11)	C(150)-C(160)	1.393(11)
C(17)-C(18)	1.360(10)	C(170)-C(180)	1.333(10)
C(21)-C(22)	1.363(10)	C(210)-C(260)	1.376(11)
C(21)-C(26)	1.364(10)	C(210)-C(220)	1.386(11)
C(22)-C(23)	1.352(11)	C(220)-C(230)	1.401(12)
C(23)-C(24)	1.391(12)	C(230)-C(240)	1.366(14)
C(24)-C(25)	1.393(13)	C(240)-C(250)	1.362(13)
C(25)-C(26)	1.420(11)	C(250)-C(260)	1.392(12)
C(31)-C(36)	1.372(11)	C(310)-C(360)	1.388(11)
C(31)-C(32)	1.387(11)	C(310)-C(320)	1.421(11)
C(32)-C(33)	1.410(12)	C(320)-C(330)	1.377(11)
C(33)-C(34)	1.371(14)	C(330)-C(340)	1.364(15)
C(34)-C(35)	1.337(14)	C(340)-C(350)	1.388(15)
C(35)-C(36)	1.403(13)	C(350)-C(360)	1.374(11)
C(41)-C(42)	1.371(11)	C(410)-C(420)	1.368(12)
C(41)-C(46)	1.375(12)	C(410)-C(460)	1.399(11)
C(42)-C(43)	1.446(14)	C(420)-C(430)	1.361(15)
C(43)-C(44)	1.349(16)	C(430)-C(440)	1.373(17)
C(44)-C(45)	1.334(16)	C(440)-C(450)	1.376(18)
C(45)-C(46)	1.411(13)	C(450)-C(460)	1.413(13)
C(51)-C(56)	1.386(11)	C(510)-C(520)	1.350(11)
C(51)-C(52)	1.424(11)	C(510)-C(560)	1.373(11)
C(52)-C(53)	1.395(12)	C(520)-C(530)	1.381(12)
C(53)-C(54)	1.392(14)	C(530)-C(540)	1.381(14)
C(54)-C(55)	1.324(13)	C(540)-C(550)	1.361(14)
C(55)-C(56)	1.395(11)	C(550)-C(560)	1.384(12)
C(61)-C(62)	1.387(11)	C(610)-C(620)	1.377(10)
C(61)-C(66)	1.395(10)	C(610)-C(660)	1.386(10)
C(62)-C(63)	1.402(11)	C(620)-C(630)	1.374(10)
C(63)-C(64)	1.362(12)	C(630)-C(640)	1.375(11)
C(64)-C(65)	1.349(12)	C(640)-C(650)	1.392(11)
C(65)-C(66)	1.394(11)	C(650)-C(660)	1.376(10)

Table B.10. Complete List of Bond Angles [deg] for 3.35.

C(6)-C(1)-C(2)	120.3(7)	C(44)-C(43)-C(42)	119.2(12)
C(6)-C(1)-C(17)	119.2(7)	C(45)-C(44)-C(43)	121.4(13)
C(2)-C(1)-C(17)	120.5(7)	C(44)-C(45)-C(46)	120.1(13)
C(3)-C(2)-C(1)	120.4(7)	C(41)-C(46)-C(45)	121.0(11)
C(3)-C(2)-C(21)	119.2(7)	C(56)-C(51)-C(52)	120.2(7)
C(1)-C(2)-C(21)	120.4(7)	C(56)-C(51)-C(5)	119.9(8)
C(2)-C(3)-C(4)	120.2(7)	C(52)-C(51)-C(5)	119.9(8)
C(2)-C(3)-C(31)	121.3(7)	C(53)-C(52)-C(51)	116.4(9)
C(4)-C(3)-C(31)	118.5(7)	C(54)-C(53)-C(52)	121.8(10)
C(3)-C(4)-C(5)	119.1(7)	C(55)-C(54)-C(53)	121.2(10)
C(3)-C(4)-C(41)	119.7(7)	C(54)-C(55)-C(56)	119.9(10)
C(5)-C(4)-C(41)	121.2(7)	C(51)-C(56)-C(55)	120.6(9)
C(6)-C(5)-C(4)	120.3(7)	C(62)-C(61)-C(66)	119.3(8)
C(6)-C(5)-C(51)	122.1(7)	C(62)-C(61)-C(6)	119.6(8)
C(4)-C(5)-C(51)	117.6(7)	C(66)-C(61)-C(6)	121.0(8)
C(1)-C(6)-C(5)	119.5(7)	C(61)-C(62)-C(63)	120.4(8)
C(1)-C(6)-C(61)	121.7(7)	C(64)-C(63)-C(62)	118.6(10)
C(5)-C(6)-C(61)	118.7(7)	C(65)-C(64)-C(63)	122.2(10)
C(16)-C(11)-C(12)	118.2(8)	C(64)-C(65)-C(66)	120.4(9)
C(16)-C(11)-C(18)	121.2(8)	C(65)-C(66)-C(61)	119.1(9)
C(12)-C(11)-C(18)	120.6(8)	C(60)-C(10)-C(20)	121.1(7)
C(13)-C(12)-C(11)	120.8(9)	C(60)-C(10)-C(170)	119.4(6)
C(12)-C(13)-C(14)	120.0(10)	C(20)-C(10)-C(170)	119.5(7)
C(13)-C(14)-C(15)	120.6(10)	C(10)-C(20)-C(30)	118.1(7)
C(16)-C(15)-C(14)	118.3(10)	C(10)-C(20)-C(210)	121.6(7)
C(15)-C(16)-C(11)	122.1(9)	C(30)-C(20)-C(210)	120.3(7)
C(18)-C(17)-C(1)	123.9(7)	C(20)-C(30)-C(40)	120.3(7)
C(18)-C(17)-Br(1)	120.2(6)	C(20)-C(30)-C(310)	120.0(8)
C(1)-C(17)-Br(1)	115.9(6)	C(40)-C(30)-C(310)	119.6(8)
C(17)-C(18)-C(11)	126.9(7)	C(50)-C(40)-C(30)	120.8(7)
C(17)-C(18)-Br(2)	119.4(6)	C(50)-C(40)-C(410)	118.5(7)
C(11)-C(18)-Br(2)	113.7(6)	C(30)-C(40)-C(410)	120.7(7)
C(22)-C(21)-C(26)	120.2(8)	C(40)-C(50)-C(60)	119.0(7)
C(22)-C(21)-C(2)	119.1(8)	C(40)-C(50)-C(510)	120.6(7)
C(26)-C(21)-C(2)	120.7(8)	C(60)-C(50)-C(510)	120.2(6)
C(23)-C(22)-C(21)	122.2(9)	C(10)-C(60)-C(50)	120.6(7)
C(22)-C(23)-C(24)	118.1(9)	C(10)-C(60)-C(610)	119.3(7)
C(23)-C(24)-C(25)	122.5(9)	C(50)-C(60)-C(610)	120.0(7)
C(24)-C(25)-C(26)	116.2(9)	C(160)-C(110)-C(120)	118.7(8)
C(21)-C(26)-C(25)	120.7(9)	C(160)-C(110)-C(180)	123.4(7)
C(36)-C(31)-C(32)	117.3(9)	C(120)-C(110)-C(180)	117.8(8)
C(36)-C(31)-C(3)	120.8(8)	C(130)-C(120)-C(110)	120.5(9)
C(32)-C(31)-C(3)	121.9(8)	C(140)-C(130)-C(120)	119.0(9)
C(31)-C(32)-C(33)	119.6(10)	C(130)-C(140)-C(150)	120.8(9)
C(34)-C(33)-C(32)	120.0(11)	C(160)-C(150)-C(140)	118.0(9)
C(35)-C(34)-C(33)	122.0(12)	C(110)-C(160)-C(150)	123.1(8)
C(34)-C(35)-C(36)	117.4(12)	C(180)-C(170)-C(10)	124.1(7)
C(31)-C(36)-C(35)	123.6(10)	C(180)-C(170)-Br(3)	121.5(6)
C(42)-C(41)-C(46)	118.4(9)	C(10)-C(170)-Br(3)	114.4(6)
C(42)-C(41)-C(4)	121.7(10)	C(170)-C(180)-C(110)	125.6(7)
C(46)-C(41)-C(4)	119.9(9)	C(170)-C(180)-Br(4)	119.7(6)
C(41)-C(42)-C(43)	119.9(11)	C(110)-C(180)-Br(4)	114.7(6)

Table B.10. Complete List of Bond Angles [deg] for 3.35 (continued).

C(260)-C(210)-C(220)	119.9(8)
C(260)-C(210)-C(20)	122.0(8)
C(220)-C(210)-C(20)	118.1(9)
C(210)-C(220)-C(230)	119.2(10)
C(240)-C(230)-C(220)	119.4(10)
C(250)-C(240)-C(230)	122.0(11)
C(240)-C(250)-C(260)	118.8(11)
C(210)-C(260)-C(250)	120.7(9)
C(360)-C(310)-C(320)	117.7(8)
C(360)-C(310)-C(30)	121.5(8)
C(320)-C(310)-C(30)	120.7(8)
C(330)-C(320)-C(310)	119.9(10)
C(340)-C(330)-C(320)	120.9(11)
C(330)-C(340)-C(350)	120.4(11)
C(360)-C(350)-C(340)	119.3(12)
C(350)-C(360)-C(310)	121.7(10)
C(420)-C(410)-C(460)	118.4(9)
C(420)-C(410)-C(40)	121.1(9)
C(460)-C(410)-C(40)	120.4(9)
C(430)-C(420)-C(410)	122.1(12)
C(420)-C(430)-C(440)	119.5(16)
C(430)-C(440)-C(450)	121.6(16)
C(440)-C(450)-C(460)	117.9(14)
C(410)-C(460)-C(450)	120.5(11)
C(520)-C(510)-C(560)	119.0(9)
C(520)-C(510)-C(50)	120.2(9)
C(560)-C(510)-C(50)	120.7(9)
C(510)-C(520)-C(530)	120.2(10)
C(540)-C(530)-C(520)	120.8(11)
C(550)-C(540)-C(530)	119.1(11)
C(540)-C(550)-C(560)	119.3(11)
C(510)-C(560)-C(550)	121.5(10)
C(620)-C(610)-C(660)	119.3(7)
C(620)-C(610)-C(60)	119.2(7)
C(660)-C(610)-C(60)	121.5(7)
C(630)-C(620)-C(610)	120.7(8)
C(620)-C(630)-C(640)	119.9(9)
C(630)-C(640)-C(650)	120.3(8)
C(660)-C(650)-C(640)	119.2(8)
C(650)-C(660)-C(610)	120.6(8)

Table B.11. Crystal Data and Structure Refinement Parameters for 3.39 and 3.40.

	3.39	3.40
Empirical formula	$C_{18}H_{22}O$	$C_{46}H_{40}$
Molecular weight	254.36	592.78
Description	colourless rock	colourless plate
Crystal size, mm	0.50 X 0.50 X 0.30	0.20 x 0.14 x 0.02
Temperature, K	100(2)	173(2)
Wavelength, Å	(Mo-Kα) 0.71073	0.71073
Crystal system	monoclinic	monoclinic
Space group	$P2_1$	$C2$
a, Å	7.476(2)	47.379(16)
b, Å	11.482(4)	11.616(4)
c, Å	17.239(6)	12.000(4)
α, deg.	90.0	90.0
β, deg.	90.340(5)	90.436(7)
γ, deg.	90.0	90.0
Volume, Å^3	1479.8(8)	6604(4)
Z	4	8
Calcd Density, g/cm^3	1.142	1.192
Abs Coeff, mm^{-1}	0.068	0.067
Scan Mode	ω & ϕ scans	ω & ϕ scans
F(000)	552	2528
θ-range, deg.	1.77 to 25.35	1.70 to 19.77
Index ranges	$-9 \le h \le 8$	$-44 \le h \le 44$
	$-13 \le k \le 13$	$-11 \le k \le 11$
	$-20 \le l \le 18$	$-11 \le l \le 11$
No. Reflect. collected	9727	14282
No. Independent reflect.	4555	5824
R(int)	0.0324	0.3289
Data / Restraints / Param.	4555 / 1 / 335	5824 / 1 / 226
Goodness-of-fit on F^2	1.195	0.959
Final *R* indices (I>2σ(I))*	*R*1 = 0.0814;	*R*1 = 0.1424;
	w*R*2 = 0.2744	w*R*2 = 0.3145
R indices (all data)*	*R*1 = 0.0838;	*R*1 = 0.3209
	w*R*2 = 0.2763	w*R*2 = 0.4218
Mean shift/error	0.000	0.000
Max. shift/error	0.001	0.001
Ratio Min:Max Trans.	0.812570	0.618956
Extinction coeff	0.020(5)	0.094(7)
Largest diff. Peak, e/Å^3	0.426	0.638
Largest diff. Hole, e/Å^3	-0.382	-0.458

Refinement method: Full-matrix least-squares on F^2,
Weighting Scheme: $w = 1/[\sigma^2Fo^2+(0.0597((Fo^2+2Fc^2)/3))^2]$

*$R1 = \Sigma(||Fo|-|Fc||)/\Sigma|Fo|$; $wR2 = [\Sigma[w(Fo^2-Fc^2)^2]/\Sigma[w(Fo^2)^2]]^{0.5}$; $P=(Fo^2+2Fc^2)/3$

Table B.12. Atomic coordinates (x 10^4) and equivalent isotropic displacement parameters (A^2 x 10^3) for 3.39. U(eq) is defined as 1/3rd of the trace of the orthogonalized Uij tensor.

	x	y	z	U(eq)
C(1A)	1242(8)	3678(5)	6687(3)	18(1)
O(2A)	309(6)	1584(3)	6502(2)	21(1)
C(2A)	-32(8)	2631(5)	6922(3)	19(1)
C(3A)	-1927(8)	3103(6)	6657(4)	23(1)
C(4A)	-1517(8)	4326(5)	6345(3)	23(1)
C(5A)	-1012(9)	5104(5)	7047(4)	32(2)
C(6A)	882(9)	4662(5)	7265(4)	23(1)
C(7A)	276(8)	4144(5)	5931(3)	20(1)
C(8A)	226(9)	3324(6)	5247(3)	26(1)
C(9A)	1124(9)	5287(6)	5633(4)	29(1)
C(10A)	3191(8)	3319(5)	6602(4)	24(1)
C(11A)	40(8)	2391(5)	7752(3)	18(1)
C(12A)	44(8)	2193(5)	8458(3)	21(1)
C(13A)	78(13)	2006(7)	9282(4)	20(1)
C(14A)	881(12)	1045(6)	9628(4)	22(2)
C(15A)	967(12)	962(6)	10432(5)	23(2)
C(16A)	249(14)	1841(8)	10889(4)	31(2)
C(17A)	-554(12)	2802(7)	10543(5)	27(2)
C(18A)	-640(12)	2885(6)	9739(5)	25(2)
C(13)	11(13)	2055(8)	9299(4)	20(1)
C(14)	-896(12)	1108(6)	9610(4)	22(2)
C(15)	-1008(11)	975(6)	10409(5)	23(2)
C(16)	-214(14)	1790(8)	10898(4)	31(2)
C(17)	692(13)	2737(7)	10588(5)	27(2)
C(18)	805(12)	2869(6)	9788(5)	25(2)
C(1B)	4117(9)	-1310(5)	7012(4)	24(1)
O(2B)	3240(6)	684(4)	7405(2)	27(1)
C(2B)	4584(8)	-217(5)	7498(3)	18(1)
C(3B)	6366(8)	203(5)	7131(3)	22(1)
C(4B)	6743(8)	-722(6)	6504(4)	24(1)
C(5B)	7235(10)	-1850(7)	6917(4)	37(2)
C(6B)	5471(10)	-2270(6)	7261(4)	32(2)
C(7B)	4834(8)	-999(5)	6187(4)	23(1)
C(8B)	3952(9)	46(6)	5781(4)	27(1)
C(9B)	4747(10)	-2019(6)	5612(4)	31(2)
C(10B)	2161(10)	-1674(7)	7067(4)	36(2)
C(11B)	4722(8)	-438(5)	8335(3)	19(1)
C(12B)	4810(8)	-521(5)	9036(3)	20(1)
C(13B)	4773(13)	-577(7)	9870(4)	17(1)
C(14B)	5539(11)	-1521(6)	10252(5)	22(2)
C(15B)	5585(12)	-1550(7)	11058(5)	26(2)
C(16B)	4864(13)	-635(8)	11482(4)	22(2)
C(17B)	4098(12)	309(7)	11100(5)	25(2)
C(18B)	4052(12)	338(6)	10294(5)	25(2)
C(13')	5043(13)	-572(8)	9865(4)	17(1)
C(14')	4325(11)	-1503(6)	10273(5)	22(2)
C(15')	4399(12)	-1514(7)	11079(5)	26(2)
C(16')	5192(13)	-594(8)	11476(4)	22(2)
C(17')	5910(12)	337(7)	11068(5)	25(2)
C(18')	5836(12)	349(6)	10262(5)	25(2)

Table B.13. Complete List of Bond Lengths [Å] for 3.39.

C(1A)-C(10A)	1.522(8)	C(1B)-C(10B)	1.525(9)
C(1A)-C(6A)	1.531(8)	C(1B)-C(2B)	1.548(8)
C(1A)-C(7A)	1.579(8)	C(1B)-C(6B)	1.555(9)
C(1A)-C(2A)	1.588(8)	C(1B)-C(7B)	1.564(9)
O(2A)-C(2A)	1.427(7)	O(2B)-C(2B)	1.451(7)
C(2A)-C(11A)	1.459(8)	C(2B)-C(11B)	1.468(8)
C(2A)-C(3A)	1.582(8)	C(2B)-C(3B)	1.554(9)
C(3A)-C(4A)	1.536(8)	C(3B)-C(4B)	1.543(9)
C(4A)-C(7A)	1.537(9)	C(4B)-C(5B)	1.522(9)
C(4A)-C(5A)	1.550(9)	C(4B)-C(7B)	1.558(8)
C(5A)-C(6A)	1.548(9)	C(5B)-C(6B)	1.528(10)
C(7A)-C(8A)	1.509(9)	C(7B)-C(8B)	1.535(9)
C(7A)-C(9A)	1.547(8)	C(7B)-C(9B)	1.536(8)
C(11A)-C(12A)	1.238(8)	C(11B)-C(12B)	1.214(9)
C(12A)-C(13A)	1.436(8)	C(12B)-C(13')	1.440(8)
C(12A)-C(13)	1.459(8)	C(12B)-C(13B)	1.441(9)
C(13A)-C(14A)	1.3900	C(13B)-C(14B)	1.3900
C(13A)-C(18A)	1.3900	C(13B)-C(18B)	1.3900
C(14A)-C(15A)	1.3900	C(14B)-C(15B)	1.3900
C(15A)-C(16A)	1.3900	C(15B)-C(16B)	1.3900
C(16A)-C(17A)	1.3900	C(16B)-C(17B)	1.3900
C(17A)-C(18A)	1.3900	C(17B)-C(18B)	1.3900
C(13)-C(14)	1.3900	C(13')-C(14')	1.3900
C(13)-C(18)	1.3900	C(13')-C(18')	1.3900
C(14)-C(15)	1.3900	C(14')-C(15')	1.3900
C(15)-C(16)	1.3900	C(15')-C(16')	1.3900
C(16)-C(17)	1.3900	C(16')-C(17')	1.3900
C(17)-C(18)	1.3900	C(17')-C(18')	1.3900

Table B.14. Complete List of Bond Angles [deg] for 3.39.

C(10A)-C(1A)-C(6A)	115.7(5)	C(17)-C(18)-C(13)	120.0
C(10A)-C(1A)-C(7A)	116.5(5)	C(10B)-C(1B)-C(2B)	113.7(6)
C(6A)-C(1A)-C(7A)	101.9(5)	C(10B)-C(1B)-C(6B)	114.3(6)
C(10A)-C(1A)-C(2A)	113.3(5)	C(2B)-C(1B)-C(6B)	106.3(5)
C(6A)-C(1A)-C(2A)	106.5(5)	C(10B)-C(1B)-C(7B)	116.9(5)
C(7A)-C(1A)-C(2A)	101.2(4)	C(2B)-C(1B)-C(7B)	103.3(5)
C(2A)-O(2A)-H(2A)	109.5	C(6B)-C(1B)-C(7B)	100.8(5)
O(2A)-C(2A)-C(11A)	109.5(4)	C(2B)-O(2B)-H(2B)	109.5
O(2A)-C(2A)-C(3A)	107.8(4)	O(2B)-C(2B)-C(11B)	106.1(5)
C(11A)-C(2A)-C(3A)	112.0(5)	O(2B)-C(2B)-C(1B)	111.4(5)
O(2A)-C(2A)-C(1A)	113.5(5)	C(11B)-C(2B)-C(1B)	113.9(5)
C(11A)-C(2A)-C(1A)	112.0(5)	O(2B)-C(2B)-C(3B)	109.2(5)
C(3A)-C(2A)-C(1A)	101.8(4)	C(11B)-C(2B)-C(3B)	113.4(5)
C(4A)-C(3A)-C(2A)	103.5(5)	C(1B)-C(2B)-C(3B)	102.9(5)
H(3AA)-C(3A)-H(3AB)	109.0	C(4B)-C(3B)-C(2B)	103.4(5)
C(3A)-C(4A)-C(7A)	102.4(4)	C(5B)-C(4B)-C(3B)	107.6(5)
C(3A)-C(4A)-C(5A)	107.5(5)	C(5B)-C(4B)-C(7B)	102.1(5)
C(7A)-C(4A)-C(5A)	103.4(5)	C(3B)-C(4B)-C(7B)	102.4(5)
C(6A)-C(5A)-C(4A)	102.6(5)	C(4B)-C(5B)-C(6B)	104.1(5)
H(5AA)-C(5A)-H(5AB)	109.2	C(5B)-C(6B)-C(1B)	103.3(5)
C(1A)-C(6A)-C(5A)	104.4(5)	C(8B)-C(7B)-C(9B)	106.6(5)
C(8A)-C(7A)-C(4A)	115.5(5)	C(8B)-C(7B)-C(4B)	113.0(5)
C(8A)-C(7A)-C(9A)	106.2(5)	C(9B)-C(7B)-C(4B)	114.6(5)
C(4A)-C(7A)-C(9A)	113.5(5)	C(8B)-C(7B)-C(1B)	116.4(5)
C(8A)-C(7A)-C(1A)	116.3(5)	C(9B)-C(7B)-C(1B)	113.5(5)
C(4A)-C(7A)-C(1A)	93.4(4)	C(4B)-C(7B)-C(1B)	92.6(4)
C(9A)-C(7A)-C(1A)	112.0(5)	C(12B)-C(11B)-C(2B)	174.4(6)
C(12A)-C(11A)-C(2A)	178.0(6)	C(11B)-C(12B)-C(13')	175.6(7)
C(11A)-C(12A)-C(13A)	177.8(7)	C(11B)-C(12B)-C(13B)	175.4(6)
C(11A)-C(12A)-C(13)	175.5(6)	C(13')-C(12B)-C(13B)	8.1(7)
C(13A)-C(12A)-C(13)	3.1(6)	C(14B)-C(13B)-C(18B)	120.0
C(14A)-C(13A)-C(18A)	120.0	C(14B)-C(13B)-C(12B)	119.8(6)
C(14A)-C(13A)-C(12A)	123.3(6)	C(18B)-C(13B)-C(12B)	120.1(6)
C(18A)-C(13A)-C(12A)	116.6(6)	C(15B)-C(14B)-C(13B)	120.0
C(13A)-C(14A)-C(15A)	120.0	C(14B)-C(15B)-C(16B)	120.0
C(16A)-C(15A)-C(14A)	120.0	C(17B)-C(16B)-C(15B)	120.0
C(15A)-C(16A)-C(17A)	120.0	C(16B)-C(17B)-C(18B)	120.0
C(16A)-C(17A)-C(18A)	120.0	C(17B)-C(18B)-C(13B)	120.0
C(17A)-C(18A)-C(13A)	120.0	C(14')-C(13')-C(18')	120.0
C(14)-C(13)-C(18)	120.0	C(14')-C(13')-C(12B)	119.3(6)
C(14)-C(13)-C(12A)	118.6(6)	C(18')-C(13')-C(12B)	120.5(6)
C(18)-C(13)-C(12A)	121.3(6)	C(15')-C(14')-C(13')	120.0
C(13)-C(14)-C(15)	120.0	C(14')-C(15')-C(16')	120.0
C(16)-C(15)-C(14)	120.0	C(17')-C(16')-C(15')	120.0
C(15)-C(16)-C(17)	120.0	C(16')-C(17')-C(18')	120.0
C(16)-C(17)-C(18)	120.0	C(17')-C(18')-C(13')	120.0

Table B.15. Atomic coordinates (x 10^4) and equivalent isotropic displacement parameters (A^2 x 10^3) for 3.40. U(eq) is defined as 1/3rd of the trace of the orthogonalized Uij tensor.

	x	y	z	U(eq)
C(1)	1437(3)	-5630(14)	11381(13)	43(9)
C(2)	1377(3)	-4530(12)	11770(13)	22(7)
C(3)	1101(4)	-4226(12)	12023(13)	27(7)
C(4)	885(3)	-5023(17)	11886(14)	46(9)
C(5)	944(3)	-6123(15)	11497(15)	66(10)
C(6)	1220(4)	-6426(11)	11244(14)	27(7)
C(9)	1908(6)	-6180(20)	10180(20)	60(9)
C(11)	1755(5)	-6080(20)	11310(20)	39(8)
C(12)	1923(6)	-6380(20)	12200(20)	51(8)
C(13)	2221(9)	-6620(30)	11610(40)	120(16)
C(14)	2136(7)	-7930(30)	11040(30)	108(11)
C(15)	1940(6)	-7660(20)	10060(20)	85(10)
C(16)	2202(7)	-5890(30)	10480(30)	95(10)
C(17)	2223(6)	-4750(20)	10780(20)	72(9)
C(18)	2428(8)	-6250(30)	9780(30)	142(15)
C(19)	1763(7)	-5640(30)	9210(20)	82(11)
C(21)	1602(4)	-3622(13)	11946(16)	71(11)
C(22)	1660(4)	-2833(15)	11108(12)	30(7)
C(23)	1871(4)	-2015(14)	11261(14)	64(10)
C(24)	2024(4)	-1988(16)	12253(17)	53(9)
C(25)	1966(4)	-2777(19)	13091(13)	106(13)
C(26)	1755(4)	-3595(15)	12938(14)	67(10)
C(31)	1013(4)	-2961(11)	12386(15)	40(8)
C(32)	882(4)	-2239(14)	11615(11)	49(9)
C(33)	812(3)	-1120(13)	11913(13)	36(7)
C(34)	872(4)	-722(12)	12981(14)	48(8)
C(35)	1003(4)	-1443(16)	13751(11)	97(13)
C(36)	1073(3)	-2563(14)	13453(13)	43(8)
C(41)	583(3)	-4683(14)	12218(18)	42(8)
C(42)	377(5)	-4624(18)	11390(13)	87(12)
C(43)	99(4)	-4370(20)	11668(17)	141(17)
C(44)	28(3)	-4178(19)	12770(20)	96(13)
C(45)	234(5)	-4237(19)	13602(14)	90(12)
C(46)	512(4)	-4490(16)	13324(15)	69(10)
C(51)	704(3)	-6969(12)	11424(16)	43(8)
C(52)	594(4)	-7371(14)	10421(12)	48(9)
C(53)	383(4)	-8203(14)	10421(12)	54(9)
C(54)	283(3)	-8632(14)	11424(16)	42(8)
C(55)	393(4)	-8230(15)	12427(12)	73(11)
C(56)	604(4)	-7399(14)	12427(12)	44(8)
C(61)	1278(4)	-7633(12)	10839(16)	58(10)
C(62)	1222(3)	-7948(14)	9742(14)	36(8)
C(63)	1247(4)	-9093(16)	9419(12)	71(11)
C(64)	1327(4)	-9922(12)	10194(16)	47(9)
C(65)	1383(4)	-9607(15)	11291(14)	54(9)
C(66)	1358(4)	-8462(17)	11614(12)	56(10)
C(10)	3572(3)	-4864(15)	13613(14)	36(8)
C(20)	3794(4)	-4089(11)	13726(14)	56(10)
C(30)	4067(3)	-4431(14)	13477(13)	25(7)

Table B.15. Atomic coordinates (x 10^4) and equivalent isotropic displacement parameters (A^2 x 10^3) for 3.40. U(eq) is defined as 1/3rd of the trace of the orthogonalized Uij tensor (continued).

	x	y	z	U(eq)
C(40)	4119(3)	-5547(16)	13113(13)	36(8)
C(50)	3897(4)	-6321(12)	13000(14)	34(8)
C(60)	3623(3)	-5980(13)	13249(14)	55(9)
C(90)	3118(7)	-4540(30)	14710(30)	83(11)
C(110)	3270(6)	-4580(20)	13810(20)	52(9)
C(120)	3078(7)	-4120(30)	13040(30)	94(13)
C(130)	2807(6)	-3820(20)	13460(20)	56(9)
C(140)	2670(6)	-5130(20)	13590(30)	99(10)
C(150)	2823(9)	-5600(40)	14670(40)	168(19)
C(160)	2870(6)	-3570(20)	14580(20)	73(8)
C(170)	2979(6)	-2310(20)	14580(30)	100(11)
C(180)	2616(6)	-3400(30)	15330(30)	99(11)
C(190)	3232(7)	-4670(30)	15820(30)	94(12)
C(210)	3734(4)	-2898(12)	14151(16)	34(8)
C(220)	3778(4)	-2592(15)	15259(14)	67(10)
C(230)	3742(4)	-1456(17)	15592(12)	53(9)
C(240)	3662(4)	-626(13)	14819(17)	81(12)
C(250)	3617(4)	-931(15)	13712(15)	75(11)
C(260)	3653(4)	-2068(17)	13378(12)	47(9)
C(310)	4295(3)	-3518(11)	13540(15)	29(7)
C(320)	4413(4)	-3243(13)	14569(12)	46(8)
C(330)	4631(4)	-2444(16)	14637(12)	65(10)
C(340)	4730(3)	-1918(14)	13676(16)	56(9)
C(350)	4612(4)	-2192(15)	12647(13)	51(9)
C(360)	4394(4)	-2992(14)	12579(11)	53(9)
C(410)	4419(3)	-5847(14)	12813(17)	55(10)
C(420)	4646(4)	-5900(15)	13551(11)	60(10)
C(430)	4914(3)	-6166(15)	13162(13)	50(8)
C(440)	4954(3)	-6378(15)	12035(14)	53(8)
C(450)	4727(4)	-6324(16)	11297(11)	66(9)
C(460)	4459(3)	-6059(15)	11686(15)	65(10)
C(510)	3965(3)	-7511(11)	12656(14)	28(7)
C(520)	4138(4)	-8186(15)	13333(11)	52(9)
C(530)	4224(3)	-9266(15)	12972(14)	64(9)
C(540)	4137(4)	-9672(12)	11934(15)	77(11)
C(550)	3965(4)	-8997(14)	11258(11)	32(7)
C(560)	3879(3)	-7917(13)	11618(13)	39(7)
C(610)	3387(3)	-6832(14)	13059(16)	44(8)
C(620)	3348(4)	-7713(17)	13826(13)	82(12)
C(630)	3138(4)	-8531(14)	13648(15)	58(9)
C(640)	2968(4)	-8467(15)	12702(17)	86(12)
C(650)	3007(4)	-7586(17)	11935(13)	49(8)

Table B.16. Complete List of Bond Lengths [Å] for 3.40.

C(1)-C(2)	1.3900	C(10)-C(20)	1.3900
C(1)-C(6)	1.3900	C(10)-C(60)	1.3900
C(1)-C(11)	1.60(3)	C(10)-C(110)	1.49(3)
C(2)-C(3)	1.3900	C(20)-C(30)	1.3900
C(2)-C(21)	1.512(17)	C(20)-C(210)	1.503(18)
C(3)-C(4)	1.3900	C(30)-C(40)	1.3900
C(3)-C(31)	1.590(17)	C(30)-C(310)	1.514(17)
C(4)-C(5)	1.3900	C(40)-C(50)	1.3900
C(4)-C(41)	1.54(2)	C(40)-C(410)	1.510(18)
C(5)-C(6)	1.3900	C(50)-C(60)	1.3900
C(5)-C(51)	1.505(17)	C(50)-C(510)	1.478(17)
C(6)-C(61)	1.509(18)	C(60)-C(610)	1.509(18)
C(9)-C(16)	1.47(4)	C(90)-C(110)	1.30(4)
C(9)-C(19)	1.49(3)	C(90)-C(190)	1.44(4)
C(9)-C(11)	1.54(3)	C(90)-C(160)	1.63(4)
C(9)-C(15)	1.73(4)	C(90)-C(150)	1.87(5)
C(11)-C(12)	1.38(3)	C(110)-C(120)	1.40(4)
C(12)-C(13)	1.61(4)	C(120)-C(130)	1.42(4)
C(13)-C(16)	1.61(4)	C(130)-C(160)	1.41(3)
C(13)-C(14)	1.71(4)	C(130)-C(140)	1.66(4)
C(14)-C(15)	1.52(3)	C(140)-C(150)	1.57(4)
C(16)-C(17)	1.38(4)	C(160)-C(180)	1.52(4)
C(16)-C(18)	1.42(4)	C(160)-C(170)	1.54(3)
C(21)-C(22)	1.3900	C(210)-C(220)	1.3900
C(21)-C(26)	1.3900	C(210)-C(260)	1.3900
C(22)-C(23)	1.3900	C(220)-C(230)	1.3900
C(23)-C(24)	1.3900	C(230)-C(240)	1.3900
C(24)-C(25)	1.3900	C(240)-C(250)	1.3900
C(25)-C(26)	1.3900	C(250)-C(260)	1.3900
C(31)-C(32)	1.3900	C(310)-C(320)	1.3900
C(31)-C(36)	1.3900	C(310)-C(360)	1.3900
C(32)-C(33)	1.3900	C(320)-C(330)	1.3900
C(33)-C(34)	1.3900	C(330)-C(340)	1.3900
C(34)-C(35)	1.3900	C(340)-C(350)	1.3900
C(35)-C(36)	1.3900	C(350)-C(360)	1.3900
C(41)-C(42)	1.3900	C(410)-C(420)	1.3900
C(41)-C(46)	1.3900	C(410)-C(460)	1.3900
C(42)-C(43)	1.3900	C(420)-C(430)	1.3900
C(43)-C(44)	1.3900	C(430)-C(440)	1.3900
C(44)-C(45)	1.3900	C(440)-C(450)	1.3900
C(45)-C(46)	1.3900	C(450)-C(460)	1.3900
C(51)-C(52)	1.3900	C(510)-C(520)	1.3900
C(51)-C(56)	1.3900	C(510)-C(560)	1.3900
C(52)-C(53)	1.3900	C(520)-C(530)	1.3900
C(53)-C(54)	1.3900	C(530)-C(540)	1.3900
C(54)-C(55)	1.3900	C(540)-C(550)	1.3900
C(55)-C(56)	1.3900	C(550)-C(560)	1.3900
C(61)-C(62)	1.3900	C(610)-C(620)	1.3900
C(61)-C(66)	1.3900	C(610)-C(660)	1.3900
C(62)-C(63)	1.3900	C(620)-C(630)	1.3900
C(63)-C(64)	1.3900	C(630)-C(640)	1.3900
C(64)-C(65)	1.3900	C(640)-C(650)	1.3900
C(65)-C(66)	1.3900	C(650)-C(660)	1.3900

Table B.17. Complete List of Bond Angles [deg] for 3.40.

C(2)-C(1)-C(6)	120.0	C(33)-C(34)-C(35)	120.0
C(2)-C(1)-C(11)	120.8(15)	C(36)-C(35)-C(34)	120.0
C(6)-C(1)-C(11)	118.1(15)	C(35)-C(36)-C(31)	120.0
C(3)-C(2)-C(1)	120.0	C(42)-C(41)-C(46)	120.0
C(3)-C(2)-C(21)	117.1(14)	C(42)-C(41)-C(4)	118.5(16)
C(1)-C(2)-C(21)	122.9(14)	C(46)-C(41)-C(4)	121.4(16)
C(2)-C(3)-C(4)	120.0	C(43)-C(42)-C(41)	120.0
C(2)-C(3)-C(31)	123.0(13)	C(44)-C(43)-C(42)	120.0
C(4)-C(3)-C(31)	116.8(13)	C(43)-C(44)-C(45)	120.0
C(5)-C(4)-C(3)	120.0	C(46)-C(45)-C(44)	120.0
C(5)-C(4)-C(41)	120.9(14)	C(45)-C(46)-C(41)	120.0
C(3)-C(4)-C(41)	119.0(14)	C(52)-C(51)-C(56)	120.0
C(4)-C(5)-C(6)	120.0	C(52)-C(51)-C(5)	123.3(14)
C(4)-C(5)-C(51)	117.7(14)	C(56)-C(51)-C(5)	116.6(14)
C(6)-C(5)-C(51)	122.2(14)	C(53)-C(52)-C(51)	120.0
C(5)-C(6)-C(1)	120.0	C(52)-C(53)-C(54)	120.0
C(5)-C(6)-C(61)	118.6(14)	C(53)-C(54)-C(55)	120.0
C(1)-C(6)-C(61)	121.4(14)	C(56)-C(55)-C(54)	120.0
C(16)-C(9)-C(19)	121(3)	C(55)-C(56)-C(51)	120.0
C(16)-C(9)-C(11)	103(2)	C(62)-C(61)-C(66)	120.0
C(19)-C(9)-C(11)	116(2)	C(62)-C(61)-C(6)	121.1(14)
C(16)-C(9)-C(15)	100(2)	C(66)-C(61)-C(6)	118.5(14)
C(19)-C(9)-C(15)	113(2)	C(63)-C(62)-C(61)	120.0
C(11)-C(9)-C(15)	101(2)	C(64)-C(63)-C(62)	120.0
C(12)-C(11)-C(9)	113(2)	C(63)-C(64)-C(65)	120.0
C(12)-C(11)-C(1)	125(2)	C(66)-C(65)-C(64)	120.0
C(9)-C(11)-C(1)	122(2)	C(65)-C(66)-C(61)	120.0
C(11)-C(12)-C(13)	102(3)	C(20)-C(10)-C(60)	120.0
C(16)-C(13)-C(12)	104(3)	C(20)-C(10)-C(110)	124.6(17)
C(16)-C(13)-C(14)	97(3)	C(60)-C(10)-C(110)	115.3(17)
C(12)-C(13)-C(14)	97(3)	C(10)-C(20)-C(30)	120.0
C(15)-C(14)-C(13)	106(3)	C(10)-C(20)-C(210)	118.9(14)
C(14)-C(15)-C(9)	101(2)	C(30)-C(20)-C(210)	121.0(14)
C(17)-C(16)-C(18)	113(3)	C(40)-C(30)-C(20)	120.0
C(17)-C(16)-C(9)	111(3)	C(40)-C(30)-C(310)	122.9(14)
C(18)-C(16)-C(9)	120(3)	C(20)-C(30)-C(310)	117.0(14)
C(17)-C(16)-C(13)	106(3)	C(30)-C(40)-C(50)	120.0
C(18)-C(16)-C(13)	108(3)	C(30)-C(40)-C(410)	117.2(14)
C(9)-C(16)-C(13)	97(3)	C(50)-C(40)-C(410)	122.7(14)
C(22)-C(21)-C(26)	120.0	C(40)-C(50)-C(60)	120.0
C(22)-C(21)-C(2)	120.1(14)	C(40)-C(50)-C(510)	117.7(14)
C(26)-C(21)-C(2)	119.9(14)	C(60)-C(50)-C(510)	122.2(14)
C(23)-C(22)-C(21)	120.0	C(50)-C(60)-C(10)	120.0
C(22)-C(23)-C(24)	120.0	C(50)-C(60)-C(610)	118.1(15)
C(23)-C(24)-C(25)	120.0	C(10)-C(60)-C(610)	121.9(15)
C(26)-C(25)-C(24)	120.0	C(110)-C(90)-C(190)	124(3)
C(25)-C(26)-C(21)	120.0	C(110)-C(90)-C(160)	110(3)
C(32)-C(31)-C(36)	120.0	C(190)-C(90)-C(160)	115(3)
C(32)-C(31)-C(3)	119.5(13)	C(110)-C(90)-C(150)	112(3)
C(36)-C(31)-C(3)	120.5(13)	C(190)-C(90)-C(150)	103(3)
C(33)-C(32)-C(31)	120.0	C(160)-C(90)-C(150)	85(2)
C(32)-C(33)-C(34)	120.0	C(90)-C(110)-C(120)	100(3)

Table B.17. Complete List of Bond Angles [deg] for 3.40 (continued).

C(90)-C(110)-C(10)	133(3)	C(330)-C(340)-C(350)	120.0
C(120)-C(110)-C(10)	126(3)	C(360)-C(350)-C(340)	120.0
C(110)-C(120)-C(130)	116(3)	C(350)-C(360)-C(310)	120.0
C(160)-C(130)-C(120)	102(3)	C(420)-C(410)-C(460)	120.0
C(160)-C(130)-C(140)	100(2)	C(420)-C(410)-C(40)	125.7(14)
C(120)-C(130)-C(140)	100(2)	C(460)-C(410)-C(40)	114.3(14)
C(150)-C(140)-C(130)	103(3)	C(410)-C(420)-C(430)	120.0
C(140)-C(150)-C(90)	98(3)	C(420)-C(430)-C(440)	120.0
C(130)-C(160)-C(180)	116(3)	C(450)-C(440)-C(430)	120.0
C(130)-C(160)-C(170)	105(2)	C(460)-C(450)-C(440)	120.0
C(180)-C(160)-C(170)	98(2)	C(450)-C(460)-C(410)	120.0
C(130)-C(160)-C(90)	95(2)	C(520)-C(510)-C(560)	120.0
C(180)-C(160)-C(90)	127(3)	C(520)-C(510)-C(50)	119.5(13)
C(170)-C(160)-C(90)	114(2)	C(560)-C(510)-C(50)	120.2(13)
C(220)-C(210)-C(260)	120.0	C(510)-C(520)-C(530)	120.0
C(220)-C(210)-C(20)	122.1(14)	C(540)-C(530)-C(520)	120.0
C(260)-C(210)-C(20)	117.6(14)	C(530)-C(540)-C(550)	120.0
C(210)-C(220)-C(230)	120.0	C(560)-C(550)-C(540)	120.0
C(240)-C(230)-C(220)	120.0	C(550)-C(560)-C(510)	120.0
C(230)-C(240)-C(250)	120.0	C(620)-C(610)-C(660)	120.0
C(260)-C(250)-C(240)	120.0	C(620)-C(610)-C(60)	119.0(15)
C(250)-C(260)-C(210)	120.0	C(660)-C(610)-C(60)	120.9(15)
C(320)-C(310)-C(360)	120.0	C(630)-C(620)-C(610)	120.0
C(320)-C(310)-C(30)	119.2(13)	C(620)-C(630)-C(640)	120.0
C(360)-C(310)-C(30)	120.7(13)	C(650)-C(640)-C(630)	120.0
C(330)-C(320)-C(310)	120.0	C(640)-C(650)-C(660)	120.0
C(340)-C(330)-C(320)	120.0	C(650)-C(660)-C(610)	120.0

Table B.18. Crystal Data and Structure Refinement Parameters for 1.139, 4.38 and 4.44.

	1.139	4.38	4.44
Empirical formula	$C_{55}H_{37}F_9O_6$	$C_{53}H_{40}Fe$	$C_{53}H_{40}Cl_6FeSb$
Molecular weight	964.85	732.70	1067.15
Description	red plate	red-orange prism	dark blue prism
Crystal size, mm	0.22 X 0.17 X 0.06	0.20 X 0.18 X 0.10	0.09 X 0.10 X 0.12
Temperature, K	210(2)	267(2)	210(2)
Wavelength, Å	(Mo-Kα) 0.71073	(Mo-Kα) 0.71073	(Mo-Kα) 0.71073
Crystal system	monoclinic	triclinic	monoclinic
Space group	$P2_1/n$	$P(\bar{1})$	$P2_1/n$
a, Å	11.3060(2)	9.7962(1)	10.806(?)
b, Å	21.2346(4)	11.0580(0)	11.9269(1)
c, Å	20.9158(1)	18.8717(2)	39.0821(3)
α, deg.	90.000(0)	87.795(1)	90.000(0)
β, deg.	104.773(1)	89.927(1)	96.256(1)
γ, deg.	90.000(0)	69.973(1)	90.000(0)
Volume, Å^3	4855.44(1)	1919.18(3)	5007.13(6)
Z	4	2	4
Calcd Density, g/cm^3	1.320	1.268	1.416
Abs. Coeff., mm^{-1}	0.108	0.430	1.183
Scan Mode	ω-scans	ω-scans	ω-scans
F(000)	1984	768	2148
θ-range, deg.	1.39 to 23.00	1.08 to 22.50	1.05 to 22.50
Index ranges	$-14 \le h \le 14$	$-8 \le h \le 12$	$-12 \le h \le 13$
	$-26 \le k \le 24$	$-13 \le k \le 13$	$-14 \le k \le 14$
	$-26 \le l \le 26$	$-23 \le l \le 23$	$-48 \le l \le 48$
No. Reflect. collected	29358	11499	20633
No. Independent Reflect.	6741	4906	6520
R(int)	0.0719	0.0273	0.1034
Data / Restraints / Param.	6696 / 15 / 687	4887 / 0 / 488	6520 / 0 / 551
Goodness-of-fit on F^2	1.052	1.054	0.784
Final *R* indices (I>2σ(I))*	*R*1 = 0.0613;	*R*1 = 0.0354;	*R*1 = 0.0365;
	w*R*2 = 0.1237	w*R*2 = 0.0793	w*R*2 = 0.0759
R indices (all data)*	*R*1 = 0.1102;	*R*1 = 0.0492;	*R*1 = 0.0620;
	w*R*2 = 0.1483	w*R*2 = 0.0865	w*R*2 = 0.0807
Mean shift/error	<0.001	<0.000	<0.000
Max. shift/error	<0.001	<0.000	<0.000
Rel. Trans. (max., min.)	1.0000, 0.8216	0.9766, 0.8498	0.9145, 0.5922
Extinction coefficient	0.0037(3)	0.0031(5)	0. 00051(10)
Largest diff. Peak, e/Å^3	0.231	0.289	0.565
Largest diff. Hole, e/Å^3	-0.302	-0.337	-0.516

Refinement method: Full-matrix least-squares on F^2,
Weighting Scheme: $w = 1/[\sigma^2Fo^2+(0.0597((Fo^2+2Fc^2)/3))^2]$

*$R1 = \Sigma(||Fo|-|Fc||)/\Sigma|Fo|$; $wR2 = [\Sigma[w(Fo^2-Fc^2)^2]/\Sigma[w(Fo^2)^2]]^{0.5}$; $P=(Fo^2+2Fc^2)/3$)

Table B.19. Atomic coordinates (x 10^4) and equivalent isotropic displacement parameters (A^2 x 10^3) for 1.139. U(eq) is defined as 1/3rd of the trace of the orthogonalized Uij tensor.

	x	y	z	U(eq)
O(1)	12021(3)	2106(2)	8727(2)	94(1)
O(2)	11644(3)	2368(1)	7656(2)	78(1)
O(3)	7373(8)	1295(4)	3522(5)	118(3)
O(4)	5759(12)	1506(5)	2685(4)	88(4)
O(3A)	4741(11)	1393(5)	2622(5)	100(4)
O(4A)	6766(13)	1510(7)	2967(9)	104(5)
O(5)	6318(3)	2327(2)	5077(2)	112(1)
O(6)	5531(3)	2136(2)	4024(1)	92(1)
F(1)	12175(3)	937(2)	8106(2)	138(1)
F(2)	13000(3)	1426(2)	7449(1)	128(1)
F(3)	13859(2)	1403(2)	8472(1)	115(1)
F(4)	6411(6)	316(3)	3719(3)	272(4)
F(5)	4799(6)	400(3)	3052(3)	242(3)
F(6)	6257(7)	172(2)	2728(3)	239(3)
F(7)	4914(15)	1085(6)	4723(8)	166(5)
F(8)	4609(16)	1754(8)	5408(7)	142(7)
F(9)	3583(9)	1770(12)	4415(7)	192(8)
F(7A)	4227(18)	1261(7)	4343(11)	129(6)
F(8A)	4712(18)	1436(14)	5325(11)	148(11)
F(9A)	3508(17)	2061(9)	4645(12)	161(10)
C(1)	7330(3)	2735(1)	6760(1)	32(1)
C(2)	7873(3)	2135(1)	6831(1)	32(1)
C(3)	8507(3)	1841(1)	6413(2)	34(1)
C(4)	9132(3)	2136(1)	5989(1)	34(1)
C(5)	9204(3)	2789(1)	5871(1)	32(1)
C(6)	8399(3)	3262(1)	5978(1)	31(1)
C(7)	7472(3)	3218(1)	6319(1)	32(1)
C(11)	6459(3)	2861(1)	7185(2)	36(1)
C(12)	5215(3)	2797(2)	6924(2)	47(1)
C(13)	4414(3)	2887(2)	7320(2)	61(1)
C(14)	4857(4)	3044(2)	7975(2)	61(1)
C(15)	6096(4)	3113(2)	8238(2)	52(1)
C(16)	6904(3)	3021(1)	7847(2)	42(1)
C(21)	7735(3)	1743(1)	7410(2)	35(1)
C(22)	6686(3)	1416(2)	7420(2)	47(1)
C(23)	6633(4)	1078(2)	7979(2)	58(1)
C(24)	7610(4)	1069(2)	8522(2)	59(1)
C(25)	8649(4)	1398(2)	8518(2)	57(1)
C(26)	8723(3)	1735(2)	7959(2)	45(1)
C(31)	8552(4)	1131(2)	6446(2)	48(1)
C(32)	7503(4)	807(2)	6141(2)	73(1)
C(33)	7507(8)	153(3)	6161(3)	121(3)
C(34)	8524(11)	-162(3)	6479(4)	151(5)
C(35)	9568(8)	155(3)	6777(3)	123(3)
C(36)	9594(4)	809(2)	6766(2)	71(1)
C(41)	9863(3)	1704(1)	5661(2)	40(1)
C(42)	9275(4)	1372(2)	5104(2)	58(1)

Table B.19. Atomic coordinates (x 10^4) and equivalent isotropic displacement parameters (A^2 x 10^3) for 1.139. U(eq) is defined as 1/3rd of the trace of the orthogonalized Uij tensor (continued).

	x	y	z	U(eq)
C(43)	9936(6)	955(2)	4813(2)	81(1)
C(44)	11161(6)	873(2)	5095(3)	94(2)
C(45)	11750(4)	1204(2)	5644(3)	78(1)
C(46)	11102(4)	1628(2)	5926(2)	56(1)
C(51)	10218(3)	2987(1)	5569(2)	33(1)
C(52)	10151(3)	2900(2)	4903(2)	41(1)
C(53)	11149(3)	3042(2)	4661(2)	46(1)
C(54)	12212(3)	3267(2)	5080(2)	50(1)
C(55)	12273(3)	3373(2)	5733(2)	48(1)
C(56)	11274(3)	3231(2)	5978(2)	43(1)
C(61)	8532(3)	3900(2)	5687(2)	38(1)
C(62)	8047(3)	4013(2)	5022(2)	55(1)
C(63)	8145(4)	4612(2)	4769(3)	80(2)
C(64)	8737(5)	5080(2)	5176(4)	95(2)
C(65)	9240(5)	4968(2)	5834(3)	88(2)
C(66)	9133(4)	4378(2)	6092(2)	58(1)
C(71)	6614(3)	3769(1)	6249(2)	37(1)
C(72)	5697(3)	3836(2)	5672(2)	46(1)
C(73)	4910(3)	4346(2)	5593(2)	61(1)
C(74)	5037(4)	4788(2)	6085(3)	66(1)
C(75)	5940(4)	4727(2)	6655(2)	58(1)
C(76)	6731(3)	4220(2)	6745(2)	44(1)
C(80)	12093(4)	2042(2)	8146(2)	67(1)
C(81)	12794(5)	1457(3)	8043(2)	85(1)
C(82)	6450(14)	1176(6)	3140(6)	80(4)
C(82A)	5738(16)	1207(8)	2891(11)	72(7)
C(83)	5905(8)	517(4)	3164(5)	134(2)
C(84)	5598(4)	2093(2)	4638(2)	61(1)
C(85)	4576(6)	1700(3)	4773(3)	91(2)

Table B.20. Complete List of Bond lengths [Å] and angles [deg] for 1.139.

O(1)-C(80)	1.247(5)	C(33)-C(34)	1.349(10)
O(2)-C(80)	1.232(5)	C(34)-C(35)	1.363(10)
O(3)-C(82)	1.169(14)	C(35)-C(36)	1.390(7)
O(4)-C(82)	1.276(13)	C(41)-C(46)	1.378(5)
O(3A)-C(82A)	1.19(2)	C(41)-C(42)	1.380(5)
O(4A)-C(82A)	1.30(2)	C(42)-C(43)	1.395(6)
O(5)-C(84)	1.172(4)	C(43)-C(44)	1.371(7)
O(6)-C(84)	1.269(5)	C(44)-C(45)	1.365(7)
F(1)-C(81)	1.330(6)	C(45)-C(46)	1.385(5)
F(2)-C(81)	1.324(5)	C(51)-C(56)	1.380(4)
F(3)-C(81)	1.310(5)	C(51)-C(52)	1.388(4)
F(4)-C(83)	1.231(8)	C(52)-C(53)	1.382(4)
F(5)-C(83)	1.238(8)	C(53)-C(54)	1.380(5)
F(6)-C(83)	1.309(9)	C(54)-C(55)	1.367(5)
F(7)-C(85)	1.372(14)	C(55)-C(56)	1.387(4)
F(8)-C(85)	1.32(2)	C(61)-C(62)	1.381(5)
F(9)-C(85)	1.189(10)	C(61)-C(66)	1.385(5)
F(7A)-C(85)	1.28(2)	C(62)-C(63)	1.393(5)
F(8A)-C(85)	1.26(2)	C(63)-C(64)	1.368(7)
F(9A)-C(85)	1.40(2)	C(64)-C(65)	1.370(7)
C(1)-C(2)	1.404(4)	C(65)-C(66)	1.381(5)
C(1)-C(7)	1.414(4)	C(71)-C(72)	1.383(4)
C(1)-C(11)	1.510(4)	C(71)-C(76)	1.393(4)
C(2)-C(3)	1.412(4)	C(72)-C(73)	1.383(5)
C(2)-C(21)	1.510(4)	C(73)-C(74)	1.375(6)
C(3)-C(4)	1.411(4)	C(74)-C(75)	1.363(5)
C(3)-C(31)	1.509(4)	C(75)-C(76)	1.382(5)
C(4)-C(5)	1.415(4)	C(80)-C(81)	1.519(6)
C(4)-C(41)	1.510(4)	C(82)-C(83)	1.535(14)
C(5)-C(6)	1.411(4)	C(82A)-C(83)	1.57(2)
C(5)-C(51)	1.503(4)	C(84)-C(85)	1.510(6)
C(6)-C(7)	1.414(4)		
C(6)-C(61)	1.506(4)		
C(7)-C(71)	1.504(4)		
C(11)-C(12)	1.379(4)		
C(11)-C(16)	1.389(4)		
C(12)-C(13)	1.388(5)		
C(13)-C(14)	1.374(5)		
C(14)-C(15)	1.377(5)		
C(15)-C(16)	1.387(4)		
C(21)-C(22)	1.379(4)		
C(21)-C(26)	1.383(4)		
C(22)-C(23)	1.386(5)		
C(23)-C(24)	1.369(5)		
C(24)-C(25)	1.369(5)		
C(25)-C(26)	1.392(4)		
C(31)-C(36)	1.379(5)		
C(31)-C(32)	1.380(5)		
C(32)-C(33)	1.389(7)		

Table B.21. Complete List of Bond Angles [deg] for 1.139.

C(2)-C(1)-C(7)	127.4(3)	C(45)-C(44)-C(43)	121.3(4)
C(2)-C(1)-C(11)	115.5(3)	C(44)-C(45)-C(46)	119.7(5)
C(7)-C(1)-C(11)	117.0(3)	C(41)-C(46)-C(45)	119.9(4)
C(1)-C(2)-C(3)	127.7(3)	C(56)-C(51)-C(52)	119.3(3)
C(1)-C(2)-C(21)	117.0(2)	C(56)-C(51)-C(5)	118.5(3)
C(3)-C(2)-C(21)	115.2(3)	C(52)-C(51)-C(5)	122.2(3)
C(4)-C(3)-C(2)	127.5(3)	C(53)-C(52)-C(51)	119.9(3)
C(4)-C(3)-C(31)	117.1(3)	C(54)-C(53)-C(52)	120.1(3)
C(2)-C(3)-C(31)	115.4(3)	C(55)-C(54)-C(53)	120.4(3)
C(3)-C(4)-C(5)	127.1(3)	C(54)-C(55)-C(56)	119.6(3)
C(3)-C(4)-C(41)	115.8(3)	C(51)-C(56)-C(55)	120.7(3)
C(5)-C(4)-C(41)	116.9(3)	C(62)-C(61)-C(66)	119.6(3)
C(6)-C(5)-C(4)	127.1(3)	C(62)-C(61)-C(6)	120.6(3)
C(6)-C(5)-C(51)	117.4(3)	C(66)-C(61)-C(6)	119.8(3)
C(4)-C(5)-C(51)	115.5(3)	C(61)-C(62)-C(63)	119.6(4)
C(5)-C(6)-C(7)	128.5(3)	C(64)-C(63)-C(62)	120.0(5)
C(5)-C(6)-C(61)	116.2(2)	C(63)-C(64)-C(65)	120.8(4)
C(7)-C(6)-C(61)	115.3(3)	C(64)-C(65)-C(66)	119.6(5)
C(1)-C(7)-C(6)	126.8(3)	C(65)-C(66)-C(61)	120.4(4)
C(1)-C(7)-C(71)	116.8(3)	C(72)-C(71)-C(76)	119.2(3)
C(6)-C(7)-C(71)	116.2(3)	C(72)-C(71)-C(7)	119.1(3)
C(12)-C(11)-C(16)	119.5(3)	C(76)-C(71)-C(7)	121.7(3)
C(12)-C(11)-C(1)	120.1(3)	C(73)-C(72)-C(71)	120.1(4)
C(16)-C(11)-C(1)	120.4(3)	C(74)-C(73)-C(72)	120.2(4)
C(11)-C(12)-C(13)	120.3(3)	C(75)-C(74)-C(73)	120.1(4)
C(14)-C(13)-C(12)	120.1(4)	C(74)-C(75)-C(76)	120.6(4)
C(13)-C(14)-C(15)	120.0(3)	C(75)-C(76)-C(71)	119.8(3)
C(14)-C(15)-C(16)	120.3(4)	O(2)-C(80)-O(1)	129.4(4)
C(15)-C(16)-C(11)	119.8(3)	O(2)-C(80)-C(81)	117.5(4)
C(22)-C(21)-C(26)	119.8(3)	O(1)-C(80)-C(81)	113.1(4)
C(22)-C(21)-C(2)	123.7(3)	F(3)-C(81)-F(2)	106.7(4)
C(26)-C(21)-C(2)	116.4(3)	F(3)-C(81)-F(1)	106.0(5)
C(21)-C(22)-C(23)	119.7(4)	F(2)-C(81)-F(1)	106.0(4)
C(24)-C(23)-C(22)	120.6(4)	F(3)-C(81)-C(80)	113.3(4)
C(25)-C(24)-C(23)	119.9(3)	F(2)-C(81)-C(80)	113.3(5)
C(24)-C(25)-C(26)	120.3(4)	F(1)-C(81)-C(80)	111.1(4)
C(21)-C(26)-C(25)	119.6(3)	O(3)-C(82)-O(4)	131.3(14)
C(36)-C(31)-C(32)	120.3(4)	O(3)-C(82)-C(83)	118.1(11)
C(36)-C(31)-C(3)	122.2(4)	O(4)-C(82)-C(83)	110.5(12)
C(32)-C(31)-C(3)	117.5(4)	O(3A)-C(82A)-O(4A)	127(2)
C(31)-C(32)-C(33)	119.3(5)	O(3A)-C(82A)-C(83)	120(2)
C(34)-C(33)-C(32)	120.4(7)	O(4A)-C(82A)-C(83)	113(2)
C(33)-C(34)-C(35)	120.7(7)	F(4)-C(83)-F(5)	108.3(8)
C(34)-C(35)-C(36)	120.3(7)	F(5)-C(83)-F(6)	103.1(9)
C(31)-C(36)-C(35)	119.0(5)	F(4)-C(83)-C(82)	104.6(9)
C(46)-C(41)-C(42)	120.1(3)	F(5)-C(83)-C(82)	124.8(9)
C(46)-C(41)-C(4)	120.4(3)	F(6)-C(83)-C(82)	106.9(8)
C(42)-C(41)-C(4)	119.5(3)	F(4)-C(83)-C(82A)	130.5(11)
C(41)-C(42)-C(43)	119.8(4)	F(5)-C(83)-C(82A)	95.5(9)
C(44)-C(43)-C(42)	119.2(4)	F(6)-C(83)-C(82A)	107.4(10)

Table B.21. Complete List of Bond Angles [deg] for 1.139 (continued).

O(5)-C(84)-O(6)	127.8(4)
O(5)-C(84)-C(85)	120.0(4)
O(6)-C(84)-C(85)	112.2(4)
F(8A)-C(85)-F(7A)	105(2)
F(9)-C(85)-F(8)	113.6(12)
F(9)-C(85)-F(7)	108.0(13)
F(8)-C(85)-F(7)	102.9(10)
F(8A)-C(85)-F(9A)	108(2)
F(7A)-C(85)-F(9A)	99.7(13)
F(9)-C(85)-C(84)	117.3(8)
F(8A)-C(85)-C(84)	119.8(11)
F(7A)-C(85)-C(84)	112.6(8)
F(8)-C(85)-C(84)	108.1(8)
F(7)-C(85)-C(84)	105.7(8)
F(9A)-C(85)-C(84)	109.0(11)

Table B.22. Atomic coordinates (x 10^4) and equivalent isotropic displacement parameters (A^2 x 10^3) for 4.38. U(eq) is defined as 1/3rd of the trace of the orthogonalized Uij tensor.

	x	y	z	U(eq)
Fe(1)	2211(1)	13164(1)	13203(1)	33(1)
C(1)	3614(3)	10119(2)	12922(1)	24(1)
C(2)	4003(3)	8926(2)	13235(1)	24(1)
C(3)	5104(3)	7791(2)	12936(1)	26(1)
C(4)	5239(3)	7538(2)	12235(1)	25(1)
C(5)	4278(3)	8352(2)	11663(1)	25(1)
C(6)	3802(3)	9656(2)	11653(1)	24(1)
C(7)	4293(3)	10360(2)	12227(1)	26(1)
C(11)	2455(3)	11231(2)	13219(1)	25(1)
C(12)	1143(3)	12001(2)	12862(2)	34(1)
C(13)	273(3)	12897(3)	13339(2)	38(1)
C(14)	1026(3)	12706(3)	13987(2)	40(1)
C(15)	2362(3)	11686(2)	13921(1)	35(1)
C(16)	3754(4)	13948(3)	13421(3)	71(1)
C(17)	2369(4)	14903(3)	13434(2)	52(1)
C(18)	1714(4)	14983(3)	12764(2)	60(1)
C(19)	2694(6)	14086(4)	12341(2)	79(1)
C(20)	3959(5)	13454(4)	12737(3)	87(2)
C(21)	3286(3)	8718(2)	13916(1)	28(1)
C(22)	1935(3)	8574(3)	13888(2)	40(1)
C(23)	1223(4)	8412(3)	14505(2)	56(1)
C(24)	1866(4)	8378(3)	15152(2)	59(1)
C(25)	3216(4)	8494(3)	15194(2)	53(1)
C(26)	3927(3)	8668(3)	14579(1)	39(1)
C(31)	6122(3)	6882(2)	13477(1)	28(1)
C(32)	7480(3)	6949(3)	13600(2)	41(1)
C(33)	8388(3)	6179(3)	14125(2)	55(1)
C(34)	7957(4)	5317(3)	14528(2)	53(1)
C(35)	6626(3)	5209(3)	14403(2)	45(1)
C(36)	5700(3)	5990(2)	13886(1)	37(1)
C(41)	6400(3)	6330(2)	12000(1)	26(1)
C(42)	6351(3)	5106(2)	12172(1)	37(1)
C(43)	7441(3)	4010(3)	11962(2)	47(1)
C(44)	8592(3)	4112(3)	11568(2)	49(1)
C(45)	8649(3)	5307(3)	11392(2)	48(1)
C(46)	7556(3)	6412(3)	11599(1)	39(1)
C(51)	3891(3)	7624(2)	11085(1)	26(1)
C(52)	3263(3)	6703(3)	11255(2)	38(1)
C(53)	2932(3)	6001(3)	10725(2)	48(1)
C(54)	3235(3)	6208(3)	10028(2)	46(1)
C(55)	3844(3)	7124(3)	9851(2)	43(1)
C(56)	4173(3)	7831(3)	10376(1)	34(1)
C(61)	2777(3)	10518(2)	11108(1)	24(1)
C(62)	1480(3)	10360(2)	10911(1)	31(1)
C(63)	541(3)	11206(3)	10420(2)	38(1)
C(64)	887(3)	12213(3)	10108(2)	41(1)

Table B.22. Atomic coordinates (x 10^4) and equivalent isotropic displacement parameters (A^2 x 10^3) for 4.38. U(eq) is defined as 1/3rd of the trace of the orthogonalized Uij tensor (continued).

	x	y	z	U(eq)
C(65)	2163(3)	12387(3)	10294(1)	39(1)
C(66)	3089(3)	11561(2)	10795(1)	33(1)
C(71)	5928(3)	10122(2)	12261(1)	28(1)
C(72)	6611(3)	10242(3)	2884(1)	40(1)
C(73)	8057(3)	10150(3)	12896(2)	51(1)
C(74)	8859(3)	9935(3)	12284(2)	52(1)
C(75)	8200(3)	9812(3)	11659(2)	48(1)
C(76)	6757(3)	9905(3)	11646(1)	36(1)

Table B.23. Complete List of Bond Lengths [Å] for 4.38.

Fe(1)-C(19)	2.028(3)	C(44)-C(45)	1.370(4)
Fe(1)-C(16)	2.033(3)	C(45)-C(46)	1.389(4)
Fe(1)-C(14)	2.033(3)	C(51)-C(52)	1.387(3)
Fe(1)-C(13)	2.033(3)	C(51)-C(56)	1.393(4)
Fe(1)-C(12)	2.037(3)	C(52)-C(53)	1.393(4)
Fe(1)-C(20)	2.039(3)	C(53)-C(54)	1.376(4)
Fe(1)-C(18)	2.042(3)	C(54)-C(55)	1.371(4)
Fe(1)-C(17)	2.045(3)	C(55)-C(56)	1.389(4)
Fe(1)-C(15)	2.049(3)	C(61)-C(62)	1.394(3)
Fe(1)-C(11)	2.068(2)	C(61)-C(66)	1.401(3)
C(1)-C(2)	1.353(3)	C(62)-C(63)	1.387(4)
C(1)-C(11)	1.486(3)	C(63)-C(64)	1.382(4)
C(1)-C(7)	1.526(3)	C(64)-C(65)	1.376(4)
C(2)-C(3)	1.478(3)	C(65)-C(66)	1.386(4)
C(2)-C(21)	1.511(3	C(71)-C(72)	1.386(4)
C(3)-C(4)	1.360(3)	C(71)-C(76)	1.395(4)
C(3)-C(31)	1.512(3)	C(72)-C(73)	1.385(4)
C(4)-C(5)	1.487(3)	C(73)-C(74)	1.378(4)
C(4)-C(41)	1.509(3)	C(74)-C(75)	1.379(4)
C(5)-C(6)	1.355(3)	C(75)-C(76)	1.383(4)
C(5)-C(51)	1.502(3)		
C(6)-C(61)	1.499(3)		
C(6)-C(7)	1.527(3)		
C(7)-C(71)	1.533(3)		
C(11)-C(15)	1.428(3)		
C(11)-C(12)	1.428(4)		
C(12)-C(13)	1.417(4)		
C(13)-C(14)	1.400(4)		
C(14)-C(15)	1.414(4)		
C(16)-C(20)	1.409(6)		
C(16)-C(17)	1.406(5)		
C(17)-C(18)	1.406(5)		
C(18)-C(19)	1.396(5)		
C(19)-C(20)	1.397(6)		
C(21)-C(22)	1.388(4)		
C(21)-C(26)	1.390(4)		
C(22)-C(23)	1.394(4)		
C(23)-C(24)	1.368(5)		
C(24)-C(25)	1.374(5)		
C(25)-C(26)	1.393(4)		
C(31)-C(32)	1.378(4)		
C(31)-C(36)	1.400(4)		
C(32)-C(33)	1.385(4)		
C(33)-C(34)	1.373(5)		
C(34)-C(35)	1.371(4)		
C(35)-C(36)	1.386(4)		
C(41)-C(46)	1.389(4)		
C(41)-C(42)	1.396(4)		
C(42)-C(43)	1.384(4)		
C(43)-C(44)	1.384(4)		

Table B.24. Complete List of Bond Angles [deg] for 4.38.

C(19)-Fe(1)-C(16)	67.8(2)	C(3)-C(2)-C(21)	117.5(2)
C(19)-Fe(1)-C(14)	159.7(2)	C(4)-C(3)-C(2)	124.9(2)
C(16)-Fe(1)-C(14)	121.3(2)	C(4)-C(3)-C(31)	120.4(2)
C(19)-Fe(1)-C(13)	123.8(2)	C(2)-C(3)-C(31)	114.7(2)
C(16)-Fe(1)-C(13)	154.6(2)	C(3)-C(4)-C(5)	124.7(2)
C(14)-Fe(1)-C(13)	40.27(11)	C(3)-C(4)-C(41)	119.5(2)
C(19)-Fe(1)-C(12)	108.0(2)	C(5)-C(4)-C(41)	115.8(2)
C(16)-Fe(1)-C(12)	164.02(14)	C(6)-C(5)-C(4)	122.7(2)
C(14)-Fe(1)-C(12)	68.11(11)	C(6)-C(5)-C(51)	122.2(2)
C(13)-Fe(1)-C(12)	40.75(10)	C(4)-C(5)-C(51)	115.2(2)
C(19)-Fe(1)-C(20)	40.2(2)	C(5)-C(6)-C(61)	124.7(2)
C(16)-Fe(1)-C(20)	40.5(2)	C(5)-C(6)-C(7)	120.6(2)
C(14)-Fe(1)-C(20)	157.7(2)	C(61)-C(6)-C(7)	114.8(2)
C(13)-Fe(1)-C(20)	161.7(2)	C(1)-C(7)-C(6)	107.5(2)
C(12)-Fe(1)-C(20)	126.5(2)	C(1)-C(7)-C(71)	115.6(2)
C(19)-Fe(1)-C(18)	40.1(2)	C(6)-C(7)-C(71)	115.6(2)
C(16)-Fe(1)-C(18)	67.8(2)	C(15)-C(11)-C(12)	106.2(2)
C(14)-Fe(1)-C(18)	123.04(13)	C(15)-C(11)-C(1)	127.9(2)
C(13)-Fe(1)-C(18)	105.49(13)	C(12)-C(11)-C(1)	125.8(2)
C(12)-Fe(1)-C(18)	119.63(13)	C(15)-C(11)-Fe(1)	68.99(14)
C(20)-Fe(1)-C(18)	67.6(2)	C(12)-C(11)-Fe(1)	68.50(14)
C(19)-Fe(1)-C(17)	67.53(14)	C(1)-C(11)-Fe(1)	130.5(2)
C(16)-Fe(1)-C(17)	40.34(14)	C(13)-C(12)-C(11)	108.8(2)
C(14)-Fe(1)-C(17)	106.75(12)	C(13)-C(12)-Fe(1)	69.5(2)
C(13)-Fe(1)-C(17)	118.79(12)	C(11)-C(12)-Fe(1)	70.79(14)
C(12)-Fe(1)-C(17)	153.99(12)	C(14)-C(13)-C(12)	108.0(2)
C(20)-Fe(1)-C(17)	67.70(14)	C(14)-C(13)-Fe(1)	69.9(2)
C(18)-Fe(1)-C(17)	40.24(13)	C(12)-C(13)-Fe(1)	69.8(2)
C(19)-Fe(1)-C(15)	158.3(2)	C(13)-C(14)-C(15)	108.3(2)
C(16)-Fe(1)-C(15)	109.88(14)	C(13)-C(14)-Fe(1)	69.9(2)
C(14)-Fe(1)-C(15)	40.54(11)	C(15)-C(14)-Fe(1)	70.3(2)
C(13)-Fe(1)-C(15)	67.96(11)	C(14)-C(15)-C(11)	108.7(2)
C(12)-Fe(1)-C(15)	67.95(11)	C(14)-C(15)-Fe(1)	69.1(2)
C(20)-Fe(1)-C(15)	123.9(2)	C(11)-C(15)-Fe(1)	70.42(14)
C(18)-Fe(1)-C(15)	160.88(13)	C(20)-C(16)-C(17)	107.8(4)
C(17)-Fe(1)-C(15)	125.70(12)	C(20)-C(16)-Fe(1)	70.0(2)
C(19)-Fe(1)-C(11)	122.36(13)	C(17)-C(16)-Fe(1)	70.3(2)
C(16)-Fe(1)-C(11)	127.33(12)	C(18)-C(17)-C(16)	107.9(3)
C(14)-Fe(1)-C(11)	68.56(10)	C(18)-C(17)-Fe(1)	69.8(2)
C(13)-Fe(1)-C(11)	68.66(10)	C(16)-C(17)-Fe(1)	69.4(2)
C(12)-Fe(1)-C(11)	40.71(10)	C(19)-C(18)-C(17)	107.8(4)
C(20)-Fe(1)-C(11)	110.21(12)	C(19)-C(18)-Fe(1)	69.4(2)
C(18)-Fe(1)-C(11)	155.75(12)	C(17)-C(18)-Fe(1)	70.0(2)
C(17)-Fe(1)-C(11)	163.37(12)	C(20)-C(19)-C(18)	108.8(4)
C(15)-Fe(1)-C(11)	40.60(10)	C(20)-C(19)-Fe(1)	70.3(2)
C(2)-C(1)-C(11)	121.5(2)	C(18)-C(19)-Fe(1)	70.5(2)
C(2)-C(1)-C(7)	121.1(2)	C(19)-C(20)-C(16)	107.7(3)
C(11)-C(1)-C(7)	117.3(2)	C(19)-C(20)-Fe(1)	69.5(2)
C(1)-C(2)-C(3)	122.8(2)	C(16)-C(20)-Fe(1)	69.5(2)
C(1)-C(2)-C(21)	119.7(2)	C(22)-C(21)-C(26)	118.1(2)

Table B.24. Complete List of Bond Angles [deg] for 4.38 (continued).

C(22)-C(21)-C(2)	119.5(2)
C(26)-C(21)-C(2)	122.5(2)
C(21)-C(22)-C(23)	121.1(3)
C(24)-C(23)-C(22)	119.9(3)
C(23)-C(24)-C(25)	120.1(3)
C(24)-C(25)-C(26)	120.3(3)
C(21)-C(26)-C(25)	120.5(3)
C(32)-C(31)-C(36)	118.2(2)
C(32)-C(31)-C(3)	120.3(2)
C(36)-C(31)-C(3)	121.5(2)
C(31)-C(32)-C(33)	120.9(3)
C(34)-C(33)-C(32)	120.4(3)
C(35)-C(34)-C(33)	119.7(3)
C(34)-C(35)-C(36)	120.3(3)
C(35)-C(36)-C(31)	120.4(3)
C(46)-C(41)-C(42)	117.9(2)
C(46)-C(41)-C(4)	120.2(2)
C(42)-C(41)-C(4)	121.9(2)
C(43)-C(42)-C(41)	120.9(3)
C(42)-C(43)-C(44)	120.3(3)
C(45)-C(44)-C(43)	119.4(3)
C(44)-C(45)-C(46)	120.6(3)
C(41)-C(46)-C(45)	120.8(3)
C(52)-C(51)-C(56)	118.5(2)
C(52)-C(51)-C(5)	119.9(2)
C(56)-C(51)-C(5)	121.6(2)
C(51)-C(52)-C(53)	120.3(3)
C(54)-C(53)-C(52)	120.4(3)
C(55)-C(54)-C(53)	119.9(3)
C(54)-C(55)-C(56)	120.1(3)
C(55)-C(56)-C(51)	120.8(3)
C(62)-C(61)-C(66)	117.5(2)
C(62)-C(61)-C(6)	122.8(2)
C(66)-C(61)-C(6)	119.6(2)
C(63)-C(62)-C(61)	120.9(2)
C(64)-C(63)-C(62)	120.5(3)
C(65)-C(64)-C(63)	119.6(3)
C(64)-C(65)-C(66)	120.1(3)
C(65)-C(66)-C(61)	121.3(3)
C(72)-C(71)-C(76)	117.3(2)
C(72)-C(71)-C(7)	121.7(2)
C(76)-C(71)-C(7)	120.7(2)
C(73)-C(72)-C(71)	121.4(3)
C(74)-C(73)-C(72)	120.6(3)
C(73)-C(74)-C(75)	118.9(3)
C(74)-C(75)-C(76)	120.5(3)
C(75)-C(76)-C(71)	121.3(3)

Table B.25. Atomic coordinates (x 10^4) and equivalent isotropic displacement parameters (A^2 x 10^3) for 4.44. U(eq) is defined as 1/3rd of the trace of the orthogonalized Uij tensor.

	x	y	z	U(eq)
Fe(1)	8281(1)	3110(1)	6690(1)	32(1)
Sb(1)	6758(1)	3092(1)	8067(1)	40(1)
Cl(1)	6402(1)	4441(1)	8492(1)	59(1)
Cl(2)	7129(1)	1711(1)	7653(1)	59(1)
Cl(3)	8627(1)	4015(1)	7969(1)	63(1)
Cl(4)	4864(1)	2198(1)	8146(1)	63(1)
Cl(5)	5685(1)	4254(1)	7638(1)	72(1)
Cl(6)	7828(1)	1978(1)	8504(1)	64(1)
C(1)	10727(3)	2586(3)	6288(1)	26(1)
C(2)	11767(4)	1922(3)	6312(1)	28(1)
C(3)	12452(3)	1687(3)	6012(1)	27(1)
C(4)	12636(3)	2446(3)	5762(1)	29(1)
C(5)	12173(3)	3610(3)	5746(1)	31(1)
C(6)	11041(4)	3927(3)	5833(1)	0(1)
C(7)	10157(3)	3045(3)	5949(1)	30(1)
C(11)	10207(3)	2947(3)	6607(1)	30(1)
C(12)	9940(3)	2296(3)	6894(1)	35(1)
C(13)	9482(4)	3005(4)	7137(2)	43(2)
C(14)	9440(4)	4103(4)	7010(2)	44(2)
C(15)	9856(4)	4088(3)	6674(1)	39(2)
C(16)	6953(4)	3442(8)	6285(2)	94(3)
C(17)	6563(4)	3889(4)	6593(2)	74(3)
C(18)	6423(4)	2992(6)	6798(2)	64(2)
C(19)	6749(5)	2053(4)	6644(3)	78(3)
C(20)	7068(5)	2303(8)	6330(3)	91(3)
C(21)	12302(4)	1470(4)	6647(2)	33(2)
C(22)	12080(4)	351(4)	6743(2)	49(2)
C(23)	12573(6)	-51(5)	7062(2)	64(2)
C(24)	13291(6)	632(7)	7282(2)	82(2)
C(25)	13537(5)	1750(7)	7195(2)	77(2)
C(26)	13030(5)	2162(5)	6875(2)	52(2)
C(31)	13036(4)	544(3)	6002(1)	28(1)
C(32)	12505(4)	-267(3)	5779(2)	36(2)
C(33)	13082(4)	-1300(4)	5754(2)	46(2)
C(34)	14168(5)	-1534(4)	5940(2)	51(2)
C(35)	14717(5)	-756(4)	6168(2)	58(2)
C(36)	14142(4)	290(4)	6196(2)	45(2)
C(41)	13431(4)	2119(3)	5485(2)	30(1)
C(42)	12923(4)	1978(4)	5150(2)	38(2)
C(43)	13654(4)	1610(3)	4898(2)	51(2)
C(44)	14899(6)	1412(4)	4982(2)	56(2)
C(45)	15421(5)	1588(5)	5310(2)	59(2)
C(46)	14707(4)	1939(3)	5562(2)	47(2)
C(51)	13022(4)	4462(3)	5607(2)	34(2)
C(52)	12675(4)	5030(4)	5305(2)	49(2)
C(53)	13504(5)	5787(4)	5175(2)	66(2)
C(54)	14645(6)	5946(4)	5334(2)	69(3)

Table B.25. Atomic coordinates (x 10^4) and equivalent isotropic displacement parameters (A^2 x 10^3) for 4.44. U(eq) is defined as 1/3rd of the trace of the orthogonalized Uij tensor (continued).

	x	y	z	U(eq)
C(55)	15001(5)	5404(4)	5641(2)	75(3)
C(56)	14184(4)	4635(3)	5774(2)	50(2)
C(61)	10581(4)	5106(3)	5833(2)	43(2)
C(62)	9405(5)	5351(4)	5668(2)	60(2)
C(63)	8936(7)	6451(6)	5671(2)	106(4)
C(64)	9630(10)	7273(5)	5843(3)	119(5)
C(65)	10766(7)	7046(4)	6002(2)	87(3)
C(66)	11261(5)	5954(3)	5997(2)	60(2)
C(71)	9722(3)	2176(3)	5675(2)	28(1)
C(72)	9312(4)	1121(4)	5761(2)	38(2)
C(73)	8804(4)	383(4)	5507(2)	46(2)
C(74)	8723(4)	664(4)	5170(2)	46(2)
C(75)	9127(4)	1694(4)	5076(2)	50(2)
C(76)	9619(4)	2439(4)	5326(2)	39(2)

Table B.26. Complete List of Bond lengths [Å] for 4.44.

Fe(1)-C(14)	2.048(5)	C(34)-C(35)	1.376(8)
Fe(1)-C(20)	2.054(7)	C(35)-C(36)	1.404(6)
Fe(1)-C(16)	2.055(7)	C(41)-C(42)	1.373(8)
Fe(1)-C(13)	2.063(6)	C(41)-C(46)	1.395(7)
Fe(1)-C(15)	2.069(4)	C(42)-C(43)	1.398(6)
Fe(1)-C(19)	2.073(5)	C(43)-C(44)	1.370(8)
Fe(1)-C(17)	2.074(5)	C(44)-C(45)	1.357(9)
Fe(1)-C(18)	2.102(4)	C(45)-C(46)	1.382(7)
Fe(1)-C(12)	2.117(4)	C(51)-C(56)	1.367(8)
Fe(1)-C(11)	2.150(3)	C(51)-C(52)	1.376(8)
Sb(1)-Cl(4)	2.3589(11)	C(52)-C(53)	1.404(6)
Sb(1)-Cl(6)	2.363(2)	C(53)-C(54)	1.331(9)
Sb(1)-Cl(3)	2.3673(10)	C(54)-C(55)	1.380(10)
Sb(1)-Cl(2)	2.3730(13)	C(55)-C(56)	1.411(6)
Sb(1)-Cl(1)	2.3742(13)	C(61)-C(66)	1.368(7)
Sb(1)-Cl(5)	2.377(2)	C(61)-C(62)	1.393(8)
C(1)-C(2)	1.369(5)	C(62)-C(63)	1.407(7)
C(1)-C(11)	1.487(6)	C(63)-C(64)	1.367(12)
C(1)-C(7)	1.502(7)	C(64)-C(65)	1.342(12)
C(2)-C(21)	1.475(7)	C(65)-C(66)	1.409(7)
C(2)-C(3)	1.479(6)	C(71)-C(72)	1.387(6)
C(3)-C(4)	1.362(6)	C(71)-C(76)	1.393(8)
C(3)-C(31)	1.504(5)	C(72)-C(73)	1.392(7)
C(4)-C(5)	1.475(5)	C(73)-C(74)	1.355(8)
C(4)-C(41)	1.506(6)	C(74)-C(75)	1.367(7)
C(5)-C(6)	1.360(4)	C(75)-C(76)	1.382(7)
C(5)-C(51)	1.510(5)		
C(6)-C(61)	1.491(5)		
C(6)-C(7)	1.523(5)		
C(7)-C(71)	1.527(7)		
C(11)-C(12)	1.421(6)		
C(11)-C(15)	1.446(5)		
C(12)-C(13)	1.400(6)		
C(13)-C(14)	1.398(6)		
C(14)-C(15)	1.433(7)		
C(16)-C(20)	1.372(9)		
C(16)-C(17)	1.422(10)		
C(17)-C(18)	1.356(8)		
C(18)-C(19)	1.338(7)		
C(19)-C(20)	1.343(10)		
C(21)-C(26)	1.393(8)		
C(21)-C(22)	1.414(6)		
C(22)-C(23)	1.386(9)		
C(23)-C(24)	1.364(9)		
C(24)-C(25)	1.408(9)		
C(25)-C(26)	1.399(9)		
C(31)-C(36)	1.378(7)		
C(31)-C(32)	1.384(6)		
C(32)-C(33)	1.389(5)		
C(33)-C(34)	1.340(8)		

Table B.27. Complete List of Bond Angles [deg] for 4.44.

C(14)-Fe(1)-C(20)	172.4(3)	Cl(3)-Sb(1)-Cl(2)	90.13(4)
C(14)-Fe(1)-C(16)	133.5(3)	Cl(4)-Sb(1)-Cl(1)	90.26(4)
C(20)-Fe(1)-C(16)	39.0(3)	Cl(6)-Sb(1)-Cl(1)	88.80(5)
C(14)-Fe(1)-C(13)	39.8(2)	Cl(3)-Sb(1)-Cl(1)	90.23(4)
C(20)-Fe(1)-C(13)	147.9(3)	Cl(2)-Sb(1)-Cl(1)	178.58(6)
C(16)-Fe(1)-C(13)	170.2(3)	Cl(4)-Sb(1)-Cl(5)	89.58(5)
C(14)-Fe(1)-C(15)	40.7(2)	Cl(6)-Sb(1)-Cl(5)	178.42(6)
C(20)-Fe(1)-C(15)	135.2(3)	Cl(3)-Sb(1)-Cl(5)	88.53(6)
C(16)-Fe(1)-C(15)	112.1(2)	Cl(2)-Sb(1)-Cl(5)	91.72(6)
C(13)-Fe(1)-C(15)	67.4(2)	Cl(1)-Sb(1)-Cl(5)	89.66(6)
C(14)-Fe(1)-C(19)	146.4(3)	C(2)-C(1)-C(11)	119.4(5)
C(20)-Fe(1)-C(19)	38.0(3)	C(2)-C(1)-C(7)	121.8(4)
C(16)-Fe(1)-C(19)	64.3(3)	C(11)-C(1)-C(7)	118.5(3)
C(13)-Fe(1)-C(19)	117.3(3)	C(1)-C(2)-C(21)	120.8(4)
C(15)-Fe(1)-C(19)	172.7(3)	C(1)-C(2)-C(3)	122.1(5)
C(14)-Fe(1)-C(17)	109.1(2)	C(21)-C(2)-C(3)	116.9(4)
C(20)-Fe(1)-C(17)	66.0(2)	C(4)-C(3)-C(2)	124.5(3)
C(16)-Fe(1)-C(17)	40.3(3)	C(4)-C(3)-C(31)	119.2(3)
C(13)-Fe(1)-C(17)	130.5(3)	C(2)-C(3)-C(31)	116.2(4)
C(15)-Fe(1)-C(17)	117.7(2)	C(3)-C(4)-C(5)	125.6(3)
C(19)-Fe(1)-C(17)	64.3(2)	C(3)-C(4)-C(41)	118.9(3)
C(14)-Fe(1)-C(18)	116.7(2)	C(5)-C(4)-C(41)	115.4(4)
C(20)-Fe(1)-C(18)	63.5(2)	C(6)-C(5)-C(4)	124.1(3)
C(16)-Fe(1)-C(18)	64.3(2)	C(6)-C(5)-C(51)	120.1(3)
C(13)-Fe(1)-C(18)	110.6(2)	C(4)-C(5)-C(51)	115.7(3)
C(15)-Fe(1)-C(18)	148.2(2)	C(5)-C(6)-C(61)	124.8(3)
C(19)-Fe(1)-C(18)	37.4(2)	C(5)-C(6)-C(7)	119.6(3)
C(17)-Fe(1)-C(18)	37.9(2)	C(61)-C(6)-C(7)	115.6(3)
C(14)-Fe(1)-C(12)	66.3(2)	C(1)-C(7)-C(6)	107.7(4)
C(20)-Fe(1)-C(12)	119.7(2)	C(1)-C(7)-C(71)	115.9(3)
C(16)-Fe(1)-C(12)	150.5(3)	C(6)-C(7)-C(71)	114.6(4)
C(13)-Fe(1)-C(12)	39.1(2)	C(12)-C(11)-C(15)	106.9(4)
C(15)-Fe(1)-C(12)	66.7(2)	C(12)-C(11)-C(1)	129.3(3)
C(19)-Fe(1)-C(12)	112.9(2)	C(15)-C(11)-C(1)	123.8(4)
C(17)-Fe(1)-C(12)	168.1(3)	C(12)-C(11)-Fe(1)	69.3(2)
C(18)-Fe(1)-C(12)	132.9(2)	C(15)-C(11)-Fe(1)	67.0(2)
C(14)-Fe(1)-C(11)	66.9(2)	C(1)-C(11)-Fe(1)	127.8(4)
C(20)-Fe(1)-C(11)	114.3(2)	C(13)-C(12)-C(11)	108.8(4)
C(16)-Fe(1)-C(11)	120.5(2)	C(13)-C(12)-Fe(1)	68.4(3)
C(13)-Fe(1)-C(11)	65.9(2)	C(11)-C(12)-Fe(1)	71.8(3)
C(15)-Fe(1)-C(11)	40.02(13)	C(14)-C(13)-C(12)	109.1(4)
C(19)-Fe(1)-C(11)	135.2(2)	C(14)-C(13)-Fe(1)	69.5(4)
C(17)-Fe(1)-C(11)	151.1(2)	C(12)-C(13)-Fe(1)	72.5(3)
C(18)-Fe(1)-C(11)	170.5(2)	C(13)-C(14)-C(15)	108.1(4)
C(12)-Fe(1)-C(11)	38.9(2)	C(13)-C(14)-Fe(1)	70.7(3)
Cl(4)-Sb(1)-Cl(6)	90.80(5)	C(15)-C(14)-Fe(1)	70.4(3)
Cl(4)-Sb(1)-Cl(3)	178.04(6)	C(14)-C(15)-C(11)	107.1(4)
Cl(6)-Sb(1)-Cl(3)	91.10(5)	C(14)-C(15)-Fe(1)	68.9(2)
Cl(4)-Sb(1)-Cl(2)	89.43(4)	C(11)-C(15)-Fe(1)	73.0(2)
Cl(6)-Sb(1)-Cl(2)	89.82(5)	C(20)-C(16)-C(17)	107.1(6)

Table B.27. Complete List of Bond Angles [deg] for 4.44 (continued).

C(20)-C(16)-Fe(1)	70.5(4)	C(64)-C(63)-C(62)	119.6(8)
C(17)-C(16)-Fe(1)	70.6(4)	C(65)-C(64)-C(63)	20.6(6)
C(18)-C(17)-C(16)	105.5(5)	C(64)-C(65)-C(66)	120.7(7)
C(18)-C(17)-Fe(1)	72.2(3)	C(61)-C(66)-C(65)	120.3(6)
C(16)-C(17)-Fe(1)	69.1(3)	C(72)-C(71)-C(76)	116.6(5)
C(19)-C(18)-C(17)	110.0(6)	C(72)-C(71)-C(7)	121.9(5)
C(19)-C(18)-Fe(1)	70.2(2)	C(76)-C(71)-C(7)	121.3(4)
C(17)-C(18)-Fe(1)	69.9(2)	C(71)-C(72)-C(73)	120.9(5)
C(18)-C(19)-C(20)	109.4(6)	C(74)-C(73)-C(72)	121.0(4)
C(18)-C(19)-Fe(1)	72.5(3)	C(73)-C(74)-C(75)	119.6(6)
C(20)-C(19)-Fe(1)	70.2(3)	C(74)-C(75)-C(76)	119.9(6)
C(19)-C(20)-C(16)	108.0(6)	C(75)-C(76)-C(71)	122.0(4)
C(19)-C(20)-Fe(1)	71.8(4)		
C(16)-C(20)-Fe(1)	70.5(5)		
C(26)-C(21)-C(22)	119.4(6)		
C(26)-C(21)-C(2)	119.4(4)		
C(22)-C(21)-C(2)	121.2(5)		
C(23)-C(22)-C(21)	120.3(6)		
C(24)-C(23)-C(22)	119.8(6)		
C(23)-C(24)-C(25)	121.6(7)		
C(26)-C(25)-C(24)	118.8(7)		
C(21)-C(26)-C(25)	120.2(6)		
C(36)-C(31)-C(32)	117.9(4)		
C(36)-C(31)-C(3)	121.7(5)		
C(32)-C(31)-C(3)	120.2(5)		
C(31)-C(32)-C(33)	120.4(5)		
C(34)-C(33)-C(32)	121.3(5)		
C(33)-C(34)-C(35)	120.0(4)		
C(34)-C(35)-C(36)	119.2(6)		
C(31)-C(36)-C(35)	121.1(5)		
C(42)-C(41)-C(46)	118.1(4)		
C(42)-C(41)-C(4)	121.1(4)		
C(46)-C(41)-C(4)	120.8(6)		
C(41)-C(42)-C(43)	120.8(5)		
C(44)-C(43)-C(42)	120.1(7)		
C(45)-C(44)-C(43)	119.7(5)		
C(44)-C(45)-C(46)	120.9(6)		
C(45)-C(46)-C(41)	120.5(7)		
C(56)-C(51)-C(52)	119.1(4)		
C(56)-C(51)-C(5)	119.4(5)		
C(52)-C(51)-C(5)	121.4(5)		
C(51)-C(52)-C(53)	120.0(6)		
C(54)-C(53)-C(52)	121.2(7)		
C(53)-C(54)-C(55)	119.6(5)		
C(54)-C(55)-C(56)	119.9(6)		
C(51)-C(56)-C(55)	120.0(6)		
C(66)-C(61)-C(62)	118.6(4)		
C(66)-C(61)-C(6)	122.3(5)		
C(62)-C(61)-C(6)	119.0(5)		
C(61)-C(62)-C(63)	120.2(6)		

APPENDIX C: Supplementary Computational Data

Cartesian Coordinates, Total Energies and Lowest Vibrational Frequencies

Potential Energy Surface Scans

$C_5Ph_5^-$ D_5-symmetry (AM1)
HF=0.205231
Low frequencies --- 19.5981

C	2.528718	0.821630	0.000000
C	0.000000	1.214343	0.000000
C	-2.528718	0.821630	0.000000
C	-1.154908	0.375252	0.000000
C	-0.713773	-0.982424	0.000000
C	0.000000	2.658851	0.000000
C	-1.562833	-2.151056	0.000000
C	0.713773	-0.982424	0.000000
C	1.562833	-2.151056	0.000000
C	1.154908	0.375252	0.000000
C	3.218490	-4.429872	0.000000
C	1.313281	-3.224978	0.873374
C	2.661310	-2.245578	-0.873374
C	3.478149	-3.372722	-0.871717
C	2.132842	-4.350144	0.871717
H	0.451028	-3.166686	1.554565
H	2.872322	-1.407513	-1.554565
H	4.332417	-3.428270	-1.561092
H	1.921689	-5.179767	1.561092
H	3.863825	-5.318098	0.000000
C	-3.218490	-4.429872	0.000000
C	-1.313281	-3.224978	-0.873374
C	-2.661310	-2.245578	0.873374
C	-3.478149	-3.372722	0.871717
C	-2.132842	-4.350144	-0.871717
H	-0.451028	-3.166686	-1.554565
H	-2.872322	-1.407513	1.554565
H	-4.332417	-3.428270	1.561092
H	-1.921689	-5.179767	-1.561092
H	-3.863825	-5.318098	0.000000
C	-5.207626	1.692060	0.000000
C	-2.958062	1.837135	0.873374
C	-3.472963	0.252432	-0.873374
C	-4.796318	0.684185	-0.871717
C	-4.282456	2.265688	0.871717
H	-2.226221	2.296795	1.554565
H	-3.151073	-0.549606	-1.554565
H	-5.520086	0.226998	-1.561092
H	-4.599269	3.060979	1.561092
H	-6.251800	2.031333	0.000000
C	0.000000	5.475622	0.000000
C	0.833128	3.380990	0.873374
C	-0.833128	3.380990	-0.873374
C	-0.831445	4.772994	-0.871717
C	0.831445	4.772994	0.871717
H	1.496442	2.827011	1.554565
H	-1.496442	2.827011	-1.554565
H	-1.489912	5.320060	-1.561092
H	1.489912	5.320060	1.561092
H	0.000000	6.573531	0.000000
C	5.207626	1.692060	0.000000
C	2.958062	1.837135	-0.873374
C	3.472963	0.252432	0.873374
C	4.796318	0.684185	0.871717
C	4.282456	2.265688	-0.871717

H	2.226221	2.296795	-1.554565
H	3.151073	-0.549606	1.554565
H	5.520086	0.226998	1.561092
H	4.599269	3.060979	-1.561092
H	6.251800	2.031333	0.000000

$C_5Ph_5^-$ TS-1 (AM1)

HF=0.2078882
Low frequencies --- -29.6791

C	0.000963	-2.635955	0.000085
C	0.000421	-1.187091	-0.000010
C	0.392597	-3.354653	1.141367
C	-0.389942	-3.355096	-1.141167
C	-1.151274	-0.350369	-0.009542
C	1.151489	-0.349506	0.009491
C	-0.389413	-4.747997	-1.139413
C	0.393110	-4.747554	1.139796
H	0.701402	-2.802515	2.041151
H	-0.699010	-2.803308	-2.041076
C	0.002079	-5.449488	0.000211
C	-0.716390	1.007533	-0.000195
C	0.715590	1.008069	-0.000065
C	-2.524954	-0.811876	0.039480
C	2.525517	-0.809991	-0.039375
H	-0.698037	-5.296070	-2.040680
H	0.702110	-5.295277	2.041146
H	0.002751	-6.547545	0.000940
C	-1.582605	2.160008	0.036416
C	1.580945	2.161187	-0.036767
C	3.271828	-0.707716	-1.225212
C	3.137690	-1.374841	1.091034
C	-3.135785	-1.380205	-1.089910
C	-3.272164	-0.707392	1.224558
C	4.454193	-1.827469	1.035312
C	4.588493	-1.158995	-1.276530
H	2.803074	-0.262940	-2.115339
H	2.562851	-1.459504	2.024918
C	2.766541	2.197920	0.720243
C	1.274932	3.274930	-0.841203
C	-2.768281	2.195755	-0.720517
C	-1.277369	3.274086	0.840684
C	-4.588490	-1.159639	1.276049
C	-4.451952	-1.833788	-1.034008
H	-2.560158	-1.466838	-2.023128
H	-2.804390	-0.260106	2.113943
C	5.184047	-1.721237	-0.147735
H	4.918502	-2.269986	1.927766
H	5.160025	-1.072254	-2.211330
C	2.121161	4.378452	-0.884759
C	3.610721	3.303432	0.672888
H	3.023732	1.329716	1.346809
H	0.346833	3.263041	-1.432671
C	-2.124421	4.376980	0.884154
C	-3.613284	3.300641	-0.673248
H	-3.024865	1.327276	-1.346951
H	-0.349221	3.262969	1.432088
C	-5.182773	-1.725199	0.148239

H	-5.160800	-1.070964	2.210192
H	-4.915238	-2.278939	-1.925683
H	6.221586	-2.078320	-0.190682
C	3.293253	4.399235	-0.128675
H	1.864273	5.237926	-1.519995
H	4.533082	3.311017	1.270702
C	-3.296581	4.396787	0.128148
H	-1.868133	5.236730	1.519258
H	-4.535692	3.307457	-1.270999
H	-6.220057	-2.083011	0.191288
H	3.960183	5.270321	-0.165434
H	-3.964160	5.267378	0.164838

$C_5Ph_5^-$ 1a (AM1)

HF=0.2067873
Low frequencies --- 24.2220

C	0.008381	-2.654909	-0.000004
C	0.003567	-1.212119	0.001141
C	0.894778	-3.378275	0.819003
C	-0.872416	-3.382998	-0.820822
C	-1.151254	-0.372571	-0.014984
C	1.153034	-0.365197	0.016212
C	-0.867420	-4.774534	-0.819723
C	0.900175	-4.769793	0.814764
H	1.594141	-2.825470	1.464780
H	-1.575742	-2.834003	-1.465533
C	0.018990	-5.476101	-0.003266
C	-0.720850	0.982367	-0.001601
C	0.713993	0.986903	0.001939
C	-2.528530	-0.828969	0.039703
C	2.533245	-0.812679	-0.037733
H	-1.565828	-5.322858	-1.467605
H	1.602733	-5.314363	1.461323
H	0.023122	-6.573766	-0.004541
C	-1.569723	2.146754	0.081455
C	1.555646	2.156464	-0.082067
C	3.151077	-1.066467	-1.272804
C	3.279058	-1.001639	1.137254
C	-3.273576	-1.023568	-1.134862
C	-3.144292	-1.085740	1.275199
C	4.603439	-1.430422	1.077144
C	4.475539	-1.495307	-1.329028
H	2.575384	-0.922379	-2.198956
H	2.804391	-0.808201	2.110881
C	2.718717	2.281409	0.697530
C	1.236081	3.204686	-0.966388
C	-2.734373	2.263350	-0.697094
C	-1.255798	3.198285	0.963890
C	-4.466005	-1.522897	1.332251
C	-4.595189	-1.460704	-1.073926
H	-2.800588	-0.827652	-2.108817
H	-2.569234	-0.937146	2.201035
C	5.205983	-1.678386	-0.155522
H	5.174681	-1.573827	2.005055
H	4.946115	-1.689894	-2.303077
C	2.049189	4.329051	-1.065050
C	3.531372	3.407238	0.594252

H	2.986758	1.468990	1.389973
H	0.323452	3.123409	-1.576135
C	-2.075748	4.317735	1.061719
C	-3.553884	3.384271	-0.594647
H	-2.998034	1.448368	-1.388198
H	-0.342053	3.123602	1.572817
C	-5.195692	-1.711559	0.159151
H	-4.935003	-1.719621	2.306633
H	-5.165883	-1.608365	-2.001507
H	6.249909	-2.016175	-0.201691
C	3.201738	4.436380	-0.286205
H	1.782162	5.136365	-1.761551
H	4.437969	3.483299	1.211058
C	-3.229753	4.416753	0.283934
H	-1.813011	5.127721	1.756747
H	-4.461559	3.453787	-1.210639
H	-6.237442	-2.055915	0.205956
H	3.843419	5.323378	-0.366871
H	-3.876859	5.299857	0.363966

$C_5Ph_5^-$ TS-2 (AM1)

HF=0.2073634
Low frequencies --- -24.8723

C	-0.827249	2.530409	-0.037343
C	-0.396239	1.155450	0.014352
C	-1.935868	2.982708	0.700488
C	-0.142044	3.465306	-0.837284
C	0.964692	0.710428	0.006598
C	-1.228129	-0.001769	0.026272
C	-0.550771	4.793602	-0.895204
C	-2.344347	4.311720	0.636909
H	-2.485356	2.267040	1.330767
H	0.732835	3.128599	-1.415109
C	-1.654984	5.224661	-0.159940
C	0.966805	-0.707489	0.006321
C	-0.392766	-1.156505	0.014321
C	2.136831	1.560486	0.072579
C	-2.678780	-0.003987	-0.036639
H	-0.000544	5.506751	-1.525186
H	-3.215396	4.642447	1.220097
H	-1.977735	6.272660	-0.208285
C	2.141515	-1.554073	0.072968
C	-0.819652	-2.532764	-0.037539
C	-3.336743	-0.004935	-1.277089
C	-3.454450	-0.005355	1.134388
C	3.007060	1.680164	-1.022968
C	2.430710	2.280474	1.243043
C	-4.846035	-0.007593	1.065182
C	-4.728530	-0.007173	-1.342370
H	-2.738560	-0.003882	-2.200204
H	-2.949422	-0.004635	2.111913
C	-1.926374	-2.988605	0.700977
C	-0.131973	-3.465448	-0.837945
C	3.009927	-1.675537	-1.023825
C	2.439786	-2.268676	1.245697
C	3.561162	3.090689	1.313588
C	4.138576	2.489537	-0.947811

H	2.786027	1.123703	-1.945529
H	1.752763	2.197966	2.105291
C	-5.487571	-0.008514	-0.172773
H	-5.439760	-0.008645	1.990056
H	-5.229722	-0.007899	-2.320576
C	-0.536519	-4.795042	-0.895664
C	-2.330689	-4.318907	0.637595
H	-2.477748	-2.274686	1.331594
H	0.741503	-3.125947	-1.416266
C	3.572665	-3.075454	1.317142
C	4.143893	-2.481495	-0.947792
H	2.785563	-1.123413	-1.948165
H	1.763350	-2.184672	2.108998
C	4.419919	3.197328	0.219799
H	3.777732	3.647745	2.235988
H	4.811503	2.570104	-1.813011
H	-6.584453	-0.010280	-0.226081
C	-1.638905	-5.229637	-0.159728
H	0.015610	-5.506436	-1.525967
H	-3.200328	-4.652414	1.221307
C	4.429560	-3.183951	0.222024
H	3.792667	-3.628288	2.241274
H	4.815296	-2.563552	-1.814044
H	5.312028	3.834917	0.278051
H	-1.958323	-6.278667	-0.207882
H	5.323573	-3.818815	0.280988

$C_5Ph_5^-$ 1b (AM1)

HF=0.2073634
Low frequencies --- -24.8723

C	-1.559368	2.154525	-0.081152
C	-0.715809	0.986387	0.002562
C	-2.725050	2.275297	0.695280
C	-1.239438	3.205496	-0.962095
C	0.719013	0.983945	-0.000233
C	-1.152750	-0.366538	0.016028
C	-2.054699	4.328300	-1.060702
C	-3.539847	3.399567	0.592053
H	-2.993394	1.460760	1.385139
H	-0.324882	3.127562	-1.569404
C	-3.209830	4.431406	-0.285111
C	1.151512	-0.370287	-0.014301
C	-0.002045	-1.211535	0.000701
C	1.566512	2.149346	0.082639
C	-2.532133	-0.816503	-0.038390
H	-1.787326	5.137741	-1.754600
H	-4.448455	3.472265	1.206307
H	-3.853200	5.317177	-0.365750
C	2.529410	-0.824780	0.039555
C	-0.004202	-2.654390	-0.000153
C	-3.150516	-1.067045	-1.273857
C	-3.276501	-1.011401	1.136540
C	2.728467	2.269015	-0.699417
C	1.253632	3.198862	0.967799
C	-4.599901	-1.443155	1.076015
C	-4.474029	-1.498764	-1.330504
H	-2.576039	-0.918022	-2.199985

H	-2.801657	-0.819744	2.110433
C	-0.884610	-3.379315	0.823787
C	0.874068	-3.380661	-0.825273
C	3.273947	-1.018332	-1.135480
C	3.146183	-1.081165	1.274634
C	2.072108	4.319466	1.064872
C	3.546530	3.391072	-0.597698
H	2.991257	1.455457	-1.392534
H	0.341864	3.121742	1.579362
C	-5.202942	-1.688049	-0.157023
H	-5.169972	-1.591350	2.003893
H	-4.945050	-1.690742	-2.304855
C	0.872250	-4.772206	-0.823661
C	-0.886840	-4.770882	0.820084
H	-1.581867	-2.827814	1.472927
H	1.572988	-2.830139	-1.473469
C	4.468310	-1.517138	1.330823
C	4.596007	-1.454260	-1.075444
H	2.800265	-0.822514	-2.109114
H	2.571514	-0.933404	2.200841
C	3.223502	4.421576	0.283613
H	1.810301	5.127892	1.762062
H	4.452145	3.463062	-1.216432
H	-6.246057	-2.028291	-0.203504
C	-0.008346	-5.475445	-0.002328
H	1.568506	-5.319225	-1.474951
H	-1.584732	-5.316815	1.470531
C	5.197482	-1.704877	0.157244
H	4.938058	-1.713634	2.304889
H	5.166251	-1.601260	-2.003412
H	3.869433	5.305598	0.363042
H	-0.009970	-6.573122	-0.003198
H	6.239548	-2.048378	0.203354

C_5Ph_5- D_{5h}-symmetry (AM1)

HF=0.2138095
Low frequencies --- -38.8599 -38.8545 -37.9197 -35.6115 -35.6096

C	2.530356	0.822162	0.000000
C	0.000000	1.210805	0.000000
C	-2.530356	0.822162	0.000000
C	-1.151544	0.374159	0.000000
C	-0.711693	-0.979562	0.000000
C	0.000000	2.660574	0.000000
C	-1.563846	-2.152449	0.000000
C	0.711693	-0.979562	0.000000
C	1.563846	-2.152449	0.000000
C	1.151544	0.374159	0.000000
C	3.216613	-4.427288	0.000000
C	1.985633	-2.732989	1.206759
C	1.985633	-2.732989	-1.206759
C	2.804510	-3.860077	-1.205183
C	2.804510	-3.860077	1.205183
H	1.661121	-2.286337	2.157738
H	1.661121	-2.286337	-2.157738
H	3.127081	-4.304058	-2.157324
H	3.127081	-4.304058	2.157324
H	3.862029	-5.315627	0.000000

C	-3.216613	-4.427288	0.000000
C	-1.985633	-2.732989	-1.206759
C	-1.985633	-2.732989	1.206759
C	-2.804510	-3.860077	1.205183
C	-2.804510	-3.860077	-1.205183
H	-1.661121	-2.286337	-2.157738
H	-1.661121	-2.286337	2.157738
H	-3.127081	-4.304058	2.157324
H	-3.127081	-4.304058	-2.157324
H	-3.862029	-5.315627	0.000000
C	-5.204590	1.691074	0.000000
C	-3.212822	1.043909	1.206759
C	-3.212822	1.043909	-1.206759
C	-4.537793	1.474418	-1.205183
C	-4.537793	1.474418	1.205183
H	-2.687750	0.873303	2.157738
H	-2.687750	0.873303	-2.157738
H	-5.059723	1.644004	-2.157324
H	-5.059723	1.644004	2.157324
H	-6.248895	2.030389	0.000000
C	0.000000	5.472429	0.000000
C	0.000000	3.378161	1.206759
C	0.000000	3.378161	-1.206760
C	0.000000	4.771318	-1.205183
C	0.000000	4.771318	1.205183
H	0.000000	2.826067	2.157738
H	0.000000	2.826067	-2.157738
H	0.000000	5.320108	-2.157324
H	0.000000	5.320108	2.157324
H	0.000000	6.570477	0.000000
C	5.204590	1.691074	0.000000
C	3.212822	1.043909	-1.206759
C	3.212822	1.043909	1.206759
C	4.537793	1.474418	1.205183
C	4.537793	1.474418	-1.205183
H	2.687750	0.873303	-2.157738
H	2.687750	0.873303	2.157738
H	5.059723	1.644004	2.157324
H	5.059723	1.644004	-2.157324
H	6.248895	2.030389	0.000000

C_5Ph_5- C_{2v}-symmetry (AM1)

HF=0.2142658
Low frequencies --- -87.4221 -55.6275 -28.3385 -26.1436

C	0.000000	1.555199	-2.072124
C	0.000000	1.150482	0.457219
C	0.000000	0.000000	2.758388
C	0.000000	0.000000	1.317007
C	0.000000	-1.150482	0.457219
C	0.000000	2.560684	0.803625
C	0.000000	-2.560684	0.803625
C	0.000000	-0.711709	-0.891761
C	0.000000	-1.555199	-2.072124
C	0.000000	0.711709	-0.891761
C	0.000000	-3.180412	-4.366080
C	1.206863	-1.969504	-2.657308
C	-1.206863	-1.969504	-2.657308

C	-1.205217	-2.775044	-3.794048
C	1.205217	-2.775044	-3.794048
H	2.157925	-1.650174	-2.206912
H	-2.157925	-1.650174	-2.206912
H	-2.157726	-3.091923	-4.241422
H	2.157726	-3.091923	-4.241422
H	0.000000	-3.815365	-5.262054
C	0.000000	-5.310186	1.392543
C	-1.207536	-3.262547	0.953317
C	1.207536	-3.262547	0.953317
C	1.205340	-4.624699	1.245480
C	-1.205340	-4.624699	1.245480
H	-2.158221	-2.722210	0.836120
H	2.158221	-2.722210	0.836120
H	2.157888	-5.161168	1.358629
H	-2.157888	-5.161168	1.358629
H	0.000000	-6.384294	1.621075
C	0.000000	0.000000	5.607543
C	0.000000	-1.197753	3.505680
C	0.000000	1.197753	3.505680
C	0.000000	1.197918	4.896172
C	0.000000	-1.197918	4.896172
H	0.000000	-2.168033	2.989331
H	0.000000	2.168033	2.989331
H	0.000000	2.155361	5.436827
H	0.000000	-2.155361	5.436827
H	0.000000	0.000000	6.704475
C	0.000000	5.310186	1.392543
C	1.207536	3.262547	0.953317
C	-1.207536	3.262547	0.953317
C	-1.205340	4.624699	1.245480
C	1.205340	4.624699	1.245480
H	2.158221	2.722210	0.836120
H	-2.158221	2.722210	0.836120
H	-2.157888	5.161168	1.358629
H	2.157888	5.161168	1.358629
H	0.000000	6.384294	1.621075
C	0.000000	3.180412	-4.366080
C	-1.206863	1.969504	-2.657308
C	1.206863	1.969504	-2.657308
C	1.205217	2.775044	-3.794048
C	-1.205217	2.775044	-3.794048
H	-2.157925	1.650174	-2.206912
H	2.157925	1.650174	-2.206912
H	2.157726	3.091923	-4.241422
H	-2.157726	3.091923	-4.241422
H	0.000000	3.815365	-5.262054

C_5Ph_4H- C_2-symmetry (AM1)

HF=0.1617098
Low frequencies --- 22.6204

C	0.881364	2.334415	1.679742
C	0.264656	0.660809	-0.205110
C	-0.264656	-0.660809	-0.205110
C	-0.427729	-1.072606	1.160980
C	0.000000	0.000000	1.983148
C	0.427729	1.072606	1.160980

C	0.586697	1.441563	-1.376530
C	-0.586697	-1.441563	-1.376530
H	0.000000	0.000000	3.070189
C	-0.881364	-2.334415	1.679742
C	1.730322	4.794762	2.772526
C	1.535277	2.390376	2.927440
C	0.662987	3.546234	0.997383
C	1.084155	4.757080	1.536807
C	1.951936	3.604153	3.463854
H	1.717229	1.454554	3.475854
H	0.151724	3.523228	0.022861
H	0.903181	5.691063	0.985946
H	2.461152	3.624358	4.437838
H	2.060459	5.751716	3.196430
C	1.224396	2.954844	-3.665890
C	1.816975	2.117088	-1.476956
C	-0.317172	1.544798	-2.449230
C	0.000000	2.293151	-3.579501
C	2.130413	2.863021	-2.609346
H	2.526326	2.054048	-0.638051
H	-1.279611	1.015001	-2.385838
H	-0.719277	2.361355	-4.407842
H	3.097206	3.382367	-2.670334
H	1.473465	3.543556	-4.558409
C	-1.224396	-2.954844	-3.665890
C	-1.816975	-2.117088	-1.476956
C	0.317172	-1.544798	-2.449230
C	0.000000	-2.293151	-3.579501
C	-2.130413	-2.863021	-2.609346
H	-2.526326	-2.054048	-0.638051
H	1.279611	-1.015001	-2.385838
H	0.719277	-2.361355	-4.407842
H	-3.097206	-3.382367	-2.670334
H	-1.473465	-3.543556	-4.558409
C	-1.730322	-4.794762	2.772526
C	-1.535277	-2.390376	2.927440
C	-0.662987	-3.546234	0.997383
C	-1.084155	-4.757080	1.536807
C	-1.951936	-3.604153	3.463854
H	-1.717229	-1.454554	3.475854
H	-0.151724	-3.523228	0.022861
H	-0.903181	-5.691063	0.985946
H	-2.461152	-3.624358	4.437838
H	-2.060459	-5.751716	3.196430

C_5Ph_4H- TS-1 (AM1)

HF=0.1656664
Low frequencies --- -28.8749

C	2.498180	-1.664444	-0.028449
C	1.143754	-1.154346	-0.031346
C	3.013096	-2.290708	1.119850
C	3.306399	-1.605478	-1.175069
C	0.703086	0.206303	-0.044223
C	-0.000554	-1.982334	0.004197
C	4.595919	-2.133101	-1.165102
C	4.301267	-2.819318	1.125953
H	2.383369	-2.353555	2.019412

H	2.905123	-1.150678	-2.092637
C	-0.724405	0.203730	-0.031376
C	-1.161311	-1.162292	-0.014210
C	1.548138	1.375154	0.054349
H	0.005325	-3.068757	0.007403
C	5.099322	-2.739377	-0.015073
H	5.217456	-2.074443	-2.069700
H	4.691404	-3.300177	2.034023
C	-1.560726	1.378570	-0.018242
C	-2.495923	-1.692041	-0.069642
H	6.116398	-3.153082	-0.008250
C	2.589535	1.613208	-0.857331
C	1.348660	2.306885	1.091021
C	2.163366	3.428337	1.209829
C	3.405432	2.735571	-0.733898
H	2.760124	0.897996	-1.674836
H	0.529969	2.136309	1.806223
C	-2.694739	1.453475	0.812464
C	-1.260627	2.488317	-0.830010
C	-2.788150	-2.934598	0.529462
C	-3.538232	-1.027343	-0.744013
C	3.197215	3.647757	0.298907
H	1.992140	4.144183	2.026125
H	4.217186	2.901569	-1.456068
C	-2.061470	3.626440	-0.808484
C	-3.492343	2.593391	0.830875
H	-2.946850	0.587636	1.443322
H	-0.372340	2.446311	-1.478370
C	-4.813503	-1.578008	-0.810528
C	-4.064594	-3.482186	0.457707
H	-1.988160	-3.470155	1.061095
H	-3.328700	-0.057708	-1.221009
H	3.840960	4.531767	0.395400
C	-3.180536	3.685765	0.021346
H	-1.808894	4.483071	-1.449241
H	-4.372651	2.632709	1.487893
C	-5.085715	-2.808005	-0.211156
H	-5.611695	-1.040855	-1.342394
H	-4.270082	-4.451804	0.933067
H	-3.810622	4.584453	0.037863
H	-6.092704	-3.240723	-0.266161

C_5Ph_4H- 2a (AM1)

HF=0.1623729
Low frequencies --- 24.6297

C	2.455856	-1.734549	-0.043476
C	1.126887	-1.189700	-0.052746
C	2.685823	-3.019375	0.493310
C	3.561237	-1.042017	-0.572807
C	0.710780	0.182449	-0.050617
C	-0.049951	-1.986231	-0.050758
C	4.833695	-1.603529	-0.560479
C	3.958474	-3.578557	0.498795
H	1.839780	-3.578880	0.918203
H	3.408877	-0.040699	-1.003310
C	-0.708446	0.219580	-0.037789
C	-1.183493	-1.139918	-0.053061

C	1.585073	1.339420	0.019438
H	-0.074436	-3.072363	-0.089250
C	5.042060	-2.874734	-0.026585
H	5.680815	-1.040529	-0.977637
H	4.112535	-4.580740	0.923444
C	-1.522317	1.407114	0.064743
C	-2.535157	-1.622919	-0.123074
H	6.046655	-3.316143	-0.019053
C	2.028637	1.981473	-1.148818
C	2.002535	1.843114	1.261808
C	2.837606	2.956335	1.331941
C	2.863529	3.094355	-1.074552
H	1.710948	1.591622	-2.127363
H	1.661146	1.347203	2.182423
C	-2.606517	1.456152	0.962288
C	-1.253393	2.549705	-0.708836
C	-2.867035	-2.879031	0.424353
C	-3.556796	-0.894603	-0.762472
C	3.270304	3.585721	0.165460
H	3.155648	3.339983	2.311605
H	3.202133	3.586753	-1.996947
C	-2.033252	3.696677	-0.585786
C	-3.383750	2.603500	1.081921
H	-2.834664	0.563818	1.564790
H	-0.407180	2.530047	-1.412468
C	-4.850256	-1.398429	-0.845784
C	-4.161683	-3.379690	0.335765
H	-2.084307	-3.463557	0.929360
H	-3.316307	0.087572	-1.197298
H	3.927610	4.463597	0.222682
C	-3.101128	3.730508	0.309347
H	-1.803700	4.579948	-1.198395
H	-4.224158	2.622279	1.790094
C	-5.161658	-2.643364	-0.298447
H	-5.631921	-0.812046	-1.349452
H	-4.398149	-4.361285	0.770412
H	-3.714353	4.635777	0.406491
H	-6.182967	-3.039102	-0.366818

C_5Ph_4H- TS-2 (AM1)

HF=0.1623742
Low frequencies --- 24.6291

C	2.533569	-1.625303	-0.121518
C	1.182190	-1.141620	-0.052133
C	3.557169	-0.894795	-0.755307
C	2.863559	-2.884000	0.421230
C	0.708303	0.218196	-0.035618
C	0.047675	-1.986862	-0.049921
C	4.158046	-3.385137	0.333216
C	4.850473	-1.399138	-0.838108
H	3.318356	0.089401	-1.186458
H	2.079406	-3.470316	0.921924
C	-0.710810	0.182654	-0.047928
C	-1.128339	-1.189176	-0.050844
C	1.523438	1.405247	0.064483
H	0.071099	-3.072976	-0.089701
C	5.159907	-2.646711	-0.295611

H	4.392948	-4.368747	0.764145
H	5.633525	-0.811179	-1.337780
C	-1.583182	1.341027	0.022586
C	-2.457881	-1.732491	-0.043930
H	6.181079	-3.042876	-0.363594
C	1.265312	2.540408	-0.723382
C	2.598187	1.460521	0.972813
C	3.376347	2.607549	1.089770
C	2.046162	3.687045	-0.603110
H	0.426093	2.515638	-1.435153
H	2.817985	0.573572	1.586196
C	-2.007661	1.838834	1.265001
C	-2.018682	1.989869	-1.144888
C	-2.690230	-3.017907	0.490417
C	-3.561487	-1.037895	-0.574267
C	3.104363	3.727452	0.303161
H	4.209180	2.631636	1.806672
H	1.825133	4.564728	-1.226775
C	-2.852833	3.103290	-1.069931
C	-2.841656	2.952798	1.335852
H	-1.672615	1.337683	2.185113
H	-1.695409	1.605066	-2.123602
C	-4.834579	-1.598026	-0.565278
C	-3.963520	-3.575707	0.492524
H	-1.845639	-3.579031	0.916062
H	-3.407040	-0.036042	-1.002810
H	3.718345	4.632450	0.398146
C	-3.266585	3.588712	0.170050
H	-3.185454	3.600721	-1.991799
H	-3.165116	3.331797	2.315553
C	-5.045316	-2.869898	-0.033836
H	-5.680287	-1.033460	-0.983188
H	-4.119470	-4.578409	0.915263
H	-3.923350	4.466953	0.227786
H	-6.050401	-3.310236	-0.028962

C_5Ph_4H- 2b (AM1)

HF=0.1623742
Low frequencies --- 24.6291

C	2.533569	-1.625303	-0.121518
C	1.182190	-1.141620	-0.052133
C	3.557169	-0.894795	-0.755307
C	2.863559	-2.884000	0.421230
C	0.708303	0.218196	-0.035618
C	0.047675	-1.986862	-0.049921
C	4.158046	-3.385137	0.333216
C	4.850473	-1.399138	-0.838108
H	3.318356	0.089401	-1.186458
H	2.079406	-3.470316	0.921924
C	-0.710810	0.182654	-0.047928
C	-1.128339	-1.189176	-0.050844
C	1.523438	1.405247	0.064483
H	0.071099	-3.072976	-0.089701
C	5.159907	-2.646711	-0.295611
H	4.392948	-4.368747	0.764145
H	5.633525	-0.811179	-1.337780
C	-1.583182	1.341027	0.022586

C	-2.457881	-1.732491	-0.043930
H	6.181079	-3.042876	-0.363594
C	1.265312	2.540408	-0.723382
C	2.598187	1.460521	0.972813
C	3.376347	2.607549	1.089770
C	2.046162	3.687045	-0.603110
H	0.426093	2.515638	-1.435153
H	2.817985	0.573572	1.586196
C	-2.007661	1.838834	1.265001
C	-2.018682	1.989869	-1.144888
C	-2.690230	-3.017907	0.490417
C	-3.561487	-1.037895	-0.574267
C	3.104363	3.727452	0.303161
H	4.209180	2.631636	1.806672
H	1.825133	4.564728	-1.226775
C	-2.852833	3.103290	-1.069931
C	-2.841656	2.952798	1.335852
H	-1.672615	1.337683	2.185113
H	-1.695409	1.605066	-2.123602
C	-4.834579	-1.598026	-0.565278
C	-3.963520	-3.575707	0.492524
H	-1.845639	-3.579031	0.916062
H	-3.407040	-0.036042	-1.002810
H	3.718345	4.632450	0.398146
C	-3.266585	3.588712	0.170050
H	-3.185454	3.600721	-1.991799
H	-3.165116	3.331797	2.315553
C	-5.045316	-2.869898	-0.033836
H	-5.680287	-1.033460	-0.983188
H	-4.119470	-4.578409	0.915263
H	-3.923350	4.466953	0.227786
H	-6.050401	-3.310236	-0.028962

C_5Ph_4H- C_s-symmetry (AM1)

HF=0.1629713
Low frequencies --- -25.1334

H	3.091416	-0.082897	0.000000
C	1.183109	-0.041649	1.155547
C	-0.182905	-0.031631	0.707955
C	-0.182905	-0.031631	-0.707955
C	1.183109	-0.041649	-1.155547
C	2.005164	-0.041524	0.000000
C	1.682681	-0.081648	2.500605
C	-1.359247	0.052544	1.550435
C	-1.359247	0.052544	-1.550435
C	1.682681	-0.081648	-2.500605
C	2.721898	-0.179867	-5.125611
C	0.931029	-0.622948	-3.561761
C	2.973049	0.406918	-2.793954
C	3.482512	0.355955	-4.086617
C	1.443608	-0.667324	-4.853608
H	-0.076779	-1.014902	-3.355070
H	3.577323	0.837497	-1.982403
H	4.490698	0.743244	-4.291525
H	0.836904	-1.092635	-5.665776
H	3.124611	-0.217361	-6.145679
C	-3.651264	0.235567	-3.171356

C	-2.236984	-1.036001	-1.679468
C	-1.650759	1.234660	-2.252419
C	-2.785798	1.323078	-3.054339
C	-3.372477	-0.943315	-2.481510
H	-2.018582	-1.966743	-1.135617
H	-0.967321	2.091760	-2.161625
H	-3.000944	2.254712	-3.596361
H	-4.050955	-1.803397	-2.569942
H	-4.546874	0.307819	-3.802550
C	-3.651264	0.235567	3.171356
C	-1.650759	1.234660	2.252419
C	-2.236984	-1.036001	1.679468
C	-3.372477	-0.943315	2.481510
C	-2.785798	1.323078	3.054339
H	-0.967321	2.091760	2.161625
H	-2.018582	-1.966743	1.135617
H	-4.050955	-1.803397	2.569942
H	-3.000944	2.254712	3.596361
H	-4.546874	0.307819	3.802550
C	2.721898	-0.179867	5.125611
C	0.931029	-0.622948	3.561761
C	2.973049	0.406918	2.793954
C	3.482512	0.355955	4.086617
C	1.443608	-0.667324	4.853608
H	-0.076779	-1.014902	3.355070
H	3.577323	0.837497	1.982403
H	4.490698	0.743244	4.291525
H	0.836904	-1.092635	5.665776
H	3.124611	-0.217361	6.145679

C_5Ph_4H- C_{2V}-symmetry (AM1)

HF=0.1740782
Low frequencies --- -41.5103 -36.7469 -31.9535 -29.2825

C	0.000000	1.566758	-1.330206
C	0.000000	1.148400	1.197761
C	0.000000	0.000000	2.027225
C	0.000000	-1.148400	1.197761
C	0.000000	-0.711108	-0.160581
C	0.000000	0.711108	-0.160581
C	0.000000	2.515400	1.674736
H	0.000000	0.000000	3.112563
C	0.000000	-2.515400	1.674736
C	0.000000	-1.566758	-1.330206
C	0.000000	-5.158661	2.638636
C	-1.206403	-3.190713	1.920827
C	1.206403	-3.190713	1.920827
C	1.204934	-4.499511	2.398747
C	-1.204934	-4.499511	2.398747
H	-2.156925	-2.671635	1.730107
H	2.156925	-2.671635	1.730107
H	2.157187	-5.015272	2.585664
H	-2.157187	-5.015272	2.585664
H	0.000000	-6.190756	3.013545
C	0.000000	-3.232163	-3.597468
C	1.206469	-1.992366	-1.909329
C	-1.206469	-1.992366	-1.909329
C	-1.205099	-2.816772	-3.032040

C	1.205099	-2.816772	-3.032040
H	2.157345	-1.665624	-1.463999
H	-2.157345	-1.665624	-1.463999
H	-2.157456	-3.140888	-3.474423
H	2.157456	-3.140888	-3.474423
H	0.000000	-3.882765	-4.481916
C	0.000000	3.232163	-3.597468
C	1.206469	1.992366	-1.909329
C	-1.206469	1.992366	-1.909329
C	-1.205099	2.816772	-3.032040
C	1.205099	2.816772	-3.032040
H	2.157345	1.665624	-1.463999
H	-2.157345	1.665624	-1.463999
H	-2.157456	3.140888	-3.474423
H	2.157456	3.140888	-3.474423
H	0.000000	3.882765	-4.481916
C	0.000000	5.158661	2.638636
C	1.206403	3.190713	1.920827
C	-1.206403	3.190713	1.920827
C	-1.204934	4.499511	2.398747
C	1.204934	4.499511	2.398747
H	2.156925	2.671635	1.730107
H	-2.156925	2.671635	1.730107
H	-2.157187	5.015272	2.585664
H	2.157187	5.015272	2.585664
H	0.000000	6.190756	3.013545

C_5Ph_4H- C_s-symmetry; alpha-ring (AM1)

HF=0.1691061
Low frequencies --- -40.1349 -35.1295 -31.6135 -7.7929

C	0.927350	1.804286	0.000000
C	-0.882636	-1.448617	0.000000
C	0.335467	-0.686939	0.000000
C	0.000000	0.689643	0.000000
C	-1.427385	0.796536	0.000000
C	-1.957534	-0.507144	0.000000
C	-1.067138	-2.869890	0.000000
C	1.700103	-1.180235	0.000000
H	-3.016839	-0.747073	0.000000
C	-2.207407	2.017020	0.000000
C	-1.493772	-5.675781	0.000000
C	-2.369315	-3.421633	0.000000
C	0.010040	-3.780476	0.000000
C	-0.200742	-5.154440	0.000000
C	-2.575446	-4.795468	0.000000
H	-3.239986	-2.751003	0.000000
H	1.041197	-3.397520	0.000000
H	0.662442	-5.835536	0.000000
H	-3.600944	-5.191895	0.000000
H	-1.657998	-6.760295	0.000000
C	4.361627	-2.088440	0.000000
C	2.379342	-1.412499	1.207249
C	2.379342	-1.412499	-1.207249
C	3.697845	-1.862392	-1.205271
C	3.697845	-1.862392	1.205271
H	1.855894	-1.234176	2.157892
H	1.855894	-1.234176	-2.157892

H	4.217120	-2.038306	-2.157793
H	4.217120	-2.038306	2.157793
H	5.401463	-2.441424	0.000000
C	2.715829	3.974262	0.000000
C	1.383685	2.358093	1.206730
C	1.383685	2.358093	-1.206730
C	2.269860	3.433103	-1.205162
C	2.269860	3.433103	1.205162
H	1.032398	1.931923	2.157671
H	1.032398	1.931923	-2.157671
H	2.618575	3.856191	-2.157631
H	2.618575	3.856191	2.157631
H	3.414535	4.821404	0.000000
C	-3.752898	4.366513	0.000000
C	-2.602102	2.616503	1.206751
C	-2.602102	2.616503	-1.206751
C	-3.367329	3.780694	-1.205182
C	-3.367329	3.780694	1.205182
H	-2.297276	2.155267	2.157425
H	-2.297276	2.155267	-2.157425
H	-3.667286	4.239821	-2.157615
H	-3.667286	4.239821	2.157615
H	-4.355192	5.284692	0.000000

C_5Ph_4H- C_s-symmetry; beta-ring (AM1)

HF=0.1733176
Low frequencies --- -53.2254 -39.3024 -14.4511

C	1.893233	-1.040704	0.000000
C	-0.635678	-1.509327	0.000000
C	-1.804365	-0.718332	0.000000
C	-1.419770	0.646055	0.000000
C	0.000000	0.702234	0.000000
C	0.511321	-0.639564	0.000000
C	-0.719643	-2.957431	0.000000
H	-2.825029	-1.088751	0.000000
C	-2.348801	1.757785	0.000000
C	0.720191	1.962483	0.000000
C	-4.190577	3.883374	0.000000
C	-2.819383	2.300175	1.206714
C	-2.819383	2.300175	-1.206714
C	-3.730716	3.353665	-1.205189
C	-3.730716	3.353665	1.205189
H	-2.456333	1.883377	2.157492
H	-2.456333	1.883377	-2.157492
H	-4.088394	3.769418	-2.157602
H	-4.088394	3.769418	2.157602
H	-4.908674	4.714070	0.000000
C	2.039775	4.446389	0.000000
C	1.056782	2.597023	-1.207305
C	1.056782	2.597023	1.207305
C	1.710673	3.827211	1.205211
C	1.710673	3.827211	-1.205211
H	0.796210	2.109176	-2.157891
H	0.796210	2.109176	2.157891
H	1.967143	4.311955	2.157646
H	1.967143	4.311955	-2.157646
H	2.553457	5.416911	0.000000

H	-0.737347	-3.121396	2.157728
C	-1.007602	-5.755564	0.000000
C	-0.793910	-3.672023	-1.207267
C	-0.935736	-5.057836	-1.205284
H	-0.991560	-5.603406	-2.157775
H	-1.119843	-6.847901	0.000000
C	-0.793910	-3.672023	1.207267
H	-0.737347	-3.121396	-2.157728
H	-0.991560	-5.603406	2.157775
C	-0.935736	-5.057836	1.205284
C	4.626638	-1.842869	0.000000
C	2.947448	-0.101185	0.000000
C	2.272891	-2.401246	0.000000
C	3.606633	-2.792597	0.000000
C	4.281363	-0.492808	0.000000
H	2.722530	0.974739	0.000000
H	1.501508	-3.184333	0.000000
H	3.856581	-3.863331	0.000000
H	5.070088	0.273286	0.000000
H	5.679087	-2.151683	0.000000

C_5Ph_4O C_2-symmetry (AM1)

HF=0.1987691
Low frequencies --- 15.7521

C	1.581000	-0.079317	2.558444
C	2.001782	-0.055408	0.000000
C	1.083954	-0.042617	-1.202752
C	-0.203942	0.000927	-0.747538
C	-0.203942	0.000927	0.747538
C	1.083954	-0.042617	1.202752
O	3.226815	-0.065532	0.000000
C	1.581000	-0.079317	-2.558444
C	-1.435171	0.065901	-1.518043
C	-1.435171	0.065901	1.518043
C	2.548527	-0.150495	-5.192727
C	2.822930	0.494212	-2.878751
C	0.835935	-0.695044	-3.577418
C	1.318246	-0.729582	-4.883410
C	3.298218	0.459844	-4.187305
H	3.428139	0.963376	-2.086769
H	-0.137027	-1.152877	-3.337573
H	0.724742	-1.215933	-5.671410
H	4.271238	0.914320	-4.425465
H	2.927297	-0.177046	-6.224727
C	-3.814528	0.198978	-2.986283
C	-1.872577	1.288970	-2.044990
C	-2.198881	-1.090191	-1.733268
C	-3.382526	-1.020725	-2.465375
C	-3.058579	1.351507	-2.774861
H	-1.276858	2.199546	-1.882532
H	-1.862080	-2.052088	-1.318692
H	-3.977060	-1.931318	-2.630346
H	-3.396656	2.314742	-3.184672
H	-4.749983	0.251418	-3.562222
C	-3.814528	0.198978	2.986283
C	-1.872577	1.288970	2.044990
C	-2.198881	-1.090191	1.733268

C	-3.382526	-1.020725	2.465375
C	-3.058579	1.351507	2.774861
H	-1.276858	2.199546	1.882532
H	-1.862080	-2.052088	1.318692
H	-3.977060	-1.931318	2.630346
H	-3.396656	2.314742	3.184672
H	-4.749983	0.251418	3.562222
C	2.548527	-0.150495	5.192727
C	0.835935	-0.695044	3.577418
C	2.822930	0.494212	2.878751
C	3.298218	0.459844	4.187305
C	1.318246	-0.729582	4.883410
H	-0.137027	-1.152877	3.337573
H	3.428139	0.963376	2.086769
H	4.271238	0.914320	4.425465
H	0.724742	-1.215933	5.671410
H	2.927297	-0.177046	6.224727

C_5Ph_4O C_s-symmetry (AM1)

HF=0.1989157
Low frequencies --- 19.2738

C	1.581000	-0.079317	2.558444
C	2.001782	-0.055408	0.000000
C	1.083954	-0.042617	-1.202752
C	-0.203942	0.000927	-0.747538
C	-0.203942	0.000927	0.747538
C	1.083954	-0.042617	1.202752
O	3.226815	-0.065532	0.000000
C	1.581000	-0.079317	-2.558444
C	-1.435171	0.065901	-1.518043
C	-1.435171	0.065901	1.518043
C	2.548527	-0.150495	-5.192727
C	2.822930	0.494212	-2.878751
C	0.835935	-0.695044	-3.577418
C	1.318246	-0.729582	-4.883410
C	3.298218	0.459844	-4.187305
H	3.428139	0.963376	-2.086769
H	-0.137027	-1.152877	-3.337573
H	0.724742	-1.215933	-5.671410
H	4.271238	0.914320	-4.425465
H	2.927297	-0.177046	-6.224727
C	-3.814528	0.198978	-2.986283
C	-1.872577	1.288970	-2.044990
C	-2.198881	-1.090191	-1.733268
C	-3.382526	-1.020725	-2.465375
C	-3.058579	1.351507	-2.774861
H	-1.276858	2.199546	-1.882532
H	-1.862080	-2.052088	-1.318692
H	-3.977060	-1.931318	-2.630346
H	-3.396656	2.314742	-3.184672
H	-4.749983	0.251418	-3.562222
C	-3.814528	0.198978	2.986283
C	-1.872577	1.288970	2.044990
C	-2.198881	-1.090191	1.733268
C	-3.382526	-1.020725	2.465375
C	-3.058579	1.351507	2.774861
H	-1.276858	2.199546	1.882532

H	-1.862080	-2.052088	1.318692
H	-3.977060	-1.931318	2.630346
H	-3.396656	2.314742	3.184672
H	-4.749983	0.251418	3.562222
C	2.548527	-0.150495	5.192727
C	0.835935	-0.695044	3.577418
C	2.822930	0.494212	2.878751
C	3.298218	0.459844	4.187305
C	1.318246	-0.729582	4.883410
H	-0.137027	-1.152877	3.337573
H	3.428139	0.963376	2.086769
H	4.271238	0.914320	4.425465
H	0.724742	-1.215933	5.671410
H	2.927297	-0.177046	6.224727

C_5Ph_4O C_{2v}-symmetry (AM1)

HF=0.2044654
Low frequencies --- -24.8743 -20.7126 -17.2474 -15.5558

C	0.000000	2.559303	1.568724
C	0.000000	0.000000	1.993839
C	0.000000	-1.197739	1.069529
C	0.000000	-0.749524	-0.216614
C	0.000000	0.749524	-0.216614
C	0.000000	1.197739	1.069529
O	0.000000	0.000000	3.216693
C	0.000000	-2.559303	1.568724
C	0.000000	-1.535395	-1.439704
C	0.000000	1.535395	-1.439704
C	0.000000	-5.180146	2.551300
C	-1.210501	-3.220463	1.818332
C	1.210501	-3.220463	1.818332
C	1.207015	-4.525711	2.306647
C	-1.207015	-4.525711	2.306647
H	-2.164249	-2.706163	1.630128
H	2.164249	-2.706163	1.630128
H	2.160440	-5.038395	2.501174
H	-2.160440	-5.038395	2.501174
H	0.000000	-6.209638	2.937822
C	0.000000	-3.054147	-3.790068
C	1.210533	-1.919286	-2.032289
C	-1.210533	-1.919286	-2.032289
C	-1.207075	-2.675323	-3.203157
C	1.207075	-2.675323	-3.203157
H	2.164263	-1.623651	-1.570955
H	-2.164263	-1.623651	-1.570955
H	-2.160553	-2.973787	-3.663177
H	2.160553	-2.973787	-3.663177
H	0.000000	-3.650855	-4.713858
C	0.000000	3.054147	-3.790068
C	1.210533	1.919286	-2.032289
C	-1.210533	1.919286	-2.032289
C	-1.207075	2.675323	-3.203157
C	1.207075	2.675323	-3.203157
H	2.164263	1.623651	-1.570955
H	-2.164263	1.623651	-1.570955
H	-2.160553	2.973787	-3.663177
H	2.160553	2.973787	-3.663177

H	0.000000	3.650855	-4.713858
C	0.000000	5.180146	2.551300
C	-1.210501	3.220463	1.818332
C	1.210501	3.220463	1.818332
C	1.207015	4.525711	2.306647
C	-1.207015	4.525711	2.306647
H	-2.164249	2.706163	1.630128
H	2.164249	2.706163	1.630128
H	2.160440	5.038395	2.501174
H	-2.160440	5.038395	2.501174
H	0.000000	6.209638	2.937822

C_5Ph_4O C_s-symmetry; alpha-ring (AM1)

HF=0.2032147
Low frequencies --- -48.0886 -25.1372 -15.4854

C	-2.197916	2.024206	0.000000
C	-1.929853	-0.554160	0.000000
C	-0.727400	-1.483863	0.000000
C	0.393966	-0.696981	0.000000
C	0.000000	0.747310	0.000000
C	-1.356892	0.842716	0.000000
O	-3.119786	-0.842717	0.000000
C	-3.835770	4.293904	0.000000
C	1.801077	-1.063676	0.000000
C	0.969078	1.831830	0.000000
H	-2.295734	2.149511	2.164141
C	-2.612740	2.596284	-1.210494
C	-0.847151	-2.925885	0.000000
H	-3.750430	4.170228	-2.160335
C	-3.427683	3.726855	-1.206964
C	-2.612740	2.596284	1.210494
H	-4.479670	5.185320	0.000000
H	-3.750430	4.170228	2.160335
H	-2.295734	2.149511	-2.164141
C	-3.427683	3.726855	1.206964
C	4.523684	-1.715145	0.000000
C	2.488573	-1.229123	1.211016
C	2.488573	-1.229123	-1.211016
C	3.844071	-1.553274	-1.207044
C	3.844071	-1.553274	1.207044
H	1.955011	-1.101735	2.164628
H	1.955011	-1.101735	-2.164628
H	4.377555	-1.680049	-2.160653
H	4.377555	-1.680049	2.160653
H	5.593866	-1.968681	0.000000
C	2.819888	3.930663	0.000000
C	1.435287	2.362072	1.210617
C	1.435287	2.362072	-1.210617
C	2.357305	3.407178	-1.207076
C	2.357305	3.407178	1.207076
H	1.071061	1.952590	2.164341
H	1.071061	1.952590	-2.164341
H	2.718943	3.819286	-2.160596
H	2.718943	3.819286	2.160596
H	3.547278	4.755517	0.000000
C	-1.074205	-5.740213	0.000000
C	-2.107301	-3.552339	0.000000

C	0.294060	-3.748112	0.000000
C	0.181529	-5.136040	0.000000
C	-2.216056	-4.940705	0.000000
H	-3.032320	-2.953922	0.000000
H	1.299768	-3.300358	0.000000
H	1.090968	-5.754888	0.000000
H	-3.213186	-5.405836	0.000000
H	-1.163400	-6.836032	0.000000

C_5Ph_4O C_s-symmetry; beta-ring (AM1)

HF=0.2090796
Low frequencies --- -60.8496 -22.4867

C	2.366184	1.700842	0.000000
C	1.722467	-0.803749	0.000000
C	0.396331	-1.525431	0.000000
C	-0.622740	-0.607208	0.000000
C	0.000000	0.766620	0.000000
C	1.359315	0.656045	0.000000
O	2.842640	-1.296698	0.000000
C	0.409167	-2.976545	0.000000
C	-2.050869	-0.879608	0.000000
C	-0.694769	2.046554	0.000000
C	0.540323	-5.773781	0.000000
C	0.444641	-3.683627	1.210949
C	0.444641	-3.683627	-1.210949
C	0.508657	-5.075726	-1.207027
C	0.508657	-5.075726	1.207027
H	0.427141	-3.135505	2.164489
H	0.427141	-3.135505	-2.164489
H	0.538388	-5.623310	-2.160547
H	0.538388	-5.623310	2.160547
H	0.595242	-6.872108	0.000000
C	3.841531	3.195791	1.206975
H	4.228663	3.584258	2.160337
H	5.103828	4.476499	0.000000
H	2.482130	1.809281	-2.164007
C	4.331342	3.693879	0.000000
C	2.863898	2.202559	1.210604
H	4.228663	3.584258	-2.160337
H	2.482130	1.809281	2.164007
C	2.863898	2.202559	-1.210604
C	3.841531	3.195791	-1.206975
C	-1.930757	4.557988	0.000000
C	-1.004619	2.681854	-1.211381
C	-1.004619	2.681854	1.211381
C	-1.621765	3.931646	1.207068
C	-1.621765	3.931646	-1.207068
H	-0.757776	2.191736	-2.164855
H	-0.757776	2.191736	2.164855
H	-1.860993	4.425182	2.160662
H	-1.860993	4.425182	-2.160662
H	-2.414634	5.545688	0.000000
C	-4.822449	-1.466298	0.000000
C	-2.521568	-2.207003	0.000000
C	-3.015641	0.142224	0.000000
C	-4.378584	-0.145740	0.000000
C	-3.883680	-2.495779	0.000000

H	-1.814682	-3.050988	0.000000
H	-2.718757	1.201020	0.000000
H	-5.105988	0.679761	0.000000
H	-4.215474	-3.544808	0.000000
H	-5.898303	-1.692789	0.000000

C_5Ph_4O TS-1 (AM1)

HF=0.2013279
Low frequencies --- -22.8020

C	0.036116	-1.993235	-0.043686
O	0.058305	-3.216769	-0.074712
C	-1.180757	-1.094760	-0.030258
C	1.219595	-1.051811	-0.007397
C	-2.527628	-1.620476	-0.081871
C	-0.752519	0.200210	0.018989
C	0.744490	0.227217	0.026118
C	2.585125	-1.529710	-0.013827
C	-3.548594	-0.896427	-0.716430
C	-2.827432	-2.867679	0.487522
C	-1.552407	1.413168	0.055749
C	1.499731	1.468527	0.060780
C	3.395479	-1.354441	-1.146176
C	3.110951	-2.191747	1.106216
C	-4.124130	-3.373481	0.428594
C	-4.843291	-1.407584	-0.772129
H	-3.321368	0.079075	-1.173145
H	-2.031475	-3.449824	0.976910
C	-2.177608	1.811438	1.245619
C	-1.702172	2.196957	-1.096990
C	1.576037	2.217329	1.243589
C	2.159910	1.926225	-1.088115
C	4.423540	-2.658247	1.095546
C	4.707344	-1.823188	-1.150699
H	2.988541	-0.849523	-2.035781
H	2.479699	-2.343249	1.995256
C	-5.134586	-2.645389	-0.199419
H	-4.348832	-4.352011	0.877845
H	-5.636300	-0.831766	-1.271450
C	-2.468814	3.360077	-1.057382
C	-2.940469	2.977389	1.279037
H	-2.066353	1.199561	2.153214
H	-1.211901	1.891792	-2.033353
C	2.879782	3.119153	-1.053145
C	2.300034	3.407770	1.272459
H	1.061845	1.863033	2.149320
H	2.110197	1.339711	-2.017648
C	5.224584	-2.473972	-0.031046
H	4.826213	-3.175006	1.979043
H	5.334429	-1.680582	-2.043036
H	-6.157192	-3.047195	-0.244979
C	-3.087790	3.752706	0.129244
H	-2.582521	3.970058	-1.965636
H	-3.427827	3.284221	2.216180
C	2.951303	3.861083	0.125505
H	3.393961	3.473223	-1.958770
H	2.356634	3.989743	2.204144
H	6.260324	-2.843355	-0.037635

H	-3.690507	4.672170	0.158064
H	3.521025	4.801450	0.150768

$C_5Ph_4H_2$ C_2-symmetry (AM1)

HF=0.2225989
Low frequencies --- 20.4361

C	0.022661	-2.538399	1.680645
C	0.000000	0.000000	2.102128
C	0.000000	1.187726	1.167290
C	0.001677	0.739775	-0.128897
C	-0.001677	-0.739775	-0.128897
C	0.000000	-1.187726	1.167290
H	0.107400	-6.177101	3.103874
C	-0.022661	2.538399	1.680645
C	0.020032	1.525870	-1.352353
C	-0.020032	-1.525870	-1.352353
C	-0.084403	5.153365	2.703482
C	0.576055	2.838136	2.915937
C	-0.654122	3.570274	0.968406
C	-0.684210	4.866387	1.477990
C	0.546136	4.135769	3.419693
H	1.077890	2.043485	3.487720
H	-1.126316	3.347091	-0.002035
H	-1.182842	5.664704	0.908747
H	1.022513	4.357897	4.385895
H	-0.107400	6.177101	3.103874
C	0.062852	3.024051	-3.718539
C	-1.157633	1.722894	-2.087458
C	1.219023	2.087584	-1.813252
C	1.237110	2.832432	-2.991243
C	-1.133196	2.468607	-3.264516
H	-2.101235	1.281811	-1.733631
H	2.146576	1.939090	-1.240758
H	2.181881	3.269218	-3.346620
H	-2.060643	2.616330	-3.836921
H	0.079955	3.610586	-4.648438
C	-0.062852	-3.024051	-3.718539
C	-1.219023	-2.087584	-1.813252
C	1.157633	-1.722894	-2.087458
C	1.133196	-2.468607	-3.264516
C	-1.237110	-2.832432	-2.991243
H	-2.146576	-1.939090	-1.240758
H	2.101235	-1.281811	-1.733631
H	2.060643	-2.616330	-3.836921
H	-2.181881	-3.269218	-3.346620
H	-0.079955	-3.610586	-4.648438
C	0.084403	-5.153365	2.703482
C	0.654122	-3.570274	0.968406
C	-0.576055	-2.838136	2.915937
C	-0.546136	-4.135769	3.419693
C	0.684210	-4.866387	1.477990
H	1.126316	-3.347091	-0.002035
H	-1.077890	-2.043485	3.487720
H	-1.022513	-4.357897	4.385895
H	1.182842	-5.664704	0.908747
H	0.910361	-0.009856	2.752673
H	-0.910361	0.009856	2.752673

$C_5Ph_4H_2$ C_s-symmetry (AM1)

HF=0.2226959
Low frequencies --- 20.6406

C	1.679995	-0.071474	2.538333
C	2.101579	-0.044208	0.000000
C	1.166967	-0.031152	-1.187974
C	-0.128518	0.009059	-0.739766
C	-0.128518	0.009059	0.739766
C	1.166967	-0.031152	1.187974
H	3.102745	-0.205263	6.176247
C	1.679995	-0.071474	-2.538333
C	-1.351809	0.067789	-1.524275
C	-1.351809	0.067789	1.524275
C	2.702471	-0.168600	-5.152891
C	2.935724	0.483664	-2.837388
C	0.947575	-0.678089	-3.571057
C	1.456821	-0.725617	-4.866827
C	3.439321	0.436391	-4.134475
H	3.524742	0.964357	-2.042369
H	-0.038547	-1.117247	-3.349184
H	0.871198	-1.204253	-5.665546
H	4.421733	0.878788	-4.355723
H	3.102745	-0.205263	-6.176247
C	-3.717138	0.187345	-3.019499
C	-1.797736	1.289627	-2.047073
C	-2.102206	-1.093619	-1.757367
C	-3.278433	-1.031301	-2.502028
C	-2.975519	1.345790	-2.790553
H	-1.214499	2.205110	-1.868576
H	-1.760812	-2.054337	-1.344087
H	-3.862340	-1.946308	-2.679121
H	-3.319492	2.308478	-3.196303
H	-4.646526	0.234548	-3.605197
C	-3.717138	0.187345	3.019499
C	-1.797736	1.289627	2.047073
C	-2.102206	-1.093619	1.757367
C	-3.278433	-1.031301	2.502028
C	-2.975519	1.345790	2.790553
H	-1.214499	2.205110	1.868576
H	-1.760812	-2.054337	1.344087
H	-3.862340	-1.946308	2.679121
H	-3.319492	2.308478	3.196303
H	-4.646526	0.234548	3.605197
C	2.702471	-0.168600	5.152891
C	0.947575	-0.678089	3.571057
C	2.935724	0.483664	2.837388
C	3.439321	0.436391	4.134475
C	1.456821	-0.725617	4.866827
H	-0.038547	-1.117247	3.349184
H	3.524742	0.964357	2.042369
H	4.421733	0.878788	4.355723
H	0.871198	-1.204253	5.665546
H	2.742885	-0.960564	0.000000
H	2.761037	0.860295	0.000000

$C_5Ph_4H_2$ C_{2v}-symmetry (AM1)

HF=0.2266833
Low frequencies --- -25.9986 -24.9050 -13.4358 -5.2619

C	0.000000	2.539903	1.668719
C	0.000000	0.000000	2.095000
C	0.000000	-1.183134	1.154920
C	0.000000	-0.741362	-0.138704
C	0.000000	0.741362	-0.138704
C	0.000000	1.183134	1.154920
H	0.000000	6.169099	3.096410
C	0.000000	-2.539903	1.668719
C	0.000000	-1.541606	-1.352908
C	0.000000	1.541606	-1.352908
C	0.000000	-5.145521	2.694681
C	-1.209845	-3.198430	1.928151
C	1.209845	-3.198430	1.928151
C	1.206878	-4.495291	2.438426
C	-1.206878	-4.495291	2.438426
H	-2.163015	-2.688982	1.723885
H	2.163015	-2.688982	1.723885
H	2.160220	-5.006396	2.637446
H	-2.160220	-5.006396	2.637446
H	0.000000	-6.169099	3.096410
C	0.000000	-3.087250	-3.688061
C	1.209684	-1.932412	-1.942957
C	-1.209684	-1.932412	-1.942957
C	-1.206801	-2.701422	-3.105260
C	1.206801	-2.701422	-3.105260
H	2.163029	-1.629229	-1.486026
H	-2.163029	-1.629229	-1.486026
H	-2.160088	-3.003837	-3.562685
H	2.160088	-3.003837	-3.562685
H	0.000000	-3.693943	-4.605032
C	0.000000	3.087250	-3.688061
C	1.209684	1.932412	-1.942957
C	-1.209684	1.932412	-1.942957
C	-1.206801	2.701422	-3.105260
C	1.206801	2.701422	-3.105260
H	2.163029	1.629229	-1.486026
H	-2.163029	1.629229	-1.486026
H	-2.160088	3.003837	-3.562685
H	2.160088	3.003837	-3.562685
H	0.000000	3.693943	-4.605032
C	0.000000	5.145521	2.694681
C	-1.209845	3.198430	1.928151
C	1.209845	3.198430	1.928151
C	1.206878	4.495291	2.438426
C	-1.206878	4.495291	2.438426
H	-2.163015	2.688982	1.723885
H	2.163015	2.688982	1.723885
H	2.160220	5.006396	2.637446
H	-2.160220	5.006396	2.637446
H	-0.909587	0.000000	2.746164
H	0.909587	0.000000	2.746164

$C_5Ph_4H_2$ C_s-symmetry; alpha-ring (AM1)

HF=0.2250493
Low frequencies --- -28.3126 -21.6082 -14.8273

C	-2.116433	2.149769	0.000000
C	-2.046925	-0.423400	0.000000
C	-0.902697	-1.417344	0.000000
C	0.283776	-0.726985	0.000000
C	0.000000	0.727426	0.000000
C	-1.353046	0.916057	0.000000
H	-1.986786	-6.668010	0.000000
C	-3.620397	4.511876	0.000000
C	1.647314	-1.232775	0.000000
C	1.036869	1.747644	0.000000
H	-2.199321	2.285293	2.163151
C	-2.496652	2.746611	-1.209897
C	-1.175092	-2.836751	0.000000
H	-3.537752	4.386164	-2.160222
C	-3.244818	3.922453	-1.206877
C	-2.496652	2.746611	1.209897
H	-4.209936	5.440073	0.000000
H	-3.537752	4.386164	2.160222
H	-2.199321	2.285293	-2.163151
C	-3.244818	3.922453	1.206877
C	4.287890	-2.167252	0.000000
C	2.314894	-1.469710	1.210197
C	2.314894	-1.469710	-1.210197
C	3.628835	-1.934443	-1.206768
C	3.628835	-1.934443	1.206768
H	1.798071	-1.284517	2.163429
H	1.798071	-1.284517	-2.163429
H	4.146429	-2.115343	-2.160224
H	4.146429	-2.115343	2.160224
H	5.325354	-2.531626	0.000000
C	3.023798	3.721061	0.000000
C	1.538858	2.246655	1.209692
C	1.538858	2.246655	-1.209692
C	2.527577	3.228778	-1.206822
C	2.527577	3.228778	1.206822
H	1.149803	1.860174	2.163098
H	1.149803	1.860174	-2.163098
H	2.916542	3.615314	-2.160091
H	2.916542	3.615314	2.160091
H	3.804032	4.495755	0.000000
C	-1.758718	-5.592551	0.000000
C	-2.506536	-3.294391	0.000000
C	-0.145764	-3.791377	0.000000
C	-0.436108	-5.154296	0.000000
C	-2.792809	-4.656009	0.000000
H	-3.337147	-2.572649	0.000000
H	0.906041	-3.464030	0.000000
H	0.386187	-5.885090	0.000000
H	-3.839610	-4.993931	0.000000
H	-2.685363	-0.541506	-0.911285
H	-2.685363	-0.541506	0.911285

$C_5Ph_4H_2$ C_s-symmetry; beta-ring (AM1)

HF=0.2312708
Low frequencies --- -60.2759 -29.5981

C	2.286004	1.862990	0.000000
C	1.885863	-0.672851	0.000000
C	0.620337	-1.497473	0.000000
C	-0.486398	-0.680298	0.000000
C	0.000000	0.729373	0.000000
C	1.368663	0.737981	0.000000
H	-5.629629	-2.284227	0.000000
C	0.784273	-2.940166	0.000000
C	-1.881022	-1.096221	0.000000
C	-0.802549	1.944802	0.000000
C	1.223810	-5.706613	0.000000
C	0.896538	-3.639833	1.210474
C	0.896538	-3.639833	-1.210474
C	1.114103	-5.016386	-1.206931
C	1.114103	-5.016386	1.206931
H	0.809389	-3.097064	2.163382
H	0.809389	-3.097064	-2.163382
H	1.199832	-5.558158	-2.160390
H	1.199832	-5.558158	2.160390
H	1.396880	-6.792571	0.000000
C	3.641338	3.468920	1.206860
H	3.993608	3.889326	2.160200
H	4.799653	4.844747	0.000000
H	2.386943	1.985766	-2.163131
C	4.091652	4.003420	0.000000
C	2.742840	2.403514	1.209898
H	3.993608	3.889326	-2.160200
H	2.386943	1.985766	2.163131
C	2.742840	2.403514	-1.209898
C	3.641338	3.468920	-1.206860
C	-2.258005	4.338217	0.000000
C	-1.169435	2.551073	-1.210420
C	-1.169435	2.551073	1.210420
C	-1.894556	3.741229	1.206882
C	-1.894556	3.741229	-1.206882
H	-0.882161	2.083079	-2.163562
H	-0.882161	2.083079	2.163562
H	-2.178040	4.210801	2.160239
H	-2.178040	4.210801	-2.160239
H	-2.827823	5.278638	0.000000
C	-4.581697	-1.952877	0.000000
C	-2.218845	-2.462736	0.000000
C	-2.941524	-0.174691	0.000000
C	-4.269689	-0.595277	0.000000
C	-3.545878	-2.884535	0.000000
H	-1.432053	-3.231997	0.000000
H	-2.747309	0.907684	0.000000
H	-5.074626	0.154603	0.000000
H	-3.772825	-3.960900	0.000000
H	2.504346	-0.881978	0.909171
H	2.504346	-0.881978	-0.909171

$C_5Ph_4H_2$ TS-1 (AM1)

HF=0.224236
Low frequencies --- -26.2157

C	-2.494617	-1.735071	-0.072998
C	-1.158365	-1.185305	-0.039945
C	-3.545616	-1.042353	-0.694336
C	-2.759918	-2.987880	0.505243
C	0.053787	-2.088940	-0.046425
C	-0.745146	0.121968	-0.018856
C	-4.042856	-3.527285	0.466210
C	-4.827009	-1.587435	-0.733598
H	-3.349656	-0.059014	-1.151672
H	-1.949367	-3.545848	0.997087
C	1.212392	-1.120001	-0.044813
C	0.736305	0.162616	-0.020672
C	-1.563753	1.323595	0.012486
C	-5.079923	-2.829745	-0.153476
H	-4.237886	-4.507083	0.926398
H	-5.640619	-1.032984	-1.224107
H	0.067155	-2.737989	-0.957394
H	0.085716	-2.741033	0.862697
H	-6.092031	-3.258230	-0.183882
C	2.575208	-1.614666	-0.028771
C	1.497652	1.398705	0.033169
C	-2.115764	1.770989	1.221216
C	-1.802195	2.050997	-1.162303
C	3.384776	-1.532398	-1.169775
C	3.088486	-2.207022	1.134575
C	1.356071	2.263811	1.128399
C	2.382575	1.742006	-0.998063
C	-2.580973	3.206235	-1.125641
C	-2.895063	2.926221	1.251085
H	-1.932460	1.205296	2.146768
H	-1.368003	1.708546	-2.113278
C	4.391191	-2.700498	1.155258
C	4.686427	-2.030475	-1.144431
H	2.988405	-1.076957	-2.089385
H	2.458595	-2.274415	2.033939
C	3.114321	2.926387	-0.932107
C	2.093105	3.444186	1.192020
H	0.650848	2.007298	1.933708
H	2.499986	1.070348	-1.861410
C	-3.128706	3.645484	0.079424
H	-2.761076	3.773076	-2.050824
H	-3.325717	3.270090	2.202911
C	5.192356	-2.613456	0.016783
H	4.787864	-3.158472	2.073227
H	5.315182	-1.961623	-2.044258
C	2.973327	3.778038	0.162774
H	3.805527	3.187301	-1.746711
H	1.977625	4.114493	2.056227
H	-3.742278	4.557568	0.105760
H	6.220363	-3.003264	0.035256
H	3.553371	4.710648	0.214338

Table C.1. Energies (a.u.) of the Principal Stationary Points on the *Rigid* Potentail Energy Surface (RHF level of theory) of the C_6Ph_6 Rearrangement, M_0 (90°) to M_1 (180°).

Dihedral Angle	*E* (a.u.)					
	RHF/ STO-3G	RHF/ 3-21G	RHF/ 3-21G*	RHF/ 6-31G(d)	RHF/ 6-31G(d,p)	RHF/ cc-pVDZ
90	-1588.40	-1598.99	-1598.99	-1607.96	-1608.01	-1608.08
100	-1588.39	-1598.99	-1598.99	-1607.95	-1608.01	-1608.08
110	-1588.38	-1598.97	-1598.97	-1607.94	-1608.00	-1608.06
120	-1588.35	-1598.95	-1598.95	-1607.92	-1607.97	-1608.04
130	-1588.32	-1598.91	-1598.91	-1607.88	-1607.94	-1608.01
140	-1588.26	-1598.86	-1598.86	-1607.83	-1607.89	-1607.96
150	-1588.19	-1598.80	-1598.80	-1607.76	-1607.82	-1607.89
160	-1588.09	-1598.70	-1598.70	-1607.68	-1607.73	-1607.80
170	-1587.95	-1598.58	-1598.58	-1607.56	-1607.62	-1607.69
180	-1587.77	n.a.	n.a.	-1607.41	-1607.47	-1607.54

Table C.2. Relative Energies (kcal mol^{-1}) of the Principal Stationary Points on the *Rigid* Potential Energy Surface (RHF level of theory) of the C_6Ph_6 Rearrangement, M_0 (90°) to M_1 (180°).

Dihedral Angle	ΔE (kcal mol^{-1})					
	RHF/ STO-3G	RHF/ 3-21G	RHF/ 3-21G*	RHF/ 6-31G(d)	RHF/ 6-31G(d,p)	RHF/ cc-pVDZ
90	0.00	0.00	0.00	0.00	0.00	0.00
100	2.77	2.69	2.69	2.57	2.57	2.56
110	11.38	10.93	10.93	10.57	10.55	10.50
120	26.76	25.37	25.37	24.84	24.79	24.65
130	50.58	47.35	47.35	46.88	46.79	46.47
140	84.98	78.73	78.73	78.56	78.38	77.80
150	132.34	121.59	121.59	121.54	121.18	120.23
160	195.51	178.95	178.95	177.00	176.36	174.95
170	279.51	255.59	255.63	248.17	247.32	245.31
180	395.21	n.a.	n.a.	341.13	340.17	337.22

Table C.3. Energies (Hartrees) of the Principal Stationary Points on the *Rigid* Potential Energy Surface (HDFT level of theory) of the C_6Ph_6 Rearrangement, M_0 (90°) to M_1 (180°).

Dihedral Angle	*E* (a.u.)						
	AM1	B3PW91/ STO-3G	B3PW91/ 3-21G	B3PW91/ 3-21G*	B3PW91/ 6-31G(d)	B3PW91/ 6-31G(d,p)	B3PW91/ cc-pVDZ
90	0.32280	-1598.34	-1609.04	-1609.04	-1617.93	-1617.97	-1618.04
100	0.32614	-1598.34	-1609.03	-1609.03	-1617.93	-1617.97	-1618.03
110	0.33638	-1598.33	-1609.02	-1609.02	-1617.91	-1617.96	-1618.02
120	0.35453	-1598.31	-1609.00	-1609.00	-1617.90	-1617.94	-1618.01
130	0.38338	-1598.27	-1608.98	-1608.98	-1617.87	-1617.91	-1617.98
140	0.42666	-1598.23	-1608.94	-1608.94	-1617.83	-1617.87	-1617.94
150	0.48660	-1598.17	-1608.88	-1608.88	-1617.77	-1617.82	-1617.88
160	0.56283	-1598.08	-1608.80	-1608.80	-1617.69	-1617.74	-1617.81
170	0.65395	-1597.96	-1608.70	-1608.70	-1617.60	-1617.64	-1617.71
180	0.74127	-1597.94	-1608.68	-1608.68	-1617.61	-1617.66	-1617.72

Table C.4. Relative Energies (kcal mol^{-1}) of the Principal Stationary Points on the *Rigid* Potentail Energy Surface (semi-empirical and HDFT levels of theory) of the C_6Ph_6 Rearrangement: M_0 (90°) to M_1 (180°).

Dihedral Angle	ΔE (kcal mol^{-1})						
	AM1	B3PW91/ STO-3G	B3PW91/ 3-21G	B3PW91/ 3-21G*	B3PW91/ 6-31G(d)	B3PW91/ 6-31G(d,p)	B3PW91/ cc-pVDZ
90	0.00	0.00	0.00	0.00	0.00	0.00	0.00
100	2.10	2.33	2.16	2.16	2.11	2.11	2.14
110	8.52	9.54	8.77	8.77	8.67	8.63	8.75
120	19.91	22.38	20.36	20.36	20.34	20.26	20.41
130	38.01	42.14	38.07	38.07	38.38	38.21	38.26
140	65.17	70.65	63.52	63.52	64.38	64.04	63.85
150	102.79	110.35	98.83	98.83	100.01	99.43	98.93
160	150.62	164.47	147.22	147.22	146.83	145.95	145.19
170	207.80	237.97	212.78	212.78	207.91	206.80	205.71
180	262.59	253.65	222.37	222.37	200.22	199.41	197.56

Table C.5. Energies (Hartrees and kcal mol^{-1}) of the Principal Stationary Points on the *Relaxed* Potentail Energy Surface (AM1 Hamiltonian) of the C_6Ph_6 Rearrangement: M_0 (90°) to M_1 (180°).

Dihedral Angle	E (a.u.)	ΔE (kcal mol^{-1})
90	0.3148022	0.00
100	0.3148333	0.02
110	0.3149271	0.08
120	0.3151861	0.24
130	0.3160454	0.78
140	0.3179663	1.99
150	0.3213582	4.11
160	0.3263375	7.24
170	0.3325743	11.15
180	0.3381831	14.67

C_6Ph_6, D_6-symmetry (AM1)

HF=0.3147954

6	0.000000	2.876592	0.000000
6	0.000000	1.406126	0.000000
6	0.000000	-1.406126	0.000000
6	1.217741	0.703063	0.000000
6	-1.217741	0.703063	0.000000
6	-1.217741	-0.703063	0.000000
6	1.217741	-0.703063	0.000000
6	2.491202	1.438296	0.000000
6	-2.491202	1.438296	0.000000
6	-2.491202	-1.438296	0.000000
6	2.491202	-1.438296	0.000000
6	0.000000	-2.876592	0.000000
6	0.000000	5.676416	0.000000
6	-0.005138	3.583670	1.209491
6	0.005138	3.583670	-1.209491
6	0.005171	4.977589	-1.206741
6	-0.005171	4.977589	1.206741
1	-0.009292	3.035018	2.162742
1	0.009292	3.035018	-2.162742
1	0.009302	5.525785	-2.160070
1	-0.009302	5.525785	2.160070
1	0.000000	6.775934	0.000000
6	-4.915920	2.838208	0.000000
6	-3.106118	1.787386	1.209491
6	-3.100981	1.796285	-1.209491
6	-4.308133	2.493273	-1.206741
6	-4.313304	2.484316	1.206741
1	-2.633048	1.509462	2.162742
1	-2.623756	1.525556	-2.162742
1	-4.780820	2.770948	-2.160070
1	-4.790121	2.754837	2.160070
1	-5.868131	3.387967	0.000000
6	-4.915920	-2.838208	0.000000
6	-3.106118	-1.787386	-1.209491
6	-3.100981	-1.796285	1.209491
6	-4.308133	-2.493273	1.206741
6	-4.313304	-2.484316	-1.206741
1	-2.633048	-1.509462	-2.162742
1	-2.623756	-1.525556	2.162742
1	-4.780820	-2.770948	2.160070
1	-4.790121	-2.754837	-2.160070
1	-5.868131	-3.387967	0.000000
6	4.915920	2.838208	0.000000
6	3.100981	1.796285	1.209491
6	3.106118	1.787386	-1.209491
6	4.313304	2.484316	-1.206741
6	4.308133	2.493273	1.206741
1	2.623756	1.525556	2.162742
1	2.633048	1.509462	-2.162742
1	4.790121	2.754837	-2.160070
1	4.780820	2.770948	2.160070
1	5.868131	3.387967	0.000000
6	0.000000	-5.676416	0.000000
6	-0.005138	-3.583670	-1.209491

6	0.005138	-3.583670	1.209491
6	0.005171	-4.977589	1.206741
6	-0.005171	-4.977589	-1.206741
1	-0.009292	-3.035018	-2.162742
1	0.009292	-3.035018	2.162742
1	0.009302	-5.525785	2.160070
1	-0.009302	-5.525785	-2.160070
1	0.000000	-6.775934	0.000000
6	4.915920	-2.838208	0.000000
6	3.106118	-1.787386	1.209491
6	3.100981	-1.796285	-1.209491
6	4.308133	-2.493273	-1.206741
6	4.313304	-2.484316	1.206741
1	2.633048	-1.509462	2.162742
1	2.623756	-1.525556	-2.162742
1	4.780820	-2.770948	-2.160070
1	4.790121	-2.754837	2.160070
1	5.868131	-3.387967	0.000000

C_6Ph_6-M_0, D_{6h}-symmetry (AM1)

HF= 0.3147964

6	0.000000	1.405895	0.000000
6	1.217541	0.702947	0.000000
6	1.217541	-0.702947	0.000000
6	0.000000	-1.405895	0.000000
6	-1.217541	-0.702947	0.000000
6	-1.217541	0.702947	0.000000
6	0.000000	2.876617	0.000000
6	2.491223	1.438308	0.000000
6	2.491223	-1.438308	0.000000
6	0.000000	-2.876617	0.000000
6	-2.491223	-1.438308	0.000000
6	-2.491223	1.438308	0.000000
6	0.000000	3.583731	1.209459
6	3.103602	1.791865	1.209459
6	3.103602	-1.791865	1.209459
6	0.000000	-3.583731	1.209459
6	-3.103602	-1.791865	1.209459
6	-3.103602	1.791865	-1.209459
6	0.000000	3.583731	-1.209459
6	3.103602	1.791865	-1.209459
6	3.103602	-1.791865	-1.209459
6	0.000000	-3.583731	-1.209459
6	-3.103602	-1.791865	-1.209459
6	-3.103602	1.791865	1.209459
6	0.000000	4.977500	1.206588
6	4.310642	2.488750	1.206588
6	4.310642	-2.488750	1.206588
6	0.000000	-4.977500	1.206588
6	-4.310642	-2.488750	1.206588
6	-4.310642	2.488750	-1.206588
6	0.000000	4.977500	-1.206588
6	4.310642	2.488750	-1.206588
6	4.310642	-2.488750	-1.206588
6	0.000000	-4.977500	-1.206588
6	-4.310642	-2.488750	-1.206588

6	-4.310642	2.488750	1.206588
6	0.000000	5.676318	0.000000
6	4.915836	2.838159	0.000000
6	4.915836	-2.838159	0.000000
6	0.000000	-5.676318	0.000000
6	-4.915836	-2.838159	0.000000
6	-4.915836	2.838159	0.000000
1	0.000000	3.035207	2.162817
1	2.628566	1.517604	2.162817
1	2.628566	-1.517604	2.162817
1	0.000000	-3.035207	2.162817
1	-2.628566	-1.517604	2.162817
1	-2.628566	1.517604	-2.162817
1	0.000000	3.035207	-2.162817
1	2.628566	1.517604	-2.162817
1	2.628566	-1.517604	-2.162817
1	0.000000	-3.035207	-2.162817
1	-2.628566	-1.517604	-2.162817
1	-2.628566	1.517604	2.162817
1	0.000000	5.525684	2.159948
1	4.785382	2.762842	2.159948
1	4.785382	-2.762842	2.159948
1	0.000000	-5.525684	2.159948
1	-4.785382	-2.762842	2.159948
1	-4.785382	2.762842	-2.159948
1	0.000000	5.525684	-2.159948
1	4.785382	2.762842	-2.159948
1	4.785382	-2.762842	-2.159948
1	0.000000	-5.525684	-2.159948
1	-4.785382	-2.762842	-2.159948
1	-4.785382	2.762842	2.159948
1	0.000000	6.775824	0.000000
1	5.868036	3.387912	0.000000
1	5.868036	-3.387912	0.000000
1	0.000000	-6.775824	0.000000
1	-5.868036	-3.387912	0.000000
1	-5.868036	3.387912	0.000000

C_6Ph_6-M_1, C_{2v}-symmetry (AM1)

HF= 0.3421427

6	0.000000	0.000000	1.590554
6	0.000000	1.205403	0.836898
6	0.000000	-1.205403	0.836898
6	0.000000	1.201387	-0.575048
6	0.000000	-1.201387	-0.575048
6	0.000000	0.000000	-1.292304
6	0.000000	0.000000	3.073966
6	0.000000	2.572178	1.390594
6	0.000000	-2.572178	1.390594
6	1.211616	3.246479	1.609402
6	-1.211616	3.246479	1.609402
6	1.211616	-3.246479	1.609402
6	-1.211616	-3.246479	1.609402
6	1.207143	4.563910	2.064052
6	-1.207143	4.563910	2.064052
6	1.207143	-4.563910	2.064052
6	-1.207143	-4.563910	2.064052

6	0.000000	5.223656	2.293716
6	0.000000	-5.223656	2.293716
6	0.000000	0.000000	5.948725
6	0.000000	1.191076	5.231139
6	0.000000	-1.191076	5.231139
6	0.000000	1.184083	3.837377
6	0.000000	-1.184083	3.837377
6	0.000000	2.468413	-1.327093
6	0.000000	-2.468413	-1.327093
6	0.000000	0.000000	-2.762018
6	1.209497	3.068759	-1.701572
6	-1.209497	3.068759	-1.701572
6	1.209497	-3.068759	-1.701572
6	-1.209497	-3.068759	-1.701572
6	1.206667	4.252358	-2.437658
6	-1.206667	4.252358	-2.437658
6	1.206667	-4.252358	-2.437658
6	-1.206667	-4.252358	-2.437658
6	0.000000	4.845783	-2.806979
6	0.000000	-4.845783	-2.806979
6	1.209635	0.000000	-3.469193
6	-1.209635	0.000000	-3.469193
6	1.206823	0.000000	-4.863005
6	-1.206823	0.000000	-4.863005
6	0.000000	0.000000	-5.561972
1	2.164270	2.729438	1.422683
1	-2.164270	2.729438	1.422683
1	2.164270	-2.729438	1.422683
1	-2.164270	-2.729438	1.422683
1	2.160346	5.084733	2.237017
1	-2.160346	5.084733	2.237017
1	2.160346	-5.084733	2.237017
1	-2.160346	-5.084733	2.237017
1	0.000000	6.263983	2.649826
1	0.000000	-6.263983	2.649826
1	0.000000	0.000000	7.047211
1	0.000000	2.155050	5.761916
1	0.000000	-2.155050	5.761916
1	0.000000	2.181330	3.383057
1	0.000000	-2.181330	3.383057
1	2.162622	2.602594	-1.411531
1	-2.162622	2.602594	-1.411531
1	2.162622	-2.602594	-1.411531
1	-2.162622	-2.602594	-1.411531
1	2.160045	4.717292	-2.727923
1	-2.160045	4.717292	-2.727923
1	2.160045	-4.717292	-2.727923
1	-2.160045	-4.717292	-2.727923
1	0.000000	5.778800	-3.388654
1	0.000000	-5.778800	-3.388654
1	2.162857	0.000000	-2.920437
1	-2.162857	0.000000	-2.920437
1	2.160245	0.000000	-5.411059
1	-2.160245	0.000000	-5.411059
1	0.000000	0.000000	-6.661479

C_6Ph_6-M_3, C_{2v}-symmetry (AM1)

HF=0.3836412

6	0.000000	2.583887	1.584308
6	0.000000	1.270777	0.872836
6	0.000000	-1.232258	-0.542280
6	0.000000	1.232258	-0.542280
6	0.000000	0.000000	1.532483
6	0.000000	-1.270777	0.872836
6	0.000000	0.000000	-1.215762
6	0.000000	2.370494	-1.482144
6	0.000000	0.000000	3.000019
6	0.000000	-2.583887	1.584308
6	0.000000	0.000000	-2.693937
6	0.000000	-2.370494	-1.482144
6	0.000000	5.177013	2.872217
6	0.000000	2.755092	2.982934
6	0.000000	3.806651	0.877813
6	0.000000	5.059404	1.487269
6	0.000000	4.001323	3.611225
1	0.000000	1.933306	3.704071
1	0.000000	3.866048	-0.214856
1	0.000000	5.961019	0.856153
1	0.000000	4.041887	4.711171
1	0.000000	6.159995	3.361854
6	0.000000	-5.177013	2.872217
6	0.000000	-3.806651	0.877813
6	0.000000	-2.755092	2.982934
6	0.000000	-4.001323	3.611225
6	0.000000	-5.059404	1.487269
1	0.000000	-3.866048	-0.214856
1	0.000000	-1.933306	3.704071
1	0.000000	-4.041887	4.711171
1	0.000000	-5.961019	0.856153
1	0.000000	-6.159995	3.361854
6	0.000000	0.000000	5.796833
6	1.217489	0.000000	3.706623
6	-1.217489	0.000000	3.706623
6	-1.209013	0.000000	5.100831
6	1.209013	0.000000	5.100831
1	2.168567	0.000000	3.154945
1	-2.168567	0.000000	3.154945
1	-2.160845	0.000000	5.652473
1	2.160845	0.000000	5.652473
1	0.000000	0.000000	6.896683
6	0.000000	-4.414322	-3.398031
6	1.212152	-2.878338	-1.977609
6	-1.212152	-2.878338	-1.977609
6	-1.207198	-3.900328	-2.925136
6	1.207198	-3.900328	-2.925136
1	2.164574	-2.468492	-1.610744
1	-2.164574	-2.468492	-1.610744
1	-2.160256	-4.297528	-3.304212
1	2.160256	-4.297528	-3.304212
1	0.000000	-5.219397	-4.146964
6	0.000000	4.414322	-3.398031
6	1.212152	2.878338	-1.977609
6	-1.212152	2.878338	-1.977609
6	-1.207198	3.900328	-2.925136
6	1.207198	3.900328	-2.925136
1	2.164574	2.468492	-1.610744
1	-2.164574	2.468492	-1.610744

1	-2.160256	4.297528	-3.304212
1	2.160256	4.297528	-3.304212
1	0.000000	5.219397	-4.146964
6	0.000000	0.000000	-5.494903
6	-1.209594	0.000000	-3.401954
6	1.209594	0.000000	-3.401954
6	1.206807	0.000000	-4.795809
6	-1.206807	0.000000	-4.795809
1	-2.162512	0.000000	-2.852642
1	2.162512	0.000000	-2.852642
1	2.160271	0.000000	-5.343724
1	-2.160271	0.000000	-5.343724
1	0.000000	0.000000	-6.594376

C_6Ph_6-M_4, D_{2h}-symmetry (AM1)

HF=0.3726176

6	0.000000	2.964256	0.000000
6	0.000000	1.479315	0.000000
6	0.000000	-1.479315	0.000000
6	-1.188163	0.709312	0.000000
6	1.188163	0.709312	0.000000
6	1.188163	-0.709312	0.000000
6	-1.188163	-0.709312	0.000000
6	-2.545418	1.290607	0.000000
6	2.545418	1.290607	0.000000
6	2.545418	-1.290607	0.000000
6	-2.545418	-1.290607	0.000000
6	0.000000	-2.964256	0.000000
6	0.000000	5.845500	0.000000
6	1.181781	3.732292	0.000000
6	-1.181781	3.732292	0.000000
6	-1.189607	5.126241	0.000000
6	1.189607	5.126241	0.000000
1	2.182625	3.287768	0.000000
1	-2.182625	3.287768	0.000000
1	-2.154441	5.655564	0.000000
1	2.154441	5.655564	0.000000
1	0.000000	6.943894	0.000000
6	0.000000	-5.845500	0.000000
6	-1.181781	-3.732292	0.000000
6	1.181781	-3.732292	0.000000
6	1.189607	-5.126241	0.000000
6	-1.189607	-5.126241	0.000000
1	-2.182625	-3.287768	0.000000
1	2.182625	-3.287768	0.000000
1	2.154441	-5.655564	0.000000
1	-2.154441	-5.655564	0.000000
1	0.000000	-6.943894	0.000000
6	-5.150753	2.320456	0.000000
6	-3.209902	1.539096	1.211994
6	-3.209902	1.539096	-1.211994
6	-4.503602	2.057619	-1.207245
6	-4.503602	2.057619	1.207245
1	-2.702172	1.327514	2.164517
1	-2.702172	1.327514	-2.164517
1	-5.015659	2.255636	-2.160309
1	-5.015659	2.255636	2.160309

1	-6.171467	2.729306	0.000000
6	5.150753	2.320456	0.000000
6	3.209902	1.539096	1.211994
6	3.209902	1.539096	-1.211994
6	4.503602	2.057619	-1.207245
6	4.503602	2.057619	1.207245
1	2.702172	1.327514	2.164517
1	2.702172	1.327514	-2.164517
1	5.015659	2.255636	-2.160309
1	5.015659	2.255636	2.160309
1	6.171467	2.729306	0.000000
6	-5.150753	-2.320456	0.000000
6	-3.209902	-1.539096	1.211994
6	-3.209902	-1.539096	-1.211994
6	-4.503602	-2.057619	-1.207245
6	-4.503602	-2.057619	1.207245
1	-2.702172	-1.327514	2.164517
1	-2.702172	-1.327514	-2.164517
1	-5.015659	-2.255636	-2.160309
1	-5.015659	-2.255636	2.160309
1	-6.171467	-2.729306	0.000000
6	5.150753	-2.320456	0.000000
6	3.209902	-1.539096	1.211994
6	3.209902	-1.539096	-1.211994
6	4.503602	-2.057619	-1.207245
6	4.503602	-2.057619	1.207245
1	2.702172	-1.327514	2.164517
1	2.702172	-1.327514	-2.164517
1	5.015659	-2.255636	-2.160309
1	5.015659	-2.255636	2.160309
1	6.171467	-2.729306	0.000000

C_6Ph_6-M_7, D_{3h}-symmetry (AM1)

HF=0.4528652

6	0.000000	-2.965742	0.000000
6	0.000000	-1.454803	0.000000
6	0.000000	1.395435	0.000000
6	-1.208482	-0.697717	0.000000
6	1.208482	-0.697717	0.000000
6	1.259896	0.727401	0.000000
6	-1.259896	0.727401	0.000000
6	-2.478400	-1.430905	0.000000
6	2.478400	-1.430905	0.000000
6	2.568408	1.482871	0.000000
6	-2.568408	1.482871	0.000000
6	0.000000	2.861810	0.000000
6	0.000000	-5.895875	0.000000
6	1.163585	-3.768550	0.000000
6	-1.163585	-3.768550	0.000000
6	-1.178681	-5.164147	0.000000
6	1.178681	-5.164147	0.000000
1	2.187874	-3.395854	0.000000
1	-2.187874	-3.395854	0.000000
1	-2.149781	-5.682765	0.000000
1	2.149781	-5.682765	0.000000
1	0.000000	-6.993530	0.000000
6	5.105977	2.947937	0.000000

6	2.681867	2.891969	0.000000
6	3.845452	0.876580	0.000000
6	5.061623	1.561306	0.000000
6	3.882942	3.602841	0.000000
1	1.846959	3.592681	0.000000
1	4.034833	-0.196827	0.000000
1	5.996309	0.979618	0.000000
1	3.846529	4.703147	0.000000
1	6.056575	3.496765	0.000000
6	-5.105977	2.947937	0.000000
6	-3.845452	0.876580	0.000000
6	-2.681867	2.891969	0.000000
6	-3.882942	3.602841	0.000000
6	-5.061623	1.561306	0.000000
1	-4.034833	-0.196827	0.000000
1	-1.846959	3.592681	0.000000
1	-3.846529	4.703147	0.000000
1	-5.996309	0.979618	0.000000
1	-6.056575	3.496765	0.000000
6	-4.899444	-2.828695	0.000000
6	-3.090169	-1.784110	1.220510
6	-3.090169	-1.784110	-1.220510
6	-4.297765	-2.481316	-1.210382
6	-4.297765	-2.481316	1.210382
1	-2.611733	-1.507885	2.170739
1	-2.611733	-1.507885	-2.170739
1	-4.776452	-2.757686	-2.161399
1	-4.776452	-2.757686	2.161399
1	-5.851982	-3.378644	0.000000
6	0.000000	5.657391	0.000000
6	0.000000	3.568220	-1.220510
6	0.000000	3.568220	1.220510
6	0.000000	4.962631	1.210382
6	0.000000	4.962631	-1.210382
1	0.000000	3.015769	-2.170739
1	0.000000	3.015769	2.170739
1	0.000000	5.515371	2.161399
1	0.000000	5.515371	-2.161399
1	0.000000	6.757287	0.000000
6	4.899444	-2.828695	0.000000
6	3.090169	-1.784110	1.220510
6	3.090169	-1.784110	-1.220510
6	4.297765	-2.481316	-1.210382
6	4.297765	-2.481316	1.210382
1	2.611733	-1.507885	2.170739
1	2.611733	-1.507885	-2.170739
1	4.776452	-2.757686	-2.161399
1	4.776452	-2.757686	2.161399
1	5.851982	-3.378644	0.000000

C_6Ph_6, D_6-symmetry (B3PW91/6-31G(d,p))

HF=-1617.97821368
Low frequencies --- 22.1417 22.7405 28.2469
ZPE = 0.585390 (Hartree/Particle)

6	0.000000	2.905761	0.000000
6	0.000000	1.410331	0.000000
6	0.000000	-1.410331	0.000000

6	1.221382	0.705165	0.000000
6	-1.221382	0.705165	0.000000
6	-1.221382	-0.705165	0.000000
6	1.221382	-0.705165	0.000000
6	2.516463	1.452880	0.000000
6	-2.516463	1.452880	0.000000
6	-2.516463	-1.452880	0.000000
6	2.516463	-1.452880	0.000000
6	0.000000	-2.905761	0.000000
6	0.000000	5.715633	0.000000
6	-0.500293	3.621716	1.094455
6	0.500293	3.621716	-1.094455
6	0.497149	5.014091	-1.096693
6	-0.497149	5.014091	1.096693
1	-0.897156	3.079944	1.947953
1	0.897156	3.079944	-1.947953
1	0.887173	5.551521	-1.956798
1	-0.887173	5.551521	1.956798
1	0.000000	6.802115	0.000000
6	-4.949883	2.857816	0.000000
6	-3.386645	1.377592	1.094455
6	-2.886352	2.244125	-1.094455
6	-4.093756	2.937589	-1.096693
6	-4.590904	2.076502	1.096693
1	-3.115888	0.763012	1.947953
1	-2.218732	2.316932	-1.947953
1	-4.364172	3.544075	-1.956798
1	-5.251345	2.007447	1.956798
1	-5.890804	3.401058	0.000000
6	-4.949883	-2.857816	0.000000
6	-3.386645	-1.377592	-1.094455
6	-2.886352	-2.244125	1.094455
6	-4.093756	-2.937589	1.096693
6	-4.590904	-2.076502	-1.096693
1	-3.115888	-0.763012	-1.947953
1	-2.218732	-2.316932	1.947953
1	-4.364172	-3.544075	1.956798
1	-5.251345	-2.007447	-1.956798
1	-5.890804	-3.401058	0.000000
6	4.949883	2.857816	0.000000
6	2.886352	2.244125	1.094455
6	3.386645	1.377592	-1.094455
6	4.590904	2.076502	-1.096693
6	4.093756	2.937589	1.096693
1	2.218732	2.316932	1.947953
1	3.115888	0.763012	-1.947953
1	5.251345	2.007447	-1.956798
1	4.364172	3.544075	1.956798
1	5.890804	3.401058	0.000000
6	0.000000	-5.715633	0.000000
6	-0.500293	-3.621716	-1.094455
6	0.500293	-3.621716	1.094455
6	0.497149	-5.014091	1.096693
6	-0.497149	-5.014091	-1.096693
1	-0.897156	-3.079944	-1.947953
1	0.897156	-3.079944	1.947953
1	0.887173	-5.551521	1.956798
1	-0.887173	-5.551521	-1.956798
1	0.000000	-6.802115	0.000000
6	4.949883	-2.857816	0.000000

6	3.386645	-1.377592	1.094455
6	2.886352	-2.244125	-1.094455
6	4.093756	-2.937589	-1.096693
6	4.590904	-2.076502	1.096693
1	3.115888	-0.763012	1.947953
1	2.218732	-2.316932	-1.947953
1	4.364172	-3.544075	-1.956798
1	5.251345	-2.007447	1.956798
1	5.890804	-3.401058	0.000000

C_6Ph_6, C_1-symmetry (B3PW91/6-31G(d,p))

HF=-1617.9779821

6	2.541045	1.338443	-0.001911
6	1.239124	0.656120	-0.014022
6	3.372319	1.298825	-1.129780
6	2.971442	2.021241	1.144048
6	0.050348	1.408517	-0.002178
6	1.183514	-0.749651	-0.020752
6	4.211468	2.657379	1.157373
6	4.610070	1.939183	-1.112053
1	3.045334	0.754983	-2.028457
1	2.322632	2.059022	2.031670
6	-0.061800	-1.405057	-0.017390
6	-1.195053	0.753686	-0.002880
6	0.110733	2.876615	-0.000386
6	2.428483	-1.530901	-0.021730
6	5.031947	2.618714	0.030380
1	4.540937	3.192316	2.060026
1	5.255732	1.904236	-2.001647
6	-1.250791	-0.652221	-0.012130
6	-0.121482	-2.872924	-0.006566
6	-2.438355	1.537173	-0.009669
1	6.009411	3.122053	0.042763
6	2.786446	-2.292751	-1.142508
6	3.264284	-1.531863	1.103652
6	0.654187	3.564575	-1.094179
6	-0.358507	3.603974	1.102206
6	-2.553361	-1.333029	0.006604
6	4.440355	-2.279576	1.103861
6	3.965616	-3.035803	-1.138384
1	2.129733	-2.305363	-2.025042
1	2.991817	-0.931007	1.984173
6	0.423103	-3.596936	1.063219
6	-0.708023	-3.566441	-1.074426
6	-0.288441	4.995862	1.106445
6	0.717120	4.956747	-1.087178
1	1.039010	2.998520	-1.955774
1	-0.791621	3.070373	1.961477
6	-2.768996	2.331204	-1.116492
6	-3.299037	1.510345	1.096423
6	4.793746	-3.031368	-0.016369
1	5.091210	-2.273313	1.990325
1	4.239908	-3.629351	-2.022675
6	-0.752125	-4.959307	-1.067998
6	0.370701	-4.989532	1.068033
1	0.900966	-3.058988	1.895989
1	-1.144313	-3.003609	-1.913487

6	0.247261	5.674598	0.012293
1	-0.659451	5.558498	1.975504
1	1.142951	5.488358	-1.950610
6	-2.955540	-2.061692	1.134499
6	-3.399489	-1.274023	-1.109446
6	-4.472414	2.262282	1.091372
6	-3.945957	3.077621	-1.118341
1	-2.091076	2.367505	-1.982314
1	-3.048181	0.884214	1.965731
1	5.722843	-3.619342	-0.014757
6	-0.215313	-5.673125	0.003067
1	-1.214549	-5.494740	-1.909981
1	0.797689	-5.548904	1.913161
1	0.299946	6.772838	0.016846
6	-4.629886	-1.928402	-1.092743
6	-4.188503	-2.711428	1.147122
1	-2.290971	-2.122539	2.009130
1	-3.091179	-0.701106	-1.996635
6	-4.798792	3.045496	-0.015409
1	-5.142470	2.234488	1.962991
1	-4.198678	3.696184	-1.991838
1	-0.253207	-6.771973	0.007441
6	-5.027131	-2.646611	0.034776
1	-5.288583	-1.875211	-1.971822
1	-4.497085	-3.279472	2.036847
1	-5.725856	3.636664	-0.018146
1	-5.998800	-3.161069	0.046395

C_6Ph_6-M_0, D_{6h}-symmetry (B3PW91/6-31G(d,p))

HF=-1617.97355235
Low frequencies --- -42.3748 -32.9344 -32.9344

6	0.000000	1.407632	0.000000
6	1.219045	0.703816	0.000000
6	1.219045	-0.703816	0.000000
6	0.000000	-1.407632	0.000000
6	-1.219045	-0.703816	0.000000
6	-1.219045	0.703816	0.000000
6	0.000000	2.903748	0.000000
6	2.514720	1.451874	0.000000
6	2.514720	-1.451874	0.000000
6	0.000000	-2.903748	0.000000
6	-2.514720	-1.451874	0.000000
6	-2.514720	1.451874	0.000000
6	0.000000	3.618176	1.202794
6	3.133432	1.809088	1.202794
6	3.133432	-1.809088	1.202794
6	0.000000	-3.618176	1.202794
6	-3.133432	-1.809088	1.202794
6	-3.133432	1.809088	-1.202794
6	0.000000	3.618176	-1.202794
6	3.133432	1.809088	-1.202794
6	3.133432	-1.809088	-1.202794
6	0.000000	-3.618176	-1.202794
6	-3.133432	-1.809088	-1.202794
6	-3.133432	1.809088	1.202794
6	0.000000	5.011022	1.204006
6	4.339672	2.505511	1.204006

6	4.339672	-2.505511	1.204006
6	0.000000	-5.011022	1.204006
6	-4.339672	-2.505511	1.204006
6	-4.339672	2.505511	-1.204006
6	0.000000	5.011022	-1.204006
6	4.339672	2.505511	-1.204006
6	4.339672	-2.505511	-1.204006
6	0.000000	-5.011022	-1.204006
6	-4.339672	-2.505511	-1.204006
6	-4.339672	2.505511	1.204006
6	0.000000	5.712096	0.000000
6	4.946820	2.856048	0.000000
6	4.946820	-2.856048	0.000000
6	0.000000	-5.712096	0.000000
6	-4.946820	-2.856048	0.000000
6	-4.946820	2.856048	0.000000
1	0.000000	3.075486	2.143983
1	2.663449	1.537743	2.143983
1	2.663449	-1.537743	2.143983
1	0.000000	-3.075486	2.143983
1	-2.663449	-1.537743	2.143983
1	-2.663449	1.537743	-2.143983
1	0.000000	3.075486	-2.143983
1	2.663449	1.537743	-2.143983
1	2.663449	-1.537743	-2.143983
1	0.000000	-3.075486	-2.143983
1	-2.663449	-1.537743	-2.143983
1	-2.663449	1.537743	2.143983
1	0.000000	5.548867	2.148162
1	4.805460	2.774433	2.148162
1	4.805460	-2.774434	2.148162
1	0.000000	-5.548867	2.148162
1	-4.805460	-2.774433	2.148162
1	-4.805460	2.774434	-2.148162
1	0.000000	5.548867	-2.148162
1	4.805460	2.774433	-2.148162
1	4.805460	-2.774434	-2.148162
1	0.000000	-5.548867	-2.148162
1	-4.805460	-2.774433	-2.148162
1	-4.805460	2.774433	2.148162
1	0.000000	6.798500	0.000000
1	5.887674	3.399250	0.000000
1	5.887674	-3.399250	0.000000
1	0.000000	-6.798500	0.000000
1	-5.887674	-3.399250	0.000000
1	-5.887674	3.399250	0.000000

C_6Ph_6-M_1, C_{2v}-symmetry (B3PW91/6-31G(d,p))

HF=-1617.94762852
Low frequencies --- -90.8727 -21.8429 -14.7682

6	0.000000	0.000000	1.602359
6	0.000000	1.212264	0.838594
6	0.000000	-1.212264	0.838594
6	0.000000	1.203629	-0.573229
6	0.000000	-1.203629	-0.573229
6	0.000000	0.000000	-1.289104
6	0.000000	0.000000	3.126091

6	0.000000	2.601981	1.405400
6	0.000000	-2.601981	1.405400
6	1.204143	3.278241	1.635216
6	-1.204143	3.278241	1.635216
6	1.204143	-3.278241	1.635216
6	-1.204143	-3.278241	1.635216
6	1.204598	4.584802	2.117004
6	-1.204598	4.584802	2.117004
6	1.204598	-4.584802	2.117004
6	-1.204598	-4.584802	2.117004
6	0.000000	5.241328	2.364269
6	0.000000	-5.241328	2.364269
6	0.000000	0.000000	6.009178
6	0.000000	1.187281	5.288813
6	0.000000	-1.187281	5.288813
6	0.000000	1.183840	3.896991
6	0.000000	-1.183840	3.896991
6	0.000000	2.484249	-1.354197
6	0.000000	-2.484249	-1.354197
6	0.000000	0.000000	-2.784665
6	1.202180	3.081563	-1.747815
6	-1.202180	3.081563	-1.747815
6	1.202180	-3.081563	-1.747815
6	-1.202180	-3.081563	-1.747815
6	1.203685	4.249179	-2.507155
6	-1.203685	4.249179	-2.507155
6	1.203685	-4.249179	-2.507155
6	-1.203685	-4.249179	-2.507155
6	0.000000	4.837532	-2.889285
6	0.000000	-4.837532	-2.889285
6	1.202728	0.000000	-3.499193
6	-1.202728	0.000000	-3.499193
6	1.203868	0.000000	-4.891932
6	-1.203868	0.000000	-4.891932
6	0.000000	0.000000	-5.593159
1	2.144148	2.764724	1.454468
1	-2.144148	2.764724	1.454468
1	2.144148	-2.764724	1.454468
1	-2.144148	-2.764724	1.454468
1	2.148521	5.091562	2.298441
1	-2.148521	5.091562	2.298441
1	2.148521	-5.091562	2.298441
1	-2.148521	-5.091562	2.298441
1	0.000000	6.260320	2.740831
1	0.000000	-6.260320	2.740831
1	0.000000	0.000000	7.095604
1	0.000000	2.144135	5.804041
1	0.000000	-2.144135	5.804041
1	0.000000	2.148762	3.428410
1	0.000000	-2.148762	3.428410
1	2.143860	2.625673	-1.455130
1	-2.143860	2.625673	-1.455130
1	2.143860	-2.625673	-1.455130
1	-2.143860	-2.625673	-1.455130
1	2.148093	4.698310	-2.802431
1	-2.148093	4.698310	-2.802431
1	2.148093	-4.698310	-2.802431
1	-2.148093	-4.698310	-2.802431
1	0.000000	5.747526	-3.482815
1	0.000000	-5.747526	-3.482815

1	2.143648	0.000000	-2.956205
1	-2.143648	0.000000	-2.956205
1	2.148232	0.000000	-5.429484
1	-2.148232	0.000000	-5.429484
1	0.000000	0.000000	-6.679555

C_6Ph_6-M_3, C_{2v}-symmetry (B3PW91/6-31G(d,p))

HF=-1617.9079617

6	0.000000	2.628610	1.604394
6	0.000000	1.278615	0.859473
6	0.000000	-1.234566	-0.566453
6	0.000000	1.234566	-0.566453
6	0.000000	0.000000	1.522609
6	0.000000	-1.278615	0.859473
6	0.000000	0.000000	-1.239188
6	0.000000	2.403209	-1.510289
6	0.000000	0.000000	3.012035
6	0.000000	-2.628610	1.604394
6	0.000000	0.000000	-2.745133
6	0.000000	-2.403209	-1.510289
6	0.000000	5.229685	2.896374
6	0.000000	2.806016	3.010107
6	0.000000	3.857448	0.903650
6	0.000000	5.107670	1.514481
6	0.000000	4.053213	3.630908
1	0.000000	1.979597	3.687559
1	0.000000	3.881363	-0.165895
1	0.000000	5.990210	0.880384
1	0.000000	4.081756	4.717284
1	0.000000	6.201777	3.381393
6	0.000000	-5.229685	2.896374
6	0.000000	-3.857448	0.903650
6	0.000000	-2.806016	3.010107
6	0.000000	-4.053213	3.630908
6	0.000000	-5.107670	1.514481
1	0.000000	-3.881363	-0.165895
1	0.000000	-1.979597	3.687559
1	0.000000	-4.081756	4.717284
1	0.000000	-5.990210	0.880384
1	0.000000	-6.201777	3.381393
6	0.000000	0.000000	5.812044
6	1.208187	0.000000	3.719734
6	-1.208187	0.000000	3.719734
6	-1.207820	0.000000	5.112274
6	1.207820	0.000000	5.112274
1	2.145074	0.000000	3.170825
1	-2.145074	0.000000	3.170825
1	-2.149909	0.000000	5.653453
1	2.149909	0.000000	5.653453
1	0.000000	0.000000	6.898437
6	0.000000	-4.517997	-3.358481
6	1.204254	-2.932498	-1.990489
6	-1.204254	-2.932498	-1.990489
6	-1.204356	-3.984956	-2.901905
6	1.204356	-3.984956	-2.901905
1	2.144222	-2.528664	-1.625642
1	-2.144222	-2.528664	-1.625642

1	-2.148424	-4.389096	-3.257034
1	2.148424	-4.389096	-3.257034
1	0.000000	-5.339946	-4.068737
6	0.000000	4.517997	-3.358481
6	1.204254	2.932498	-1.990489
6	-1.204254	2.932498	-1.990489
6	-1.204356	3.984956	-2.901905
6	1.204356	3.984956	-2.901905
1	2.144222	2.528664	-1.625642
1	-2.144222	2.528664	-1.625642
1	-2.148424	4.389096	-3.257034
1	2.148424	4.389096	-3.257034
1	0.000000	5.339946	-4.068737
6	0.000000	0.000000	-5.557588
6	-1.200905	0.000000	-3.462614
6	1.200905	0.000000	-3.462614
6	1.203042	0.000000	-4.855158
6	-1.203042	0.000000	-4.855158
1	-2.143439	0.000000	-2.922311
1	2.143439	0.000000	-2.922311
1	2.147968	0.000000	-5.391819
1	-2.147968	0.000000	-5.391819
1	0.000000	0.000000	-6.644017

C_6Ph_6-M_4, D_{2h}-symmetry (B3PW91/6-31G(d,p))

HF=-1617.9164779

6	0.000000	3.019268	0.000000
6	0.000000	1.490033	0.000000
6	0.000000	-1.490033	0.000000
6	-1.194536	0.709175	0.000000
6	1.194536	0.709175	0.000000
6	1.194536	-0.709175	0.000000
6	-1.194536	-0.709175	0.000000
6	-2.568904	1.316848	0.000000
6	2.568904	1.316848	0.000000
6	2.568904	-1.316848	0.000000
6	-2.568904	-1.316848	0.000000
6	0.000000	-3.019268	0.000000
6	0.000000	5.913348	0.000000
6	1.180957	3.798465	0.000000
6	-1.180957	3.798465	0.000000
6	-1.184842	5.190332	0.000000
6	1.184842	5.190332	0.000000
1	2.148978	3.340966	0.000000
1	-2.148978	3.340966	0.000000
1	-2.143511	5.702138	0.000000
1	2.143511	5.702138	0.000000
1	0.000000	6.999734	0.000000
6	0.000000	-5.913348	0.000000
6	-1.180957	-3.798465	0.000000
6	1.180957	-3.798465	0.000000
6	1.184842	-5.190332	0.000000
6	-1.184842	-5.190332	0.000000
1	-2.148978	-3.340966	0.000000
1	2.148978	-3.340966	0.000000
1	2.143511	-5.702138	0.000000
1	-2.143511	-5.702138	0.000000

1	0.000000	-6.999734	0.000000
6	-5.133969	2.460989	0.000000
6	-3.226568	1.596626	1.203676
6	-3.226568	1.596626	-1.203676
6	-4.496090	2.168447	-1.204639
6	-4.496090	2.168447	1.204639
1	-2.724284	1.387542	2.143800
1	-2.724284	1.387542	-2.143800
1	-4.987060	2.388446	-2.148691
1	-4.987060	2.388446	2.148691
1	-6.123250	2.909917	0.000000
6	5.133969	2.460989	0.000000
6	3.226568	1.596626	1.203676
6	3.226568	1.596626	-1.203676
6	4.496090	2.168447	-1.204639
6	4.496090	2.168447	1.204639
1	2.724284	1.387542	2.143800
1	2.724284	1.387542	-2.143800
1	4.987060	2.388446	-2.148691
1	4.987060	2.388446	2.148691
1	6.123250	2.909917	0.000000
6	-5.133969	-2.460989	0.000000
6	-3.226568	-1.596626	1.203676
6	-3.226568	-1.596626	-1.203676
6	-4.496090	-2.168447	-1.204639
6	-4.496090	-2.168447	1.204639
1	-2.724284	-1.387542	2.143800
1	-2.724284	-1.387542	-2.143800
1	-4.987060	-2.388446	-2.148691
1	-4.987060	-2.388446	2.148691
1	-6.123250	-2.909917	0.000000
6	5.133969	-2.460989	0.000000
6	3.226568	-1.596626	1.203676
6	3.226568	-1.596626	-1.203676
6	4.496090	-2.168447	-1.204639
6	4.496090	-2.168447	1.204639
1	2.724284	-1.387542	2.143800
1	2.724284	-1.387542	-2.143800
1	4.987060	-2.388446	-2.148691
1	4.987060	-2.388446	2.148691
1	6.123250	-2.909917	0.000000

C_6Ph_6-M_7, D_{3h}-symmetry (B3PW91/6-31G(d,p))

HF=-1617.8460376

6	0.000000	-3.034608	0.000000
6	0.000000	-1.463735	0.000000
6	0.000000	1.405248	0.000000
6	-1.216981	-0.702624	0.000000
6	1.216981	-0.702624	0.000000
6	1.267632	0.731868	0.000000
6	-1.267632	0.731868	0.000000
6	-2.504157	-1.445776	0.000000
6	2.504157	-1.445776	0.000000
6	2.628047	1.517304	0.000000
6	-2.628047	1.517304	0.000000
6	0.000000	2.891551	0.000000
6	0.000000	-5.971106	0.000000

6	1.167263	-3.844847	0.000000
6	-1.167263	-3.844847	0.000000
6	-1.174769	-5.237870	0.000000
6	1.174769	-5.237870	0.000000
1	2.146981	-3.430244	0.000000
1	-2.146981	-3.430244	0.000000
1	-2.140241	-5.736704	0.000000
1	2.140241	-5.736704	0.000000
1	0.000000	-7.057380	0.000000
6	5.171130	2.985553	0.000000
6	2.746103	2.933302	0.000000
6	3.913366	0.911544	0.000000
6	5.123513	1.601555	0.000000
6	3.948744	3.636315	0.000000
1	1.897188	3.574462	0.000000
1	4.044168	-0.144218	0.000000
1	6.038252	1.014849	0.000000
1	3.898011	4.721855	0.000000
1	6.111870	3.528690	0.000000
6	-5.171130	2.985553	0.000000
6	-3.913366	0.911544	0.000000
6	-2.746103	2.933302	0.000000
6	-3.948744	3.636315	0.000000
6	-5.123513	1.601555	0.000000
1	-4.044168	-0.144218	0.000000
1	-1.897188	3.574462	0.000000
1	-3.898011	4.721855	0.000000
1	-6.038252	1.014849	0.000000
1	-6.111870	3.528690	0.000000
6	-4.925880	-2.843958	0.000000
6	-3.115015	-1.798455	1.209932
6	-3.115015	-1.798455	-1.209932
6	-4.320518	-2.494452	-1.208841
6	-4.320518	-2.494452	1.208841
1	-2.638164	-1.523145	2.145689
1	-2.638164	-1.523145	-2.145689
1	-4.790012	-2.765515	-2.150297
1	-4.790012	-2.765515	2.150297
1	-5.866735	-3.387161	0.000000
6	0.000000	5.687916	0.000000
6	0.000000	3.596909	-1.209932
6	0.000000	3.596909	1.209932
6	0.000000	4.988905	1.208841
6	0.000000	4.988905	-1.208841
1	0.000000	3.046290	-2.145689
1	0.000000	3.046290	2.145689
1	0.000000	5.531030	2.150297
1	0.000000	5.531030	-2.150297
1	0.000000	6.774321	0.000000
6	4.925880	-2.843958	0.000000
6	3.115015	-1.798455	1.209932
6	3.115015	-1.798455	-1.209932
6	4.320518	-2.494452	-1.208841
6	4.320518	-2.494452	1.208841
1	2.638164	-1.523145	2.145689
1	2.638164	-1.523145	-2.145689
1	4.790012	-2.765515	-2.150297
1	4.790012	-2.765515	2.150297
1	5.866735	-3.387161	0.000000

$C_6Ph_5(CCPh)$, C_1-symmetry propeller (B3PW91/6-31G(d,p))

HF=-1694.10784423
Low frequencies --- 16.1173 19.3288 22.8915
ZPE = 0.595507 (Hartree/Particle)

6	0.957479	-2.504461	-0.005659
6	0.184248	-1.228541	0.006244
6	-1.221539	1.224712	-0.000091
6	-1.221530	-1.224708	0.000120
6	0.886051	0.000009	0.000049
6	0.184240	1.228553	-0.006168
6	-1.925777	0.000000	0.000003
6	-1.965774	-2.521131	-0.018261
6	2.309820	0.000014	0.000072
6	0.957465	2.504477	0.005755
6	-3.420232	-0.000008	-0.000023
6	-1.965792	2.521129	0.018260
6	2.436367	-4.890498	-0.029590
6	1.743539	-2.868339	1.094707
6	0.927456	-3.351323	-1.119647
6	1.663309	-4.533336	-1.132827
6	2.473026	-4.054707	1.085751
1	1.780139	-2.214906	1.961686
1	0.322765	-3.078983	-1.979389
1	1.630564	-5.177554	-2.007131
1	3.070250	-4.326179	1.952085
1	3.005631	-5.815960	-0.038021
6	-3.356978	-4.961121	-0.060654
6	-1.892482	-3.405188	1.065081
6	-2.746307	-2.880657	-1.123833
6	-3.433616	-4.091200	-1.146740
6	-2.585035	-4.613043	1.046088
1	-1.285488	-3.142460	1.926558
1	-2.815441	-2.202917	-1.969621
1	-4.032151	-4.353707	-2.014778
1	-2.518424	-5.284717	1.897604
1	-3.895346	-5.904675	-0.076760
6	-6.229661	-0.000024	-0.000072
6	-4.135988	-0.508142	1.091169
6	-4.135956	0.508117	-1.091240
6	-5.528251	0.504904	-1.093319
6	-5.528284	-0.504944	1.093200
1	-3.594278	-0.909996	1.942379
1	-3.594221	0.909977	-1.942432
1	-6.065741	0.900683	-1.950703
1	-6.065798	-0.900729	1.950565
1	-7.316111	-0.000029	-0.000091
6	-3.357018	4.961107	0.060594
6	-1.892459	3.405188	-1.065078
6	-2.746377	2.880648	1.123798
6	-3.433696	4.091185	1.146676
6	-2.585023	4.613037	-1.046114
1	-1.285425	3.142467	-1.926529
1	-2.815542	2.202906	1.969583
1	-4.032272	4.353686	2.014687
1	-2.518381	5.284713	-1.897627
1	-3.895395	5.904657	0.076677
6	2.436351	4.890515	0.029722

6	1.743549	2.868357	-1.094593
6	0.927418	3.351338	1.119743
6	1.663270	4.533350	1.132941
6	2.473034	4.054726	-1.085620
1	1.780168	2.214926	-1.961572
1	0.322709	3.078995	1.979473
1	1.630507	5.177567	2.007246
1	3.070276	4.326199	-1.951942
1	3.005614	5.815977	0.038166
6	3.526610	-0.000014	0.000059
6	4.948104	-0.000006	-0.000006
6	7.751169	0.000013	-0.000141
6	5.661652	1.212576	0.037960
6	5.661665	-1.212578	-0.038037
6	7.051585	-1.206441	-0.037908
6	7.051573	1.206458	0.037694
1	5.110565	2.147245	0.066623
1	5.110588	-2.147255	-0.066645
1	7.592755	-2.148095	-0.067837
1	7.592732	2.148119	0.067571
1	8.837526	0.000020	-0.000194

C_6Ph_5(CCPh), C_{2v}-symmetry (B3PW91/6-31G(d,p))

HF=-1694.1042444

6	0.000000	0.000000	-3.422781
6	0.000000	0.000000	-1.927206
6	0.000000	0.000000	0.881288
6	0.000000	1.222164	-1.224063
6	0.000000	-1.222164	-1.224063
6	0.000000	-1.226193	0.179056
6	0.000000	1.226193	0.179056
6	0.000000	2.520007	-1.968471
6	0.000000	-2.520007	-1.968471
6	0.000000	-2.503839	0.952465
6	0.000000	2.503839	0.952465
6	0.000000	0.000000	2.304391
6	0.000000	0.000000	-6.230566
6	-1.203132	0.000000	-4.136830
6	1.203132	0.000000	-4.136830
6	1.204094	0.000000	-5.529645
6	-1.204094	0.000000	-5.529645
1	-2.144067	0.000000	-3.593859
1	2.144067	0.000000	-3.593859
1	2.148113	0.000000	-6.067752
1	-2.148113	0.000000	-6.067752
1	0.000000	0.000000	-7.316978
6	0.000000	0.000000	3.520956
6	0.000000	0.000000	4.942441
6	0.000000	0.000000	7.745455
6	0.000000	1.213122	5.655969
6	0.000000	-1.213122	5.655969
6	0.000000	-1.207048	7.045886
6	0.000000	1.207048	7.045886
1	0.000000	2.148216	5.104830
1	0.000000	-2.148216	5.104830
1	0.000000	-2.149204	7.587005
1	0.000000	2.149204	7.587005

1	0.000000	0.000000	8.831826
6	0.000000	4.966073	-3.345775
6	-1.203283	3.141378	-2.319056
6	1.203283	3.141378	-2.319056
6	1.204218	4.355196	-3.002384
6	-1.204218	4.355196	-3.002384
1	-2.144374	2.669039	-2.051583
1	2.144374	2.669039	-2.051583
1	2.148182	4.824285	-3.266154
1	-2.148182	4.824285	-3.266154
1	0.000000	5.913040	-3.878297
6	0.000000	-4.966073	-3.345775
6	-1.203283	-3.141378	-2.319056
6	1.203283	-3.141378	-2.319056
6	1.204218	-4.355196	-3.002384
6	-1.204218	-4.355196	-3.002384
1	-2.144374	-2.669039	-2.051583
1	2.144374	-2.669039	-2.051583
1	2.148182	-4.824285	-3.266154
1	-2.148182	-4.824285	-3.266154
1	0.000000	-5.913040	-3.878297
6	0.000000	-4.879968	2.444033
6	-1.204282	-3.105431	1.333080
6	1.204282	-3.105431	1.333080
6	1.204909	-4.285893	2.072481
6	-1.204909	-4.285893	2.072481
1	-2.144431	-2.640218	1.050651
1	2.144431	-2.640218	1.050651
1	2.148750	-4.741562	2.359280
1	-2.148750	-4.741562	2.359280
1	0.000000	-5.801844	3.019120
6	0.000000	4.879968	2.444033
6	-1.204282	3.105431	1.333080
6	1.204282	3.105431	1.333080
6	1.204909	4.285893	2.072481
6	-1.204909	4.285893	2.072481
1	-2.144431	2.640218	1.050651
1	2.144431	2.640218	1.050651
1	2.148750	4.741562	2.359280
1	-2.148750	4.741562	2.359280
1	0.000000	5.801844	3.019120

C_6Ph_5Fc, C_1-symmetry (B3LYP/lanl2dz)

HF=-1896.5088615

6	0.0000000	0.0000000	0.0000000
6	0.0000000	0.0000000	1.4536012
6	1.4004721	0.0000000	-0.3970338
6	1.3580831	0.0582960	1.9234918
26	1.0991792	-1.7016022	0.7834350
6	2.2274637	0.0663998	0.7752525
6	1.6609618	-3.3577333	1.9853150
6	1.6644032	-3.4016975	-0.3496420
6	0.2983887	-3.5149554	1.5420593
6	2.5056821	-3.2868918	0.8173952
6	0.3008418	-3.5410039	0.0984868
6	-1.1535140	0.0370108	-0.9588344
6	-2.4115186	-0.5876973	-0.6820545

6	-0.9909782	0.6956719	-2.2234656
6	-3.3810507	-0.7341145	-1.7100163
6	-2.8312094	-0.9969637	0.7056428
6	-1.9830239	0.5720032	-3.2358071
6	0.1766988	1.6086251	-2.4873760
6	-3.1545589	-0.1909693	-3.0002922
6	-4.6950037	-1.4143359	-1.4241153
6	-2.9148153	-2.3397368	1.1233470
6	-3.2652030	0.0101443	1.5985338
6	-1.8316812	1.2847851	-4.5539219
6	0.3562400	2.7602028	-1.6894221
6	1.0863666	1.3741167	-3.5418762
6	-4.1985952	-0.3368960	-4.0740368
6	-4.8518770	-2.8032219	-1.6133326
6	-5.8031265	-0.6654729	-0.9738875
6	-3.3989192	-2.6701639	2.4017322
6	-3.7502769	-0.3129327	2.8781671
6	-1.5917370	0.5655454	-5.7441089
6	-1.9500636	2.6896090	-4.6270573
6	1.4160193	3.6509940	-1.9336428
6	2.1517874	2.2577916	-3.7858049
6	-4.3312234	-1.5427878	-4.7944292
6	-5.0651518	0.7333592	-4.3846354
6	-6.0832660	-3.4322732	-1.3569435
6	-7.0363726	-1.2895397	-0.7148543
6	-3.8155957	-1.6591892	3.2877001
6	-1.4666245	1.2318554	-6.9762484
6	-1.8296204	3.3599370	-5.8569011
6	2.3215329	3.4029547	-2.9833231
6	-5.3005725	-1.6768127	-5.8045228
6	-6.0376564	0.6032392	-5.3914835
6	-7.1820246	-2.6768327	-0.9052502
6	-1.5860805	2.6334271	-7.0384693
6	-6.1590700	-0.6029777	-6.1075682

C_6Ph_5Fc, C_s-symmetry (B3LYP/lanl2dz)

HF=-1896.50608227
Low frequencies --- -22.2114
ZPE = 0.655730 (Hartree/Particle)

6	0.579481	-0.105456	1.225767
6	0.579481	-0.105456	-1.225767
6	0.180026	1.258405	1.220038
6	0.180026	1.258405	-1.220038
6	-0.081684	1.929136	0.000000
6	0.450415	4.404122	0.000000
6	-1.877812	3.721480	0.000000
1	1.508170	4.150088	0.000000
6	0.056692	5.754043	0.000000
6	-2.276869	5.069994	0.000000
1	-2.631549	2.936792	0.000000
1	0.812087	6.536609	0.000000
6	-1.309734	6.093038	0.000000
1	-3.335498	5.320385	0.000000
1	-1.615661	7.136803	0.000000
6	-0.511316	3.371326	0.000000
6	1.244883	2.515797	3.144699
6	1.244883	2.515797	-3.144699

6	-1.171486	2.305412	3.098195
6	-1.171486	2.305412	-3.098195
1	2.218175	2.312858	2.703842
1	2.218175	2.312858	-2.703842
6	1.160611	3.249024	4.341410
6	1.160611	3.249024	-4.341410
6	-1.261188	3.036297	4.296323
6	-1.261188	3.036297	-4.296323
1	-2.078879	1.945158	2.618604
1	-2.078879	1.945158	-2.618604
1	2.068910	3.612927	4.816434
1	2.068910	3.612927	-4.816434
6	-0.094128	3.511604	4.924032
6	-0.094128	3.511604	-4.924032
1	-2.236303	3.236531	4.734761
1	-2.236303	3.236531	-4.734761
1	-0.161183	4.078753	5.849691
1	-0.161183	4.078753	-5.849691
6	0.081000	2.031635	2.509782
6	0.081000	2.031635	-2.509782
6	2.345707	-0.929477	2.816262
6	2.345707	-0.929477	-2.816262
6	0.042528	-0.927704	3.582245
6	0.042528	-0.927704	-3.582245
1	3.077368	-0.741814	2.033878
1	3.077368	-0.741814	-2.033878
6	2.764944	-1.426419	4.063087
6	2.764944	-1.426419	-4.063087
6	0.455714	-1.428966	4.829116
6	0.455714	-1.428966	-4.829116
1	-1.011759	-0.735734	3.401526
1	-1.011759	-0.735734	-3.401526
1	3.821027	-1.613929	4.243285
1	3.821027	-1.613929	-4.243285
6	1.819479	-1.682105	5.075592
6	1.819479	-1.682105	-5.075592
1	-0.282055	-1.616472	5.605811
1	-0.282055	-1.616472	-5.605811
1	2.139990	-2.067160	6.040817
1	2.139990	-2.067160	-6.040817
6	0.979756	-0.679613	2.556720
6	0.979756	-0.679613	-2.556720
6	0.782072	-2.350755	0.000000
6	0.781006	-3.241539	1.159513
6	0.781006	-3.241539	-1.159513
26	-0.929627	-3.642422	0.000000
6	0.812733	-4.606204	0.718340
6	0.812733	-4.606204	-0.718340
1	0.756406	-2.957647	2.193086
1	0.756406	-2.957647	-2.193086
1	0.826262	-5.472761	1.364301
1	0.826262	-5.472761	-1.364301
6	-2.637204	-4.672014	0.721615
6	-2.637204	-4.672014	-0.721615
6	-2.682586	-2.452256	0.000000
1	-2.612186	-5.546800	1.356683
1	-2.612186	-5.546800	-1.356683
6	-2.664261	-3.299373	1.168052
6	-2.664261	-3.299373	-1.168052
1	-2.678754	-1.370907	0.000000

1	-2.660585	-2.965599	2.196152
1	-2.660585	-2.965599	-2.196152
6	0.675146	-0.849306	0.000000

4.15, C_7Ph_7H, C_s-symmetry (AM1)

ΔH_f = 248.028 kcal/mol
Low frequencies --- 25.03

H	-2.4950611	0.0000000	-1.6030088
C	-1.2609648	-1.2138901	-0.3384146
C	-0.1053294	-1.4957974	0.3117689
C	0.0161564	2.6675629	1.1960942
C	1.1042129	-0.6793968	0.1806082
C	2.3623296	1.4368571	0.0481168
C	1.1042129	0.6793968	0.1806082
C	-1.4259720	0.0000000	-1.2154144
C	0.0161564	-2.6675629	1.1960942
C	-0.1053294	1.4957974	0.3117689
C	-2.4747964	2.0257753	-0.1893903
C	-2.4747964	-2.0257753	-0.1893903
C	-1.2609648	1.2138901	-0.3384146
C	2.3623296	-1.4368571	0.0481168
C	-0.5768253	0.0000000	-2.4502919
C	0.8627178	0.0000000	-4.8595124
C	-0.2125099	-1.2065951	-3.0617251
C	-0.2125099	1.2065951	-3.0617251
C	0.5043467	1.2054704	-4.2571065
C	0.5043467	-1.2054704	-4.2571065
H	-0.4869258	-2.1623046	-2.5875874
H	-0.4869258	2.1623046	-2.5875874
H	0.7872044	2.1600778	-4.7244467
H	0.7872044	-2.1600778	-4.7244467
H	1.4264973	0.0000000	-5.8033666
C	-4.8229932	3.5331064	0.0771199
C	-3.0150927	2.2800599	1.0786223
C	-3.1269585	2.5317207	-1.3235453
C	-4.2909496	3.2848835	-1.1882610
C	-4.1837871	3.0281669	1.2087429
H	-2.5027788	1.8929790	1.9732776
H	-2.7135761	2.3327614	-2.3243791
H	-4.7914393	3.6822467	-2.0833561
H	-4.5996443	3.2207775	2.2085409
H	-5.7438924	4.1248438	0.1814457
C	0.2683024	4.8748053	2.8999347
C	0.0738445	2.4864586	2.5853399
C	0.0859944	3.9632026	0.6683640
C	0.2118553	5.0605175	1.5191903
C	0.1983567	3.5868603	3.4309896
H	0.0223433	1.4706193	3.0044536
H	0.0427116	4.1115826	-0.4208135
H	0.2665294	6.0749126	1.0975299
H	0.2427401	3.4384957	4.5197361
H	0.3686163	5.7415183	3.5690098
C	4.7468558	2.8772953	-0.2294585
C	2.7276587	1.9657442	-1.1971479
C	3.1982817	1.6404267	1.1534292
C	4.3847847	2.3581820	1.0130807
C	3.9166230	2.6803160	-1.3324816

H	2.0712266	1.8098565	-2.0691271
H	2.9133986	1.2325473	2.1346364
H	5.0357822	2.5131701	1.8856974
H	4.2004726	3.0878724	-2.3135543
H	5.6853319	3.4393837	-0.3391369
C	4.7468558	-2.8772953	-0.2294585
C	3.1982817	-1.6404267	1.1534292
C	2.7276587	-1.9657442	-1.1971479
C	3.9166230	-2.6803160	-1.3324816
C	4.3847847	-2.3581820	1.0130807
H	2.9133986	-1.2325473	2.1346364
H	2.0712266	-1.8098565	-2.0691271
H	4.2004726	-3.0878724	-2.3135543
H	5.0357822	-2.5131701	1.8856974
H	5.6853319	-3.4393837	-0.3391369
C	0.2683024	-4.8748053	2.8999347
C	0.0859944	-3.9632026	0.6683640
C	0.0738445	-2.4864586	2.5853399
C	0.1983567	-3.5868603	3.4309896
C	0.2118553	-5.0605175	1.5191903
H	0.0427116	-4.1115826	-0.4208135
H	0.0223433	-1.4706193	3.0044536
H	0.2427401	-3.4384957	4.5197361
H	0.2665294	-6.0749126	1.0975299
H	0.3686163	-5.7415183	3.5690098
C	-4.8229932	-3.5331064	0.0771199
C	-3.1269585	-2.5317207	-1.3235453
C	-3.0150927	-2.2800599	1.0786223
C	-4.1837871	-3.0281669	1.2087429
C	-4.2909496	-3.2848835	-1.1882610
H	-2.7135761	-2.3327614	-2.3243791
H	-2.5027788	-1.8929790	1.9732776
H	-4.5996443	-3.2207775	2.2085409
H	-4.7914393	-3.6822467	-2.0833561
H	-5.7438924	-4.1248438	0.1814457

1.139, $C_7Ph_7^+$, C_1-symmetry (AM1)

ΔH_f = 419.521 kcal/mol
Low frequencies --- 10.88

C1	1.4406418	-0.6868070	-0.2242413
C2	0.6583161	-1.2341191	0.8086536
C3	-0.6309252	-0.8494744	1.2158662
C4	2.3838476	1.0451489	-1.6777587
C5	-1.5202355	0.0147429	0.5449182
C6	-1.1442221	-1.4756359	2.4566926
C7	-1.2220512	0.9494632	-0.4580998
C8	-2.9366294	-0.0555717	0.9771820
C9	-2.3655839	1.7166998	-1.0061367
C10	0.0469258	1.2828916	-0.9774880
C11	2.6705556	-1.4311811	-0.5824957
C12	1.2685562	-2.3585684	1.5583802
C13	1.2259377	0.5242838	-0.9120492
C14	0.1233020	2.5590907	-1.7268852
C15	-4.5254212	3.1377871	-2.0667704
C16	-2.7991369	2.8976551	-0.3911412
C17	-3.0178475	1.2496729	-2.1555820
C18	-4.0953849	1.9608231	-2.6803655

C19	-3.8762031	3.6045486	-0.9238044
H1	-2.2897312	3.2692916	0.5104248
H2	-2.6839303	0.3221965	-2.6434046
H3	-4.6070244	1.5902465	-3.5818906
H4	-4.2129575	4.5334306	-0.4383990
H5	-5.3766004	3.6975279	-2.4845253
C20	0.2748201	4.9859541	-3.1041914
C21	0.3751268	3.7487943	-1.0293934
C22	-0.0521090	2.5903907	-3.1157164
C23	0.0224671	3.8032082	-3.7992336
C24	0.4517909	4.9564938	-1.7204899
H6	0.5143779	3.7321456	0.0614987
H7	-0.2488202	1.6594638	-3.6681111
H8	-0.1180265	3.8238486	-4.8909055
H9	0.6523978	5.8886663	-1.1703192
H10	0.3346210	5.9421346	-3.6468583
C25	-5.6103491	-0.2056301	1.7757106
C26	-3.4154908	0.7855911	1.9894759
C27	-3.8020087	-0.9730321	0.3662051
C28	-5.1352056	-1.0435645	0.7664814
C29	-4.7495891	0.7068643	2.3860192
H11	-2.7399649	1.5057446	2.4745224
H12	-3.4334616	-1.6354104	-0.4307774
H13	-5.8130656	-1.7635590	0.2827488
H14	-5.1219784	1.3680922	3.1835069
H15	-6.6638954	-0.2645077	2.0901519
C30	2.4193716	-4.4759025	2.9729017
C31	1.0390164	-3.6801929	1.1543210
C32	2.0767548	-2.1012898	2.6734959
C33	2.6473368	-3.1604130	3.3775579
C34	1.6165323	-4.7335223	1.8614568
H16	0.4074018	-3.8887960	0.2782417
H17	2.2592572	-1.0660153	2.9972753
H18	3.2792768	-2.9549899	4.2552428
H19	1.4367200	-5.7707543	1.5394329
H20	2.8728137	-5.3101983	3.5302767
C35	4.9648149	-2.8594580	-1.2935841
C36	3.8746513	-1.2085230	0.0962877
C37	2.6191350	-2.3729383	-1.6199491
C38	3.7653638	-3.0836735	-1.9704029
C39	5.0175006	-1.9222776	-0.2618900
H21	3.9195700	-0.4716729	0.9121707
H22	1.6770003	-2.5530243	-2.1581358
H23	3.7215833	-3.8234927	-2.7844186
H24	5.9626088	-1.7432982	0.2735213
H25	5.8688333	-3.4220950	-1.5738055
C40	-2.0955145	-2.6183955	4.8228303
C41	-1.7942455	-2.7152829	2.4258358
C42	-0.9719302	-0.8092807	3.6782022
C43	-1.4467848	-1.3834478	4.8557664
C44	-2.2686004	-3.2817948	3.6081582
H26	-1.9302975	-3.2429536	1.4699730
H27	-0.4623765	0.1648845	3.7105589
H28	-1.3085693	-0.8586069	5.8135315
H29	-2.7803993	-4.2560501	3.5793384
H30	-2.4702934	-3.0686100	5.7551375
C45	4.5722011	2.0358693	-3.1054754
C46	3.3081494	1.8904512	-1.0495369
C47	2.5602037	0.6977089	-3.0231691
C48	3.6538243	1.1928833	-3.7316592

C49	4.3975009	2.3835807	-1.7657448
H31	3.1749830	2.1690291	0.0061424
H32	1.8396852	0.0316702	-3.5205932
H33	3.7904779	0.9159393	-4.7882981
H34	5.1204465	3.0495267	-1.2700142
H35	5.4342820	2.4264727	-3.6681089

1.139, $C_7Ph_7^+$, D_{7h}-symmetry (AM1)

ΔH_f = 419.711 kcal/mol
Low frequencies --- 11.18

C44	0.0000000	0.0000000	-3.1049836
C2	0.0000000	0.0000000	-1.6210815
C3	1.2674126	0.0000000	-1.0107278
C4	-1.2674126	0.0000000	-1.0107278
C5	-1.5804376	0.0000000	0.3607246
C20	-2.4275739	0.0000000	-1.9359256
C14	-3.0271351	0.0000000	0.6909238
C8	1.5804376	0.0000000	0.3607246
C9	-0.7033609	0.0000000	1.4605440
C32	3.0271351	0.0000000	0.6909238
C1	-1.3472019	0.0000000	2.7974935
C12	0.7033609	0.0000000	1.4605440
C38	2.4275739	0.0000000	-1.9359256
C26	1.3472019	0.0000000	2.7974935
C6	-2.5598751	0.0000000	5.3156355
C7	-1.6520938	-1.2119652	3.4306081
C10	-1.6520938	1.2119652	3.4306081
C11	-2.2568719	1.2077332	4.6864428
C13	-2.2568719	-1.2077332	4.6864428
H1	-1.4154017	-2.1670827	2.9391118
H2	-1.4154017	2.1670827	2.9391118
H3	-2.4946665	2.1624314	5.1802285
H4	-2.4946665	-2.1624314	5.1802285
H5	-3.0376466	0.0000000	6.3077382
C15	-5.7519872	0.0000000	1.3128535
C16	-3.7122210	1.2119652	0.8472902
C17	-3.7122210	-1.2119652	0.8472902
C18	-5.0711452	-1.2077332	1.1574558
C19	-5.0711452	1.2077332	1.1574558
H6	-3.1803787	2.1670827	0.7259007
H7	-3.1803787	-2.1670827	0.7259007
H8	-5.6054648	-2.1624314	1.2794108
H9	-5.6054648	2.1624314	1.2794108
H10	-6.8255300	0.0000000	1.5578827
C21	-4.6127356	0.0000000	-3.6785339
C22	-2.9769701	-1.2119652	-2.3740545
C23	-2.9769701	1.2119652	-2.3740545
C24	-4.0667427	1.2077332	-3.2431191
C25	-4.0667427	-1.2077332	-3.2431191
H11	-2.5504657	-2.1670827	-2.0339285
H12	-2.5504657	2.1670827	-2.0339285
H13	-4.4952338	2.1624314	-3.5848293
H14	-4.4952338	-2.1624314	-3.5848293
H15	-5.4736500	0.0000000	-4.3650903
C27	2.5598751	0.0000000	5.3156355
C28	1.6520938	-1.2119652	3.4306081
C29	1.6520938	1.2119652	3.4306081

C30	2.2568719	1.2077332	4.6864428
C31	2.2568719	-1.2077332	4.6864428
H16	1.4154017	-2.1670827	2.9391118
H17	1.4154017	2.1670827	2.9391118
H18	2.4946665	2.1624314	5.1802285
H19	2.4946665	-2.1624314	5.1802285
H20	3.0376466	0.0000000	6.3077382
C33	5.7519872	0.0000000	1.3128535
C34	3.7122210	-1.2119652	0.8472902
C35	3.7122210	1.2119652	0.8472902
C36	5.0711452	1.2077332	1.1574558
C37	5.0711452	-1.2077332	1.1574558
H21	3.1803787	-2.1670827	0.7259007
H22	3.1803787	2.1670827	0.7259007
H23	5.6054648	2.1624314	1.2794108
H24	5.6054648	-2.1624314	1.2794108
H25	6.8255300	0.0000000	1.5578827
C39	4.6127356	0.0000000	-3.6785339
C40	2.9769701	1.2119652	-2.3740545
C41	2.9769701	-1.2119652	-2.3740545
C42	4.0667427	-1.2077332	-3.2431191
C43	4.0667427	1.2077332	-3.2431191
H26	2.5504657	2.1670827	-2.0339285
H27	2.5504657	-2.1670827	-2.0339285
H28	4.4952338	-2.1624314	-3.5848293
H29	4.4952338	2.1624314	-3.5848293
H30	5.4736500	0.0000000	-4.3650903
C45	0.0000000	0.0000000	-5.8999103
C46	0.0000000	1.2119652	-3.8076877
C47	0.0000000	-1.2119652	-3.8076877
C48	0.0000000	-1.2077332	-5.2015591
C49	0.0000000	1.2077332	-5.2015591
H31	0.0000000	2.1670827	-3.2621680
H32	0.0000000	-2.1670827	-3.2621680
H33	0.0000000	-2.1624314	-5.7496198
H34	0.0000000	2.1624314	-5.7496198
H35	0.0000000	0.0000000	-7.0010612

4.35, 1,2,4,6-$C_7H_3Ph_4^+$, C_2-symmetry (AM1)

ΔH_f = 309.246 kcal/mol
Low frequencies --- -23.86

H1	0.0000000	0.0000000	3.1996308
C1	0.0000000	0.0000000	2.0843556
C2	-1.2603539	0.0184496	1.4879067
C3	1.2603539	-0.0184496	1.4879067
C4	1.5430741	-0.0200697	0.1144310
C5	2.4185585	-0.0290604	2.3934571
C6	-2.4185585	0.0290604	2.3934571
C7	-1.5430741	0.0200697	0.1144310
C8	0.7084902	0.0023998	-0.9973529
H2	2.6338828	-0.0406563	-0.1288459
H3	-2.6338828	0.0406563	-0.1288459
C9	-0.7084902	-0.0023998	-0.9973529
C10	-1.4183387	-0.0441090	-2.2896389
C11	1.4183387	0.0441090	-2.2896389
C12	-2.8550150	-0.1563429	-4.6850834
C13	-2.3400047	0.9653337	-2.6070851

C14	-1.2248094	-1.1119587	-3.1762046
C15	-1.9471221	-1.1668524	-4.3671472
C16	-3.0472191	0.9107769	-3.8056545
H4	-2.4977026	1.8064128	-1.9148299
H5	-0.5013613	-1.9055596	-2.9338679
H6	-1.7969449	-2.0112081	-5.0580850
H7	-3.7614855	1.7105707	-4.0566259
H8	-3.4203592	-0.2001869	-5.6295098
C17	2.8550150	0.1563429	-4.6850834
C18	2.3400047	-0.9653337	-2.6070851
C19	1.2248094	1.1119587	-3.1762046
C20	1.9471221	1.1668524	-4.3671472
C21	3.0472191	-0.9107769	-3.8056545
H9	2.4977026	-1.8064128	-1.9148299
H10	0.5013613	1.9055596	-2.9338679
H11	1.7969449	2.0112081	-5.0580850
H12	3.7614855	-1.7105707	-4.0566259
H13	3.4203592	0.2001869	-5.6295098
C22	4.6193397	-0.0405634	4.1213017
C23	2.4373133	-0.8814415	3.5082611
C24	3.5116187	0.8176170	2.1515412
C25	4.6030467	0.8127705	3.0167666
C26	3.5370761	-0.8882911	4.3630347
H14	1.5923651	-1.5604929	3.7015133
H15	3.5027573	1.5023471	1.2891833
H16	5.4543941	1.4854798	2.8269853
H17	3.5509682	-1.5656733	5.2315461
H18	5.4857202	-0.0445349	4.8020097
C27	-4.6193397	0.0405634	4.1213017
C28	-2.4373133	0.8814415	3.5082611
C29	-3.5116187	-0.8176170	2.1515412
C30	-4.6030467	-0.8127705	3.0167666
C31	-3.5370761	0.8882911	4.3630347
H19	-1.5923651	1.5604929	3.7015133
H20	-3.5027573	-1.5023471	1.2891833
H21	-5.4543941	-1.4854798	2.8269853
H22	-3.5509682	1.5656733	5.2315461
H23	-5.4857202	0.0445349	4.8020097

4.35, 1,2,4,6-$C_7H_3Ph_4^+$, C_1-symmetry (AM1)

ΔH_f = 309.48 kcal/mol
Low frequencies --- -21.49

C1	1.9845328	-0.5857693	0.0725424
C2	1.1430749	-1.2143215	0.9901093
C3	-0.2431192	-1.0452925	1.1157728
C4	2.7869268	0.8314408	-1.7438829
C5	-1.1303816	-0.2058683	0.4520304
H1	-0.7171631	-1.7018424	1.8861767
C6	-0.8066129	0.7727424	-0.5215961
C7	-2.5437998	-0.3859997	0.8307352
C8	-1.8657104	1.6898998	-0.9809566
C9	0.4356105	0.9850842	-1.1080250
H2	3.0492252	-0.9167658	0.0985659
C10	1.7705418	-2.1824027	1.9016607
C11	1.6811872	0.3792668	-0.8871157
C12	2.5954659	0.9665672	-3.1277301
C13	-3.7896890	3.5096596	-1.8779451

C14	-2.5461693	2.5035735	-0.0646342
C15	-2.1527989	1.7954007	-2.3504042
C16	-3.1178384	2.6967684	-2.7928176
C17	-3.5005582	3.4133894	-0.5164684
H3	-2.3277587	2.4237199	1.0114070
H4	-1.6244556	1.1579559	-3.0753892
H5	-3.3478870	2.7693936	-3.8672963
H6	-4.0270714	4.0561638	0.2063983
H7	-4.5472045	4.2270609	-2.2314266
C18	4.8899492	1.6834794	-3.3813268
H8	0.4503407	1.7922505	-1.8809904
C19	3.6463140	1.3847175	-3.9405191
H9	3.4937758	1.4791943	-5.0273041
C20	5.0832706	1.5580081	-2.0046519
H10	6.0624861	1.7987982	-1.5615252
H11	4.1988894	1.0425910	-0.1012600
C21	4.0403110	1.1287578	-1.1872495
H12	5.7182255	2.0184001	-4.0261571
H13	1.6202605	0.7247939	-3.5777290
C22	-5.1997349	-0.8399618	1.5773008
C23	-2.9237948	-0.2909817	2.1782302
C24	-3.5017303	-0.7124015	-0.1392471
C25	-4.8234365	-0.9435011	0.2378183
C26	-4.2494404	-0.5095048	2.5452077
H14	-2.1778821	-0.0324763	2.9453186
H15	-3.2107901	-0.7850788	-1.1984478
H16	-5.5710501	-1.2070271	-0.5266584
H17	-4.5459544	-0.4238941	3.6023141
H18	-6.2460817	-1.0191255	1.8713848
C27	2.9732824	-4.0157167	3.6395647
C28	1.1857424	-3.4395153	2.1172201
C29	2.9643412	-1.8521669	2.5618634
C30	3.5566233	-2.7646019	3.4314274
C31	1.7905836	-4.3517198	2.9790286
H19	0.2589663	-3.7181763	1.5919631
H20	3.4262767	-0.8648278	2.4081681
H21	4.4878846	-2.4968209	3.9551136
H22	1.3326244	-5.3409463	3.1374272
H23	3.4466857	-4.7375214	4.3242958

4.36, 1,3,5-$C_7H_4Ph_3^+$, C_1-symmetry (AM1)

ΔH_f = 279.351 kcal/mol
Low frequencies --- 18.89

C1	1.2873933	0.0100689	-0.2798187
C2	0.4611584	-0.6437956	0.6429985
C3	-0.9262975	-0.5141754	0.7837823
C4	2.0762955	1.4441587	-2.0895449
C5	-1.8297933	0.2729587	0.0772901
H1	-1.3751169	-1.1415050	1.5904068
C6	-1.5240879	1.1505978	-0.9830508
C7	-3.2410030	0.1934360	0.4746019
H2	0.7775818	-4.7338475	2.8396705
C8	-0.3139288	1.4368505	-1.5648560
H3	2.3657295	-0.2723086	-0.2241022
C9	1.1243763	-1.5801978	1.5615884
C10	0.9702916	0.9357277	-1.2686010
C11	1.9342518	1.5471297	-3.4823843

C12	1.2086790	-3.7351768	2.6652368
H4	2.8864092	-4.0625686	3.9994991
H5	-2.3981831	1.7046316	-1.3986911
C13	2.3884477	-3.3611732	3.3107615
H6	2.7497558	-0.2140528	2.0407056
H7	3.8659155	-1.8000675	3.5954739
C14	0.5730150	-2.8490787	1.7987265
C15	2.3148683	-1.2115722	2.2077310
H8	-0.3513653	-3.1570120	1.2855940
C16	2.9375280	-2.0979992	3.0828469
C17	4.1853538	2.4112499	-3.6542296
H9	-0.3444232	2.1885773	-2.3880935
C18	2.9881914	2.0231313	-4.2583760
H10	2.8749788	2.0924419	-5.3519816
C19	4.3297943	2.3163256	-2.2690446
H11	5.2722271	2.6268859	-1.7907049
H12	3.4035635	1.7673017	-0.3951904
C20	3.2845602	1.8295839	-1.4878811
H13	5.0156826	2.7922165	-4.2704050
H14	0.9981394	1.2327740	-3.9692669
C21	-5.9309038	0.0413307	1.2311177
C22	-3.5957754	0.2119484	1.8326519
C23	-4.2458589	0.0980095	-0.5011947
C24	-5.5829342	0.0162823	-0.1207004
C25	-4.9361056	0.1421093	2.2050430
H15	-2.8186816	0.3023420	2.6075638
H16	-3.9806716	0.0667358	-1.5693073
H17	-6.3668495	-0.0682191	-0.8900435
H18	-5.2095934	0.1673441	3.2718817
H19	-6.9901959	-0.0180501	1.5288247

4.2, $C_7H_6Ph^+$, C_1-symmetry (AM1)

ΔH_f = 232.520 kcal/mol
Low frequencies --- 62.50

C1	3.5640225	-0.1061078	-0.4281224
C2	2.7353259	-0.7598752	0.4849766
C3	1.3615500	-0.6959078	0.6223089
C4	-3.6730406	-0.3655704	1.0065223
C5	0.4204861	0.0423323	-0.1148419
H1	0.9338318	-1.3344398	1.4311760
C6	0.7065146	0.9025755	-1.1882273
C7	-0.9849115	-0.0974295	0.2702213
H2	3.2585249	-1.4344889	1.2023401
C8	1.9226010	1.2228397	-1.7616141
H3	4.6518427	-0.3275936	-0.3365319
C9	-1.9815492	-0.2139968	-0.7138123
C10	3.2023033	0.7769438	-1.4278060
C11	-1.3500472	-0.1164999	1.6272350
H4	-2.9696527	-0.2457167	3.0545465
H5	-4.7314061	-0.4711845	1.2964116
H6	-0.1796562	1.4115043	-1.6361286
H7	-1.7107524	-0.2205251	-1.7812208
C12	-3.3161421	-0.3542221	-0.3434603
H8	-4.0918962	-0.4568221	-1.1194425
H9	1.8778844	1.9452963	-2.6098475
C13	-2.6883580	-0.2429588	1.9890207
H10	4.0326832	1.1876937	-2.0463183

H11	-0.5839316	-0.0064607	2.4106124

1.140, $C_7Me_7^+$, C_s-symmetry (AM1)

ΔH_f = 168.537 kcal/mol
Low frequencies --- 20.70

C	1.3604115	-0.7495914	-0.3158053
C	0.6269924	-1.2609919	0.7593986
C	-0.5365624	-0.6940981	1.3223011
C	-2.9146142	-0.0296881	1.0393025
C	-1.4924216	0.0310288	0.5817724
C	0.1018748	2.6150582	-1.6087557
C	-1.2421042	0.8170360	-0.5489967
C	-0.8270781	-0.9816616	2.7531923
C	-2.4159116	1.3176957	-1.3178182
C	0.0389065	1.2778621	-0.9480362
C	2.4467666	-1.5997274	-0.8788491
C	1.1471471	-2.5183011	1.3790032
C	1.2307484	0.5652688	-0.8338686
C	2.4686761	1.2042833	-1.3695344
H	0.8701217	3.2559608	-1.1022194
H	-0.8666958	3.1702575	-1.5549899
H	0.3913019	2.5041897	-2.6853949
H	-2.1220906	1.6644184	-2.3406234
H	-2.9076976	2.1688637	-0.7784451
H	-3.1747732	0.5036669	-1.4489280
H	-3.0494470	-0.5813753	2.0004157
H	-3.5309782	-0.5608095	0.2666636
H	-3.3277324	1.0030906	1.1710213
H	0.1234522	-1.1088330	3.3324330
H	-1.4356134	-1.9170767	2.8637406
H	-1.3940317	-0.1340770	3.2176288
H	2.1897174	-2.3611006	1.7573022
H	1.1694417	-3.3369604	0.6127523
H	0.5183281	-2.8855234	2.2257695
H	3.3133816	-1.6531523	-0.1696801
H	2.8125403	-1.2148330	-1.8636689
H	2.0724235	-2.6421635	-1.0518387
H	3.3954413	0.6497926	-1.0798947
H	2.5738174	2.2442851	-0.9644899
H	2.4221049	1.2663402	-2.4873900

1.140, $C_7Me_7^+$, C_{7h}-symmetry (AM1)

ΔH_f = 181.519 kcal/mol
Low frequencies --- -192.05

C	2.4238504	0.0000000	-1.9756763
C	-1.5758484	0.0000000	0.3958035
C	-0.6730738	0.0000000	1.4788273
C	-1.2919770	0.0000000	-0.9852685
C	-0.0352206	0.0000000	-1.6244132
H	-0.6472590	0.0000000	3.7144383
C	1.3867846	0.0000000	2.8027088
C	0.7365391	0.0000000	1.4482640
C	1.2480577	0.0000000	-1.0403416
H	2.5005054	0.0000000	2.8219619
H	1.0740205	-0.9184561	3.3668292

C	1.5915231	0.0000000	0.3271284
C	-3.0410276	0.0000000	0.7283536
C	-1.3265999	0.0000000	2.8316922
H	-3.3076243	0.0000000	1.8098669
H	-3.5214078	-0.9184561	0.2979026
H	-3.5214078	0.9184561	0.2979026
H	-1.9626522	-0.9184561	2.9388867
H	-1.9626522	0.9184561	2.9388867
C	-2.4654995	0.0000000	-1.9234501
H	1.0740205	0.9184561	3.3668292
C	3.0558920	0.0000000	0.6632285
C	-0.0334000	0.0000000	-3.1268566
H	-2.4284715	-0.9184561	-2.5674083
H	-2.4284715	0.9184561	-2.5674083
H	-3.4772809	0.0000000	-1.4575712
H	0.4931534	-0.9184561	-3.4994083
H	0.4931534	0.9184561	-3.4994083
H	-1.0284741	0.0000000	-3.6274285
H	3.3019339	-0.9184561	1.2594806
H	3.3019339	0.9184561	1.2594806
H	3.7653383	0.0000000	-0.1955094
H	3.0434237	-0.9184561	-1.7962826
H	3.0434237	0.9184561	-1.7962826
H	2.1947946	0.0000000	-3.0657581

4.37, 1,3,5-$C_7H_4Me_3^+$, C_s-symmetry (AM1)

ΔH_f = 182.420 kcal/mol
Low frequencies --- -33.48

C	2.8438430	0.0000000	-0.0747782
C	1.3527084	0.0000000	-0.0213669
C	0.7035240	0.0000000	-1.2599130
C	0.7637168	0.0000000	1.2466376
C	-0.5785522	0.0000000	1.6053602
H	1.4829882	0.0000000	2.0993493
H	1.3841602	0.0000000	-2.1441795
C	-0.6530293	0.0000000	-1.5625394
C	-1.6822830	0.0000000	0.7327503
C	-0.9066923	0.0000000	3.0596543
C	-1.0084721	0.0000000	-3.0104511
C	-1.7161808	0.0000000	-0.6423223
H	-2.7362058	0.0000000	-1.0935994
H	-2.6774061	0.0000000	1.2373078
H	3.3052295	0.0000000	0.9434618
H	3.2072831	0.9071142	-0.6242739
H	3.2072831	-0.9071142	-0.6242739
H	-2.1141632	0.0000000	-3.1756183
H	-0.5793624	-0.9068826	-3.5107062
H	-0.5793624	0.9068826	-3.5107062
H	0.0090124	0.0000000	3.7008341
H	-1.5140195	-0.9072109	3.3146863
H	-1.5140195	0.9072109	3.3146863